VOLCANICLASTIC SEDIMENTATION IN A CARADOCIAN MARGINAL BASIN, NORTH WALES

D. Phil. thesis
Department of Earth Sciences
University of Oxford

Trinity, 1988

VOLUME 2: FIGURES

Geoff Orton
Wolfson College
Oxford

LIST OF FIGURES - Chapter 1

LIST OF FIGURES- Chapter 2

LIST OF FIGURES-Chapter 3

LIST OF FIGURES-Chapter 4

LIST OF FIGURES CHAPTER 5

LIST OF FIGURES: Chapt.6

LIST OF FIGURES: Chapter 7

LIST OF FIGURES: Chapter 8

Chapter 1

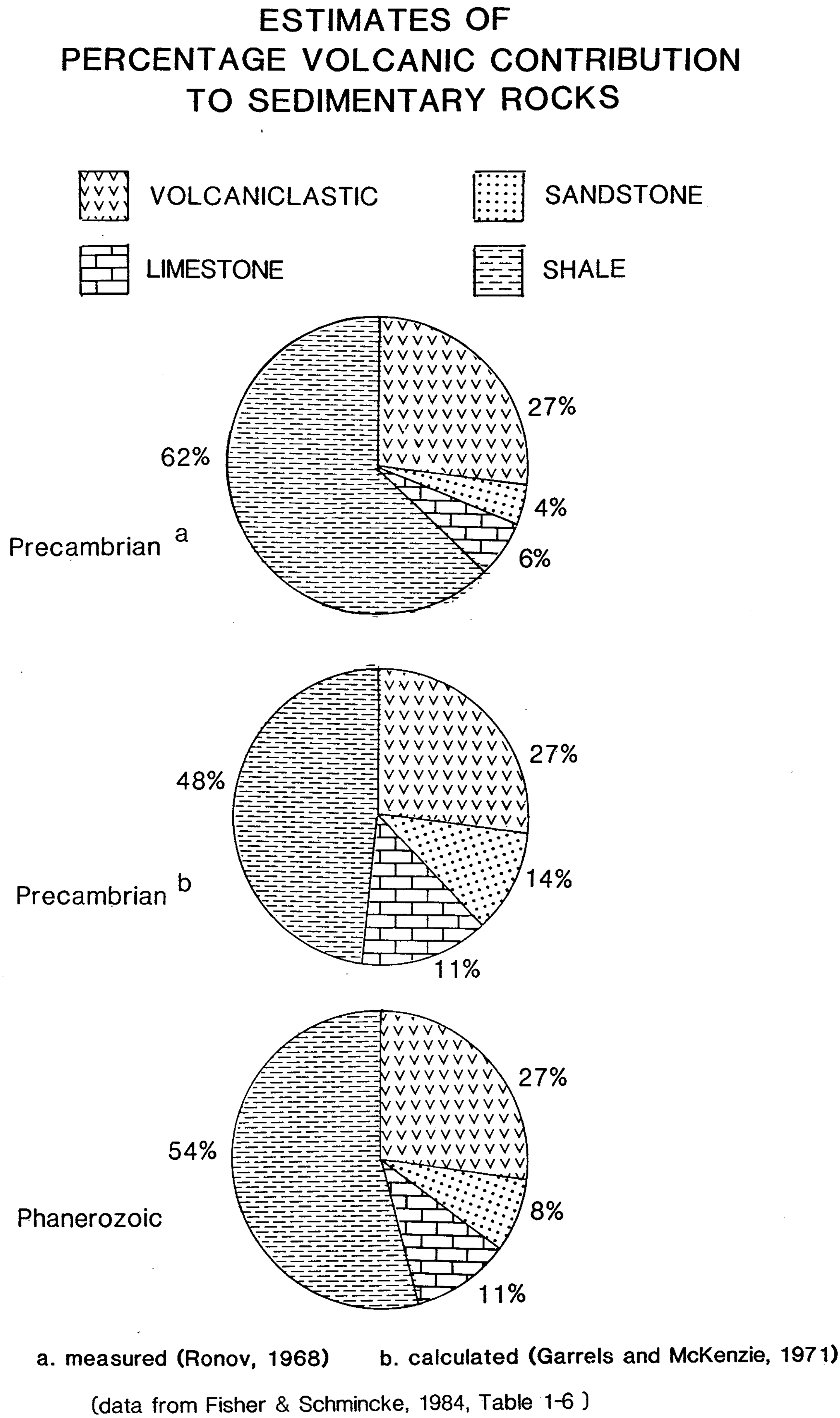

Figure 1.1 Percentage estimates of common sedimentary rocks for Precambrian and Phanerozoic time periods.

Figure 1.2A Conwy castle - a relict of the turbulent 13th century in Wales when the English attempted to eradicate the Welsh spirit.

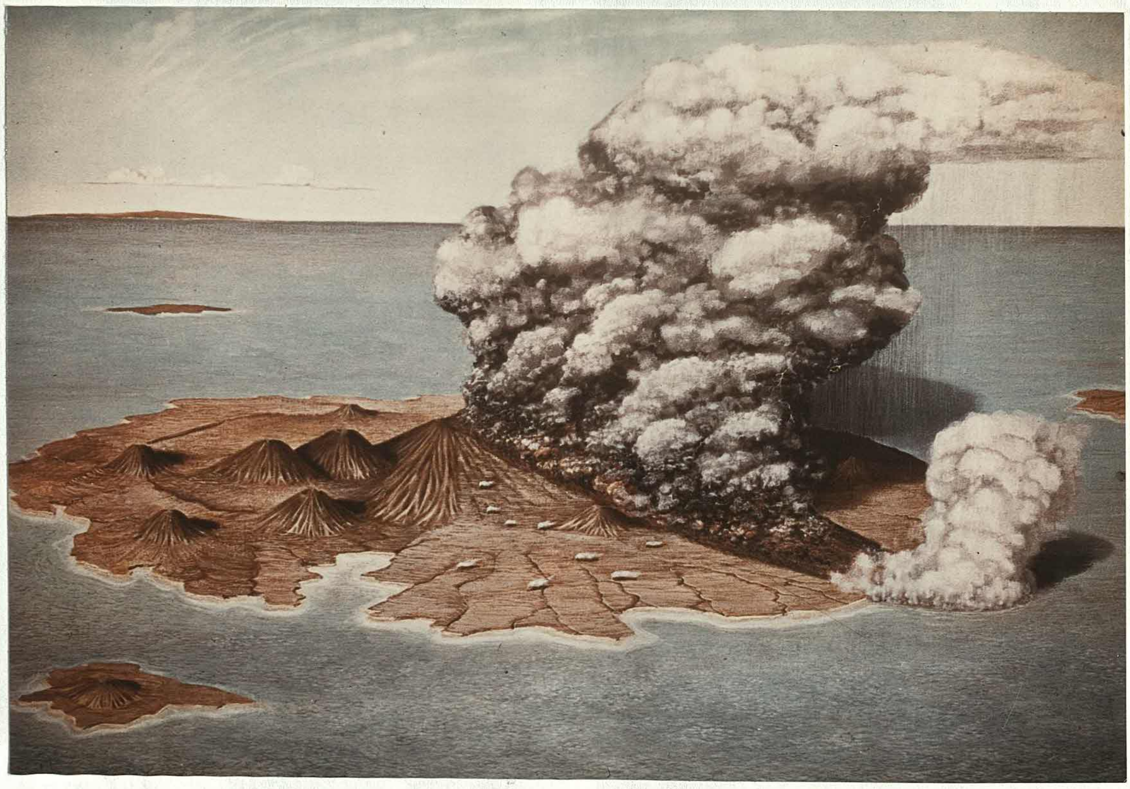

Figure 1.2B Pictorial representation of North Wales during the turbulent Caradoc period showing entry of an ash flow tuff into the sea. (from a painting by A. Oxenham, Geological Museum, London).

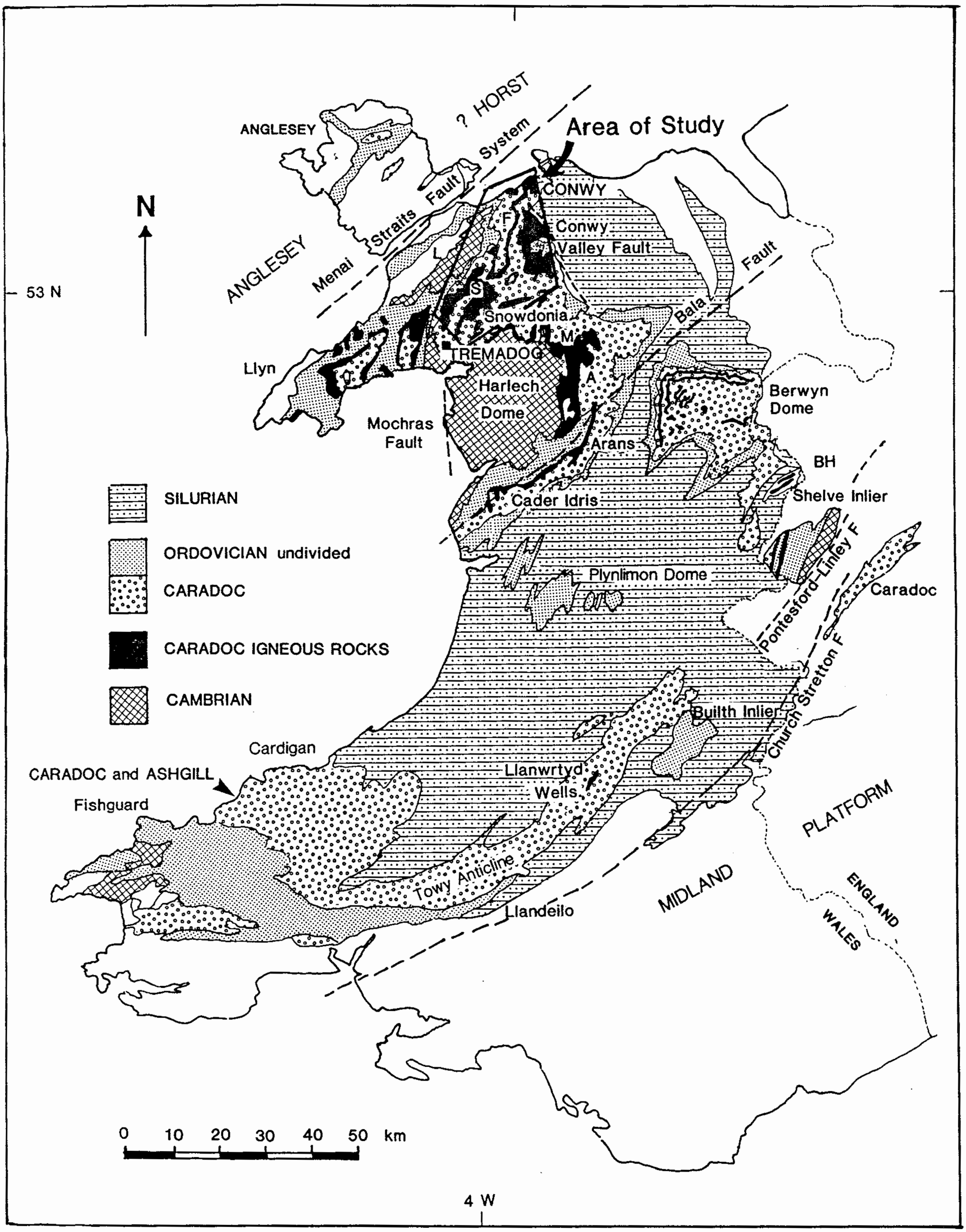

Figure 1.3 Simplified geology of the Welsh Basin showing area of study. (A - Arenigs, BH- Breidden Hills F - Foel Fras Volcanic Complex, L - Llanberis, M - Migneint, Mo - Moelwyns, S - Snowdon. Post-Silurian rocks unshaded.

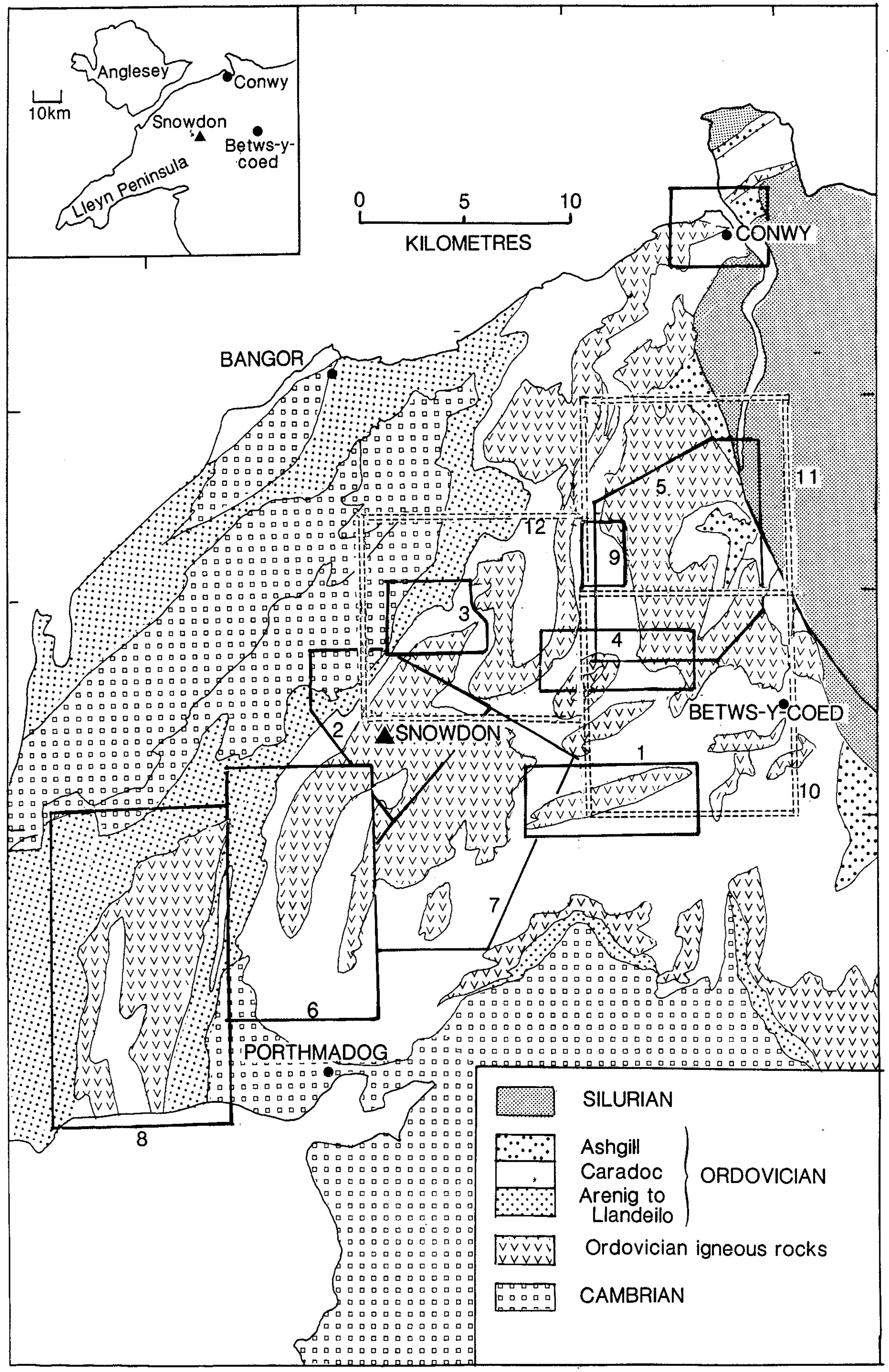

Figure 1.4 Distribution of Lower Palaeozoic rocks in Wales within area of study with index to areas for which geological maps have been published between 1922 and 1988. Areas of "academic" mapping include some coverage by officers of the British Geological Survey (BGS) that is published other than on survey map sheets. BGS maps include both those from new or revised surveys and from new compilations. Numbering of mapping areas is in chronological order. Sources as follows: 1 - H. Williams, 1922; 2 - H. Williams, 1927; 3 - D. Williams, 1930; 4 - Williams & Bulman, 1931; 5 - Davies, 1936; 6- Shackleton, 1959; 7 - Beavon, 1963; 8 - Roberts, 1967; 9 - Diggens & Romano, 1968; 10 - BGS Sheet Capel Curig and Betws-y-Coed, 1976 (1:25,000); 11 - BGS Sheet SH 76, Dolgarrog, 1981 (1:25,000); 12 - BGS Sheet Passes of Llanberis and Nant Ffrancon, 1986

ISOPACHYTE MAPS OF THE ORDOVICIAN AND CARADOCIAN ROCKS IN WALES

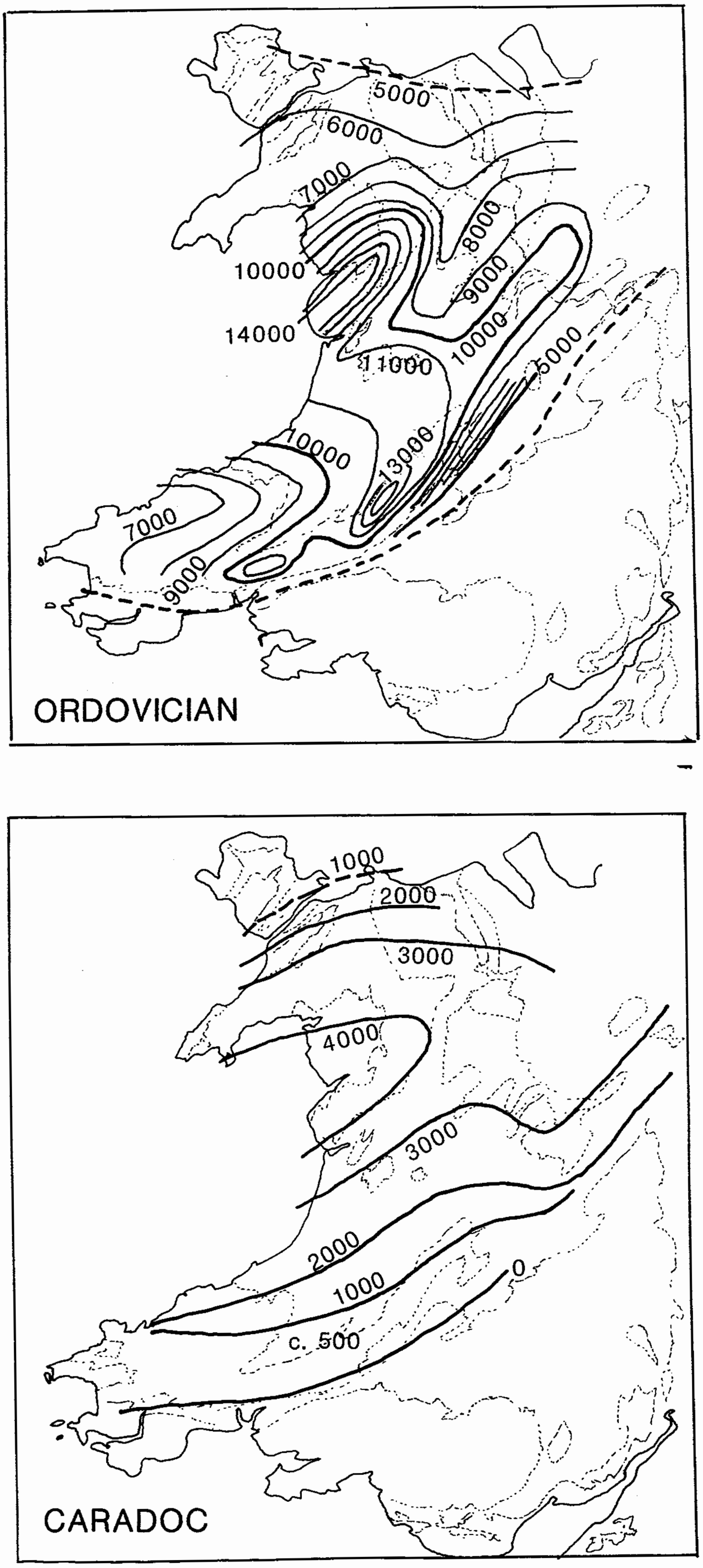

(after O.T. Jones, 1938)

Figure 1.5 Isopachytes of Ordovician and Caradocian sediments within the Welsh Basin (from O.T. Jones, 1938). Scale in feet.

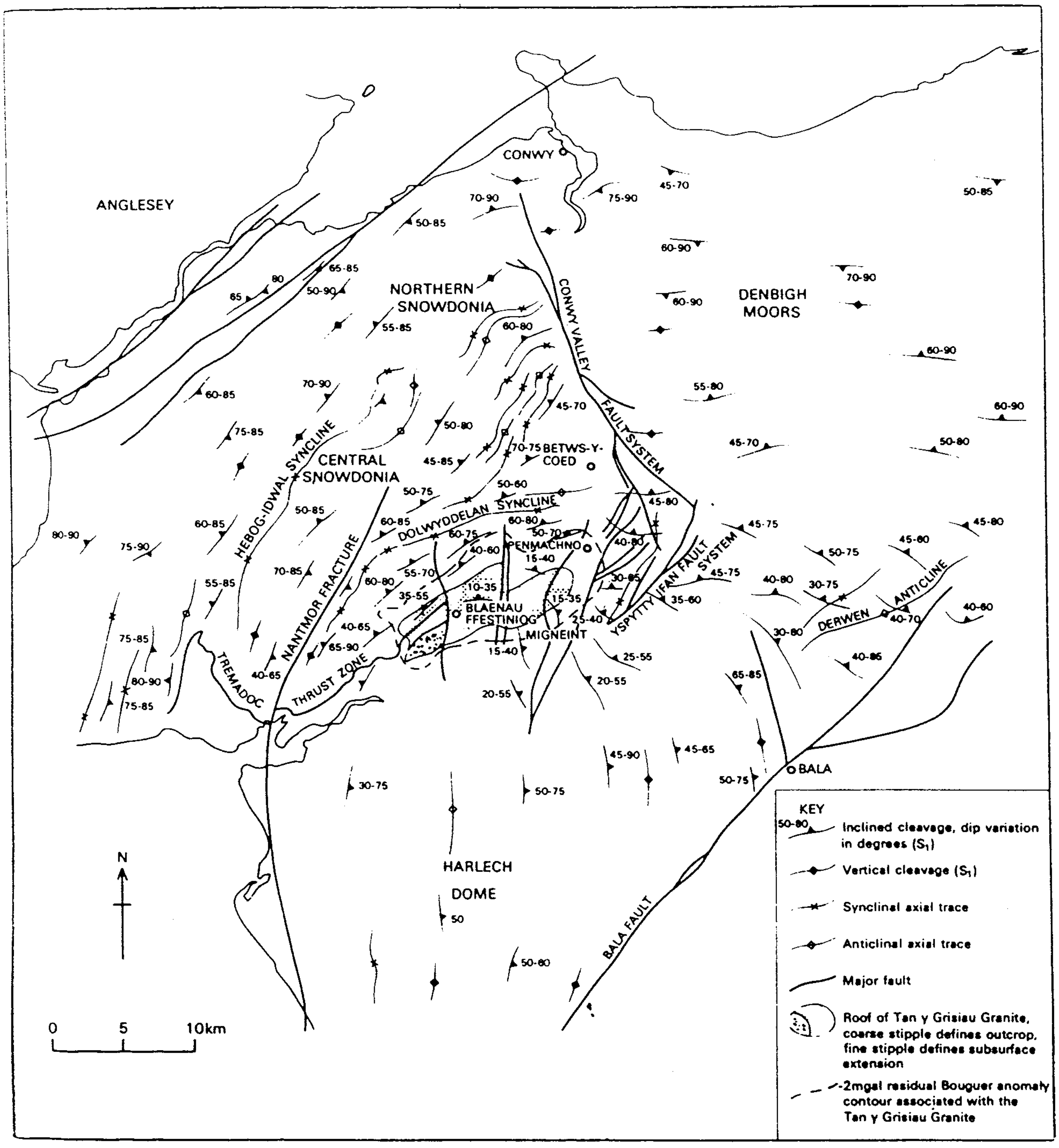

Figure 1.6 A structural map of North Wales showing a) arcuate nature of principal fold axial traces and S_1 cleavage strikes and b) distribution of mapped fault systems. Map compiled from BGS 1:50,000 Bangor sheet, and 1:25,000 sheets SH75, Capel Curig and Betws y Coed; SH76, Dolgarrog, SH65/66 Passes of Nant Francon and Llanberis and Special Snowdonia by Campbell *et al*, 1985.

Fig. 1.7a View of Tryfan anticline, showing outcop of Capel Curig Volcanic Fm. on the Peaks of Tryfan (x) as well as Gwern Gof Tuff on centre-left (arrow).

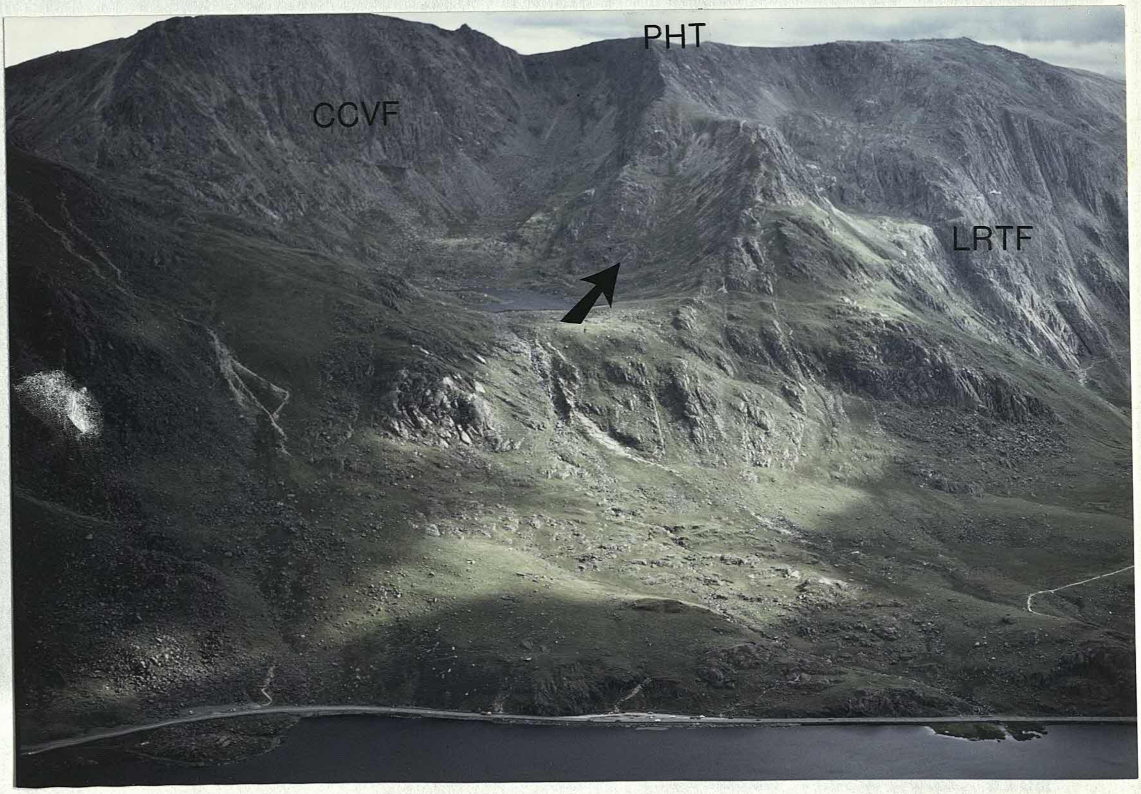

FIG. 1.7b: View of west side of Idwal syncline showing succession from Capel Curig Volcanic Fm. on Glyder Fach through Lower and Upper Cwm Eigiau Fms. to Lower Rhyolitic Tuff Fm. Pitts Head Tuff Fm is indicated by arrow.

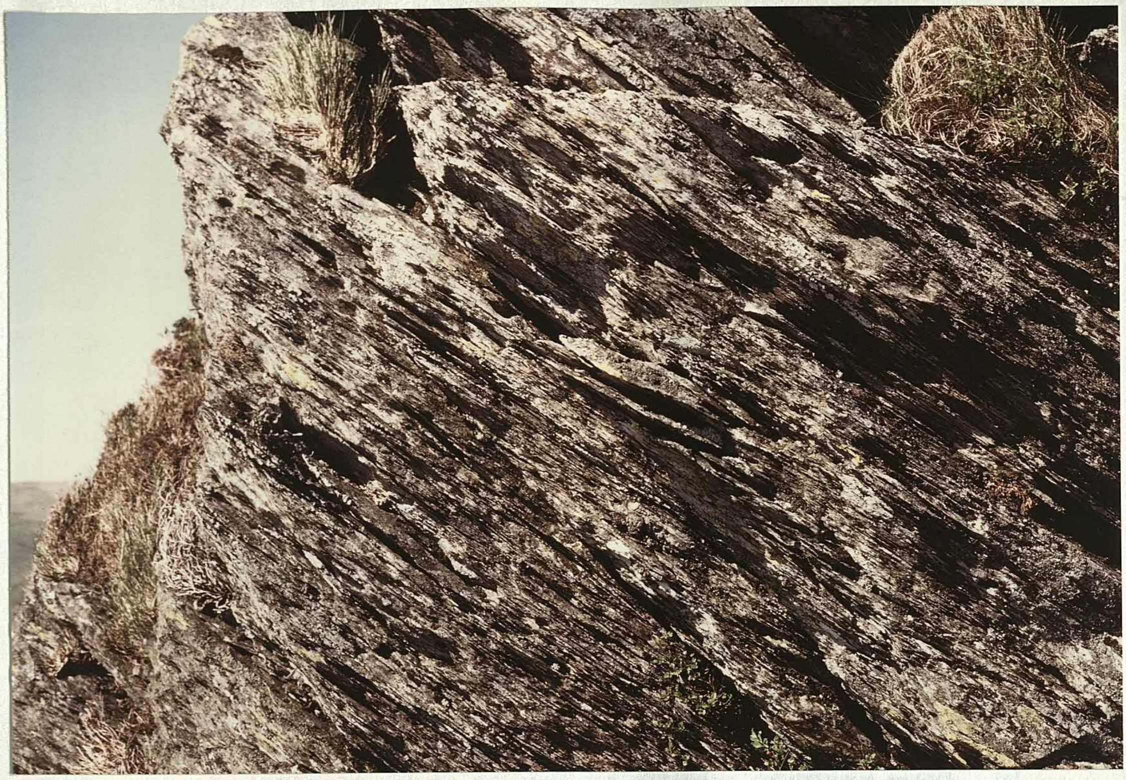

Fig. 1.8a: Pervasive slatey cleavage within mudstone. From Upper Cwm Eigiau Fm. near Pen-yr-Helgi Du.

FIG. 1.8b: Refraction of slatey cleavage as it passes into very fine-grained sandstone to coarse siltstone storm beds. From Pen-yr-ole Wen, SH 6512 6181.

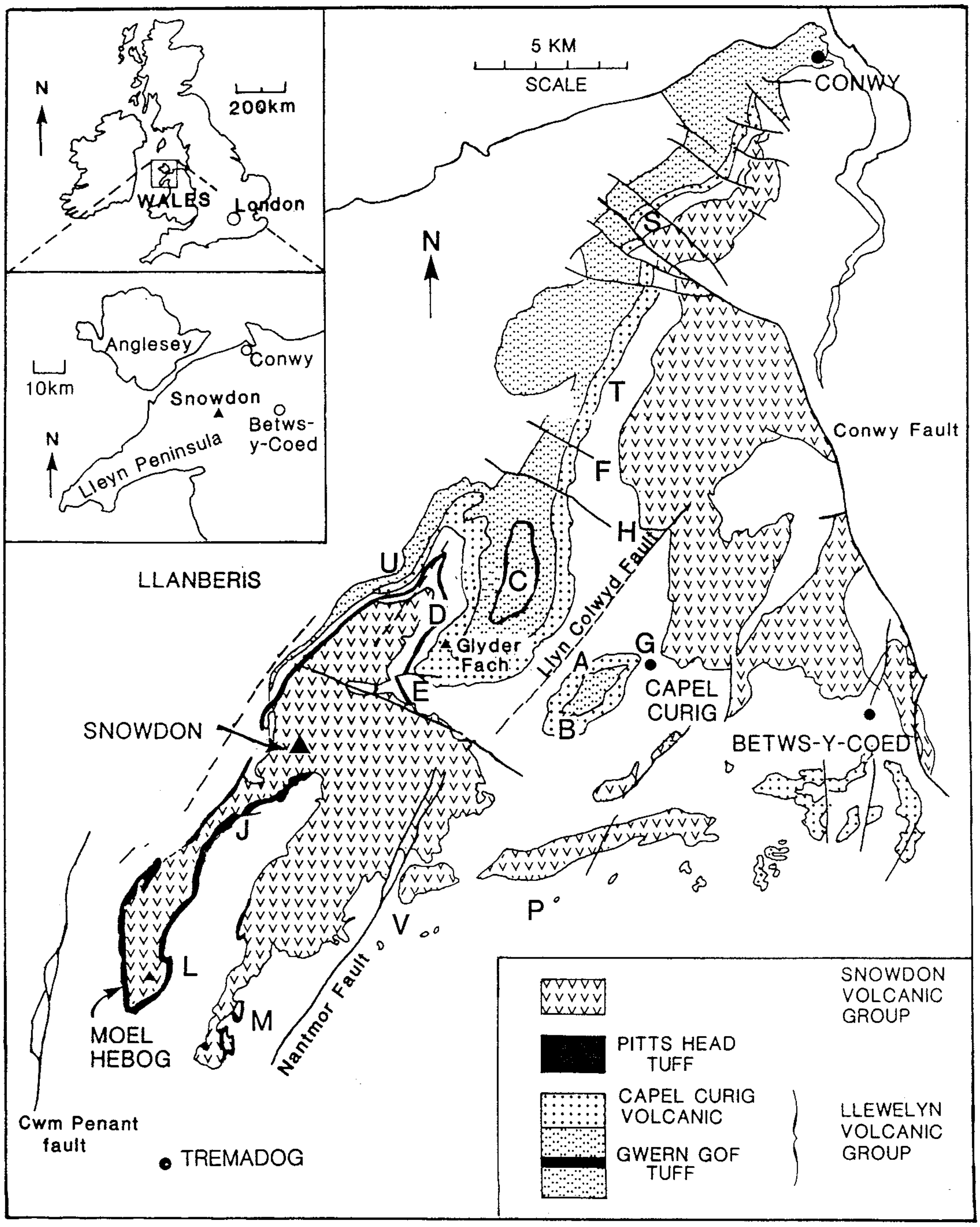

Figure 1.9 Distribution of the main volcanic successions within the area of study showing location of the various "regions" of study.

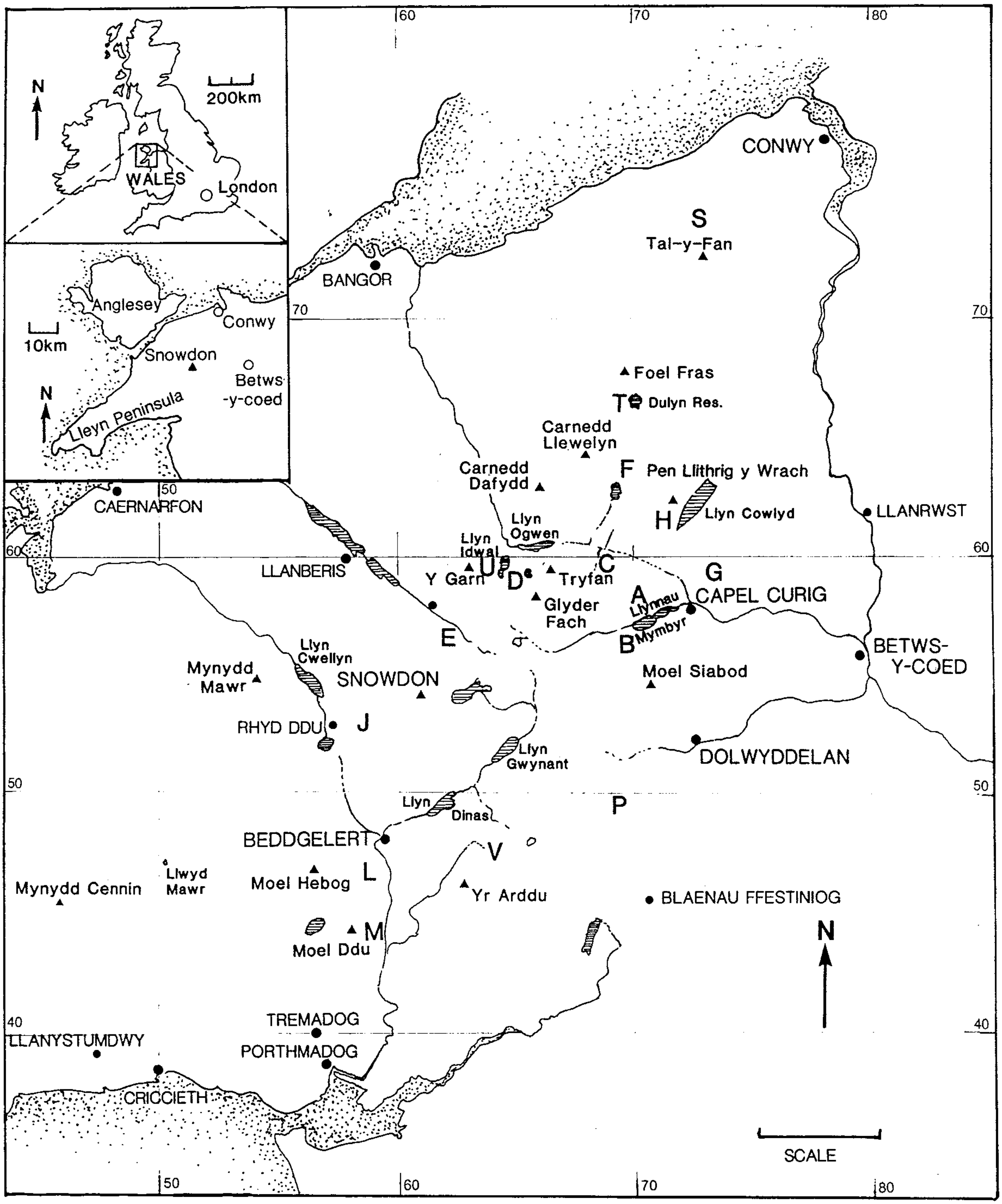

Figure 1.10 Location of place-names (towns, lakes, mountains) commonly referred to within text.

PRONUNCIATION OF WELSH

THE PRONUNCIATION OF WELSH

Welsh is fairly phonetically written and each individual letter, with one or two exceptions, represents one sound only. The number of sounds that will be new are few, and when mastered, will present little or no difficulty.

Stress. The stress generally falls on the last-but-one syllable in the word, i.e. Llanélli, eistéddfod.

The Alphabet

A (a:) (1) long as in the first *a* in H*a*lleluja.
(a) (2) short as in the second *a* in Hall*e*luja.
B as in English.
C as in 'cat' (never s). There is no k in Welsh.
CH as in Scottish 'loch'. BACH (long A)=small. [J. S. Bach has frequently figured in music howlers in Wales as a Welsh musician!]
D as in English, 'dog', 'devil', etc.
DD as 'th' in *this* (the softer sound of *th*). 'Though' in Welsh would be written 'ddo'.
E (e) (1) long sound. Pêl (a ball) like the clear vowel sound of 'a' in 'pale'.
(ɛ) (2) short as in pell-mell. Ll*a*n*e*lli (short *a*, short *e*). Pen (a head).
F as English v. Vandal in Welsh would be spelt 'fandal'.
FF as English f or ph. The Welsh for 'phone' is 'ffôn'.
G as in '*g*et'. Gêm (game).
NG as in 'ha*ng*'. Llong (a ship). In a few words such as dangos (dang-gos) and Bangor (Ban-gor) as in English 'finger'.
H as in 'help', 'hand'. Never silent. Halen (long *a*, short *e*), salt.
I (i) (1) vowel, long like *ee* in n*ee*d. Mil (a thousand) pronounced like English 'meal', short like *i* in s*i*n, DIM (nothing) pronounced like English 'dim'.
(j) (2) consonant, like *y* in *y*ard ('Iard' in Welsh). Arian (money), *I*aith (language).
J only in borrowed words such as JAM (and Jones!).
L as in 'lot'.
LL a consonant whose difficulty is much overrated, and which can easily be mastered with a little practice. Put the tip of the tongue against the roof

of the mouth and hiss. Llan ('church' or 'village') Llan-gollen, Llanelli.
M as in English 'make'.
N as in English 'not'.
O (o) (1) long, as in 'more'. (Welsh 'môr'-sea: 'tôn'-tone: the vowel has a pure vowel sound.)
(ɔ) (2) short, as in 'pot', 'not'. Ton (a wave).
P as in English 'pot'.
PH as in English 'pheasant'.
R is trilled as in 'robin', 'horrid'. fferm (a farm).
RH r accompanied by an emission of breath (h). Rhedeg (to run).
S as in '*s*at, never as in 'hi*s*'. Sosban (a saucepan).
SI as English *sh*. Siop (shop), siarad (to speak).
T as in English. Testament (testament).
TH as in '*th*ink' (not as in '*th*is'). Anthem (anthem). Athro (a teacher).
U (1) long. In South Wales generally pronounced like *i* (*ee*). In North Wales, it resembles an *ee* pronounced as far back in the throat as possible (without swallowing it entirely). E.g. *un* (pronounced as *een*) one.
(2) short. pump (pronounced pimp), punt (pron. pin-t), papur pumpunt=a £5 note.
W (u:) (1) long *oo* sound. 'ffŵl' (English 'fool'), drws (door).
(u) (2) short *oo* sound. Twc (as English 'took'). Cwm (valley). The Western 'Cwm' on Everest was so named by Mallory, 'doubtless', according to Sir John Hunt, 'from affection for his Welsh climbing haunts'.
Y (i:) (1) long clear sound similar to *ee*. This sound (normally written y) will be denoted by the symbol ɥ in the pages of this book in order to distinguish it from the obscure sound which will be written y. Dɥn (pronounced like English 'dean') a man.
(i) short clear sound similar to *i* in b*in*. Brɥn, hill (pronounced like the first syllable in 'Brinley').
(ə) (2) obscure sound like the vowels in *udder, fur*. YN (in). Both sounds are found in some words, e.g. hynnɥ (pronounced like English 'honey'), Cymrɥ (Welsh people) pronounced 'come-ree'. One of the most difficult letters for beginners, it has the clear sound generally if it occurs in the last syllable of a word or in a monosyllable, otherwise it has the

obscure sound. However, Y, YR (the), fy (my), dy (thy), yn (in) have the obscure sound.

Diphthongs

The chief vowel comes first, but both are pronounced in quick succession, e.g. ae, ai, au, ei, eu, eɥ, aw, ew, i'w, ɥw, wɥ, oe, oi, ou, ow.

ae, ai, au are pronounced like 'aye' (aye, sir) in English—the first diphthong slightly broader than the second.
ei, eu, eɥ here the *e* has the obscure *y* sound. Teigar (English 'tiger'), creu (to create). The diphthongs are similarly pronounced. Tei (a tie) as in English, tie.
aw aa-oo (the sound of *ow* in f*ow*l). The first element slightly more emphatic than the second as in Brawd (brother).
ew a slightly more difficult combination for the non-Welsh speaker. The *e* sound is an *open* one as in 'pell-mell'. The tendency to pronounce the Welsh 'dew' (a form of 'tew'-fat) as the English word 'dew' must be resisted.
iw, ɥw pronounced somewhat like '(y)ew' in English: bɥw (to live).
wɥ oo-ee, the first element longer than the second, as in 'wɥth' (eight), ŵɥ (an egg), pwɥ? (who?).
oe, oi, ou similar to *oi* in *oi*l, with the variations of *e* and *u* noted above.

Accents

A circumflex accent over a vowel shows that the vowel is a long one: tɥ̂ (tee), a house; gŵr (goor), a husband.

Figure 1.11 Guide to pronunciation of Welsh for those of foreign tongue.

Chapter 2

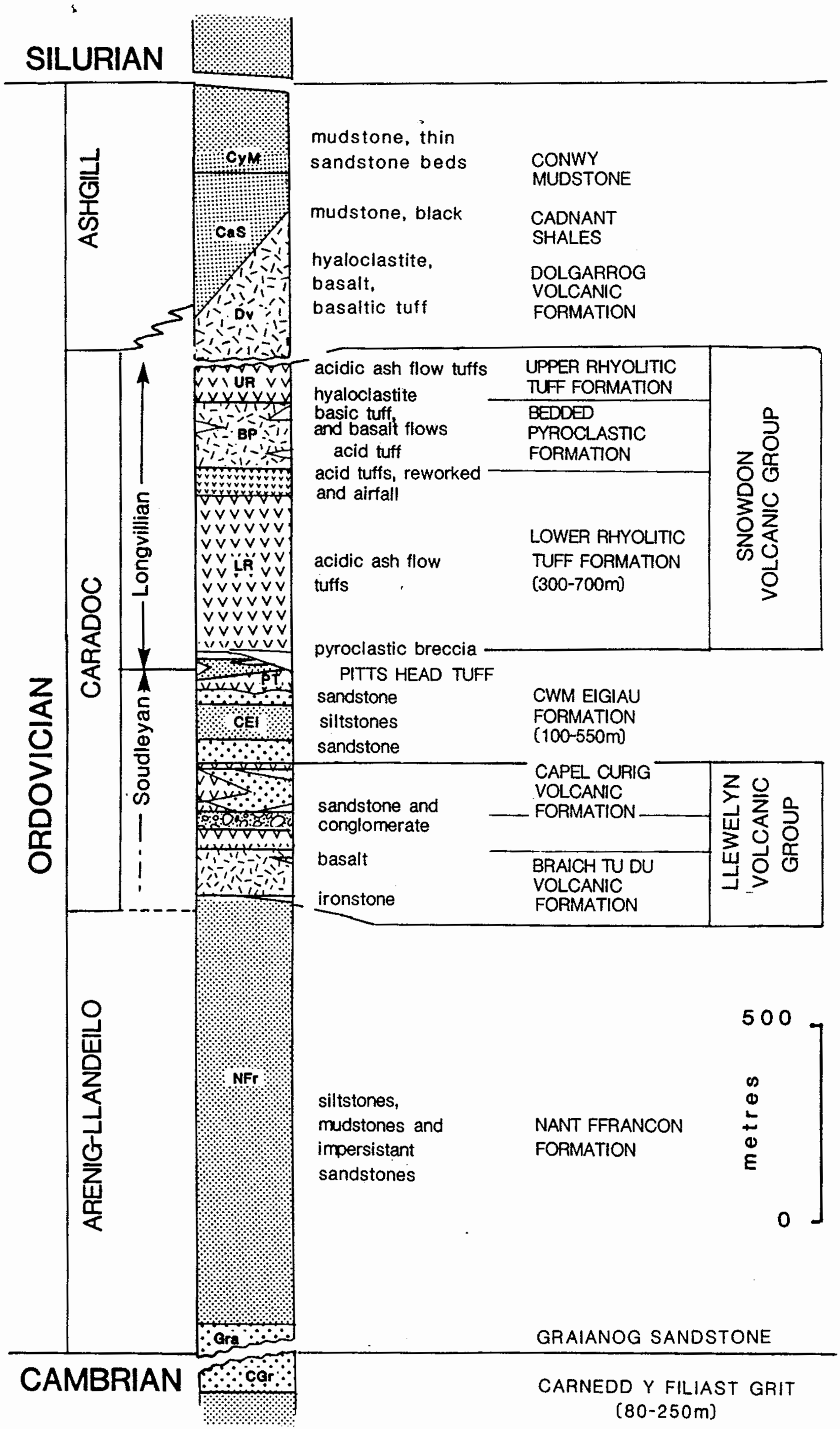

Figure 2.1 General stratigraphic column for the Ordovician System in North Wales.

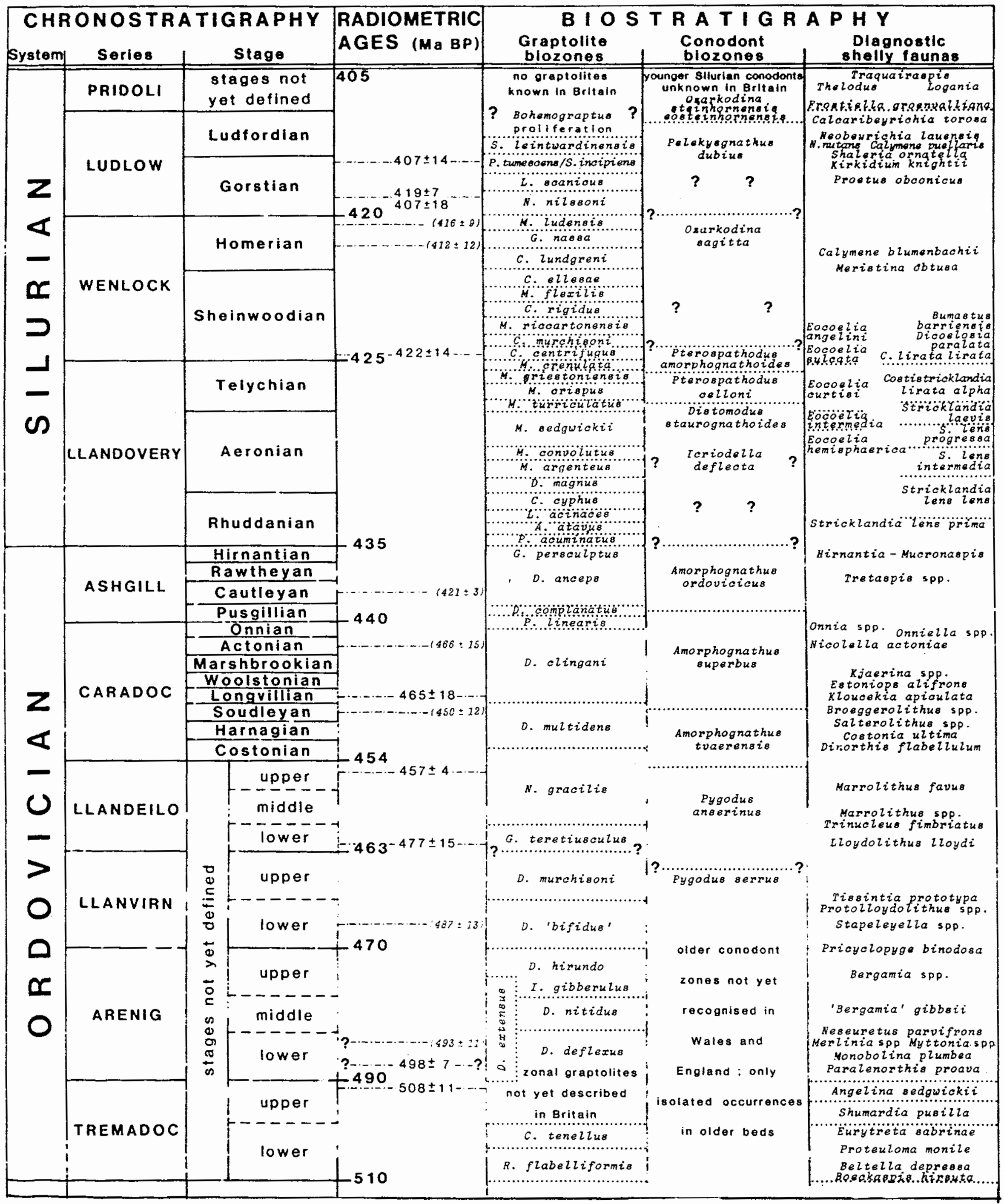

Figure 2.2 Chronostratigraphical subdivision of the Ordovician and Silurian in Wales and the Welsh Borderland. Graptolite and conodont biozones are those proved to be present in Wales and England. Chronometric ages for the base of each System and Series are interpolations; ages in the centre of this column are restricted to samples in Wales and England whose stratagraphic positions are known within close limits with analytical errors less than 2%. Shelly fauna listed (trilobites, brachiopods, ostracodes) are all taxa that occur in the region; they are not considered to be of biozonal status but are used as examples of the reasonably diagnostic correlative fauna. (from Bassett, 1984, Fig. 7).

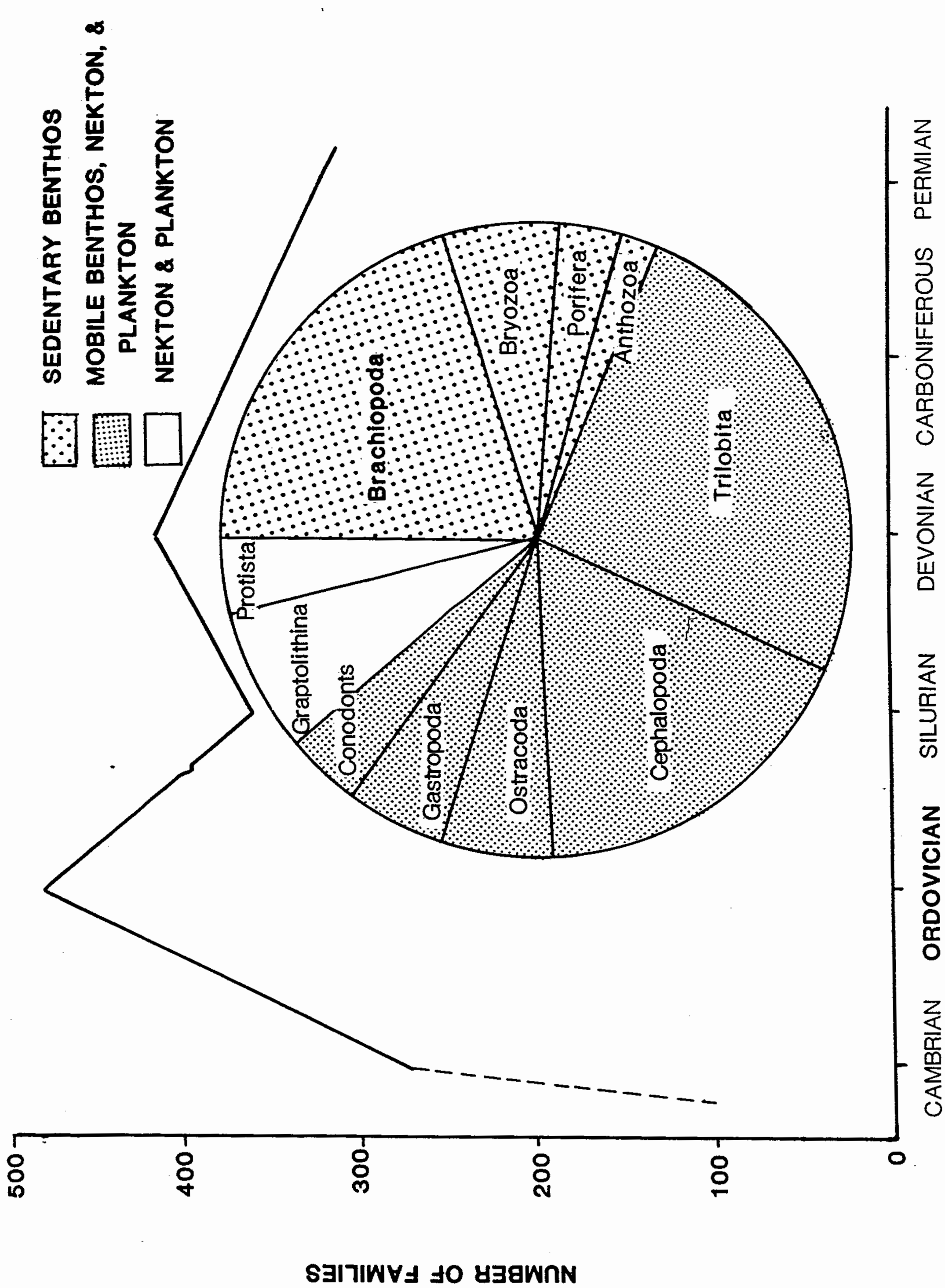

Figure 2.3 Polygonal frequency distribution of Palaeozoic families of Protista, Archaeocyatha, Porifera, Bryozoa, Coelenterata, Brachiopoda, Mollusca (archaeogastropods, nautiloids, ammonoids and bivalves), Arthropoda (decapods, ostracodes and trilobites), Echinodermata and Graptolithina; relative commonness of occurrence of principal Ordovician phyla indicated by sectors of a circle and classed according to the typical adult mode of life (from Williams, 1976)

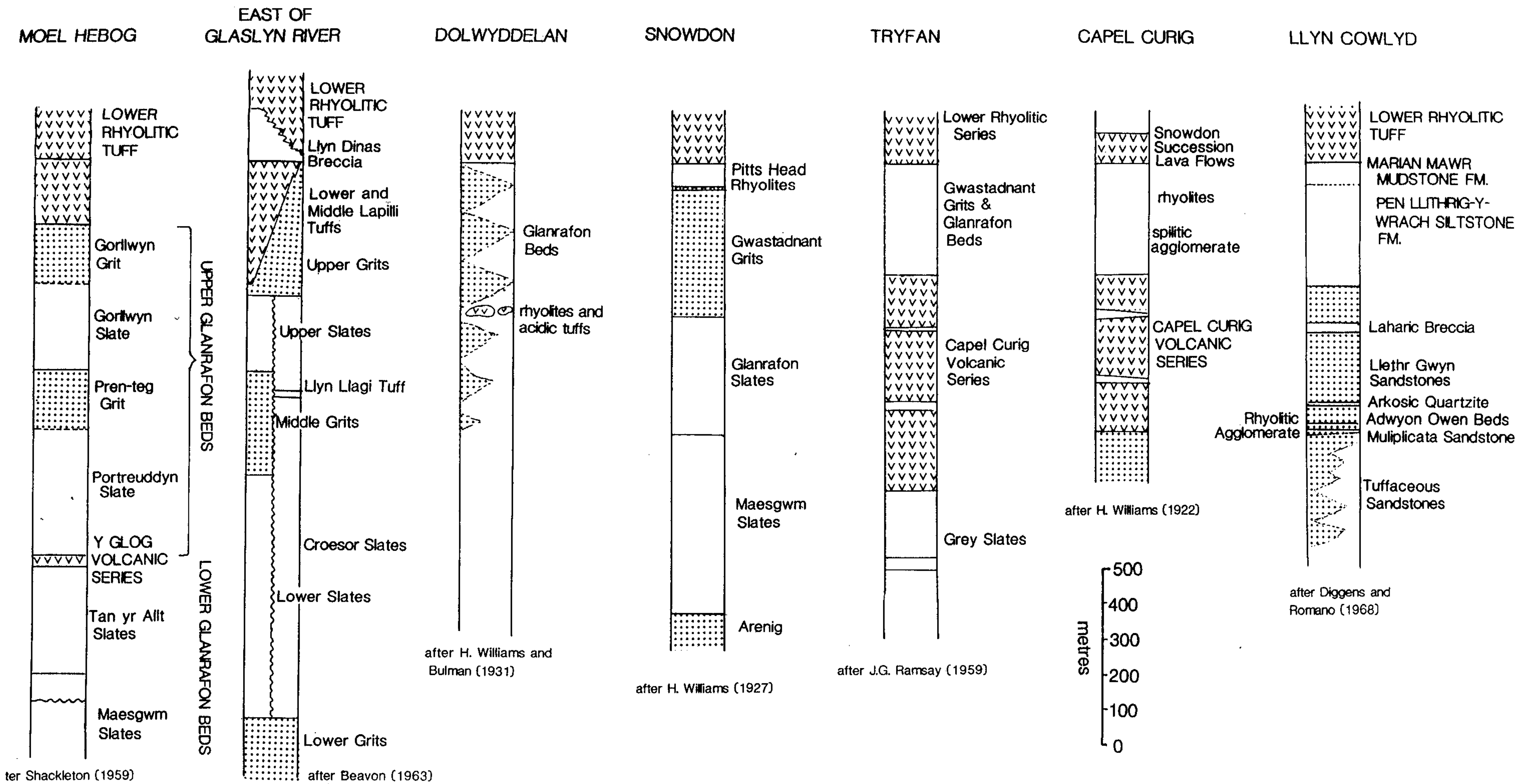

Figure 2.4 Stratigraphic schemes suggested for various portions of the Welsh basin.

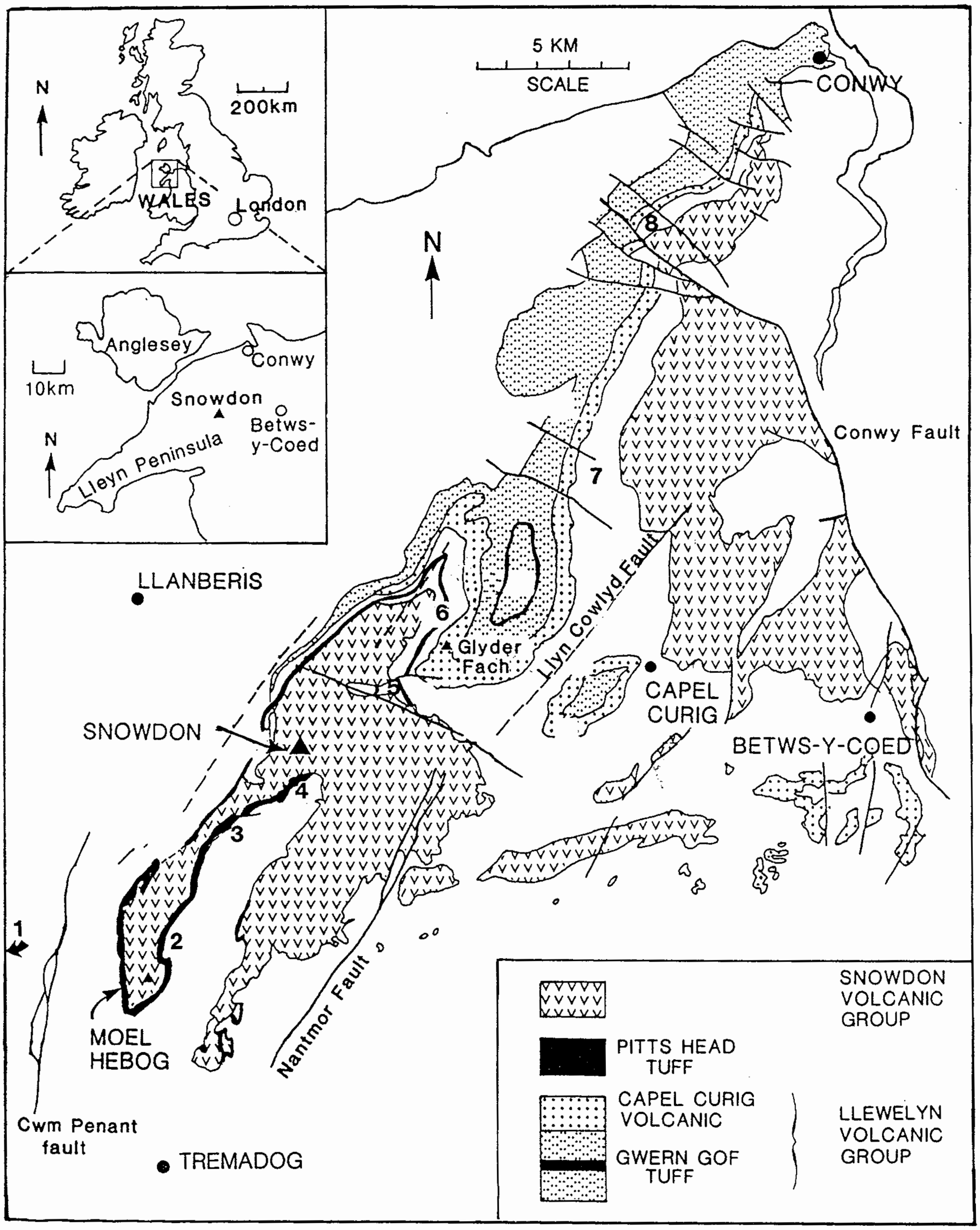

FIG. 2.5: Distribution of main volcanic units in North Wales.

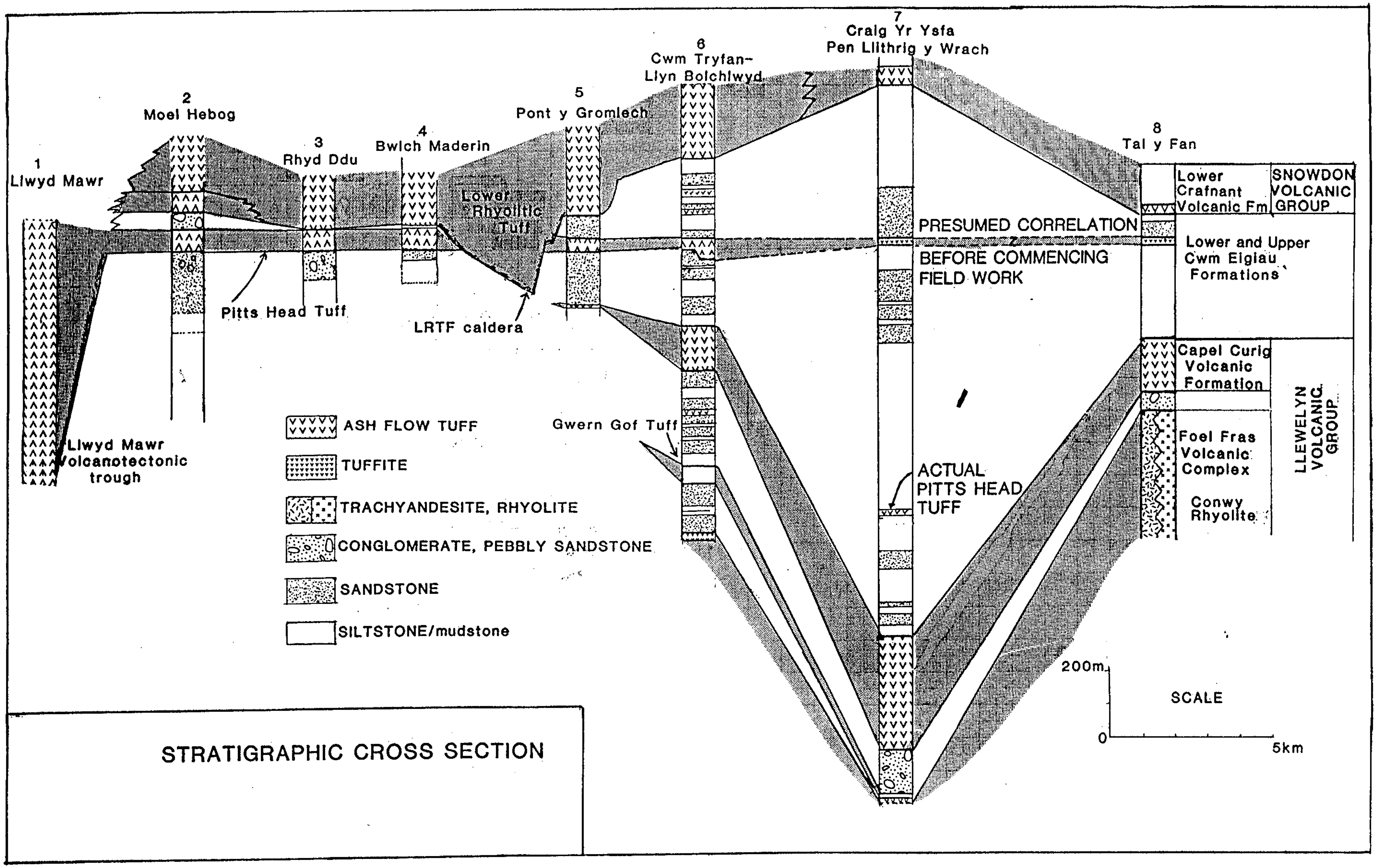

FIG. 2.6: STRATIGRAPHIC CROSS-SECTION FROM SW TO NE ACROSS NORTH WALES. See Fig. 2.5 for location of vertical profiles.

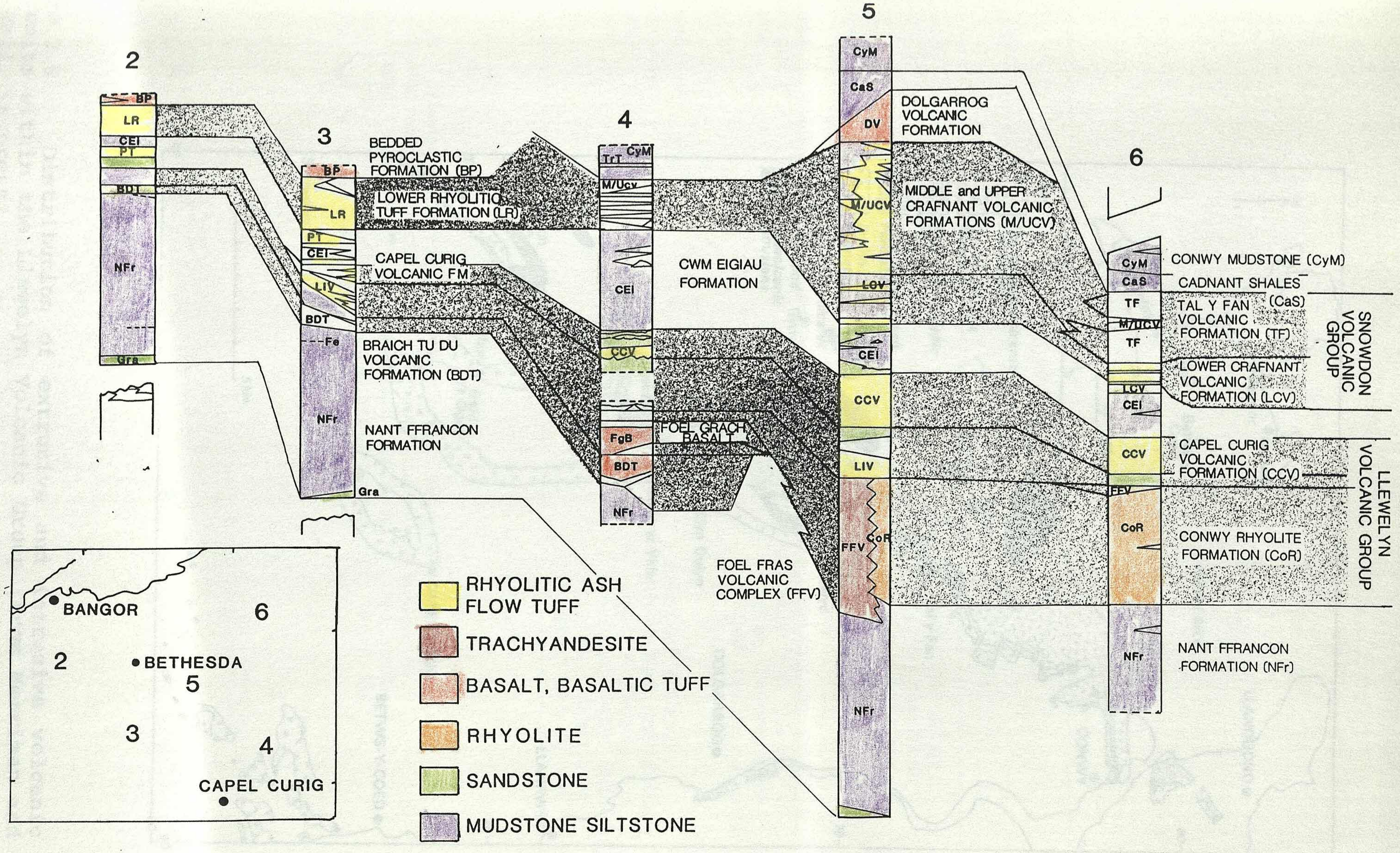

Figure 2.7 Detailed lithostratigraphic subdivision of volcanic successions in central and northeastern Snowdonia. Location of sections and stratigraphic columns from BGS 1:50,000 Bangor map sheet 106, 1985.

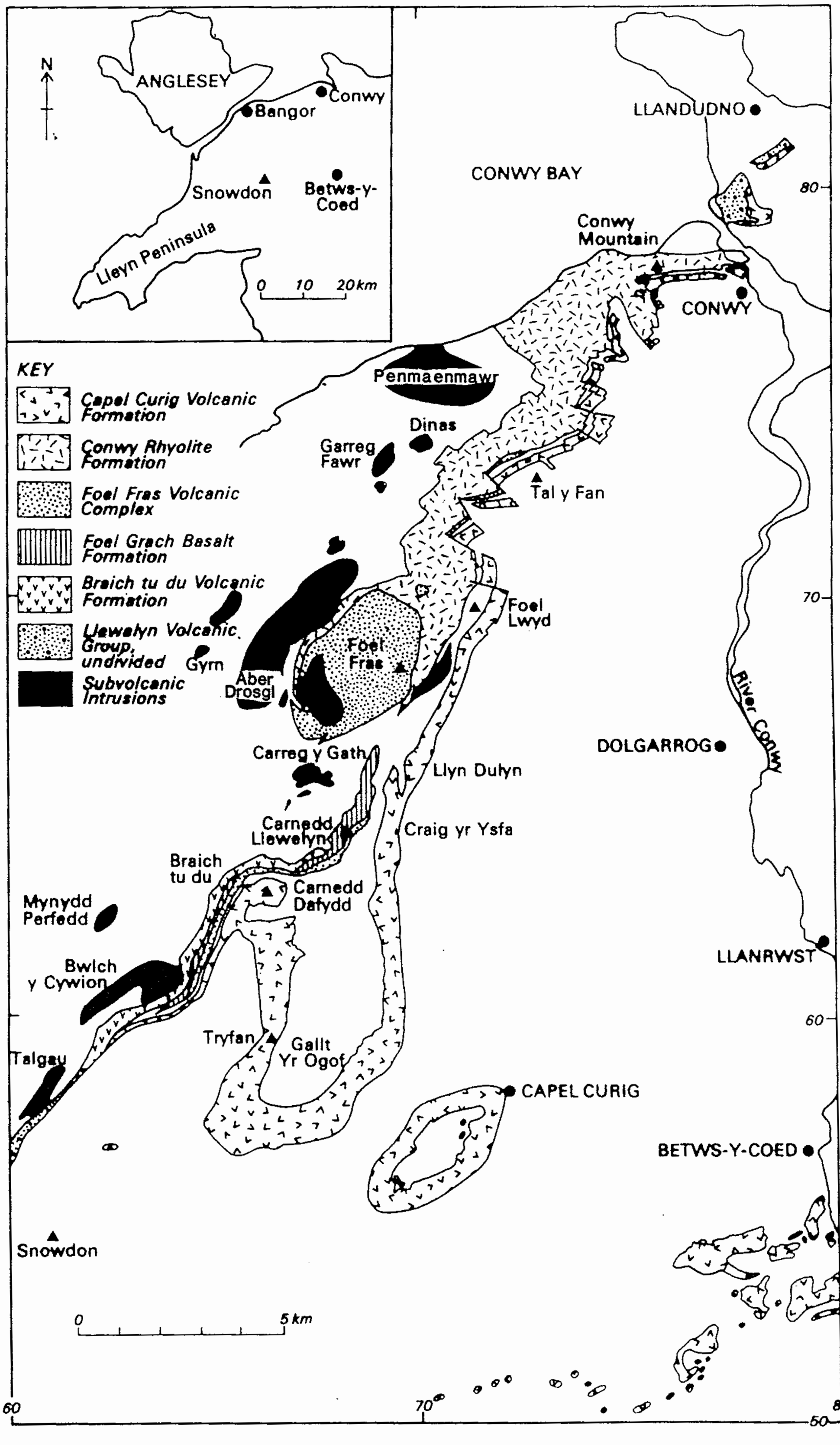

Figure 2.8 Distribution of extrusive and intrusive volcanic units within the Llewelyn Volcanic Group (from Merriman and Ball, in press).

TUFF	LATERAL EXTENT (kilometres)	THICKNESS (metres)	VOLUME (km^3)	NATURE
1st (GARTH)	45	20-150	28	primary ash flow tuff, vitric-rich
2nd (RACKS)	25	0-130	15	primary ash flow tuff, vitric rich
3rd volcanic mbr.	10	0-170	3	accumulation of thin primary ash flow tuffs, lowest flow 8-50m thick, others up to 4m thick.
4th volcanic mbr.	15	0-200	2	slumped tuffs, reworked ash flows, debris flows, accretionary lapilli tuffs, few thin primary ash flows

Fig. 2.9: Salient features of the 4 volcanic members of the Capel Curig Volcanic Formation. Data (except volumes) from Howells & Leveridge (1980). Volume of Garth tuff from Howells *et al*, 1985. Other volume estimates from this study. See Fig. 2.10 for regional variation in tuff thickness and aspect.

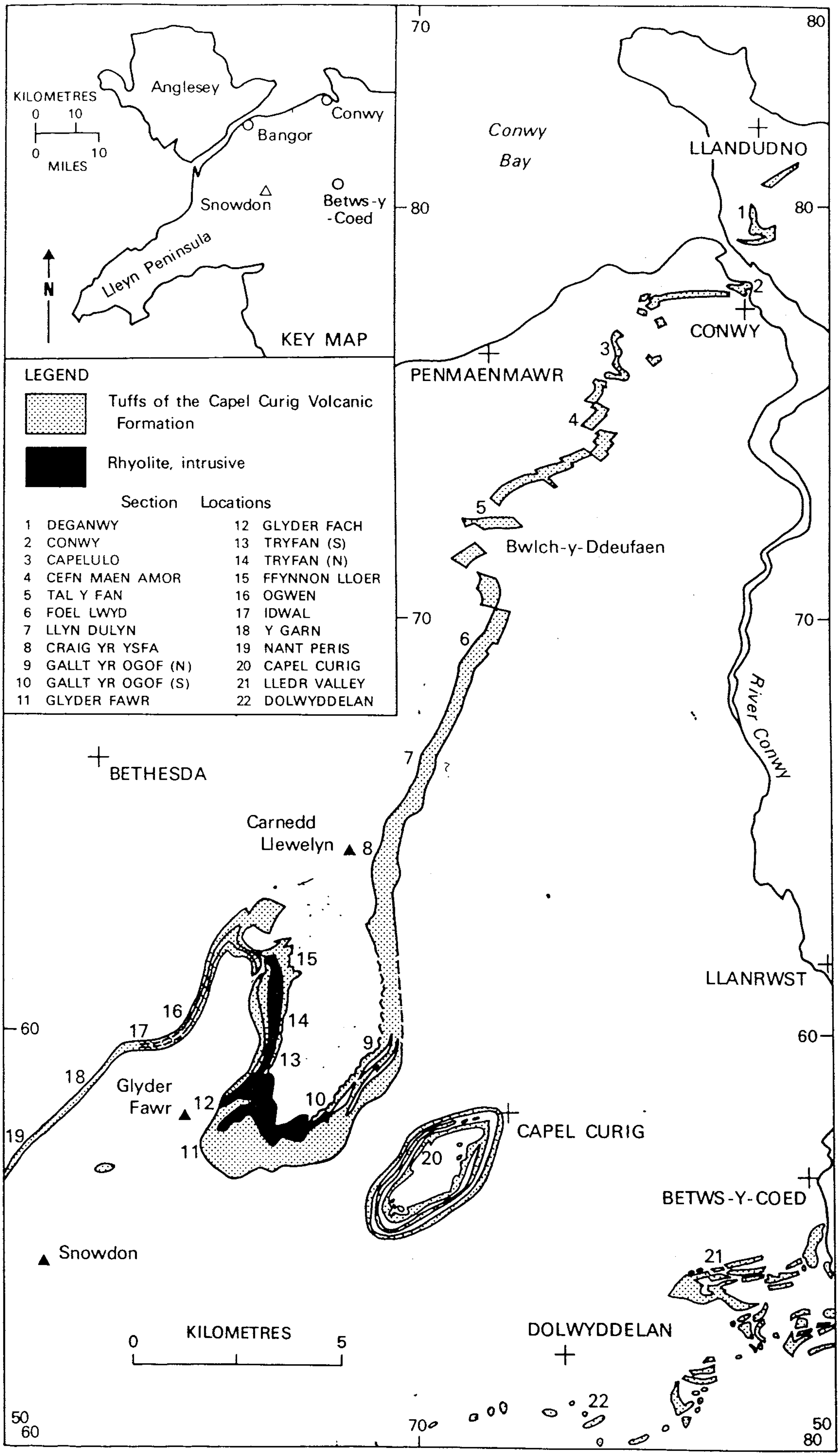

Figure 2.10a Distribution of the CCVF (from Howells and Leveridge, 1980).

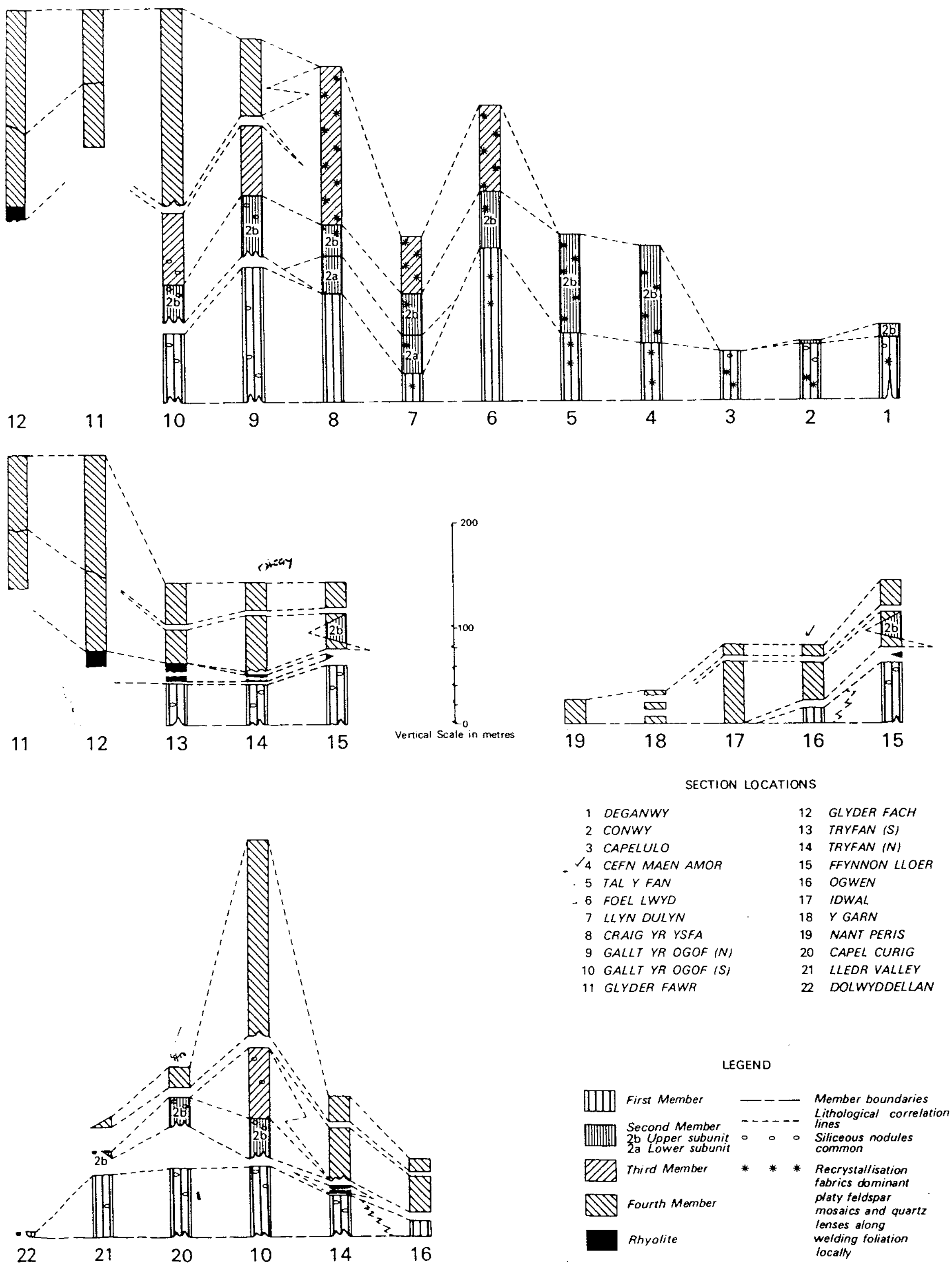

Figure 2.10b Correlation of tuff members within the CCVF (from Howells and Leveridge, 1980)

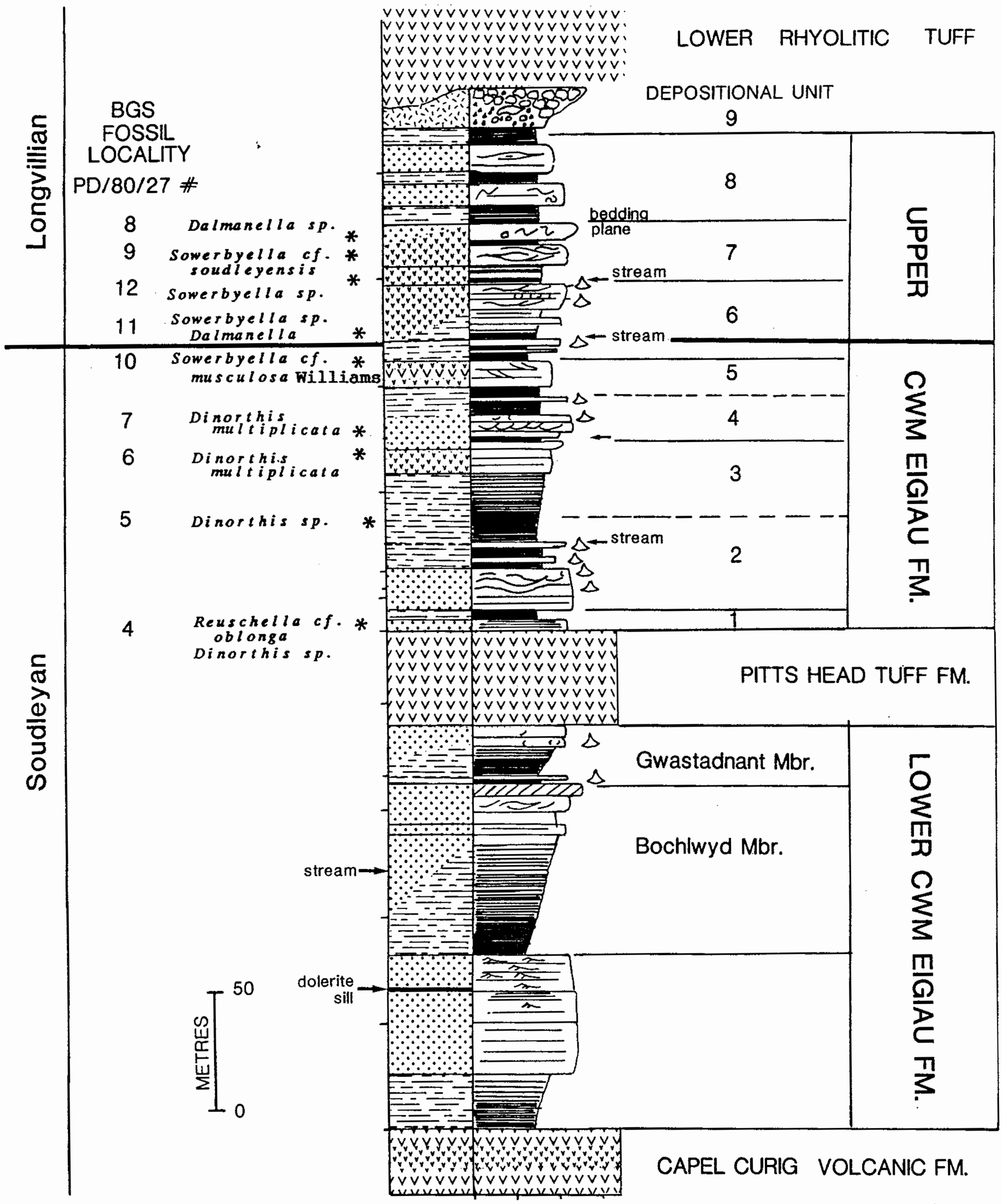

Figure 2.11 Type section of the Cwm Eigiau Formation at Llyn Bochlwyd - Cwm Cneifion. Palaeontological data from S.P. Tunnicliffe (BGS Open File report, PD/80/27).

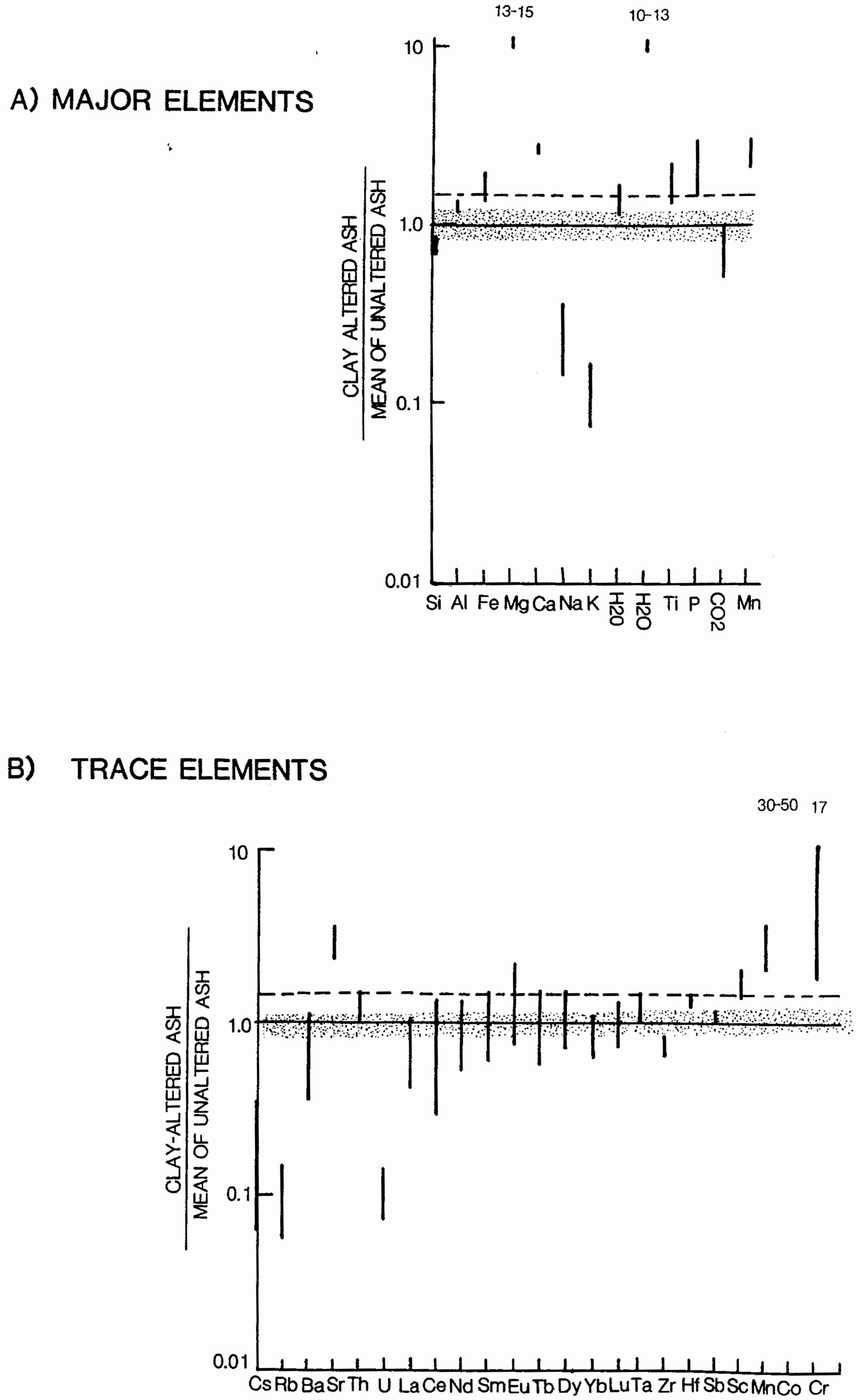

Figure 2.12 A) Major and B) Trace element concentrations in samples of clay-altered ash normalized to the concentrations found in unaltered glassy ash. Values that plot outside the shaded regions are considered analytically significant. The **horizontal dashed lines** represents the postulated limit of enrichment produced by concentration of immobile elements in an insoluble residuum. (from Zielinski, 1982, Fig. 3 and 4).

FIGURE 2.13

LOCATION AND IDENTITY OF ANALYZED
ASH FLOW TUFFS/ TUFFITES

KNOWN ASH FLOW TUFFS

TUFF	NO.	LOCATION	SECTION	GRID REF	ASH FLOW
1	10	Llynnau Mymbyr	base A2	7062 5770	1st MBR CCVF
2	8	Llynnau Mymbyr	top A2	7057 5785	2nd MBR CCVF
3	2	Gallt yr Ogof	C11	6853 5880	3rd MBR CCVF
4	6	Gallt yr Ogof	C11	6870 5875	4th MBR CCVF
51	7	Pont-y-Gromlech	------	6301 5652	Pitts Head
52	13	Bochlwyd Ridge	D1	6525 5892	Pitts Head
53	5	Llyn Idwal	Top U1	6410 5969	Pitts Head
53	2	Ogwen Cottage	--------	6501 6057	Pitts Head
54	2	Cwm Ystradllyn	--------	560 457	Pitts Head
55	4	Pont-y-Gromlech	--------	630 566	Pitts Head
56	3	Ogwen Cottage	--------	650 606	Pitts Head

UNKNOWN ASH FLOW TUFFS

TUFF	NO.	LOCATION	SECTION	GRID REF	ASH FLOW
101	2	Rolwyd	-------	7644 5086	Lledr Vall.
102	3	Nantmor Valley	V3 26.7m	6400 4910	Nantmor 1
103	2	Lledr Valley	--------	7661 5422	Lledr Valley
104	1	Moel Ddu	M1 18.6m	5871 4443	Moel Ddu 1
105	1	Carnedd Dafydd	Top F7	6570 6305	?GARTH
201	1	Lledr Valley	------	7710 5430	Lledr Vall.
202	2	Ffynnon Lloer	F9 65m	6573 6203	Ffynnon 1
203	1	Ffynnon Lloer	F9 74 m	6573 6203	Ffynnon 2
501	6	Llyn Cwm-y-fynnon	L 13	6564 5638	?Pitts Head
502	5	Penyrhelgi-du	TOP F2	6978 6312	F2
503	2	Bwlch Trimarchog	F3 69 m	7069 6273	F3
504	2	Bwlch Trimarchog	F4 28 m	7094 6265	F4
505	3	Bwlch Trimarchog	F5 56-60m	7105 6263	F5
511	3	Llyn Cowlyd	H1 24-28m	7160 6131	Cowlyd 1
512	5	Llyn Cowlyd	H4 2-10m	7158 6165	Cowlyd 2
522	2	Capel Hill	G2 20-25m	7232 5832	G2
526	10	Capel Hill	G6 10-13m	7248 5831	G6
530	1	Bochlwyd Ridge	D1, 145 m	6517 5891	rework PHT
531	3	Nantmor Valley	V2 13-15m	6384 4906	Nantmor 2
999	1	Bochlwyd Ridge	D1 74 m	6525 5892	sandstone
5111	5	Pont-y-Gromlech		6301 5652	replictes PH

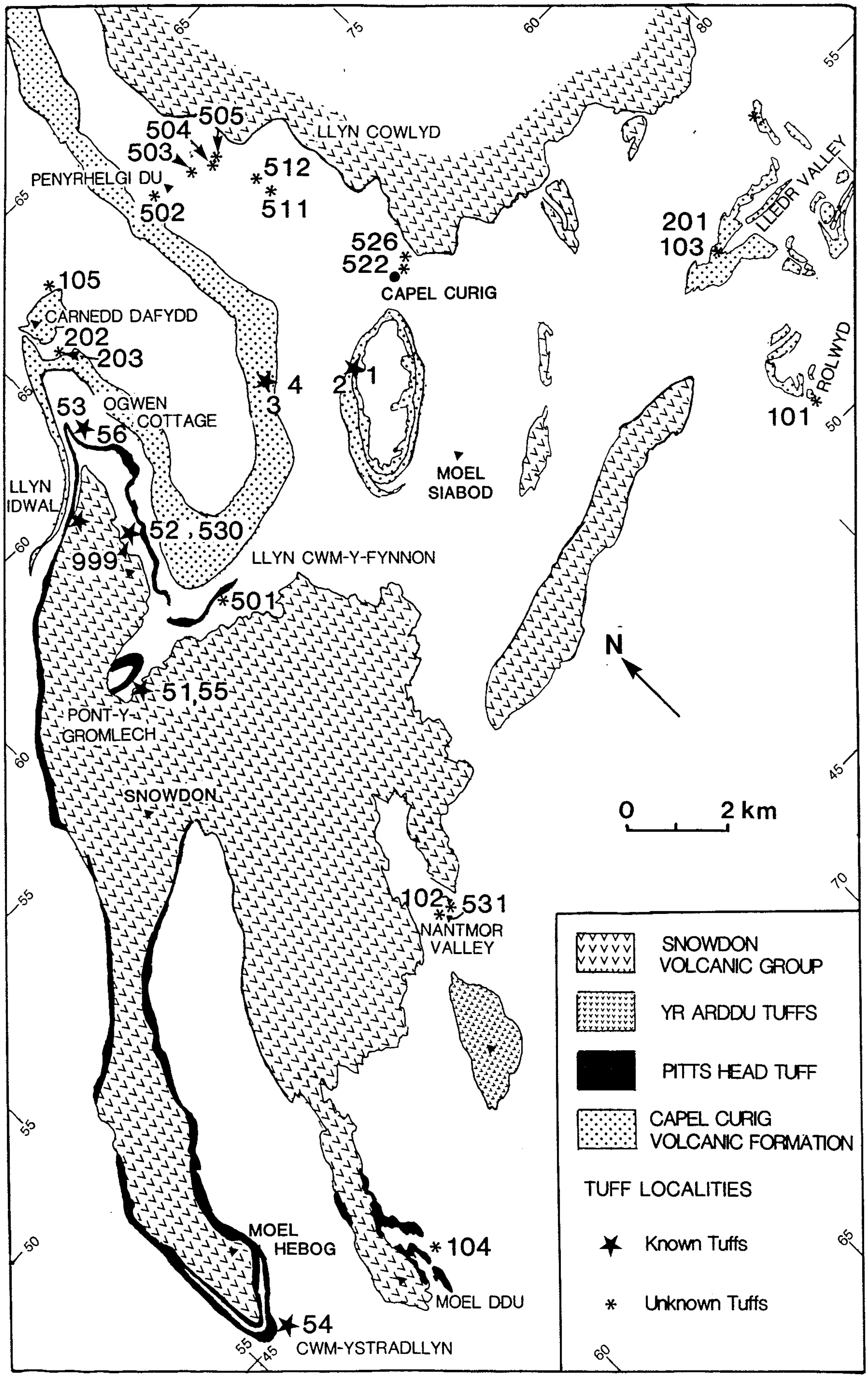

Figure 2.14 Location of ash flow tuffs analysed for major and or trace elements. See Figure 2.13 for descriptions of tuffs.

FIGURE 2.15

MAJOR ELEMENT COMPOSITION

GROUP MEANS AND STANDARD DEVIATIONS FROM NORMALIZED DATA

TUFF	SIO2		TIO2		AL2O3	
	mean	std. dev	mean	std. dev	mean	std. dev
1.00	75.0670	2.6987	.2096	.0617	13.2882	1.7611
2.00	77.0614	1.8790	.1780	.0110	11.8477	.6641
51.00	75.4880	3.5516	.2586	.0485	12.8739	1.8823
52.00	75.7133	4.0694	.2310	.0310	12.8819	2.1234
102.00	78.3432	.0000	.3765	.0000	10.0807	.0000
201.00	79.9333	.0000	.1556	.0000	11.2396	.0000
501.00	68.7226	.0000	.3058	.0000	14.6090	.0000
503.00	83.3442	.0000	.1525	.0000	8.8780	.0000
504.00	77.5803	.0000	.2128	.0000	14.1732	.0000
505.00	80.0131	1.5265	.1779	.008	10.4310	.5880
511.00	78.4818	1.6565	.1909	.031	11.6061	1.1424
512.00	78.7109	1.9095	.2047	.046	11.3504	1.0378
522.00	77.3402	2.1352	.1850	.081	10.6626	3.0850
526.00	80.1864	.8597	.1831	.0382	10.7888	.5983
530.00	59.7754	.0000	1.3578	.0000	15.416	.0000
999.00	74.4642	.0000	.4606	.0000	11.1156	.0000
1000.00	74.4227	.3002	.2333	.004	14.2270	.0611
TOTAL	76.3545	3.9230	.2382	.157	12.4458	1.8871

TUFF	CR2O3		FE2O3		MNO	
	mean	std. dev	mean	std. dev	mean	std. dev
1.00	.0000	.0000	2.5326	1.0348	.1099	.0548
2.00	.0000	.0000	2.8680	.429	.1125	.0555
51.00	.0000	.0000	2.4736	.861	.0847	.0354
52.00	.0000	.0000	2.2554	.329	.1061	.1222
102.00	.0108	.0000	6.1969	.000	.3120	.0000
201.00	.0000	.0000	2.3902	.000	.0556	.0000
501.00	.0000	.0000	4.4245	.000	.1223	.0000
503.00	.0000	.0000	2.1786	.000	.0545	.0000
504.00	.0000	.0000	1.4578	.000	.0319	.0000
505.00	.0000	.0000	3.2348	.196	.0733	.0035
511.00	.0000	.0000	2.2655	.321	.0625	.0406
512.00	.0000	.0000	2.4944	.464	.0612	.0161
522.00	.0000	.0000	2.8665	.867	.1113	.0680
526.00	.0000	.0000	1.9400	.805	.0335	.0147
530.00	.0204	.0000	8.1776	.000	.1531	.0000
999.00	.0100	.0000	5.7781	.000	.2904	.0000
1000.00	.0000	.0000	2.7204	.037	.1160	.0045
	.0007	.0032	2.6999	1.180	.0980	.0734

FIGURE 2.15 continued

GROUP MEANS AND STANDARD DEVIATIONS FROM NORMALIZED DATA

	MgO		CaO		Na2O	
	mean	std. dev	mean	std. dev	mean	std. dev
1.00	.3441	.365	.4821	.4550	1.4800	.5448
2.00	.2236	.028	.4111	.3926	1.4520	1.0356
51.00	.9280	.685	.3583	.334	2.0857	.995
52.00	.4256	.265	1.2172	2.235	3.9070	1.9316
102.00	1.6676	.000	.0968	.000	.3765	.0000
201.00	.3224	.000	.2335	.000	3.4130	.0000
501.00	1.1928	.000	2.6098	.000	5.6887	.0000
503.00	.4466	.000	.5447	.000	3.3442	.0000
504.00	.3724	.000	.3511	.000	5.5118	.0000
505.00	.5644	.002	.4331	.031	3.6259	1.2650
511.00	.5022	.121	.4397	.080	4.5484	.1743
512.00	.5308	.126	1.0370	.522	4.1226	.5933
522.00	.5183	.161	3.0637	3.423	3.9351	1.1160
526.00	.2414	.144	.4199	.090	5.7913	.7709
530.00	5.1149	.000	3.3997	.000	3.7366	.0000
999.00	.9513	.000	1.5021	.000	3.1644	.0000
1000.00	.2658	.016	.4045	.013	1.2745	.1808
TOTAL	.5358	.709	.7641	1.220	3.0282	1.8677

	K2O		P2O5	
	mean	std. dev	mean	std. dev
1.00	6.3611	.711	.1207	.0212
2.00	5.7278	1.9467	.1201	.0079
51.00	5.4225	1.3137	.0303	.0053
52.00	3.2388	1.8977	.0248	.0048
102.00	2.4852	.0000	.0646	.0000
201.00	2.1345	.0000	.1334	.0000
501.00	2.2938	.0000	.0306	.0000
503.00	.9259	.0000	.1089	.0000
504.00	.1915	.0000	.1277	.0000
505.00	1.3422	.4911	.0992	.0027
511.00	1.7706	.2827	.1216	.0287
512.00	1.3710	.8566	.1170	.0143
522.00	1.1955	.2778	.1216	.0368
526.00	.3125	.2120	.1015	.0143
530.00	2.6442	.0000	.2246	.0000
999.00	2.1530	.0000	.1001	.0000
1000.00	6.2097	.1419	.1273	.0041
TOTAL	3.7415	2.4972	.0930	.0464

FIGURE 2.16

GROUP MEANS OF MAJOR ELEMENTS COMPARING 3 KNOWN TUFFS AND UNKNOWN TUFFITES.

1 = GARTH, RACKS, and PITTS HEAD TUFFS n=30
2 = OTHER UNKNOWN TUFFS n=22

TUFFS	SiO2		TiO2		AL2O3	
	mean	std.dev.	mean	std.dev.	mean	std.dev.
1	75.6990	3.2037	.2213	.0496	12.8298	1.7775
2	78.0367	4.9596	.2529	.2536	11.3350	1.7361
TOTAL	76.6880	4.1623	.2347	.1677	12.1974	1.8957

TUFFS	CR2O3		FE2O3		MNO	
	mean	std.dev.	mean	std.dev.	mean	std.dev.
1	.0000	.0000	2.4843	.7257	.1040	.0788
2	.0014	.0048	2.8465	1.6481	.0746	.0658
TOTAL	.0006	.0032	2.6375	1.2044	.0916	.0743

TUFFS	MGO		CAO		Na2O	
	mean	std.dev.	mean	std.dev.	mean	std.dev.
1	.4680	.4463	.6905	1.3392	2.4055	1.6672
2	.7077	1.0447	.9618	1.2876	4.5089	1.4467
TOTAL	.5694	.7596	.8053	1.3118	3.2954	1.8824

TUFFS	K2O		P2O5	
	mean	std.dev.	mean	std.dev.
1	5.0270	1.9621	.0705	.0490
2	1.1633	.8535	.1107	.0362
TOTAL	3.3924	2.4908	.0875	.0481

FIGURE 2.17

COMPARISON OF 3 KNOWN TUFFS WITH UNKNOWN DISTAL PORTIONS OR "TUFFITES"

Univariate F-tests with (1,49) D. F.
F critical = 7.70 at 99% confidence level, 4.04 at 95% confidence level

Variable	Hypoth. SS	Error SS	Hypoth. MS	Error MS	F	Sig. of F
SIO2	29.68888	562.20814	29.68888	11.47364	2.58757	.114
TIO2	.00394	.14392	.00394	.00294	1.34271	.252
AL2O3	7.89146	164.82318	7.89146	3.36374	2.34604	.132
CR2O3	.00000	.00011	.00000	.00000	.37364	.544
FE2O3	.29433	42.38990	.29433	.86510	.34022	.562
MNO	.00807	.26979	.00807	.00551	1.46619	.232
MGO	.61941	7.73814	.61941	.15792	3.92229	.053
CAO	1.71005	79.18508	1.71005	1.61602	1.05818	.309
NA2O	63.69169	116.83328	63.69169	2.38435	26.71236	.000
K2O	143.59522	172.24981	143.59522	3.51530	40.84861	.000
P2O5	.02446	.07426	.02446	.00152	16.13818	.000

FIGURE 2.18

MAJOR ELEMENT COMPOSITION OF KNOWN ASH FLOW TUFFS

1 = GARTH TUFF
2 = RACKS TUFF
3 = PITTS HEAD TUFF

TUFF	SiO_2		TiO_2		Al_2O_3	
	mean	std.dev.	mean	std.dev.	mean	std.dev.
1	75.0670	2.6987	.2096	.0617	13.2882	1.7611
2	77.0614	1.8790	.1780	.0110	11.8477	.6641
3	75.6288	3.7621	.2413	.0394	12.8789	1.9714
TOTAL	75.6990	3.2037	.2213	.0496	12.8298	1.7775

TUFF	Cr_2O_3		Fe_2O_3		MnO	
	mean	std.dev.	mean	std.dev.	mean	std.dev.
1	.0000	.0000	2.5326	1.0348	.1099	.0548
2	.0000	.0000	2.8680	.4293	.1125	.0555
3	.0000	.0000	2.3372	.5696	.0981	.0974
TOTAL	.0000	.0000	2.4843	.7257	.1040	.0788

TUFF	MgO		CaO		Na_2O	
	mean	std.dev.	mean	std.dev.	mean	std.dev.
1	.3441	.3650	.4821	.4550	1.4800	.5448
2	.2236	.0283	.4111	.3926	1.4520	1.0356
3	.6140	.5118	.8951	1.7941	3.2240	1.8434
TOTAL	.4680	.4463	.6905	1.3392	2.4055	1.6672

TUFF	K_2O		P_2O_5	
	mean	std.dev.	mean	std.dev.
1	6.3611	.7117	.1207	.0212
2	5.7278	1.9467	.1201	.0079
3	4.0577	1.9820	.0268	.0055
TOTAL	5.0270	1.9621	.0705	.0490

FIGURE 2.19
COMPARISON OF MAJOR ELEMENTS FROM THREE KNOWN TUFFS

TUFFS USED PITTS HEAD TUFF
GARTH TUFF
RACKS TUFF

A) Multivariate Tests of Significance (S = 2, M = 3 1/2, N = 8)

Test Name	Value	Approx. F	Hypoth. DF	Error DF	Sig. of F
Pillais	1.36206	4.05665	20.00	38.00	.000
Hotellings	81.51933	69.29143	20.00	34.00	.000
Wilks	.00764	18.79563	20.00	36.00	.000
Roys	.98779				

Note.. F statistic for WILK'S Lambda is exact.

B) UNIVARIATE COMPARISON OF INDIVIDUAL ELEMENTS

Univariate F-tests with (2,27) D. F. F critical = 5.49 at 99% confidence interval

Variable	Hypoth. SS	Error SS	Hypoth. MS	Error MS	F	Sig. of F
SIO2	12.95513	284.68338	6.47757	10.54383	.61435	.548
TIO2	.01701	.05428	.00850	.00201	4.22926	.025
AL2O3	6.75233	84.86956	3.37616	3.14332	1.07408	.356
FE2O3	1.10321	14.17033	.55160	.52483	1.05102	.363
MNO	.00124	.17866	.00062	.00662	.09340	.911
MGO	.77770	4.99804	.38885	.18511	2.10060	.142
CAO	1.45128	50.55537	.72564	1.87242	.38754	.682
NA2O	22.97385	57.63758	11.48693	2.13473	5.38099	.011
K2O	33.50745	78.13318	16.75372	2.89382	5.78948	.008
P2O5	.06544	.00431	.03272	.00016	205.20609	.000

FIGURE 2.20

COMPARISON OF MAJOR ELEMENTS FROM KNOWN TUFFS USING TUKEY-B PROCEDURE

MULTIPLE RANGE TEST
TUKEY-B PROCEDURE

RANGES FOR THE 0.050 LEVEL - 3.20 3.50
THE RANGES ABOVE ARE TABLE RANGES.

A) Variable SIO2

ANALYSIS OF VARIANCE

SOURCE	D.F.	SUM OF SQUARES	MEAN SQUARES	F RATIO	F PROB.
BETWEEN GROUPS	2	12.9551	6.4776	.6143	.5484
WITHIN GROUPS	27	284.6834	10.5438		
TOTAL	29	297.6385			

THE VALUE ACTUALLY COMPARED WITH MEAN(J)-MEAN(I) IS..
2.2961 * RANGE * DSQRT(1/N(I) + 1/N(J))
NO TWO GROUPS ARE SIGNIFICANTLY DIFFERENT AT THE 0.050 LEVEL

B) Variable TIO2

ANALYSIS OF VARIANCE

SOURCE	D.F.	SUM OF SQUARES	MEAN SQUARES	F RATIO	F PROB.
BETWEEN GROUPS	2	.0170	.0085	4.2293	.0252
WITHIN GROUPS	27	.0543	.0020		
TOTAL	29	.0713			

THE VALUE ACTUALLY COMPARED WITH MEAN(J)-MEAN(I) IS..
0.0317 * RANGE * DSQRT(1/N(I) + 1/N(J))
(*) DENOTES PAIRS OF GROUPS SIGNIFICANTLY DIFFERENT AT THE 0.050 LEVEL

Mean	Group	Grp 2	Grp 1	Grp 3
.2096	Grp 1			
.2413	Grp 3	*		

C) VARIABLE P2O5

ANALYSIS OF VARIANCE

SOURCE	D.F.	SUM OF SQUARES	MEAN SQUARES	F RATIO	F PROB.
BETWEEN GROUPS	2	.0654	.0327	205.2061	.0000
WITHIN GROUPS	27	.0043	.0002		
TOTAL	29	.0697			

THE VALUE ACTUALLY COMPARED WITH MEAN(J)-MEAN(I) IS..
0.0089 * RANGE * DSQRT(1/N(I) + 1/N(J))
(*) DENOTES PAIRS OF GROUPS SIGNIFICANTLY DIFFERENT AT THE 0.050 LEVEL

Mean	Group	Gp 3	Gp 2	Gp 1
.1201	Grp 2	*		
.1207	Grp 1	*		

FIGURE 2.20 continued
COMPARISON OF MAJOR ELEMENTS FROM KNOWN TUFFS USING TUKEY-B PROCEDURE

D) Variable NA2O
By Variable TUFF

ANALYSIS OF VARIANCE

SOURCE	D.F.	SUM OF SQUARES	MEAN SQUARES	F RATIO	F PROB.
BETWEEN GROUPS	2	22.9739	11.4869	5.3810	.0108
WITHIN GROUPS	27	57.6376	2.1347		
TOTAL	29	80.6114			

MULTIPLE RANGE TEST
TUKEY-B PROCEDURE
RANGES FOR THE 0.050 LEVEL -

3.20 3.50
THE RANGES ABOVE ARE TABLE RANGES.
THE VALUE ACTUALLY COMPARED WITH MEAN(J)-MEAN(I) IS..
1.0331 * RANGE * DSQRT(1/N(I) + 1/N(J))
(*) DENOTES PAIRS OF GROUPS SIGNIFICANTLY DIFFERENT AT THE 0.050 LEVEL

Mean	Group	Grp 2	Grp 1	Grp 3
1.4800	Grp 1			
3.2240	Grp 3		*	

E) Variable K2O
By Variable TUFF

ANALYSIS OF VARIANCE

SOURCE	D.F.	SUM OF SQUARES	MEAN SQUARES	F RATIO	PROB.
BETWEEN GROUPS	2	33.5074	16.7537	5.7895	.0081
WITHIN GROUPS	27	78.1332	2.8938		
TOTAL	29	111.6406			

MULTIPLE RANGE TEST
TUKEY-B PROCEDURE
RANGES FOR THE 0.050 LEVEL -
3.20 3.50
THE RANGES ABOVE ARE TABLE RANGES.
THE VALUE ACTUALLY COMPARED WITH MEAN(J)-MEAN(I) IS..
1.2029 * RANGE * DSQRT(1/N(I) + 1/N(J))
(*) DENOTES PAIRS OF GROUPS SIGNIFICANTLY DIFFERENT AT THE 0.050 LEVEL

Mean	Group	Grp 3	Grp 2	Grp 1
5.7278	Grp 2			
6.3611	Grp 1	*		

FIGURE 2.21

GROUP MEANS OF TRACE ELEMENT COMPOSITION FROM VARIOUS TUFF LOCALITIES

TUFF	RB		Sr		Y	
	mean	Std.dev.	mean	Std.dev	mean	Std.dev
1.00	192.650	78.937	45.360	35.305	75.520	16.088
2.00	160.725	51.974	74.400	21.018	76.650	10.455
3.00	52.700	70.710	67.750	4.454	73.150	10.253
4.00	97.283	40.118	75.466	32.520	72.966	11.260
5.00	114.016	58.921	65.166	32.885	49.163	12.120
101.00	55.000	29.274	100.100	27.152	77.200	5.091
102.00	106.933	19.863	15.533	4.921	36.533	13.054
103.00	64.100	11.738	95.300	36.911	71.700	4.808
104.00	109.500	.000	9.800	.000	32.900	.000
105.00	130.000	.000	51.000	.000	81.200	.000
201.00	57.000	.000	63.700	.000	73.000	.000
202.00	101.400	1.979	76.900	2.969	72.400	6.646
203.00	68.000	.000	79.000	.000	78.300	.000
501.00	55.950	27.646	68.550	5.366	87.483	14.906
502.00	82.860	32.598	109.160	26.713	45.520	7.854
503.00	33.800	.282	108.550	19.586	24.900	.565
504.00	8.750	6.858	84.900	12.586	37.100	13.293
505.00	60.666	20.128	114.600	23.643	28.933	5.008
511.00	40.166	19.071	93.000	5.656	30.966	3.257
512.00	38.200	32.332	214.640	37.782	30.160	6.023
522.00	47.600	9.758	132.700	47.800	42.300	14.142
526.00	8.870	9.417	122.770	15.781	27.780	3.123
530.00	54.500	.000	223.100	.000	45.400	.000
531.00	49.333	9.882	46.433	4.077	46.666	11.430
999.00	51.500	.000	122.300	.000	20.400	.000
5111.00	163.740	.654	88.640	.594	51.980	.804
9999.00	201.300	.000	243.900	.000	15.500	.000
TOTAL	95.264	67.451	82.242	46.610	53.456	20.996

FIGURE 2.21

GROUP MEANS OF TRACE ELEMENT COMPOSITION FROM VARIOUS TUFF LOCALITIES

TUFF	Zr		Nb		Pb	
	mean	Std.dev	mean	Std.dev	mean	Std.dev
1.00	170.910	33.449	17.300	3.405	13.580	14.752
2.00	201.562	10.436	18.537	1.934	45.362	51.145
3.00	363.450	106.419	20.350	2.616	17.150	10.677
4.00	376.233	53.480	21.700	1.285	18.100	8.415
5.00	268.380	49.798	21.519	3.490	14.855	10.461
101.00	159.300	23.758	19.200	4.808	11.800	.141
102.00	164.066	46.684	13.933	2.173	195.233	119.669
103.00	172.300	10.465	15.900	1.272	8.150	.212
104.00	84.100	.000	10.600	.000	62.100	.000
105.00	148.100	.000	16.300	.000	13.300	.000
201.00	181.000	.000	16.300	.000	14.100	.000
202.00	279.950	11.950	17.050	1.484	22.550	.070
203.00	292.500	.000	18.100	.000	10.600	.000
501.00	462.250	64.527	22.000	2.766	10.300	11.252
502.00	274.880	11.294	20.800	1.234	14.560	4.852
503.00	112.050	45.184	8.350	.777	30.950	16.192
504.00	171.300	68.023	9.700	.707	6.700	1.697
505.00	88.433	9.681	8.633	.945	28.100	9.552
511.00	95.833	20.010	8.166	1.222	27.333	27.499
512.00	105.480	20.725	8.620	.988	19.720	11.506
522.00	103.250	56.780	8.000	1.697	22.000	11.313
526.00	91.550	22.776	7.820	1.141	16.360	4.532
530.00	279.800	.000	12.900	.000	7.300	.000
531.00	118.400	10.409	10.966	1.026	60.266	59.127
999.00	151.800	.000	8.800	.000	13.500	.000
5111.00	330.460	1.847	27.980	.216	6.820	1.355
9999.00	210.500	.000	20.600	.000	48.100	.000
TOTAL	225.5650	106.065	17.3057	6.231	23.295	37.459

FIGURE 2.21 continued

GROUP MEANS OF TRACE ELEMENT COMPOSITION FROM VARIOUS TUFF LOCALITIES

TUFF	Zn		Cu		Ni		Co	
	mean	Std.dev	mean	Std.dev	mean	Std.dev	mean	Std.dev
1.	53.170	16.979	3.230	1.058	3.060	2.082	12.090	4.514
2.	321.087	507.601	6.662	3.077	1.825	.820	14.212	2.009
3.	58.850	12.515	6.200	1.131	2.000	1.979	17.350	.353
4.	70.083	35.437	9.483	2.531	6.816	2.752	13.483	6.044
5.	44.472	18.183	5.063	2.897	1.661	1.989	8.130	6.706
101.	36.800	1.697	4.000	.141	1.200	.141	11.850	1.909
102.	80.533	4.708	5.733	1.893	16.900	2.364	10.733	4.178
103.	31.500	18.101	5.250	1.909	1.050	.353	7.950	2.333
104.	177.600	.000	7.100	.000	22.600	.000	18.000	.000
105.	48.200	.000	4.400	.000	1.500	.000	10.500	.000
201.	76.800	.000	3.100	.000	.900	.000	8.600	.000
202.	55.350	12.798	6.600	1.272	5.000	.424	12.400	2.969
203.	64.500	.000	7.900	.000	3.400	.000	13.900	.000
501.	66.950	29.846	13.316	12.677	2.616	1.256	8.866	.902
502.	49.800	15.556	6.060	.978	5.640	6.139	11.180	2.688
503.	49.850	5.869	4.500	2.121	1.350	1.767	11.850	.636
504.	40.550	37.547	7.200	7.071	2.650	1.060	15.400	.565
505.	42.500	8.292	9.533	1.289	2.533	.709	11.200	1.907
511.	25.766	8.957	5.166	1.401	1.400	.360	12.233	1.457
512.	31.120	2.192	9.580	7.215	1.540	.466	13.460	4.772
522.	41.750	2.050	8.700	.424	2.700	.141	11.050	3.182
526.	33.330	27.532	8.200	5.266	1.160	1.029	14.240	3.738
530.	60.500	.000	25.100	.000	42.000	.000	23.200	.000
531.	88.800	37.984	4.166	2.983	5.666	2.532	11.700	.888
999.	60.000	.000	14.000	.000	20.500	.000	22.000	.000
5111.	26.400	.514	3.280	.507	1.360	.493	11.600	.500
9999.	47.700	.000	17.100	.000	1.700	.000	1.200	.000
TOTAL	66.855	141.292	6.517	4.885	3.400	5.37	11.337	5.247

TUFF	CR		V		BA	
	mean	Std.dev	mean	Std.dev	mean	Std.dev
1.	6.520	3.342	10.480	5.075	919.080	372.642
2.	4.250	1.411	8.775	.949	1784.575	800.395
3.	6.700	.424	8.800	5.515	736.650	979.413
4.	15.766	5.485	22.950	7.877	746.216	373.974
5.	5.919	5.731	11.486	6.873	684.066	360.699
101.	4.050	.777	6.500	1.272	692.050	614.263
102.	35.766	6.133	42.466	6.414	421.300	71.378
103.	5.200	1.979	6.800	.141	440.950	158.745
104.	40.400	.000	42.400	.000	374.100	.000
105.	4.000	.000	7.500	.000	854.700	.000
201.	4.100	.000	6.900	.000	214.500	.000
202.	9.150	.070	15.700	2.121	1070.750	20.011
203.	10.000	.000	13.500	.000	695.400	.000
501.	6.883	2.914	10.450	3.721	386.716	168.259
502.	5.280	1.541	9.900	1.848	213.080	65.967
503.	8.550	2.333	13.950	3.889	187.100	18.526
504.	13.250	2.899	20.800	5.515	85.800	32.951
505.	7.733	1.517	12.633	2.730	214.833	68.779
511.	8.433	1.680	12.733	3.197	477.633	129.508
512.	9.240	2.301	15.820	3.509	226.100	127.120
522.	7.200	3.394	13.150	6.717	159.900	22.203
526.	8.330	2.461	10.470	3.017	70.550	21.261
530.	118.200	.000	132.600	.000	420.600	.000
531.	15.200	6.050	17.066	5.331	161.600	20.962
999.	51.400	.000	49.300	.000	317.100	.000
5111.	3.280	1.504	12.500	.282	1634.080	10.597
9999.	21.400	.000	21.100	.000	1002.900	.000
TOTAL	9.416	12.804	14.333	13.766	645.626	559.769

FIGURE 2.22

REPLICATE ANALYSES OF SAMPLE G075

SAMPLE	REGION	RB	SR	Y	ZR	NB	PB
G075	5111.00	164.50	88.90	52.10	329.50	27.80	8.00
G075B	5111.00	164.40	89.40	52.30	332.10	28.20	7.90
G075C	5111.00	163.20	88.70	52.70	329.00	28.10	5.30
G075D	5111.00	163.40	88.40	50.60	328.90	27.70	5.40
G075E	5111.00	163.20	87.80	52.20	332.80	28.10	7.50
	mean	163.70	88.60	52.00	330.50	28.00	6.80
	standard dev.	0.70	0.60	0.80	1.80	0.20	1.40
	percent deviation	0.43	0.68	1.54	0.54	0.71	20.59

SAMPLE	REG	ZN	CU	NI	CO	CR	V	BA
G075	5111	27.00	3.30	1.20	11.20	4.30	12.40	1624.50
G075	5111	26.20	2.60	1.80	11.50	4.30	13.00	1644.80
G075	5111	25.70	4.00	.70	11.90	1.10	12.40	1622.80
G075	5111	26.30	3.40	1.90	11.10	2.30	12.40	1644.80
G075	5111	26.80	3.10	1.20	12.30	4.40	12.30	1633.50
	mean	26.40	3.30	1.40	11.60	3.30	12.50	1634.10
	std. dev.	0.50	0.50	0.50	0.50	1.50	0.30	10.60
	percent	1.89	15.15	35.71	4.31	45.45	2.40	0.60

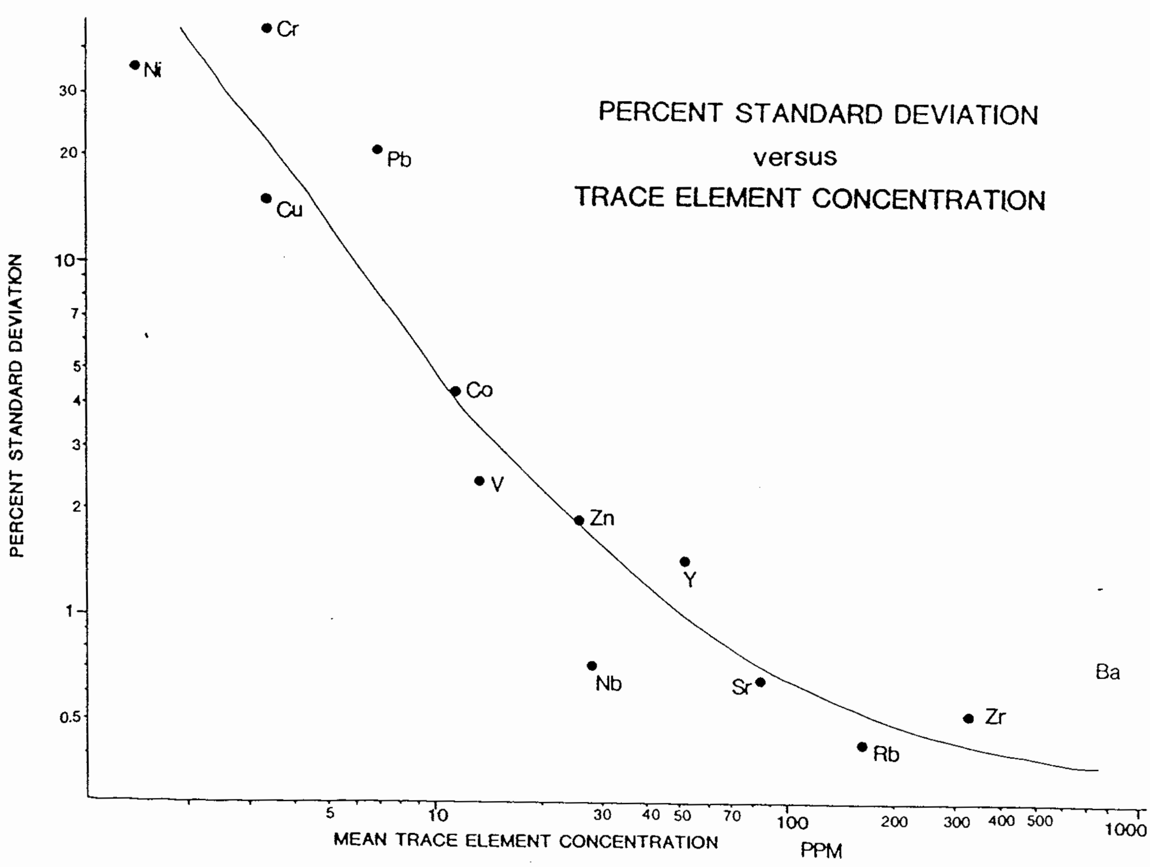

FIGURE 2.23

GROUP MEANS FROM THE PITTS HEAD TUFF FROM FOUR REGIONS

1 = Cwm Ystradllyn
2 = Pont-y-Gromlech
3 = Gribin Ridge
4 = Ogwen Cottage

TUFF	RB		SR		Y	
	mean	std. dev.	mean	std. dev	mean	std. dev
1.00	186.4000	18.5262	29.1000	1.4140	26.6500	2.7577
2.00	141.7909	35.4891	46.4727	18.1159	52.4182	14.8107
3.00	110.6692	75.1739	82.2846	41.9682	49.6077	9.9162
4.00	73.3400	23.8125	70.6900	17.8577	49.5100	8.3450
TOTAL	114.016	58.9214	65.1667	32.8851	49.1639	12.1207

TUFF	ZR		NB		PB	
	mean	std. dev	mean	std. dev	mean	std. dev
1.00	250.0500	17.0413	21.4000	3.1113	19.2500	14.3543
2.00	259.1727	69.5089	20.8273	4.0856	9.9273	6.4153
3.00	268.9385	48.361	21.5538	4.1052	20.0077	12.8073
4.00	281.4500	27.5072	22.2600	2.0222	12.7000	7.7954
TOTAL	268.3806	49.7988	21.5194	3.4905	14.8556	10.4611

TUFF	ZN		CU		NI		CO	
	mean	std. dev	mean	std. dev	mean	std. dev	mean	std. dev
1	80.4500	23.9709	8.8000	2.6870	2.3500	.3536	.9000	.7071
2	41.0182	18.0230	5.0273	2.4828	2.8818	3.1777	6.4000	7.0140
3	47.2077	15.7748	4.3385	2.0304	1.0846	.8474	10.7385	5.0283
4	37.5200	12.7497	5.3000	3.9477	.9300	.4547	8.0900	7.8333
TOT	44.4722	18.1837	5.0639	2.8979	1.6611	1.9899	8.1306	6.7062

TUFF	CR		V		BA	
	mean	std. dev	mean	std. dev	mean	std. dev
1.00	8.3500	2.1920	8.7500	.9192	1077.5000	112.0057
2.00	6.9455	8.9100	16.4455	10.8514	901.5818	408.6281
3.00	3.8923	1.2440	9.5077	2.2066	428.8231	169.6838
4.00	6.9400	5.2195	9.1500	1.6847	697.9300	306.7640
TOTAL	5.9194	5.7313	11.4861	6.8730	684.0067	360.6996

FIGURE 2.24
COMPARISON OF PITTS HEAD TUFF FROM DIFFERENT REGIONS

A) Multivariate Tests of Significance (S = 3, M = 4 1/2, N = 9)

Test Name	Value	Approx. F	Hypoth. DF	Error DF	Sig. of F
Pillais	2.06267	3.72404	39.00	66.00	.000
Hotellings	8.21224	3.93064	39.00	56.00	.000
Wilks	.02430	3.85846	39.00	59.97	.000
Roys	.82581				

B) Univariate F-tests with (3,32) D. F.   F critical = 2.90 at 95% confidence
= 4.47 at 99% confidence

Variable	Hypoth. SS	Error SS	Hypoth. MS	Error MS	F	Sig. of F
RB	35655.76922	85854.74078	11885.25641	2682.96065	4.42990	.010
SR	10560.09226	27289.90774	3520.03075	852.80962	4.12757	.014
Y	1134.00346	4007.89959	378.00115	125.24686	3.01805	.044
ZR	3316.79380	83480.46259	1105.59793	2608.76446	.42380	.737
NB	10.79826	415.63813	3.59942	12.98869	.27712	.841
PB	697.33284	3132.85605	232.44428	97.90175	2.37426	.089
ZN	3300.64563	8272.02659	1100.21521	258.50083	4.25614	.012
CU	35.33047	258.59259	11.77682	8.08102	1.45734	.245
NI	27.00627	111.57929	9.00209	3.48685	2.58172	.071
CO	225.93662	1348.11977	75.31221	42.12874	1.78767	.169
CR	87.23089	1062.44550	29.07696	33.20142	.87577	.464
V	390.97655	1262.34650	130.32552	39.44833	3.30370	.033
BA	1678883.51956	2874763.34044	559627.83985	89836.35439	6.22941	.002

C) Multivariate Tests of Significance (S = 3, M = 1/2, N = 13) Using ONLY Zr, Nb, Cr, Cu, and Y.

Test Name	Value	Approx.F	Hypoth. DF	Error DF	Sig. of F
Pillais	.66278	1.70147	15.00	90.00	.065
Hotellings	1.09438	1.94557	15.00	80.00	.030
Wilks	.43308	1.83420	15.00	77.70	.044
Roys	.46296				

FIG. 2.25:

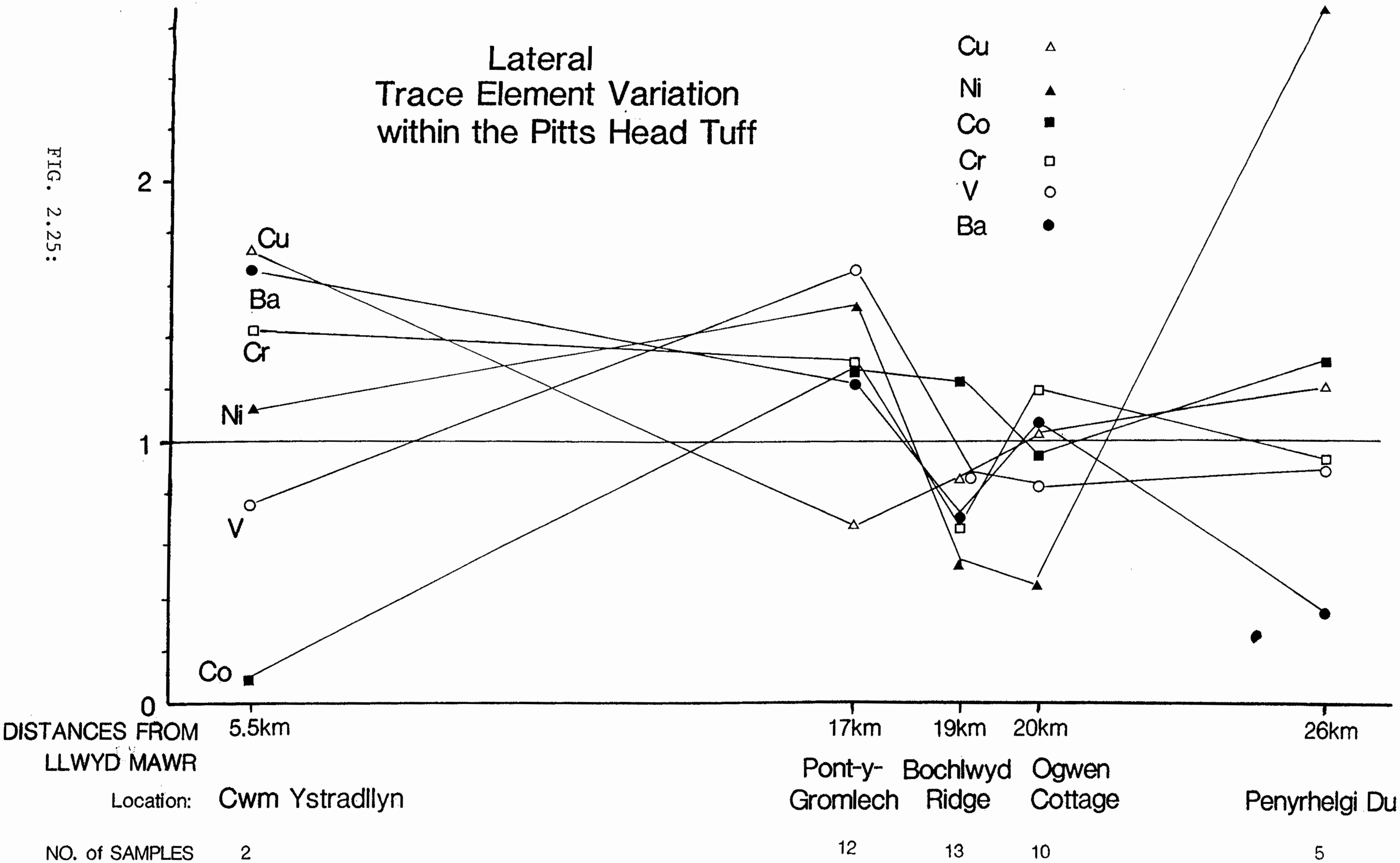

Lateral
Trace Element Variation
within the Pitts Head Tuff
Cu
Ni
Co
Cr
V
Ba
0
1
2
Cu
Ba
Cr
Ni
V
Co
DISTANCES FROM
LLWYD MAWR
5.5km
17km
19km
20km
26km
Location:
Cwm Ystradllyn
Pont-y-
Gromlech
Bochlwyd
Ridge
Ogwen
Cottage
Penyrhelgi Du
NO. of SAMPLES
2
12
13
10
5

FIG. 2.25 continued

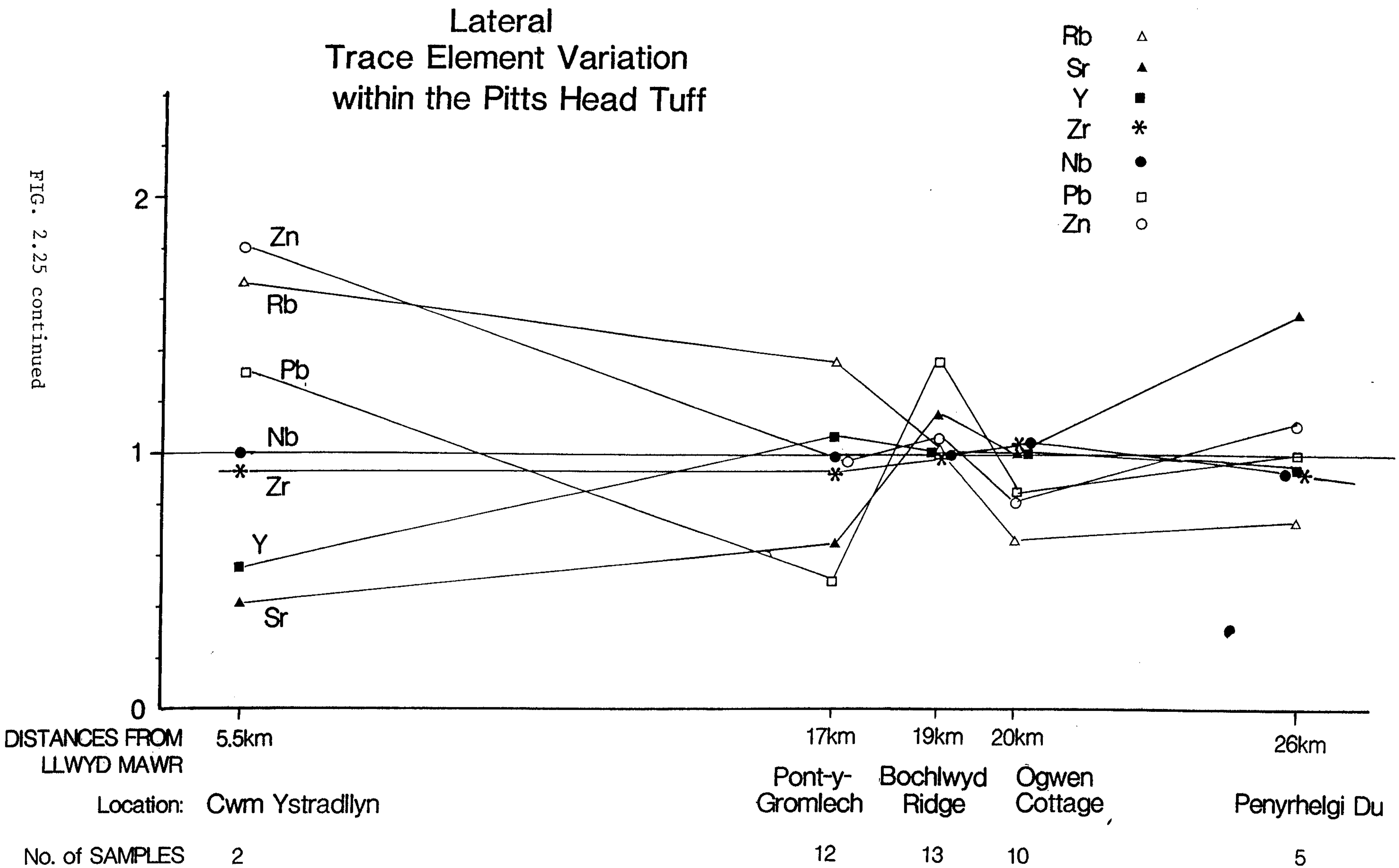

FIGURE 2.26

GROUP MEANS OF TRACE ELEMENT COMPOSITION OF KNOWN ASH FLOW TUFFS

1 = GARTH TUFF n=10
2 = RACKS TUFF n=8
3 = 3rd MEMBER CCVF n=2
4 = 4th MEMBER CCVF n=6
5 = PITTS HEAD TUFF n=36

TUFF	RB		SR		Y		ZR	
	mean	std.dev.	mean	std.dev.	mean	std.dev.	mean	std.dev.
1	192.6500	78.9379	45.3600	35.3054	75.5200	16.0888	170.9100	33.4494
2	160.7250	51.9740	74.4000	21.0180	76.6500	10.4553	201.5625	10.4361
3	52.7000	70.7107	67.7500	4.4548	73.1500	10.2530	363.4500	106.4196
4	97.2833	40.1189	75.4667	32.5202	72.9667	11.2608	376.2333	53.4809
5	114.0167	58.9214	65.1667	32.8851	49.1639	12.1207	268.3806	49.7988
TOT	129.1290	68.2177	64.2435	32.0528	60.0387	17.7340	257.5419	74.0585

	NB		PB		ZN		CU	
	mean	std.dev.	mean	std.dev.	mean	std.dev.	mean	std.dev.
1	17.3000	3.4056	13.5800	14.7529	53.1700	16.9799	3.2300	1.0584
2	18.5375	1.9346	45.3625	51.1452	321.0875	507.6018	6.6625	3.0775
3	20.3500	2.6163	17.1500	10.6773	58.8500	12.5158	6.2000	1.1314
4	21.7000	1.2853	18.1000	8.4150	70.0833	35.4370	9.4833	2.5317
5	21.5194	3.4905	14.8556	10.4611	44.4722	18.1837	5.0639	2.8979
TOT	20.4339	3.5091	18.9742	22.5620	84.5097	195.9453	5.4387	3.0535

	NI		CO		CR	
	mean	std.dev.	mean	std.dev.	mean	std.dev.
1	3.0600	2.0823	12.0900	4.5148	6.5200	3.3423
2	1.8250	.8207	14.2125	2.0096	4.2500	1.4112
3	2.0000	1.9799	17.3500	.3536	6.7000	.4243
4	6.8167	2.7520	13.4833	6.0446	15.7667	5.4851
5	1.6611	1.9899	8.1306	6.7062	5.9194	5.7313
TOT	2.4177	2.4565	10.3694	6.3406	6.7790	5.6942

	V		BA	
	mean	std.dev.	mean	std.dev.
1	10.4800	5.0758	919.0800	372.6421
2	8.7750	.9498	1784.5750	800.3959
3	8.8000	5.5154	736.6500	979.4136
4	22.9500	7.8772	746.2167	373.9746
5	11.4861	6.8730	684.0667	360.6996
TOT	11.9968	7.1149	871.6839	573.0838

FIGURE 2.27
COMPARSISON OF KNOWN TUFFS

A) Multivariate Tests of Significance (S = 4, M = 4 , N = 21 1/2)

Test Name	Value	Approx. F	Hypoth. DF	Error DF	Sig. of F
Pillais	2.52141	6.29644	52.00	192.00	.000
Hotellings	17.32214	14.49064	52.00	174.00	.000
Wilks	.00475	10.1121	52.00	176.40	.000
Roys	.90972				

B) COMPARISON OF INDIVIDUAL ELEMENTS BETWEEN 5 KNOWN TUFFS

WILKS' LAMBDA (U-STATISTIC) AND UNIVARIATE F-RATIO
WITH 4 AND 57 DEGREES OF FREEDOM

VARIABLE	WILKS' LAMBDA	F	SIGNIFICANCE
RB	0.73817	5.054	0.0015
SR	0.91699	1.290	0.2848
Y	0.46788	16.21	0.0000
ZR	0.36841	24.43	0.0000
NB	0.76165	4.459	0.0033
PB	0.79120	3.761	0.0088
ZN	0.77889	4.045	0.0059
CU	0.70966	5.830	0.0005
NI	0.60882	9.156	0.0000
CO	0.80271	3.502	0.0126
CR	0.71529	5.672	0.0006
V	0.72288	5.463	0.0009
BA	0.59631	9.647	0.0000

C) COMPARISON OF ZR USING TUKEY-B PROCEDURE
WITHIN ONEWAY ANALYSIS OF VARIANCE

Variable Zr
BY Region

THE FOLLOWING GROUPS ARE SIGNIFICANTLY DIFFERENT
AT THE 95% CONFIDENCE LEVEL

Mean	Group	Grp 1	Grp 2	Grp 5	Grp 3	Grp 4
170.9100	Grp 1					
201.5625	Grp 2					
268.3806	Grp 5	*	*			
363.4500	Grp 3	*	*	*		
376.2333	Grp 4	*	*	*		

FIGURE 2.28

GROUP MEANS OF RELATIVE PROPORTIONS OF Y,Nb Zr and Y/ZR Nb/Zr RATIOS

TUFF	PERCENT Y	PERCENT NB	PERCENT ZR	Y/ZR RATIO	NB/ZR RATIO
1	52.26582	24.00910	23.72508	0.44182	0.10133
2	49.61883	24.07123	26.30993	0.37946	0.09177
3	39.43857	21.96870	38.59273	0.20596	0.05740
4	38.05038	22.71077	39.23885	0.19786	0.05842
5	33.63831	29.53925	36.82245	0.20202	0.08186
101	52.58323	25.83561	21.58115	0.48766	0.11961
102	37.52230	28.63896	33.83874	0.25730	0.08875
103	51.96948	23.05131	24.97921	0.41775	0.09223
104	46.39030	29.89284	23.71686	0.39120	0.12604
105	56.61693	22.73044	20.65263	0.54828	0.11006
201	51.48096	22.99013	25.52891	0.40331	0.09006
202	44.52702	20.97564	34.49734	0.25835	0.06085
203	45.26012	20.92486	33.81503	0.26769	0.06188
501	39.01777	19.66287	41.31936	0.19060	0.04773
502	31.89728	29.33393	38.76878	0.16620	0.07576
503	39.42211	26.27709	34.30080	0.24078	0.07959
504	40.56628	22.21281	37.22091	0.21839	0.06058
505	45.14989	27.10153	27.74858	0.32578	0.09765
511	46.70883	24.57761	28.71356	0.33045	0.08715
512	43.86620	25.42393	30.70987	0.28733	0.08295
522	53.64879	20.25004	26.10117	0.52704	0.08596
526	45.26620	25.38195	29.35185	0.31202	0.08708
530	35.70305	20.28940	44.00755	0.16226	0.04610
531	50.13440	23.94414	25.92146	0.39215	0.09270
999	29.84201	25.74605	44.41194	0.13439	0.05797
5111	29.86689	32.15515	37.97796	0.15730	0.08467
9999	15.68826	41.70040	42.61134	0.07363	0.09786
TOTAL	40.62620	26.26535	33.10844	0.27292	0.08242

RELATIVE PROPORTIONS OF Zr, Y, & Nb for 5 "KNOWN" ASH FLOW TUFFS AND UNIDENTIFIED TUFFITES

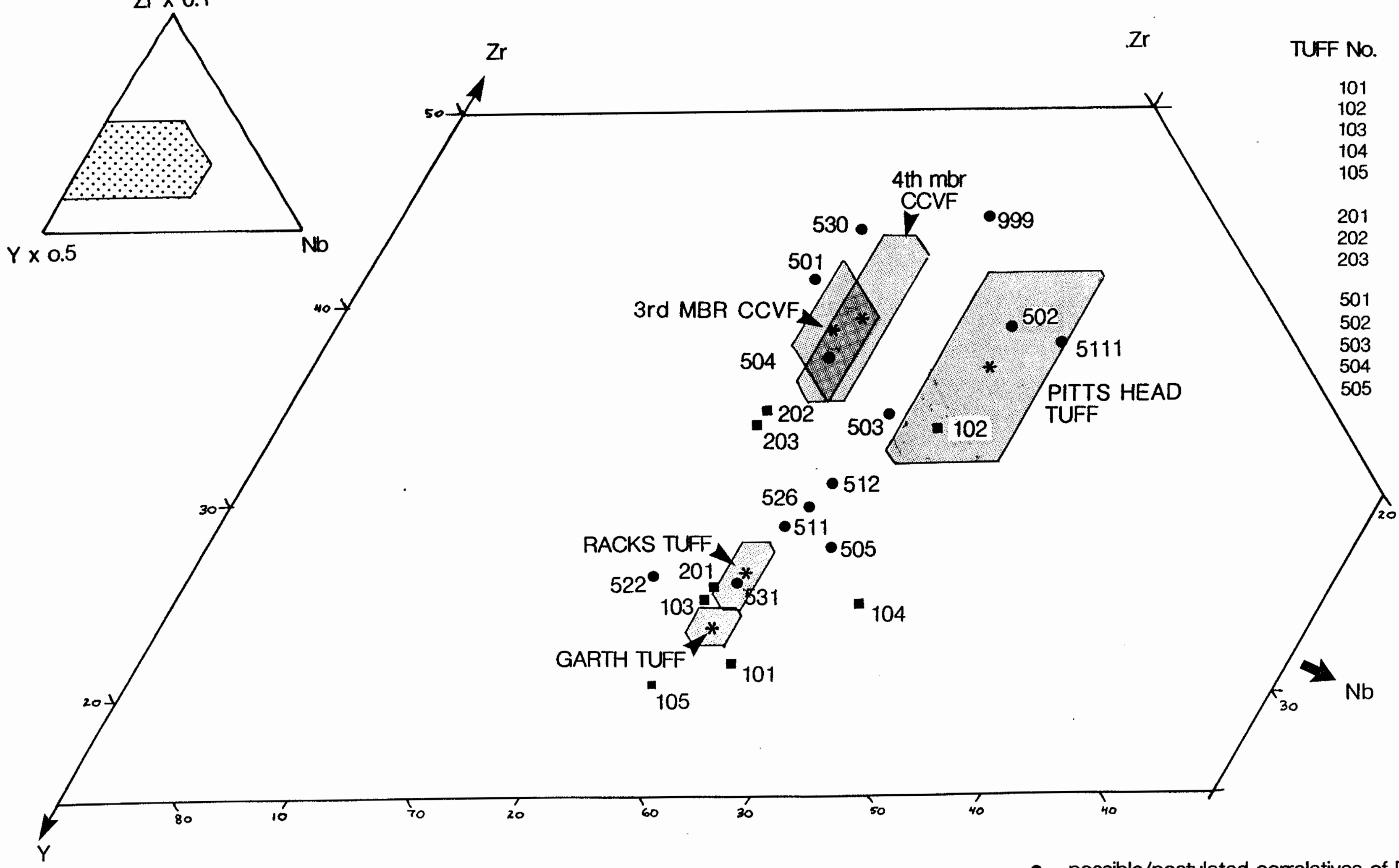

TUFF No.	ASH FLOW TUFF
101	ROLWYD
102	NANTMOR 1
103	LLEDR VALLEY TUFF 1
104	HEBOG 1
105	CARNEDD DAFYDD
201	LLEDR VALLEY TUFF 2
202	FYNNON LLOER 1
203	FYNNON LLOER 2
501	CWM Y FYNNON
502	F2
503	F3
504	F4
505	F5
511	COLWYD 1
512	COLWYD 2
522	G2
526	G6
530	REWORKED PHT
531	NANTMOR 2
999	Sandstone dyke
5111	Replicates PHT

● possible/postulated correlatives of PHT

■ possible/postulated correlatives of CCVF

FIG. 2.29a

SUMMARY TABLE OF STEPWISE DISCRIMINANT ANALYSIS OF KNOWN ASH FLOW TUFFS.

STEP	ACTION ENTERED	ACTION REMOVED	VARS IN	WILKS' LAMBDA
1	ZR		1	.36841
2	Y		2	.16764
3	NB		3	.06193
4	CR		4	.03387
5	CU		5	.02161
6	BA		6	.01580
7	CO		7	.01265
8	PB		8	.01003
9	NI		9	.00853
10	V		10	.00734
11	RB		11	.00630
12	SR		12	.00544
13	ZN		13	.00475

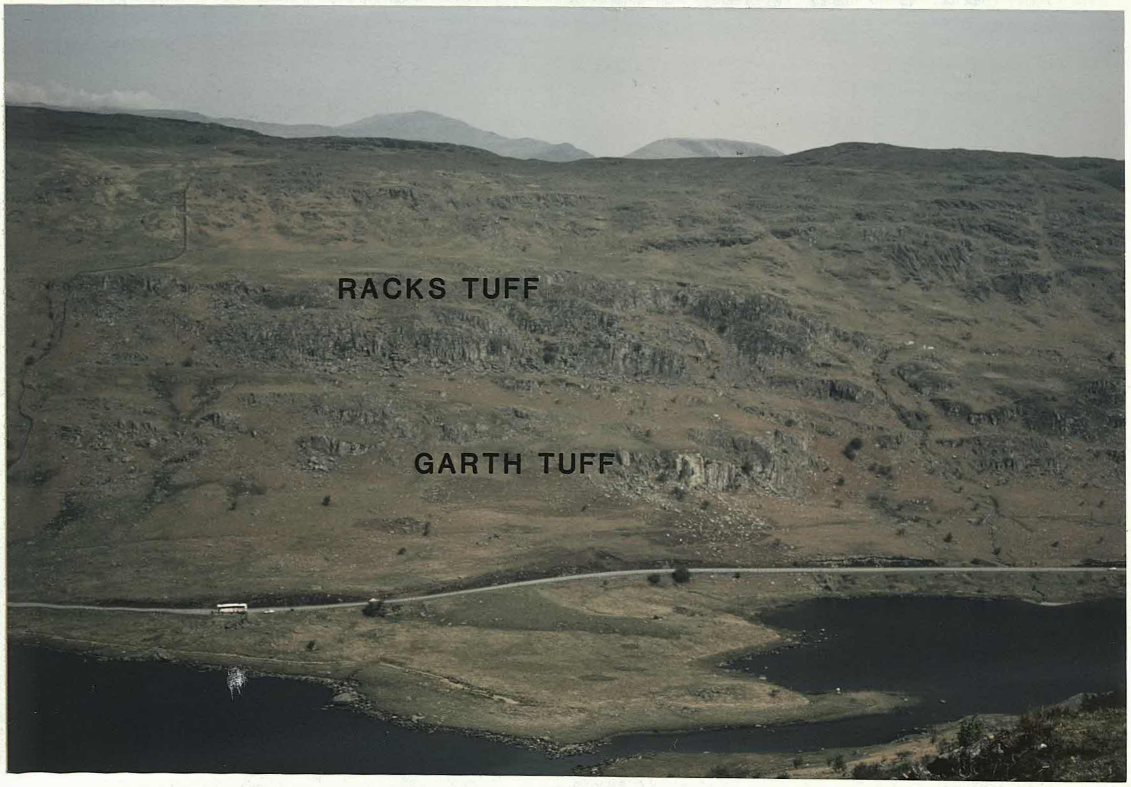

FIG. 2.29b: View of ash flow tuffs in the Capel Curig anticline: Garth tuff has 170.91 ppm Zr, 75.52 ppm Y, and 17.30 ppm Nb. Racks tuff has concentrations of 201.56 ppm, 76.65 ppm and 18.54 ppm respectively of these elements. Coach shown for scale.

FIGURE 2.30

CANONICAL DISCRIMINANT FUNCTIONS

FUNCTION	EIGENVALUE	PERCENT OF VARIANCE	CUMULATIVE PERCENT	CANONICAL CORRELATION	:	AFTER FUNCTION	WILKS' LAMBDA	CHI-SQUARED	D.F.	SIGNIFICANCE
					:	0	0.0047451	278.23	52	0.0000
1*	10.07653	58.17	58.17	0.9537919	:	1	0.0525596	153.18	36	0.0000
2*	5.75003	33.19	91.37	0.9229586	:	2	0.3547792	53.885	22	0.0002
3*	1.23371	7.12	98.49	0.7431781	:	3	0.7924728	12.095	10	0.2787
4*	0.26187	1.51	100.00	0.4555515	:					

* MARKS THE 4 CANONICAL DISCRIMINANT FUNCTIONS REMAINING IN THE ANALYSIS.

FIGURE 2.31

UNSTANDARDIZED CANONICAL DISCRIMINANT FUNCTION COEFFICIENTS CALCULATED FROM KNOWN TUFFS

	FUNC 1	FUNC 2	FUNC 3	FUNC 4
RB	0.6480880E-02	0.4365110E-02	-0.1056100E-01	0.5857400E-02
SR	0.1516370E-01	-0.1355176E-02	-0.4863696E-04	0.1464844E-01
Y	0.4502177E-01	0.8324526E-01	-0.2673714E-01	-0.5096028E-01
ZR	0.4363144E-01	-0.1340424E-01	-0.1064128E-01	-0.1466351E-01
NB	-0.6185503	-0.1351758	0.2610687	0.1877427
PB	0.1602072E-01	0.1364171E-01	0.1666850E-01	-0.2437615E-02
ZN	0.8507601E-03	0.5788406E-03	0.2540681E-02	0.4487328E-04
CU	0.3934098	0.2266912	0.1810518	0.1308333
NI	0.3357264	-0.1645347	-0.4784209	0.5799330
CO	0.1227187	0.5380648E-01	0.3890084E-01	0.5058091E-01
CR	-0.3632861E-02	-0.1309925	-0.3375427E-02	-0.7058977E-01
V	-0.2788437E-01	0.1071972E-01	0.1861705	0.1942572E-01
BA	-0.1328062E-03	0.7333046E-03	0.1437187E-02	-0.1663725E-04
(CONSTANT)	-7.236456	-0.8408309	-3.847633	-1.033417

FIGURE 2.32
CLASSIFICATION OF UNKNOWN TUFFS

	TUFF	HIGHEST PROBABILITY GROUP	P(D/G)	P(G/D)	2ND HIGHEST GROUP	P(G/D)	DISCRIMINANT SCORES...			
101	G056ROL	1	0.0030	0.8954	5	0.1046	-4.7033	1.7188	0.2635	0.0025
101	G058ROL	1	0.4117	0.9991	2	0.0009	-2.1945	3.3518	-0.4391	-0.5823
102	G090	4	0.0000	1.0000	2	0.0000	6.3688	1.0206	3.7516	5.1276
102	G091	4	0.0000	0.9999	5	0.0001	3.6024	-6.6631	0.9181	8.7062
102	G09491	4	0.0000	1.0000	5	0.0000	4.8778	-5.0105	-1.1985	7.4169
105	G095	1	0.4165	0.9999	2	0.0001	-2.1453	3.9366	-1.2719	-0.9788
103	G0111	1	0.1579	0.9781	5	0.0219	-2.8048	1.3625	-1.2292	-1.5195
103	G0112	1	0.2972	0.9835	2	0.0165	0.4422	2.8561	-1.3174	-0.5206
104	GOC2	4	0.0000	1.0000	5	0.0000	4.5726	-4.9513	-3.0572	11.5999
201	G0118	1	0.2269	0.9976	5	0.0024	-2.1671	1.7174	-1.6008	-1.9078
202	X17	3	0.0801	0.9874	4	0.0126	5.0514	0.8665	-1.5822	-0.0021
202	X18	3	0.0673	0.9642	4	0.0358	5.1620	0.9386	-0.7243	0.1473
203	X20	3	0.4342	0.9994	4	0.0006	5.1686	1.0056	-0.8864	-1.1287
501	G0147	4	0.0000	1.0000	3	0.0000	22.0193	6.2613	2.7053	-0.3182
501	G0148	3	0.1057	1.0000	4	0.0000	4.7581	-0.9111	-2.7215	-4.1387
501	X12	4	0.0000	0.9809	3	0.0191	12.6583	0.0914	-0.9755	-3.0625
501	X13	4	0.0000	0.9947	3	0.0053	10.8896	-3.9649	-2.9300	-2.9683
501	X14	3	0.0000	0.9999	4	0.0001	10.6129	-0.9562	-3.6299	-6.0454
501	X15	3	0.0024	0.9991	4	0.0009	9.4089	0.4492	-2.2432	-3.9315
502	G0127	5	0.0282	1.0000	1	0.0000	-0.6216	-3.2571	-0.7351	2.3883
502	X23	5	0.0000	1.0000	1	0.0000	0.9305	-3.4440	-1.7759	3.6128
502	X24	4	0.0000	1.0000	3	0.0000	7.2161	-3.8551	-7.8571	9.0442
502	X25	5	0.0597	0.9999	1	0.0001	1.2148	-1.4655	-0.5887	0.9205
502	X26	5	0.4193	0.9993	1	0.0007	-0.0677	-0.4206	0.4297	-0.8779
503	G0130	5	0.0134	0.9996	1	0.0003	1.5754	-0.7469	0.3774	1.5956
503	G0131	5	0.2906	0.9847	1	0.0153	-3.0858	0.0572	0.0655	0.3494
504	G0133	4	0.1099	0.9784	3	0.0216	6.9359	0.1862	1.2917	0.4973
504	G0134	5	0.9362	1.0000	1	0.0000	-2.2030	-1.6797	-0.1439	0.2841
505	G0136	1	0.0147	0.6640	5	0.3099	-0.3263	1.3689	0.3453	2.1153
505	G0137	1	0 0001	0.5340	5	0.3279	1.1428	1.0602	-0.0197	3.2222
505	G0138	2	0.0007	0.8615	1	0.1236	1.4885	1.6499	0.2925	2.9503
511	G0139	5	0.4168	0.9834	1	0.0166	-0.9717	0.2079	0.3101	0.9173
511	G0140	5	0.1760	0.8913	1	0.1087	-2.8360	0.3867	-0.2058	0.9429
511	G0141	2	0.0491	0.8615	1	0.0956	0.7258	1.7057	0.7930	0.5378
512	G0142	4	0.0000	0.7430	2	0.2570	7.9815	4.2732	3.8844	4.2817
512	G0143	5	0.0011	0.9996	1	0.0004	1.4716	-1.0247	-0.0882	2.9922
512	G0144	2	0.0000	0.9863	4	0.0111	3.4495	1.0676	0.8822	2.8831
512	G0145	5	0.0018	0.9943	1	0.0055	-0.7308	0.3179	1.1868	3.5404
512	G0146	5	0.0008	0.9174	1	0.0640	1.1752	0.4720	0.2754	2.8081
522	G043	5	0.0002	0.5388	2	0.4408	2.4065	0.4755	0.5408	1.5885
522	G044	1	0.0011	0.7245	2	0.2755	2.0021	3.5343	-1.8573	2.3662
526	G046	5	0.3061	0.9979	1	0.0021	-2.3095	-1.2357	-1.3117	1.2307
526	G047	5	0.1425	0.5583	1	0.4416	-1.2632	0.9419	-0.0537	0.9604
526	G048	1	0.0468	0.9250	2	0.0379	0.3348	1.6407	-0.2852	1.6496
526	G050	2	0.0140	0.9663	1	0.0170	1.4048	1.5433	0.9173	1.6502
526	G051	5	0.1642	0.8360	1	0.1640	-0.6475	0.1945	-0.7502	1.3857
526	G051A	5	0.3140	0.9641	1	0.0359	-1.3630	-0.1388	-0.6026	1.4661
526	G052	2	0.0000	0.9793	4	0.0205	4.9317	2.1262	2.2331	2.8023
526	G052A	2	0.0001	0.9987	4	0.0011	4.1559	1.6664	2.3104	2.3336
526	G054	5	0.0572	0.6446	1	0.3528	-0.0560	0.8419	-0.0638	1.2718
526	G055	5	0.2821	0.8958	1	0.1042	-1.0622	0.5127	0.0141	0.9356
530	G071	4	0.0000	1.0000	3	0.0000	25.5804	-16.2113	5.2628	21.5840
531	G087	2	0.2619	0.9970	1	0.0030	1.2740	2.5816	0.9162	0.8265
531	G088	1	0.2129	0.6886	5	0.3114	-1.2071	0.2848	-1.7004	0.547
531	G089	5	0.0025	1.0000	1	0.0000	-0.8563	-3.0089	-2.0017	2.8751
999	G063	4	0.0000	1.00 00	3	0.0000	1 0.8040	-7. 0765	-0.8400	11.5733

FIGURE 2.33

MULTIVARIATE COMPARSISONS OF VECTOR MEANS FROM PAIRS OF TUFF/TUFFIES

The maximum number of elements statistically possible
were used in comparisons

ELEMENTS USED IN COMPARISONS WERE (under Degrees of Freedom column):

a = Rb Sr Y Zr Nb Pb Zn Cu Ni Co Cr Ba (all)
b = Zr Y Nb Cr Cu
c = Nb Cr Pb Cu Zn
d = Zr Y Nb
e = Zr Y Nb Cr
f = Zr Nb
g = Zr Y Nb Cr CU Ba Co Pb Ni V Rb Sr

F critical (and indication of significance of F)
for 99% confidence level unless noted otherwise.

TUFFS COMPARED	HOTELLINGS T2/N-2	F estim.	DEGREES OF FREEDOM	F crit.	SIGNIF F	REGIONS STATIST. DIFFERENT
101/1	1.774	2.129	b 5,6	8.75	.192	
101/2	68.8126	54.25	b 5,4	15.52	.001	******
102/1	33.76	47.26	b 5,7	7.46	.000	******
102/2	73.131	73.13	b 5,5	10.97	.000	******
102/3	4.311	2.87	d 3,2	99.17	.269	
102/4	255.9	153.50	b 5,3	28.20	.001	******
102/PHT	40.802	78.46	a 13,25	2.94	.001	******
102/PHT	3.232	21.33	b 5,33	3.64	.000	******
102/PHT	.422	4.92	d 3,35	4.42	.006	
531/1	523.05	47.54	g 11,1	6080.	.113	
531/2	97.68	97.68	b 5,5	10.97	.000	******
531/4	60.19	36.12	b 5,3	28.24	.007	******
531/PHT	.768	5.07	b 5,33	3.62	.001	******
103/1	1.397	1.67	b 5,6	8.75	.273	
103/2	16.09	12.87	b 5,4	9.36	.014	***97.5%
104/1	51.97	51.97	b 5,5	10.97	.000	******
104/2	190.63	114.4	b 5,3	28.2	.001	******
104/4	2851	516.3	b 5,1	230.2	.033	***95%
105/1	1.287	1.287	b 5,5	10.97	.394	
105/2	45.737	27.44	b 5,3	39.3	.010	***97.5%
105/3						no univ
201/1	1.14	1.14	b 5,5	10.97	.440	
201/2	7.6342	4.58	b 5,3	28.2	.120	
202/1	44.257	53.1	b 5,6	8.75	.000	******
202/2	176.11	140.9	b 5,4	15.52	.000	******
202/3	.6065	.7706	f 2,1	4999	.627	
202/4	45.62	18.24	b 5,2	19.3	.053	***95%
203/1	25.47	25.4	b 5,5	10.97	.001	******
203/2	200.7	120.4	b 5,3	28.2	.001	******
203/4	53.56	10.71	b 5,1	5763	.228	

FIGURE 2.33 continued

MULTIVARIATE COMPARSISONS OF VECTOR MEANS FROM PAIRS OF TUFF/TUFFIES

TUFFS COMPARED	HOTELLINGS T2/N-1	F estim.	DEGREES OF FREEDOM	F crit.	SIGNIF F	REGIONS STATIST. DIFFERENT
PHT/502	1.09047	2.265	a 13,27	2.88	.035	
PHT/502	.09131	.639	b 5,35	3.55	.671	
PHT/502	.04714	.3301	b 5,35	3.55	.891	
PHT/503	1.874	3.40	a 13,24	2.99	.004	******
PHT/503	.89634	5.736	b 5,32	3.68	.001	******
PHT/503	1.18094	7.558	c 5,32	3.68	.000	******
PHT/504	1.36558	2.521	a 13,24	2.99	.024	***97.5%
PHT/504	1.00613	6.49	b 5,32	3.68	.000	******
PHT/504	.68872	4.407	c 5,32	3.68	.004	******
PHT/505	2.982	5.734	a 13,25	2.94	.000	******
PHT/505	1.809	11.94	b 5,33	3.64	.000	******
PHT/505	1.675	11.05	c 5,33	3.64	.000	******
PHT/511	2.35	4.523	a 13,25	2.94	.001	******
PHT/511	1.37	9.054	b 5,33	3.64	.000	******
PHT/512	6.404	14.77	a 13,30	2.80	.000	******
PHT/512	23.58	3.07	b 5,38	3.53	.000	******
PHT/522	6.82	16.79	a 13,22	3.08	.000	******
PHT/522	3.65	29.21	b 5,40	3.51	.000	******
PHT/526	8.62	27.87	a 13,42	2.60	.000	******
PHT/526	6.129	61.29	b 5,50	3.40	.000	******
511/503	20.064	6.68	d 3,1	5403	.275	
511/504	6.477	3.159	d 3,1	5403	.687	
511/505	15.327	3.813	e 4,1	5624	.364	
511/522	2.805	.935	d 3,1	5403	.623	
511/526	1.584	2.214	b 5,7	7.46	.164	
512/503	.70059	.1401	b 5,1	5763	.956	
512/504	6.74094	1.348	b 5,1	5763	.572	
512/505	3.19	1.27	b 5,2	99.3	.494	
512/522	28.835	5.767	b 5,1	5763	.306	
512/526	80.24	6.171	a 13,1	6140.	.306	
512/526	.29099	.5237	b 5,9	6.06	.753	
PHT/501	22.29	48.01	a 13,28	2.85	.000	******
PHT/501	14.76	106.3	b 5,36	3.6	.000	******
PHT/530	84.524	149.54	a 13,23	3.03	.000	******
PHT/530	25.05	155.3	b 5,5	10.97	.000	******

FIGURE 2.34

COMPARISON OF PITTS HEAD TUFF AND TUFF 502 at PEN Yr HELGI DU

a) Multivariate Tests of Significance (S = 1, M = 5 1/2, N = 12 1/2) using all 13 trace elements.

Test Name	Value	Exact F	Hypoth. DF	Error DF	Sig. of F
Pillais	.52164	2.26483	13.00	27.00	.035
Hotellings	1.09047	2.26483	13.00	27.00	.035
Wilks	.47836	2.26483	13.00	27.00	.035
Roys	.52164				

Note.. F statistics are exact.

b) Univariate F-tests with (1,39) D. F.

Variable	Hypoth. SS	Error SS	Hypoth. MS	Error MS	F	Sig. of F
RB	4261.77605	125761.16200	4261.77605	3224.64518	1.32163	.257
SR	8496.93678	40704.33200	8496.93678	1043.70082	8.14116	.007
Y	58.29333	5388.69106	58.29333	138.17157	.42189	.520
ZR	185.45610	87307.52439	185.45610	2238.65447	.08284	.775
NB	2.27239	432.53639	2.27239	11.09068	.20489	.653
PB	.38350	3924.38089	.38350	100.62515	.00381	.951
ZN	124.61802	12540.71222	124.61802	321.55672	.38755	.537
CU	4.35616	297.75506	4.35616	7.63475	.57057	.455
NI	69.50440	289.33756	69.50440	7.41891	9.36854	.004
CO	40.82537	1602.96439	40.82537	41.10165	.99328	.325
CR	1.79512	1159.18439	1.79512	29.72268	.06040	.807
V	11.04475	1666.98306	11.04475	42.74316	.25840	.614
BA	973880.95688	4571053.88800	973880.95688	117206.50995	8.30910	.006

FIG. 2.36 A

COMPARISON OF ABSOLUTE CONCENTRATIONS OF TRACE ELEMENTS BETWEEN PITTS HEAD TUFF and TUFF 102

Multivariate Tests of Significance (S = 1, M = 5 1/2, N = 11 1/2)

Test Name	Value	Exact F	Hypoth. DF	Error DF	Sig. of F
Pillais	.97608	78.46468	13.00	25.00	.000
Hotellings	40.80163	78.46468	13.00	25.00	.000
Wilks	.02392	78.46468	13.00	25.00	.000
Roys	.97608				

Note.. F statistics are exact.

EFFECT .. REGION (CONT.)
Univariate F-tests with (1,37) D. F.

Variable	Hypoth. SS	Error SS	Hypoth. MS	Error MS	F	Sig. of F
RB	138.94231	122299.63667	138.94231	3305.39559	.04204	.839
SR	6821.91077	37898.44667	6821.91077	1024.28234	6.66019	.014
Y	441.77797	5482.72972	441.77797	148.18188	2.98132	.093
ZR	30133.07284	91156.16306	30133.07284	2463.68008	12.23092	.001
NB	159.36669	435.88306	159.36669	11.78062	13.52787	.001
PB	90100.08752	32471.83556	90100.08752	877.61718	102.66445	.000
ZN	3601.11803	11617.01889	3601.11803	313.97348	11.46950	.002
CU	1.24105	301.08972	1.24105	8.13756	.15251	.698
NI	643.08111	149.76556	643.08111	4.04772	158.87499	.000
CO	18.76002	1608.98306	18.76002	43.48603	.43140	.515
CR	2466.98771	1224.90306	2466.98771	33.10549	74.51900	.000
V	2657.89335	1735.60972	2657.89335	46.90837	56.66139	.000
BA	191205.19692	4563836.68000	191205.19692	123346.93730	1.55014	.221

FIG. 2.36 B

COMPARISON OF TUFF 102 and PITTS HEAD TUFF USING ALL 12 TRACE ELEMENT RATIOS OVER ZR.

EFFECT .. REGION
Multivariate Tests of Significance (S = 1, M = 5 , N = 12)

Test Name	Value	Exact F	Hypoth. DF	Error DF	Sig. of F
Pillais	.98482	140.52543	12.00	26.00	.000
Hotellings	64.85789	140.52543	12.00	26.00	.000
Wilks	.01518	140.52543	12.00	26.00	.000
Roys	.98482				

Note.. F statistics are exact.

EFFECT .. REGION (CONT.)
Univariate F-tests with (1,37) D. F.

Variable	Hypoth. SS	Error SS	Hypoth. MS	Error MS	F	Sig. of F
RBR	.13675	3.67866	.13675	.09942	1.37548	.248
SRR	.06383	.61518	.06383	.01663	3.83878	.058
YR	.00846	.94472	.00846	.02553	.33136	.568
NBR	.00013	.00802	.00013	.00022	.60516	.442
PBR	5.33011	3.65283	5.33011	.09873	53.98947	.000
ZNR	.32782	.38396	.32782	.01038	31.58939	.000
CUR	.00115	.00656	.00115	.00018	6.47167	.015
NIR	.02674	.02355	.02674	.00064	42.00354	.000
COR	.00328	.05044	.00328	.00136	2.40594	.129
CRR	.11425	.19603	.11425	.00530	21.56471	.000
VR	.13321	.23007	.13321	.00622	21.42336	.000
BAR	.00969	70.61040	.00969	1.90839	.00508	.944

FIG. 2.36 C

SUMMARY TABLE OF STEPWISE DISCRIMINANT ANALYSIS
OF KNOWN TUFFS USING RATIOS OF ELEMENTS OVER ZR

STEP	ACTION ENTERED	ACTION REMOVED	VARS IN	WILKS' LAMBDA	SIG.	LABEL
1	BAR		1	.43510	.0000	
2	NBR		2	.24698	.0000	
3	YR		3	.08865	.0000	
4	NIR		4	.02858	.0000	
5	RBR		5	.01954	.0000	
6	VR		6	.01442	.0000	
7	CUR		7	.01101	.0000	
8	PBR		8	.00926	.0000	
9	CRR		9	.00762	.0000	
10	ZNR		10	.00645	.0000	
11	SRR		11	.00584	.0000	

FIG. 2.36 D

COMPARISON OF PITTS HEAD TUFF and TUFF 102 using Y/ZR and Nb/Zr RATIOS

Multivariate Tests of Significance (S = 1, M = 0, N = 17)

Test Name	Value	Exact F	Hypoth. DF	Error DF	Sig. of F
Pillais	.02021	.37127	2.00	36.00	.692
Hotellings	.02063	.37127	2.00	36.00	.692
Wilks	.97979	.37127	2.00	36.00	.692
Roys	.02021				

Note.. F statistics are exact.

FIG. 2.36 E

COMPARISON OF 3rd volcanic member of CCVF and TUFF 102 using Y/ZR and Nb/Zr RATIOS

Multivariate Tests of Significance (S = 1, M = 0, N = 0)

Test Name	Value	Exact F	Hypoth. DF	Error DF	Sig. of F
Pillais	.78782	3.71306	2.00	2.00	.212
Hotellings	3.71306	3.71306	2.00	2.00	.212
Wilks	.21218	3.71306	2.00	2.00	.212
Roys	.78782				

Note.. F statistics are exact.

FIGURE 2.37

GROUP MEANS OF TRACE ELEMENT RATIOS OVER ZR

	Rb		Sr		Y	
	mean	std.dev.	mean	std.dev.	mean	std.dev.
1	.1152	.4082	.2808	.2428	.4418	.0321
2	.7885	.2302	.3672	.0951	.3795	.0414
3	.1217	.1589	.1929	.0442	.2060	.0321
4	.2680	.1304	.2085	.1145	.1979	.0449
5	.4555	.3220	.2461	.1326	.2020	.1584
101	.3630	.2379	.6226	.0776	.4877	.0408
102	.6777	.1576	.0943	.0081	.2573	.1827
103	.3748	.0909	.5606	.2483	.4178	.0533
104	1.3020	.0000	.1165	.0000	.3912	.0000
105	.8778	.0000	.3444	.0000	.5483	.0000
201	.3149	.0000	.3519	.0000	.4033	.0000
202	.3627	.0226	.2752	.0224	.2583	.0127
203	.2325	.0000	.2701	.0000	.2677	.0000
501	.1192	.0494	.1507	.0235	.1906	.0283
502	.2994	.1155	.3962	.0933	.1662	.0328
503	.3289	.1352	1.0161	.2350	.2408	.0920
504	.0468	.0214	.5222	.1339	.2184	.0091
505	.6801	.1924	1.3088	.3338	.3258	.0214
511	.4393	.2465	.9993	.2194	.3304	.0599
512	.4185	.4405	2.0814	.4341	.2873	.0370
522	.5125	.1873	1.6642	1.3781	.5270	.4268
526	.1106	.1187	1.4013	.3389	.3120	.0448
530	.1948	.0000	.7974	.0000	.1623	.0000
531	.4199	.1027	.3961	.0673	.3922	.0730
999	.3393	.0000	.8057	.0000	.1344	.0000
5111	.4955	.0033	.2682	.0025	.1573	.0023
9999	.9563	.0000	1.1587	.0000	.0736	.0000
TOTAL	.4713	.3677	.5359	.5567	.2729	.1430

	Nb		Pb		Zn	
	mean	std.dev.	mean	std.dev.	mean	std.dev.
1	.1013	.0054	.0860	.1004	.3138	.0928
2	.0918	.0057	.2184	.2423	1.5829	2.5273
3	.0574	.0096	.0538	.0451	.1639	.0136
4	.0584	.0069	.0492	.0221	.1919	.1079
5	.0819	.0142	.0561	.0382	.1749	.0985
101	.1196	.0123	.0748	.0103	.2344	.0456
102	.0887	.0219	1.4435	1.3420	.5190	.1488
103	.0922	.0018	.0474	.0016	.1800	.0941
104	.1260	.0000	.7384	.0000	2.1118	.0000
105	.1101	.0000	.0898	.0000	.3255	.0000
201	.0901	.0000	.0779	.0000	.4243	.0000
202	.0608	.0027	.0806	.0037	.1969	.0373
203	.0619	.0000	.0362	.0000	.2205	.0000
501	.0477	.0024	.0232	.0272	.1505	.0794
502	.0758	.0051	.0534	.0184	.1803	.0508
503	.0796	.0252	.2689	.0361	.4958	.2523
504	.0606	.0199	.0403	.0061	.2097	.1359
505	.0977	.0030	.3127	.0698	.4861	.1229
511	.0872	.0182	.2707	.2716	.2680	.0601
512	.0829	.0084	.1836	.1041	.3086	.0882
522	.0860	.0308	.2155	.0090	.4700	.2386
526	.0871	.0081	.1821	.0508	.3724	.3042
530	.0461	.0000	.0261	.0000	.2162	.0000
531	.0927	.0054	.5326	.5555	.7361	.2468
999	.0580	.0000	.0889	.0000	.3953	.0000
5111	.0847	.0005	.0206	.0040	.0799	.0015
9999	.0979	.0000	.2285	.0000	.2266	.0000
TOTAL	.0824	.0182	.1508	.3098	.3594	.7253

FIG. 2.37 continued

GROUP MEANS OF TRACE ELEMENT RATIOS OVER ZR

	Cu		Ni		Co	
	mean	std.dev.	mean	std.dev.	mean	std.dev.
1	.0191	.0059	.0170	.0087	.0750	.0335
2	.0338	.0171	.0090	.0040	.0709	.0116
3	.0183	.0085	.0049	.0040	.0500	.0156
4	.0263	.0100	.0185	.0072	.0352	.0121
5	.0198	.0120	.0091	.0253	.0342	.0374
101	.0255	.0047	.0077	.0020	.0761	.0233
102	.0401	.0274	.1073	.0240	.0686	.0273
103	.0309	.0130	.0062	.0024	.0466	.0164
104	.0844	.0000	.2687	.0000	.2140	.0000
105	.0297	.0000	.0101	.0000	.0709	.0000
201	.0171	.0000	.0050	.0000	.0475	.0000
202	.0237	.0056	.0178	.0008	.0441	.0087
203	.0270	.0000	.0116	.0000	.0475	.0000
501	.0284	.0260	.0055	.0023	.0195	.0031
502	.0221	.0039	.0199	.0211	.0407	.0101
503	.0396	.0030	.0097	.0119	.1164	.0526
504	.0367	.0267	.0155	.0000	.0969	.0352
505	.1079	.0115	.0284	.0052	.1289	.0330
511	.0541	.0107	.0148	.0034	.1314	.0296
512	.0905	.0605	.0148	.0043	.1290	.0395
522	.1006	.0594	.0313	.0186	.1161	.0330
526	.0837	.0320	.0122	.0113	.1671	.0625
530	.0897	.0000	.1501	.0000	.0829	.0000
531	.0366	.0287	.0479	.0217	.0989	.0015
999	.0922	.0000	.1350	.0000	.1449	.0000
5111	.0099	.0016	.0041	.0015	.0351	.0014
9999	.0812	.0000	.0081	.0000	.0057	.0000
TOTAL	.0374	.0332	.0193	.0358	.0690	.0552

	Cr		V		Ba	
	mean	std.dev.	mean	std.dev.	mean	std.dev.
1	.0374	.0162	.0597	.0208	5.5597	2.5381
2	.0213	.0075	.0436	.0045	8.7434	3.7618
3	.0191	.0044	.0230	.0084	1.7054	2.1954
4	.0434	.0175	.0629	.0237	1.9534	.8800
5	.0311	.0716	.0517	.0794	2.6213	1.4116
101	.0261	.0088	.0407	.0019	4.6840	4.5546
102	.2342	.0905	.2710	.0693	2.6804	.6603
103	.0306	.0133	.0395	.0016	2.5920	1.0788
104	.4804	.0000	.5042	.0000	4.4483	.0000
105	.0270	.0000	.0506	.0000	5.7711	.0000
201	.0227	.0000	.0381	.0000	1.1851	.0000
202	.0327	.0011	.0563	.0100	3.8298	.2350
203	.0342	.0000	.0462	.0000	2.3774	.0000
501	.0148	.0055	.0226	.0069	.8198	.2893
502	.0193	.0058	.0360	.0065	.7711	.2284
503	.0785	.0108	.1279	.0169	1.7813	.5530
504	.0803	.0150	.1249	.0174	.5023	.0071
505	.0872	.0125	.1430	.0295	2.4096	.6527
511	.0907	.0267	.1351	.0331	5.3087	2.3826
512	.0877	.0151	.1589	.0698	2.3747	1.8245
522	.0715	.0065	.1290	.0059	1.7549	.7500
526	.0929	.0280	.1145	.0210	.8315	.3459
530	.4224	.0000	.4739	.0000	1.5032	.0000
531	.1290	.0533	.1442	.0453	1.3763	.2622
999	.3386	.0000	.3248	.0000	2.0889	.0000
5111	.0099	.0045	.0378	.0008	4.9449	.0350
9999	.1017	.0000	.1002	.0000	4.7644	.0000
TOTAL	.0585	.0819	.0833	.0885	3.0361	2.5866

FIGURE 2.38

COMPARISON OF PITTS HEAD TUFF AND SAMPLE 530

A) Multivariate Tests of Significance (S = 1, M = 5 1/2, N = 10 1/2)
USING ALL TRACE ELEMENTS

Test Name	Value	Exact F	Hypoth. DF	Error DF	Sig. of F
Pillais	.98831	149.54254	13.00	23.00	.000
Hotellings	84.52404	149.54254	13.00	23.00	.000
Wilks	.01169	149.54254	13.00	23.00	.000
Roys	.98831				

Note.. F statistics are exact.

B) Univariate F-tests with (1,35) D. F.

F critical = 7.45 at 99% confidence level, 4.13 at 95% confidence level

Variable	Hypoth. SS	Error SS	Hypoth. MS	Error MS	F	Sig. of F
RB	3446.49757	121510.51000	3446.49757	3471.72886	.99273	.326
SR	24268.80432	37850.00000	24268.80432	1081.42857	22.44143	.000
Y	13.78397	5141.90306	13.78397	146.91152	.09382	.761
ZR	126.87929	86797.25639	126.87929	2479.92161	.05116	.822
NB	72.28685	426.43639	72.28685	12.18390	5.93298	.020
PB	55.54354	3830.18889	55.54354	109.43397	.50755	.481
ZN	249.94670	11572.67222	249.94670	330.64778	.75593	.391
CU	390.59586	293.92306	390.59586	8.39780	46.51168	.000
NI	1583.24688	138.58556	1583.24688	3.95959	399.85149	.000
CO	220.95064	1574.05639	220.95064	44.97304	4.91296	.033
CR	12266.19550	1149.67639	12266.19550	32.84790	373.42408	.000
V	14272.12613	1653.32306	14272.12613	47.23780	302.13358	.000
BA	67538.61189	4553646.86000	67538.61189	130104.19600	.51911	.476

C) COMPARISON OF PITTS HEAD TUFF AND TUFF 530 USING ONLY Zr AND Y

Multivariate Tests of Significance (S = 1, M = 0, N = 16)

Test Name	Value	Exact F	Hypoth. DF	Error DF	Sig. of F
Pillais	.00427	.07292	2.00	34.00	.930
Hotellings	.00427	.07292	2.00	34.00	.930
Wilks	.99573	.07292	2.00	34.00	.930
Roys	.00427				

Note.. F statistics are exact.

FIGURE 2.39

COMPARISON OF PITTS HEAD TUFF PROPER AND
?PITTS HEAD TUFF AT LLYN CWM Y FYNNON (TUFF 501)

A) Multivariate Tests of Significance (S = 1, M = 5 1/2, N = 13)

Test Name	Value	Exact F	Hypoth. DF	Error DF	Sig. of F
Pillais	.95707	48.01754	13.00	28.00	.000
Hotellings	22.29386	48.01754	13.00	28.00	.000
Wilks	.04293	48.01754	13.00	28.00	.000
Roys	.95707				

Note.. F statistics are exact.

B) Univariate F-tests with (1,40) D. F.

Variable	Hypoth. SS	Error SS	Hypoth. MS	Error MS	F	Sig. of F
RB	17340.36571	125332.06500	17340.36571	3133.30162	5.53422	.024
SR	58.87000	37994.01500	58.87000	949.85038	.06198	.805
Y	7551.66766	6252.95139	7551.66766	156.32378	48.30786	.000
ZR	193296.14480	107615.99139	193296.14480	2690.39978	71.84663	.000
NB	1.18766	464.69639	1.18766	11.61741	.10223	.751
PB	106.73016	4463.28889	106.73016	111.58222	.95652	.334
ZN	2598.43111	16026.74722	2598.43111	400.66868	6.48524	.015
CU	350.27147	1097.53139	350.27147	27.43828	12.76579	.001
NI	4.69587	146.47389	4.69587	3.66185	1.28238	.264
CO	2.78671	1578.12972	2.78671	39.45324	.07063	.792
CR	4.77813	1192.14472	4.77813	29.80362	.16032	.691
V	5.52099	1722.55806	5.52099	43.06395	.12820	.722
BA	454716.11571	4695203.28833	454716.11571	117380.08221	3.87388	.056

Chapter 3

FIGURE 3.1A: Granulometric classification of pyroclasts and of unimodal, well sorted, pyroclastic deposits. (after Schmid, 1981).

Clast size	Pyroclast	Pyroclastic deposit: Mainly unconsolidated: tephra	Pyroclastic deposit: Mainly consolidated pyroclastic rock
	Block, Bomb	Agglomerate, bed of blocks or bomb, block tephra	Agglomerate, pyroclastic breccia
64mm			
	Lapillus	Layer, bed of lapilli or lapilli tephra	Lapillistone
2mm			
	Coarse ash grain	Coarse ash	Coarse(ash) tuff
1/16mm			
	Fine ash grain (dust)	Fine ash (dust)	Fine (ash) tuff

Figure 3.1B: Subdivision of ashes and tuffs according to their fragmental composition.

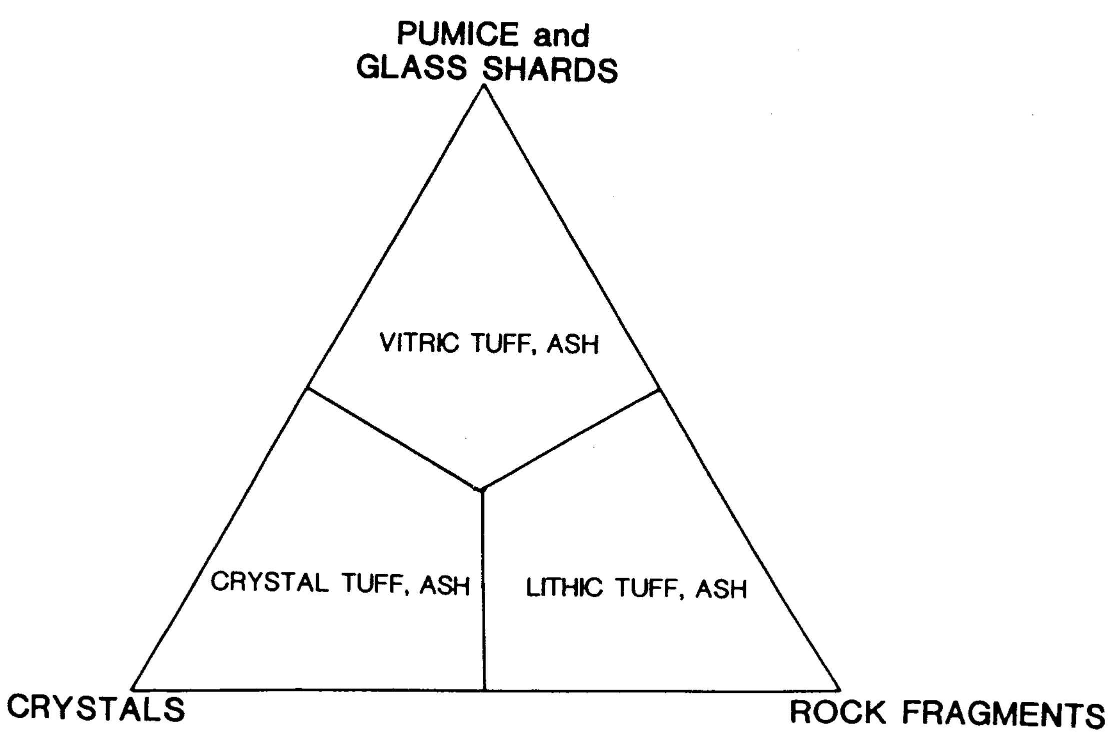

Figure 3.2a: Terms for mixed pyroclastic-epiclastic rocks.
(after Schmid, 1981).

Pyroclastic	Tuffites (mixed pyroclastic-epiclastic)	Epiclastic (volcanic and/or nonvolcanic)	Average clast size (mm)
Agglomerate, pyroclastic breccia	Tuffaceous conglomerate/breccia	Conglomerate, Breccia	64
Lapillistone			
Tuff coarse	Tuffaceous sandstone	Sandstone	2
fine	Tuffaceous siltstone	Siltstone	1/16
	Tuffaceous mudstone	Mudstone, Shale	1/256
100%	75%	25%	0% by volume

(increase)
--------------------------Pyroclasts--------------------------------

(increase) Volcanic + nonvolcanic epiclasts
-------------------------- (+ minor amounts of biogenic, chemical sedimentary and authigenic constituents)

Fig. 3.2B View of typical well bedded "tuffite" horizon consisting of white-weathering beds with a higher pyroclastic component alternating with thinner beds rich in epiclastic material. Notebook 16cm long for scale. (Cowlyd 1 tuff, section H1, 10-30m, SH 7160 6131.

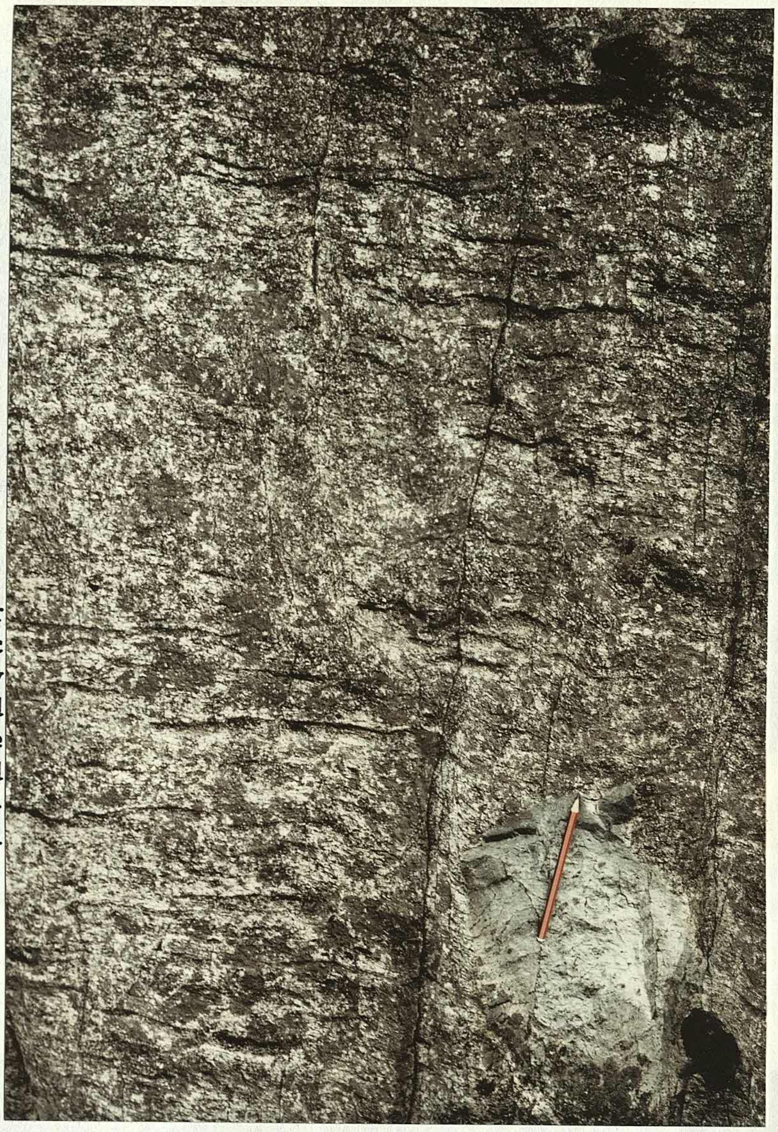

Fig. 3.3 Planar eutaxitic fabric exhibited by flattened chloritic fiamme within Pitts Head Tuff, Pont-y-Gromlech, SH 6301 5652 PH

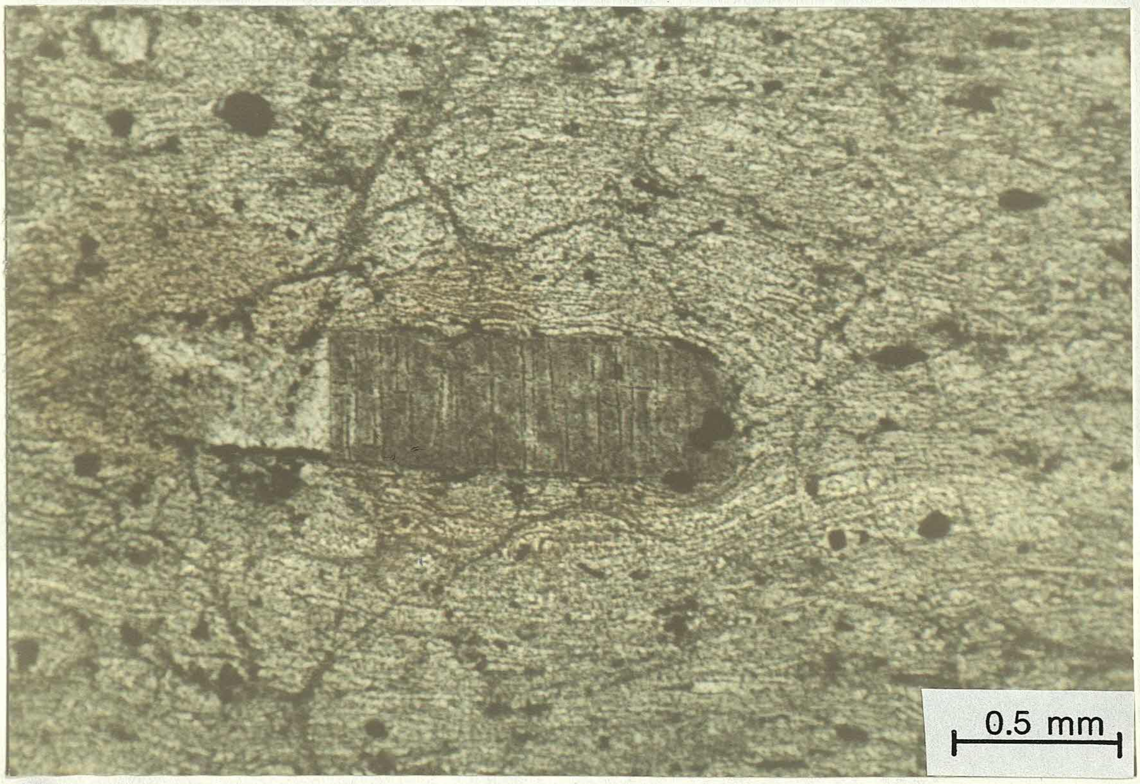

Fig. 3.4 Well developed parataxitic texture with aligned plagioclase crystal. Sample C44, 1st member of Capel Curig Volcanic Formation, Tryfan, SH 667 598. PPL.

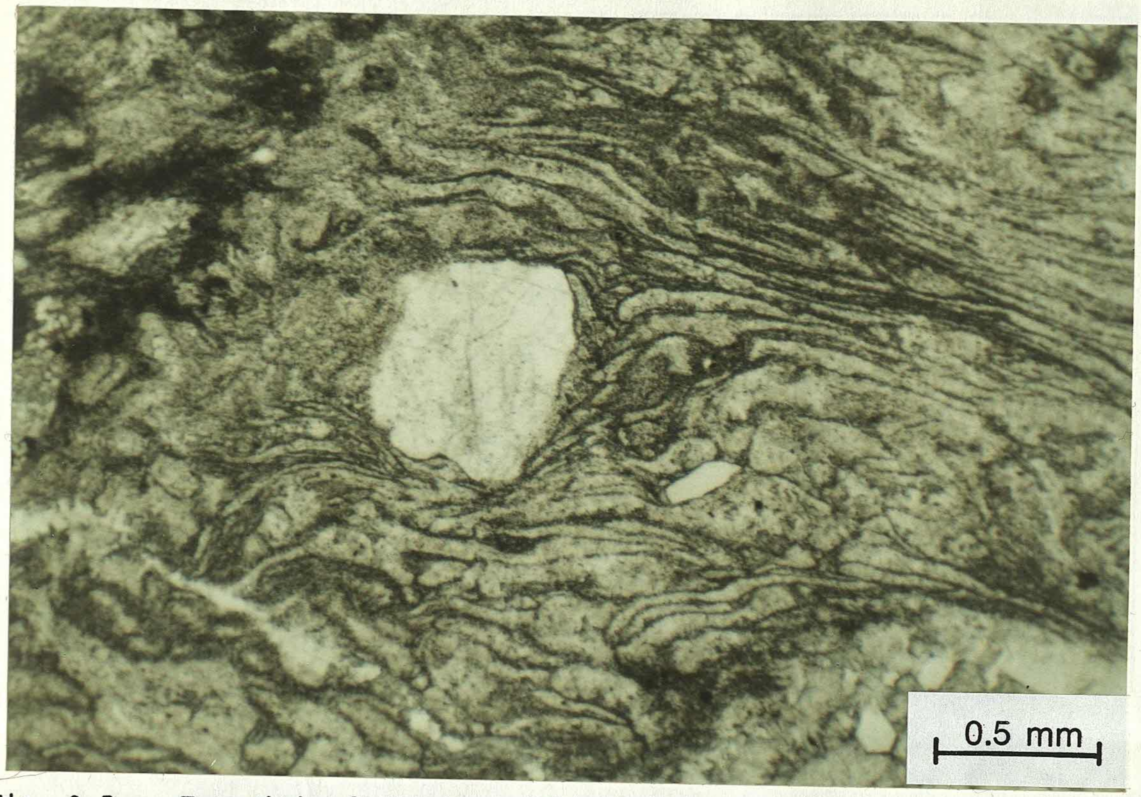

Fig. 3.5 Eutaxitic foliation within middle of Garth tuff, 28 m from base of flow. (sample G06, Capel Curig anticline, SH 7062 5770). PPL.

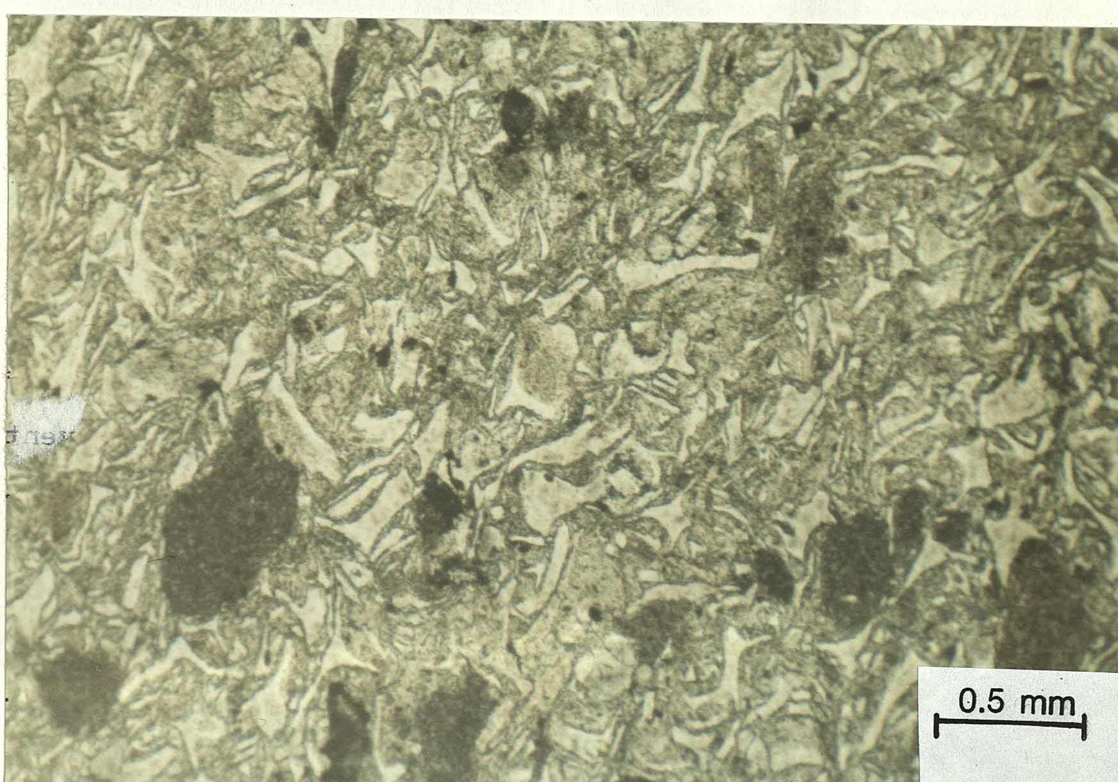

Fig. 3.6 Non-welded vitroclastic texture within top portion of Garth tuff showing slender cuspate glass shards and occasional epiclastic fragments of mudstone. (Sample G07, SH7062 5769). PPL.

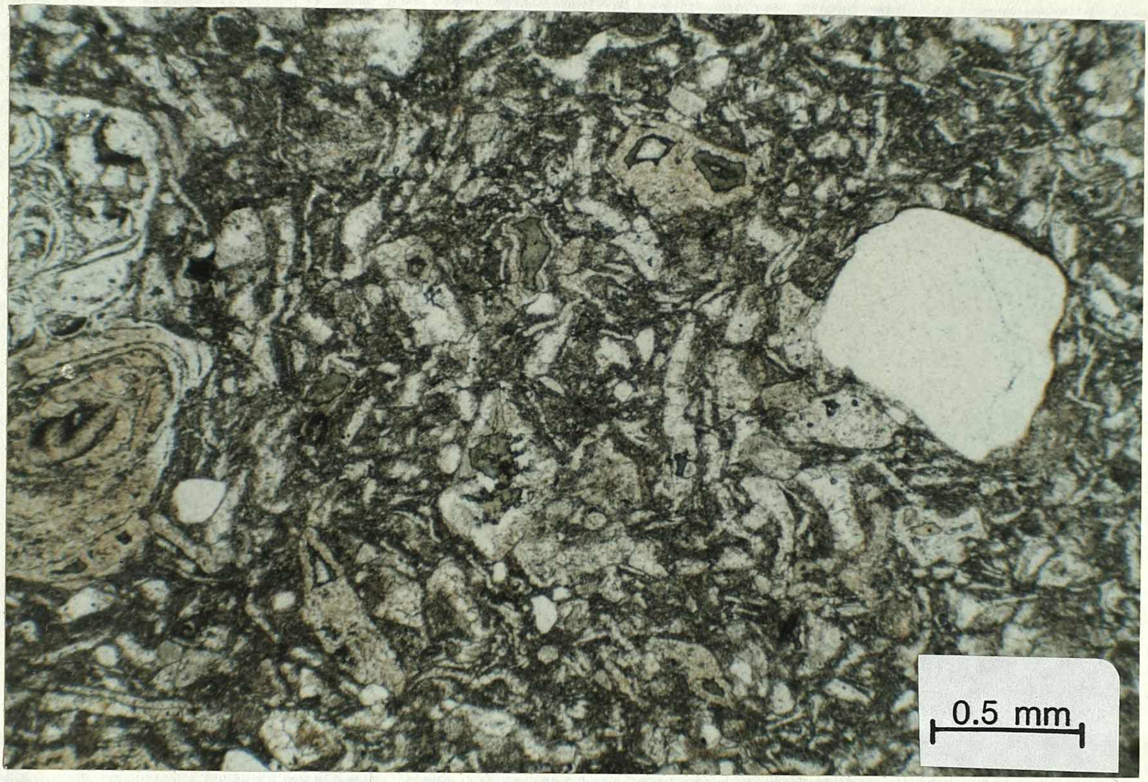

FIG. 3.7A Non-welded vitroclastic texture within reworked pyroclastic deposits from top of Garth tuff. Angular glass shards (devitrified to microcrystalline quartz), an unstrained monocrystalline quartz grain (Qm), and large glass fragment showing perlitic fracture are set in fine-grained quartz-sericite matrix. (Sample A5A, section A1, 33m, Capel Curig anticline). Plane polarised light.

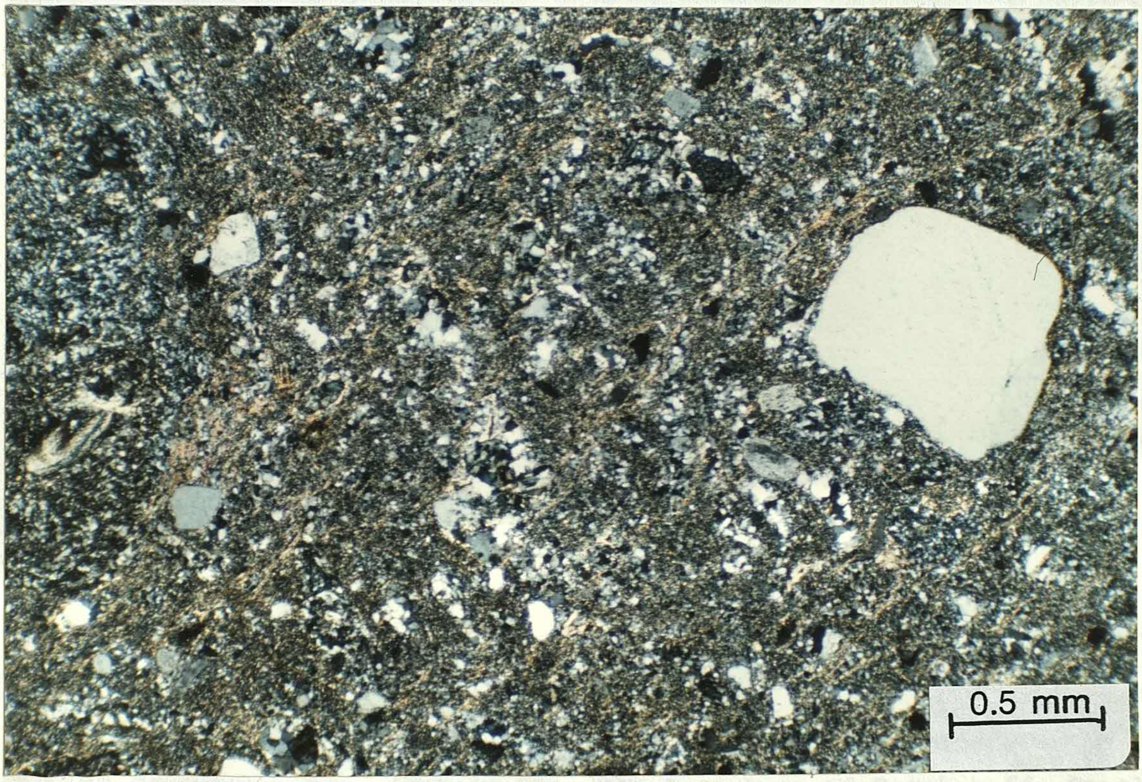

FIG. 3.7B As above in cross-polarised light.

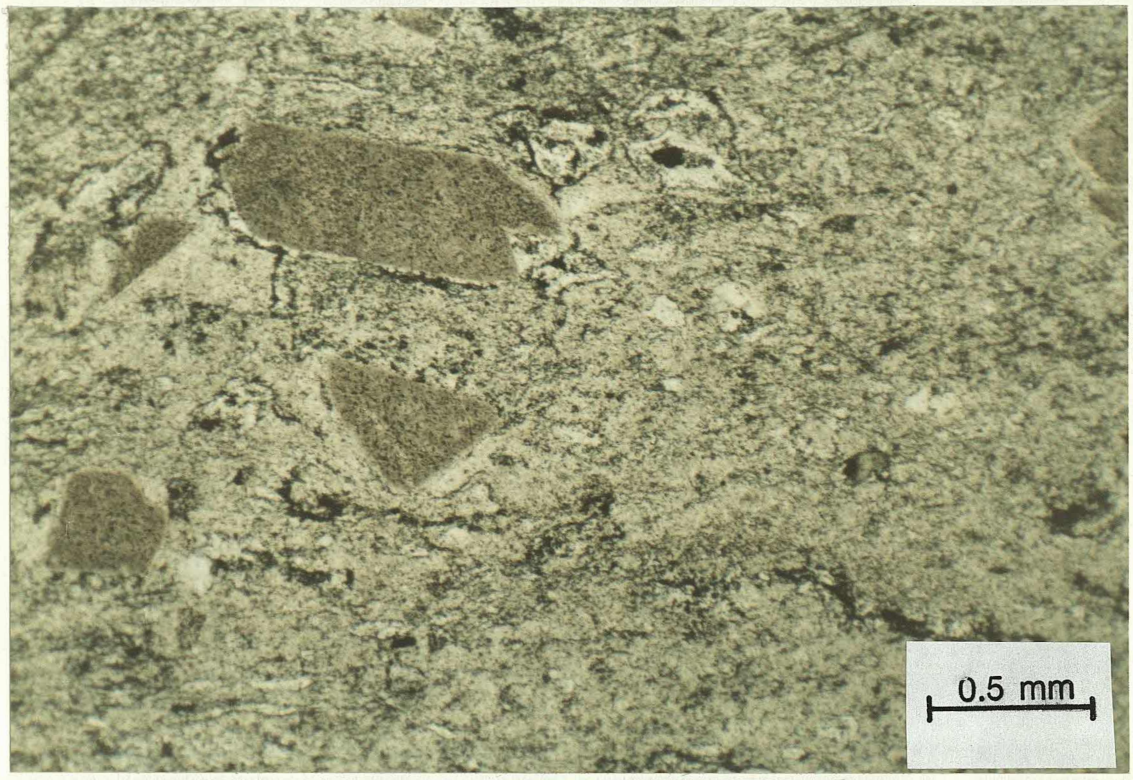

FIG. 3.8 Devitrified and recrystallized rhyolitic ash flow tuff. Subhedral to euhedral K-feldspar crystals and ghost fabric of poorly developed welding are only signs of original pyroclastic and volcanic origin. (Sample G01, 18m from base of Garth tuff, Capel Curig anticline). PPL.

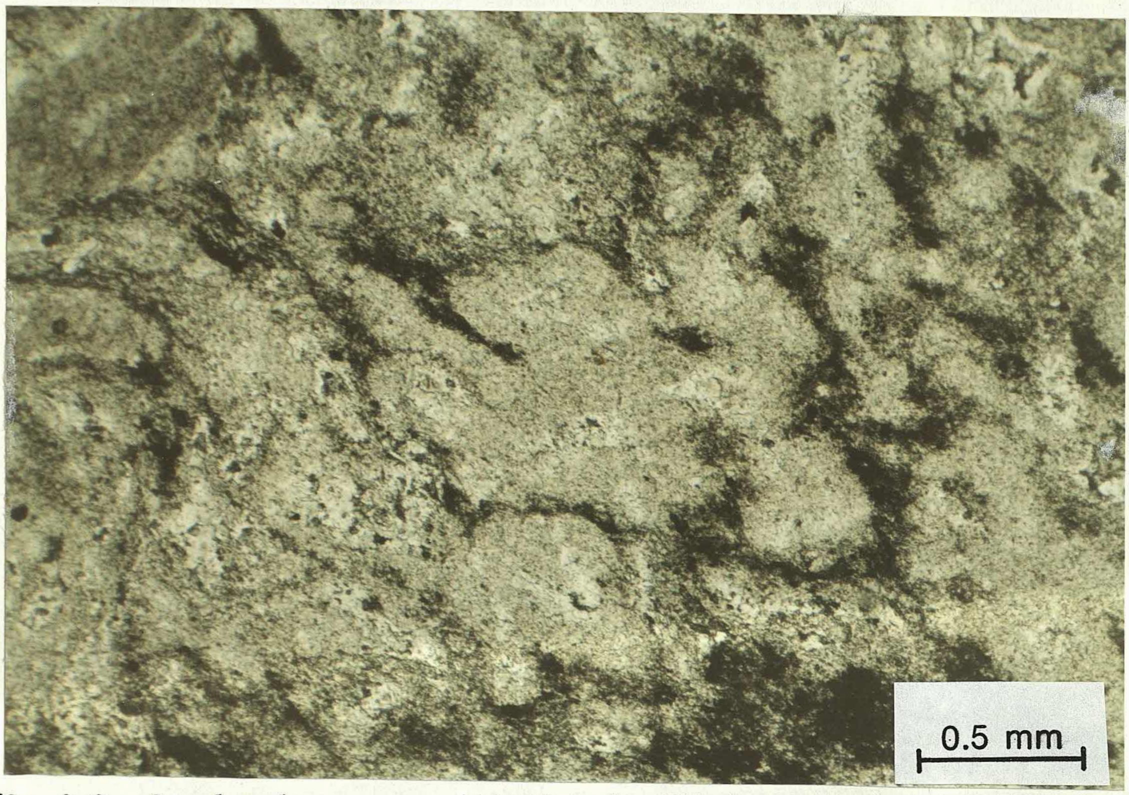

FIG. 3.9 Completely recrystallized and silicified rhyolitic ash flow tuff. Texture is optically indistinguishable from either biogenic or chemically precipitated chert in either plane polarised light or with crossed-polars. (Sample G06, 28m from base of Garth tuff, Capel Curig anticline, SH 7062 5770). XPL.

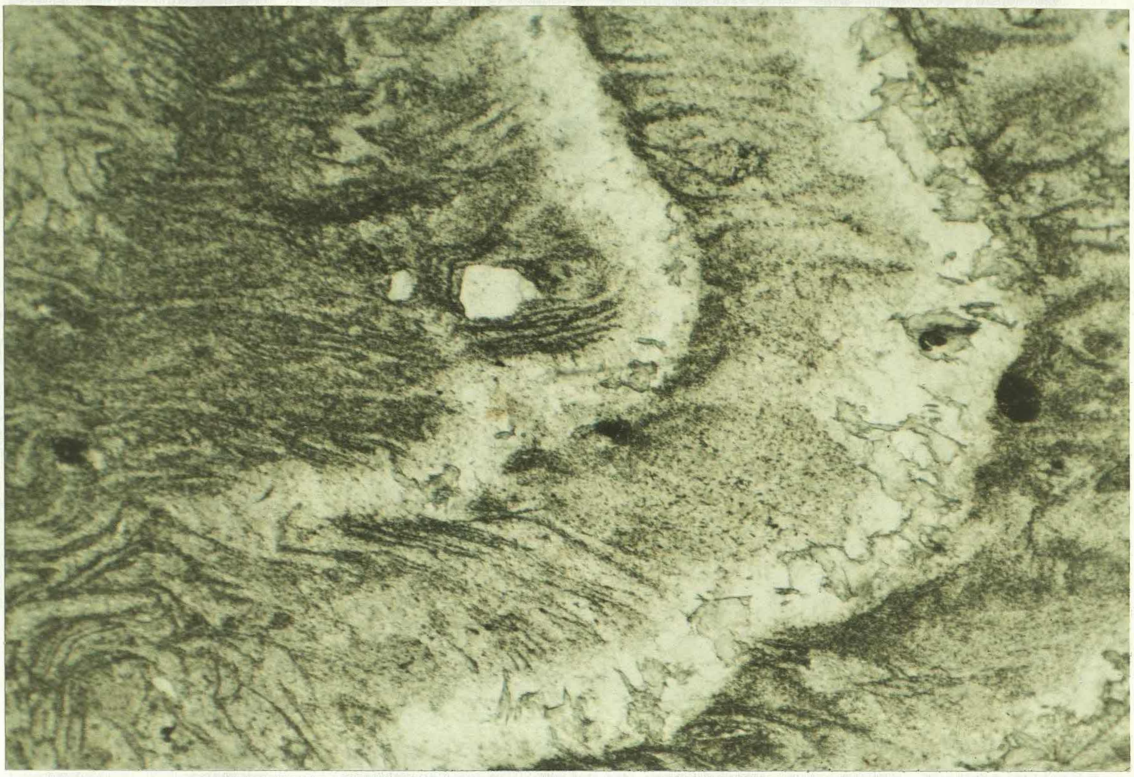

Fig. 3.10 Texture within siliceous nodule from middle of Garth Tuff. Silicification has resulted in both accentuation and destruction of welding fabric. (Sample G06, Capel Curig anticline, SH 7062 5770). PPL.

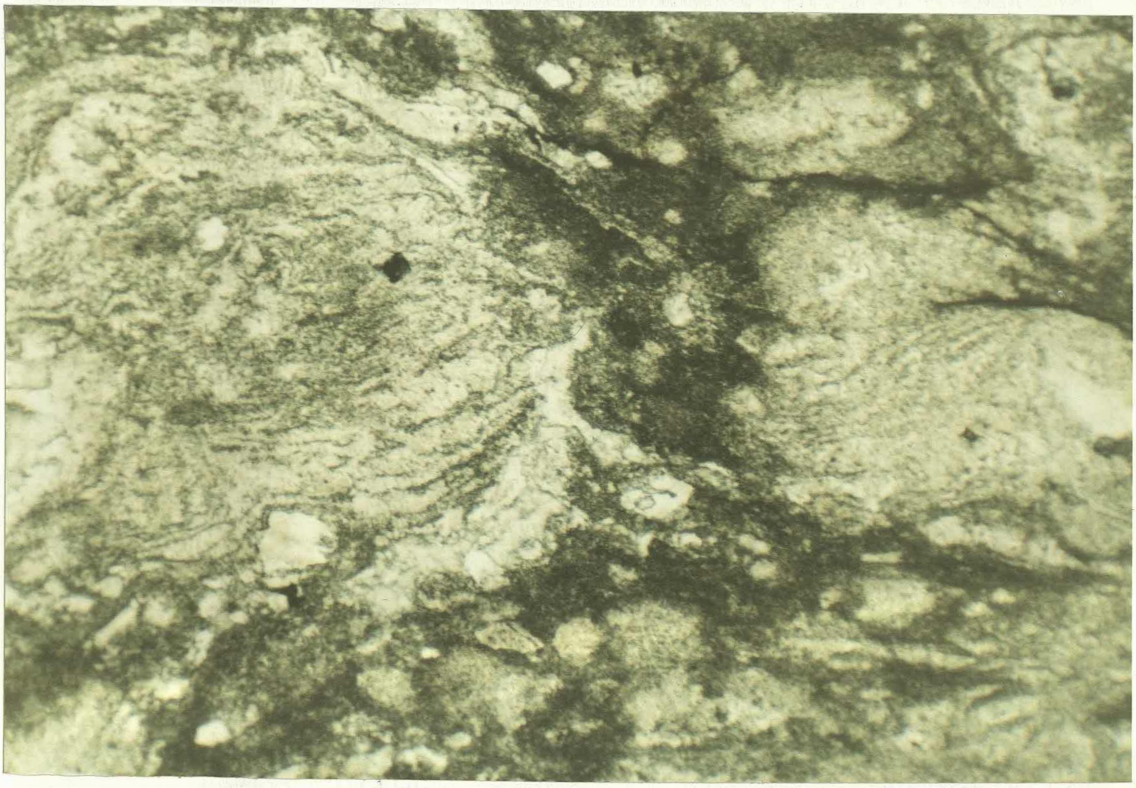

Fig. 3.11 Accentuation of welding fabric within siliceous nodule with depletion of silica between nodules. (Sample G06, Garth tuff, Capel Curig anticline, SH 7062 5770). PPL.

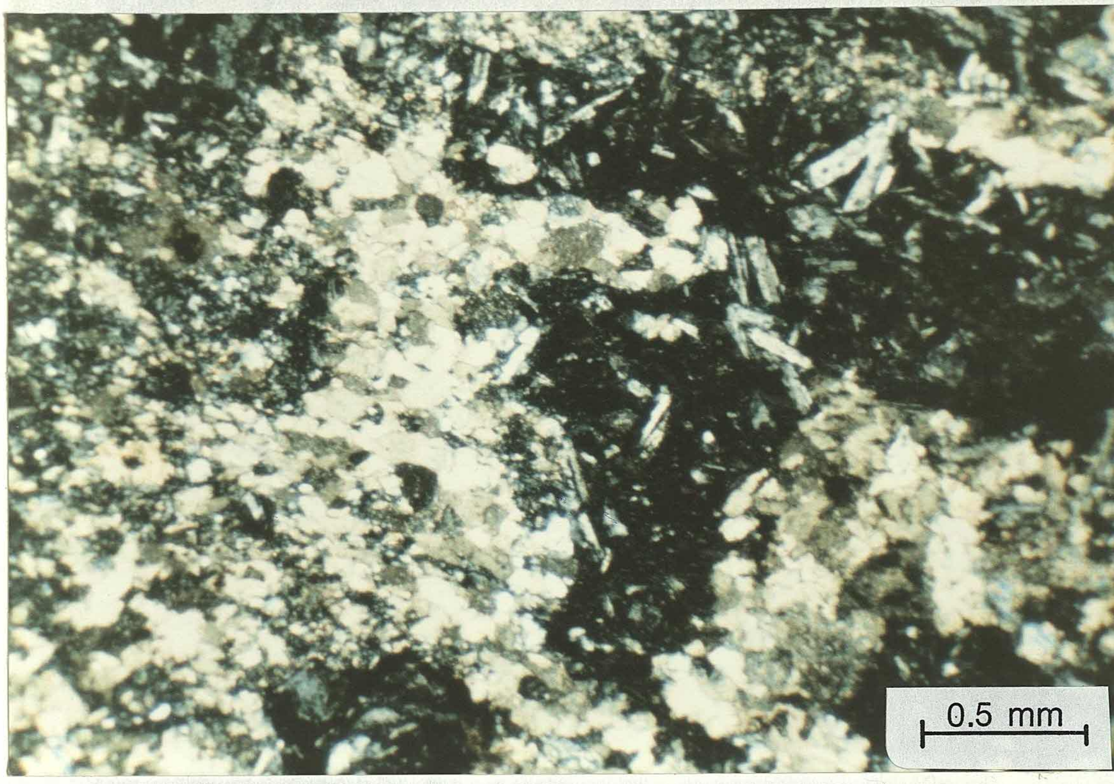

FIG. 3.12 Basaltic hyaloclastite. Felted texture of tiny plagioclase laths within chloritised basalt fragment. Surrounded by authigenic calcite and ?epidote. No evidence in thin section of pyroclastic origin. Sample D74,
GRIBIN RIDGE.

FIG. 3.13 Massive crystal and lithic-rich debris flow, 4th member of Capel Curig Volcanic Fm. Section A2, 148.1m. PH583.

FIG. 3.14: Quartzose vitric- and crystal-rich pyroclastics from barrier island deposits overlying Garth tuff. Trough cross-bedding reflects shoaling nearshore waves; vertically aggrading wave ripples (top of photo) indicate an abundant supply of loose sediment. Continued reworking on a coastline with high wave energy such as this, progressively enriches the crystal concentrations inherited from subjacent ash flow. Section A1, 43m, top of Garth tuff, Capel Curig anticline.

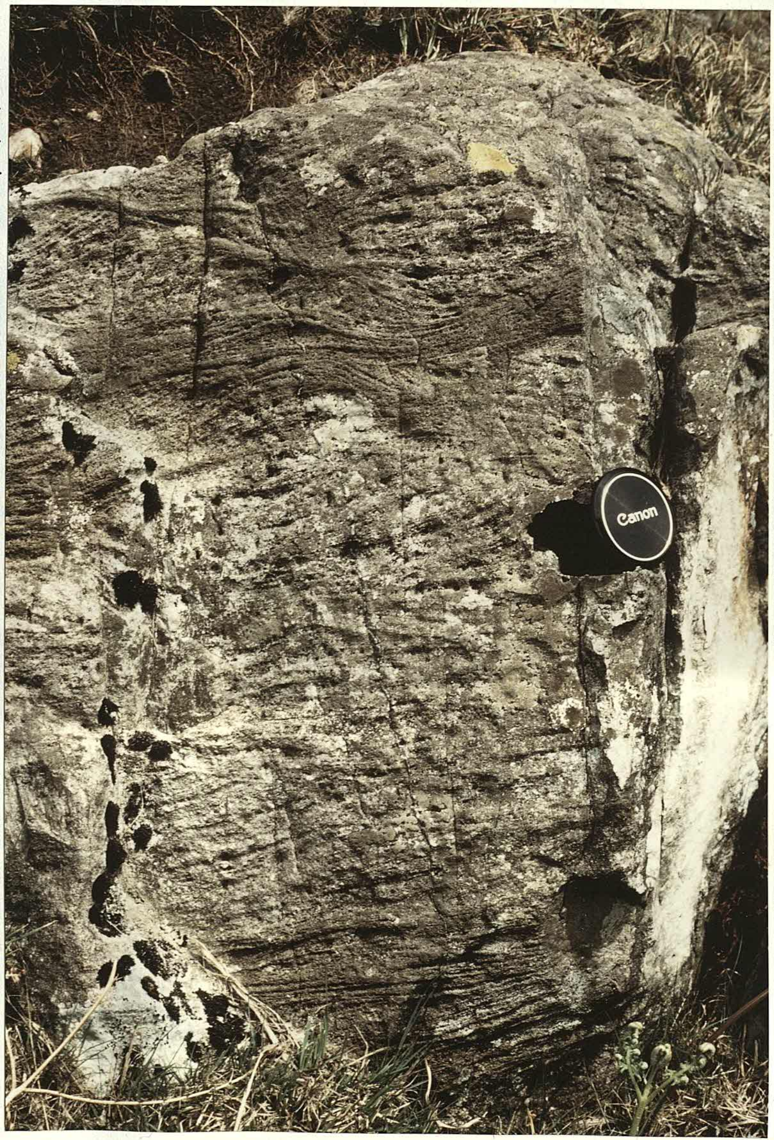

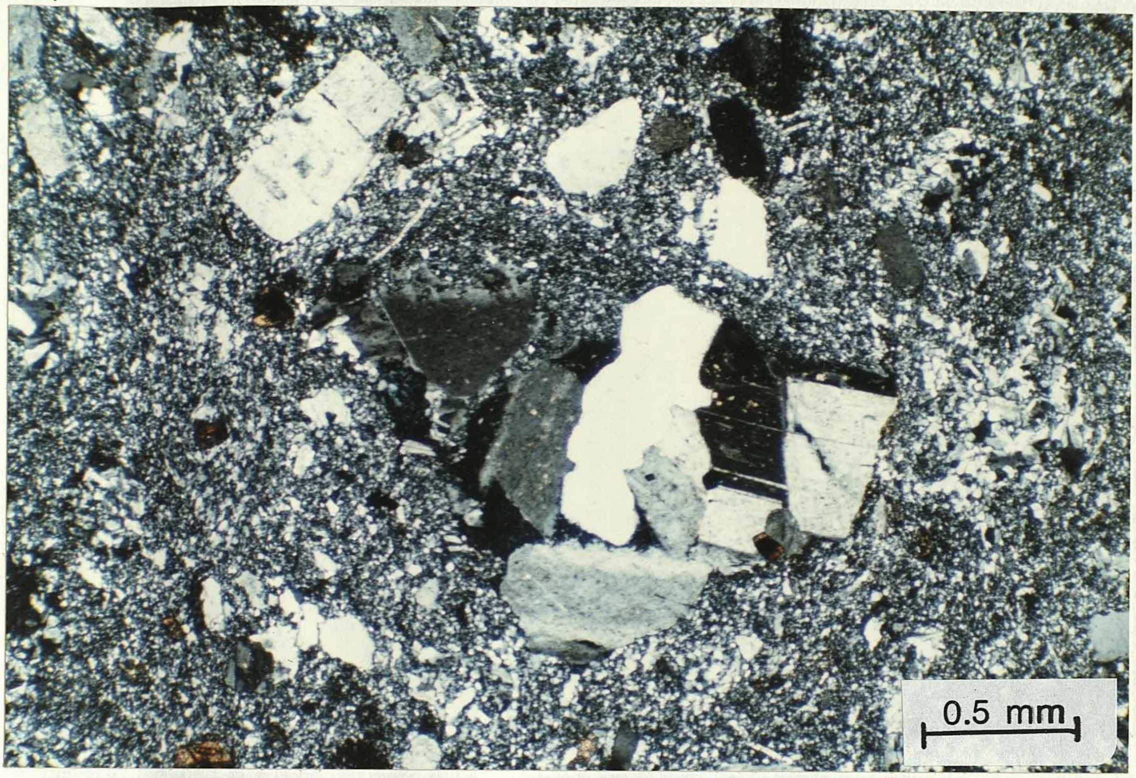

FIG. 3.15: Cluster of plagioclase and quartz crystals set in fine-grained felsitic groundmass from vitroclastic ash flow tuff, 4th member of Capel Curig Volcanic Formation, Gallt yr Ogof. Sample X8, section C12, 41m. XPL.

FIG. 3.16: Crystal-rich ash from 2-3 metre debris flow within 4th member of CCVF. Euhedral phenocrysts of dominantly plagioclase with rounded quartz crystals set in an over-exposed matrix of microcrystalline quartz. Sample A71, section A2, 154m, Capel Curig anticline. XPL.

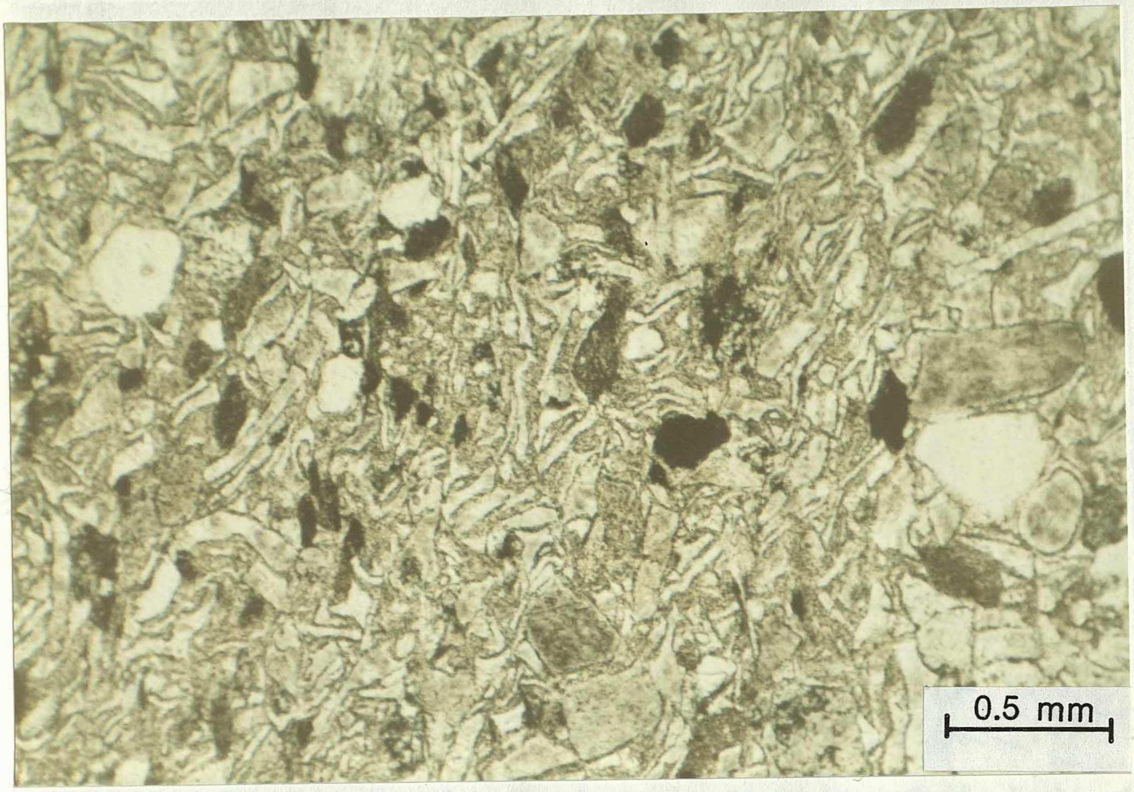

FIG. 3.17: Reworked pyroclastics overlying Garth tuff. Shards are more angular in shape than those from within ash flow tuff proper. Slight enrichment in crystal/lithic content to ≈ 30% from wave sorting. See Fig. 3.14 for sedimentary structures found at sampling location. Sample A9A, section A1, 44m. PPL.

FIG. 3.18: Tuffaceous sandstone from transgressive shoreface deposits approximately 20m above the Garth tuff. Crystal content (primarily quartz) and lithic concentration (lithified tuff fragments appearing as sericitic chert) have been enriched as the expense of glass shards. Sample A51, section A2, 28m. PPL.

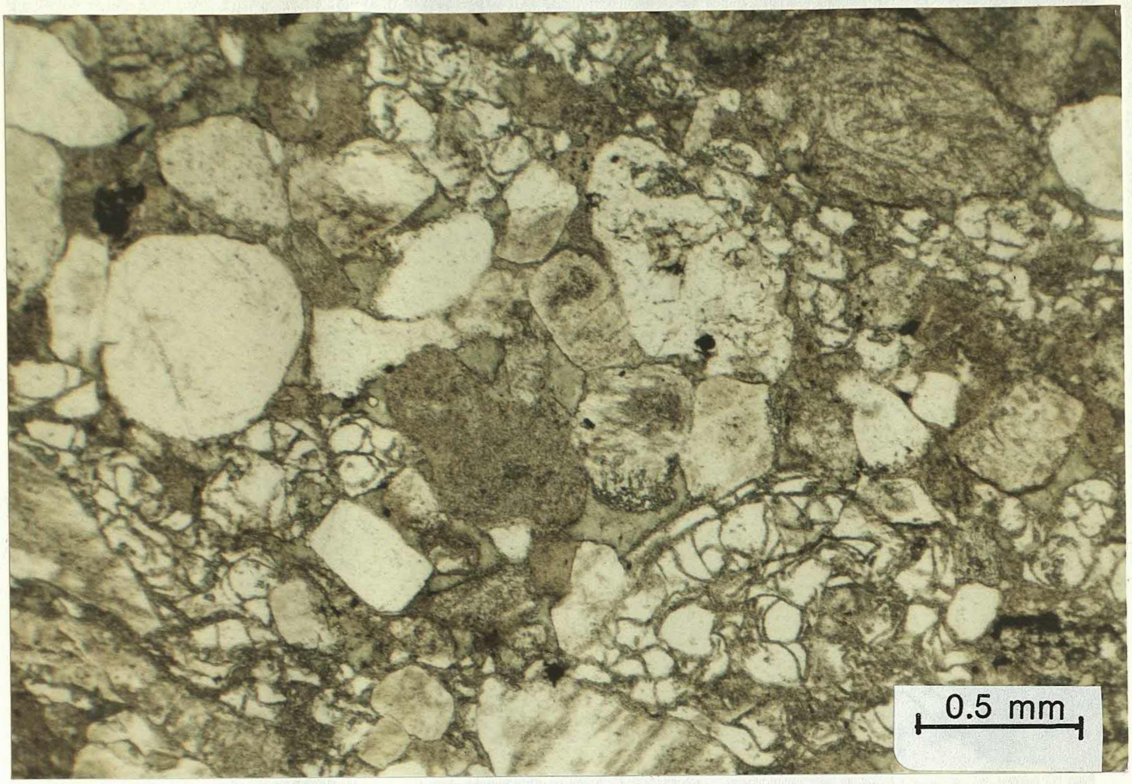

FIG. 3.19: Reworked deposits 5m above the Pitts Head Tuff, Bochlwyd ridge. Fragments of perlitically fractured glass, welded tuff, tuffaceous siltstone and large quartz crystals are set in a chloritic matrix. Sample D27, section D1, 145m. PPL.

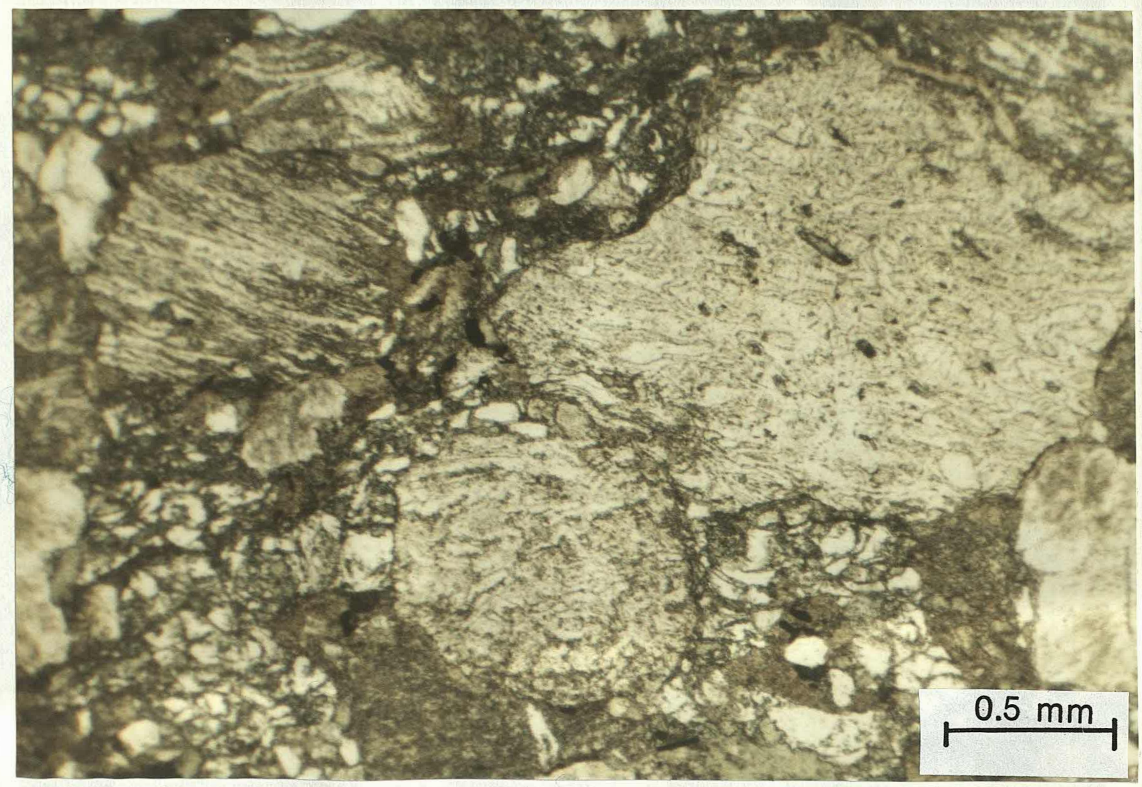

FIG. 3.20: Reworked Pitts Head tuff. Fragments of welded tuff within clay-rich matrix containing angular quartz crystals. Sample D27, section D1, 145m, PPL.

FIG. 3.21A: Trough-crossbedded rhyolitic sand-grade volcanic ash and discontinuous fine-grained ash fall horizons within Vuggy Mbr. of Ddeugwm Formation. Section C2, 19-21m. Tryfan anticline.

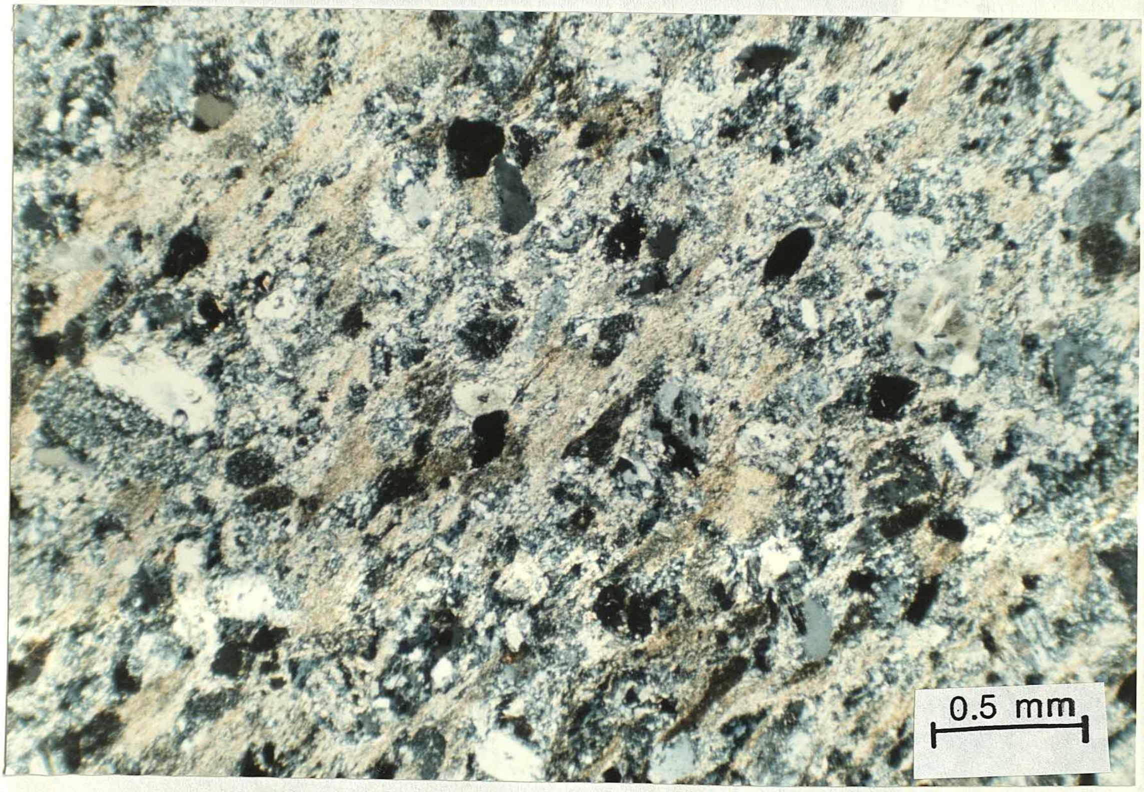

FIG. 3.21B: Complete replacement of glass shards within Vuggy Mbr. by a quartz-sericite aggregate with no hint of original pyroclastic textures. Sample C34, section C2, 18m. PPL.

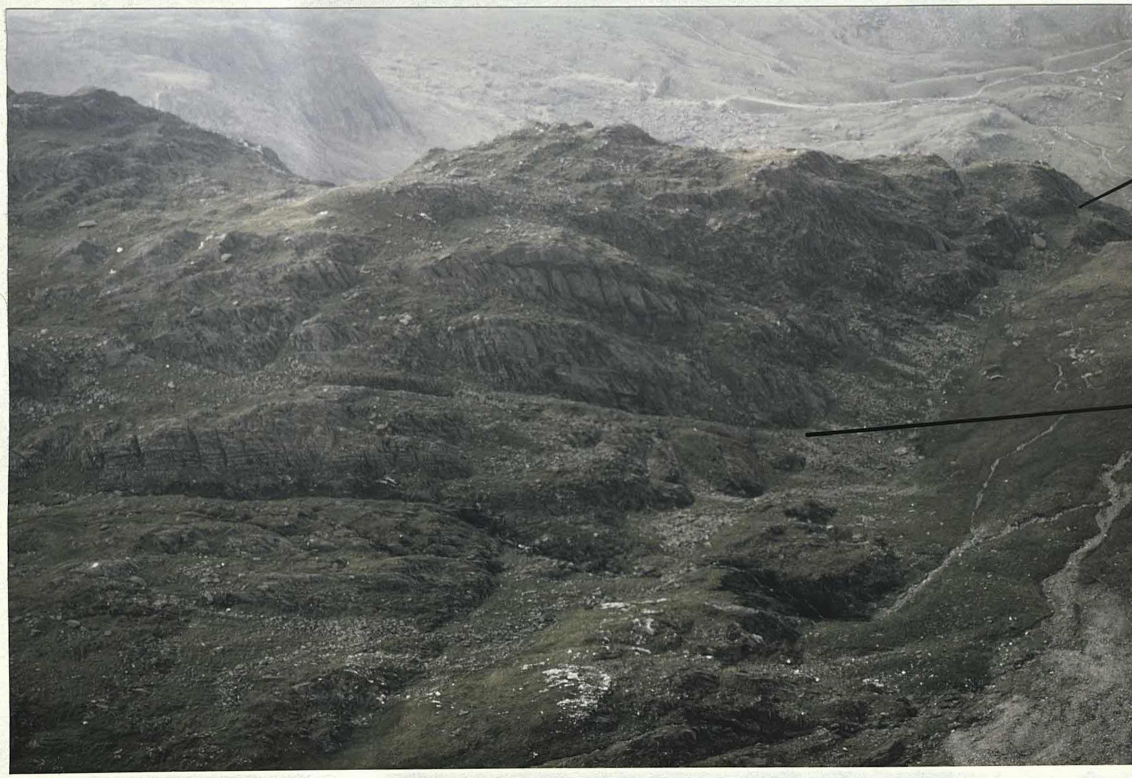

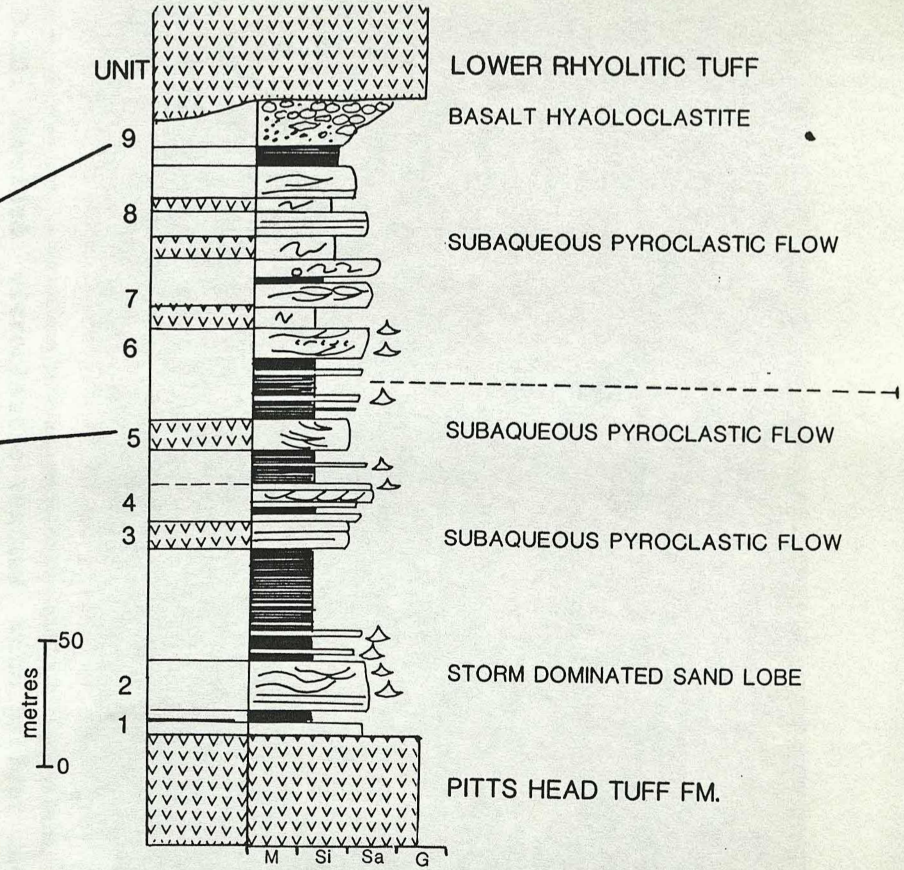

FIG. 3.22: View of type section of UPPER CWM EIGIAU FM. showing prevalence of white-weathering tuffites within depositional succession.

FIG. 3.23: Unwelded vitroclastic texture, with perfect cuspate shards, from subaqueous normally graded ash flow tuff bed on Gribin ridge. Tuff bed (70cm thick) represents one of a series of similar sediment gravity flows within a 15 m thick "tuffite" horizon. Sample D44A, Section D1, 257m. Gribin ridge. PPL.

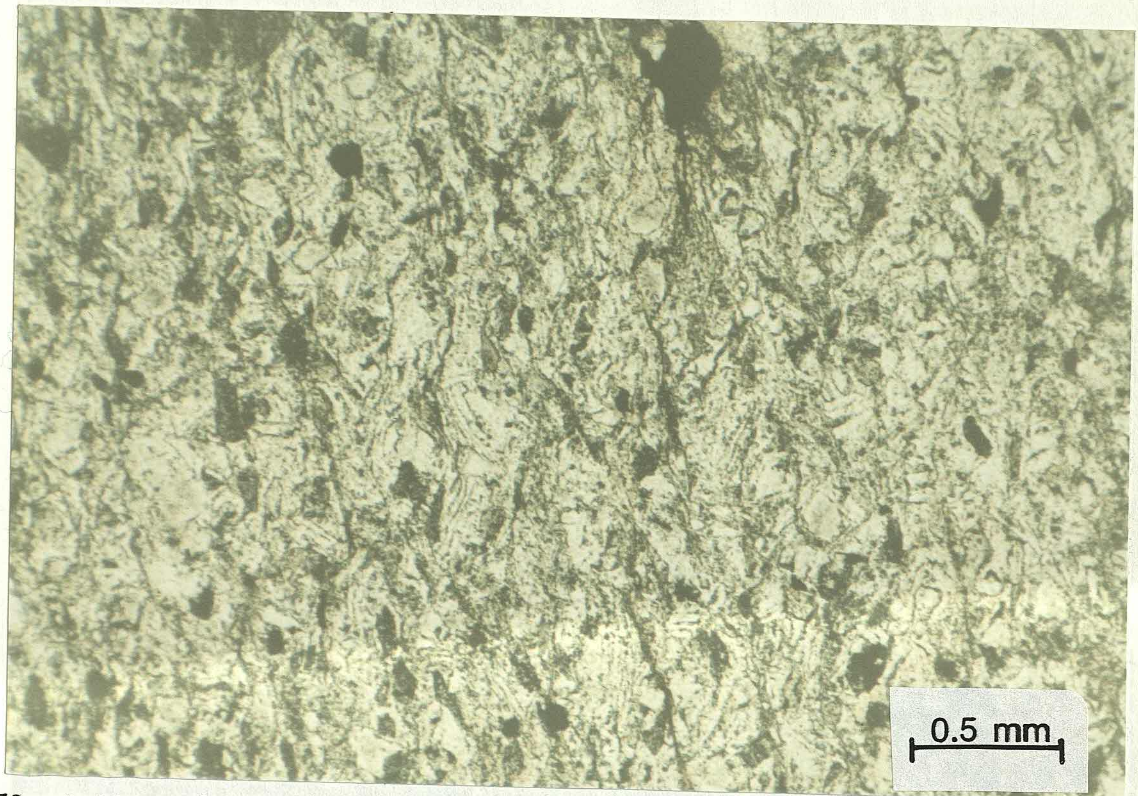

FIG. 3.24: Fine-grained silty volcanic ash. Unwelded glass shards and skeletal ?magnetite crystals are visible. Fabric observed is tectonic in origin. Sample D75, section D2, 113.7m, Cwm Cneifion. See Fig. 3.22 for location.

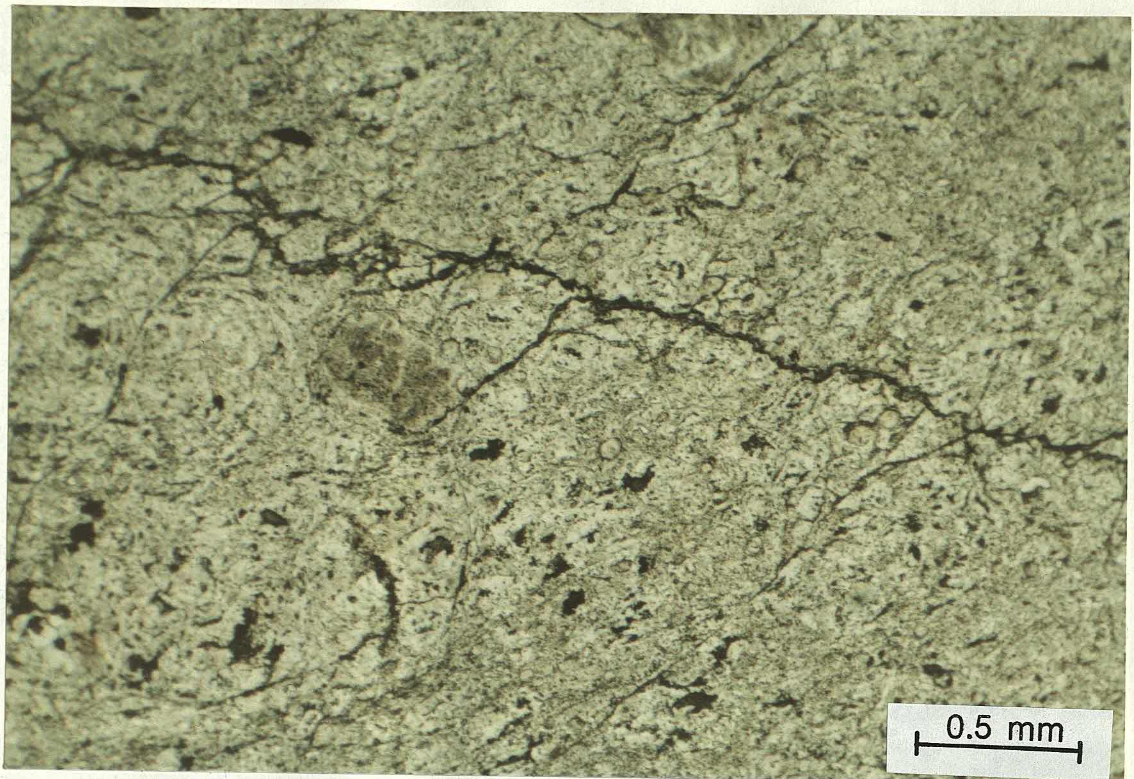

FIG: 3.25A: Small unwelded glass shards within unwelded subaqueous ash flow tuff at Bwlch Trimarchog (SH 710 626) Partial recrystallization associated with devitrification has hidden most shard texture. Sample G0130, F3 tuff, section F3, 68m. PPL.

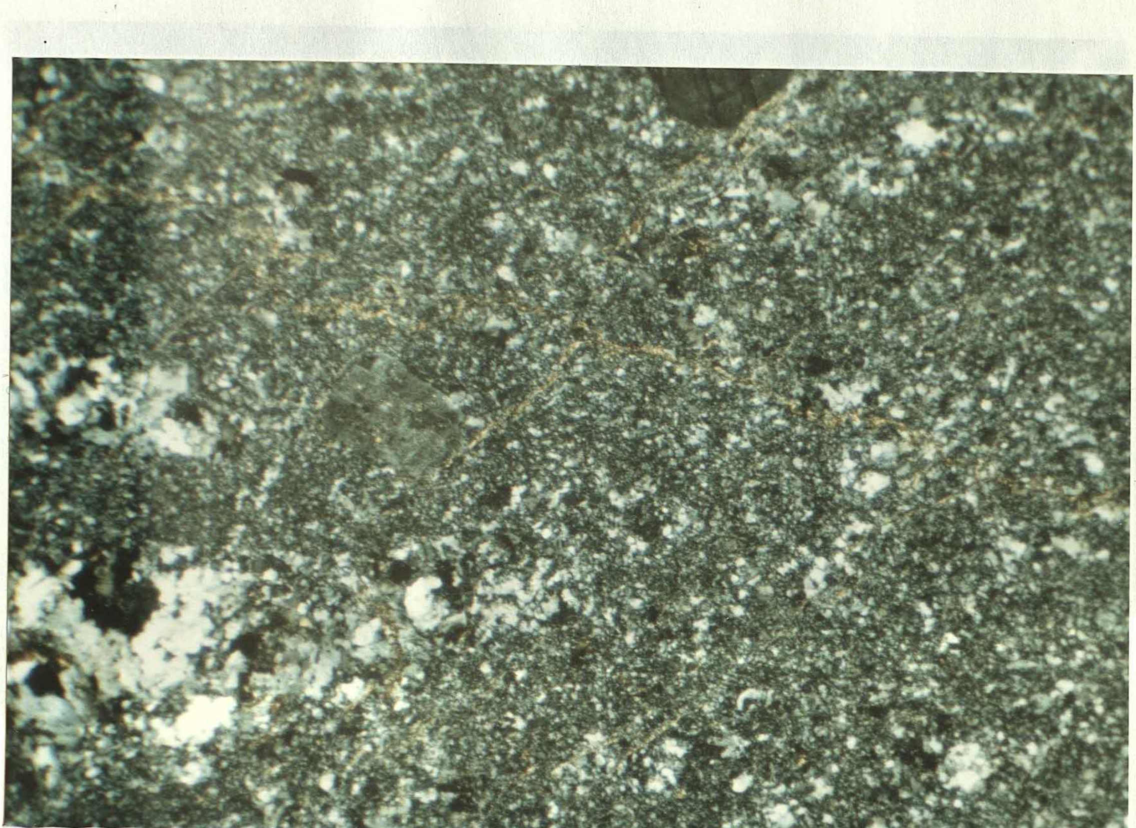

FIG. 3.25B: As above but crossed-polars. Note similarity of texture to chemically precipitated chert.

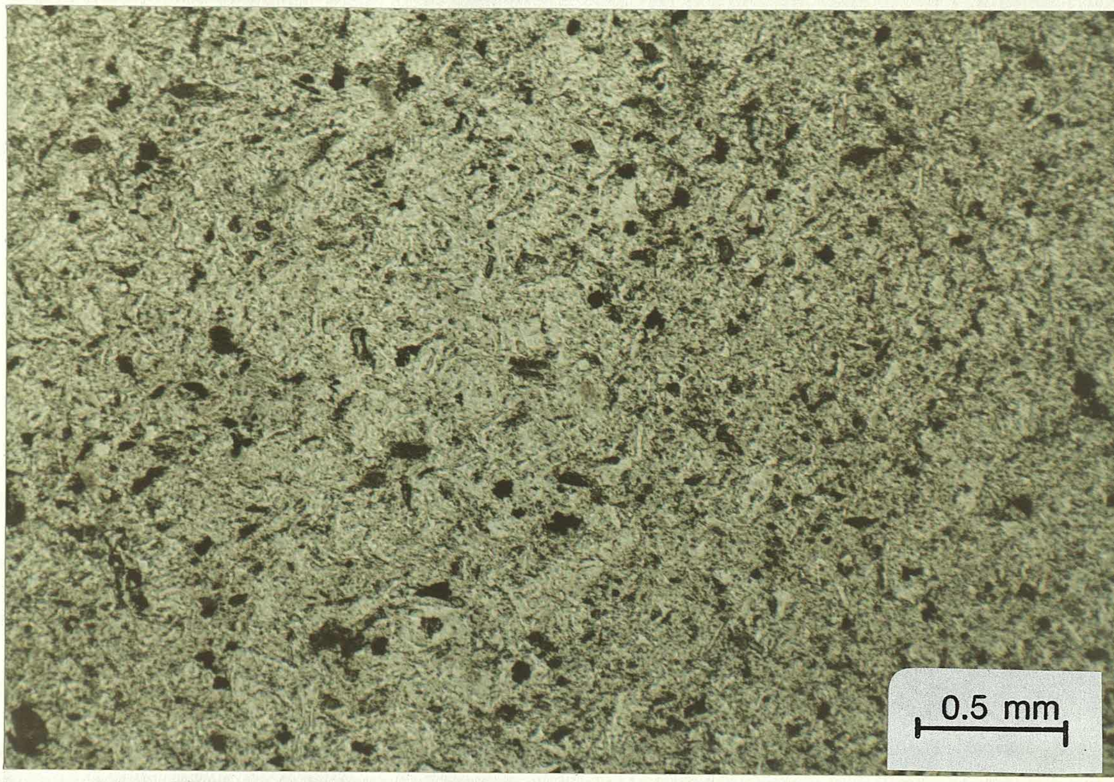

FIG. 3.26: Extremely fine grained volcanic ash from G6 tuff with minute glass shards and magnetite crystals. Sample G051. section H3, 54m, LLyn Cowlyd.

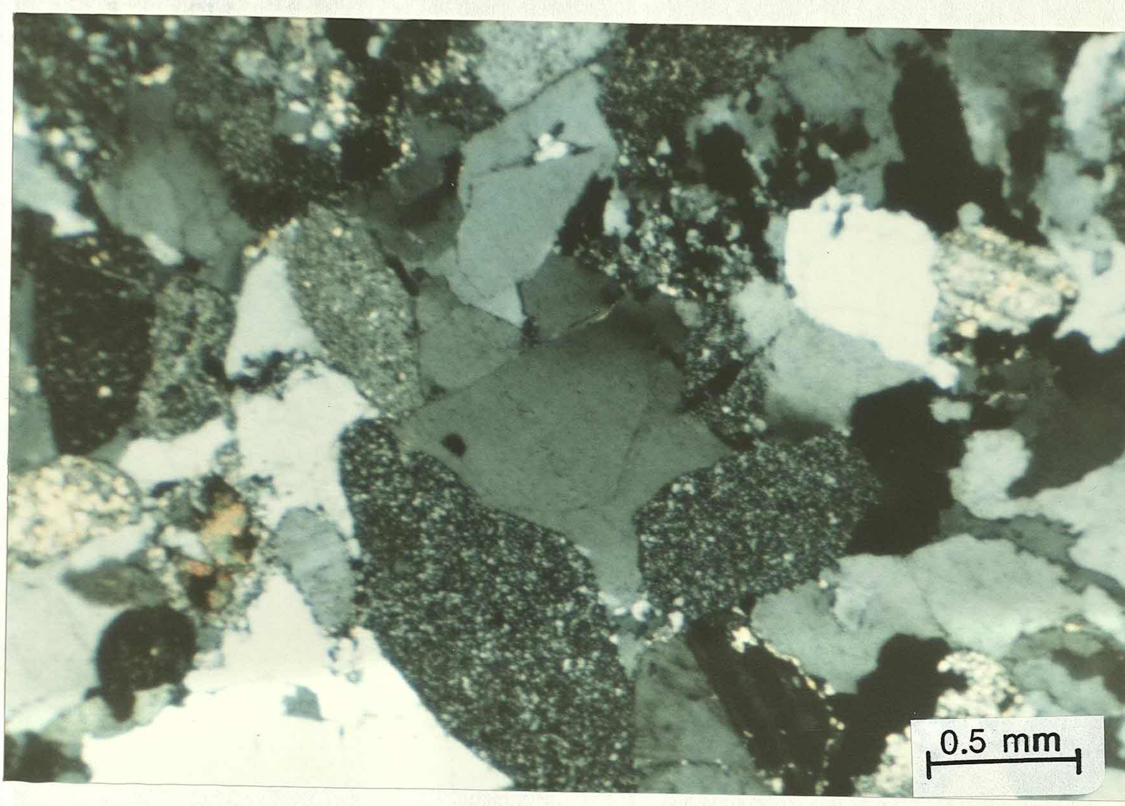

FIG. 3.27: Volcaniclastic sandstone containing nondescript "chert" and sericitic "chert" (SCHT) fragments which probably represent rhyolitic volcanic rocks. Sample S10B, section S3, 25.5m, Upper Cwm Eigiau Formation, Tal-y-fan. XPL.

OBS	REGION	SAMPLE	SECTION LOCATION	STRATIGRAPHIC UNIT	ENVIRONMENT	GRAIN SIZE	SORTING	Q F R RATIO	SANDSTONE TYPE (Okada,1971)
1	1	C34	C2 18m	Tuffite Mbr.	shallow mar.	med. ss	moderate	62:16:23	lithic arenite
2	1	C34	C2 18m	Tuffite Mbr.	shallow mar.	med. ss	moderate	43:9:47	lithic arenite
3	2	C46	C2 79m	lower Gwern Gof Mbr.	delta	med. ss	moderate	60:16:23	lithic arenite
4	2	C54	C2 123m	lower Gwern Gof Mbr.	distr. chann.	med. ss	moderate	73:23:4	feldspathic aren.
5	2	C60	C2 128m	lower Gwern Gof Mbr.	distr. chann.	med. ss	poor	54:15:30	lithic arenite
6	2	C64	C2 130.5m	lower Gwern Gof Mbr.	distr. chann.	med. ss	poor	63:19:17	feldspathic aren.
7	2	C65	C2 137m	lower Gwern Gof Mbr.	shoreface	med. ss	poor	53:21:26	lithic arenite
8	2	C66	C2 140m	lower Gwern Gof Mbr.	shoreface	med. ss	poor	57:23:20	feldspathic aren.
9	2	C67	C2 145m	upper Gwern Gof Mbr.	shallow mar.	med. ss	poor	57:16:27	lithic arenite
10	2	C69	C2 168m	upper Gwern Gof Mbr.	delta	coarse ss	very poor	32:16:52	lithic arenite
11	3	S2	S1	Llewelyn Volc. Group	alluvial fan	coarse ss	very poor	79:5:16	quartzose arenite
12	3	S6	S2 27m	Llewelyn Volc. Group	alluvial fan	v. coarse ss	very poor	66:6:28	lithic arenite
13	4	C56	C7 15.36m	Tryfan Fach Mbr.	braidplain	coarse ss	moderate	19:51:30	feldspathic aren.
14	4	C8	C1 111m	Tryfan Fach Mbr.	braidplain	granule cg.	very poor	24:24:52	lithic arenite
15	4	F10A	F1c 47m	Tryfan Fach Mbr.	alluvial fan	granule cg.	very poor	48:6:46	lithic arenite
16	4	F10B	F1c 47m	Tryfan Fach Mbr.	alluvial fan	granule cg.	very poor	34:3:63	lithic arenite
17	4	F7	F1c 22.45m	Tryfan Fach Mbr.	alluvial fan	coarse ss	very poor	59:11:30	lithic arenite
18	4	F8	F1c 28.65m	Tryfan Fach Mbr.	alluvial fan	v. coarse ss	very poor	52:12:35	lithic arenite
19	4	F9	F1c 37.35m	Tryfan Fach Mbr.	alluvial fan	coarse ss	poor	36:6:58	lithic arenite
20	5	C10	C1 154m	Magnetite Mbr.	braidplain	granule cg.	very poor	18:18:64	lithic arenite
21	5	C12	C1 160m	Magnetite Mbr.	braidplain	coarse ss	poor	46:4:50	lithic arenite
22	5	C13	C1 164.5m	Magnetite Mbr.	braidplain	v. coarse ss	very poor	12:57:31	feldspathic aren.
23	5	C14	C1 165m	Magnetite Mbr.	braidplain	med. ss	poor	40:18:43	lithic arenite
24	5	C15A	C1 167m	Magnetite Mbr.	braidplain	granule cg.	very poor	22:20:58	lithic arenite
25	5	C15B	C1 167m	Magnetite Mbr.	braidplain	granule cg.	very poor	17:25:58	lithic arenite
26	6	B30	B4 3m	Capel Curig Mbr.	shoreface	v. coarse ss	poor	56:29:15	feldspathic aren.
27	6	B32	B4 5m	Capel Curig Mbr.	shoreface	v. coarse ss	poor	53:20:27	lithic arenite
28	6	B33	B4 6.7m	Capel Curig Mbr.	shoreface	v. coarse ss	poor	65:22:12	feldspathic aren.
29	6	B33r	B4 6.7m	Capel Curig Mbr.	shoreface	v. coarse ss	very poor	71:24:5	feldspathic aren.
30	6	B34	B4 7m	Capel Curig Mbr.	shoreface	v. coarse ss	very poor	48:29:23	feldspathic aren.
31	6	B37	B4 13m	Capel Curig Mbr.	shoreface	granule cg.	very poor	51:19:30	lithic arenite
32	6	B38	B4 18m	Capel Curig Mbr.	shoreface	coarse ss	very poor	58:7:35	lithic arenite
33	6	B39	B4 28m	Capel Curig Mbr.	distr. chann.	v. coarse ss	poor	64:23:13	feldspathic aren.
34	6	C17	C1 223m	Capel Curig Mbr.	braidplain	coarse ss	very poor	48:35:17	feldspathic aren.
35	6	C20	C1 245m	Capel Curig Mbr.	braidplain	med. ss	moderate	50:27:22	feldspathic aren.
36	6	C22	C1 266m	Capel Curig Mbr.	braidplain	granule cg.	poor	28:30:43	lithic arenite
37	6	F14	F1f 83m	Capel Curig Mbr.	alluvial fan	coarse ss	very poor	40:9:51	lithic arenite
38	6	F15	F1f 89.5m	Capel Curig Mbr.	alluvial fan	med. ss	moderate	65:22:13	feldspathic aren.
39	6	F16	F1f 89.3m	Capel Curig Mbr.	alluvial fan	coarse ss	very poor	68:23:9	feldspathic aren.
40	6	F17A	F1 95.1m	Capel Curig Mbr.	alluvial fan	granule cg.	very poor	29:3:68	lithic arenite
41	6	F17A	F1 95.1m	Capel Curig Mbr.	alluvial fan	granule cg.	very poor	34:4:61	lithic arenite
42	6	T8	T1 62m	Capel Curig Mbr.	alluvial fan	v. coarse ss	poor	67:4:28	lithic arenite
43	6	T9	T1 63.5m	Capel Curig Mbr.	alluvial fan	v. coarse ss	poor	68:8:24	lithic arenite

Fig. 3.28 Stratigraphic location, depositional environment, texture and classification of 92 sandstones which were point-counted. See cross-sections in Fig. 3.104 for regional context of sampling localities.

OBS	REGION	SAMPLE	SECTION LOCATION	STRATIGRAPHIC UNIT	ENVIRONMENT	GRAIN SIZE	SORTING	Q F R RATIO	SANDSTONE TYPE (Okada,1971)
44	7	B41	B4 53m	Moel Siabod Mbr.	braidplain	med. ss	poor	54:21:25	lithic arenite
45	7	B42	B4 >pod	Moel Siabod Mbr.	braidplain	coarse ss	very poor	67:20:12	feldspathic aren.
46	7	B48	B4 base CCVF	Moel Siabod Mbr.	braidplain	coarse ss	very poor	81:13:6	feldspathic aren.
47	7	B50	B4 base CCVF	Moel Siabod Mbr.	braidplain	coarse ss	poor	75:14:12	quartzose aren.
48	7	B51	B4 base CCVF	Moel Siabod Mbr.	braidplain	coarse ss	very poor	60:15:26	lithic arenite
49	7	C143	C3 base CCVF	Moel Siabod Mbr.	braidplain	med. ss	poor	89:10:1	quartzose aren.
50	7	C144	C3 base CCVF	Moel Siabod Mbr.	braidplain	med. ss	poor	57:14:29	lithic arenite
51	7	C26	C1 300m	Moel Siabod Mbr.	braidplain	v. coarse ss	very poor	54:15:31	lithic arenite
52	7	C27	C1 305m	Moel Siabod Mbr.	braidplain	coarse ss	poor	74:23:3	feldspathic aren.
53	7	CC46	C10 base CCVF	Moel Siabod Mbr.	braidplain	v. coarse ss	very poor	22:30:48	lithic arenite
54	7	F19	F1 156m	Moel Siabod Mbr.	alluvial fan	granule cg.	very poor	44:7:49	lithic arenite
55	7	F25	F1 157.8m	Moel Siabod Mbr.	alluvial fan	granule cg.	very poor	46:7:47	lithic arenite
56	7	T11	T1 84.5m	Moel Siabod Mbr.	alluvial fan	granule cg.	very poor	63:5:32	lithic arenite
57	7	T12	T1 89.5m	Moel Siabod Mbr.	alluvial fan	granule cg.	very poor	48:7:44	lithic arenite
58**	6	T5	T1 46m	Capel Curig Mbr.	alluvial fan	coarse ss	very poor	38:9:53	lithic arenite
59	9	A18	A1 93m	Upper Racks Mbr.	shallow mar.	fine ss	moderate	53:17:30	lithic arenite
60	9	A19	A1 99m	Upper Racks Mbr.	shallow mar.	fine ss	moderate	62:13:25	lithic arenite
61	10	A40	A1 207m	4th MBR. CCVF	shallow mar.	coarse ss	very poor	55:20:25	lithic arenite
62	10	A40r	A1 207m	4th MBR. CCVF	shallow mar.	coarse ss	very poor	60:28:12	feldspathic aren.
63	10	A71	A2 154m	4th MBR. CCVF	shallow mar.	v. coarse ss	very poor	13:38:46	lithic arenite
64	11	L1	L1 86.5m	Moel Hebog Mbr.	braidplain	coarse ss	very poor	29:6:64	lithic arenite
65	11	L13	L2 112.3m	Moel Hebog Mbr.	alluvial fan	coarse ss	very poor	34:10:56	lithic arenite
66	11	L14	L2 123m	Moel Hebog Mbr.	alluvial fan	coarse ss	poor	39:11:50	lithic arenite
67	11	L16	L2 147.1m	Moel Hebog Mbr.	alluvial fan	coarse ss	poor	50:16:33	lithic arenite
68	11	L2	L1 99.5m	Moel Hebog Mbr.	alluvial fan	med. ss	poor	62:20:18	feldspathic aren.
69	11	L3	L1 156m	Moel Hebog Mbr.	alluvial fan	med. ss	poor	40:41:18	feldspathic aren.
70	12	J3	J1 6m	Cae'r Gors Mbr.	shallow mar.	coarse ss	poor	50:22:28	lithic arenite
71	12	J4	J1 46m	Cae'r Gors Mbr.	shoreface	coarse ss	poor	62:22:16	feldspathic aren.
72	13	D10	D1 44.5m	Bolchlwyd Mbr.	distr. chann.	coarse ss	moderate	83:11:5	quartzose aren.
73	13	D12	D1 42.37m	Bolchlwyd Mbr.	distr. chann.	coarse ss	poor	71:18:11	feldspathic aren.
74	13	D12r	D1 42.37m	Bolchlwyd Mbr.	distr. chann.	coarse ss	poor	75:15:10	quartzose aren.
75	13	D13	D1 42.50m	Bolchlwyd Mbr.	distr. chann.	fine ss	moderate	93:7:0	quartzose aren.
76	13	D67	D1 37m	Bolchlwyd Mbr.	distr. chann.	coarse ss	poor	73:19:8	feldspathic aren.
77	13	D68	D3 42m	Bolchlwyd Mbr.	distr. chann.	coarse ss	poor	76:8:16	quartzose aren.
78	13	D8	D1 37.5m	Bolchlwyd Mbr.	distr. chann.	v. coarse ss	poor	73:12:15	lithic arenite
79	15	J30	J4 1m	?	braidplain	v. coarse ss	poor	68:10:22	lithic arenite
80	15	J31	J4 51m	?	braidplain	coarse ss	very poor	68:6:26	lithic arenite
81	16	D27	D1 145m	Upper Cwm Eigiau Fm.	shoreface	coarse ss	very poor	33:16:51	lithic arenite
82	16	D30	D1 148m	Upper Cwm Eigiau Fm.	shoreface	coarse ss	poor	66:19:15	feldspathic aren.
83	17	D39B	D1 228m	Upper Cwm Eigiau Fm.	shallow mar.	coarse ss	moderate	71:16:13	feldspathic aren.
84	17	D45	D1 266m	Upper Cwm Eigiau Fm.	shallow mar.	coarse ss	poor	48:27:25	feldspathic aren.
85	17	D48	D1 289m	Upper Cwm Eigiau Fm.	shallow mar.	coarse ss	poor	53:33:14	feldspathic aren.
86	17	D53	D1 294m	Upper Cwm Eigiau Fm.	shallow mar.	fine ss	moderate	89:8:2	quartzose aren.
87	17	D61	D1 287m	Upper Cwm Eigiau Fm.	shallow mar.	fine ss	moderate	68:7:26	lithic arenite
88	17	D63	D1 292.4m	Upper Cwm Eigiau Fm.	shallow mar.	coarse ss	poor	26:8:66	lithic arenite
89	17	D91	D2 184m	Upper Cwm Eigiau Fm.	shallow mar.	coarse ss	poor	59:26:15	feldspathic aren.
90	99	D123	D4 4m	Bolchlwyd Mbr.	delta	coarse ss	very poor	74:14:12	feldspathic aren.
91	99	F2	F1 7.13m	Ddeugwm Fm.	shallow mar.	fine ss	moderate	53:29:18	feldspathic aren.
92	99	S10B	S3 25.5m	Upper Cwm Eigiau Fm.	shallow mar.	v. coarse ss	poor	76:12:13	quartzose aren.

VARIABLE	IDENTIFICATION
Qm	Monocrystalline quartz, flat stage extinction less than 5°
Qms	Monocrystalline quartz, strained, extinction angle » 5°.
Qp	Coarse-grained polycrystalline quartz.
Chert	fine-grained microcrystalline quartz.
Chalc	Chalcedony
PLAG	plagioclase crystals
KFELD	K-feldspar crystals
RHY	Rhyolitic volcanic fragments
BAS	Basaltic volcanic fragments
TRACH	Trachytic ?andesitic volcanic fragments
LVOTH	Unidentified volcanic lithics, mostly mafic.
SCHT	Sericitic chert fragments
SLT	Siltstone
SS	Sandstone
SOTH	Unidentified sedimentary rock fragments.
IGN	Granite or granodiorite rock fragments
META	Metamorphic rock fragments, mostly gneiss or phyllite
OPAQ	Opaque heavy minerals
HVY	Transparent heavy minerals
BIO	Detrital biotite
MUS	Detrital muscovite
HEM	Detrital hematite grains.
PERCTOT	Percentage of matrix within sandstone
Qpm	Microcrystalline quartz matrix
Qs	Quartz-sericite aggregate matrix
Chl	Chlorite matrix
Hemm	hematite matrix
Calc	Calcite cement
PF	plagioclase/total feldspar ratio
LVL	volcanic lithics/total lithics ratio.

FIG. 3.29 Explanation of variables used in point-counting. PERCTOT, PF, and LVL were determined later from point-counting data.

OBS	REGION	SAMPLE	QM	QMS	QP	CHERT	CHALC	PLAG	KFELD	RHY
1	1	C34	29.1	12.6	18.9	0.0	0.0	10.7	4.9	8.7
2	1	C34r	33.0	6.0	3.0	1.0	0.0	7.0	2.0	1.0
3	2	C46	18.6	18.3	12.5	7.6	0.0	7.2	8.0	7.6
4	2	C54	39.0	12.0	5.0	15.0	0.0	11.0	11.0	1.0
5	2	C60	35.0	12.2	6.1	0.0	0.0	6.7	8.3	0.0
6	2	C64	17.0	17.0	24.0	4.0	0.0	16.0	3.0	5.0
7	2	C65	24.0	12.0	13.0	3.0	0.0	17.0	3.0	4.0
8	2	C66	33.0	7.0	7.0	6.0	0.0	11.0	10.0	1.0
9	2	C67	40.0	6.0	5.0	5.0	0.0	10.0	6.0	2.0
10	2	C69	15.0	4.0	5.0	0.0	0.0	8.0	4.0	2.0
11	3	S2	27.6	8.4	8.0	24.0	0.0	3.2	0.8	1.2
12	3	S6	26.9	7.5	6.3	23.3	0.0	4.7	1.2	3.6
13	4	C56	3.7	5.3	6.1	2.8	0.0	38.2	10.2	17.5
14	4	C8	4.1	3.7	9.5	4.9	0.0	13.2	8.6	47.3
15	4	F10A	17.1	4.3	5.0	20.5	0.0	1.2	4.3	4.3
16	4	F10B	9.7	3.1	7.0	13.6	0.0	1.2	1.6	18.3
17	4	F7	20.4	9.8	18.0	9.8	0.0	1.6	9.4	8.2
18	4	F8	19.7	16.7	8.3	7.0	0.0	4.4	7.9	6.6
19	4	F9	11.5	4.4	13.9	4.8	0.0	2.4	3.2	16.7

OBS	REGION	SAMPLE	QM	QMS	QP	CHERT	CHALC	PLAG	KFELD	RHY
20	5	C10	2.7	0.0	15.5	0.0	0.0	6.2	11.6	53.5
21	5	C12	6.1	6.1	20.5	2.0	0.0	1.6	1.6	1.2
22	5	C13	4.0	3.5	4.0	0.0	0.0	32.2	21.6	25.6
23	5	C14	15.3	3.0	7.2	5.5	0.0	5.1	8.9	7.7
24	5	C15A	12.7	2.0	0.4	3.9	0.0	13.3	3.5	45.9
25	5	C15B	8.4	1.9	4.6	1.5	0.0	14.9	9.6	51.3
26	6	B30	8.6	35.8	8.2	2.3	0.0	23.3	5.4	5.4
27	6	B32	14.3	22.4	9.3	3.9	2.3	12.3	7.7	3.9
28	6	B33	29.4	20.0	11.8	3.9	0.0	16.5	5.9	3.9
29	6	B33r	51.8	8.3	2.2	8.3	0.7	17.4	6.5	1.1
30	6	B34	7.4	28.5	4.5	6.2	0.0	24.0	3.7	15.0
31	6	B37	8.8	26.9	4.2	4.6	6.2	15.8	3.1	11.0
32	6	B38	0.0	41.9	3.4	1.5	0.0	4.4	1.5	0.0
33	6	B39	18.2	28.8	9.8	3.9	0.4	15.8	6.7	1.8
34	6	C17	12.6	11.7	12.6	9.9	0.0	25.8	7.8	12.0
35	6	C20	14.0	8.6	9.5	14.4	0.0	2.3	23.0	11.3
36	6	C22	9.2	11.8	6.1	0.0	0.0	9.2	19.7	4.4
37	6	F14	17.8	5.8	10.4	5.4	0.0	4.1	4.6	5.0
38	6	F15	25.6	4.5	13.6	21.1	0.0	6.0	15.6	1.5
39	6	F16	39.3	15.1	10.5	1.4	0.0	15.1	7.3	0.5
40	6	F17A	7.9	2.5	9.1	8.7	0.0	2.1	1.2	33.6
41	6	F17A2	12.3	4.9	8.2	8.6	0.0	1.2	2.9	8.2
42	6	T8	43.2	4.5	3.2	11.5	0.5	3.2	0.8	3.2
43	6	T9	29.4	6.6	9.6	14.0	0.0	3.5	3.5	2.6

OBS	REGION	SAMPLE	QM	QMS	QP	CHERT	CHALC	PLAG	KFELD	RHY

FIG. 3.30: RAW PETROGRAPHIC DATA FROM 92 SAMPLES. SEE FIG. 3.29 FOR EXPLANATION OF VARIABLES. PF= PLAGIOCLASE/FELDSPAR RATIO WHEREAS LVL= VOLCANIC ROCK FRAGMENTS/ TOTAL LITHICS RATIO.

OBS	BAS	TRACH	LVOTH	SCHT	SLT	SS	SOTH	IGN	META	OPAQ	HVY	BIO
1	0.0	0.0	0.00	12.1	0.5	0.0	0.0	0.5	0.5	1.5	0.0	0.0
2	0.0	0.0	1.00	37.0	7.0	1.0	0.0	0.0	0.0	1.0	0.0	0.0
3	0.0	0.4	0.00	13.7	0.0	0.4	0.0	0.0	0.0	0.0	0.0	0.0
4	0.0	0.0	1.00	0.0	0.0	2.0	0.0	0.0	0.0	3.0	0.0	0.0
5	0.0	0.0	1.00	20.6	7.8	0.0	0.0	0.5	0.0	0.0	0.0	0.0
6	2.0	0.0	1.00	1.0	8.0	0.0	0.0	0.0	0.0	3.0	0.0	0.0
7	2.0	0.5	0.00	0.0	2.0	8.0	0.0	2.0	7.0	0.0	0.0	0.0
8	0.5	0.0	1.00	1.0	15.0	0.0	0.0	0.5	0.0	5.0	0.5	0.0
9	0.5	0.0	1.00	1.0	22.0	0.0	0.0	0.0	0.0	0.0	0.0	0.0
10	0.5	0.0	0.00	28.0	2.0	5.0	0.0	1.0	0.0	25.0	0.0	0.5
11	0.0	0.0	0.40	2.8	0.0	7.6	0.0	1.6	0.0	13.2	0.0	0.0
12	0.0	0.0	2.80	2.8	0.0	15.4	0.4	2.0	0.0	1.2	0.0	0.4
13	10.2	0.0	0.00	0.0	0.4	0.0	0.0	0.0	0.4	2.4	2.8	0.0
14	0.0	0.0	0.00	0.0	0.0	0.0	0.0	0.8	0.4	5.8	0.0	0.0
15	0.0	0.0	0.40	0.0	0.0	38.8	0.0	0.8	0.4	0.4	0.0	0.0
16	2.7	0.0	4.50	14.4	0.0	22.6	0.0	0.0	0.0	0.0	0.0	0.0
17	5.3	2.0	3.70	6.9	0.0	2.4	0.0	1.2	0.0	0.0	0.0	0.0
18	4.8	0.0	1.30	3.1	16.7	0.0	0.0	2.2	0.0	0.5	0.5	0.0
19	3.6	0.0	3.30	3.6	20.6	0.0	0.0	8.9	0.0	1.2	0.0	0.0

OBS	BAS	TRACH	LVOTH	SCHT	SLT	SS	SOTH	IGN	META	OPAQ	HVY	BIO
20	6.5	1.2	0.00	0.0	0.0	0.0	0.8	0.8	1.6	0.4	0.4	0.0
21	29.1	0.0	0.00	0.8	0.0	5.3	0.4	0.0	0.4	22.5	1.2	0.0
22	2.2	0.8	0.00	0.0	0.0	0.0	0.9	0.0	0.0	4.0	0.4	0.0
23	22.6	0.0	0.00	0.0	0.0	0.9	0.0	2.1	0.0	18.7	3.4	0.0
24	0.0	0.4	3.00	0.0	0.0	0.4	0.0	0.0	0.0	10.6	0.8	0.0
25	0.4	0.0	0.00	0.0	0.0	0.0	0.0	0.4	5.0	1.5	0.5	0.0
26	0.4	0.0	3.90	0.0	0.0	0.4	0.0	3.5	1.3	0.4	0.0	0.0
27	0.4	1.2	8.10	0.0	0.0	2.3	7.7	2.7	0.0	0.0	0.0	0.4
28	1.2	0.0	2.00	0.0	0.0	0.0	0.0	5.1	0.0	0.0	0.0	0.0
29	0.0	0.3	2.20	0.3	0.0	0.3	0.0	1.1	0.0	0.0	0.0	0.0
30	0.8	0.8	0.00	3.3	1.2	0.8	0.0	0.8	0.0	0.8	0.0	0.0
31	0.4	0.4	16.60	0.4	0.0	0.4	0.0	0.4	0.0	0.8	0.0	0.0
32	0.5	0.0	2.50	20.5	4.9	0.0	0.0	0.0	0.0	12.3	1.5	0.0
33	0.4	0.4	2.80	0.0	3.2	0.7	0.0	3.2	0.0	0.0	0.0	0.0
34	0.9	0.6	0.00	2.7	0.0	0.0	0.3	0.3	0.0	0.3	0.0	0.0
35	0.5	0.0	0.00	0.0	0.5	6.6	0.0	1.8	0.0	0.0	0.5	0.0
36	0.0	0.0	0.00	36.2	0.0	0.0	0.0	0.0	1.3	0.9	0.0	0.0
37	0.4	1.2	0.80	19.5	5.0	17.0	0.0	1.2	0.0	1.2	0.0	0.0
38	1.5	0.0	5.00	5.0	0.0	0.0	0.0	0.0	0.0	0.0	0.0	0.0
39	0.5	0.5	0.90	6.4	0.0	0.0	0.0	0.5	0.0	0.5	1.5	0.0
40	0.0	0.0	0.00	0.0	0.0	24.9	5.4	2.9	0.0	0.0	0.0	0.0
41	1.2	0.4	2.50	0.0	13.2	31.7	0.0	3.3	0.0	0.4	0.0	0.0
42	3.7	0.8	2.90	3.3	1.7	10.7	0.0	0.5	0.0	4.2	0.0	0.0
43	0.0	0.4	1.30	0.0	0.0	15.8	0.0	0.8	0.0	6.6	0.0	0.0

OBS	BAS	TRACH	LVOTH	SCHT	SLT	SS	SOTH	IGN	META	OPAQ	HVY	BIO

OBS	MUS	HEM	PERCTOT	QPM	QS	CHL	HEMM	CALC	PF	LVL
1	0.0	0.0	35.4	0.0	0.9	32.9	1.6	0.0	0.685897	0.390135
2	0.0	0.0	52.0	0.0	50.0	2.0	0.0	0.5	0.777778	0.042553
3	4.2	1.1	12.3	0.3	8.7	0.3	2.7	0.3	0.473684	0.361991
4	0.0	0.0	18.3	0.0	3.3	14.0	0.0	4.3	0.500000	0.500000
5	0.0	1.6	40.6	0.0	4.2	16.5	0.0	20.3	0.446667	0.033445
6	0.0	0.0	23.0	3.0	4.0	14.0	0.0	2.0	0.842105	0.470588
7	0.0	3.0	18.3	0.0	5.3	12.3	0.0	0.7	0.850000	0.254902
8	0.0	1.0	26.6	0.0	3.0	21.6	0.0	2.0	0.523810	0.131579
9	1.0	0.0	22.0	0.0	19.7	2.3	0.0	0.0	0.625000	0.132075
10	0.0	0.0	11.3	0.5	5.6	0.0	3.4	2.0	0.666667	0.064935
11	0.0	1.6	16.7	0.3	16.3	0.0	0.0	0.0	0.800000	0.117647
12	1.2	0.0	15.7	0.0	15.3	0.4	0.0	0.0	0.796610	0.237037
13	0.0	0.0	18.0	0.0	11.0	3.0	0.3	3.7	0.789256	0.971930
14	0.0	0.0	11.0	0.0	6.2	3.7	0.0	1.1	0.605505	0.975258
15	0.0	1.2	14.0	0.0	6.7	7.0	0.0	0.3	0.218182	0.105145
16	0.0	0.0	14.3	6.7	5.3	2.3	0.0	0.0	0.428571	0.408000
17	0.8	0.4	18.3	11.3	2.3	4.3	0.3	0.0	0.145455	0.646465
18	0.0	0.0	24.0	0.3	20.7	3.0	0.0	0.0	0.357724	0.365994
19	0.0	2.0	16.0	0.0	14.3	0.3	1.3	0.0	0.428571	0.416226

OBS	MUS	HEM	PERCTOT	QPM	QS	CHL	HEMM	CALC	PF	LVL
20	0.0	0.0	13.3	0.0	5.5	8.2	0.0	0.0	0.348315	0.950311
21	0.0	0.8	18.1	0.0	13.4	0.0	0.0	4.7	0.500000	0.814516
22	0.4	0.0	24.3	0.0	0.0	23.0	0.0	1.3	0.598513	0.969492
23	0.0	0.0	21.7	0.0	0.0	19.3	0.0	2.3	0.364286	0.90991
24	0.0	0.0	18.3	3.3	0.0	15.0	0.0	0.0	0.791667	0.99195
25	0.0	0.0	13.3	3.7	0.0	9.7	0.0	0.0	0.608163	0.90543
26	0.8	0.4	0.0	14.3	14.3	0.0	0.0	0.0	0.811847	0.65101
27	0.0	1.9	13.7	3.0	9.3	1.3	0.0	0.0	0.615000	0.51711
28	0.0	0.8	15.0	10.0	0.0	5.0	0.0	0.0	0.736607	0.58197
29	0.0	0.4	10.1	7.8	0.3	2.0	0.0	0.0	0.728033	0.67925
30	0.0	0.8	19.3	13.0	0.7	2.3	0.3	3.0	0.866426	0.73128
31	0.0	0.0	13.3	8.0	1.7	1.3	2.3	0.0	0.835979	0.95946
32	3.9	0.0	32.3	0.0	30.6	1.7	0.0	0.0	0.745763	0.10563
33	0.4	4.2	6.6	4.0	2.0	0.3	0.0	0.3	0.702222	0.43200
34	0.0	0.0	14.0	0.5	2.1	9.8	0.0	1.5	0.767857	0.80357
35	5.5	0.9	28.6	0.0	21.3	0.0	2.6	4.8	0.090909	0.57005
36	0.4	0.9	23.7	0.0	2.0	20.7	0.0	1.0	0.318339	0.10501
37	0.0	0.0	19.7	0.3	1.0	17.3	0.7	0.3	0.471264	0.14770
38	0.0	0.0	33.7	28.0	3.7	2.0	0.0	0.0	0.277778	0.61538
39	0.0	0.0	27.0	0.3	18.9	7.0	0.0	0.7	0.674107	0.25806
40	0.0	0.0	19.7	0.3	0.3	17.9	0.0	1.0	0.636364	0.50299
41	0.4	0.4	19.0	0.7	2.3	14.7	0.0	1.3	0.292683	0.20331
42	2.0	0.5	19.0	0.0	10.0	7.0	0.0	2.0	0.800000	0.39552
43	3.5	0.0	24.0	0.0	21.7	2.0	0.3	0.0	0.500000	0.20574

OBS	MUS	HEM	PERCTOT	QPM	QS	CHL	HEMM	CALC	PF	LVL

OBS	REGION	SAMPLE	QM	QMS	QP	CHERT	CHALC	PLAG	KFELD	RHY
44	7	B41	20.6	9.3	9.7	0.8	0.0	6.5	9.7	0.0
45	7	B42	24.5	12.0	6.8	1.6	0.0	4.2	9.4	2.6
46	7	B48	46.4	6.8	0.5	7.3	0.0	5.7	4.2	0.0
47	7	B50	43.3	15.9	10.4	4.0	0.0	8.5	5.0	2.0
48	7	B51	30.5	8.8	2.2	16.4	0.4	8.0	6.2	0.9
49	7	C143	51.8	5.5	2.3	8.7	0.0	2.8	4.6	0.0
50	7	C144	29.4	6.7	8.8	5.9	0.0	9.2	3.4	0.0
51	7	C26	11.3	20.8	19.7	0.5	0.0	7.3	7.3	19.0
52	7	C27	27.2	12.3	2.6	14.9	0.0	12.7	4.8	1.3
53	7	CC46	17.4	3.4	0.0	0.0	0.0	18.7	9.4	2.8
54	7	F19	16.3	6.8	11.2	6.8	0.0	2.8	4.4	13.0
55	7	F25	23.2	6.6	3.5	11.0	0.0	3.5	3.5	0.0
56	7	T11	21.8	10.3	5.6	20.9	0.0	3.4	1.3	10.7
57	7	T12	23.6	15.9	8.2	0.0	0.0	3.9	3.4	3.0
58	7	T15	24.8	10.6	1.8	0.0	0.0	6.0	2.3	7.8
59	9	A18	46.0	5.3	1.8	0.0	0.0	11.9	4.9	0.0
60	9	A19	47.3	5.3	5.3	0.0	0.0	9.5	2.4	3.0
61	10	A40	17.3	2.2	2.5	33.1	0.0	16.9	3.6	2.9
62	10	A40r	24.5	1.3	2.6	29.7	0.0	19.7	7.4	0.4
63	10	A71	9.2	2.0	4.0	0.0	0.8	28.5	9.6	4.8
64	11	L1	9.3	6.7	5.9	7.0	0.0	3.0	3.3	5.6
65	11	L13	8.3	7.9	3.2	14.2	0.0	4.7	5.5	1.6
66	11	L14	18.9	8.1	2.3	7.7	0.0	5.9	4.5	0.5
67	11	L16	12.4	12.0	4.4	19.6	0.0	10.0	5.6	4.8
68	11	L2	19.3	9.7	8.8	24.4	0.0	6.7	13.0	5.0
69	11	L3	12.7	12.4	3.7	10.5	0.0	33.7	6.7	0.4

OBS	REGION	SAMPLE	QM	QMS	QP	CHERT	CHALC	PLAG	KFELD	RHY
70	12	J3	20.4	10.4	8.0	9.0	0.0	16.9	4.0	2.0
71	12	J4	25.2	10.4	5.4	19.8	0.0	12.6	9.0	2.7
72	13	D10	30.1	28.8	5.1	17.1	0.0	6.8	4.1	1.0
73	13	D12	24.4	21.3	7.2	17.6	0.0	13.6	4.4	2.4
74	13	D12r	30.7	20.5	5.9	17.3	0.0	9.4	5.1	2.4
75	13	D13	74.2	0.0	0.5	16.3	0.0	4.3	2.4	0.0
76	13	D67	27.5	21.1	9.6	13.6	0.0	10.4	8.2	4.6
77	13	D68	40.9	10.8	12.7	8.1	0.0	5.8	2.3	6.2
78	13	D8	40.1	14.2	8.6	8.2	0.0	7.3	4.7	5.2
79	15	J30	8.5	10.4	3.9	45.2	0.0	6.2	3.5	9.3
80	15	J31	27.9	5.0	3.6	22.5	0.0	3.2	1.8	18.0
81	16	D27	15.0	3.3	3.3	7.7	0.8	8.5	6.1	44.0
82	16	D30	16.8	4.7	3.6	38.7	0.0	14.6	3.3	10.2
83	17	D39B	36.6	12.2	1.9	17.6	0.0	11.8	3.1	1.5
84	17	D45	14.7	12.0	19.6	0.0	0.0	11.6	15.1	2.7
85	17	D48	24.5	14.5	10.4	4.0	0.0	21.3	12.4	5.6
86	17	D53	47.2	2.6	0.0	37.1	0.0	4.5	3.4	1.9
87	17	D61	63.5	0.8	0.4	0.8	0.0	4.6	2.1	0.8
88	17	D63	20.7	4.4	0.7	0.0	0.0	3.6	4.4	54.2
89	17	D91	30.7	11.6	5.2	10.0	0.4	15.1	10.4	1.2
90	99	D123	41.6	9.3	6.2	17.1	0.0	8.6	5.1	3.1
91	99	F2	19.2	14.6	5.8	12.1	0.0	14.1	14.6	4.6
92	99	S10B	27.6	21.7	13.6	12.1	0.0	9.9	1.5	5.1

OBS REGION SAMPLE QM QMS QP CHERT CHALC PLAG KFELD RHY

FIG. 3.30 CONTINUED

OBS	BAS	TRACH	LVOTH	SCHT	SLT	SS	SOTH	IGN	META	OPAQ	HVY	BIO
44	0.8	0.0	0.00	18.1	0.0	0.0	0.0	0.0	0.0	22.6	0.0	0.8
45	3.1	0.0	0.00	2.1	0.0	0.5	0.0	0.0	0.0	3.6	0.0	0.0
46	0.0	0.0	0.50	0.0	2.6	1.6	0.0	0.0	0.0	14.6	0.0	0.0
47	0.5	0.0	1.50	4.0	0.0	3.0	0.0	0.5	0.0	2.0	0.5	0.0
48	1.8	0.0	2.70	5.8	10.6	0.4	1.8	0.8	0.4	1.3	0.0	0.0
49	0.0	0.0	0.50	0.0	0.5	0.0	0.0	0.0	0.0	22.0	1.5	0.0
50	0.0	0.0	2.10	13.9	9.7	0.0	0.0	0.8	0.0	9.7	0.4	0.0
51	0.4	0.4	0.00	2.6	1.5	0.0	0.0	3.6	2.6	1.8	0.0	0.0
52	0.4	0.0	0.40	0.0	0.0	0.0	0.0	0.4	0.0	19.3	3.5	0.0
53	3.0	0.0	0.00	31.1	0.0	0.0	8.9	0.0	0.0	4.3	0.0	0.0
54	0.8	0.0	2.40	4.0	6.0	8.0	7.6	4.0	0.0	4.4	0.4	0.0
55	1.3	0.4	0.00	6.1	12.3	22.8	0.0	3.1	0.0	3.1	0.0	0.0
56	0.4	0.4	0.90	5.6	0.0	11.1	0.0	0.9	0.0	0.0	6.0	0.0
57	3.4	0.0	4.70	19.3	0.0	10.3	0.0	3.0	0.0	0.0	0.0	0.0
58	0.9	0.0	2.80	26.1	12.8	0.0	0.0	0.9	0.0	2.3	0.9	0.0
59	0.4	0.0	0.40	28.8	0.0	0.0	0.0	0.0	0.0	0.0	0.0	0.0
60	0.6	0.0	1.22	10.1	8.9	0.0	0.0	0.0	0.0	0.0	0.0	0.0
61	6.0	0.0	0.00	0.4	14.0	1.1	0.0	0.4	0.0	1.1	0.0	0.0
62	0.0	0.4	0.00	10.5	0.0	0.0	0.0	0.0	0.0	0.4	0.0	0.0
63	8.0	0.0	1.20	31.7	0.0	0.0	0.0	0.0	0.0	0.0	0.4	0.0
64	40.4	1.9	1.50	0.0	9.6	1.5	0.0	3.3	0.0	0.0	0.0	0.0
65	26.6	0.8	15.00	8.7	0.0	0.0	0.0	0.8	1.7	0.0	0.0	0.0
66	36.1	0.0	0.00	0.0	11.7	0.0	0.0	0.0	0.0	3.6	0.9	0.0
67	6.8	1.6	3.2	8.8	6.0	0.0	0	0.4	0.4	0.4	0.0	0.0
68	4.2	0.4	4.6	0.0	0.0	3.3	0	0.8	0.0	0.0	0.0	0.0
69	4.5	6.8	6.4	0.0	0.0	0.0	0	0.0	0.0	0.7	0.0	0.0

OBS	BAS	TRACH	LVOTH	SCHT	SLT	SS	SOTH	IGN	META	OPAQ	HVY	BIO
70	12.4	0.0	6.5	3.5	2.0	0.0	0	0.5	0.0	5.5	0.0	0.0
71	6.3	0.0	0.0	0.0	0.0	3.2	4	0.0	0.0	3.2	0.4	0.0
72	1.3	0.0	0.7	0.0	1.4	0.0	0	0.8	0.0	0.0	0.0	0.4
73	0.8	1.2	2.0	0.0	3.2	0.0	0	1.2	0.0	1.2	0.0	0.0
74	1.2	0.4	2.0	0.0	2.8	0.0	0	1.2	0.0	0.4	0.0	0.0
75	0.0	0.0	0.0	0.0	0.0	0.0	0	0.0	0.0	1.0	0.5	0.0
76	0.0	0.0	0.7	0.0	1.8	0.0	0	0.7	0.4	0.0	0.0	1.1
77	1.9	1.6	1.9	0.0	0.0	1.2	0	2.0	0.0	0.0	0.0	0.0
78	0.0	2.2	1.3	0.0	3.9	0.0	0	1.7	0.0	0.4	0.0	0.0
79	0.8	0.8	0.8	8.9	0.0	0.8	0	0.4	0.0	0.0	1.2	0.0
80	0.0	0.0	1.4	0.0	2.3	0.0	0	0.9	0.0	11.7	1.8	0.0
81	0.0	0.0	0.0	0.0	2.4	0.0	0	0.0	0.0	1.2	0.4	0.0
82	1.1	0.0	1.1	0.0	1.8	0.0	0	0.4	0.0	0.9	0.0	0.0
83	1.5	0.0	1.1	5.3	3.1	0.0	0	0.0	0.0	0.8	0.0	0.0
84	0.9	0.0	0.0	18.2	0.0	2.2	0	0.4	0.0	0.9	0.0	0.0
85	1.2	0.0	0.0	0.0	0.0	6.8	0	0.0	0.0	0.0	0.0	0.0
86	0.4	0.0	0.0	0.0	0.0	0.0	0	0.0	0.0	0.7	1.5	0.0
87	0.0	0.0	0.0	22.8	0.0	1.2	0	0.0	0.0	2.5	0.8	0.4
88	0.0	0.0	1.5	1.1	0.0	9.1	0	0.0	0.0	0.0	0.0	0.0
89	0.0	0	0.0	11.6	2.0	0.0	0	0.0	0.0	0.0	0.4	0
90	0.8	0	1.2	1.9	0.8	1.9	0	2.0	0.0	1.2	0.0	0
91	4.6	0	0.4	7.9	0.0	0.0	0	0.0	0.4	2.1	0.0	0
92	2.2	0	2.6	0.0	0.4	0.0	0	2.2	0.0	0.0	0.8	0

OBS	BAS	TRACH	LVOTH	SCHT	SLT	SS	SOTH	IGN	META	OPAQ	HVY	BIO

OBS	MUS	HEM	PERCTOT	QPM	QS	CHL	HEMM	CALC	PF	LVL
44	0.0	0.4	17.3	0.0	14.7	1.7	1.0	0.0	0.401235	0.04233
45	27.1	0.5	40.0	0.0	2.8	35.4	1.3	0.7	0.308824	0.68675
46	10.4	0.0	36.0	0.0	35.0	1.0	0.0	0.0	0.575758	0.10638
47	0.0	0.0	33.0	0.7	26.3	2.0	0.7	3.3	0.629630	0.34783
48	0.4	1.3	24.6	20.9	3.5	0.0	1.3	0.0	0.563380	0.21429
49	0.0	0.0	27.3	0.0	26.0	1.3	0.0	0.0	0.378378	0.50000
50	0.0	0.0	20.7	0.0	20.0	0.7	0.0	0.0	0.730159	0.07925
51	1.1	0.0	8.7	0.3	2.3	6.0	0.0	0.0	0.500000	0.65781
52	0.4	0.0	24.0	12.3	7.7	3.3	0.0	0.7	0.725714	0.84000
53	0.0	0.0	24.4	22.5	1.6	1.6	0.0	0.0	0.665480	0.12664
54	0.4	0.0	17.0	2.3	6.7	8.0	0.0	0.0	0.388889	0.35371
55	0.0	0.0	24.0	3.7	20.3	0.0	0.0	0.0	0.500000	0.03696
56	0.0	0.0	22.0	0.0	1.3	20.7	0.0	0.0	0.723404	0.41333
57	0.4	0.0	22.3	0.0	11.7	10.7	0.0	0.0	0.534247	0.25400
58	0.0	0.0	24.0	0.0	22.0	2.0	0.0	0.0	0.722892	0.22417
59	0.0	0.0	25.1	0.0	18.4	0.4	0.0	6.4	0.708333	0.02703
60	6.5	0.0	43.9	0.0	24.9	0.0	2.0	16.9	0.798319	0.20235
61	0.0	0.7	11.9	0.0	3.9	8.0	0.0	0.0	0.824390	0.35887
62	0.0	3.1	23.4	0.0	18.4	5.0	0.0	0.0	0.726937	0.07080
63	0.0	0.0	13.8	0.0	8.7	5.9	0.0	0.0	0.748031	0.30635
64	0.0	1.1	11.8	0.0	1.6	8.5	2.6	0.0	0.476190	0.77429
65	0.0	0.0	12.2	0.0	0.0	10.8	0.0	1.4	0.460784	0.79710
66	0.0	0.0	26.2	0.0	0.0	26.2	0.0	0.0	0.567308	0.75776
67	2.8	0.0	16.7	0.0	0.0	16.7	0.0	0.0	0.641026	0.51250
68	0.0	0.0	22.2	0.0	22.2	0.0	0.0	0.0	0.340102	0.77596
69	1.3	0.0	11.0	0.0	11.0	0.0	0.0	0.0	0.834158	1.00000

OBS	MUS	HEM	PERCTOT	QPM	QS	CHL	HEMM	CALC	PF	LVL
70	0.0	0.0	33.0	0.7	1.0	31.3	0.0	0.0	0.808612	0.77695
71	0.0	0.0	26.0	0.0	0.0	26.0	0.0	0.0	0.583333	0.55556
72	0.7	1.0	2.7	0.0	1.3	0.0	0.0	1.3	0.623853	0.57692
73	0.0	0.0	16.7	0.0	3.7	0.0	0.3	12.7	0.755556	0.59259
74	0.4	0.0	15.9	0.0	4.6	0.0	0.0	11.3	0.648276	0.60000
75	1.4	0.0	30.0	0.0	18.7	0.0	0.0	11.3	0.641791	.
76	0.0	0.4	6.7	0.0	6.7	0.0	0.0	0.0	0.559140	0.64634
77	3.1	0.0	14.0	0.0	14.0	0.0	0.0	0.0	0.716049	0.78378
78	2.2	0.0	22.7	0.0	11.0	0.0	0.0	11.7	0.608333	0.60839
79	0.0	0.0	13.7	12.7	0.0	1.0	0.0	0.0	0.639175	0.53670
80	0.0	0.0	0.0	0.0	0.0	0.0	0.0	0.0	0.640000	0.85841
81	6.1	0.4	18.0	0.0	15.0	3.0	0.0	0.0	0.582192	0.94828
82	2.6	0.0	8.7	7.3	0.0	0.0	0.4	1.3	0.815642	0.84932
83	2.7	0.8	12.7	0.0	12.3	0.3	0.0	0.1	0.791946	0.32800
84	0.4	0.0	25.0	15.7	0.0	0.0	0.0	9.7	0.434457	0.14754
85	0.0	0.0	17.0	15.7	0.0	0.7	0.0	0.7	0.632047	0.50000
86	0.4	0.0	11.0	0.0	9.0	2.0	0.0	0.0	0.569620	1.00000
87	0.0	0.0	19.7	0.0	18.0	1.7	0.0	0.0	0.686567	0.03226
88	0.0	0.4	12.4	12.4	0.0	0.0	0.0	0.0	0.450000	0.84522
89	1.2	0.0	7.7	0	7.4	0.0	0.0	0.3	0.592157	0.081081
90	0.0	0.0	17.7	0	4.0	0.0	10.3	0.0	0.627737	0.435897
91	0.0	0.4	20.0	2	4.0	3.3	10.7	0.0	0.491289	0.536313
92	0.4	0.0	9.3	7	2.3	0.0	0.0	0.0	0.868421	0.792000

OBS	MUS	HEM	PERCTOT	QPM	QS	CHL	HEMM	CALC	PF	LVL

VARIABLE	N	MEAN	STANDARD DEVIATION	MINIMUM VALUE	MAXIMUM VALUE	STD ERROR OF MEAN
QM	92	23.57	14.05	0.00	74.20	1.47
QMS	92	10.48	7.95	0.00	41.90	0.83
QP	92	7.16	5.02	0.00	24.00	0.52
CHERT	92	9.69	9.52	0.00	45.20	0.99
CHALC	92	0.14	0.70	0.00	6.20	0.07
PLAG	92	10.09	7.56	1.20	38.20	0.79
KFELD	92	6.17	4.40	0.80	23.00	0.46
RHY	92	8.11	12.47	0.00	54.20	1.30
BAS	92	3.19	7.24	0.00	40.40	0.76
TRACH	92	0.34	0.84	0.00	6.80	0.09
LVOTH	92	1.68	2.69	0.00	16.60	0.28
SCHT	92	6.14	9.38	0.00	37.00	0.98
SLT	92	2.89	4.96	0.00	22.00	0.52
SS	92	3.38	7.19	0.00	38.80	0.75
SOTH	92	0.42	1.59	0.00	8.90	0.17
IGN	92	0.99	1.41	0.00	8.90	0.15
META	92	0.26	0.97	0.00	7.00	0.10
OPAQ	92	3.26	5.81	0.00	25.00	0.61
HVY	92	0.39	0.91	0.00	6.00	0.09
BIO	92	0.04	0.17	0.00	1.10	0.02
MUS	92	1.05	3.23	0.00	27.10	0.34
HEM	92	0.37	0.74	0.00	4.20	0.08
PERCTOT	92	20.15	8.68	2.70	52.00	0.90
QPM	92	2.78	5.68	0.00	28.00	0.59
QS	92	9.02	9.55	0.00	50.00	0.99
CHL	92	6.26	8.49	0.00	35.40	0.89
HEMM	92	0.50	1.65	0.00	10.70	0.17
CALC	92	1.64	3.74	0.00	20.30	0.39
PF	92	0.60	0.17	0.09	0.87	0.02
LVL	91	0.48	0.30	0.03	1.00	0.03

FIGURE 3.31: Mean concentration, standard deviations, and ranges of values for all detrital framework and matrix components from all volcaniclastic sandstones. Values from detrital grains represent concentration within clastic grains only, whereas matrix percentages refer to concentrations within all points counted (ie. entire sandstone). Identity of variables tabulated in Figure 3.29.

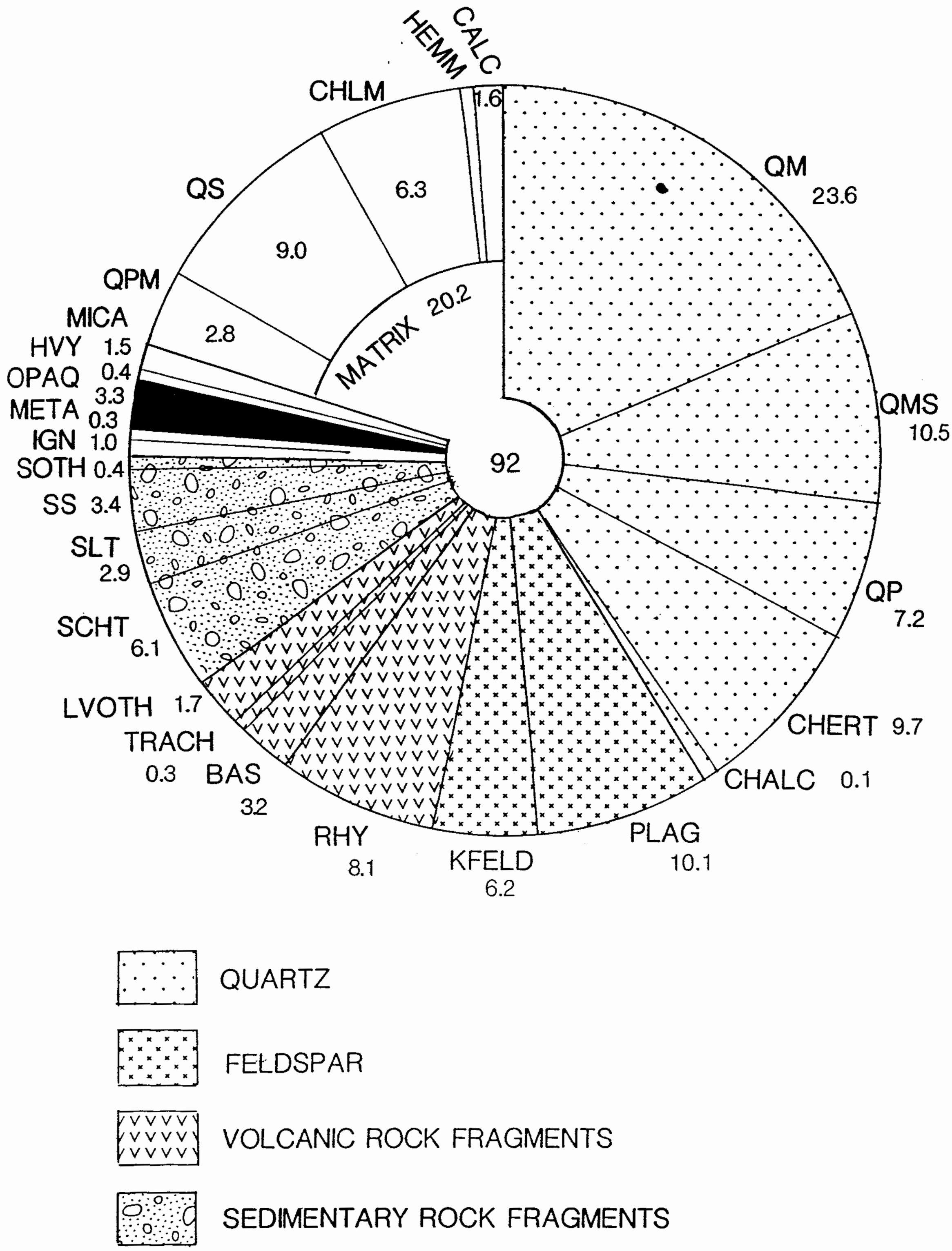

FIG. 3.32 Relative amounts of various detrital grains and matrix components within all volcaniclastic sandstones. See Fig. 3.31 for explanation of values. Sector area on circle for all variables is in relation to concentration with entire sandstone. Value in centre indicates number of samples which pie diagram was based on.

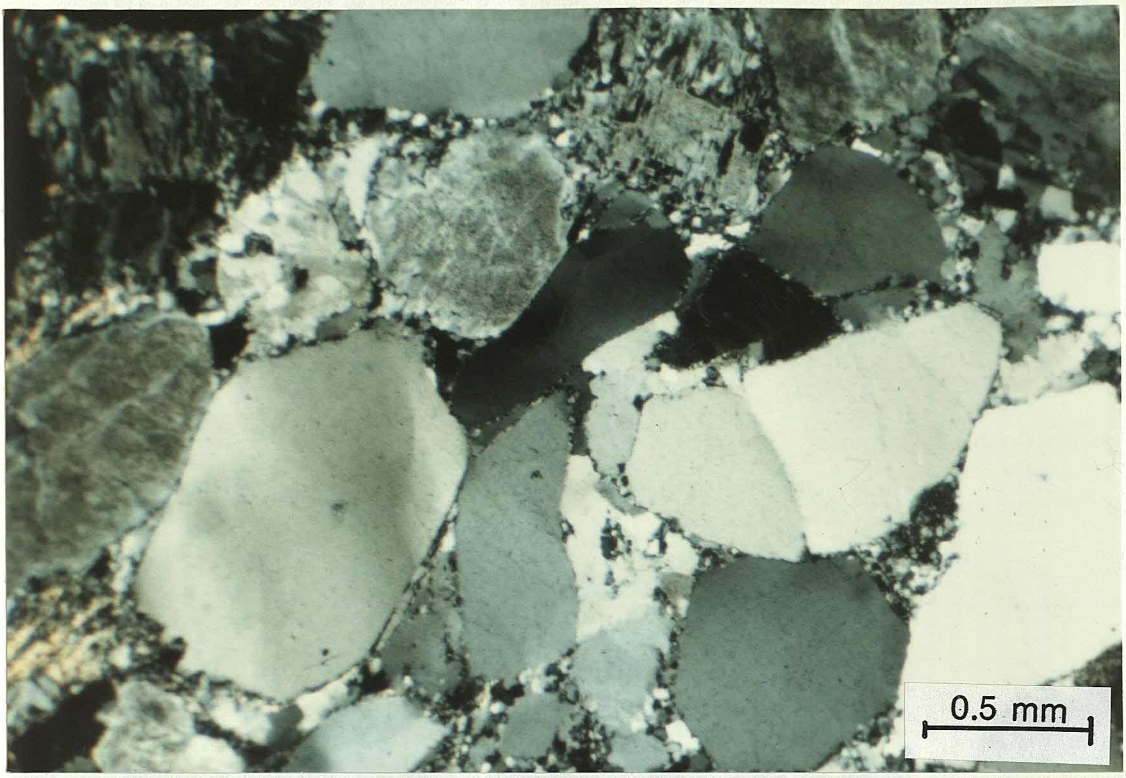

Fig. 3.34 Large crystals of strained and unstrained monocrystalline quartz (Qm, Qms), often euhedral, as well as untwinned or albitized K-feldspar (K-feld), set in matrix of microcrystalline quartz. (Sample B30, section B4, 3m).

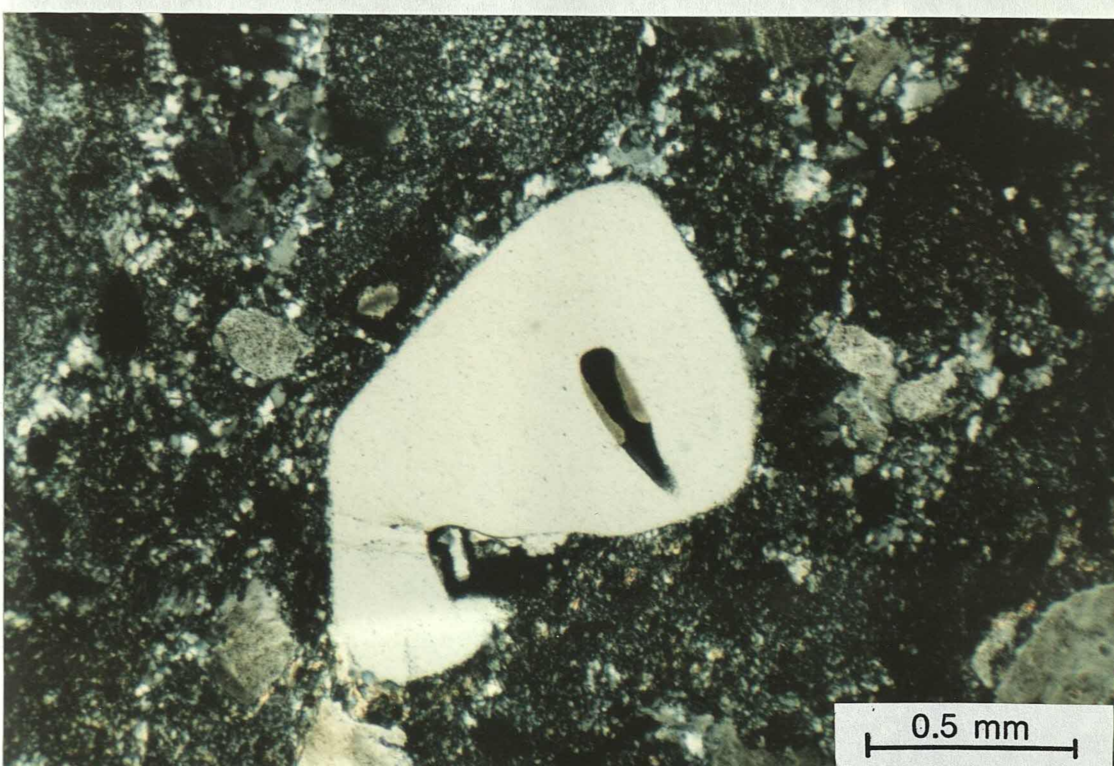

Fig. 3.35 Embayed monocrystalline quartz surrounded by "cherty" rhyolitic volcanic rock fragments. (Sample C10, section C1, 154m).

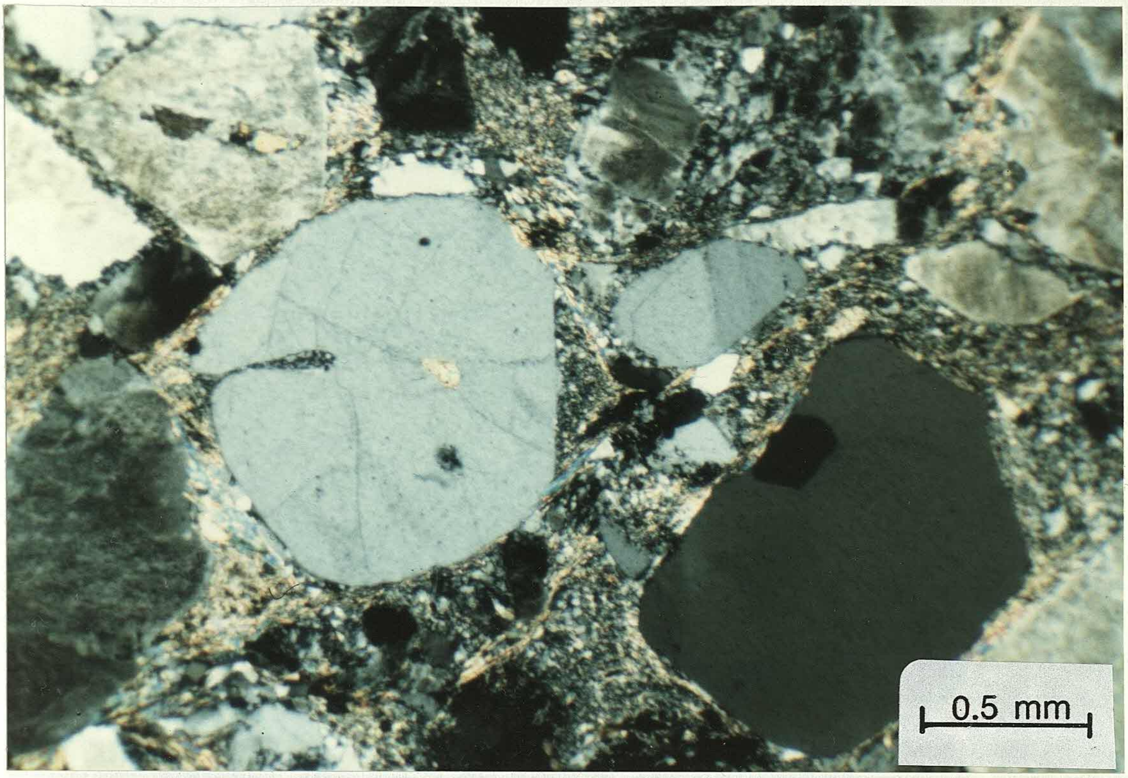

Fig. 3.36 Monocrystalline quartz crystals with either embayed margins or euhedral crystal shape with negative crystals suggesting a volcanic origin. (Sample D91, Section D2, 185m)

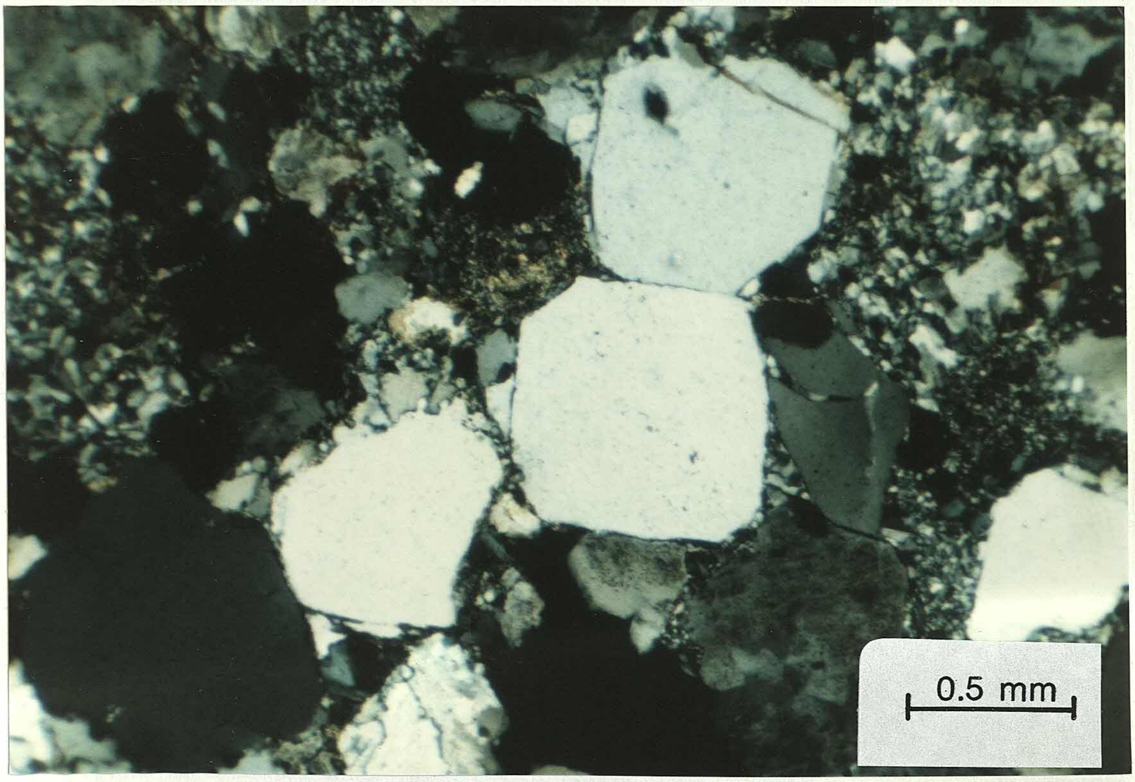

Fig. 3.37 Euhedral β-quartz habit exhibited by unstrained monocrystalline quartz crystals (Sample B33, section B4,)

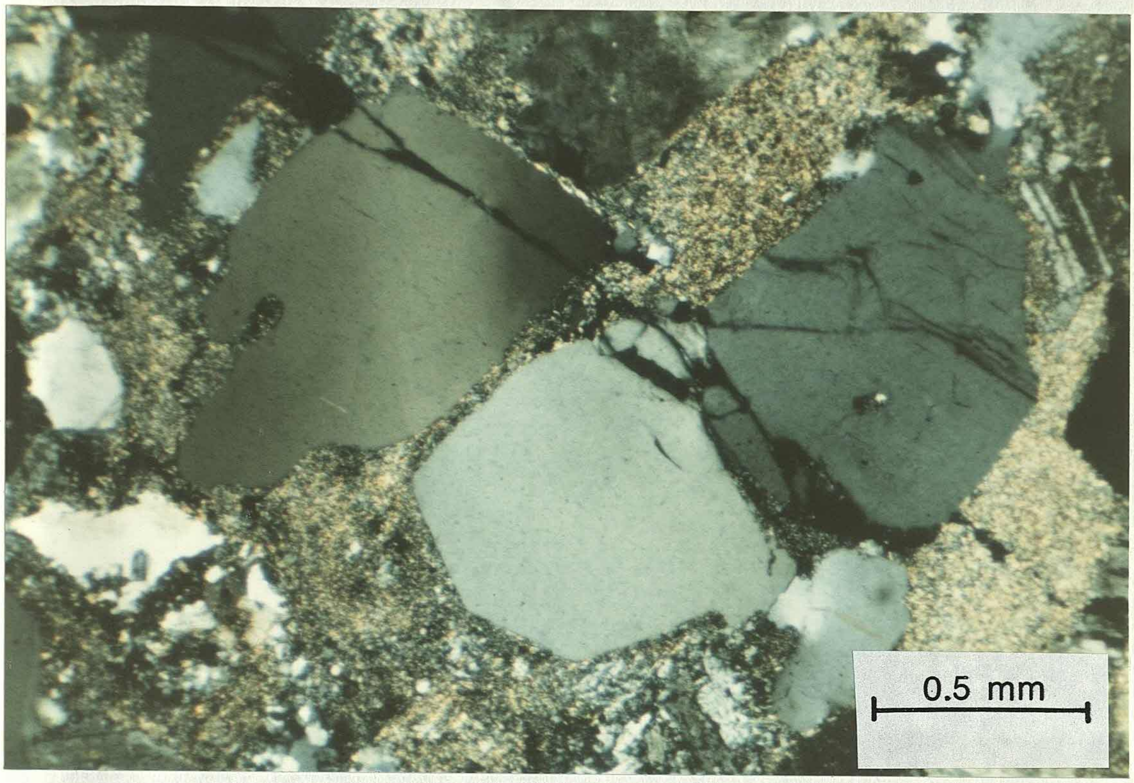

Fig. 3.38 Euhedral, embayed and fractured β-quartz of volcanic origin, surrounded by sericitic chert grains (?altered volcanic ash) (Sample B37, section B4, 6.7m, Capel Curig anticline).

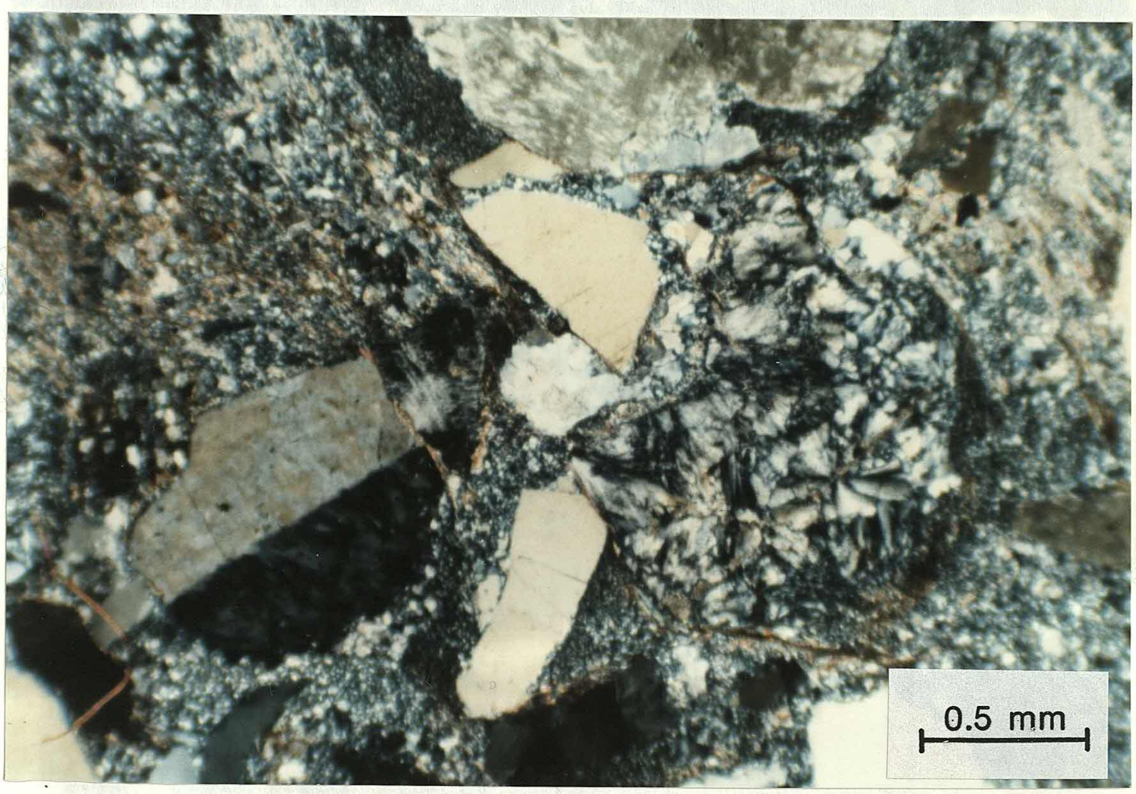

Fig. 3.41 Lithic fragment of chalcedony (CHALC: probably represents devitrified glassy rhyolite), sanidine crystal (KFELD) with simple twinning, and angular fragments of monocrystalline quartz set in a matrix of microcrystalline quartz. Sample C22, Section C1, 266m, Tryfan anticline, XPL.

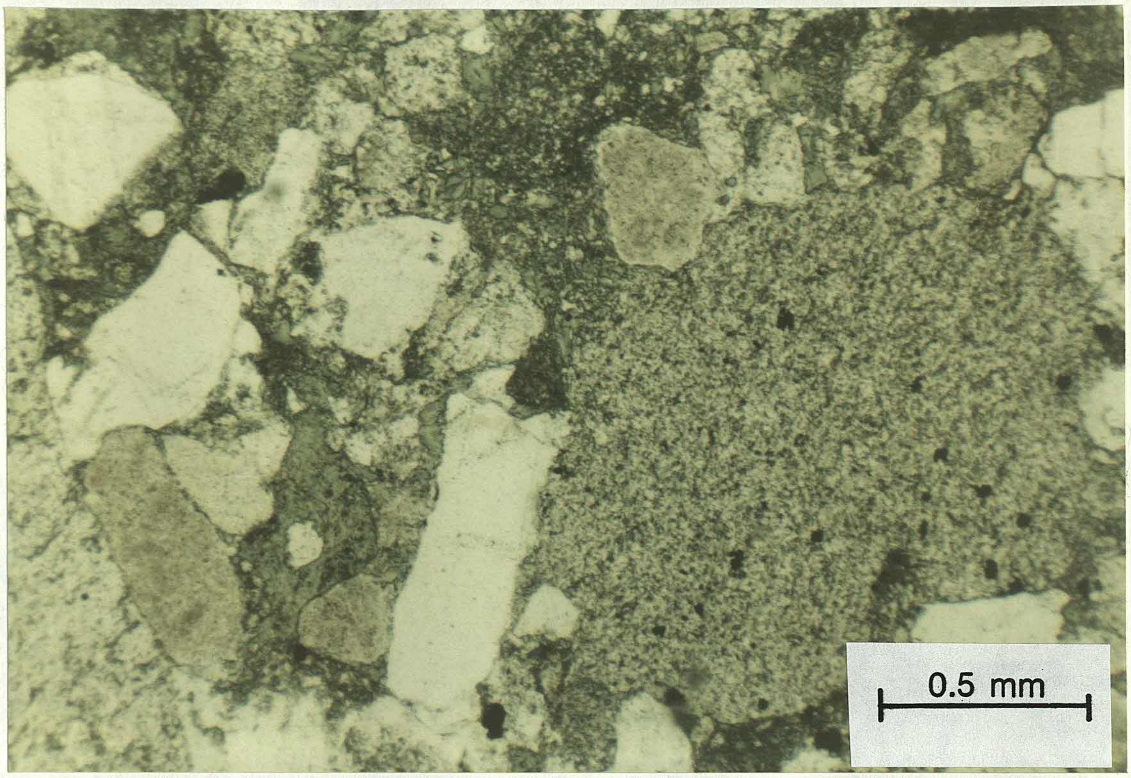

Fig. 3.39 Chert grain. PPL. Probably aphanitic felsitic volcanic rock fragment. (Sample F8, Section F1, ..m, Craig yr Ysfa.)

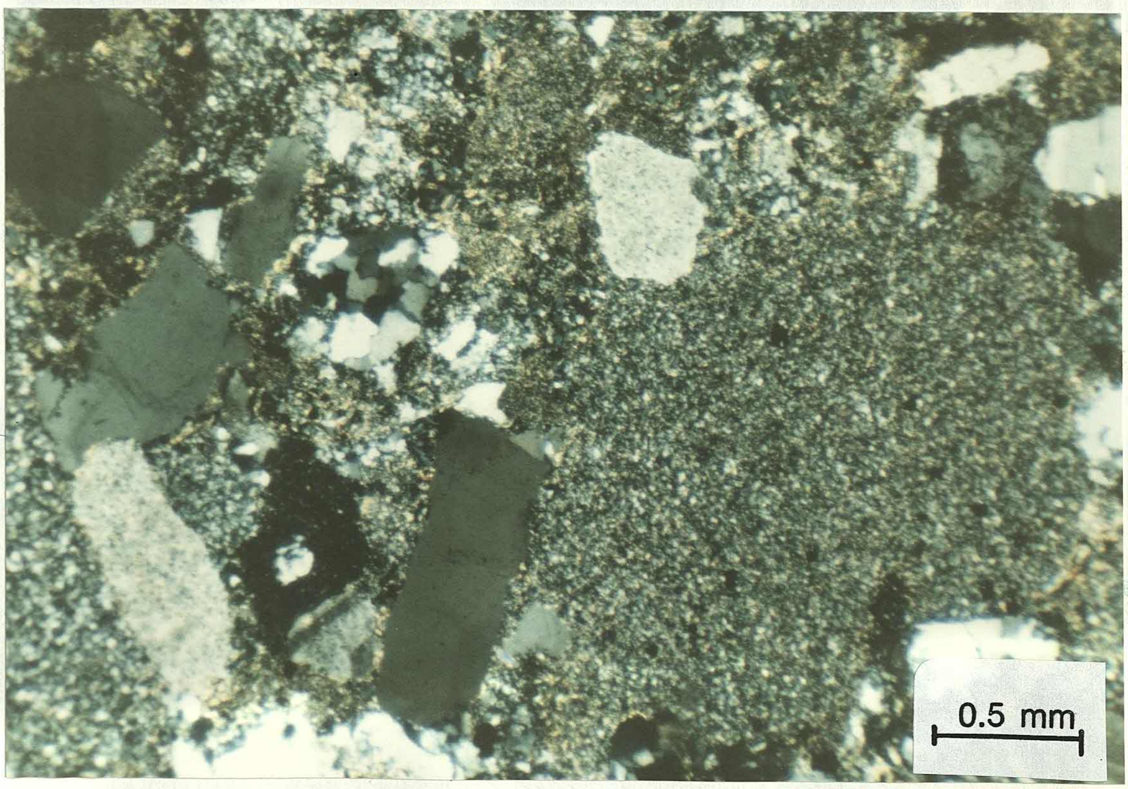

Fig. 3.40 Chert grain. XPL. As above.

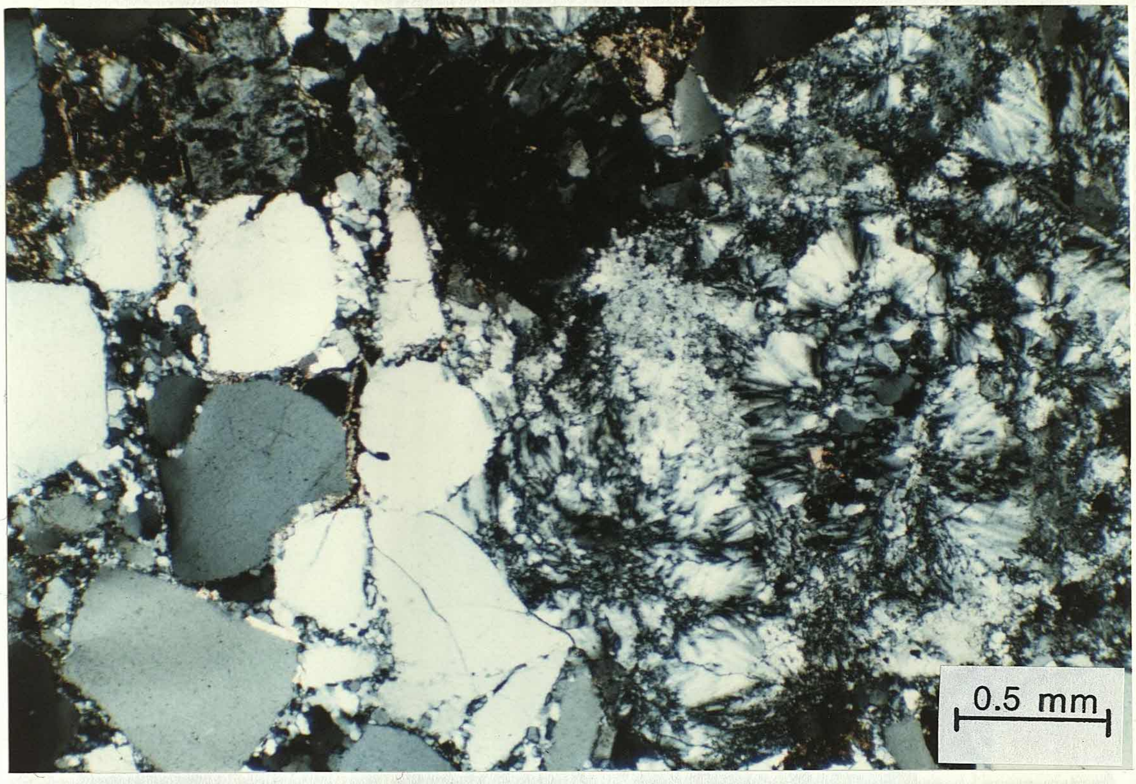

Fig. 3.42 ?Lithic fragment of chalcedony (CHALC) partially recrystallized to microcrystalline quartz (CHERT), set in a matrix of the same composition (Qpm). (Sample B34, Section B4, 13m, Capel Curig Mbr., Capel Curig anticline) XPL.

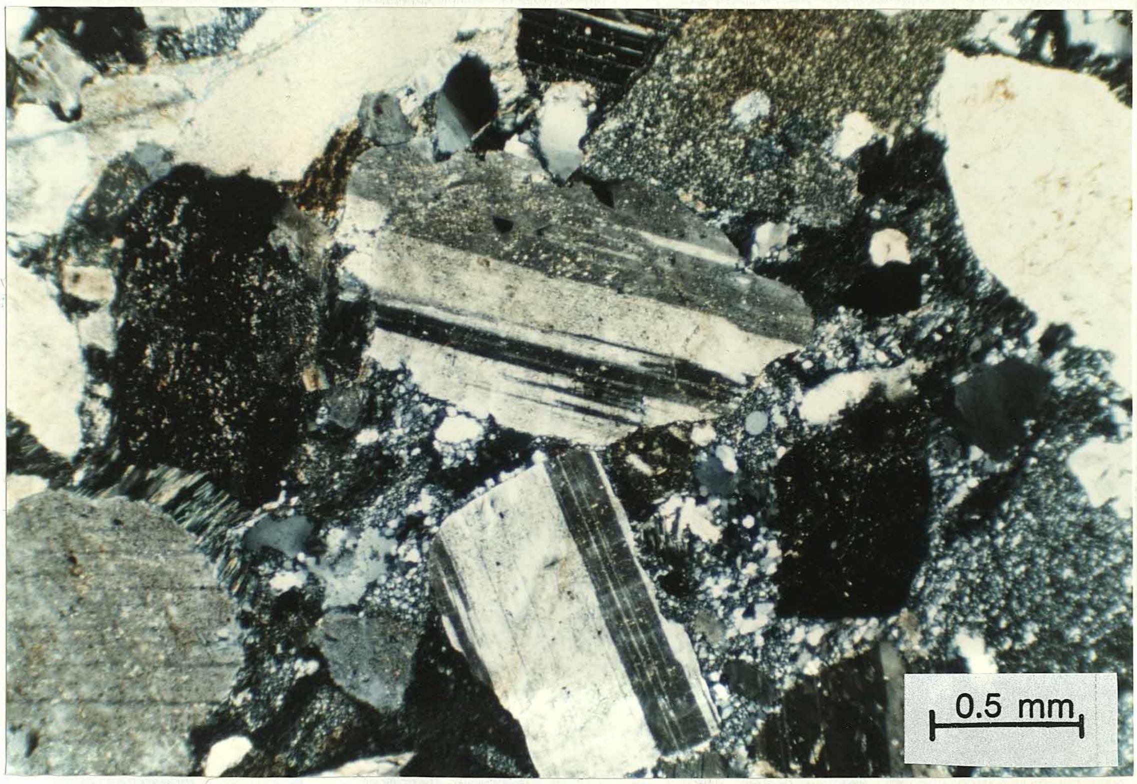

Fig. 3.43 Euhedral and subhedral crystals of plagioclase (PLAG), "chert" of volcanic origin (Lv), and monocrystalline quartz (Qm) set in a matrix of microcrystalline quartz (Qpm). (Sample C15B, Section C1, 167m, Magnetite Mbr. of Tryfan Fm.). XPL.

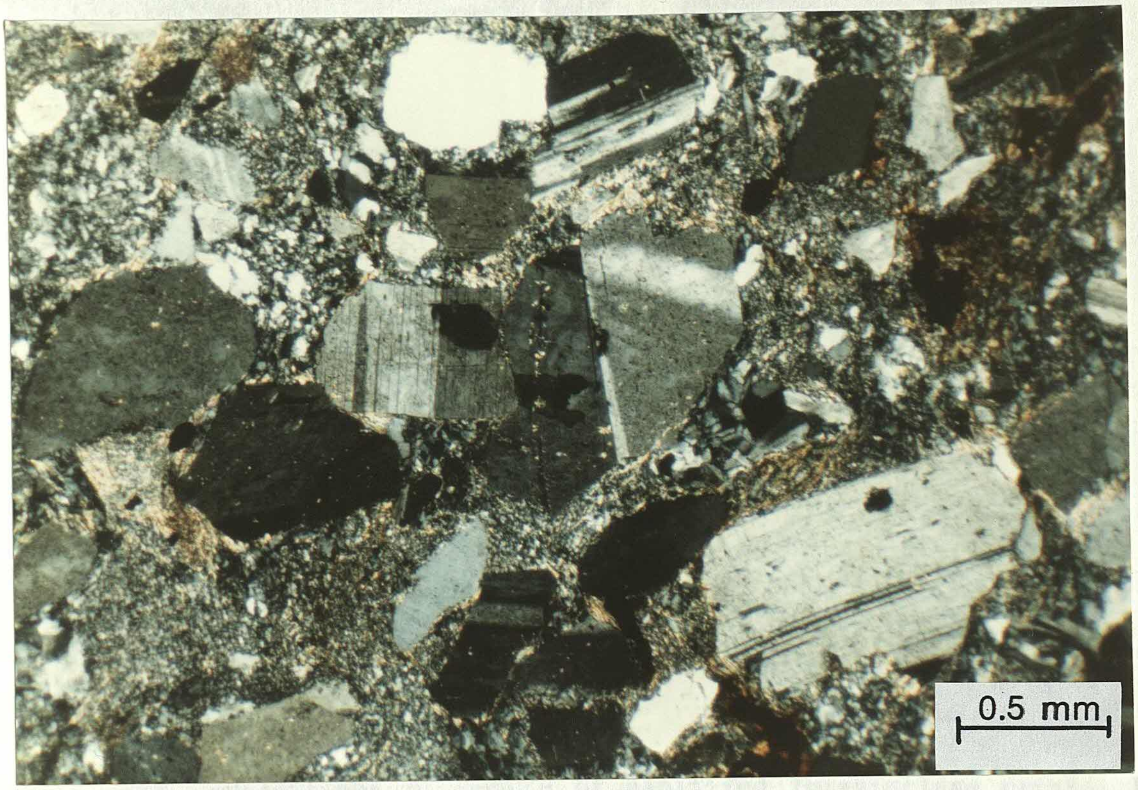

Fig. 3.44 Crystal rich volcaniclastic sandstone dominated by subhedral grains of plagioclase (PLAG) and untwinned ?K-feldspar in quartz-sericite aggregate matrix (QS). (Sample L16, Section L2, 147.1m, Hebog Mbr. of Cwm Eigiau Fm.) XPL.

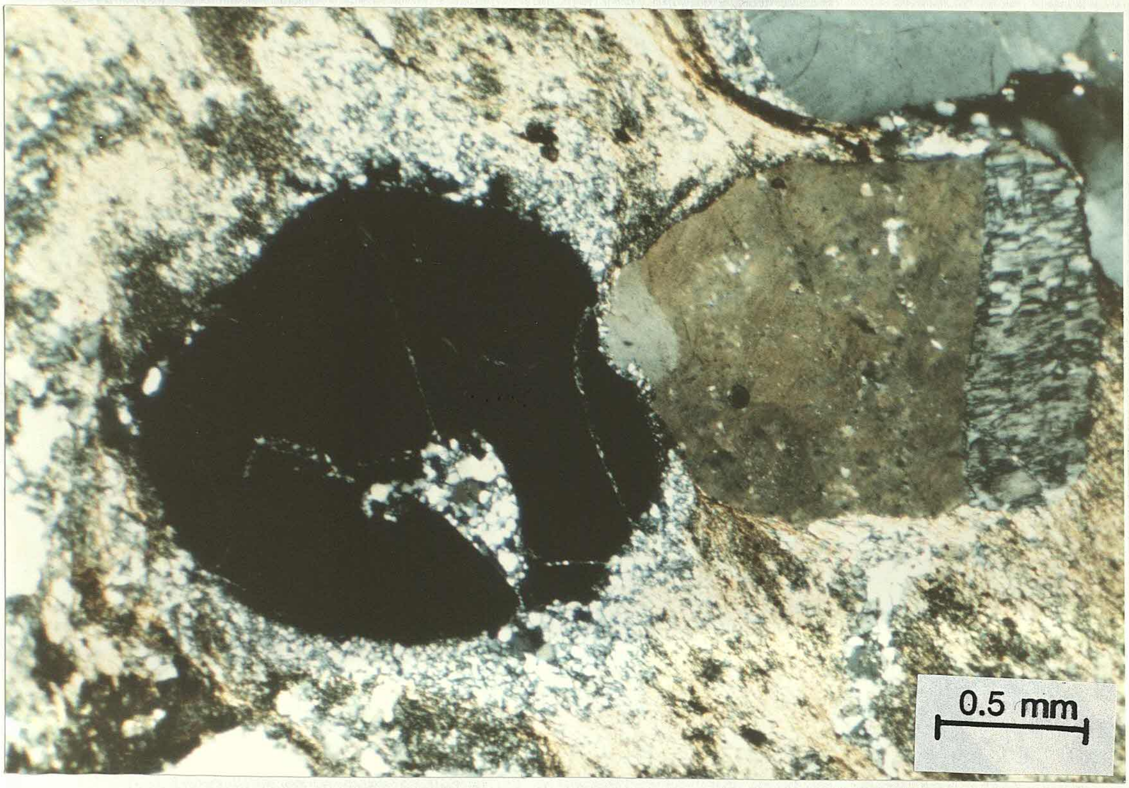

Fig. 3.45 Partially albitized crystal of simply twinned sanidine (KFELD), and fractured, embayed crystal of monocrystalline quartz (Qm). Both grains are probably of volcanic origin. (Sample C22, Section C1, 266m, Capel Curig Mbr. of Tryfan Fm.) XPL.

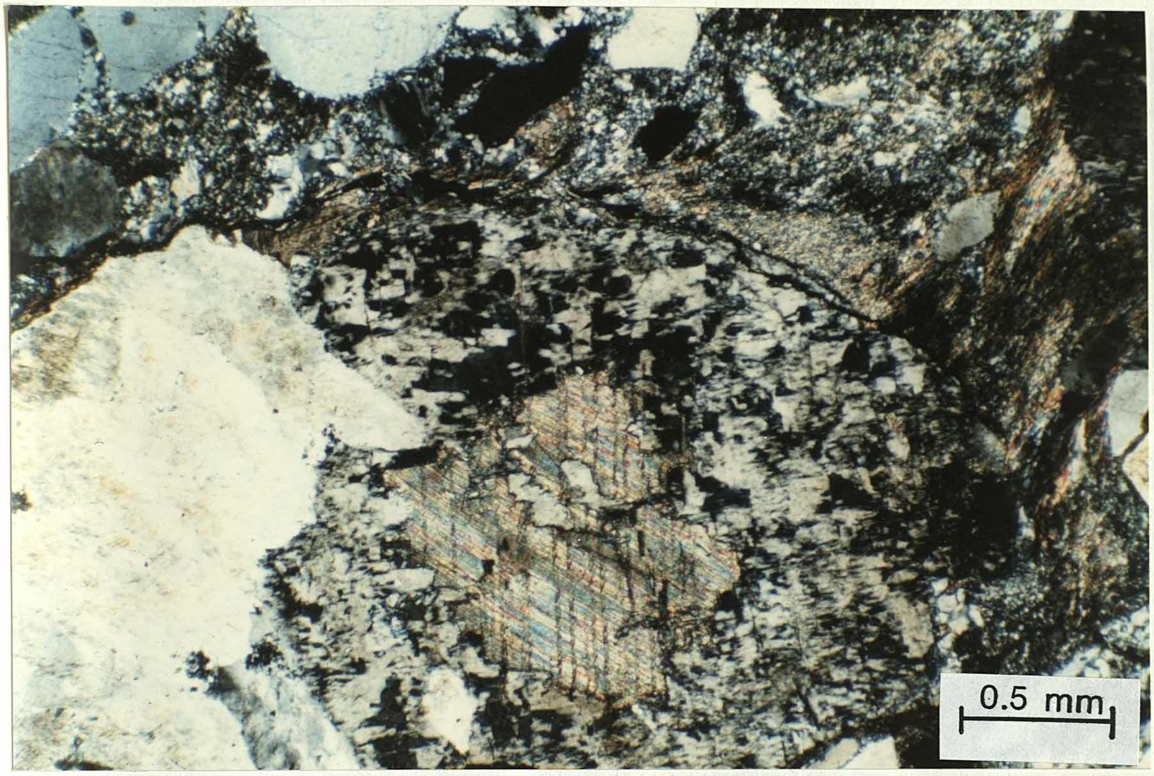

FIG. 3.46 Replacement of centre of albitized ?plagioclase crystal by calcite suggested original crystal fragment was chemically zoned. Sample C22, section C1, 266m, Capel Curig Mbr., Tryfan slopes. XPL.

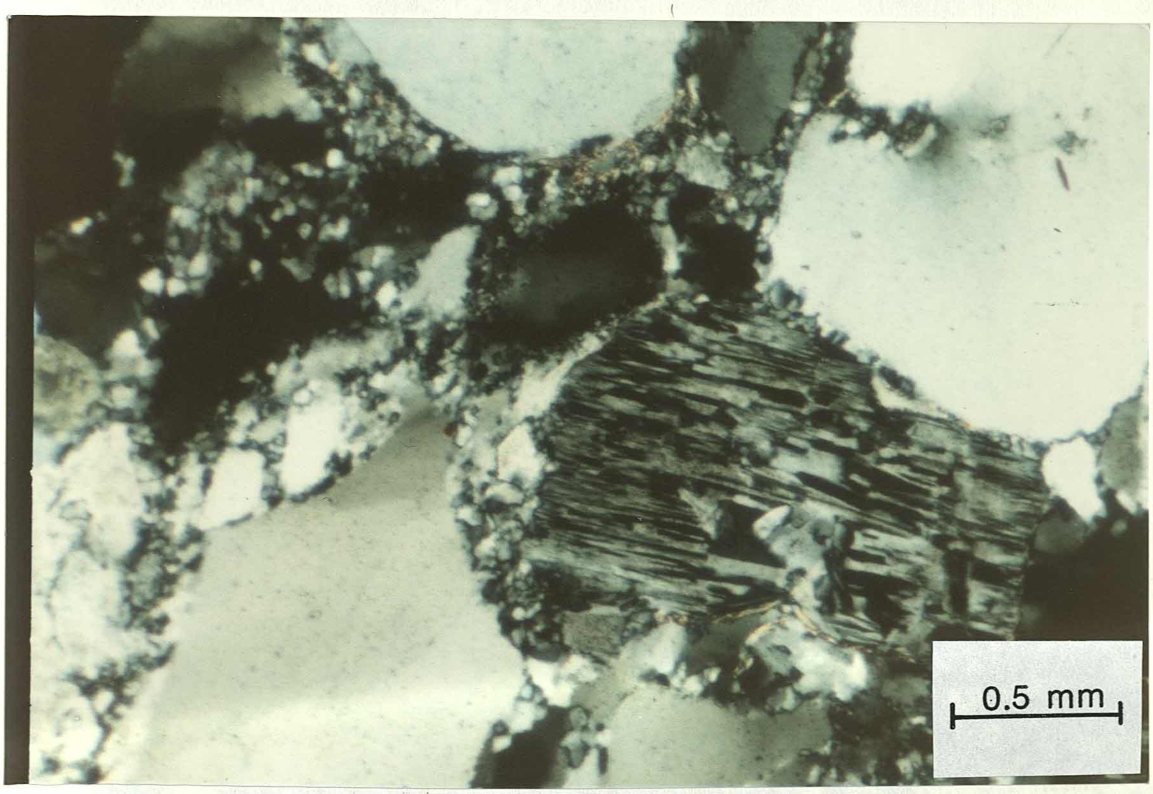

Fig. 3.47 Completely albitized crystal of K-feldspar, surrounded by monocrystalline quartz, and set in a quartz-rich matrix. (Sample B30, Section B4, Capel Curig Mbr. of Tryfan Fm.) XPL.

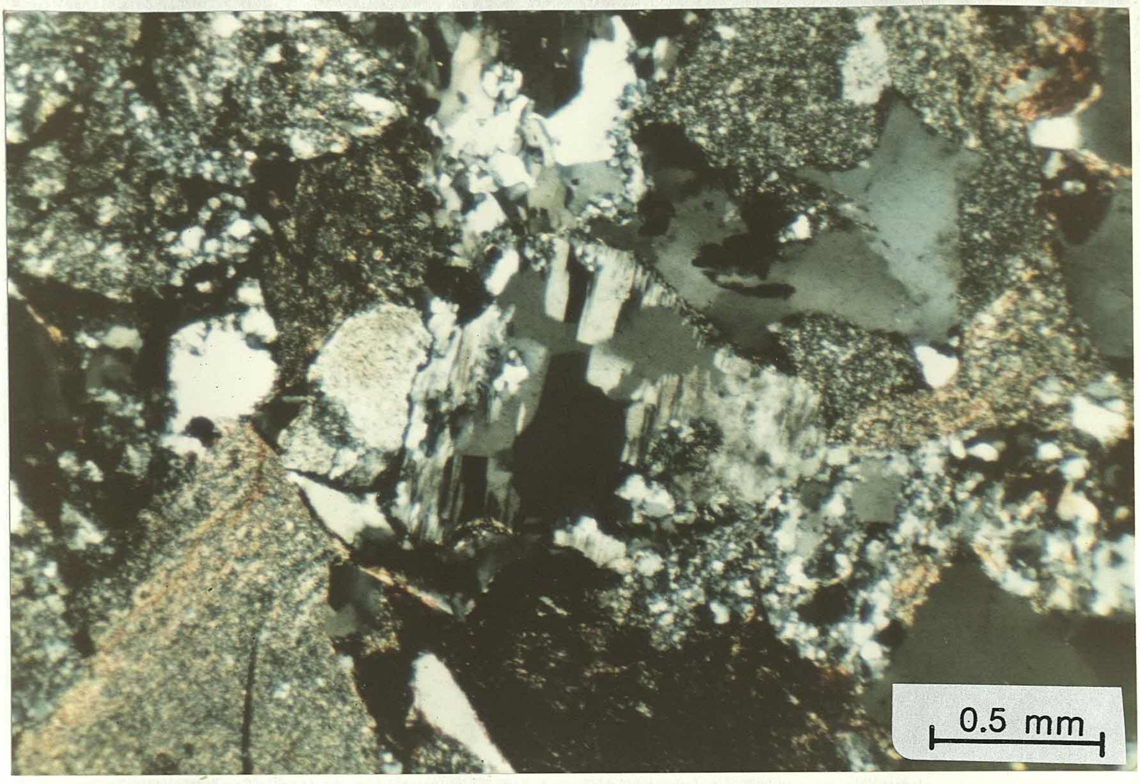

Fig. 3.48 CLast of granite consisting of monocrystalline quartz (Qm:centre, and surrounded by albitized K-feldspar (KFELD). Surrounding lithic fragments are dominantly sericitic chert (SCHT) or chert (CHERT). (SAMPLE C26, Section C1, 300m, Moel Siabod Mbr. of Tryfan Fm.) XPL.

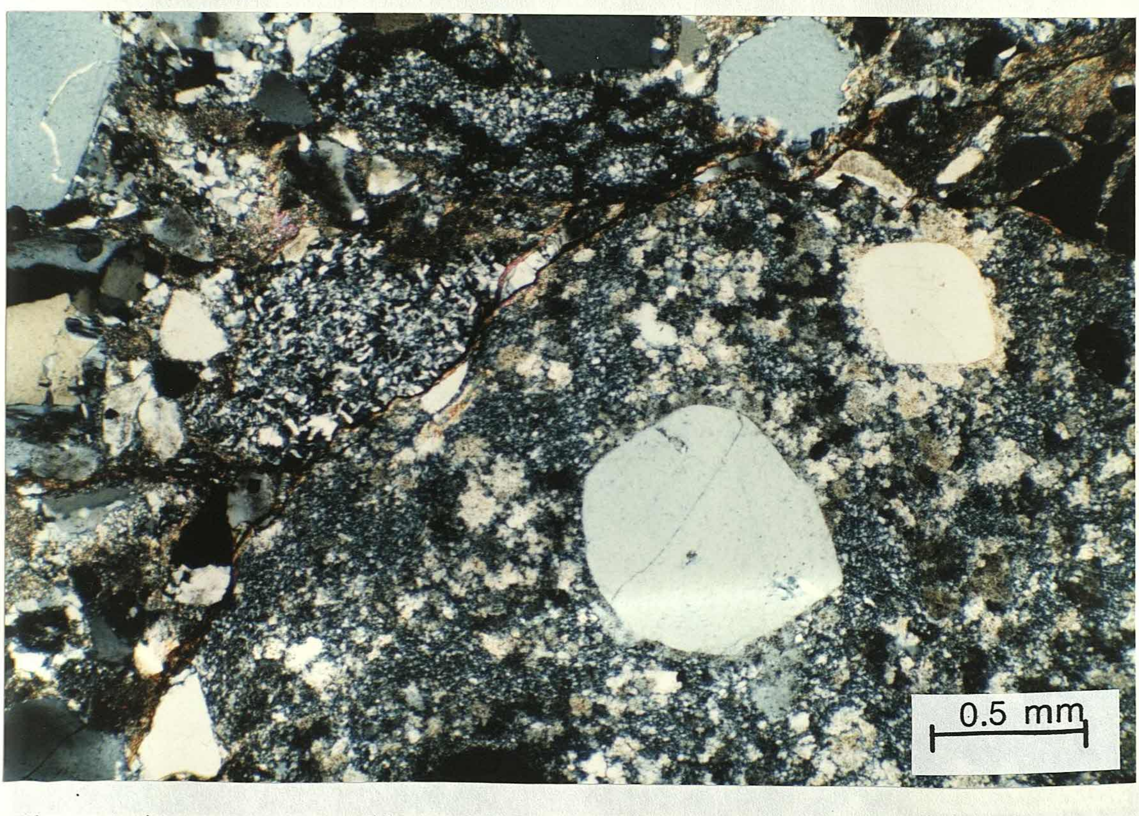

Fig. 3.49 Large well rounded lithic fragment of quartz porphyry. (Sample B32, Section B4, 5m, Capel Curig Mbr. of Tryfan Fm., Capel Curig anticline). XPL.

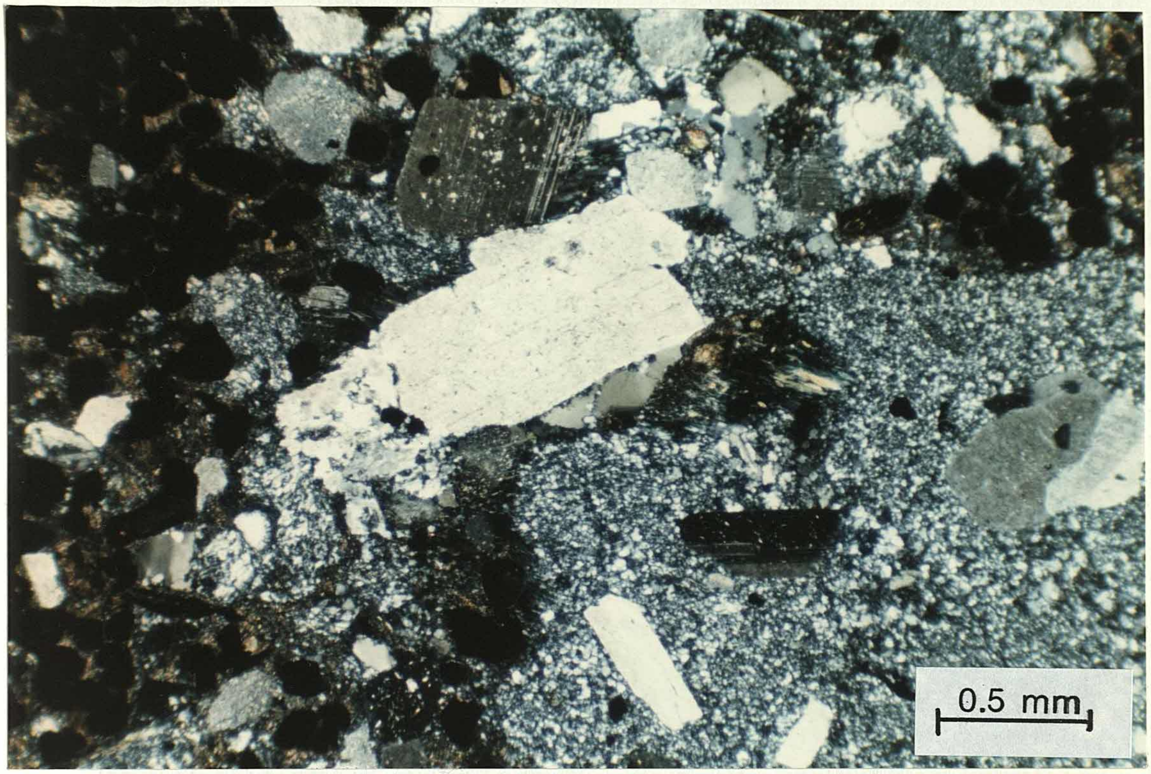

Fig. 3.50 Large, sub-rounded clast of porphyritic rhyolite (bottom right) with phenocrysts of plagioclase or K-feldspar. Surrounded by subhedral plagioclase crystals (PLAG) and small opaque grains of magnetite. Heavy minerals are **not** in hydraulic equilibrium with the larger rhyolite clast or even plagioclase crystals. (Sample C15A, Section C1, 167m, Magnetite Mbr. of Tryfan Fm.) XPL.

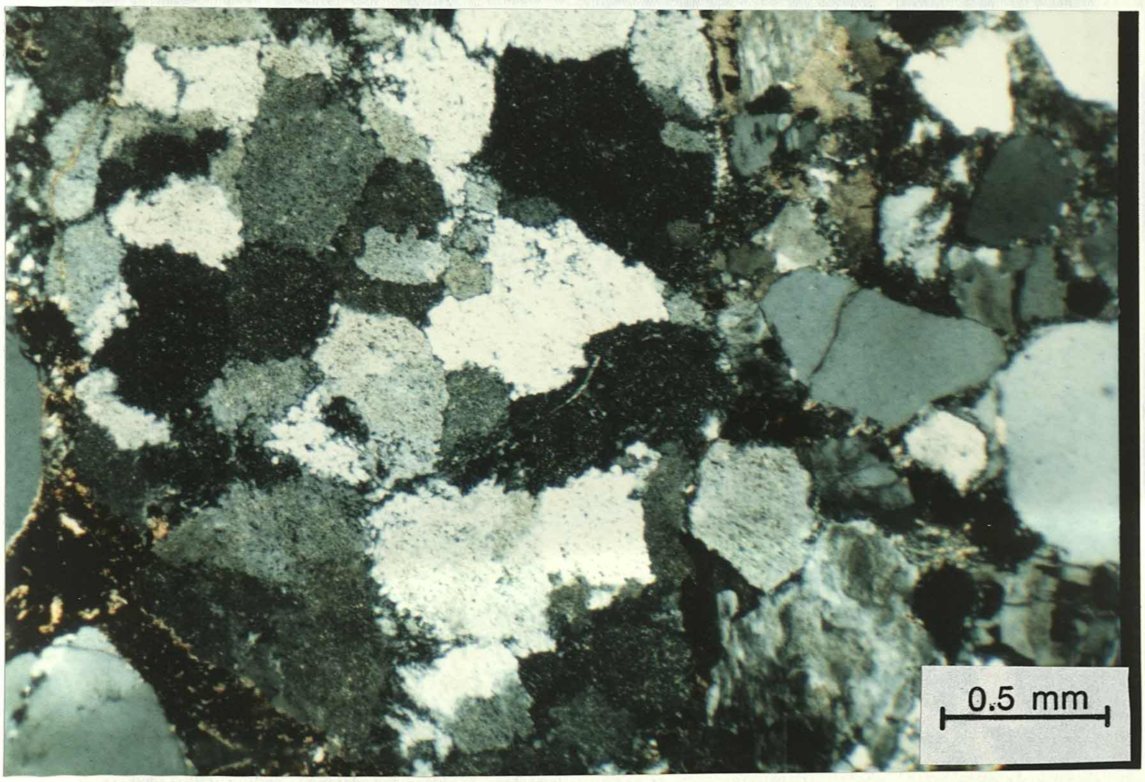

Fig. 3.51 Large lithic clast of microgranite. Portion shown consists of a apilitic intergrowth of K-feldspar. (Sample B37, Section B4, 13m, Capel Curig Mbr. of Tryfan Fm.) XPL.

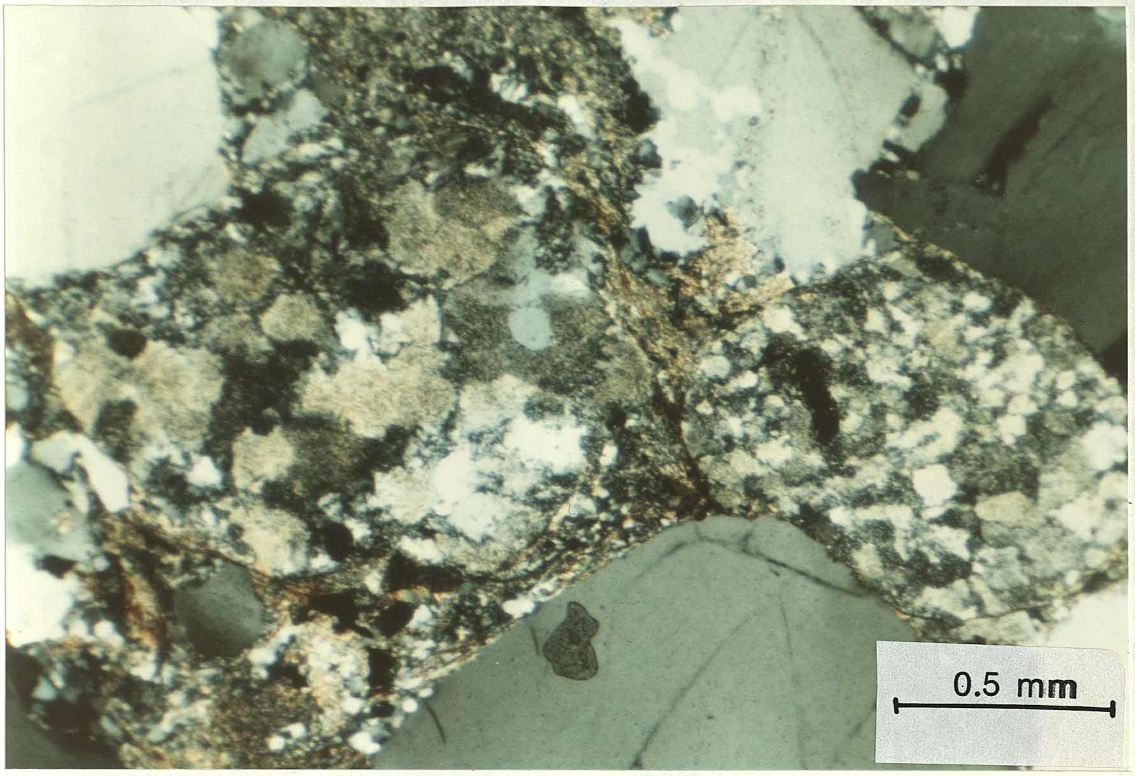

Fig. 3.52 Small lithic fragments of microgranite containing a granular intergrowth of quartz and K-feldspar. (Sample B32, Section B4, 5m, Capel Curig Mbr. of Tryfan Fm.) XPL.

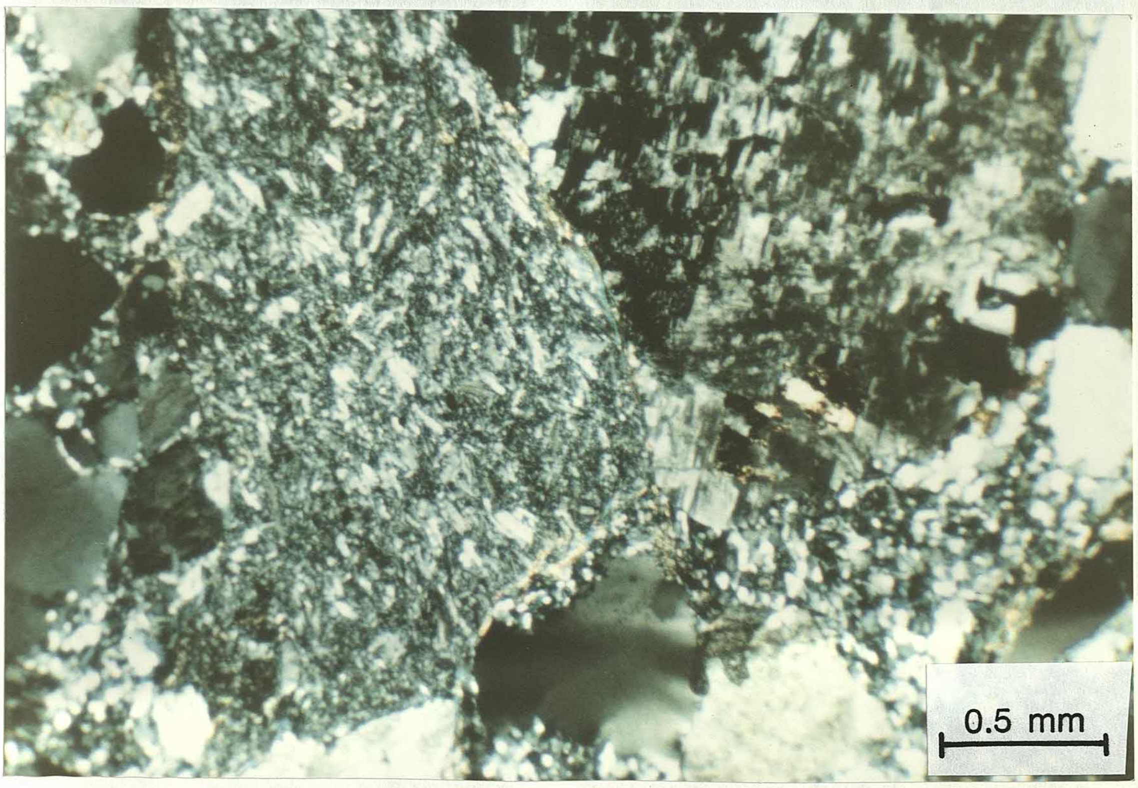

Fig. 3.53 Clast of ?Dacite with trachytic texture, and completely albitized K-feldspar fragment. (Sample B33, Section B4, 6.7m, Capel Curig Mbr. of Tryfan Fm.) XPL.

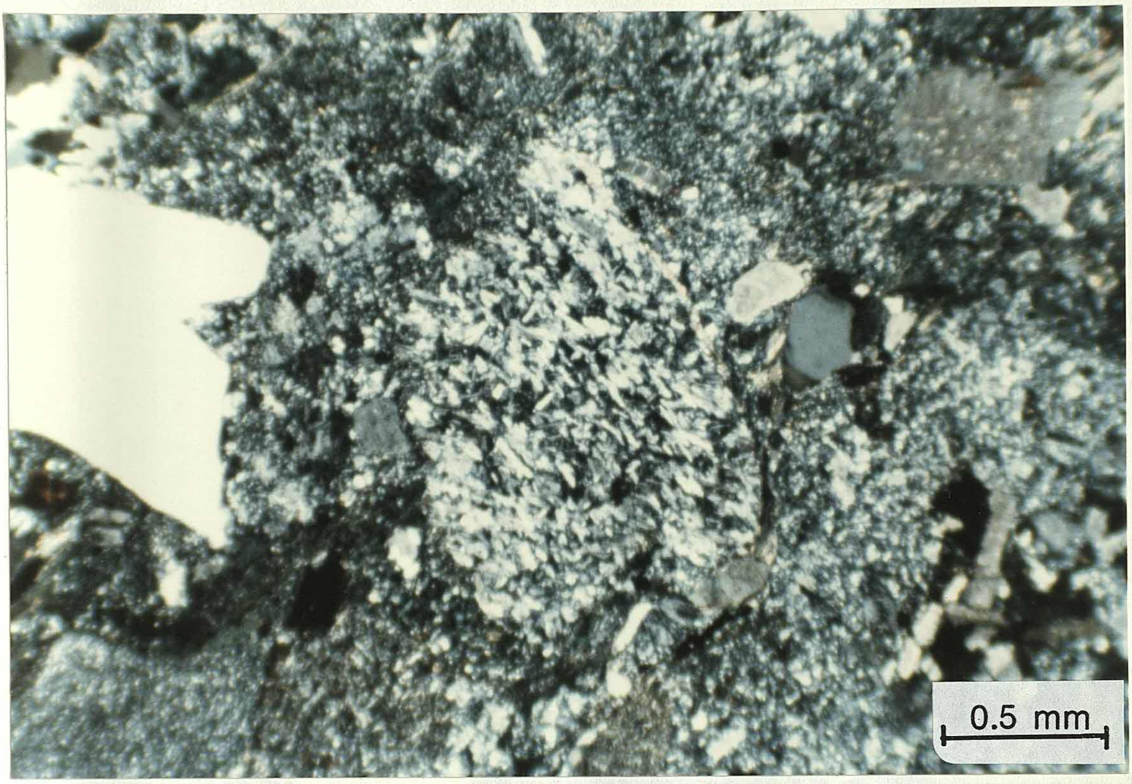

Fig. 3.54 Blurry photograph (Dept. of Earth Science, Oxford University microscope) of trachytic ?rhyolite (TRACH), volcanic "chert" (CHERT) and porphyritic rhyolite fragments (RHY), as well as crystal of monocrystalline quartz (Qm) in a matrix of microcrystalline quartz. (Sample C10, Section C1, 154m, Tryfan Fach Mbr. of Tryfan Fm.). XPL.

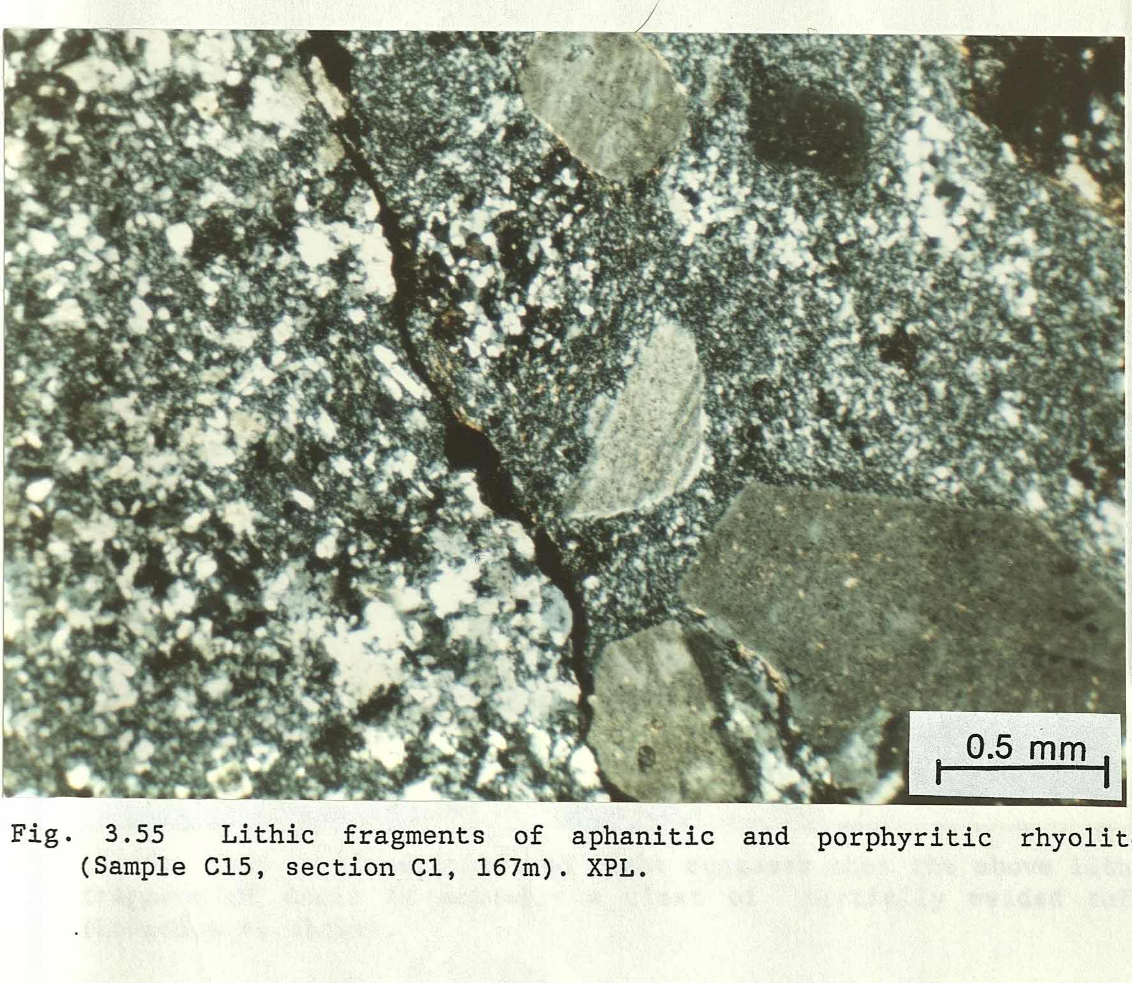

Fig. 3.55 Lithic fragments of aphanitic and porphyritic rhyolite. (Sample C15, section C1, 167m). XPL.

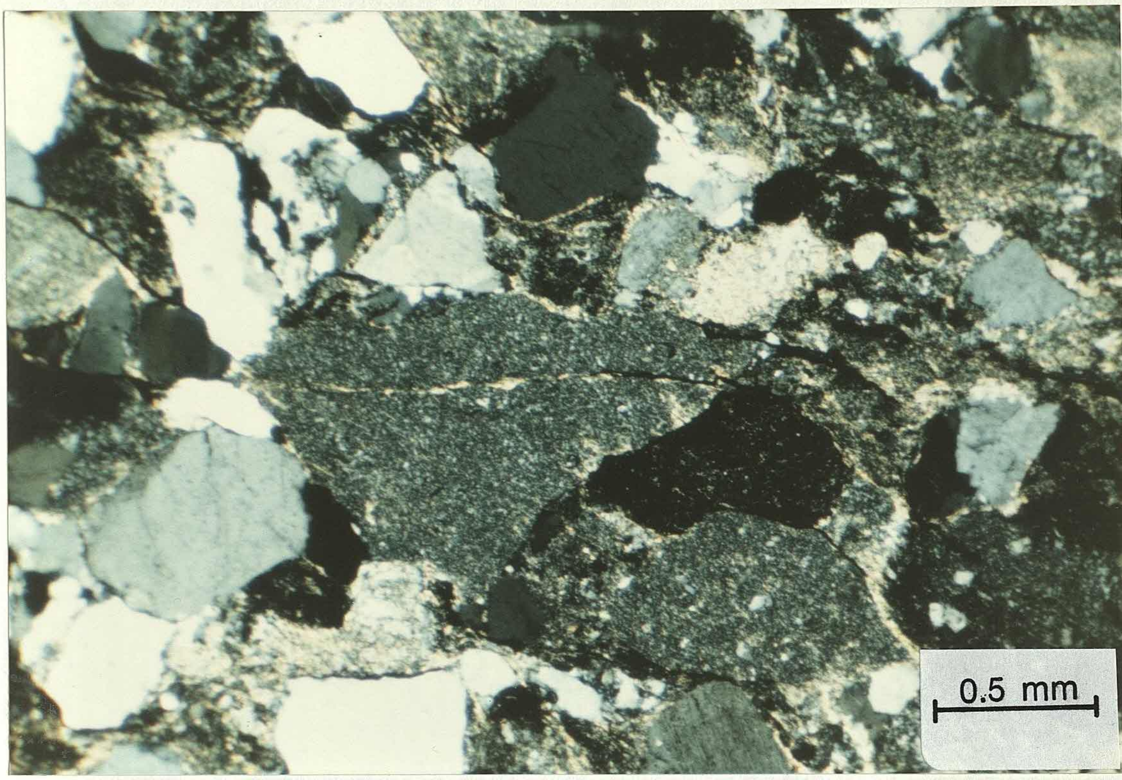

Fig. 3.56a Lithic fragment of chert (RHY). Occasional feldspar microlites as well as texture in PPL (see below) indicates a volcanic origin. (Sample S2, Section S2, Tryfan Fm., Tal-y-Fan.) XPL

Fig. 3.56b View in plane polarized light suggests that the above lithic fragment of chert is actually a clast of partially welded tuff. (Location as above).

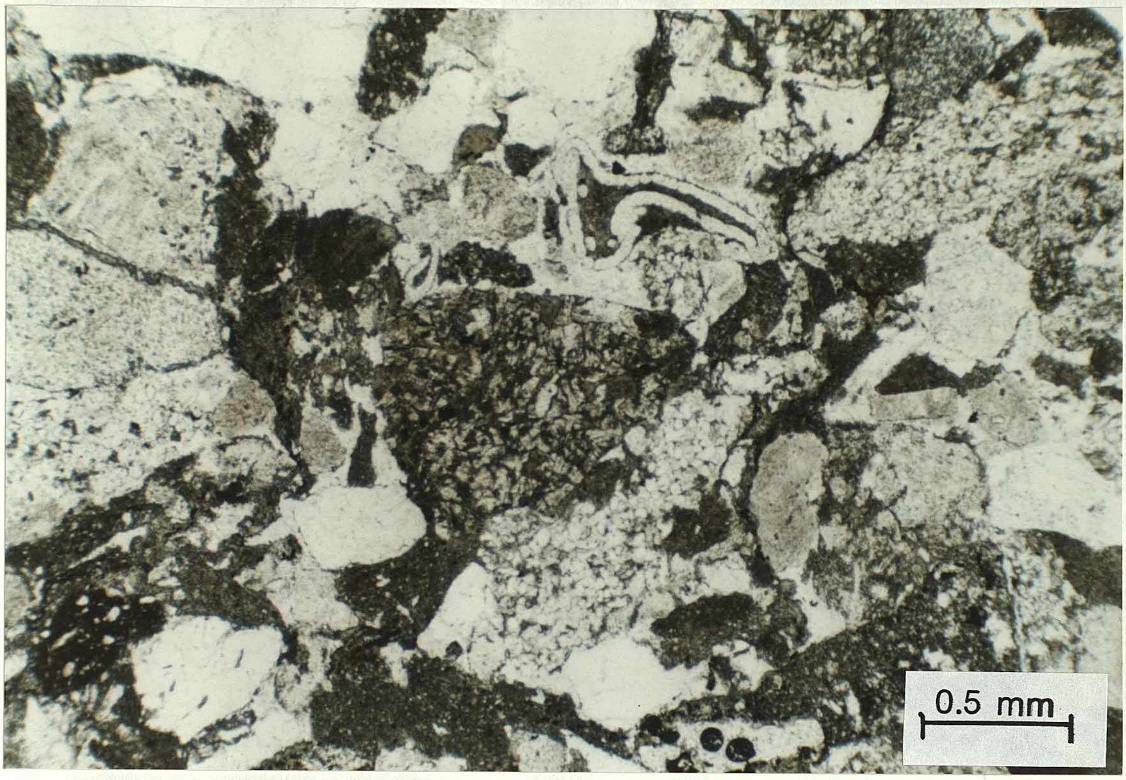

Fig. 3.57 Lithic fragments of mudstone (M) and ?basalt (BAS). At top of photo (A), ?devitrified glass shard is surrounded by microcrystalline quartz (Sample L1, section L1 86.5m, Hebog Mbr. of Lower Cwm Eigiau Fm.) PPL.

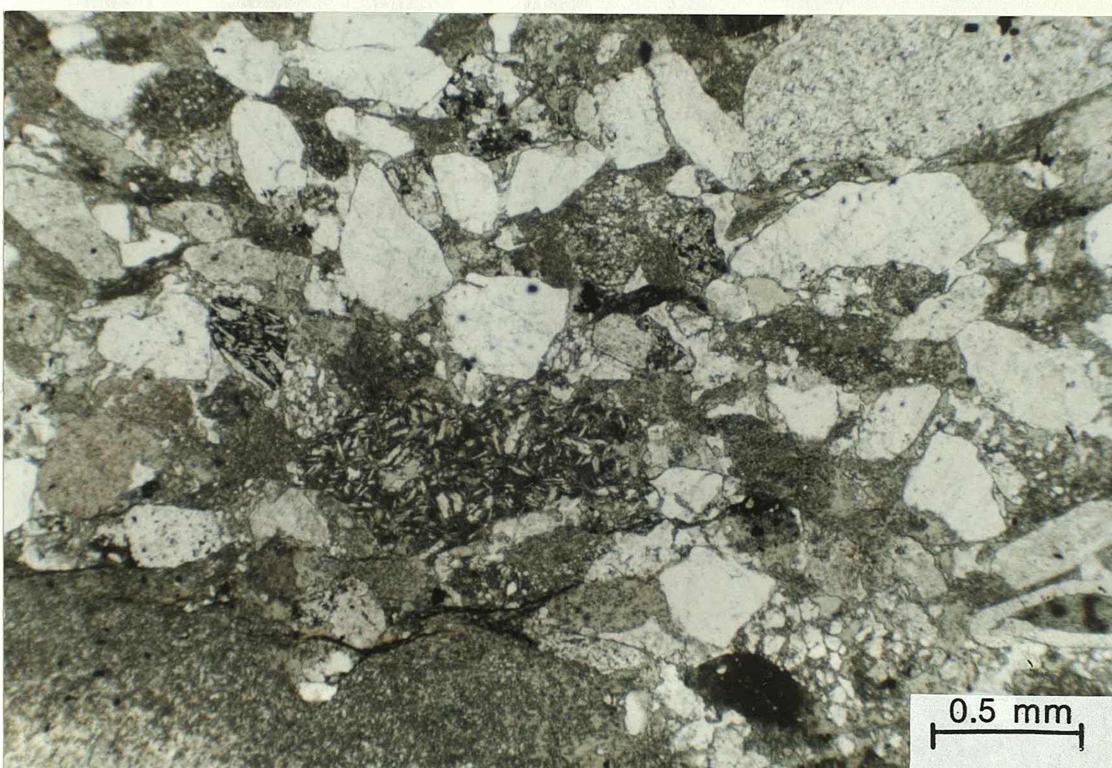

Fig. 3.58 Poorly sorted sandstone containing microlitic basalt lithic fragments (BAS), anhedral quartz crystals (Q), and rare rhyolite clasts (RHY) in clay rich matrix. (Sample L13, section L2, 112.3m, Hebog Mbr. of Lower Cwm Eigiau Fm., Hebog slopes) PPL.

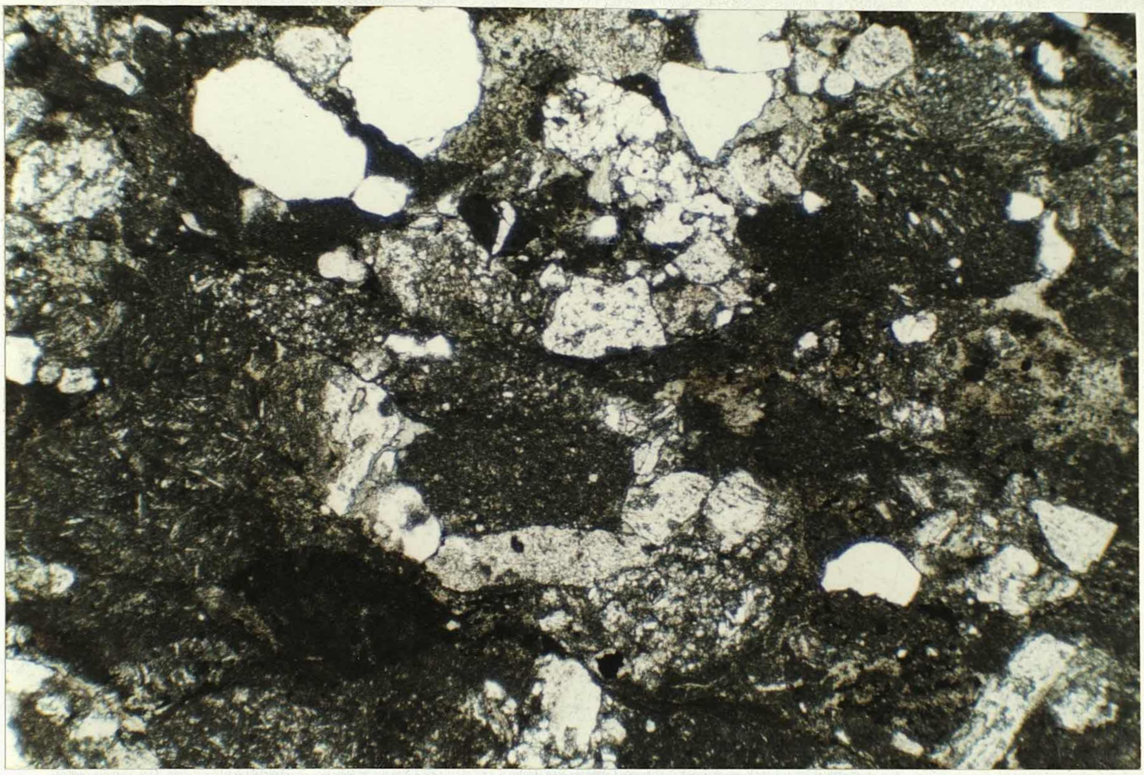

Fig. 3.59. Microlitic lithic fragments of basalt(BAS) in chloritic and clay rich matrix. (Sample L5, Section 12.56m Hebog Mbr. of Lower Cwm Eigiau Fm.)

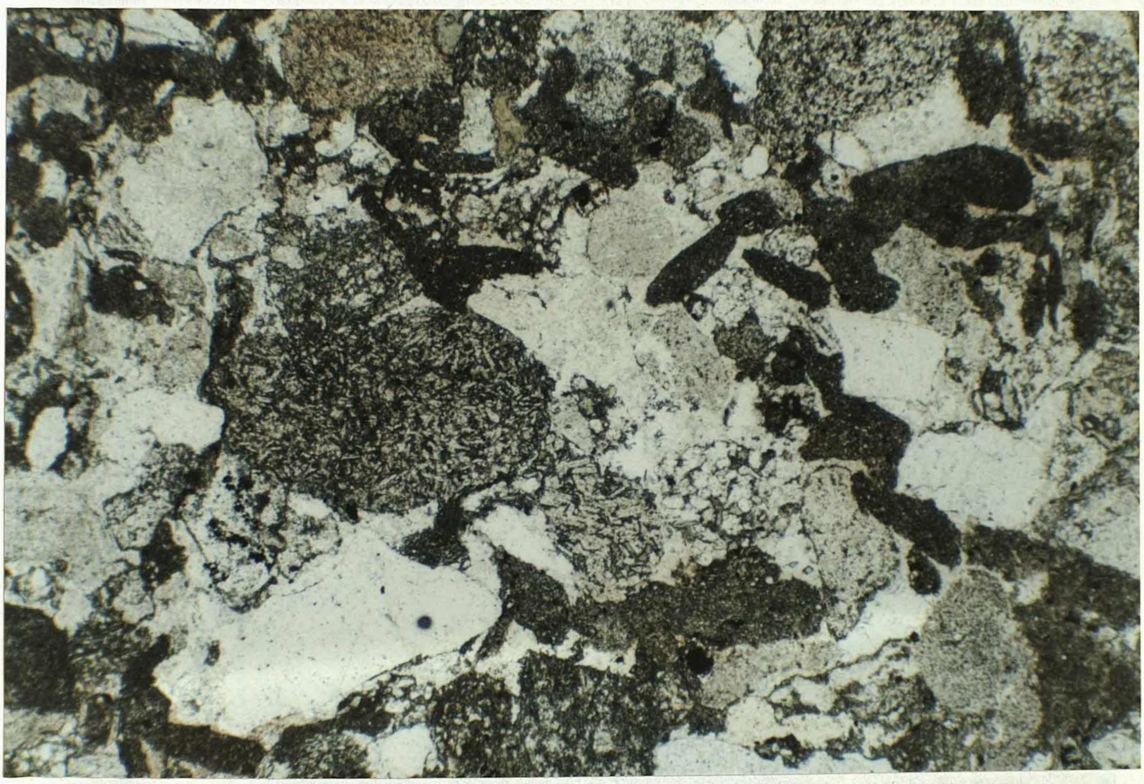

Fig. 3.60 Microlitic basalt fragments, rounded mudstone chips, plagioclase and dirty quartz in chloritic matrix. Sample L1, section L1, 86.5m. Hebog Mbr., Moel Hebog. PPL.

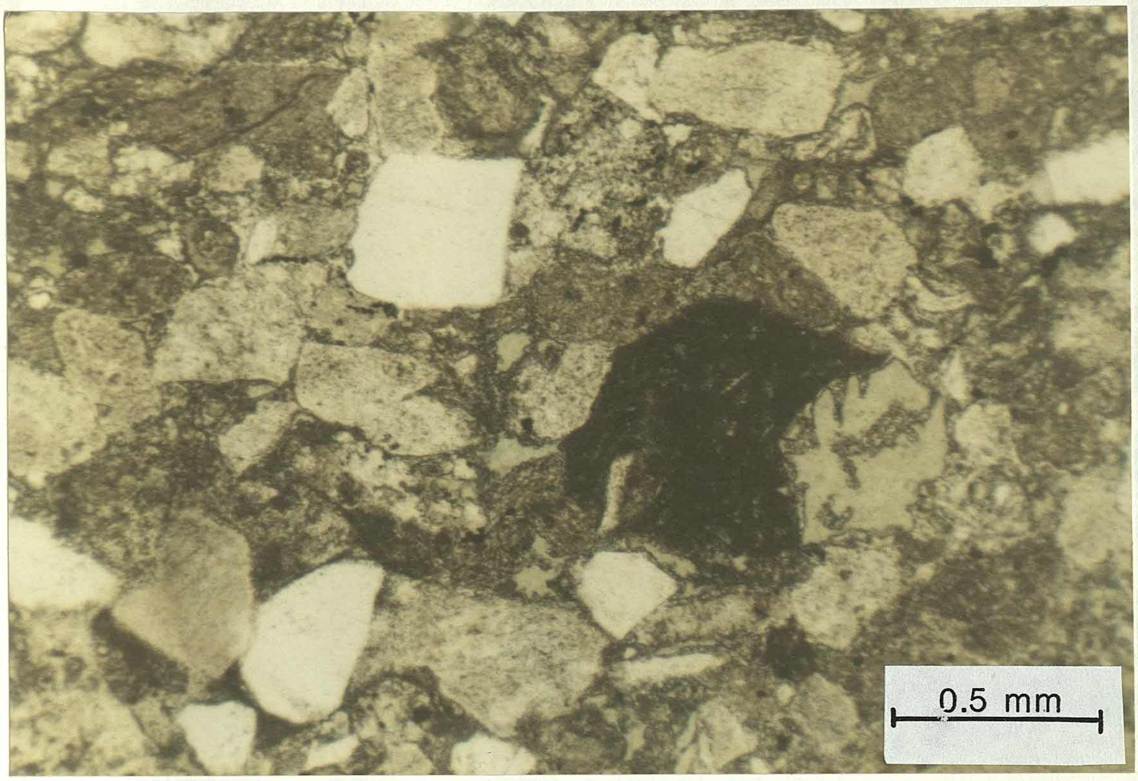

Fig. 3.61a Microlitic ?glassy basalt (BAS), sericitic mudstone (SCHT), quartz (Q) and ?untwinned plagioclase grains in chlorite/clay matrix. (Sample L16, Section L2, 147.1m, Hebog Mbr. of Lower Cwm Eigiau Fm.)

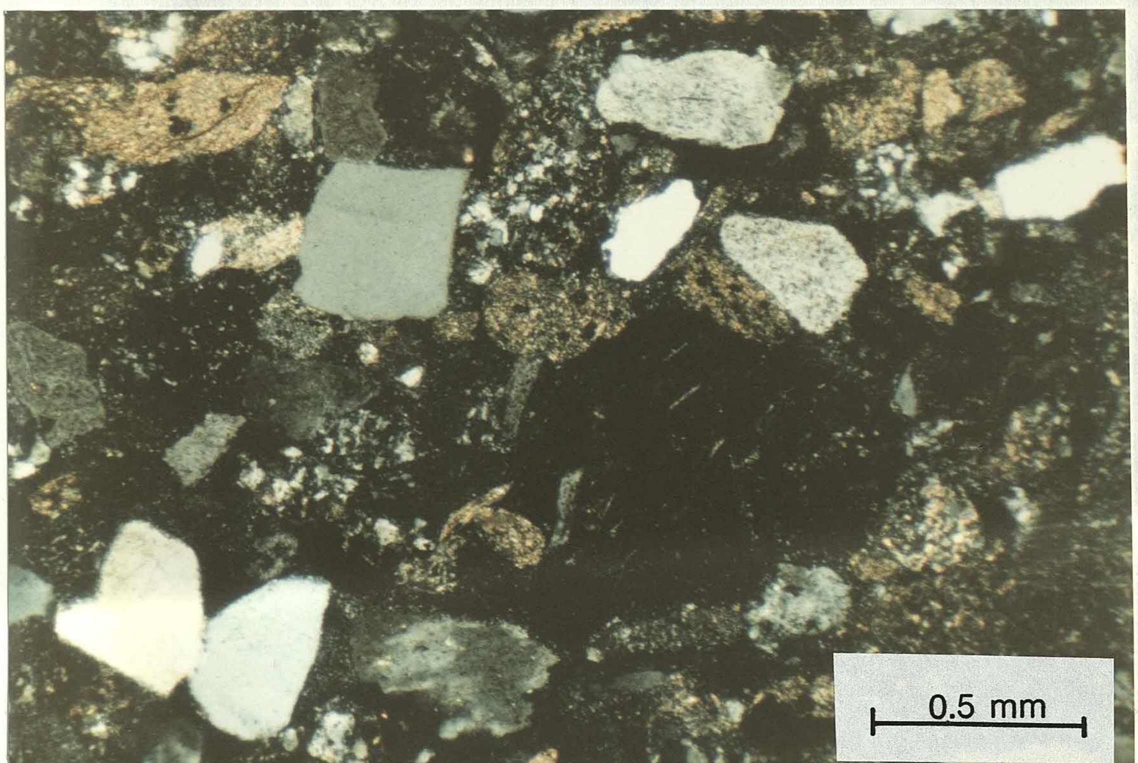

Fig. 3.61b As above, crossed polars.

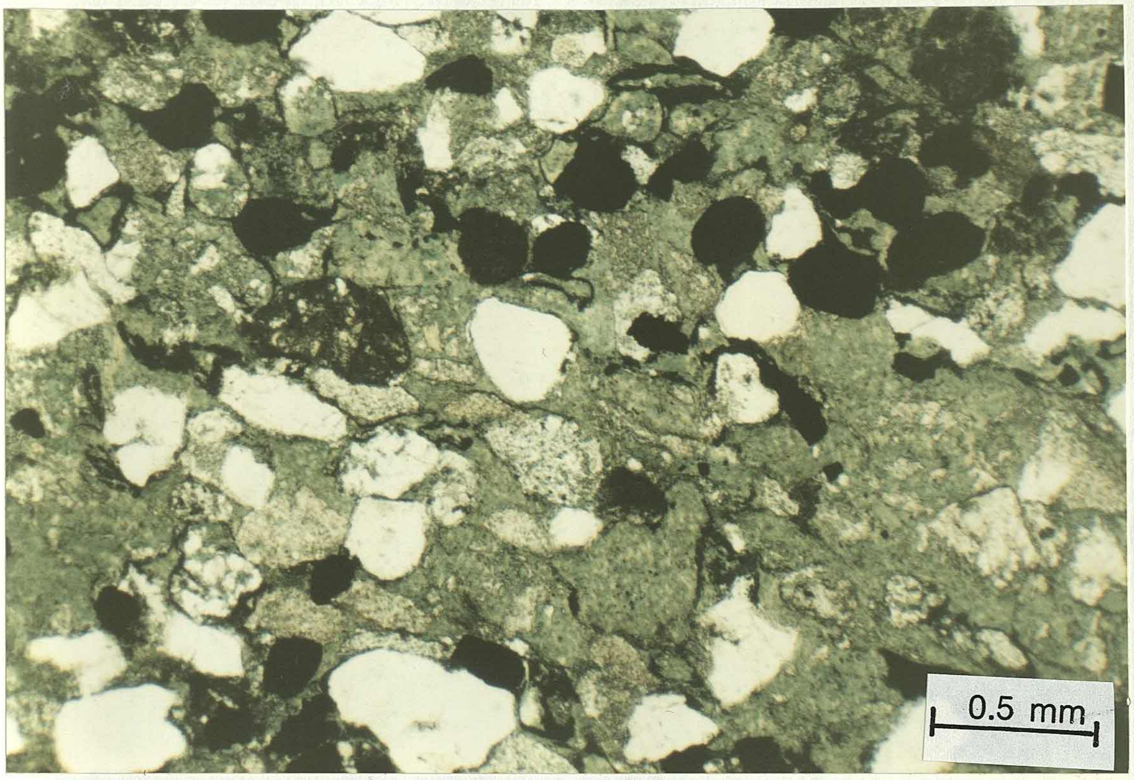

Fig. 3.62 Chloritic lithic fragments (BAS) interpreted to represent altered basalt clasts, monocrystalline quartz (Qm), and opaque magnetite grains in a matrix/cement consisting entirely of chlorite. Sample C12, section C1, 160m. Magnetite Mbr., Tryfan anticline. PPL.

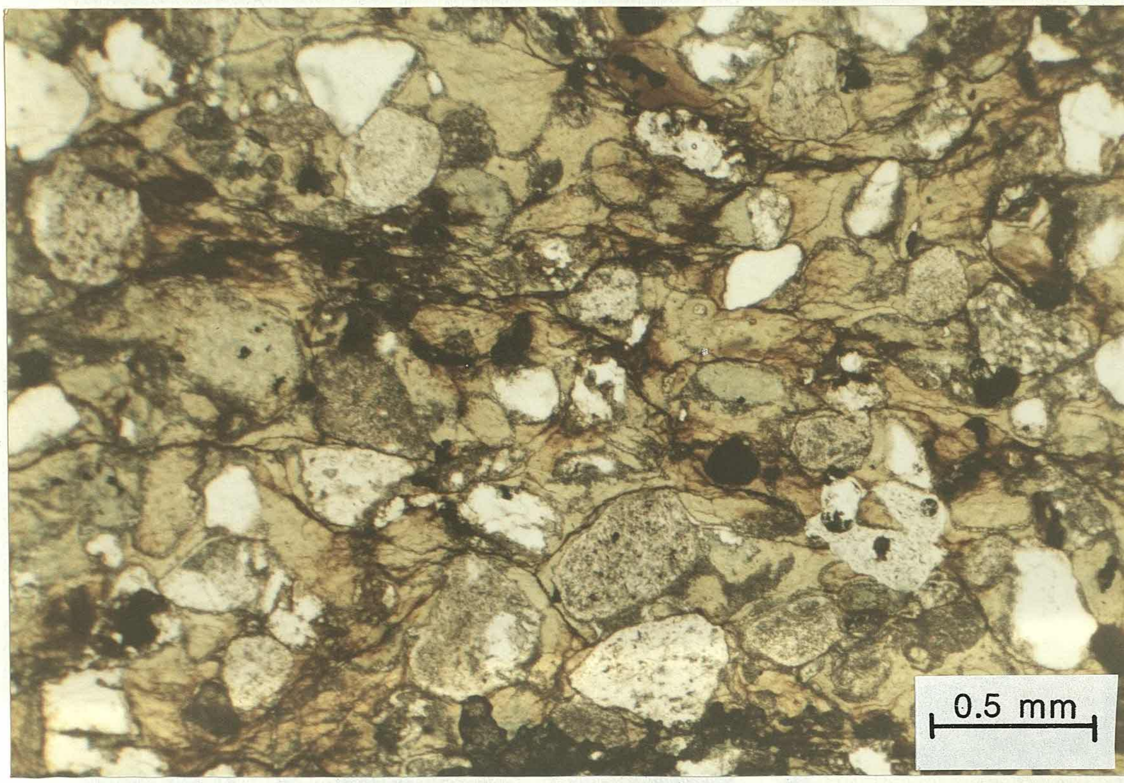

Fig. 3.63 Chlorite and haematite rich matrix, with scattered lithic fragments of microlitic or chloritic basalt (BAS) and anhedral grains of monocrystalline quartz. (Sample L15, Section L2, 144.5m, Hebog Mbr. of Lower Cwm Eigiau Fm.) PPL.

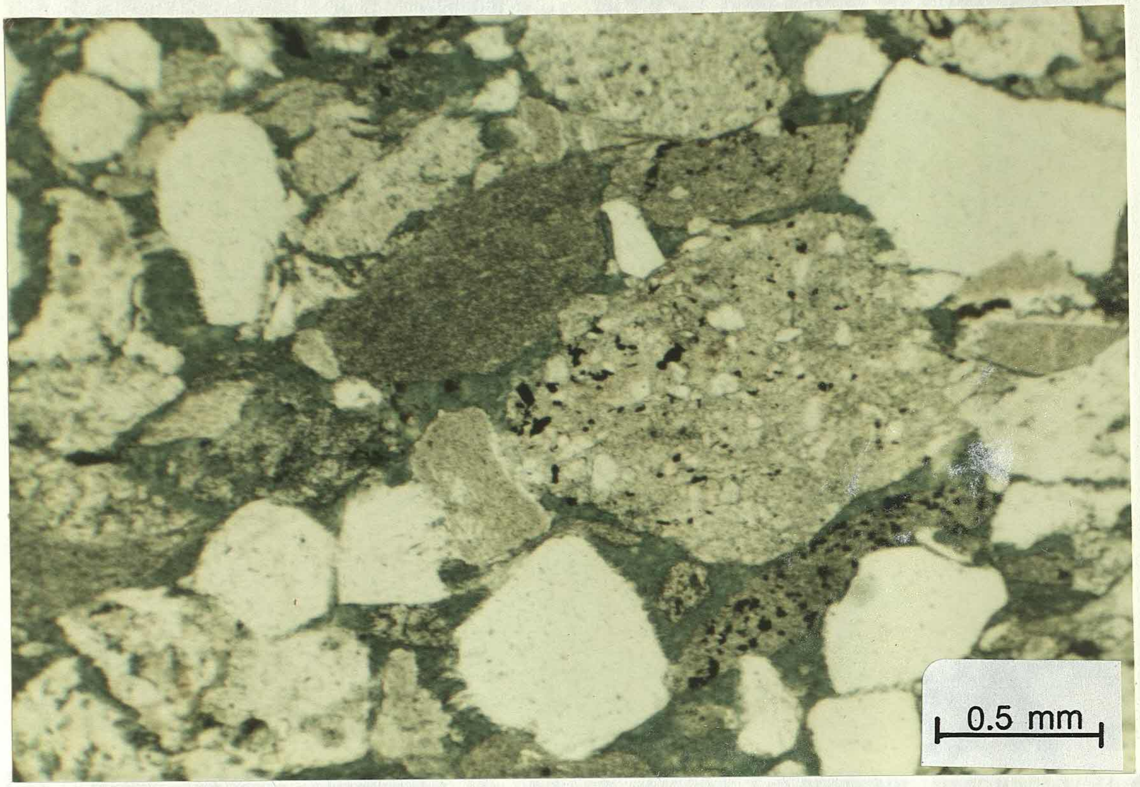

Fig. 3.64 Grains of sericitic mudstone (SCHT), tuffaceous sandstone (SS), monocrystalline quartz, and plagioclase in chlorite matrix. (Sample F17a, Section F1, 95.1m, Moel Siabod Mbr. of Tryfan Fm.)

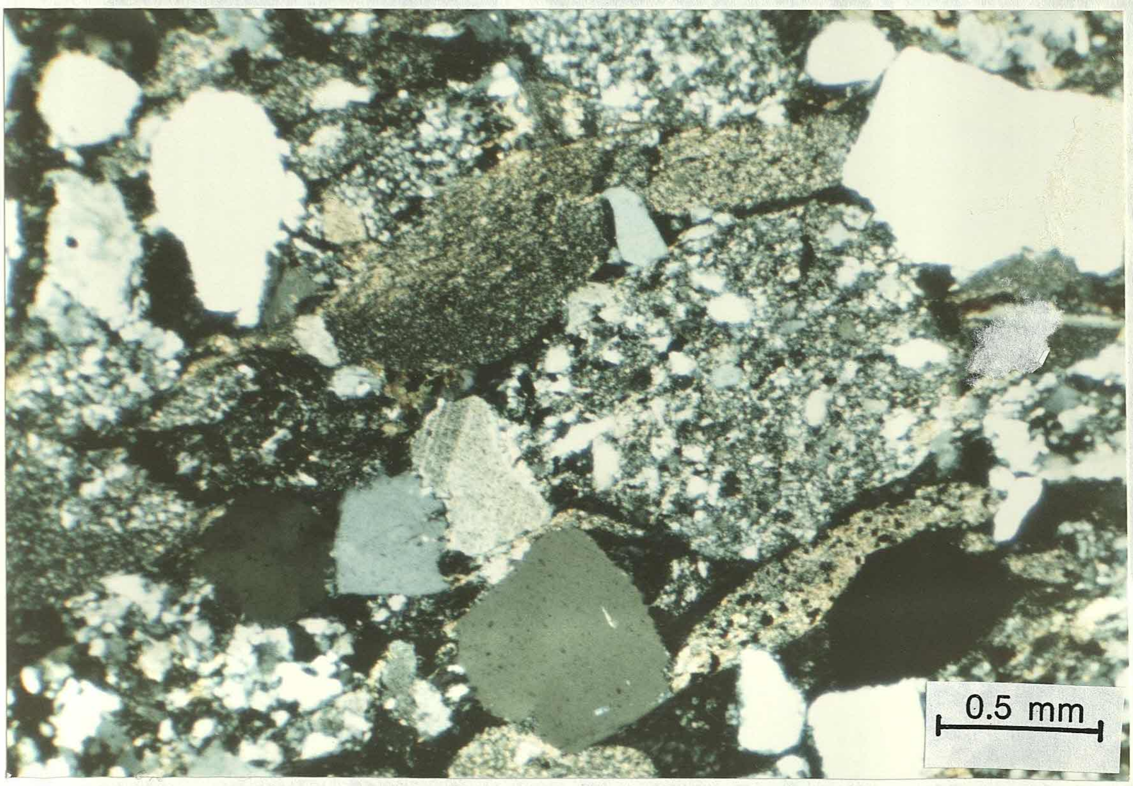

Fig. 3.64b As above. Crossed polars.

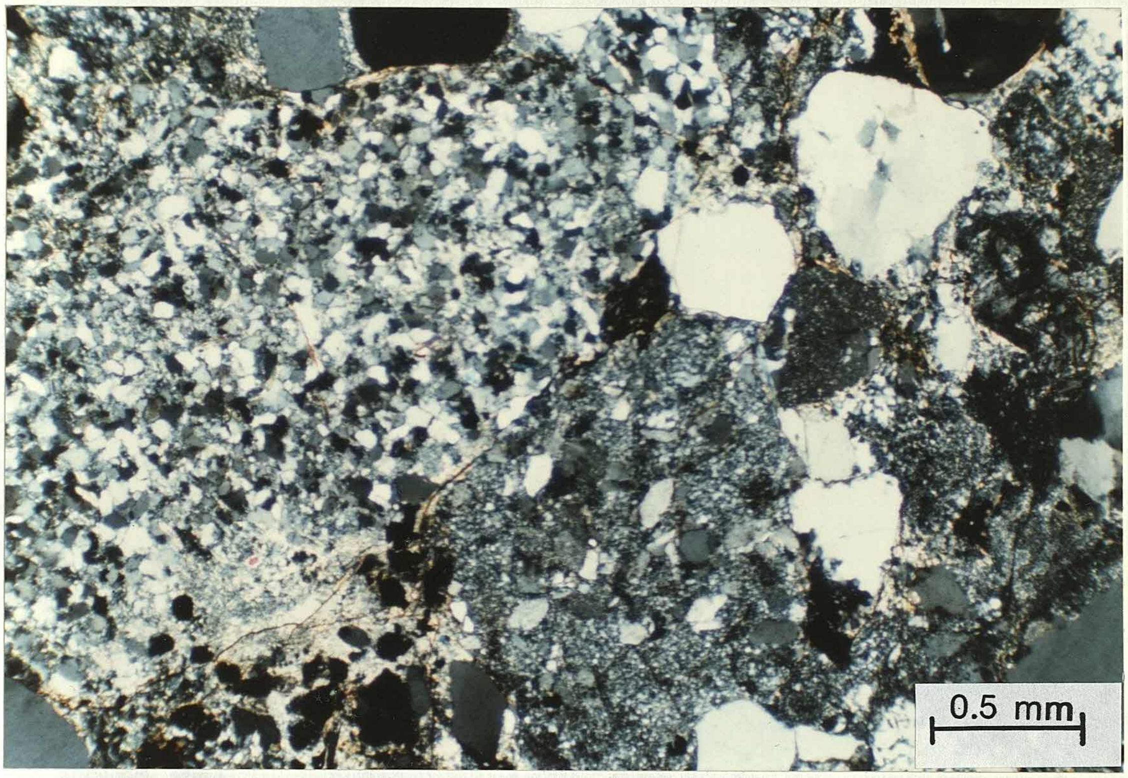

Fig. 3.65 Lithic fragments of poorly sorted tuffaceous sandstone (SS) and siltstone (SLT). (Sample F9, Section F1, 37.5m, Tryfan Fach Mbr. of Tryfan Fm.) XPL.

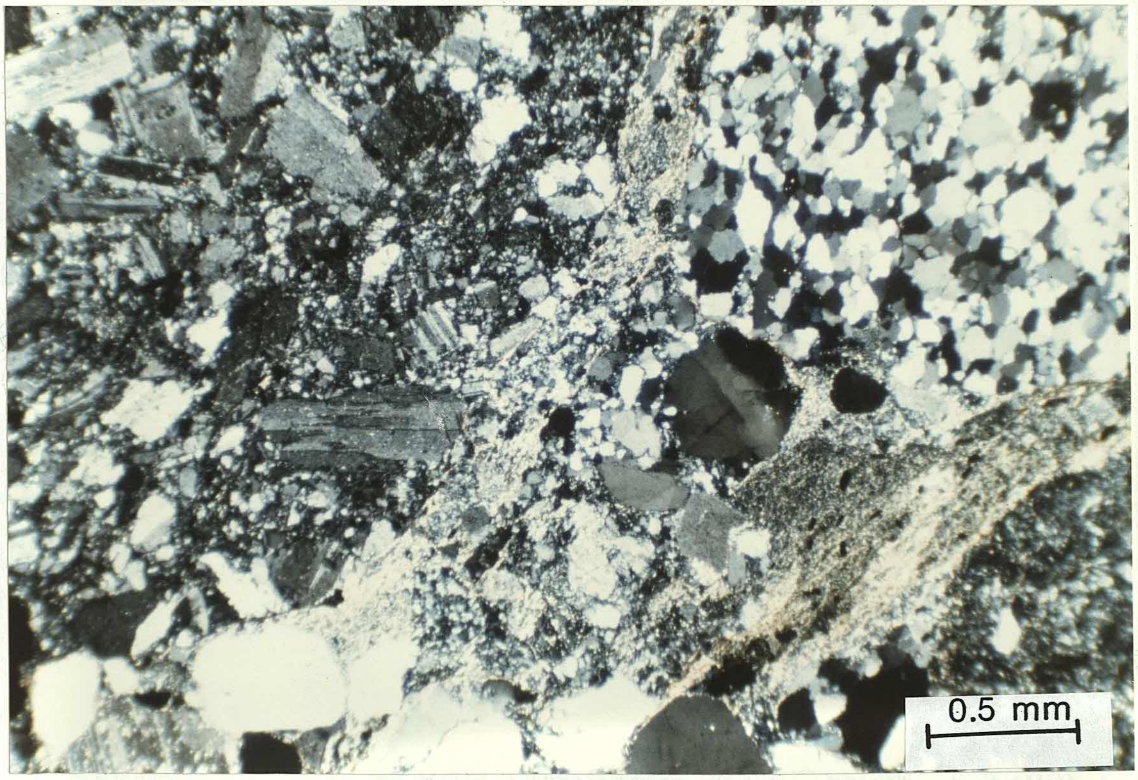

Fig. 3.66 Extremely poorly sorted lithic fragments of crystal-rich tuffaceous sandstone (SS), clast of quartzite (CHERT), and ductile fragment of sericitic mudstone(MUD) in poorly sorted quartzose matrix. (Sample F10B, Section F1, 47m, Tryfan Fach Mbr. of Tryfan Fm.) XPL.

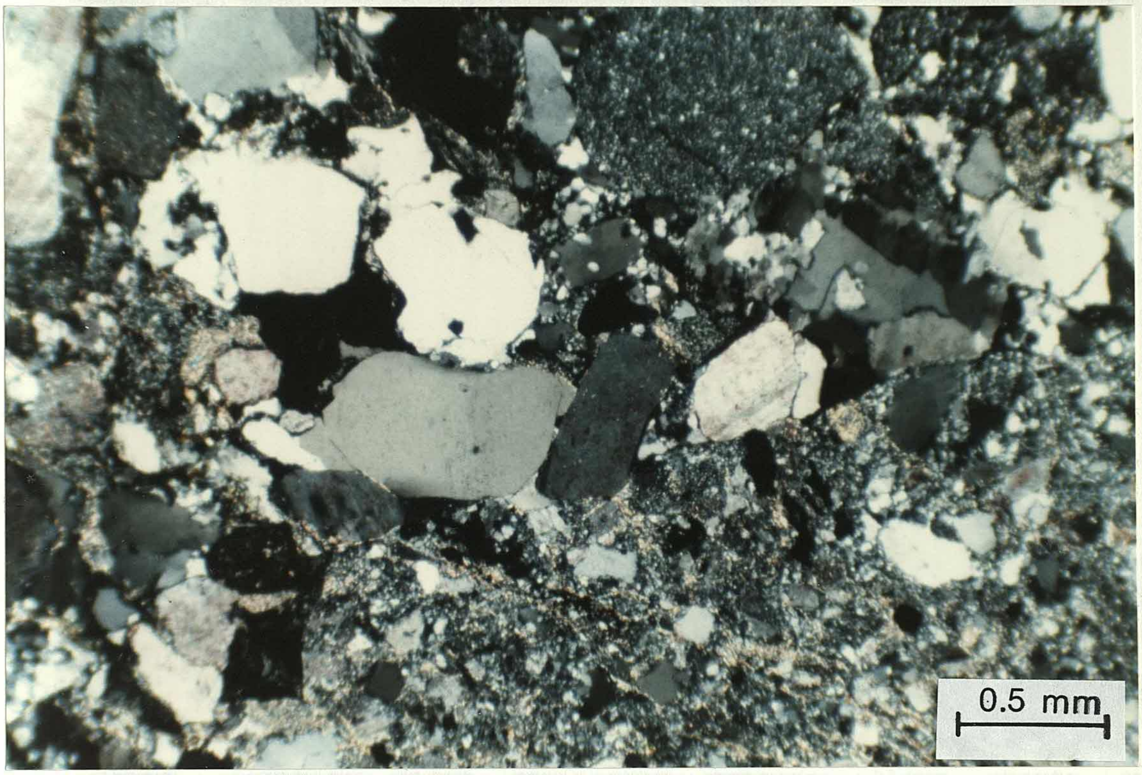

Fig. 3.67 Poorly sorted clast of tuffaceous sandstone (SS at top) surrounded by smaller fragments of monocrystalline quartz (Qm) or aphanitic rhyolite (RHY). (Sample C26, Section C1, 300m, Moel Siabod Mbr. of Tryfan Fm.) XPL.

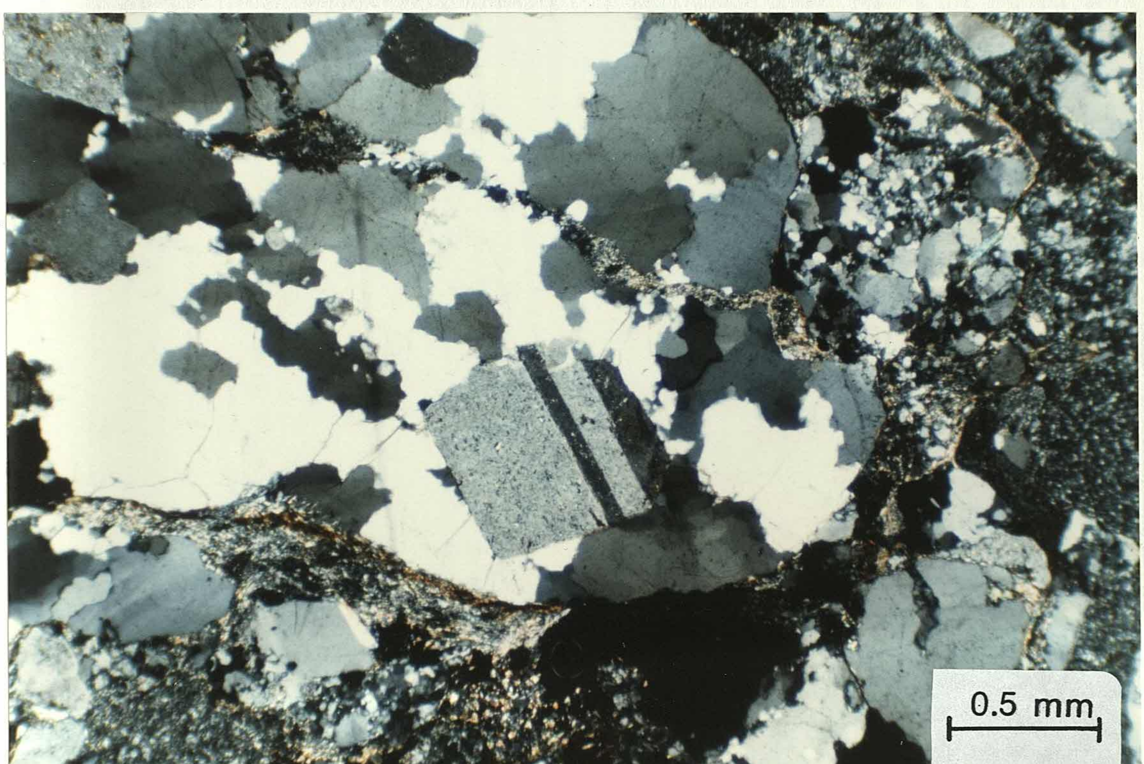

Fig. 3.68 Granite clast containing monocrystalline quartz and plagioclase. (Sample F9, Section F1, 95.1m, Tryfan Fach Mbr. of Tryfan Fm., Craig yr Ysfa). XPL.

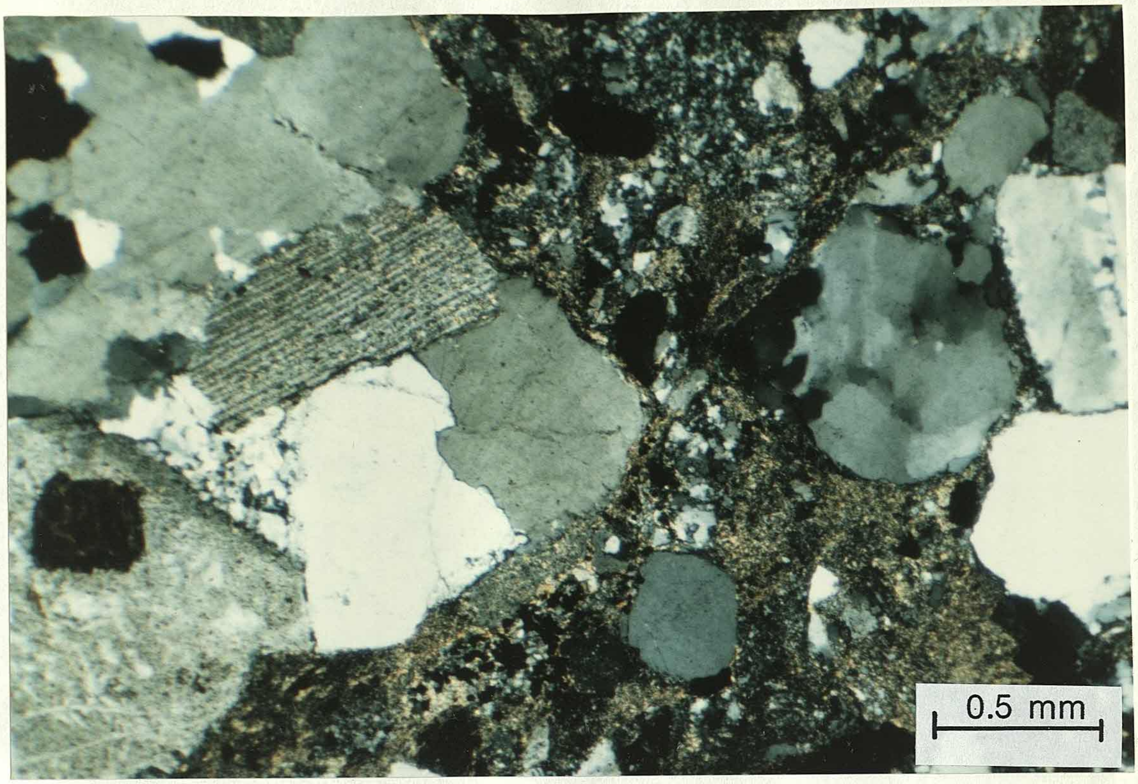

Fig. 3.69 Granite clast containing monocrystalline quartz and plagioclase. (Sample F25, Section F1, 157.8m, Tryfan Fach Mbr. of .Tryfan Fm, Craig yr Ysfa). XPL.

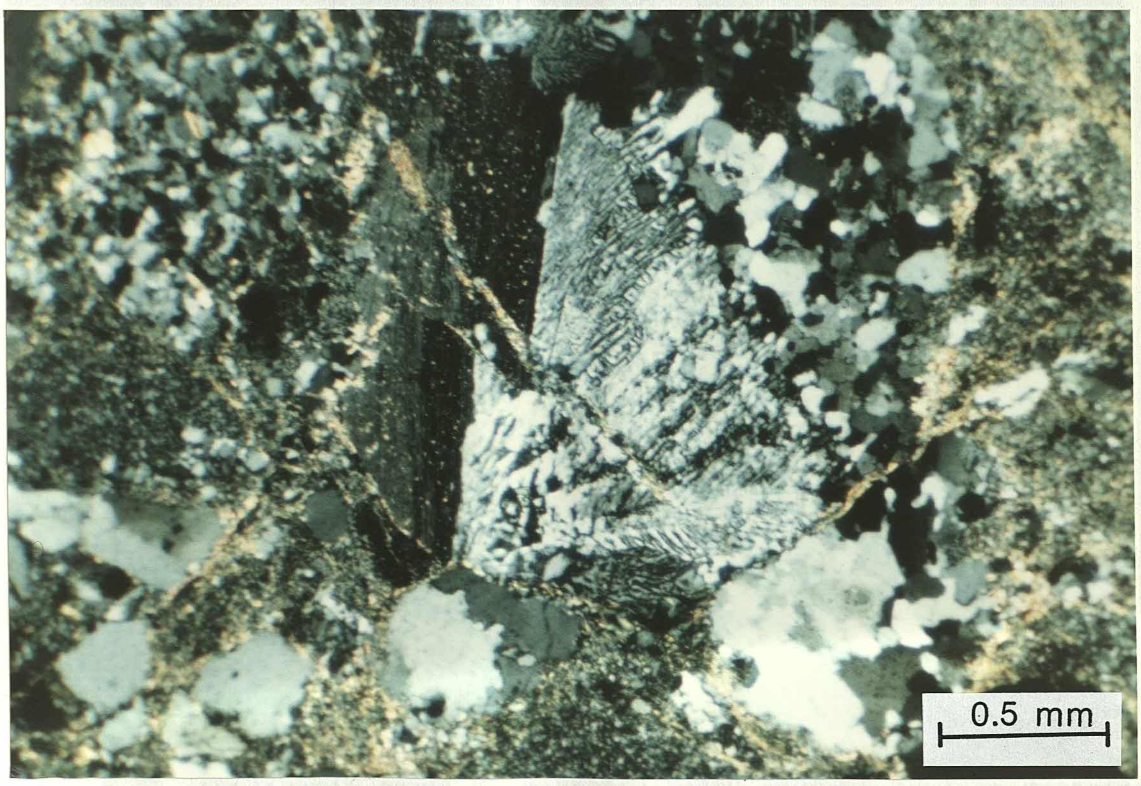

Fig. 3.70 Granophyric texture within granitic igneous fragment (Sample F19, Section F1, 95.1m, Moel Siabod Mbr. of Tryfan Fm.)

FIG. 3.71 Black opaque magnetic heavy minerals laminae along the tops of foresets of trough cross-stratification. From Magnetite Mbr., Section C1, 157m, Tryfan anticline.

FIG. 3.72 Horizontal bands of magnetic heavy mineral laminae deposited by upper flow regime flash-floods. From Magnetite Mbr., Section C1, 158.2m, Tryfan anticline.

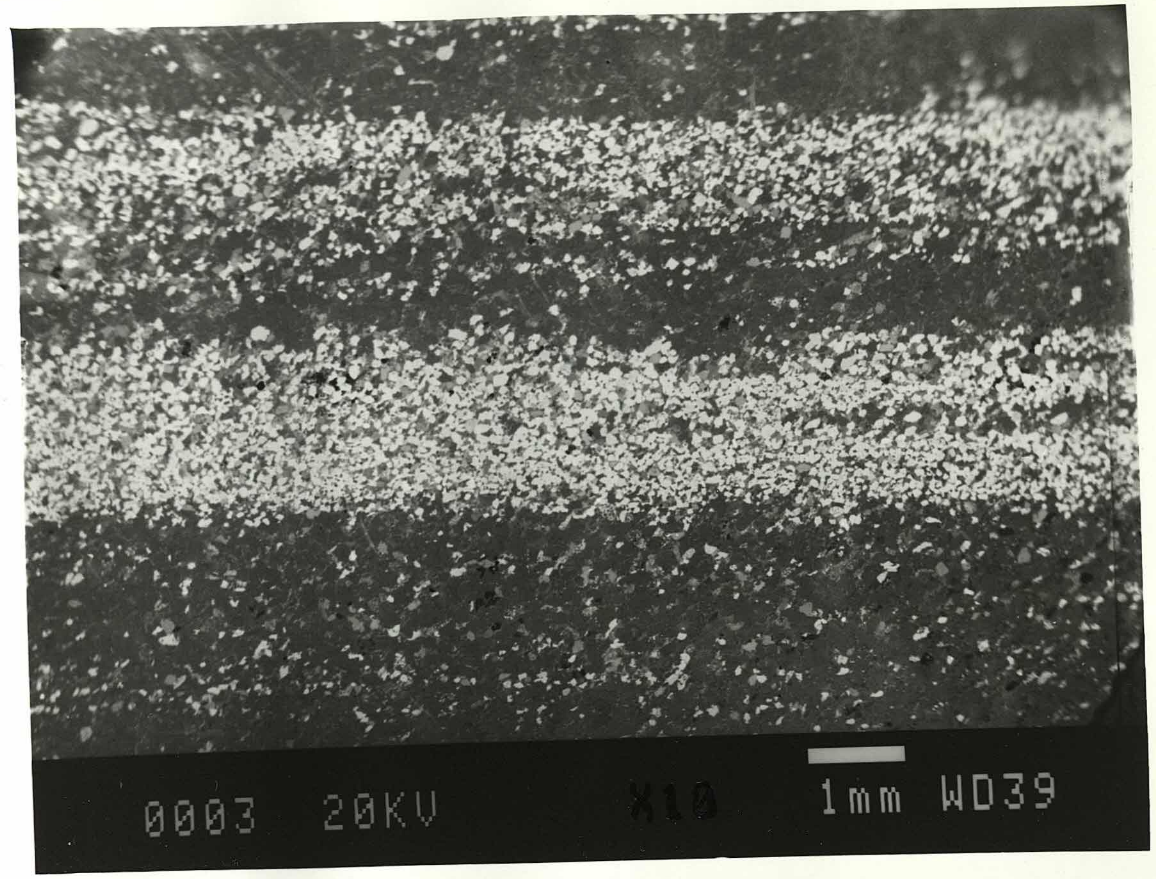

FIG. 3.73 Horizontal 2mm wide laminae of dominantly opaque heavy minerals from fluvial sandstones of Capel Curig Mbr. of Tryfan Fm., Tryfan anticline. Sample C71, Section C3, 16m. 2nd and 3rd heavy mineral laminae from sample are shown, see Fig. 4. for detail of 2nd laminae. Top of photograph is stratigraphically youngest. BSSEM.

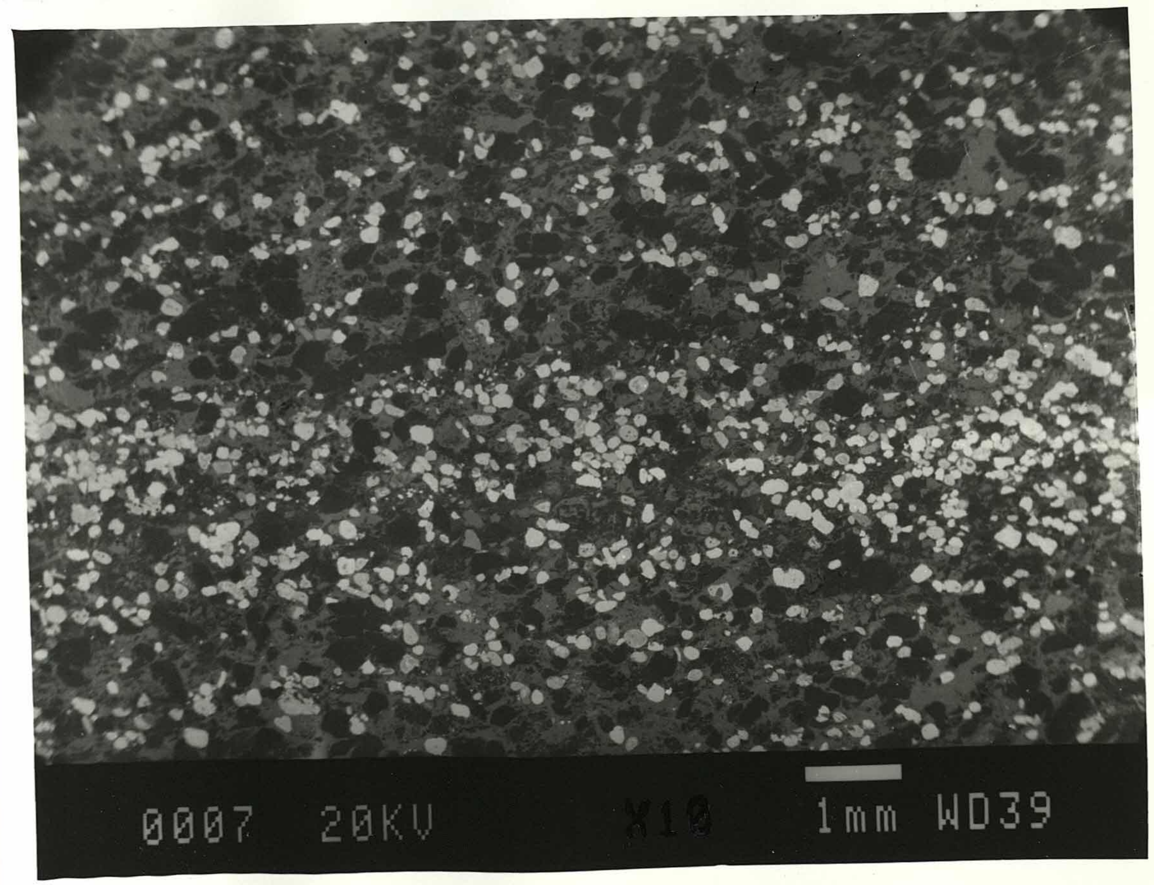

FIG. 3.74 Scattered magnetite or ilmenite (white colour) grains within fluvial sediments from Magnetite Mbr. Weak zone of concentration visible in lower-middle portion of photograph. Other detrital grains include chlorite (gray), plagioclase (dark) and quartz (dark). See Fig. 3.74 for view of similar texture on standard light microscope. Sample C12, section C1, 160m. BSSEM.

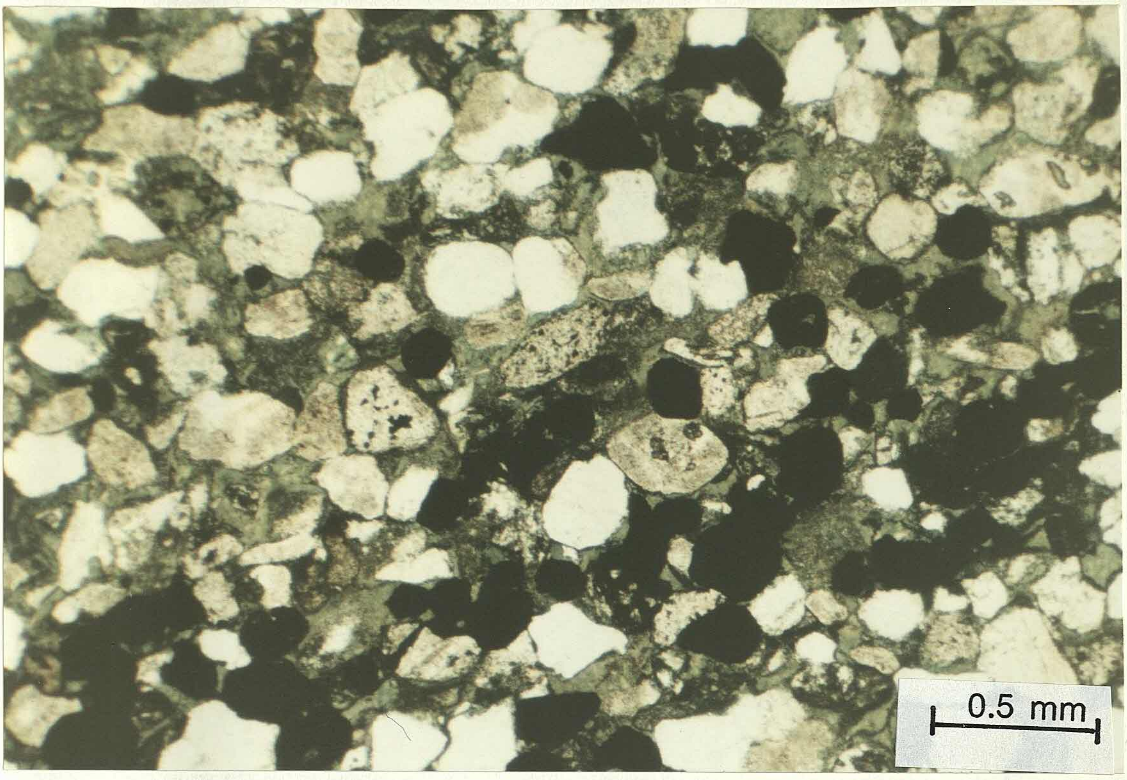

FIG. 3.75 Scattered opaque heavy minerals within fluvial sediments of Magnetite Mbr. Other detrital grains include rounded quartz (Qm), feldspar (F), and lithic fragments set in a chloritic matrix. See Fig. 3.75 for view of similar texture on back-scatter SEM. Sample C14, section C1, 165m. PPL.

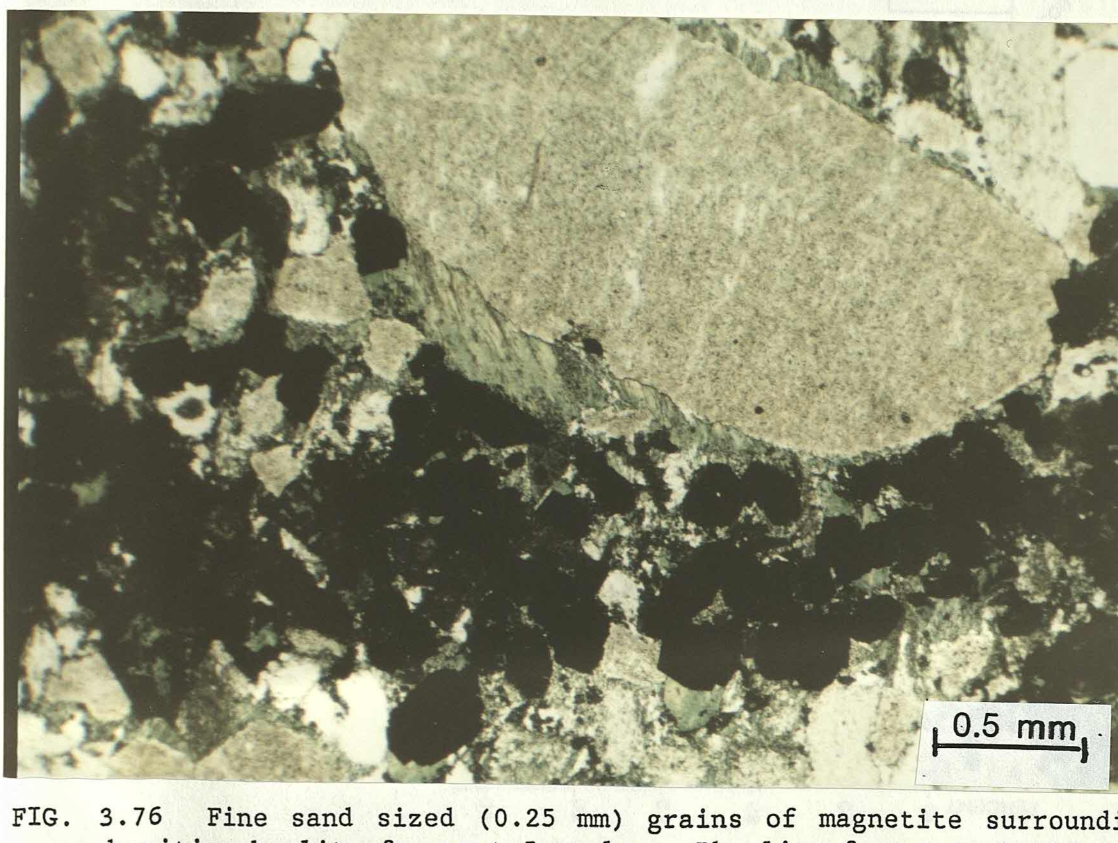

FIG. 3.76 Fine sand sized (0.25 mm) grains of magnetite surrounding aphanitic rhyolite fragment 5 mm long. Rhyolite fragment should only be about twice the size of opaque minerals if they were in hydraulic equilibrium. Sample C15a, section C1, 167m, Magnetite Mbr. PPL.

HEAVY MINERAL POPLULATION
(770 determinations)

MAGNETITE	58%
ILMENITE	12%
GARNET	7.1%
ZIRCON	4%
RUTILE	2%
APATITE	1%
SPHENE	2.6%

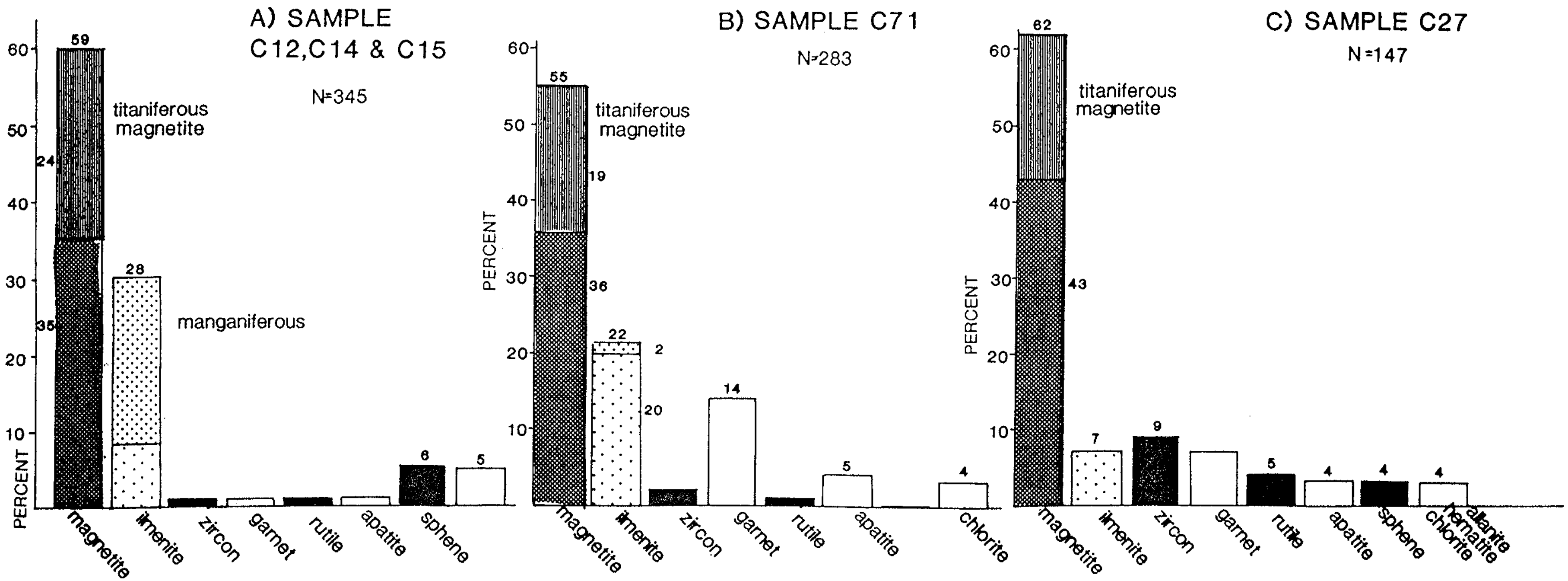

FIG. 3.77: Relative proportion of heavy minerals in sandstones examined.

FIG. 3.78 Raggy magnetite crystals(very light grey), chromite(dark grey) and euhedral zircon crystals (bright white) within heavy mineral layer. Sample C27, section C1, 305m. BSSEM.

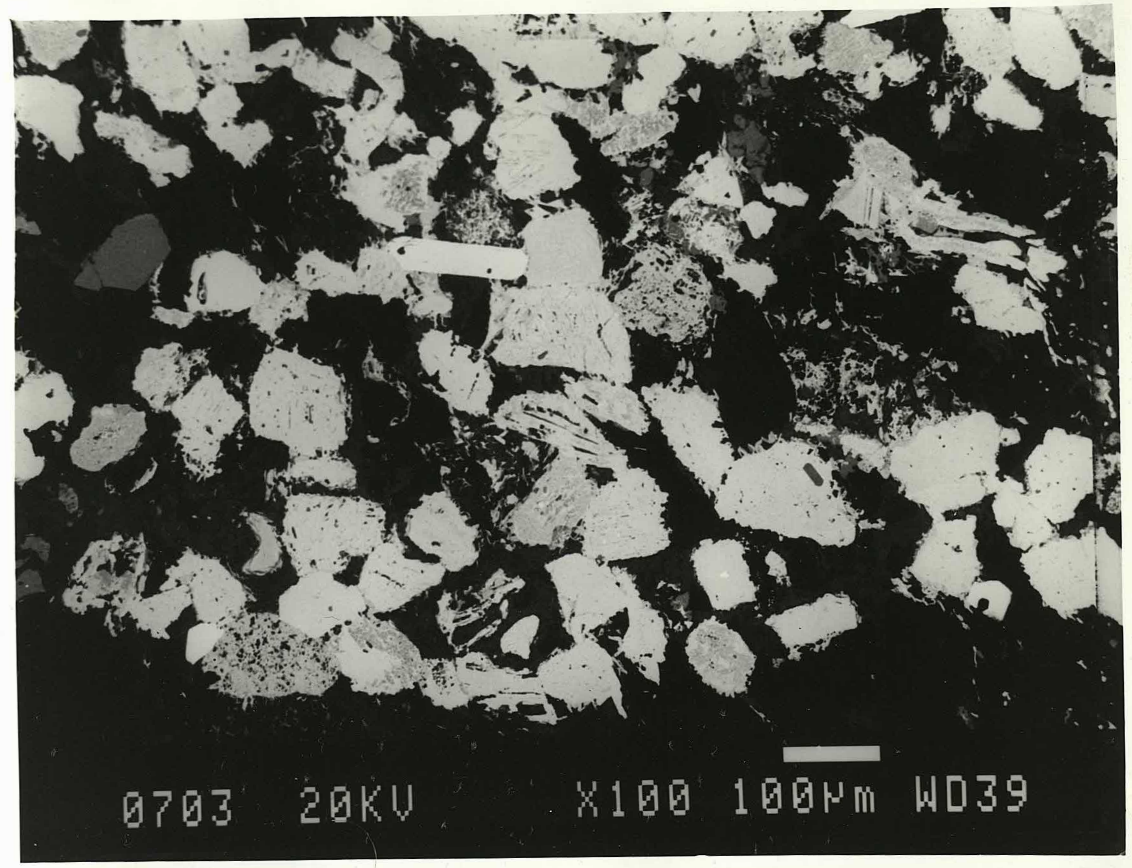

FIG. 3.79 Bipartite heavy mineral grain with euhedral magnetite (Mt) crystal(s) sutured against remnant of basalt (now chlorite: CHL) from whence it was derived. Sample C15A, section C1, 167m. BSSEM.

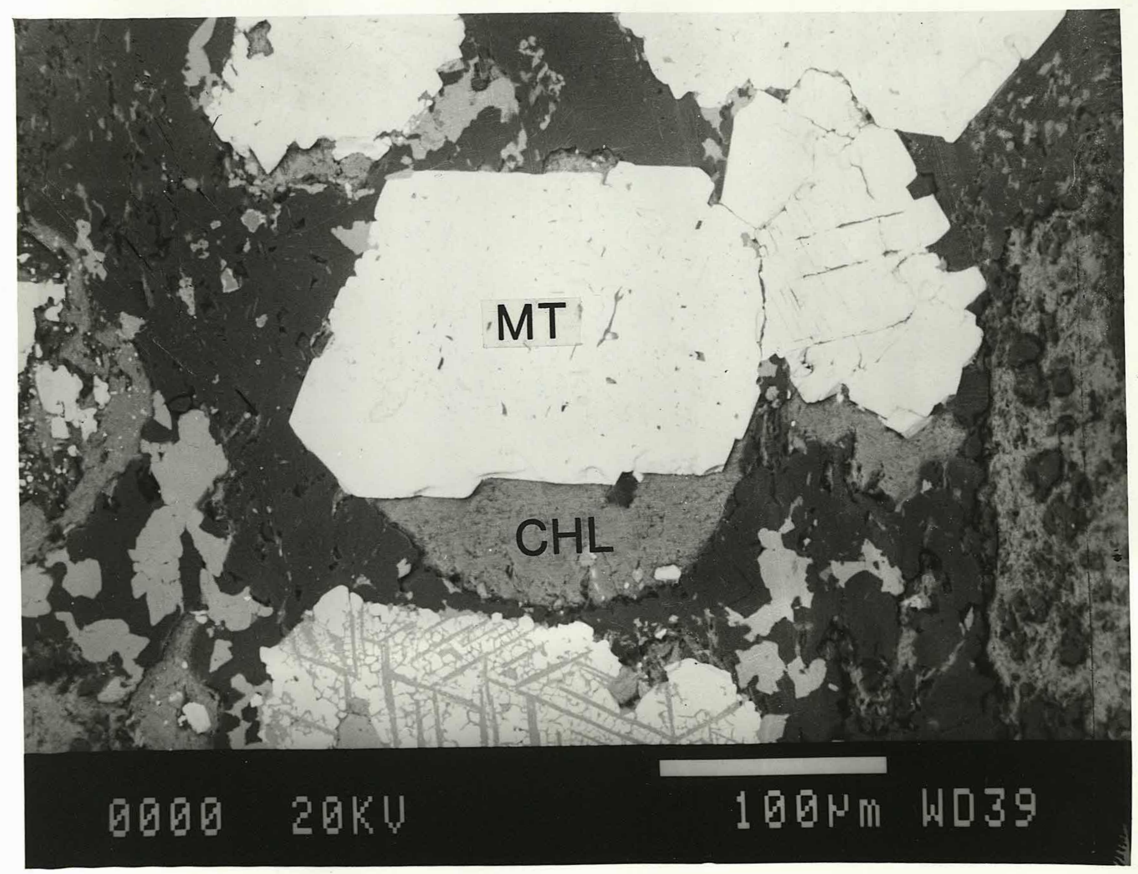

A) Typical Almandine Garnet. Sample C71 3/117 Capel Curig Mbr. Tryfan anticline

B) Typical grossular garnet. Sample C71 4/3 Capel Curig Mbr. Tryfan anticline

C) Typical spessartine C71 4/90 Capel Curig M. Tryfan anti.

	A)	B)	C)
SiO_2	35.33	36.56	36.76
Al_2O_3	21.42	23.68	21.94
TiO_2	0.12	0.00	0.34
Na_2O	0.30	0.22	0.00
CaO	1.25	23.66	5.13
MgO	3.79	0.30	1.53
Cr_2O_3	0.00	0.00	0.00
MnO	5.56	0.39	16.71
FeO	31.69	13.17	21.71
NiO	0.20	0.07	0.00
TOTAL	99.71	98.09	104.16

D) Manganiferous almandine C71 1/9

E) Typical titaniferous magnetite Sample C71 Capel Curig. Mbr. Tryfan anticline.

F) Magnetite Slightly titaniferous C29 1/1 Moel Siabod M. Tryfan anticline

	D)	E)	F)
SiO_2	36.44	0.50	1.59
Al_2O_3	21.79	0.12	1.26
TiO_2	0.00	21.92	2.09
Na_2O	0.17	0.00	0.59
CaO	4.17	0.00	0.00
MgO	3.56	0.00	0.31
Cr_2O_3	0.00	0.00	0.00
MnO	10.21	0.25	0.04
FeO	26.79	68.27	91.34
NiO	0.09	0.24	0.34
TOTAL	102.27	91.37	97.73

G) Typical Ilmenite Sample C27 2/8 Moel Siabod Mbr. Tryfan anticline

H) Altered Manganiferous Ilmenite/ Leucozene. C27 3/14B

I) Chromite C27 2/8

	G)	H)	I)
SiO_2	0.37	0.54	0.31
Al_2O_3	1.37	0.28	14.68
TiO_2	52.69	50.38	0.37
Na_2O	0.14	0.00	0.00
CaO	0.00	0.07	0.09
MgO	0.00	0.15	3.67
Cr_2O_3	0.06	0.00	49.35
MnO	0.15	22.93	7.39
FeO	45.43	28.46	25.65
NiO	0.00	0.00	0.12
TOTAL	100.25	102.89	101.74

FIG. 3.80 Representative EDS analyses for magnetite, titanomagnetite, ilmenite and garnet minerals.

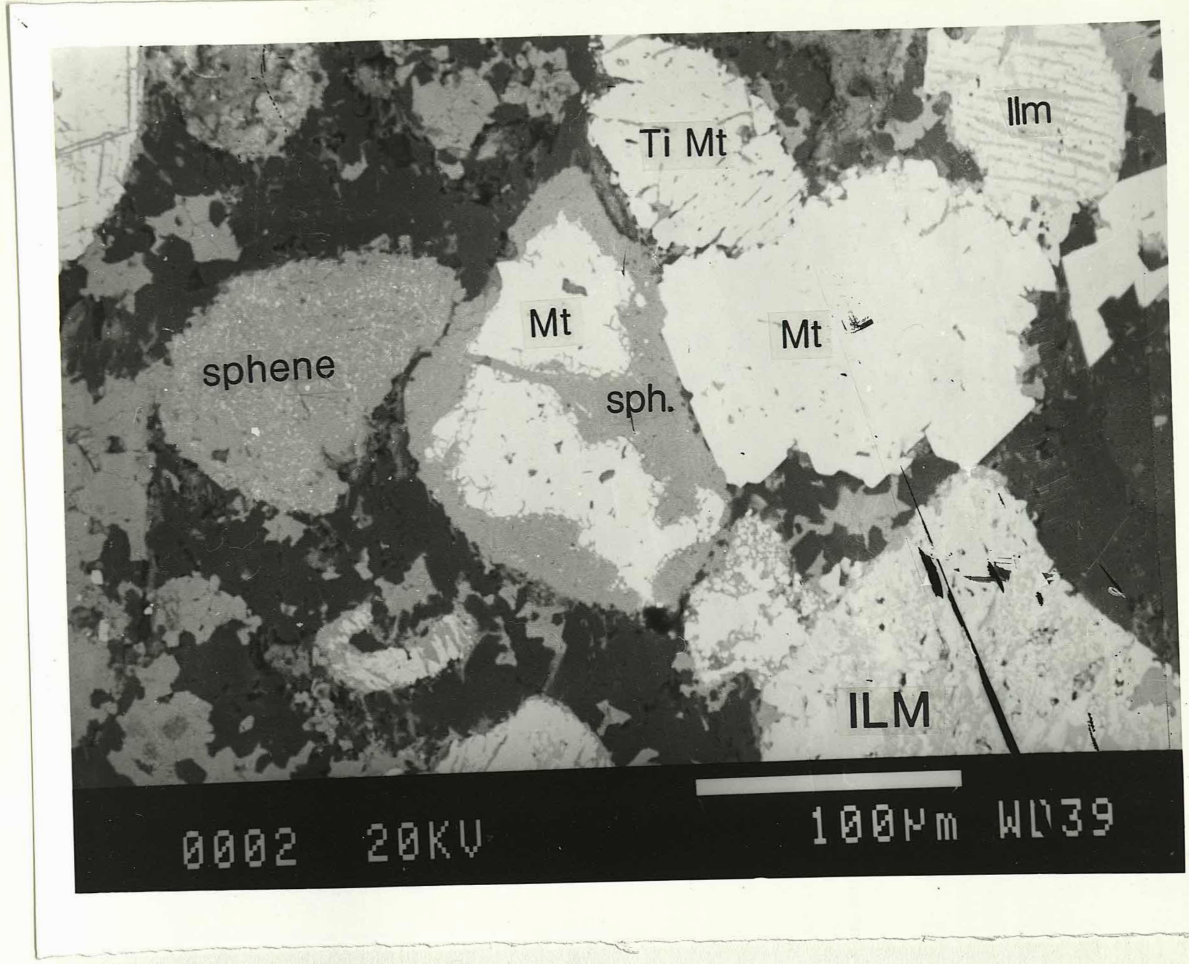

FIG. 3.81 "Symbiotic" relation ship between detrital titaniferous magnetite crystal altered to sphene and largely authigenic untitaniferous crystal (on right). Manganiferous ilmenite grain at bottom. Magnetite Mbr. Sample C15, section C1, 167m. BSSEM.

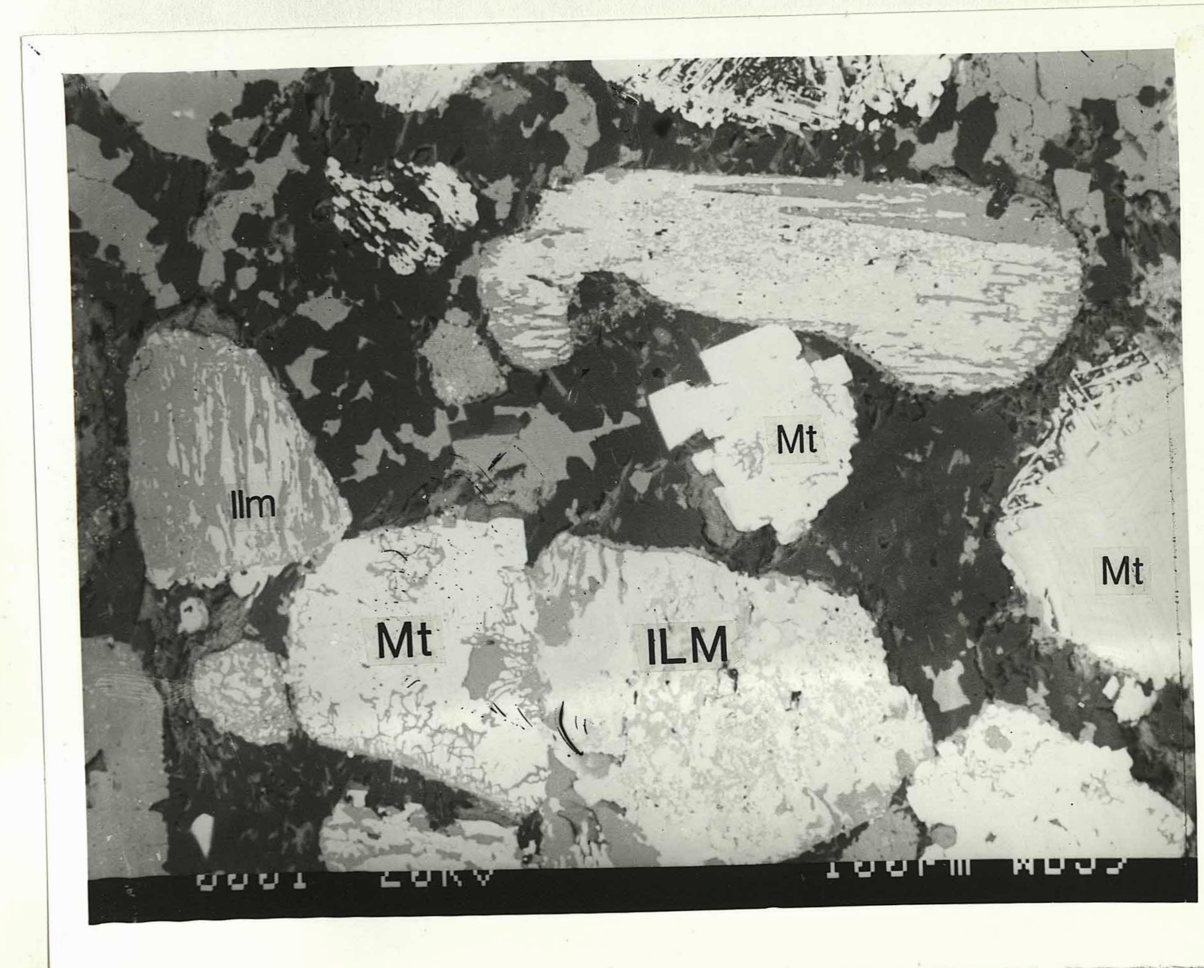

FIG. 3.82 Alteration of manganiferous magnetite (Mn Mt) and ilmenite (Ilm) to sphene (sph) along twin planes. Iron liberated precipitated locally as euhedral magnetite (Mt) overgrowth on small remnant of titaniferous magnetite. Magnetite Mbr. Sample C15, section C1, 167m. BSSEM.

ilm → leucoxene.

FIG. 3.83 More extensive replacement of ?originally titaniferous magnetite by sphene. Sphene is also a common authigenic phase in matrix. Magnetite Mbr. Sample C15, section C1, 167m. BSSEM.

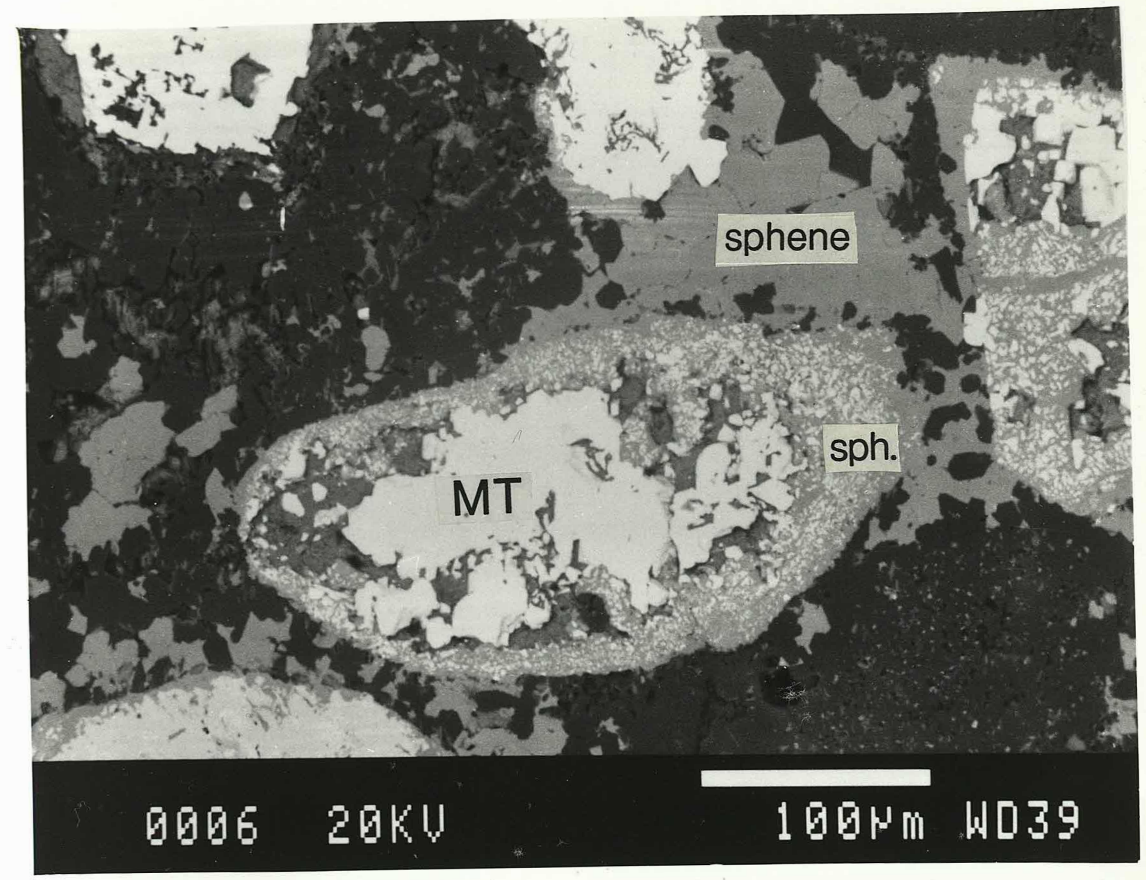

FIG. 3.84 Overgrowth of pure (only Fe) magnetite on remnant of ilmenite grain. Other detrital heavy minerals include rounded ilmenite grain and euhedral zircon crystal. Moel Siabod Mbr. Sample B41, section B4, 53m. BSSEM.

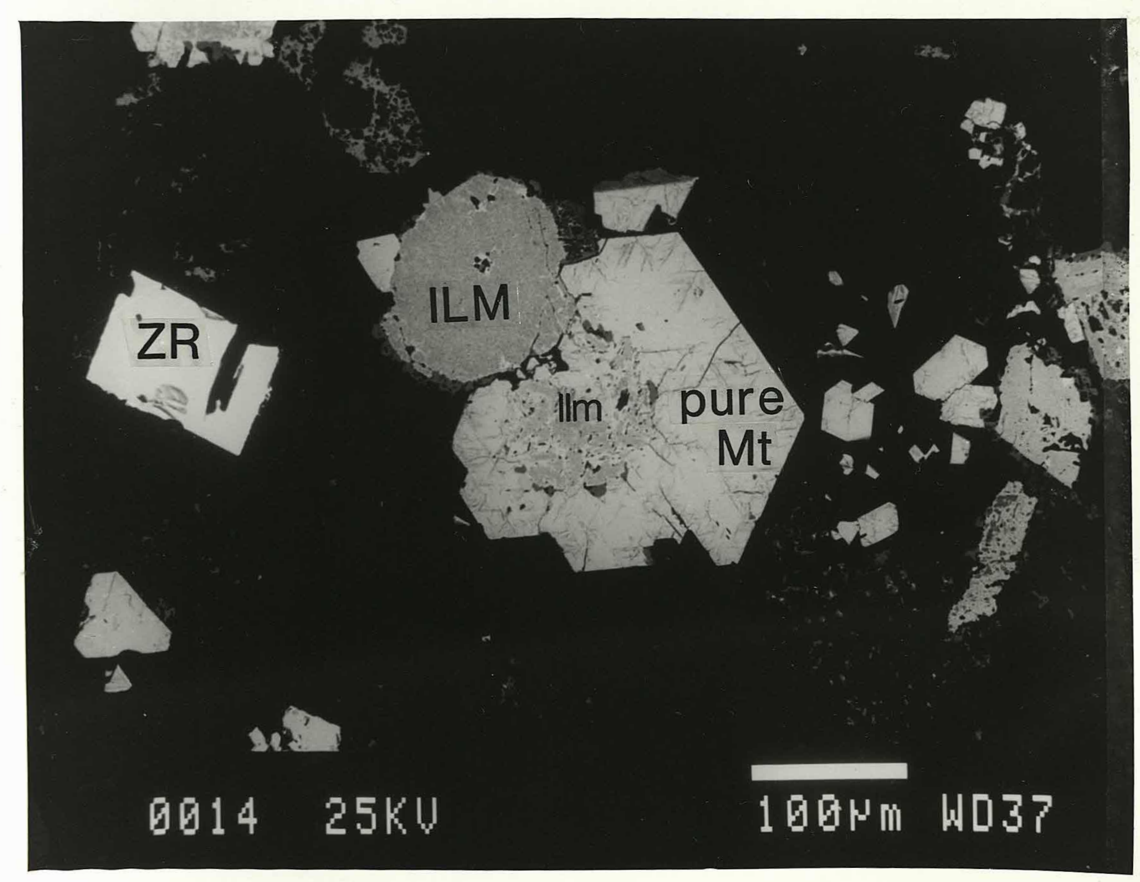

FIG. 3.85 Perfectly euhedral crystal of pure magnetite without any sign of a detrital core. Sample taken from sandstone __ m stratigraphically beneath the Capel Curig Volcanic Formation. Moel Siabod Mbr. Sample C30, section C1, 345m. BSSEM

FIG. 3.86 Stranded crystals of euhedral magnetite of varying size. Crystal show no relationship to fabric (derived from cross-stratification) within sandstone. Location as above. BSSEM.

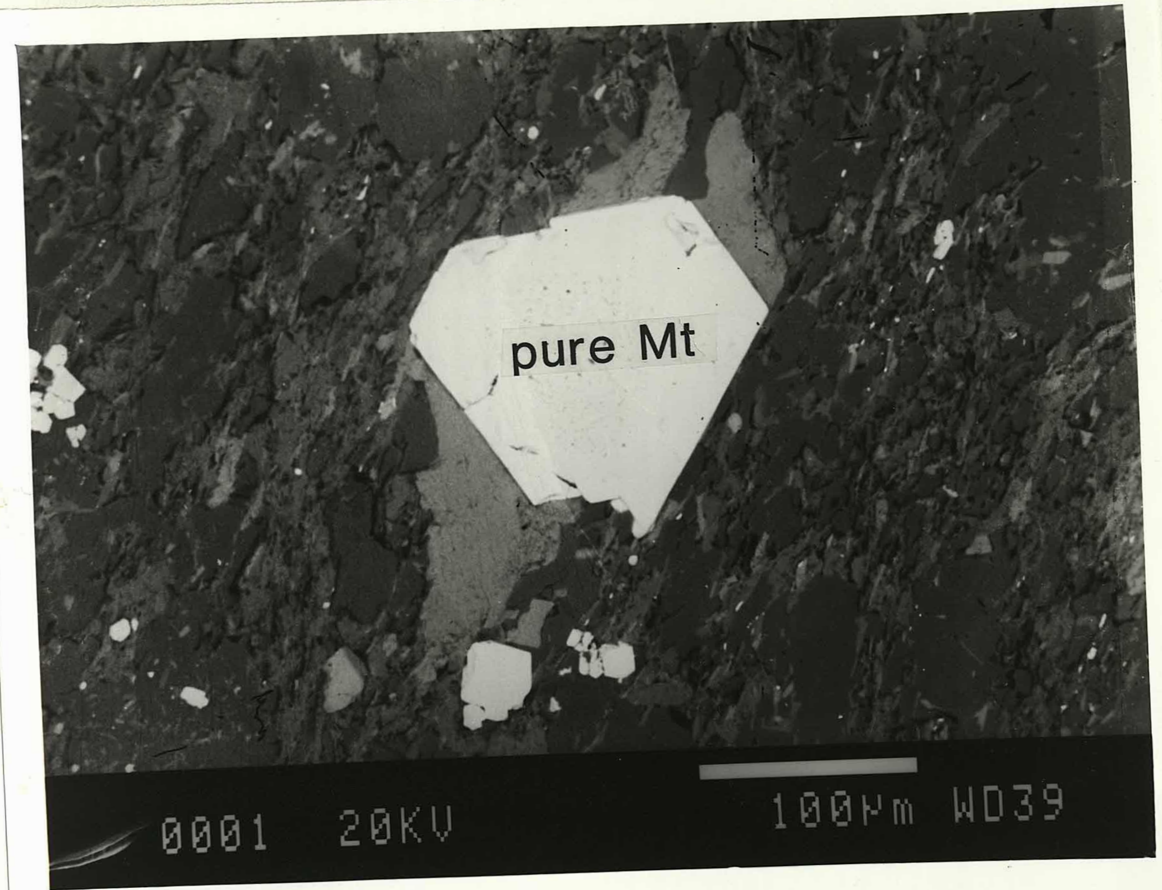

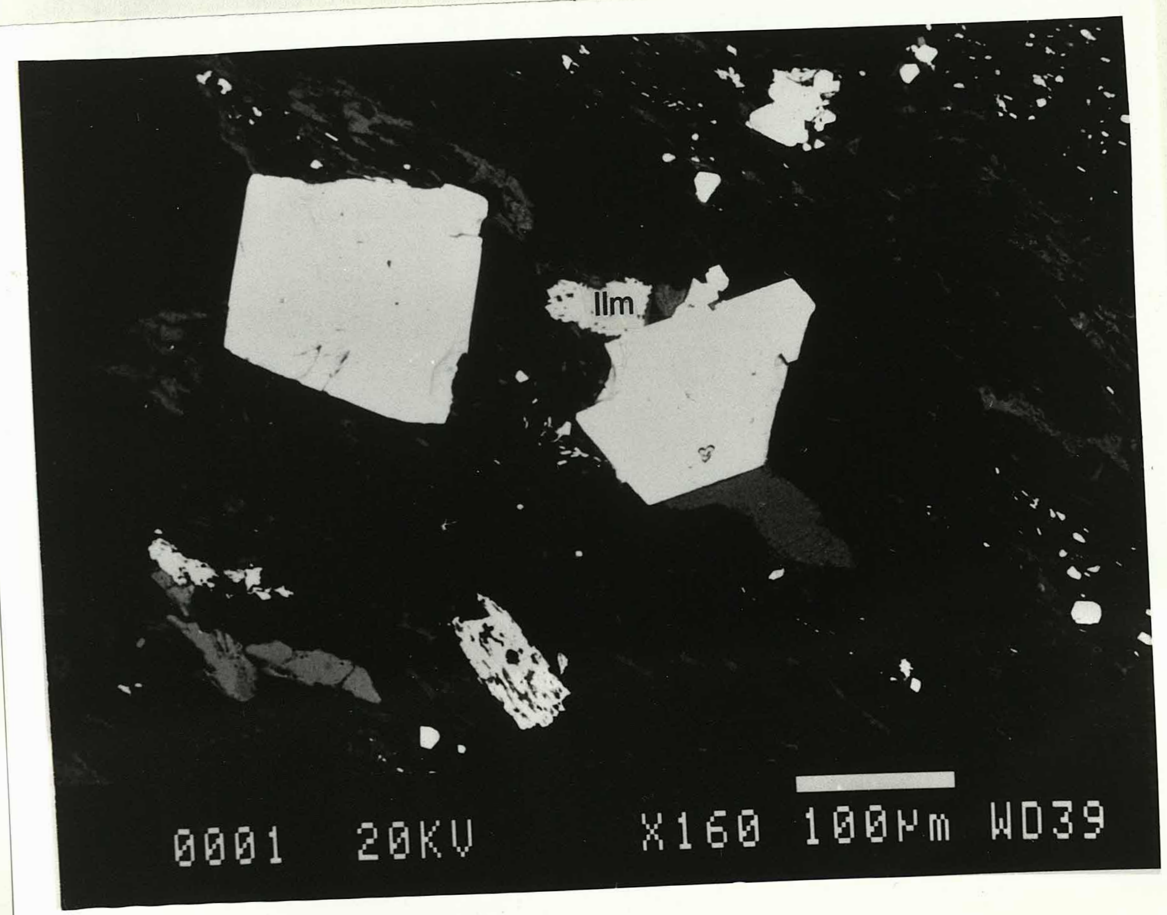

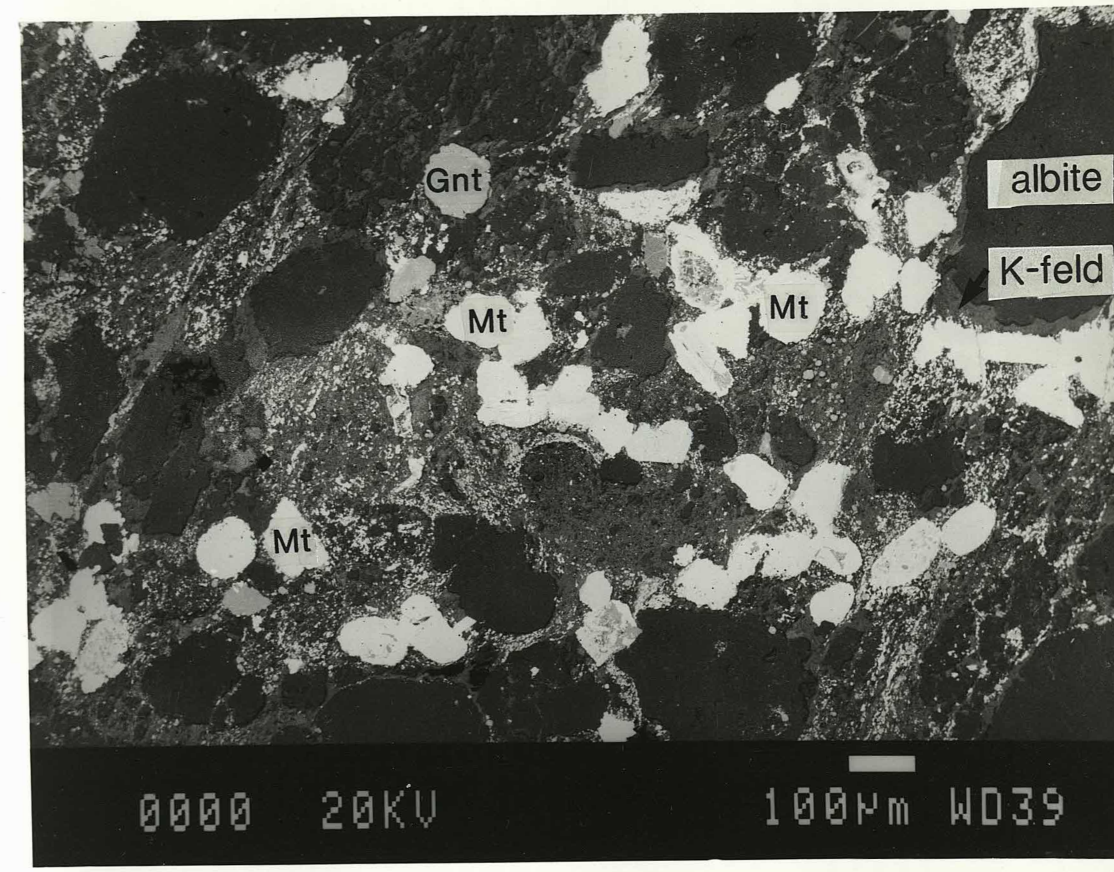

FIG. 3.89 Distribution of fine-sand grade detrital magnetite and ultrafine ?authigenic magnetite within Sample C69. The two contrasting grain size populations argues against a common origin. K-feldspar is a common authigenic phase and even forms overgrowths on albite crystals. Sample C69, section C2, 168m, Gwern Gof Mbr. BSSEM.

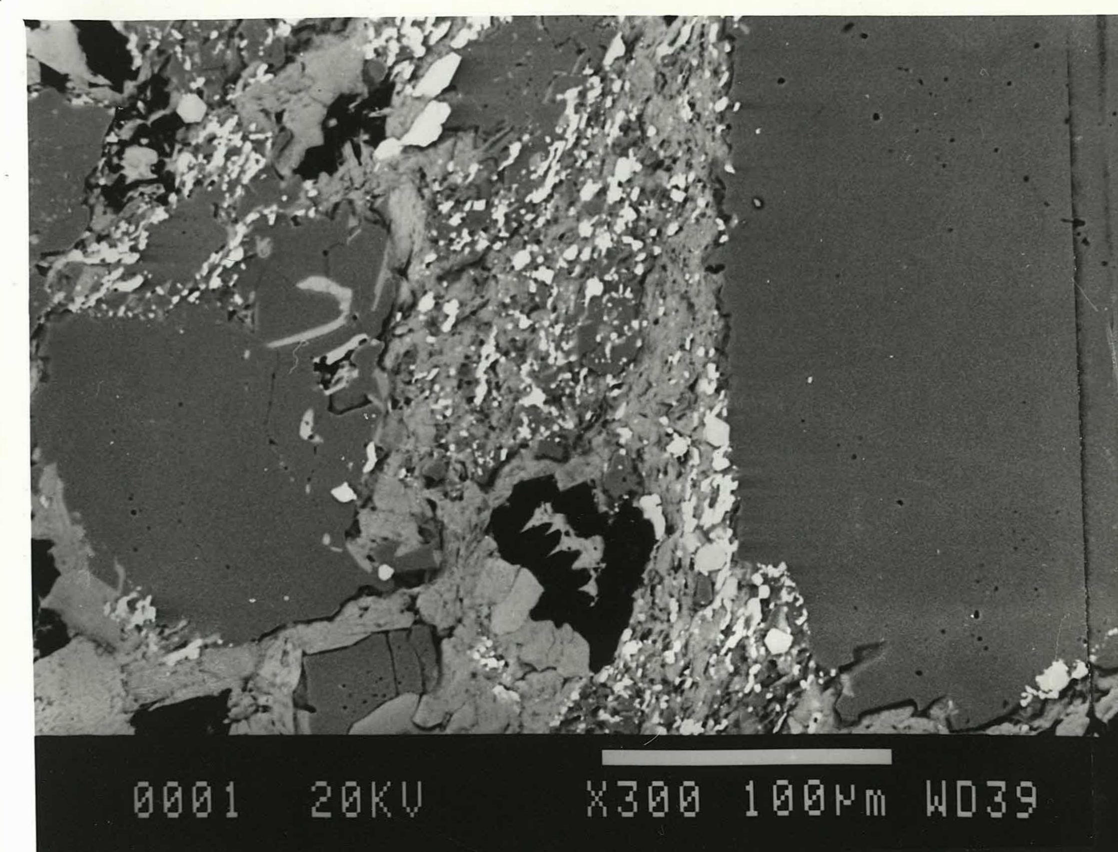

FIG. 3.90 Magnified view of euhedral fine grained magnetite crystals. Other authigenic phases include spessartine (Mn- garnet), k-feldspar and ankerite (manganiferous calcite). Source of manganese is unknown but could be derived from altered Mn-rich iron oxides. Sample C69, section C2, 168m, Gwern Gof Mbr. BSSEM.

FIG. 3.87 Black-weathering bioturbate deltaic sandstones containing approximately 15% fine-grained magnetite. section C2, 145 m, Ddeugwm ridge, Tryfan anticline.

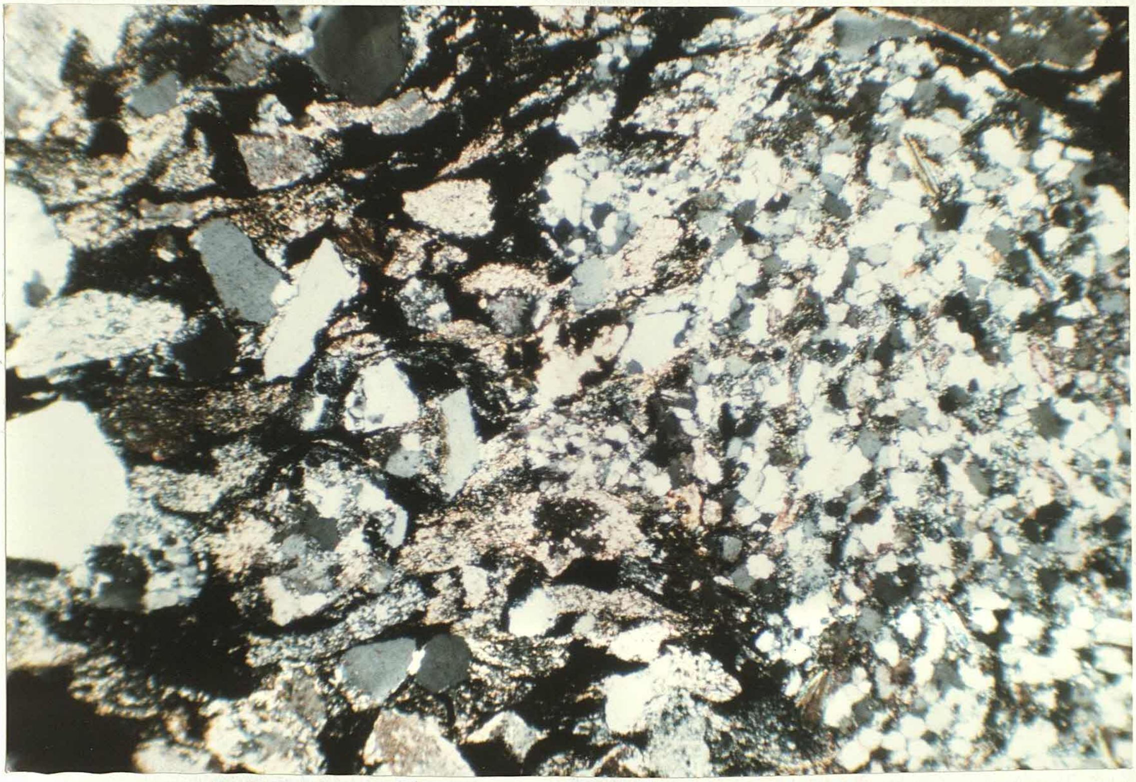

FIG. 3.88 Distribution of fine-grained magnetite. Wavy foliation is tectonic. Sample C69, section C2, 168m, Gwern Gof Mbr.

FIG. 3.91 Poorly sorted heavy mineral concentration of large manganiferous ilmenite grains (ILM), garnet (GNT), titaniferous magnetite (Ti Mt), sphene (SPH) and zircon (Zr). Sample C15, section C1, 167m, Magnetite Mbr. Tryfan anticline. BSSEM.

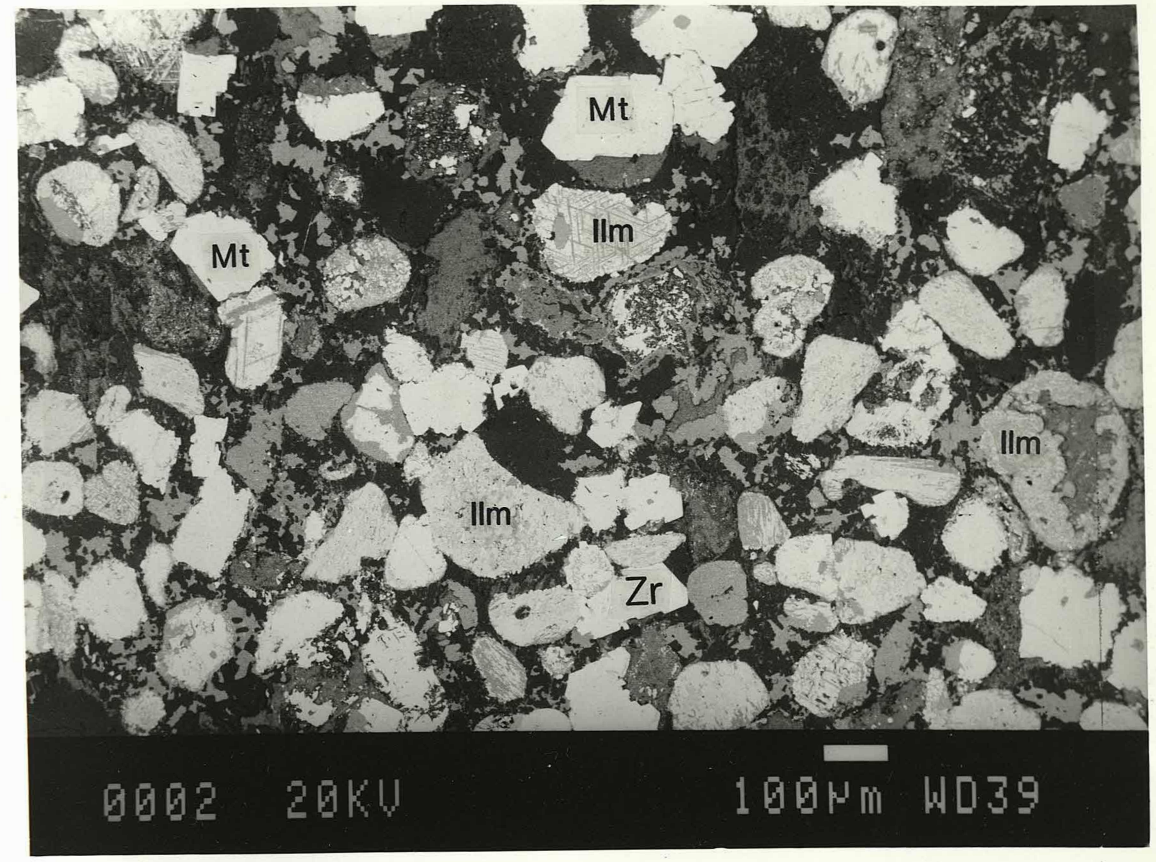

FIG. 3.92 Rounded ilmenite grains (ILM) occasionally overgrown by euhedral authigenic magnetite. Large euhedral detrital zircon crystal in upper left. Sample B41, section B4, 53m, Moel Siabod Mbr. Capel Curig anticline. BSSEM.

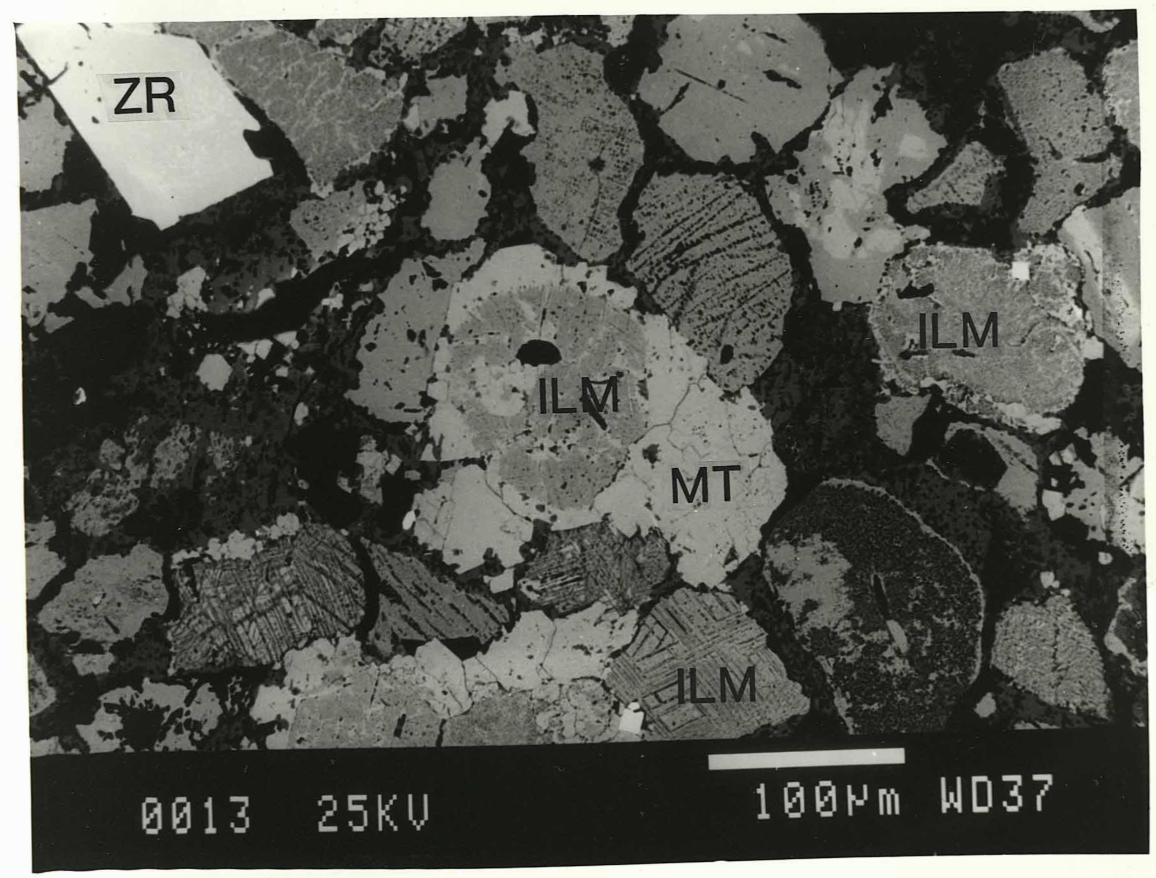

FIG. 3.93 Rounded ilmenite grain (ILM) with overgrowth of pure magnetite. Central grain of titaniferous magnetite (with Zircon seed crystal) showing exsolution textures. Sample B41, section B4, 53m, Moel Siabod Mbr. Capel Curig anticline. BSSEM.

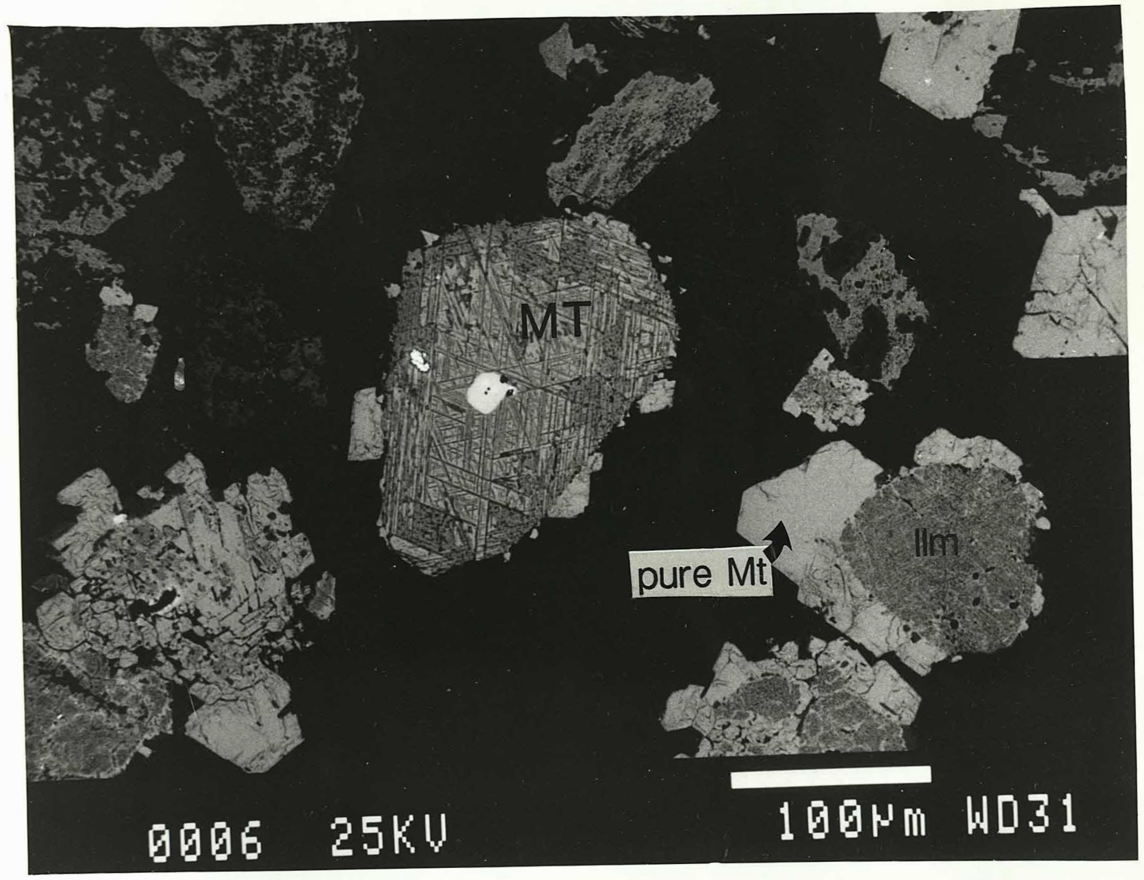

FIG. 3.94 Partial replacement of ilmenite by sphene. Matrix consists of authigenic sphene and quartz(BLACK). SAMPLE C15, section C1, 167m. Magnetite Mbr. Tryfan anticline. BSSEM.

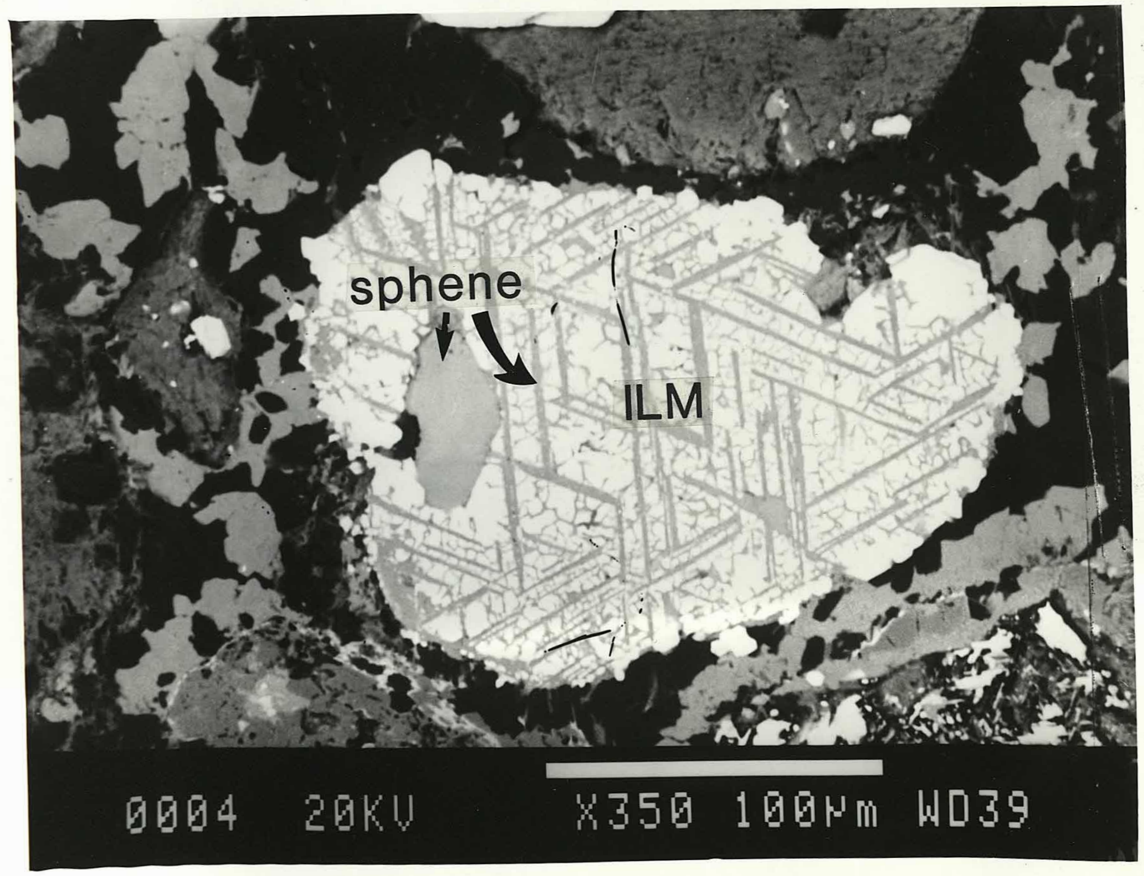

FIG. 3.95 Euhedral, partially embayed zircon crystal with leached negative crystal (lower left) and fractured zircon crystal with diasporium-rich REE along cracks (upper right). Sample B41, section B4, 53m, Moel Siabod Mbr. Capel Curig anticline. BSSEM.

FIG. 3.96 Euhedral, chemically zoned zircon crystal. Sample C12, section C1,160m, Magnetite Mbr., Tryfan anticline. BSSEM.

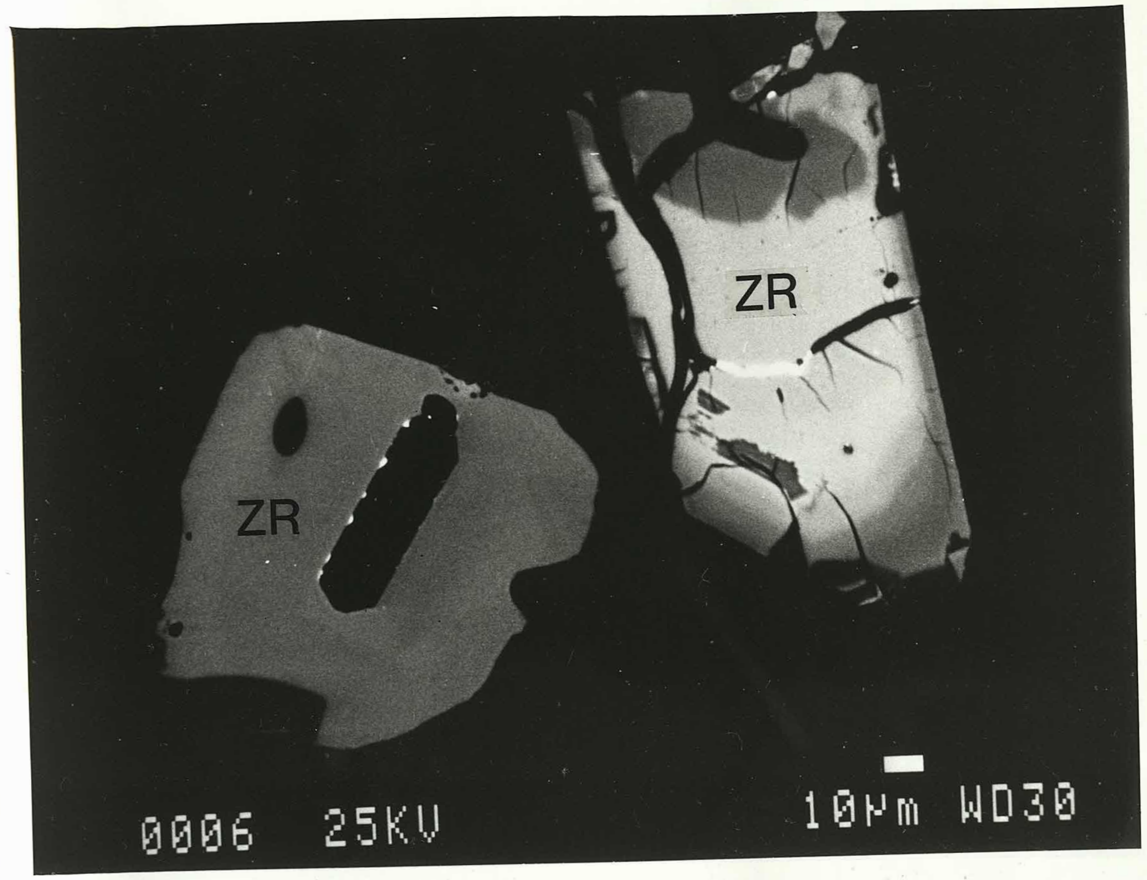

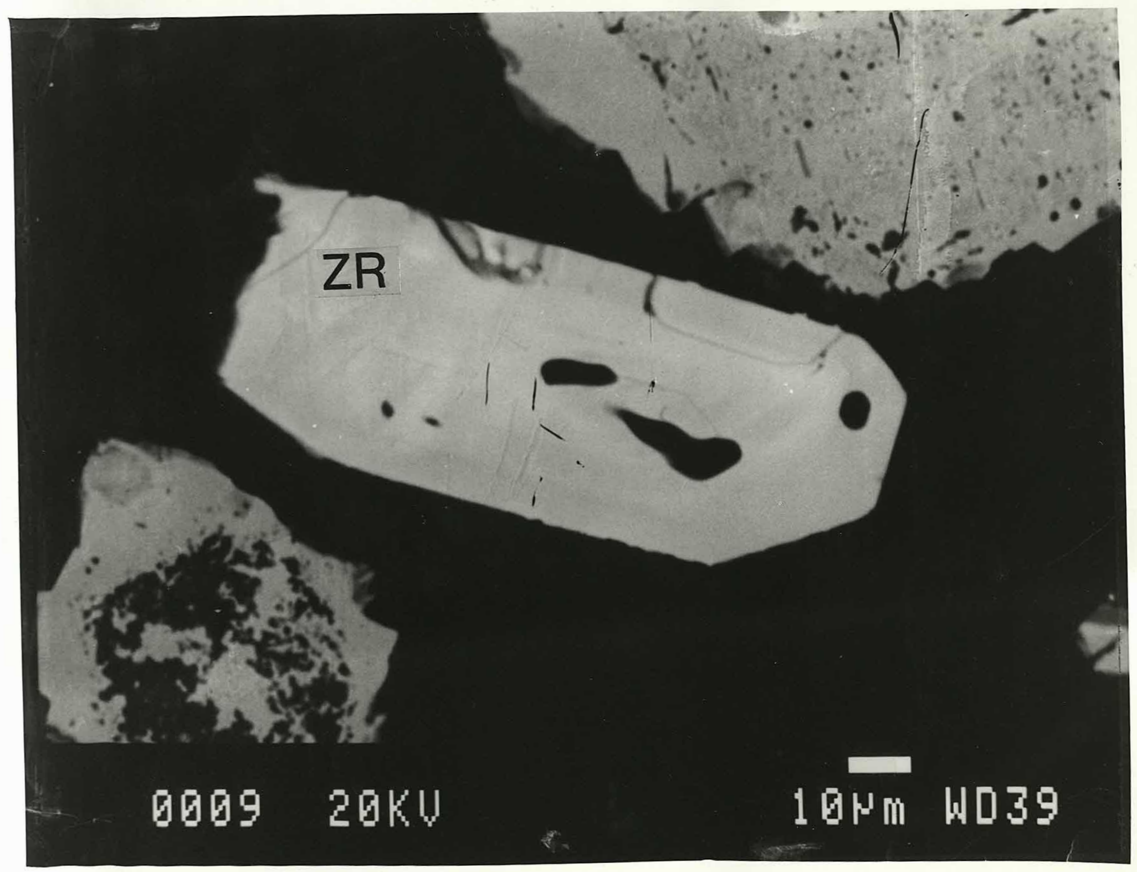

FIG. 3.97 Well-developed chemical zoning within zircon crystal. Exsolution of rare earth elements along fractures. Sample B41, section B4, 53m, Moel Siabod Mbr. Capel Curig anticline. BSSEM.

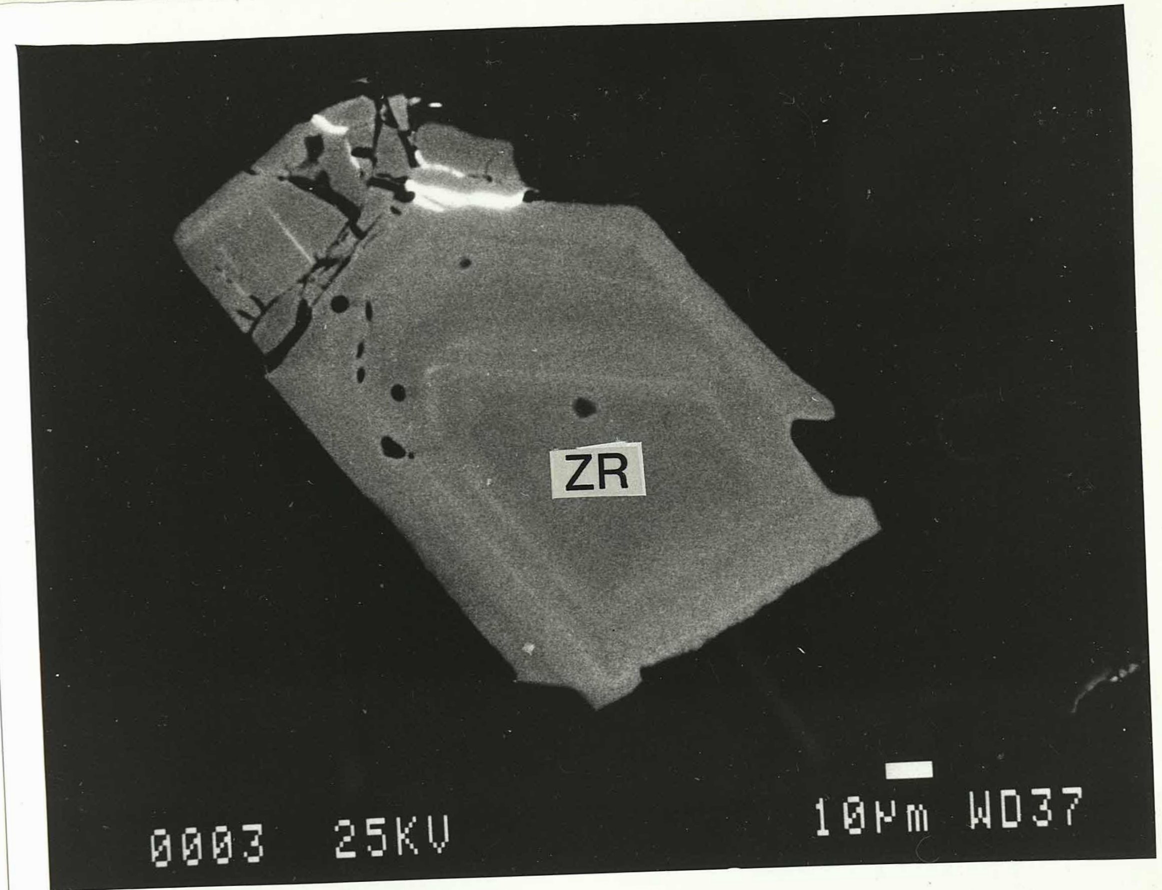

FIG. 3.98 Rare occurrence of authigenic zircon overgrowth on rounded ilmenite grain. Sample B41, section B4, 53m, Moel Siabod Mbr. Capel Curig anticline. BSSEM.

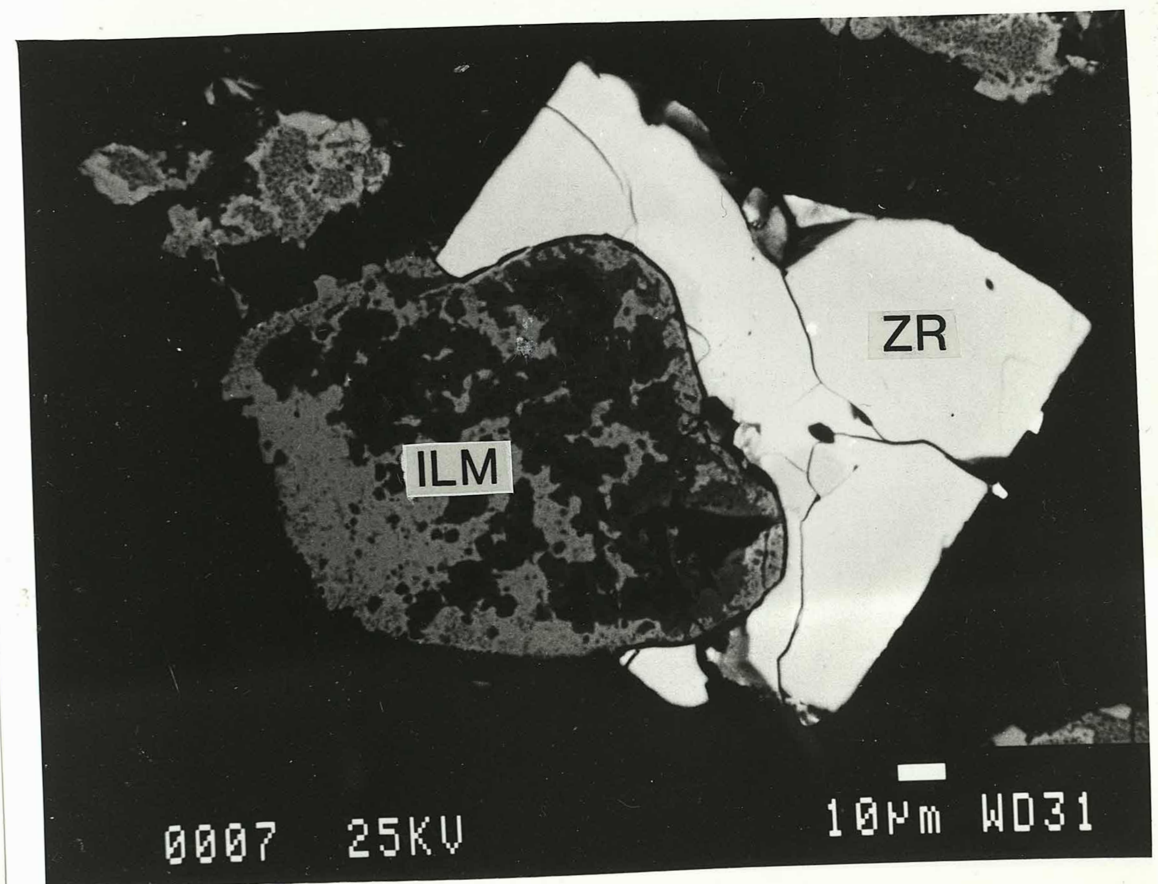

FIG. 3.99 Partially altered allanite crystal with rare earth elements in associated fractures within matrix. Sample C27, section C1, 305m, Moel Siabod Mbr., Tryfan slopes. BSSEM.

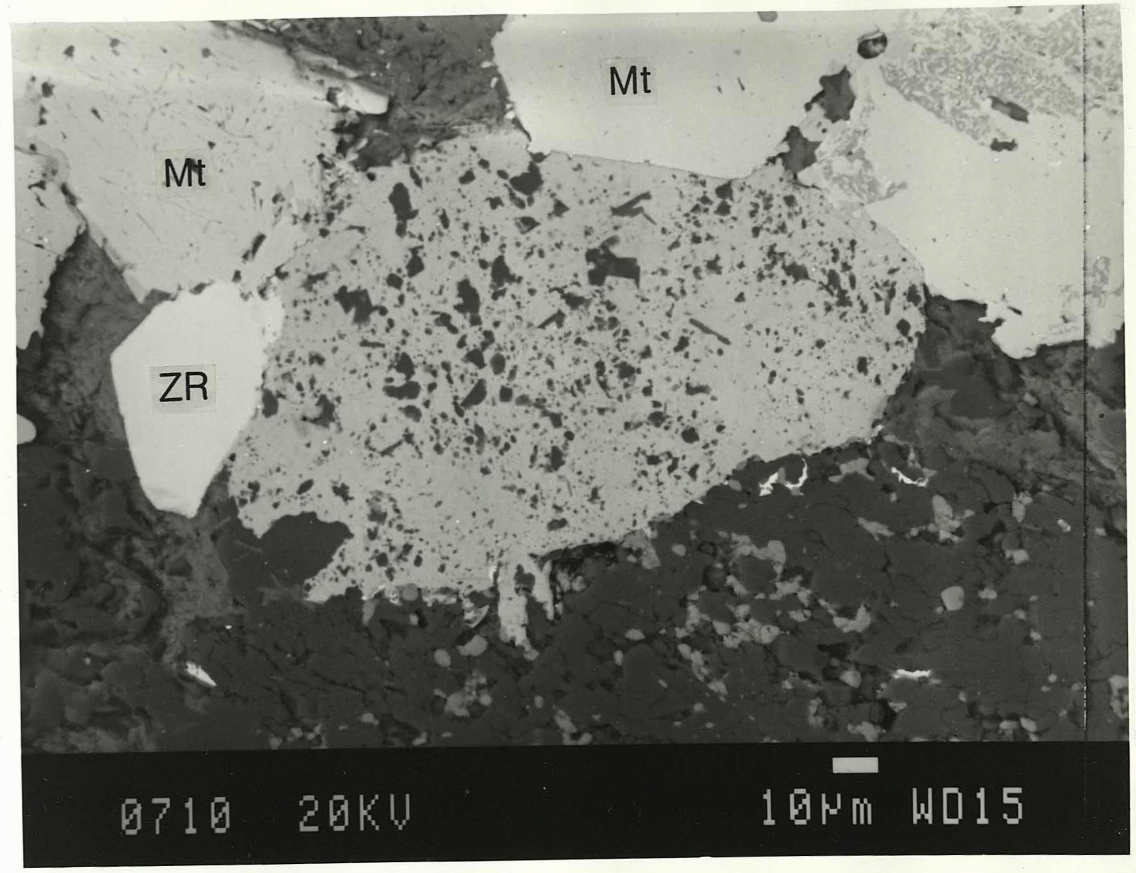

FIG. 3.100 Detail of rare earth element occurrence. Location as above.

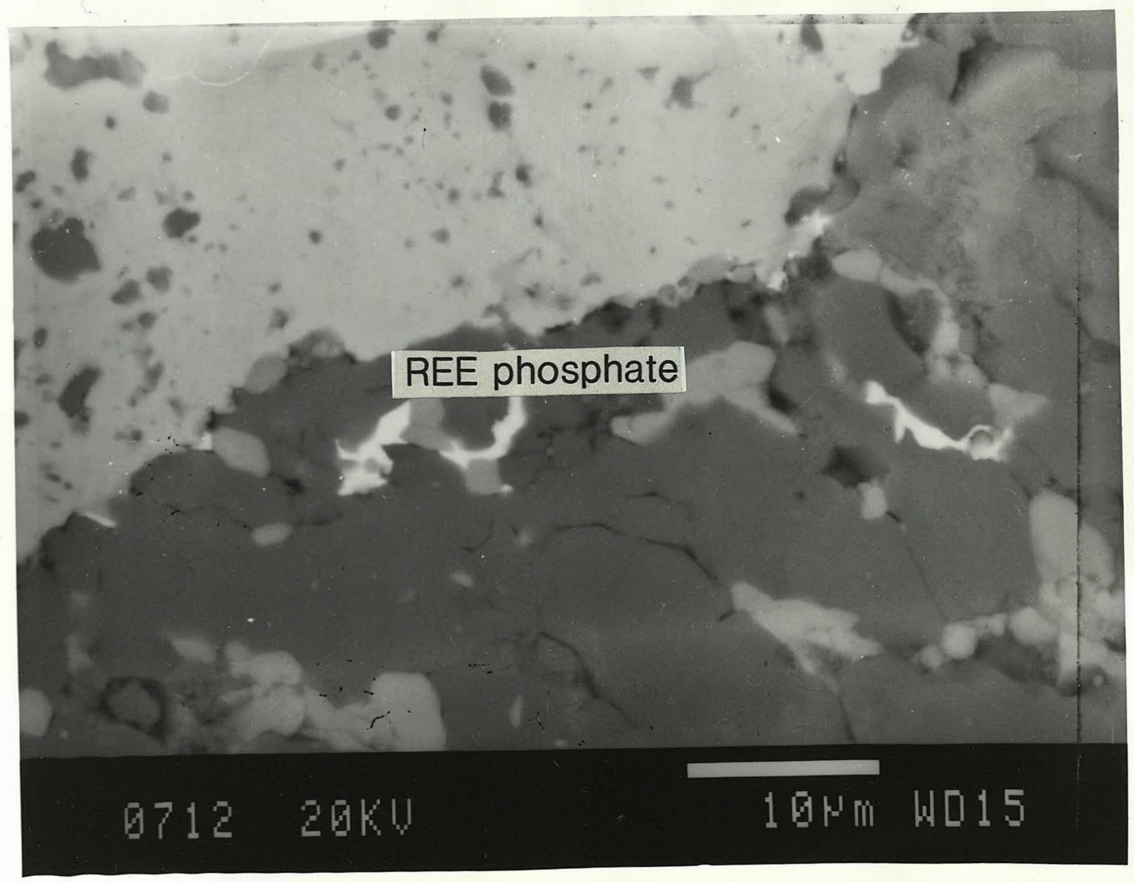

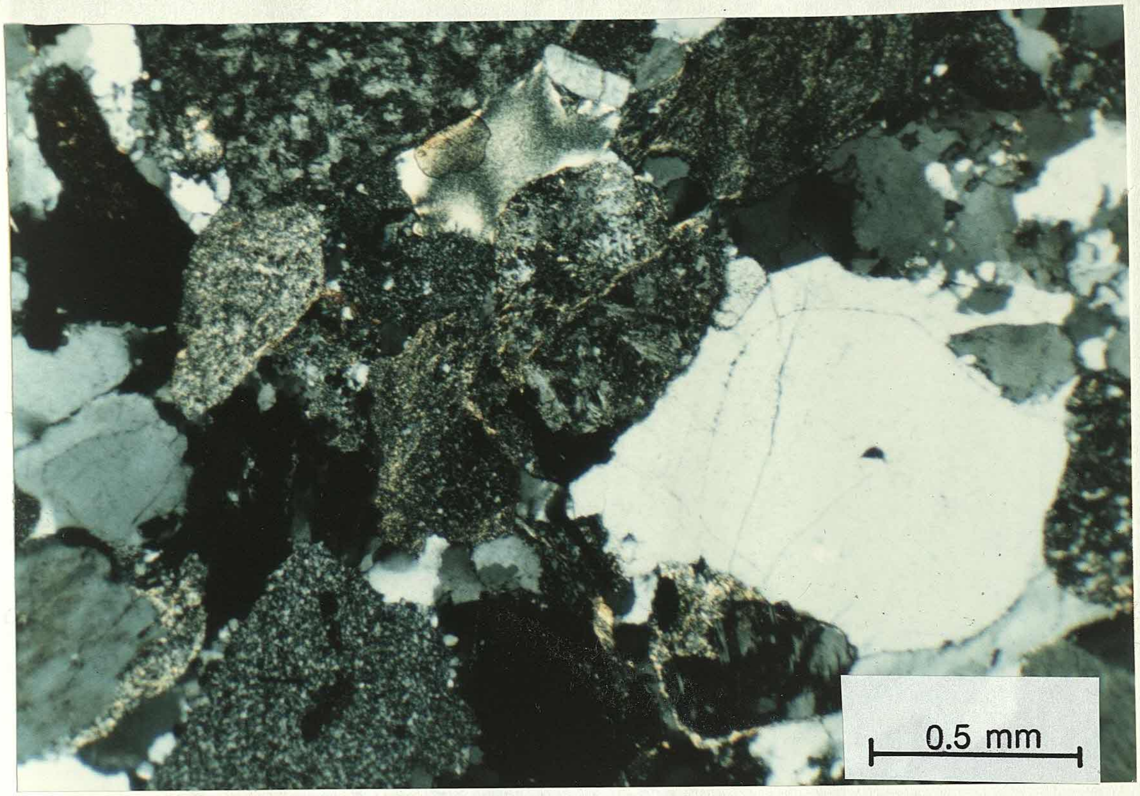

FIG. 3.101: Overgrowth on monocrystalline quartz within matrix poor quartzose volcaniclastic rock. Other detrital grains include albite, ?K-feldspar, volcanic "chert", and sericitic chert. ?Opaline cement at bottom. Section S10B, section S3, 25.5m. Upper Cwm Eigiau Fm., Tal-y-Fan. XPL.

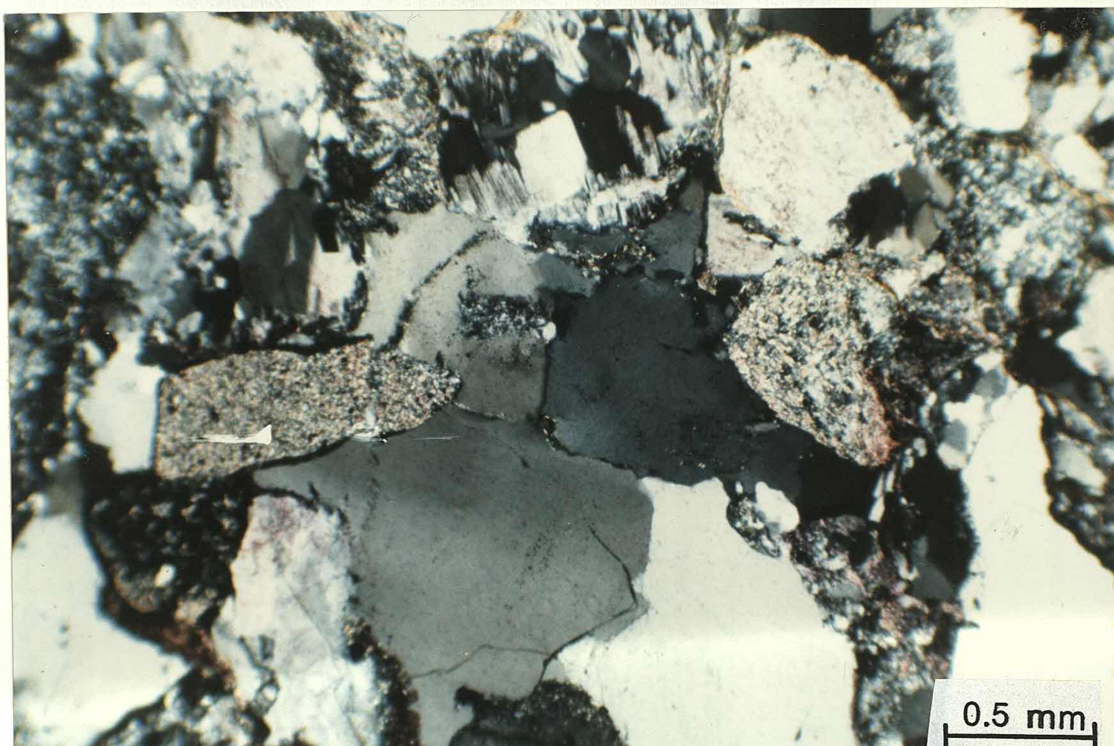

FIG. 3.102: Extensive quartz cementation within similar quartzose volcaniclastic sediment. Sample C26, section C1, 300m. Moel Siabod Mbr. of Tryfan Formation, Tryfan anticline. XPL.

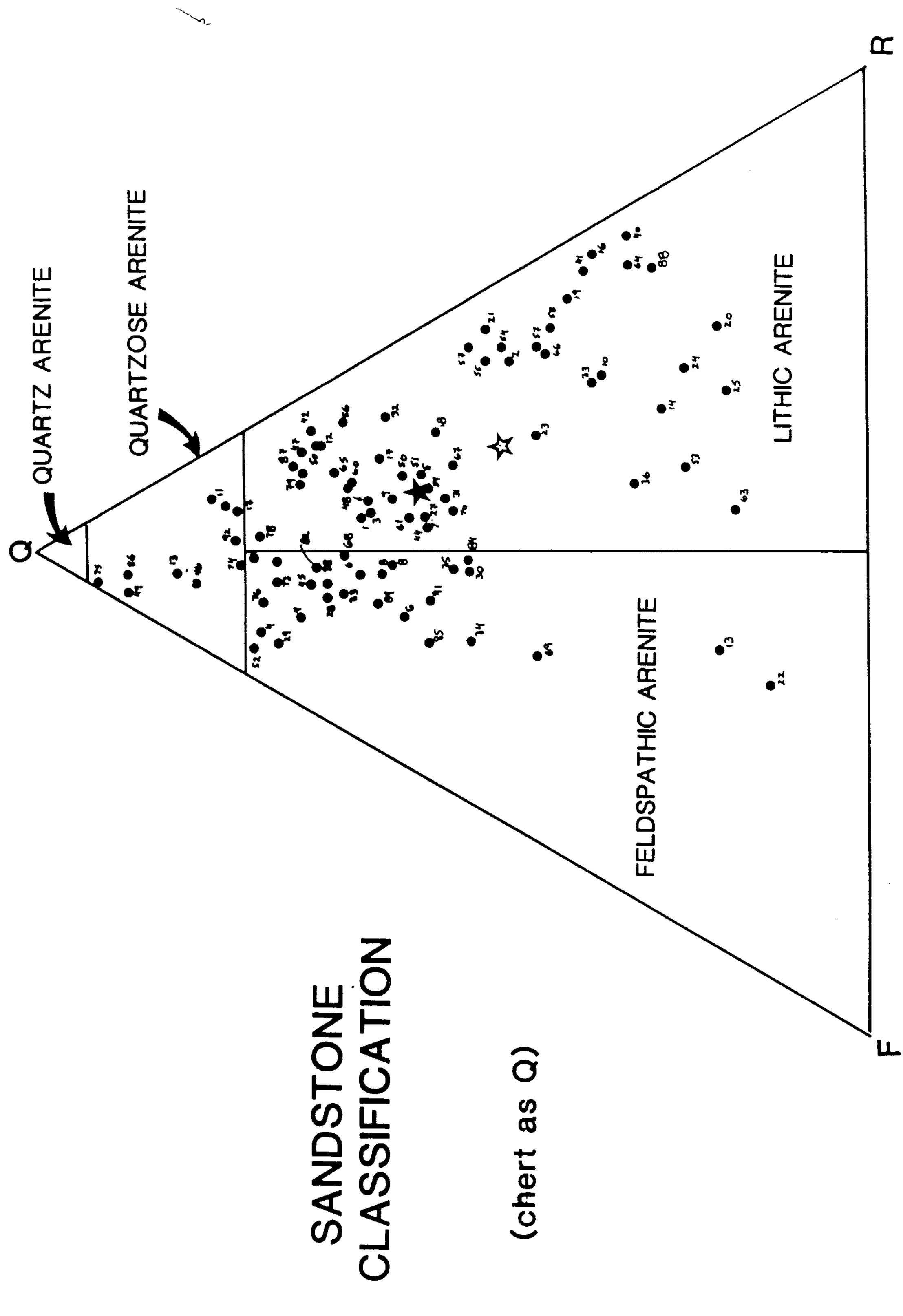

FIG. 3.103: A) Classification of sandstones with chert included as a Quartz grain. Numbers beside data points refer to observation numbers 1-92 (see Fig. 3.30 for identity). Black star denotes mean composition using this approach whereas hollow star depicts mean composition if chert included as a lithic fragment. Types of sandstones after Okada, 1971.

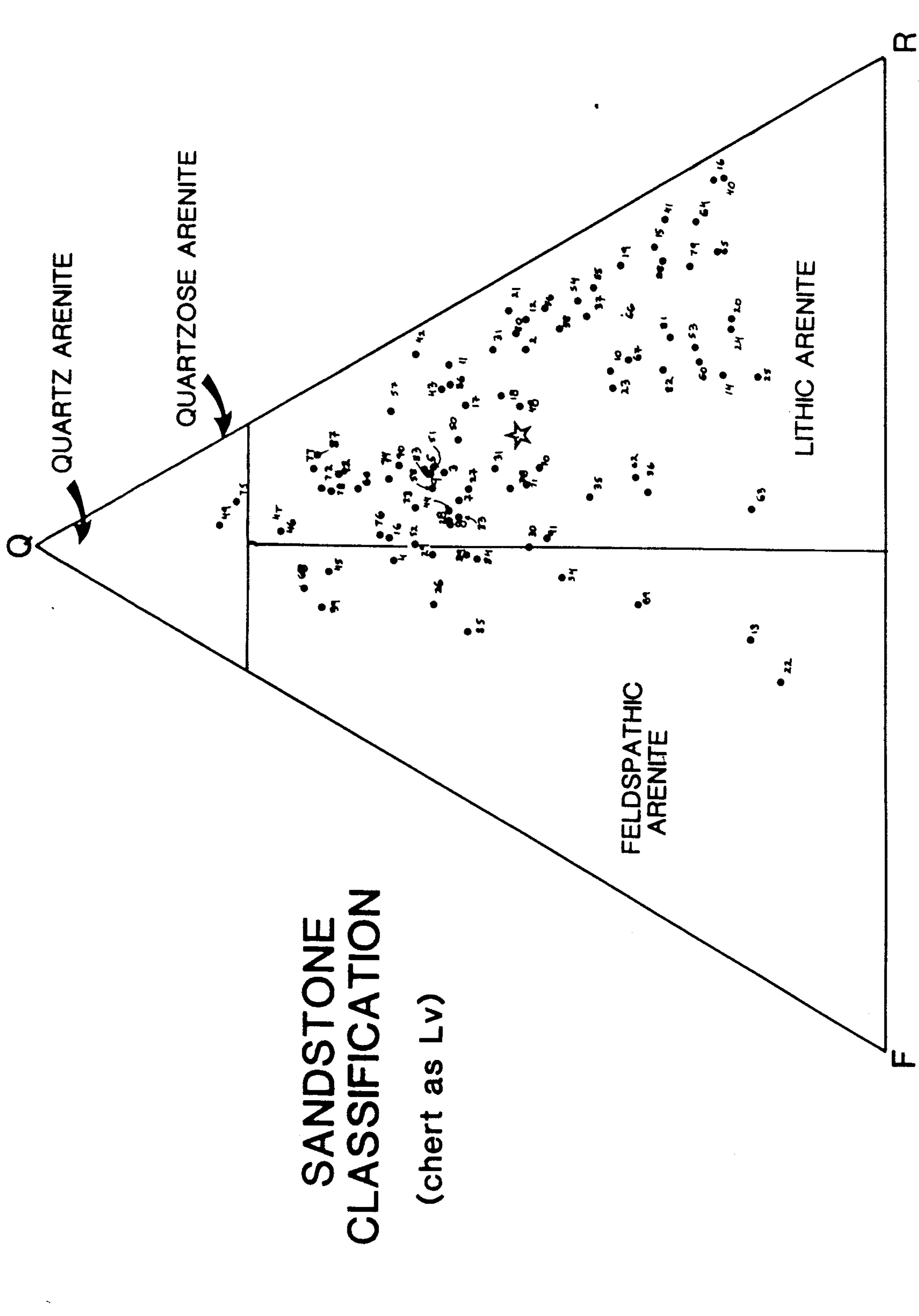

FIG. 3.103: B) Classification of sandstones with chert included as a lithic fragment. Numbers beside data points refer to observation numbers 1-92 (see Fig. 3.30 for identity). Hollow star denotes mean composition. Types of sandstones after Okada, 1971.

FIG. 3.104: A) Schematic cross-section of North Wales portion of Welsh marginal basin showing composition of sandstones for various petrogrographic units, as well as location of all samples. See Fig. 3.29 for explanation of variables and Fig. 3.31 for interpreting pie diagram. Values for important variables are show beside pie diagram; means and standard deviations for all variables are shown in Appendix 2.1. Size of pie diagram proportional to number of samples.

B) Following page. Detail showing lateral variation in sandstone petrography within various members of Llewelyn Volcanic Group.

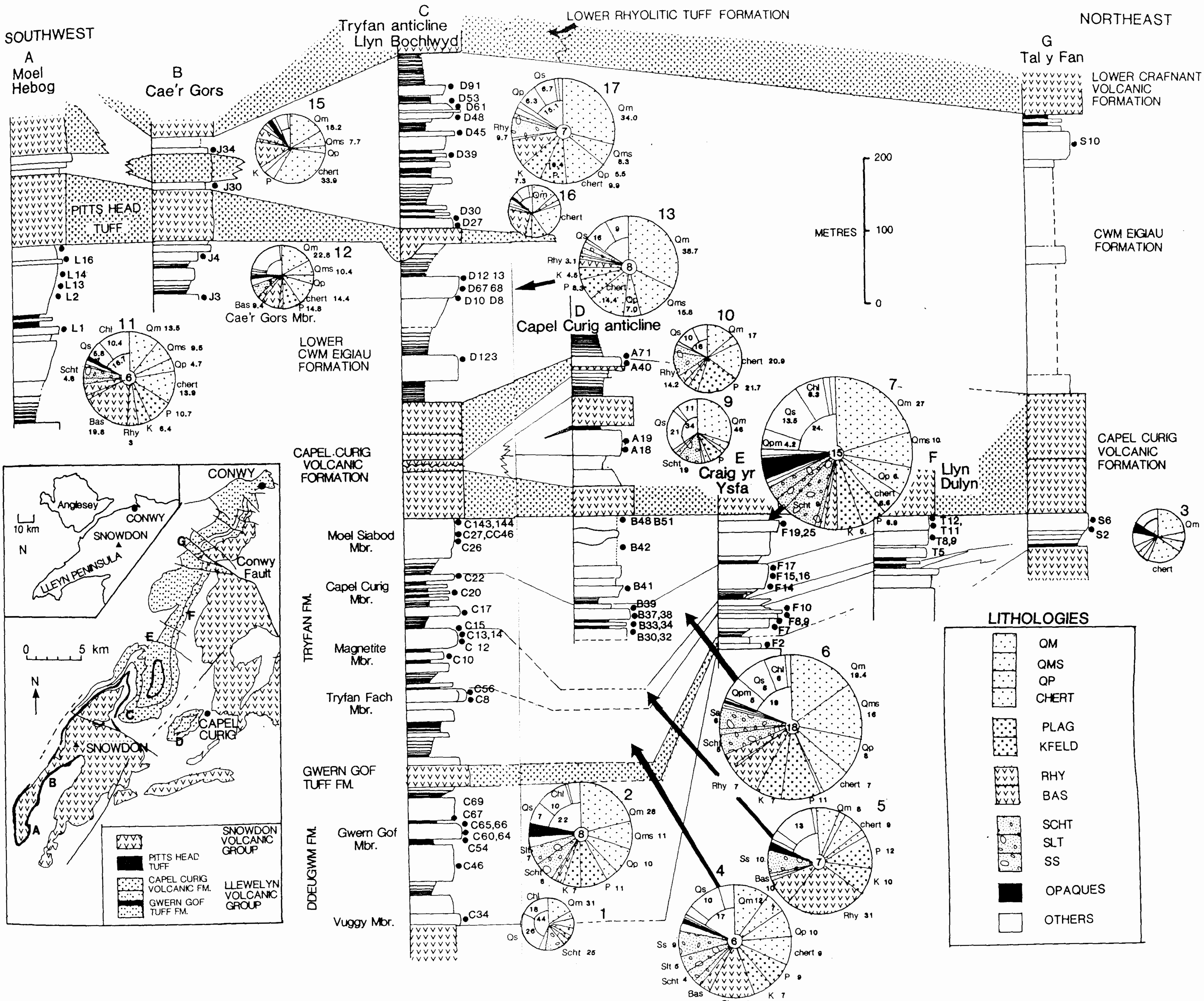

SOUTHWEST
NORTHEAST
LOWER RHYOLITIC TUFF FORMATION
A
Moel Hebog
B
Cae'r Gors
C
Tryfan anticline
Llyn Bochlwyd
D
Capel Curig anticline
E
Craig yr Ysfa
F
Llyn Dulyn
G
Tal y Fan
LOWER CRAFNANT VOLCANIC FORMATION
CWM EIGIAU FORMATION
CAPEL CURIG VOLCANIC FORMATION
PITTS HEAD TUFF
Cae'r Gors Mbr.
LOWER CWM EIGIAU FORMATION
CAPEL CURIG VOLCANIC FORMATION
TRYFAN FM.
Moel Siabod Mbr.
Capel Curig Mbr.
Magnetite Mbr.
Tryfan Fach Mbr.
GWERN GOF TUFF FM.
DDEUGWM FM.
Gwern Gof Mbr.
Vuggy Mbr.
METRES
200
100
0
LITHOLOGIES
QM
QMS
QP
CHERT
PLAG
KFELD
RHY
BAS
SCHT
SLT
SS
OPAQUES
OTHERS
CONWY
Anglesey
CONWY
10 km
N
SNOWDON
LLEYN PENINSULA
Conwy Fault
0 5 km
N
CAPEL CURIG
SNOWDON
SNOWDON VOLCANIC GROUP
PITTS HEAD TUFF
CAPEL CURIG VOLCANIC FM.
GWERN GOF TUFF FM.
LLEWELYN VOLCANIC GROUP

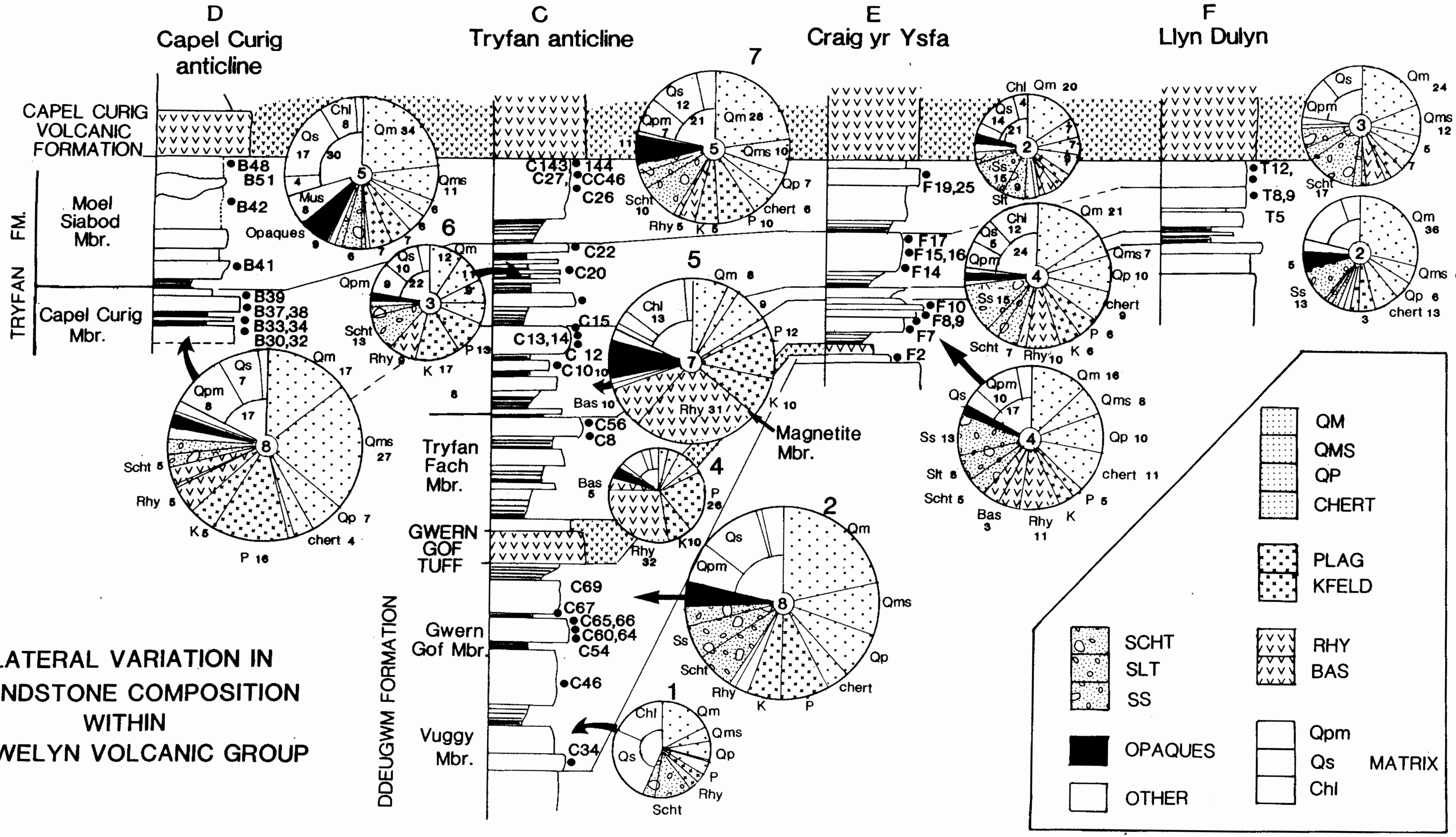

LATERAL VARIATION IN SANDSTONE COMPOSITION WITHIN LLEWELYN VOLCANIC GROUP

GRAIN PARAMETERS

(a) Q = Qm + Qms + Qp + CHALC + CHERT. where
- Q = total quartzose grains
- Qm = monocrystalline quartz, unstrained
- Qms = monocrystalline quartz, strained
- Qp = polycrstalline aphanitic quartz grains
- CHALC = chalcedony
- CHERT = CHERT

(B) F = P + K where
- F = total feldspar grains
- P = plagioclase feldspar grains
- k = potassium feldspar grains

(C) Lt = L + Qp where
- Lt = total lithic grains
- L = unstable lithic grains

(D) L = Lm + Lp + Lv + Ls where
- Lm = metamorphic lithic grains
- Lp = plutonic igneous lithic fragments
- Lv = volcanic lithic fragments
- Ls = sedimentary lithic fragments.

(E) Q2 F2 L2 PLOT: as above, with Chert as Lv.

(F) Qm3 F3 Lt PLOT, parameters as above.

(G) Qp2 Lv2 Ls2 plot , with polycrystalline quartz (chert) as Qp.

(H) Qp3 Lv3 Ls plot: with chert as Lv.

(I) Lp Lv3 Ls3: lithic parameters as above.

(J) Lp2 Lv4 Ls4: including chert as a lithic.

(K) Lvb: Lvr: LsLP PLOT where
- Lvb = basaltic volcanics
- Lvr = rhyolitic volcanics
- LsLp = sedimentary and plutonic lithics

(L) Qpm: Qs2: CHLM; plot of matrix components.

(M) Qm5: Qms5: Qp5: plot of quartz types, excluding chert

(N) Qm6 Qms6 Qp6: plot of quartz types, including chert as Qp.

FIG. 3.105a: MEANING OF VARIOUS GRAIN PARAMETERS USED IN TRIANGULAR DIAGRAMS.

VARIABLE	N	MEAN	STANDARD DEVIATION	MINIMUM VALUE	MAXIMUM VALUE	STD ERROR OF MEAN
Q	92	54.03	18.25	12.13	93.14	1.90
F	92	17.09	10.13	2.84	56.75	1.06
L	92	28.88	17.82	0.00	67.96	1.86
Q2	92	43.85	16.13	12.13	77.71	1.68
F2	92	17.09	10.13	2.84	56.75	1.06
L2	92	39.05	16.93	10.92	77.10	1.77
QM2	92	36.13	16.10	2.69	75.95	1.68
F3	92	17.09	10.13	2.84	56.75	1.06
LT	92	46.77	16.94	15.65	86.06	1.77
QP2	92	43.56	24.27	0.00	100.00	2.53
LV	92	27.73	23.44	0.00	91.30	2.44
LS	92	28.71	26.39	0.00	92.31	2.75
QP3	92	18.38	13.47	0.00	53.33	1.40
LV2	92	52.91	26.82	2.55	100.00	2.80
QM3	92	67.17	17.85	12.23	92.26	1.86
P	92	19.73	13.01	3.88	66.55	1.36
K	92	13.10	9.70	1.55	56.59	1.01
LP	91	5.62	8.08	0.00	41.80	0.85
LV3	91	48.50	30.15	2.70	100.00	3.16
LS3	91	45.88	32.02	0.00	97.30	3.36
LP2	92	4.48	8.53	0.00	46.36	0.89
LV4	92	65.03	30.25	2.70	100.00	3.15
LS4	92	34.97	30.25	0.00	97.30	3.15
LVB	92	8.68	14.67	0.00	74.23	1.53
LVR	92	53.60	28.87	1.35	100.00	3.01
LSLP	92	37.72	29.18	-0.00	97.30	3.04
QPM2	91	16.72	30.97	0.00	100.00	3.25
QS2	91	48.59	39.72	0.00	100.00	4.16
CHLM	91	34.69	36.48	0.00	100.00	3.82
QM5	92	55.58	20.66	0.00	99.33	2.15
QMS5	92	25.12	15.60	0.00	92.49	1.63
QP5	92	19.30	14.53	0.00	85.16	1.51
QM6	92	45.11	19.04	0.00	96.95	1.98
QMS6	92	20.75	14.25	0.00	89.53	1.49
QP6	92	34.15	16.98	0.00	85.16	1.77

FIGURE 3.105b : MEAN FRAMEWORK MODES OF VOLCANICLASTIC SANDSTONES. See Fig. 3.105a for explanation of grain parameters. Calculations for individual samples presented in Appendix 2.1. The means and standard deviations plotted in the following triangular diagrams are not statistically rigorous because the data sets are constant sum. Although the exact meaning of the statistical fields is ambiguous, they still provide a measure of the dispersion of the data set.

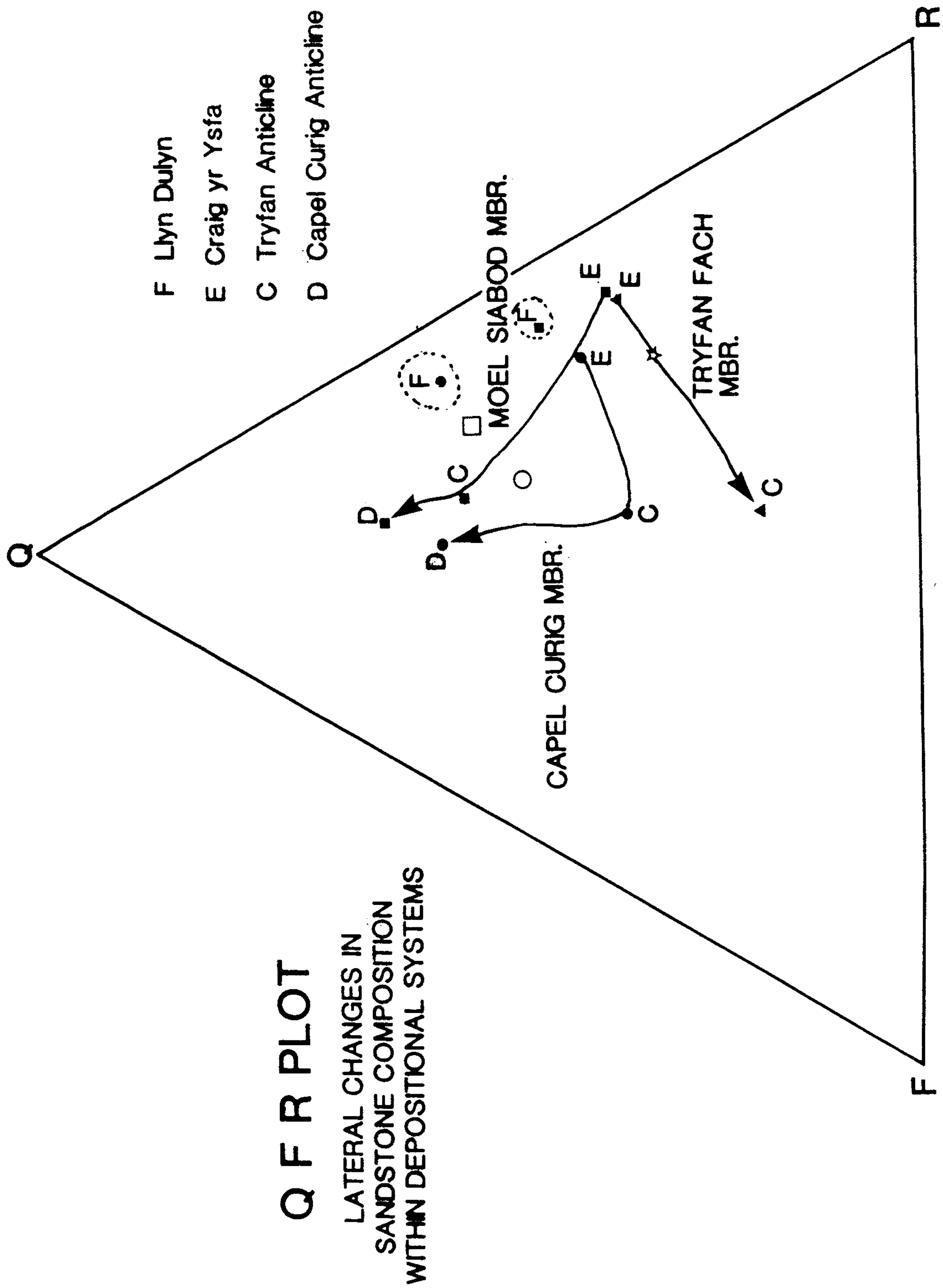

FIG. 3.106: Triangular QFR plot showing lateral changes in mean framework modes within 3 depositional systems. Data from appendix 2.1. Chert included as lithic fragment. See Figure 3.105 for explanation of grain parameters. Hollow circle, square, and asterix denotes mean composition for the Capel Curig, Moel Siabod, and Tryfan Fach depositional systems respectively.

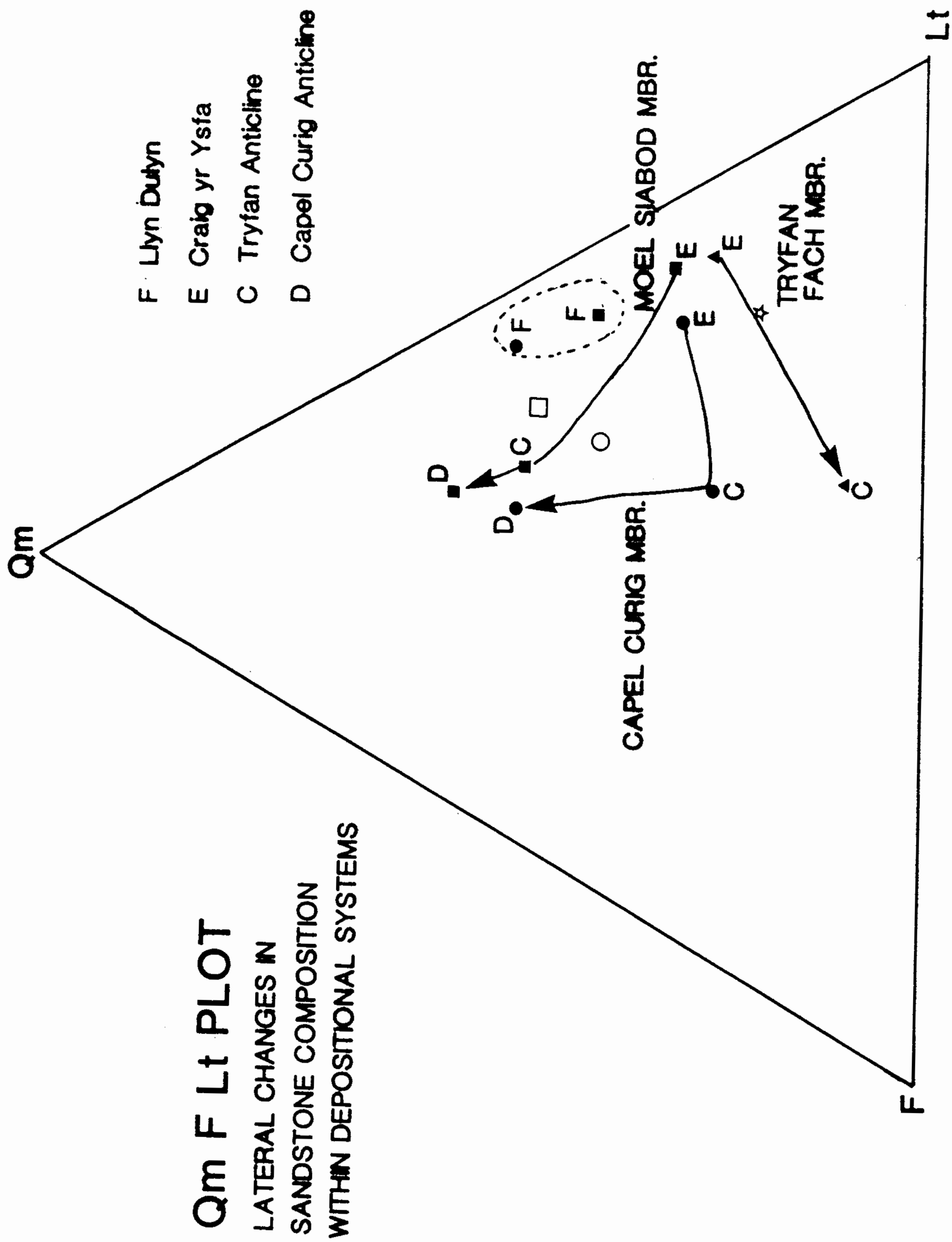

FIG. 3.107 Triangular QmFLT plot showing lateral changes in mean framework modes within 3 depositional systems. Data from appendix 2.1. Chert included as lithic fragment. See Figure 3.105 for explanation of grain parameters. Hollow circle, square, and asterix denotes mean composition for the Capel Curig, Moel Siabod, and Tryfan Fach depositional systems respectively.

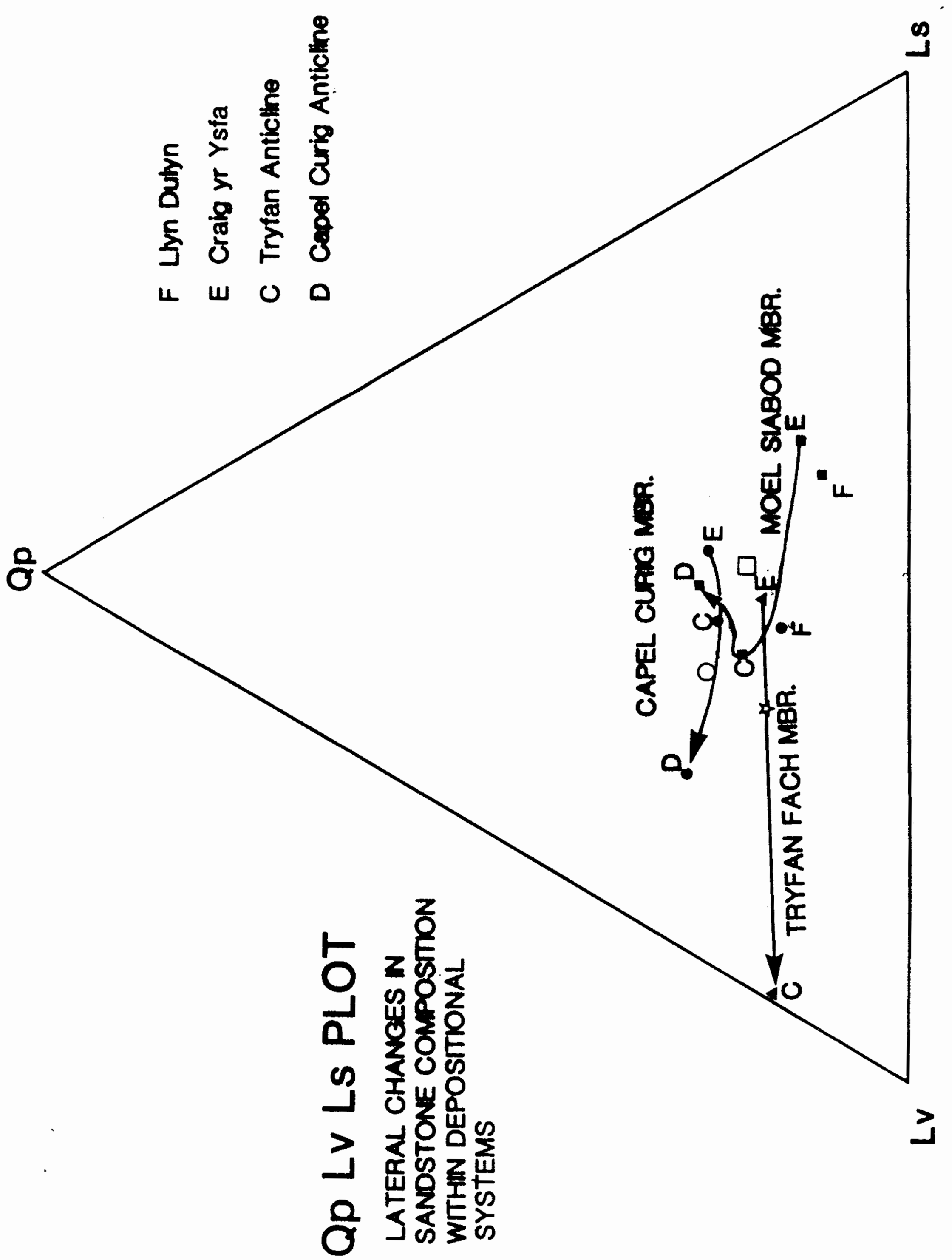

FIG. 3.108: Triangular QpLvLs plot showing lateral changes in mean framework modes within 3 depositional systems. Data from appendix 2.1. Chert included as volcanic lithic fragment. See Figure 3.105 for explanation of grain parameters. Hollow circle, square, and asterix denotes mean composition for the Capel Curig, Moel Siabod, and Tryfan Fach depositional systems respectively.

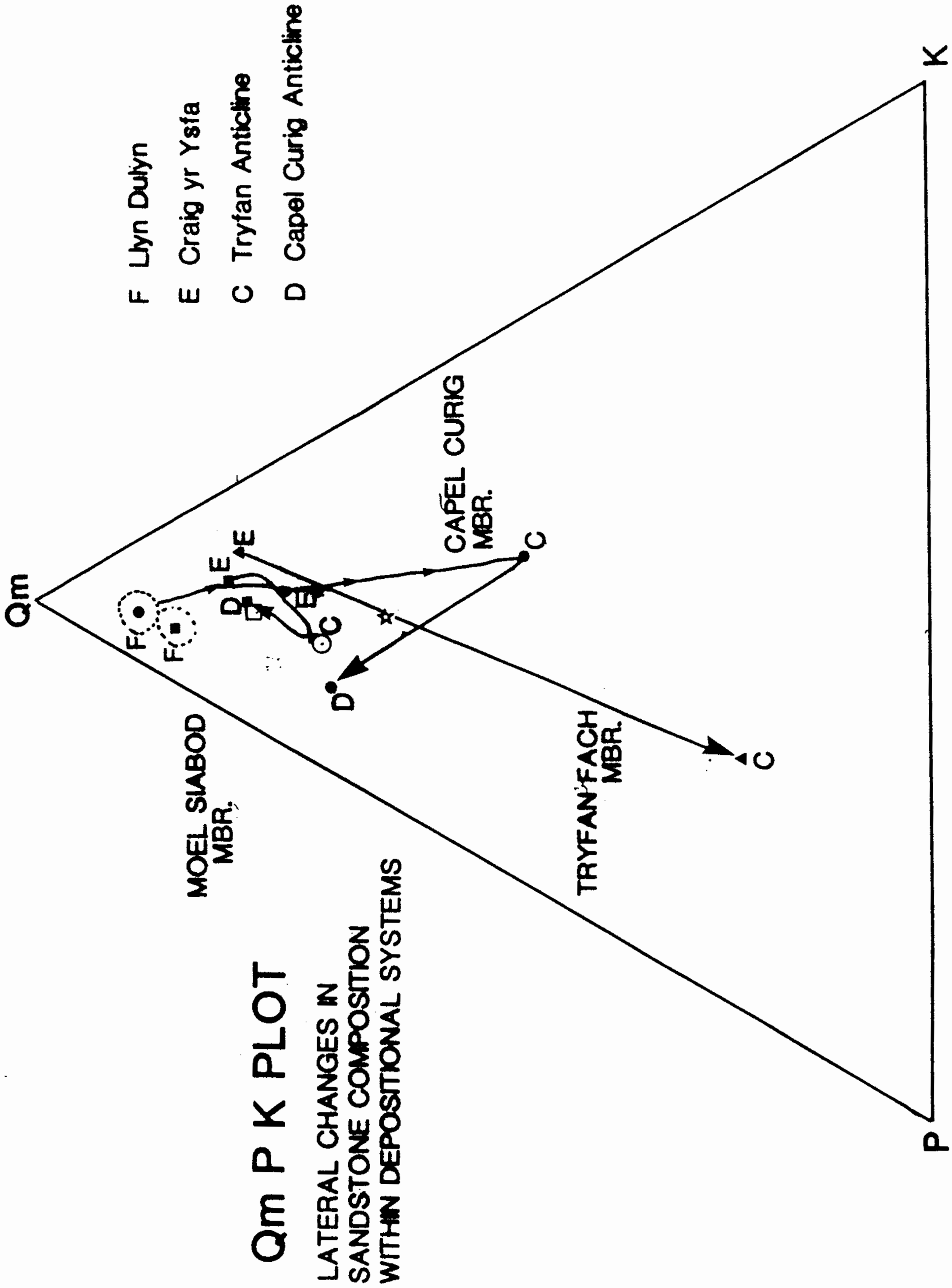

FIG. 3.109: Triangular QmPk plot showing lateral changes in mean framework modes within 3 depositional systems. Data from appendix 2.1. See Figure 3.105 for explanation of grain parameters. Hollow circle, square, and asterix denotes mean composition for the Capel Curig, Moel Siabod, and Tryfan Fach depositional systems respectively.

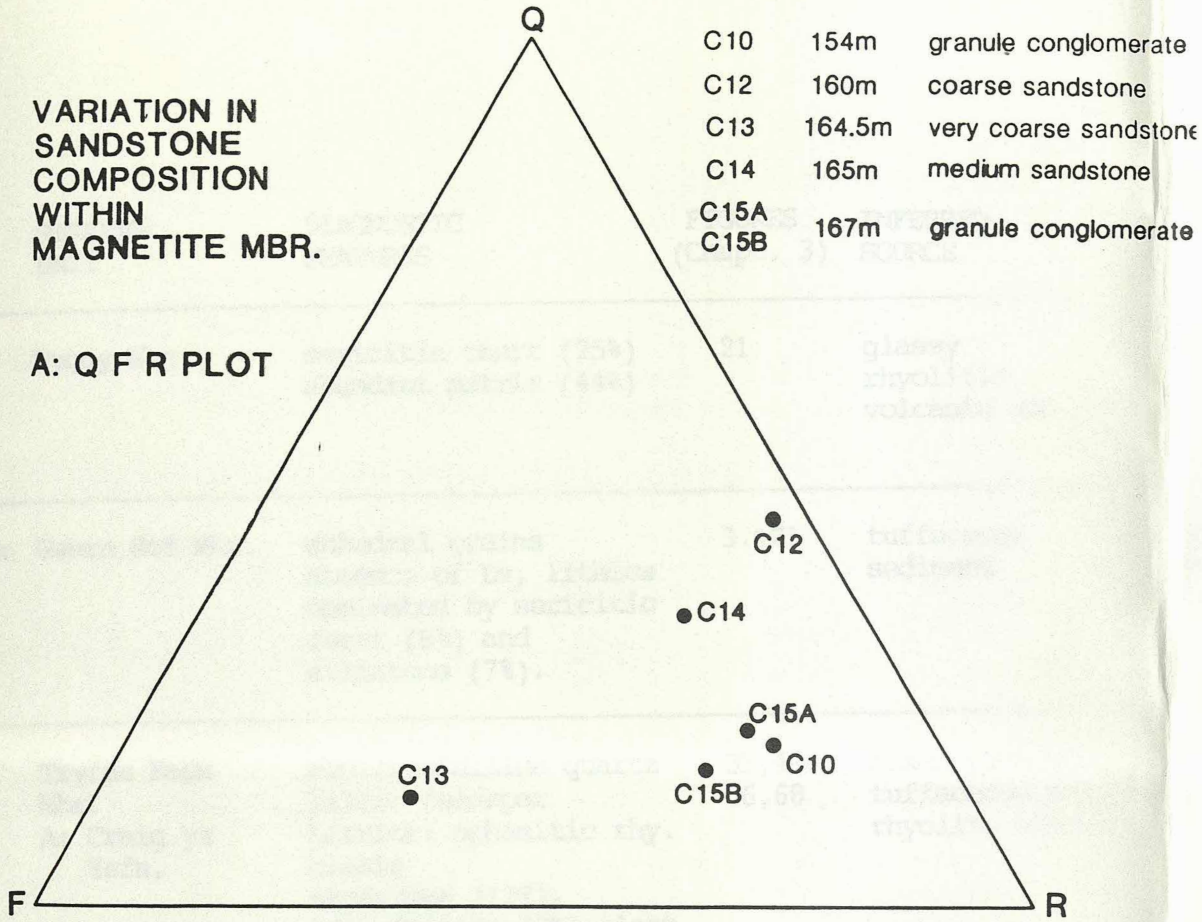

C): Small half-graben from fluvial sandstones of the Magnetite Mbr. infilled by coarse grained detritus consisting largely of euhedral plagioclase, sanidine and quartz crystals and rhyolitic rock fragments. Trough cross-stratified "background" sediments composed of basalt grains and opaque heavy minerals in a chloritic matrix. Photo illustrates the rapidity of textural and compositional variation that one should expect within a back-arc basin.

FIG. 3.110 A) QFR and B) Lvb:Lvr:Lslp plots showing variation in sandstone composition according to grain size within fluvial sandstones from the Magnetite Mbr. of the Tryfan Fm., Tryfan anticline. The total stratigraphic interval covered by sandstones is only 13m. Data from Appendix 2.1. Star denotes mean composition for Magnetite Mbr. (6 samples).

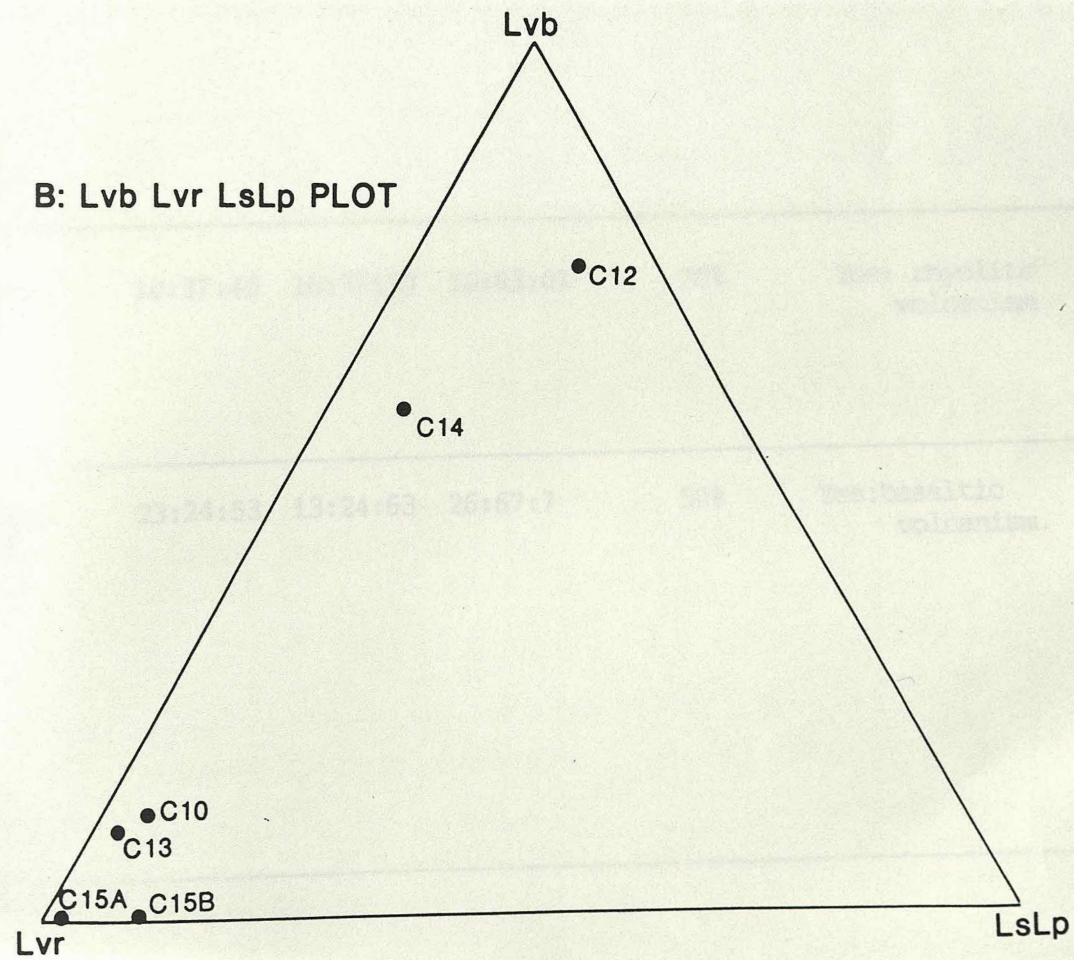

	THICK-NESS	STRATIG. UNIT	DIAGNOSTIC FEATURES	FIGURES (Chapt. 3)	INFERRED SOURCE	DIRECTION OF SOURCE	Q:F:R	Qm:F:Lt	Lvb:Lvr:LsLp	PERCENT EPI-CLASTIC	CONTEMP. VOLCANISM
1	5m	Vuggy Mbr.	sericitic chert (25%) abundant matrix (44%)	21	glassy rhyolitic volcanic ash	east	52:12:36	41:12:47	0:23:77	20%	Yes: rhyolitic
2	140m	Gwern Gof Mbr.	anhedral grains absence of Lv, lithics dominated by sericitic chert (8%) and siltstone (7%).	3.121	tuffaceous sediment	south-east	51:19:30	41:19:41	3:35:62	100%	NO
									Qp:Lv:Ls		
4	60m	Tryfan Fach Mbr. A: Craig yr Ysfa.	monocrystalline quartz little feldspar Lithics: aphanitic rhy. clasts sandstone (13%), occ. granite (3%) clast. -anhedral crystal texture.	39,40 66,68	mixed plutonic, tuffaceous sed., rhyolite source	east	39:9:57	24:8:68	17:43:40	85%	minor rhyolitic.
	60m	B: Tryfan Anticline	-less quartz -large plagioclase/ sanidine crystals. -lithic clasts dominated by porphyritic rhyolite.	54,55	crystal-rich rhyolite volcanics	south-west	18:37:45	10:37:53	16:83:01	70%	Yes: rhyolite volcanism
5	50m	Magnetite Mbr. very fine to coarse ss.	-basaltic lithics and opaque heavy minerals in chloritic matrix.	50,62 71,72	basalt lava and tuff	south-west	23:24:53	13:24:63	26:67:7	50%	Yes:basaltic volcanism.
		very coarse ss-granule conglomerate	porphyritic rhyolite, euhedral sanidine, subhedral plagioclase, microcrystalline quartz matrix.	43,125	porphyritic rhyolite						

FIG. 3.111: Summary of sandstone composition and source terrains for each petrographic unit. See text for further explanation.

	THICK-NESS	STRATIG. UNIT	DIAGNOSTIC FEATURES		INFERRED SOURCE	DIRECTION OF SOURCE	Q:F:R	Qm:F:Lt	Lvb:Lvr:LsLp	PERCENT EPI-CLASTIC	CONTEMP. VOLCANISM
6	60m	Capel Curig Mbr. A: Craig yr Ysfa	-anhedral quartz and plagioclase. -tuffaceous sandstone and siltstone lithics	64	tuffaceous sediment	north-east	38:12:50	27:12:61	13:36:42	100%	NO
	200m	B: Tryfan Anticline	-large albitized sanidine crystals. -embayed and fractured β-quartz. -common chalcedony.	41	-influence of porphyritic rhyolite source.	mostly north-east	33:30:27	24:30:46	12:53:35	90%	Minor rhyolite volcanism.
	»30m	C: Capel Curig Anticline	-abundant monocrystalline embayed, euhedral, β-quartz. -pebbles of flow banded rhyolite and aplite. -matrix entirely Qp.	34,38 42,47 49,51 52,53	-high level rhyolite intrusive. -rhyolitic volcanic ash.	south-west	54:22:24	46:22:32	16:57:18	75%	Yes: rhyolite volcanism.
7	60m to 120m	Moel Siabod Mbr.	-medium grain size, abundant anhedral quartz. -outsized quartz in Capel Curig anticline -lithic fragments dominated by sericitic chert, sandstone and siltstone.	67,69 70,102	-tuffaceous sediment. -diminished influence of quartz porphyry.	mostly north-east	51:14:36	43:14:43	5:44:52	100%	NO
9	50m	Racks Mbr.	-anhedral Qm (47%) -lithics dominated by sericitic chert (19%) and siltstone. - a lot of matrix (35%).	122	-tuffaceous quartzose sediment.	south-west	58:15:28	54:15:31	2:10:88	100%	NO
10	0 to 200m	4th Mbr. CCVF	-cherty felstic microlitic rock fragments (21%) and sericitic chert (14%). -abundant euhedral plagioclase crystals (22%).	15,16	-crystal-rich rhyolitic volcanic ash.	north-west, at Glyder Fach	22:29:49	19:29:52	10:50:40	0%	YES: crystal rich rhyolite volcanics.

FIGURE 3.111: continued

	THICK-NESS	STRATIG. UNIT	DIAGNOSTIC FEATURES		INFERRED SOURCE	DIRECTION OF SOURCE	Q:F:R	Qm:F:Lt	Lvb:Lvr:LsLp	PERCENT EPI-CLASTIC	CONTEMP. VOLCANISM
11	140m	Hebog Mbr.	-low percentage Qm (13%) -altered microlitic or aphanitic basaltic rock fragments (20%). -mudstone fragments (8%) -clay/chlorite matrix	44,57 58,59 60,61 63	-50% Basaltic lava and ash. -35% mudstone & siltstone -15% rhy. sediment.	west	28:17:54	23:17:59	39:45:16	80%	YES: minor basalt volcanism -trace rhyolite volcanism.
12	70m	Cae'r Gors Mbr.	-porphyritic basalt with plagioclase phenocrysts (12%) -rhyolitic volcanic lithics (16%) -abundant opaque heavy minerals (4%). -matrix (29%) entirely chlorite.	124 125	-basaltic lava and tuff (80%) -rhyolite intrusive(20%)	north-west	41:22:37	34:22:44	26:56:18	95%	?NO
13	40m	Bochlwyd Mbr.	-anhedral Qm (38%) and Qms (17%). -aphanitic (14%) or porphyritic (3%) rhyolite lithics. -occ. granite fragment (1%)	126 127	-hypabyssal rhyolite intrusives.	south	63:13:24	56:13:31	6:81:13	100%	?NO
15	10m	Above PHT at Cae'r gors.	-Qm quartz (18%). -"chert" (34%) and rhyolite (14%) lithic fragments.		-reworked PHT and acidic ash flows.	west	33:8:60	28:8:64	1:88:11	30%	YES: additional rhyolitic pyroclastics
16	5m	Above PHT Gribin Ridge	-Qm quartz (16%) -clasts of welded and unwelded rhyolitic ash flow tuff.	19 20	-reworked Pitts Head Tuff.	local	25:17:57	21:17:61	1:95:4	5%	YES: Pitts Head Tuff
17	240m	Upper Cwm Eigiau Fm.	-abundant Qm (34%) -rhyolite (10%), chert (10%) and sericitic chert fragments dominate lithics.	24,23 27,36	-rhyolitic ash and hypabyssal intrusives.	south-west	49:18:33	43:18:39	2:53:45	70%	YES: common explosive rhyolitic volcanism.

FIGURE 3.111: continued

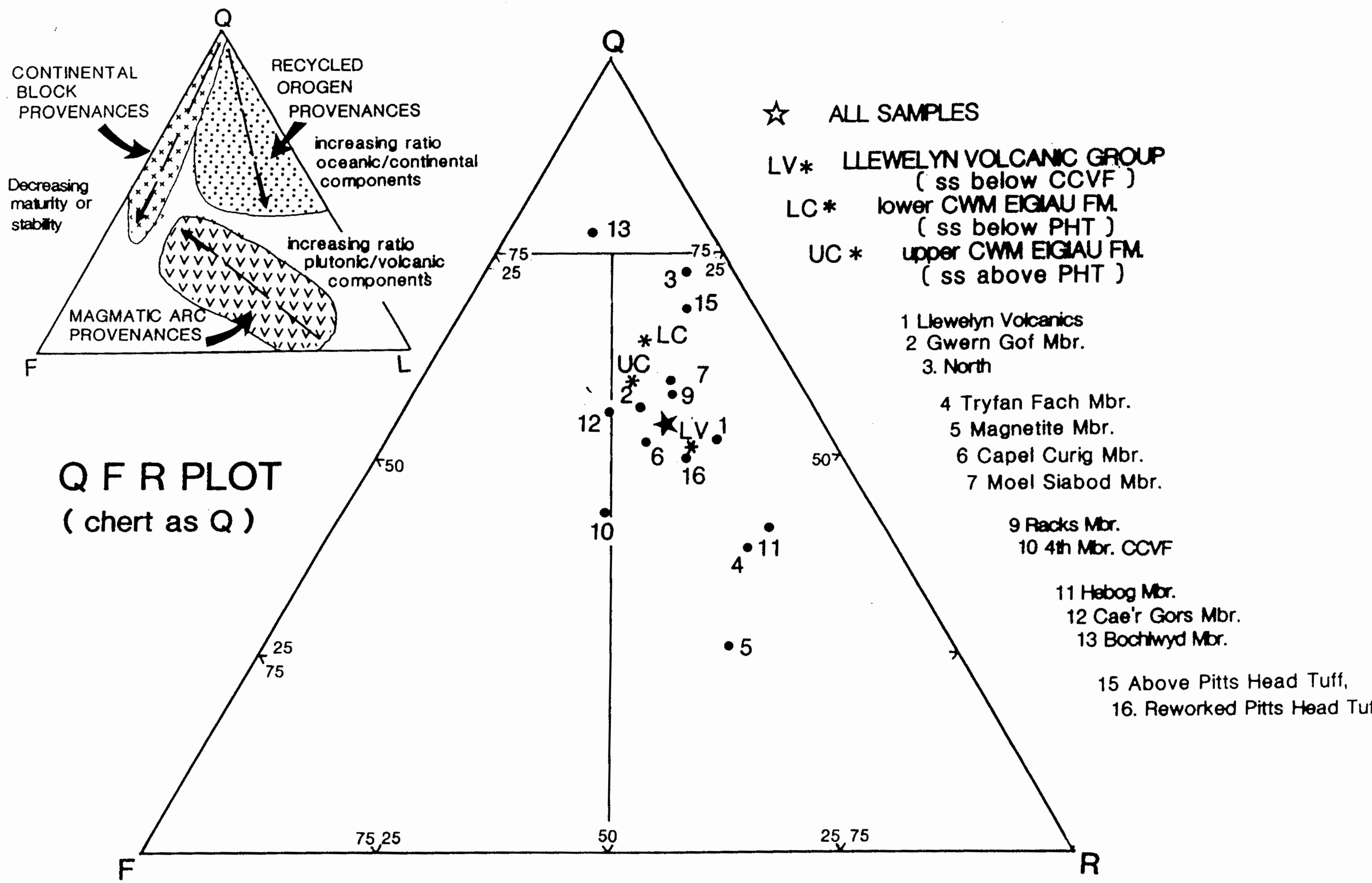

FIG. 3.112: A) QFR plot showing mean composition of all sandstones and the 17 petrographic units. Chert included with quartz. Identity of petrographic units is tabulated on the right; their regional and stratigraphic relationship can be seen graphically in Fig. 3.104. Inset triangle from Dickinson and Suczek, 1979.

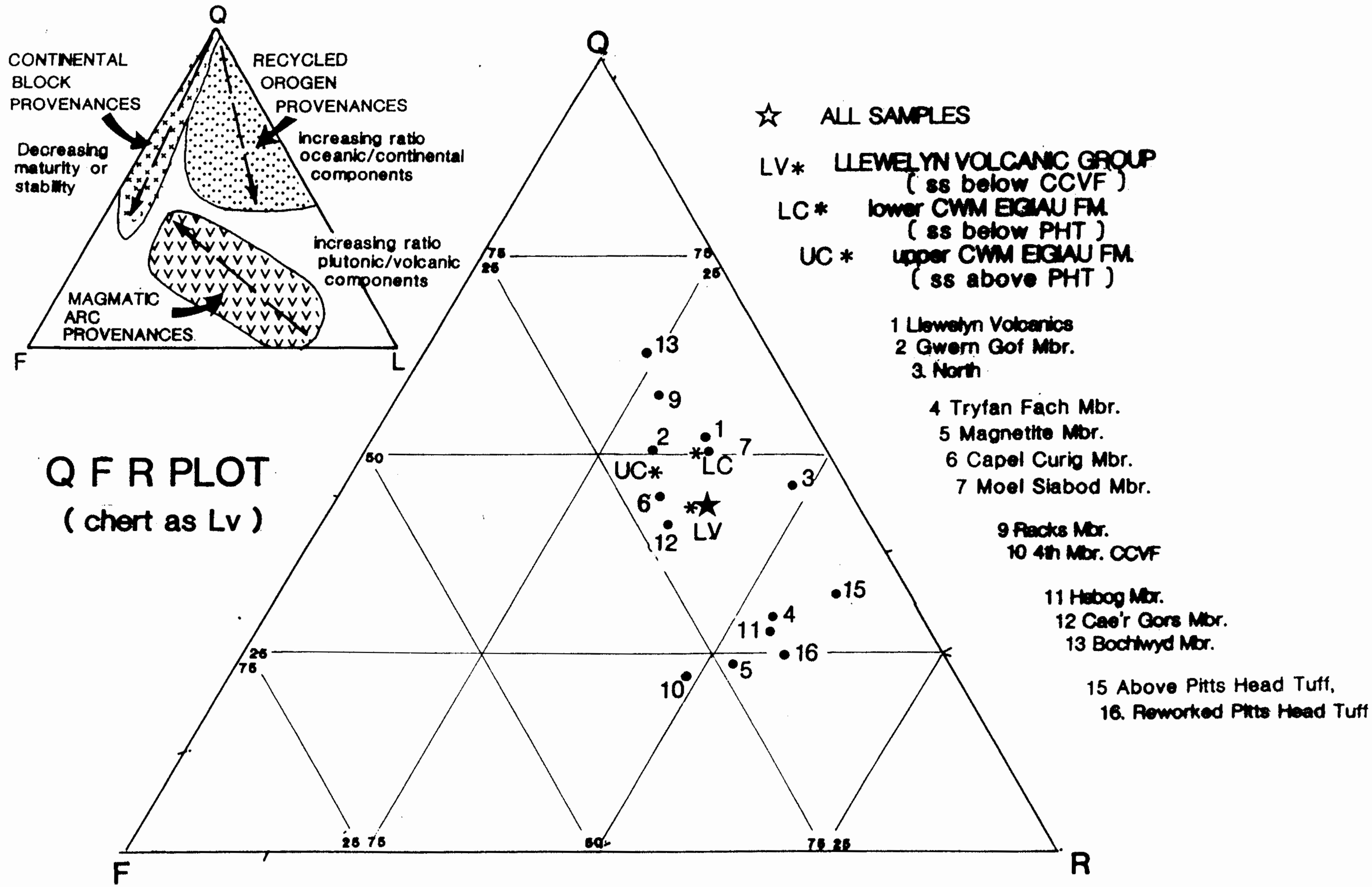

FIG. 3.112: B) QFR plot showing mean composition of all sandstones and the 17 petrographic units. Chert included with rock fragments. See Fig. 3.105 for identity of grain parameters. Identity of petrographic units is tabulated on the right; their regional and stratigraphic relationship can be seen graphically in Fig. 3.104. Inset triangle from Dickinson and Suczek, 1979.

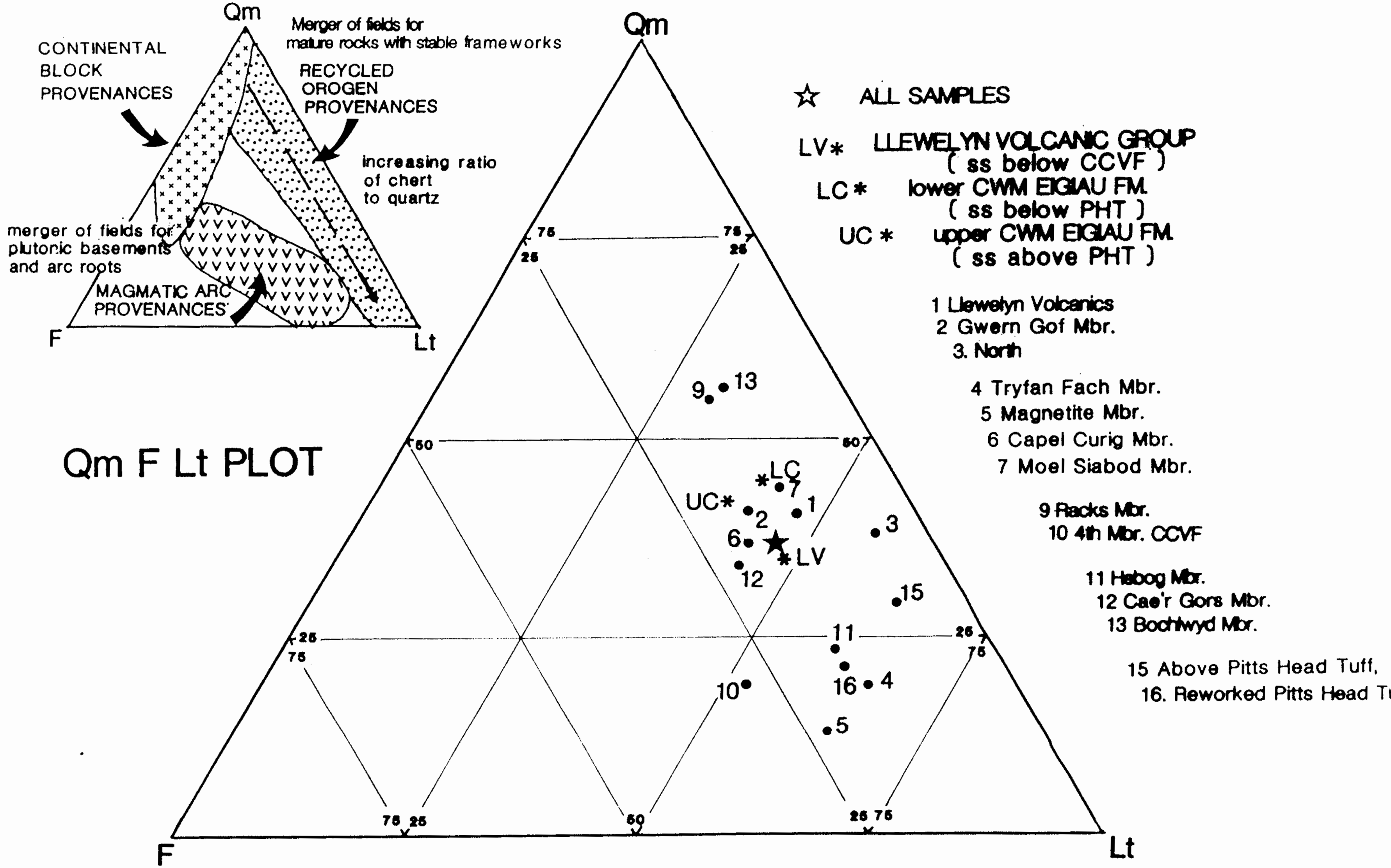

FIG. 3.113: QmFLt plot showing mean composition of all sandstones as well as the 17 petrographic units individually. See Fig. 3.105 for identity of grain parameters. Identity of petrographic units is tabulated on the right; their regional and stratigraphic relationship can be seen graphically in Fig. 3.104. Inset triangle from Dickinson and Suczek, 1979.

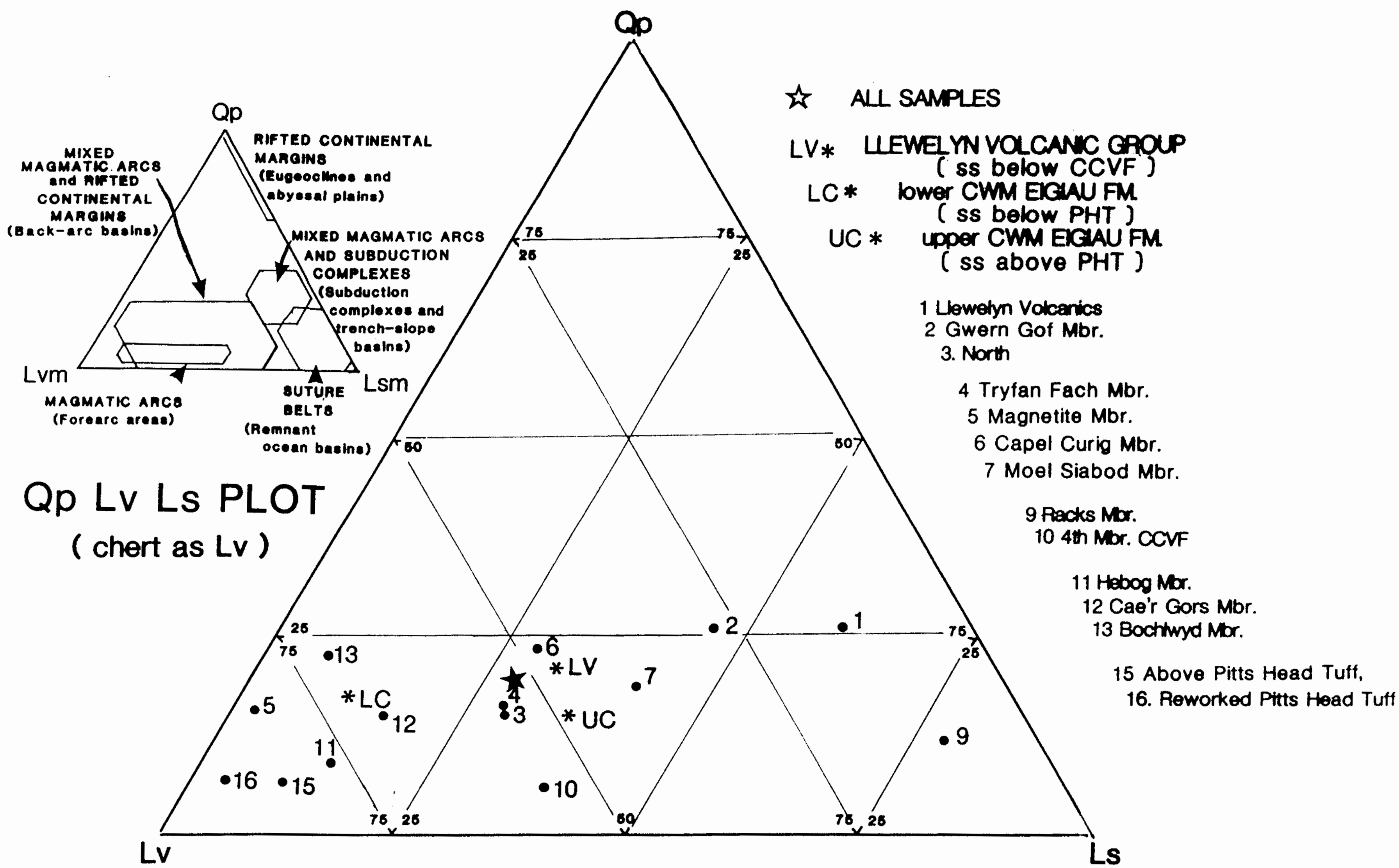

FIG. 3.114: QpLvLs plot showing mean proportion of polycrstalline lithic fragments for all 92 sandstones as well as the 17 petrographic units individually. See Fig. 3.105 for identity of grain parameters. Chert is included as a volcanic lithic. Identity of petrographic units is tabulated on the right; their regional and stratigraphic relationship can be seen graphically in Fig. 3.104. Inset triangle from Valloni and Maynard, 1981.

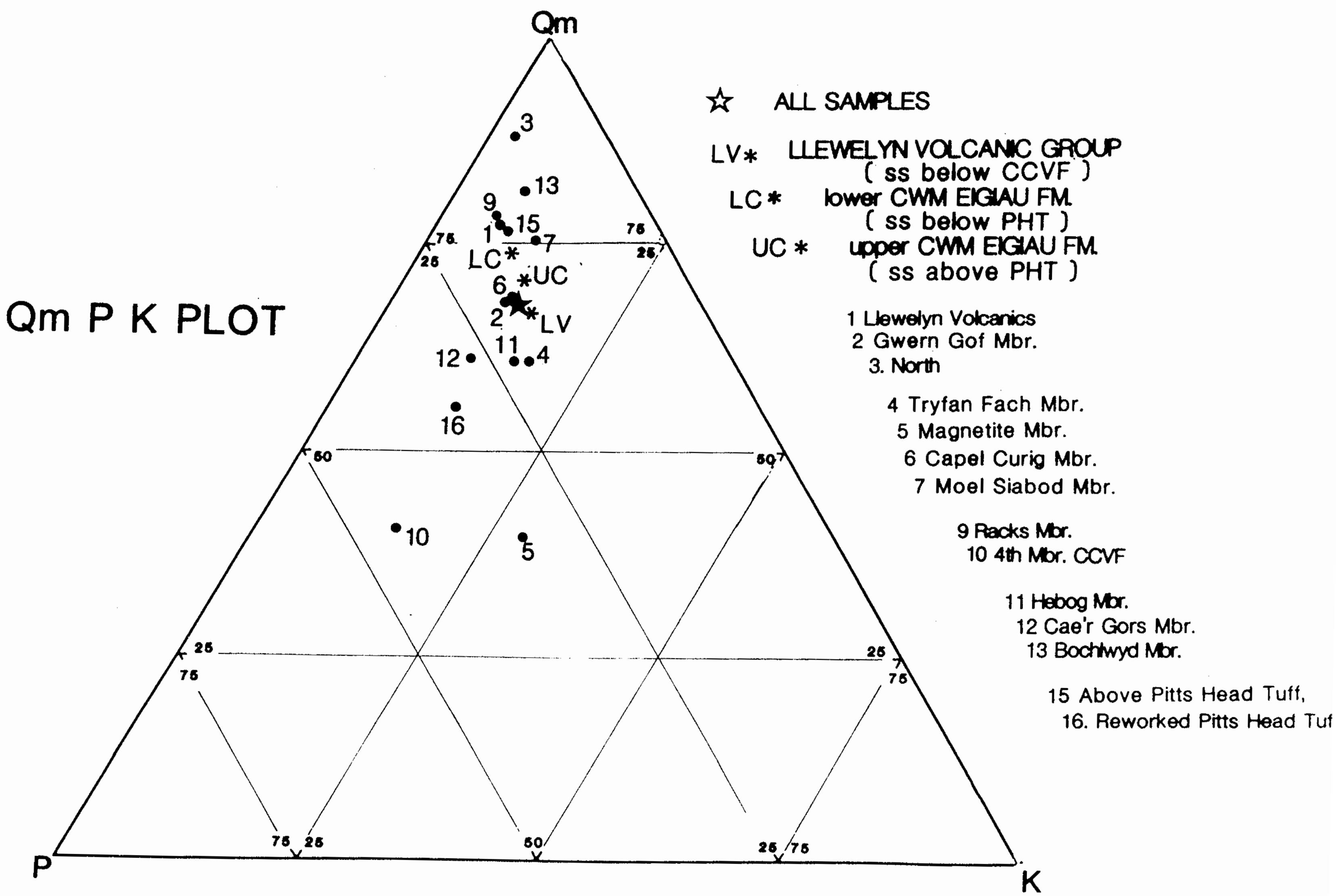

FIG. 3.115: QmPK plot showing mean proportion of monocrystalline mineral grains for all 92 sandstones as well as the 17 petrographic units individually. See Fig. 3.105 for identity of grain parameters. Identity of petrographic units is tabulated on the right; their regional and stratigraphic relationship can be seen graphically in Fig. 3.104.

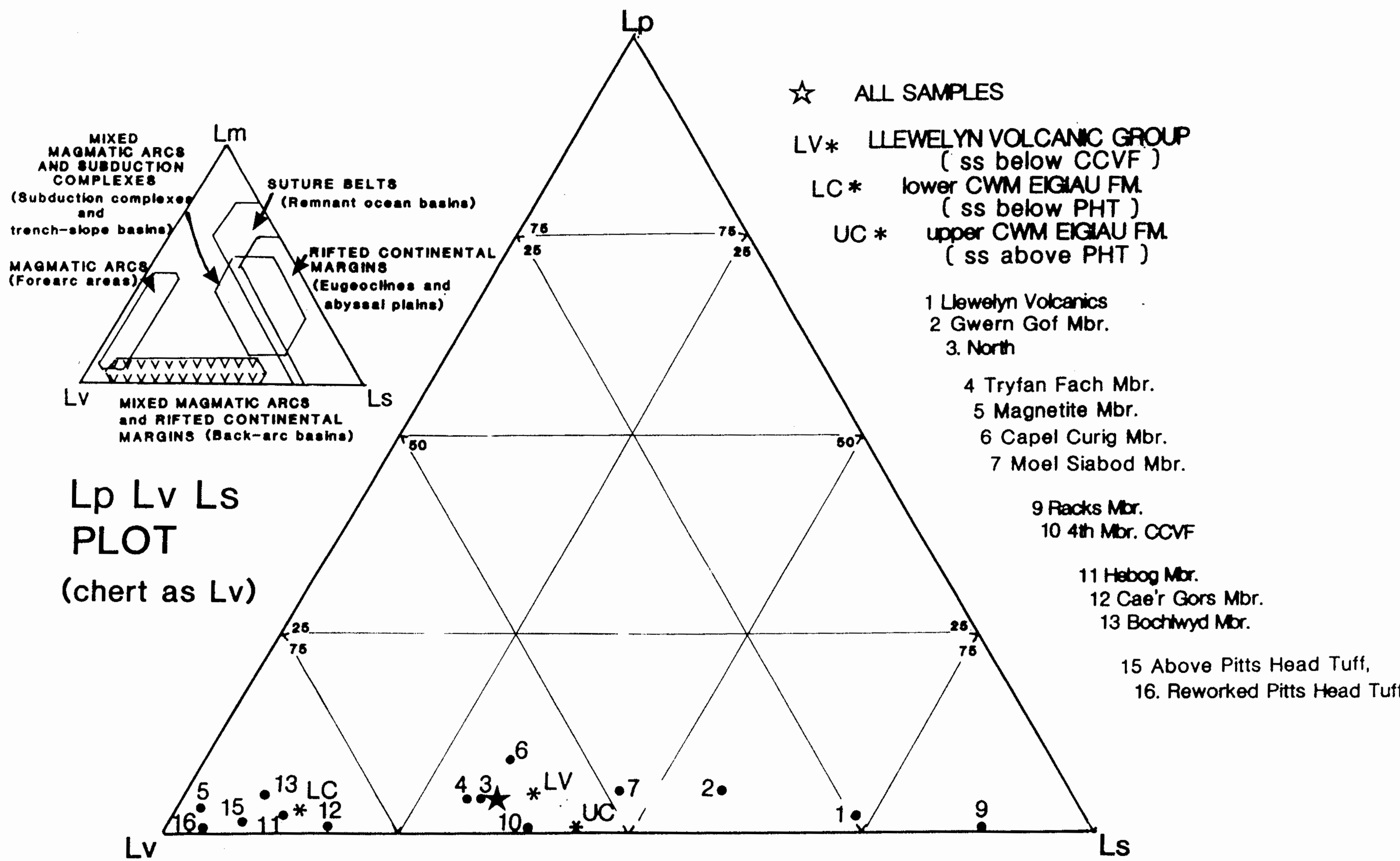

FIG. 3.116: LpLvLs plot showing mean proportion of unstable lithic fragments for all 92 sandstones as well as the 17 petrographic units individually. See Fig. 3.105 for identity of grain parameters. Identity of petrographic units is tabulated on the right; their regional and stratigraphic relationship can be seen graphically in Fig. 3.104. Inset triangle from Valloni and Maynard, 1981.

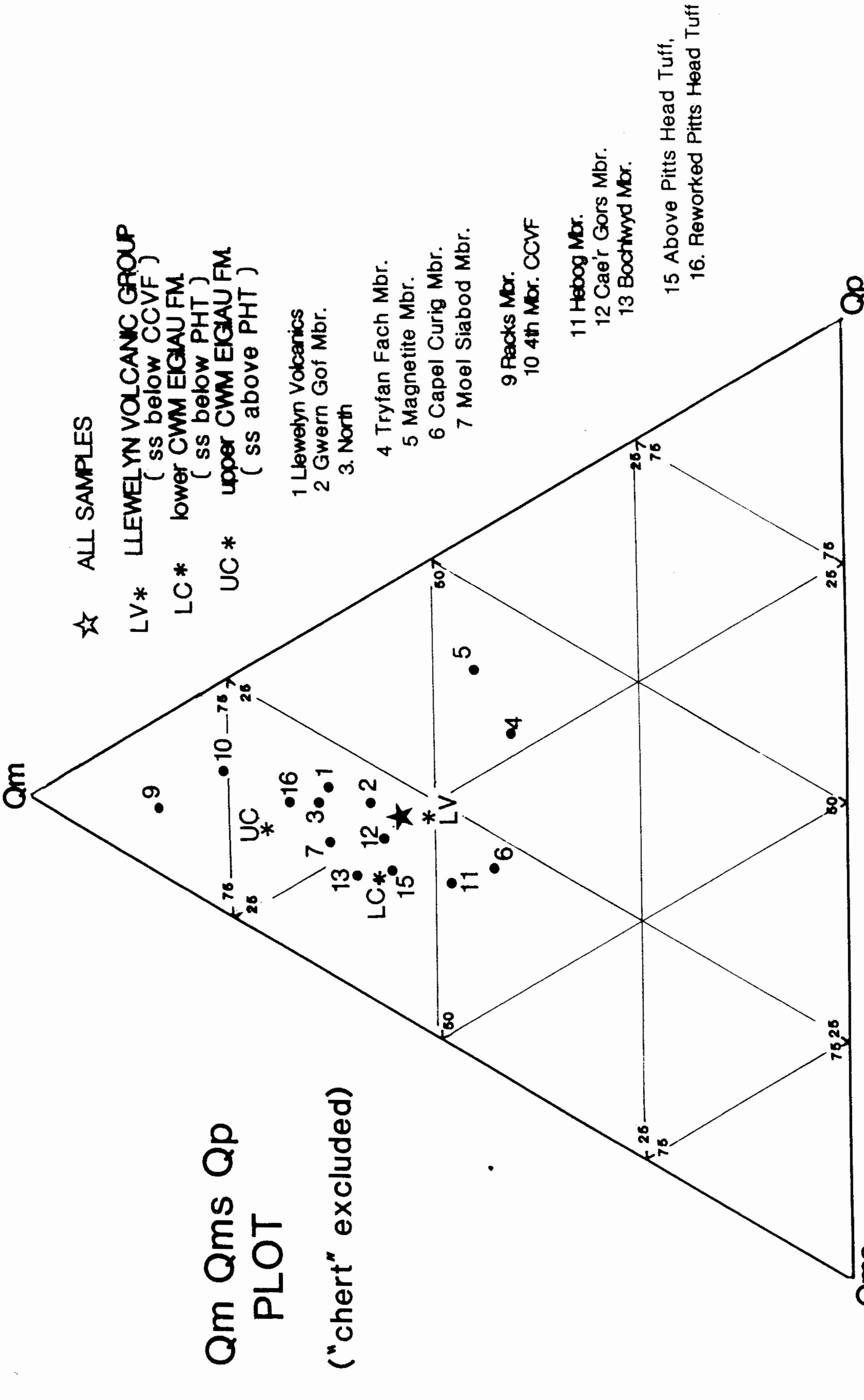

FIG. 3.117: QmQmsQp plot showing mean proprtions of quartz-types (excluding chert) for all 92 sandstones as well as the 17 petrographic units individually. See Fig. 3.105 for identity of grain parameters. Identity of petrographic units is tabulated on the right; their regional and stratigraphic relationshipcan be seen graphically in Fig. 3.104.

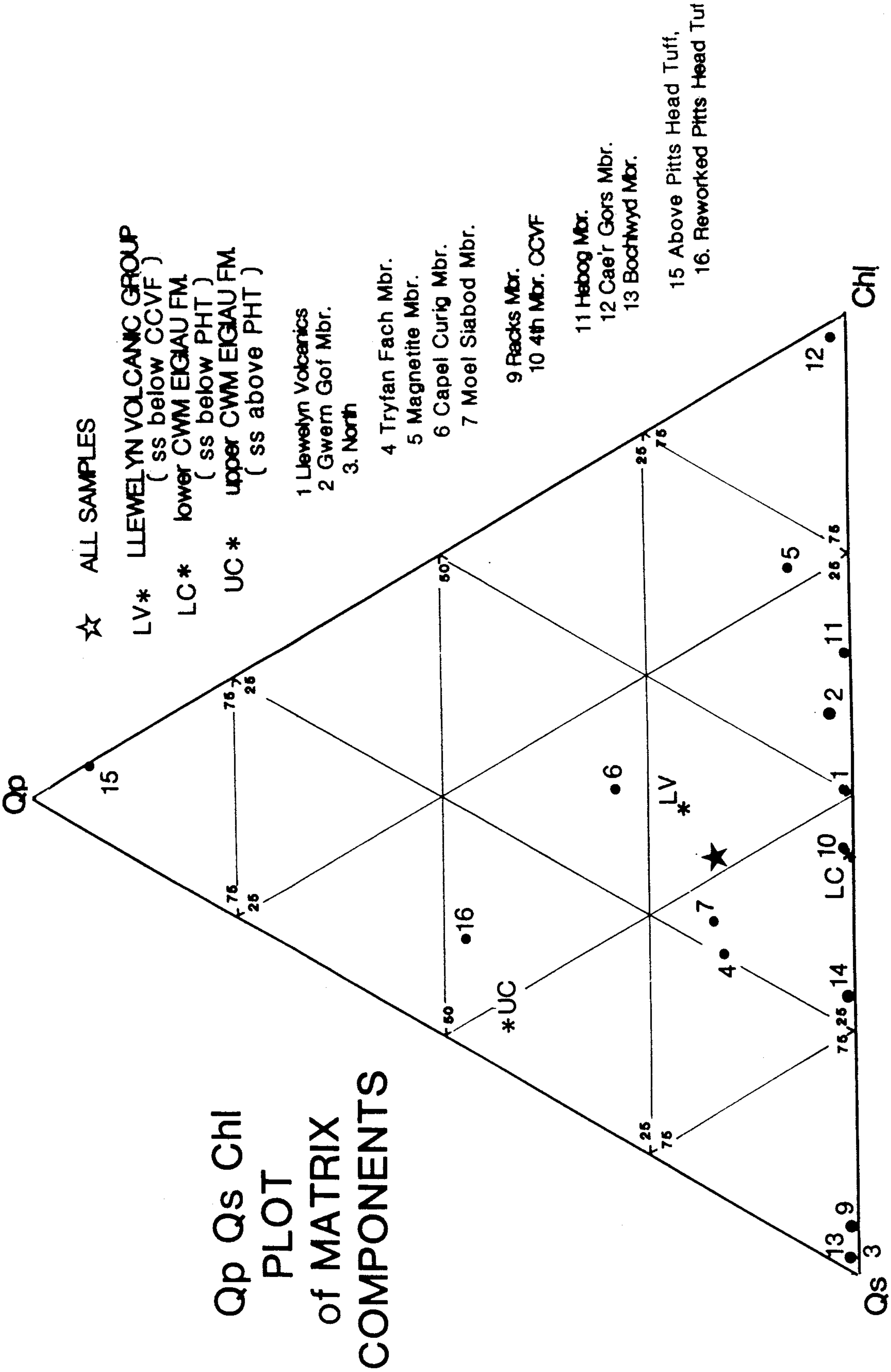

FIG. 3.118: Qp:Qs:Chl plot showing mean proprtions of various matrix components for all 92 sandstones as well as the 17 petrographic units individually. See Fig. 3.105 for identity of grain parameters. Identity of petrographic units is tabulated on the right; their regional and stratigraphic relationship can be seen graphically in Fig. 3.104.

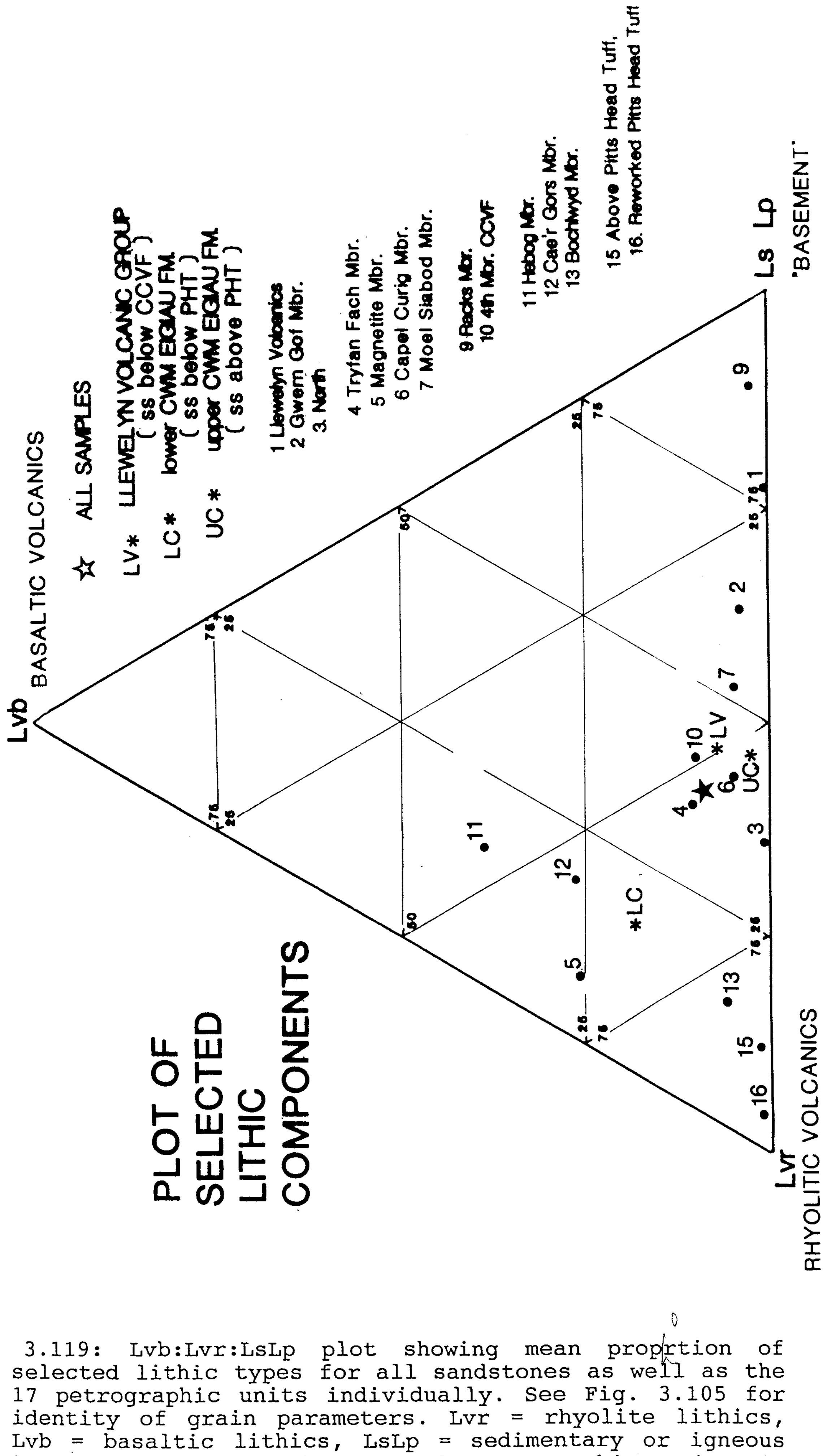

FIG. 3.119: Lvb:Lvr:LsLp plot showing mean proprtion of selected lithic types for all sandstones as well as the 17 petrographic units individually. See Fig. 3.105 for identity of grain parameters. Lvr = rhyolite lithics, Lvb = basaltic lithics, LsLp = sedimentary or igneous lithic fragments. Identity of petrographic units is tabulated on the right; their regional and stratigraphic relationship can be seen graphically in Fig. 3.104.

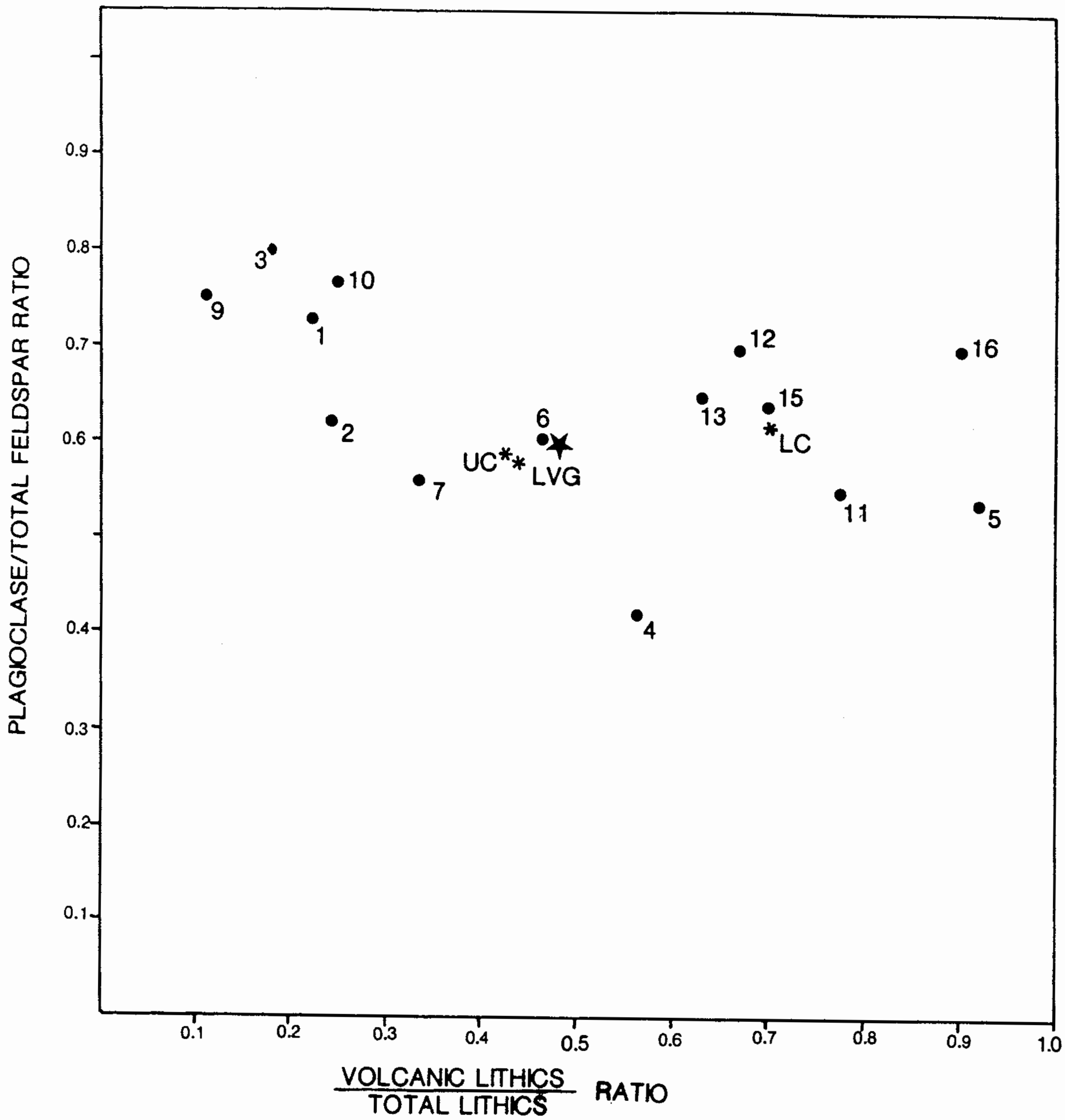

PLOT OF P/F versus Lv/L
(chert excluded)

FIG. 3.120: A) Cross-plot of plagioclase/total feldspar and lithic volcanic/total lithic ratios. Chert is excluded and sericitic chert used as a sedimentary lithic. Numbers refer to individual petrographic units. See any of previous triangular diagrams for identity. Large star denotes mean for all samples. Small stars refer to average values for various tectonic settings (data from Valloni and Maynard, 1981).

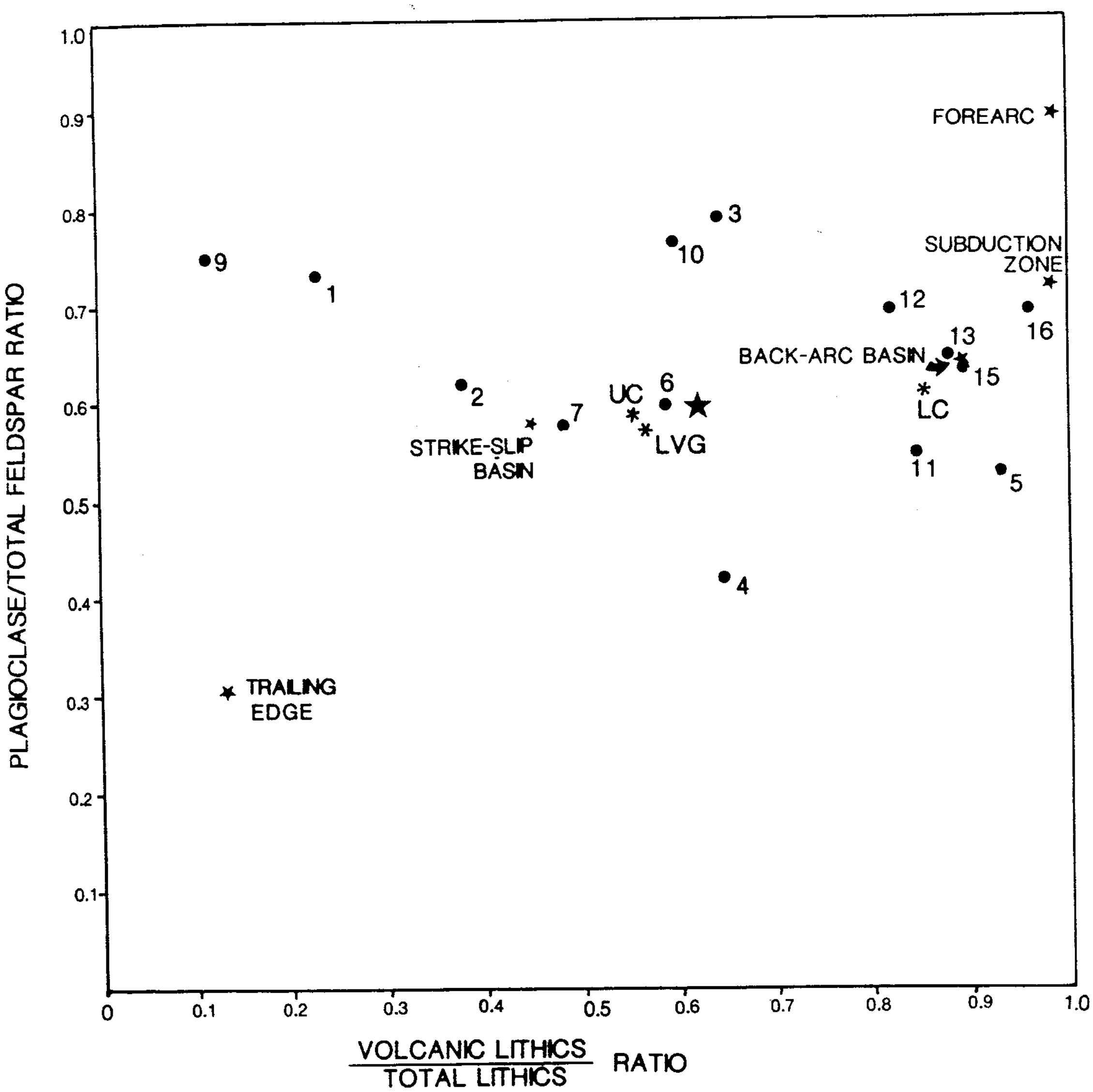

PLOT OF P/F versus Lv/L
(chert as Lv)

FIG. 3.120: B) Cross-plot of plagioclase/total feldspar and lithic volcanic/total lithic ratios. Chert is included as a volcanic lithic. See Fig. 3.120a for explanation.

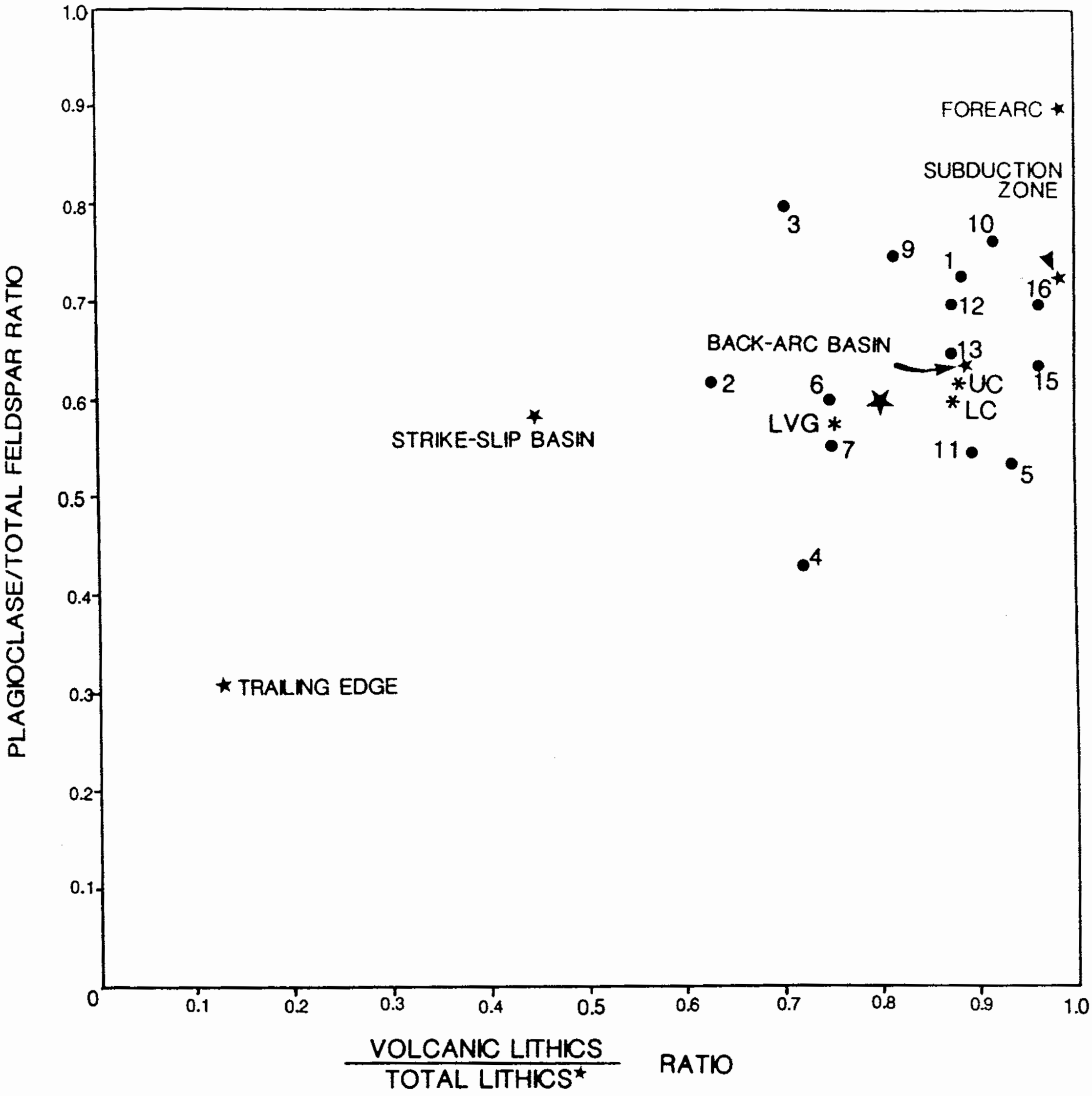

PLOT OF P/F versus Lv/L

(chert and sericitic chert as Lv)

FIG. 3.120: C) Cross-plot of plagioclase/total feldspar and lithic volcanic/total lithics ratios. Chert and sericitic chert included with volcanic rock fragments. See Fig. 3.120a for further explanation.

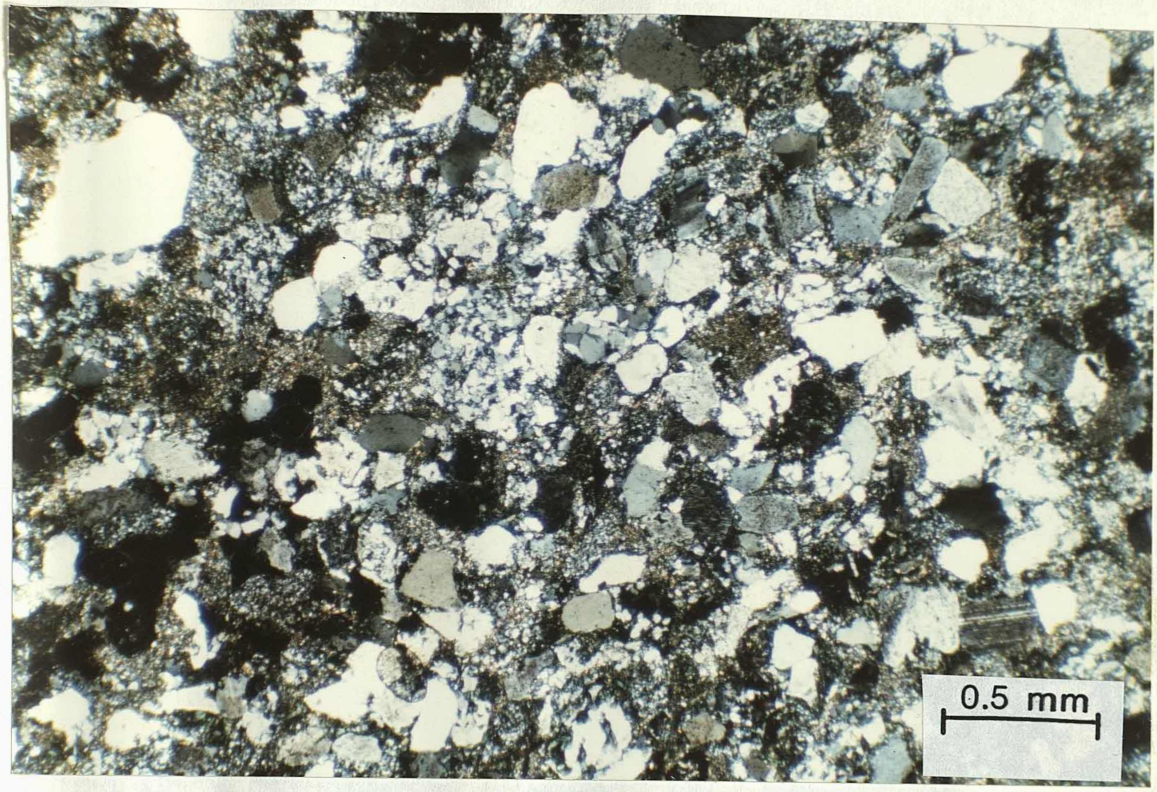

FIG. 3.121: Texture of fluvial sandstones from Gwern Gof. Mbr, Ddeugwm ridge, Tryfan anticline. Sample C54, section C2, 123m. XPL.

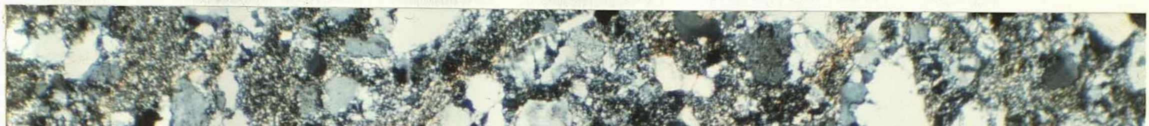

FIG. 3.122: Texture of sandstones from nearshore deposits from Racks Mbr. of Capel Curig Volcanic Formation. Compare with texture of sandstones deposited in a similarly "quiet" period (ie. the Gwern Gof Mbr., Fig. 3.121). Sample A18, section A1, 93m, Capel Curig anticline. XPL.

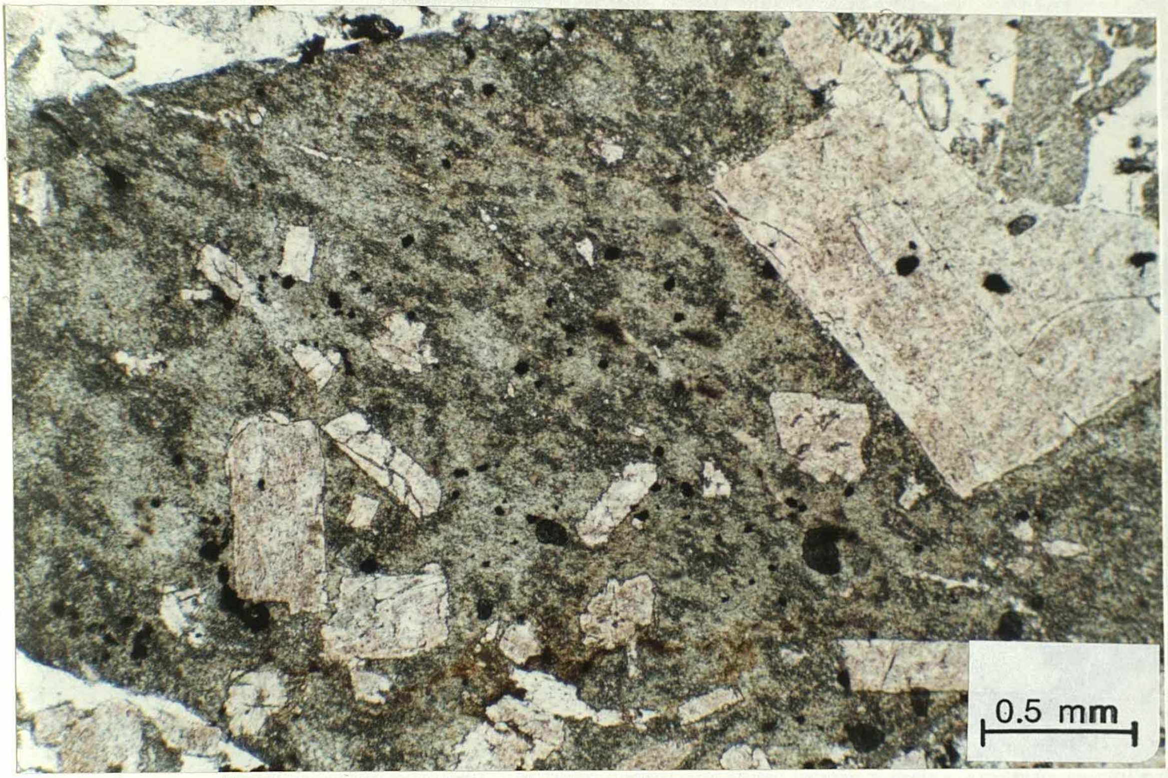

FIG. 3.123: Porphyritic basalt clast from Magnetite. Mbr., Tryfan anticline., Sample C56, section C7, 153.6m. PPL.

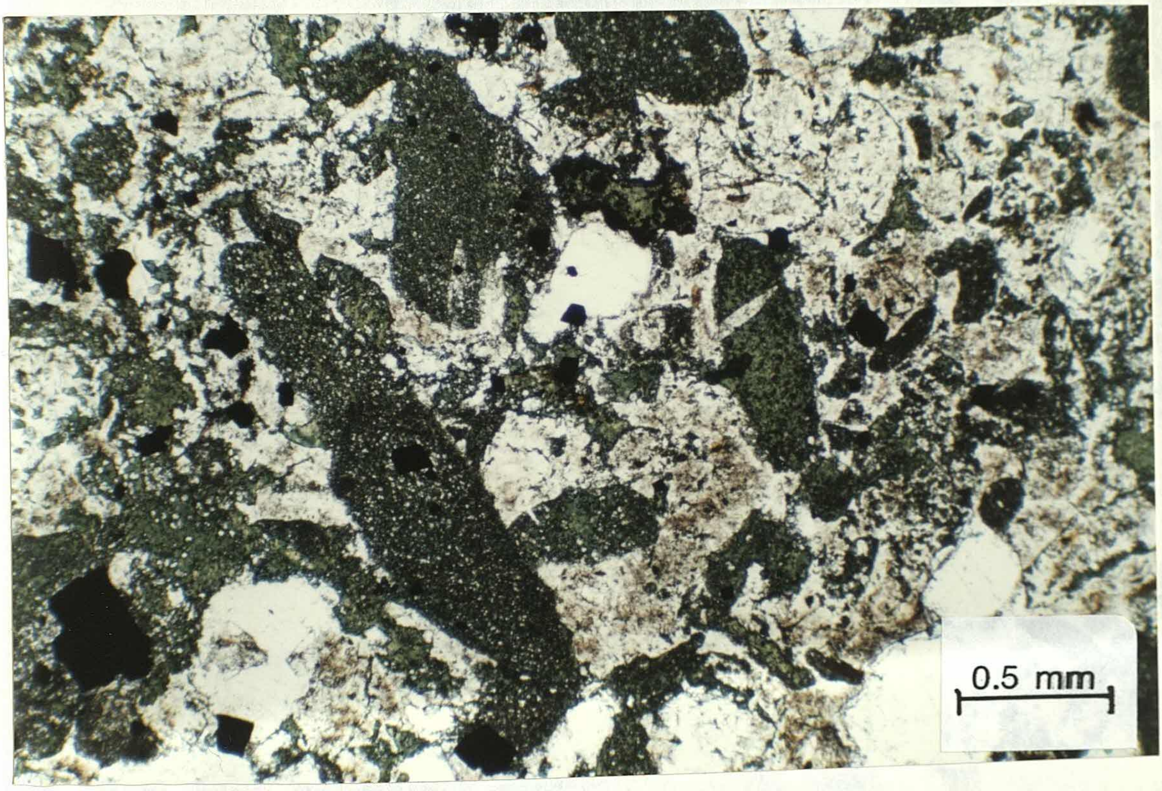

FIG. 3.124: Rounded chloritic ?mudstone or ?basalt fragments. Sample J5, section J3, 49m, Cae'r gors Mbr. near Rhyd Ddu. PPL.

FIG. 3.125: Angular quartz grains, detrital magnetite crystals, and chlorite fragments in chloritic matrix. Dispersed magnetite zone in centre represents poorly defined horizontal heavy mineral laminae. From rapidly deposited shoreface or swash bar deposits, Cae'r Gors Mbr. Sample J24, section J2, 71m. PPL.

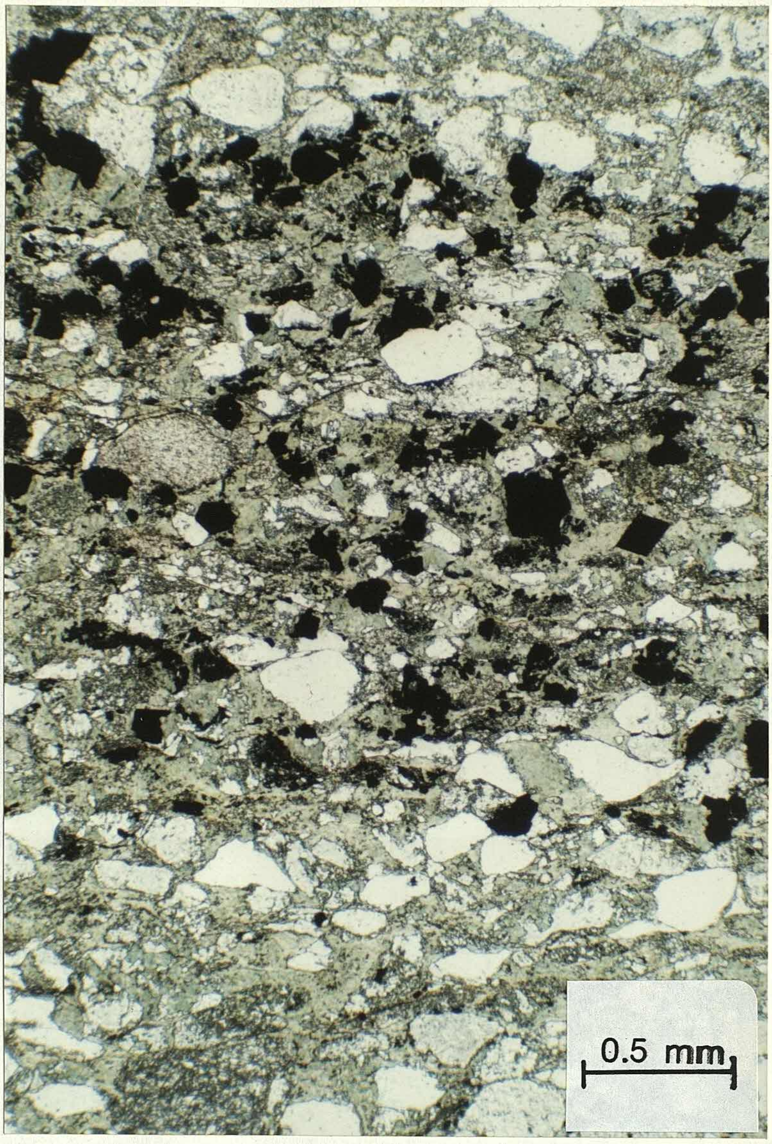

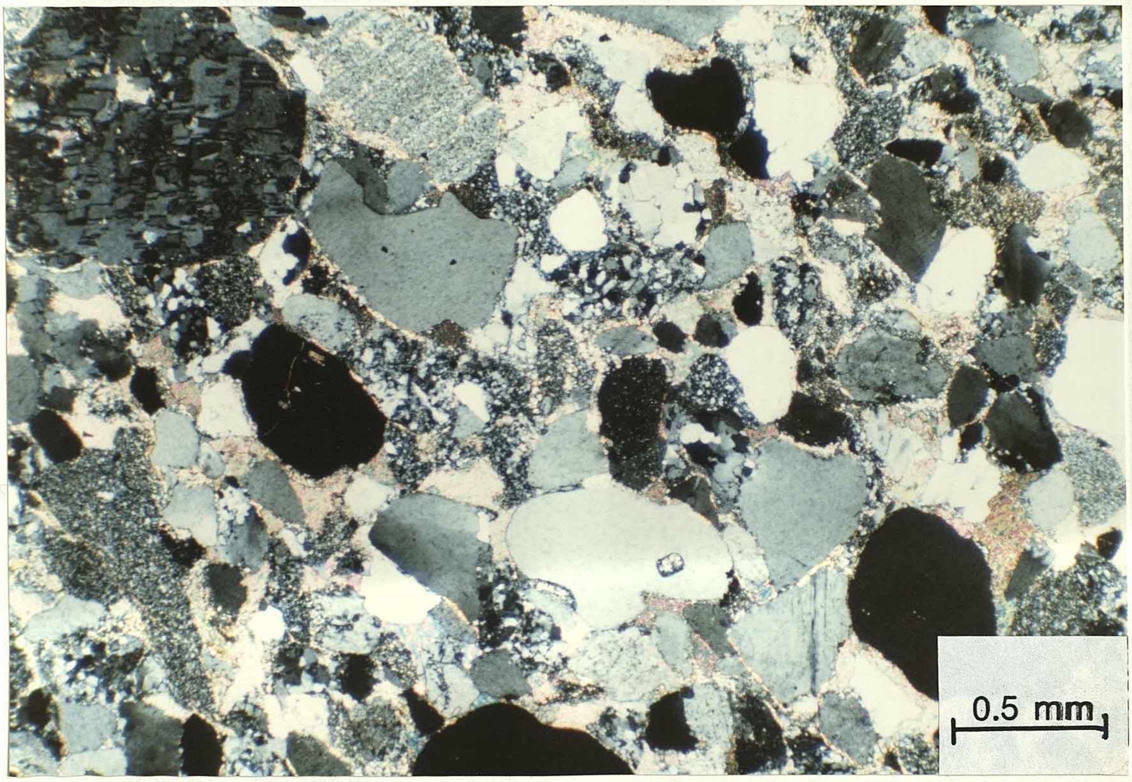

FIG. 3.126: Quartzose sandstone from distributary channel deposits of Bochlwyd Mbr., Lower Cwm Eigiau Fm., Bochlwyd ridge. Cemented by calcite. Sample D8, section D1, 37.5m. XPL.

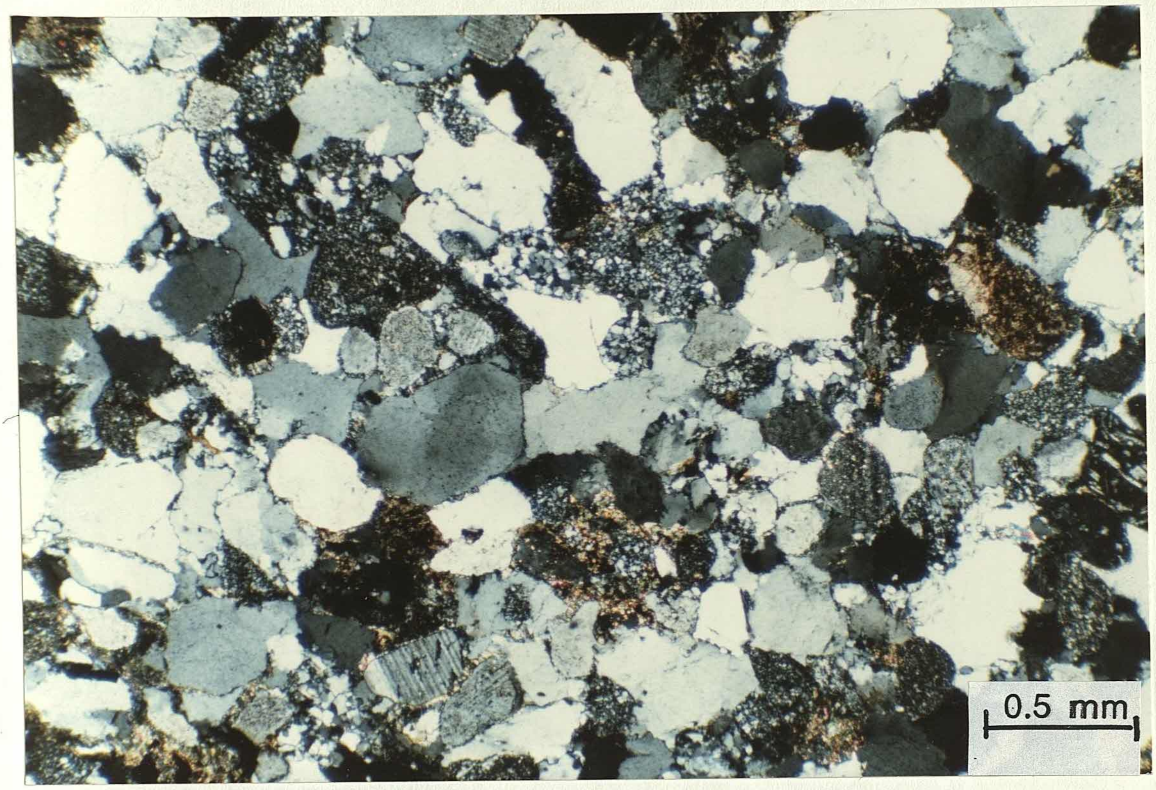

FIG. 3.127: Quartzose sandstone from fluvial deposits of Bochlwyd Mbr. Consists entirely of strained and unstrained monocrystalline quartz and chert, with occasional grains of plagioclase and sericitic chert. Cemented by quartz. Sample D10, section D1, 44.5m. XPL.

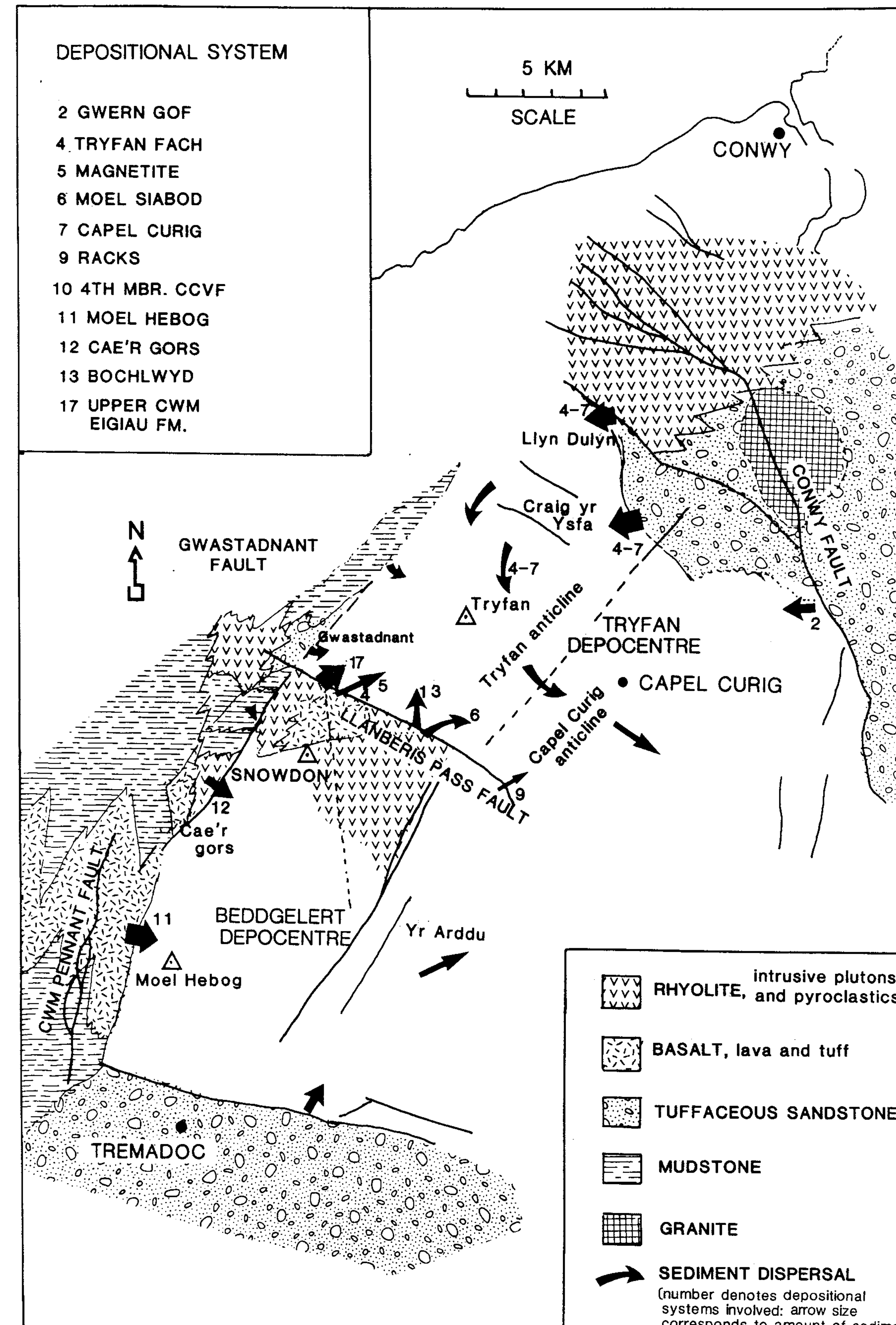

FIG. 3.128: Map depicts the distribution of the dominant source rock lithologies within basin based on petrography of derived sediment. Direction of source terrains is from analysis of paleocurrent data (Chapt. 4, 5) whereas the nature and positioning of important faults which uplifted source terrains is from a synthesis of the sedimentary and tectonic evolution of the basin (Chapt. 6). The depositional systems which were fed by the various sources are indicated beside arrows indicating patterns of sediment dispersal. The composition of the source terrain to the south is inferred from macroscopic examination of sandstones at Moel Ddu and Yr arddu (weathering aspect, pebble lithologies); no petrographic information is available from these localities.

FIG. 3.129: Variation in compositional maturity of first cycle fluvial sandstones in the Gondwana Supergroup (Permian-Triassic intracontinental rift) of Peninsular India. From Suttner and Dutta, 1987. See text for further explanation.

Figure 3.129

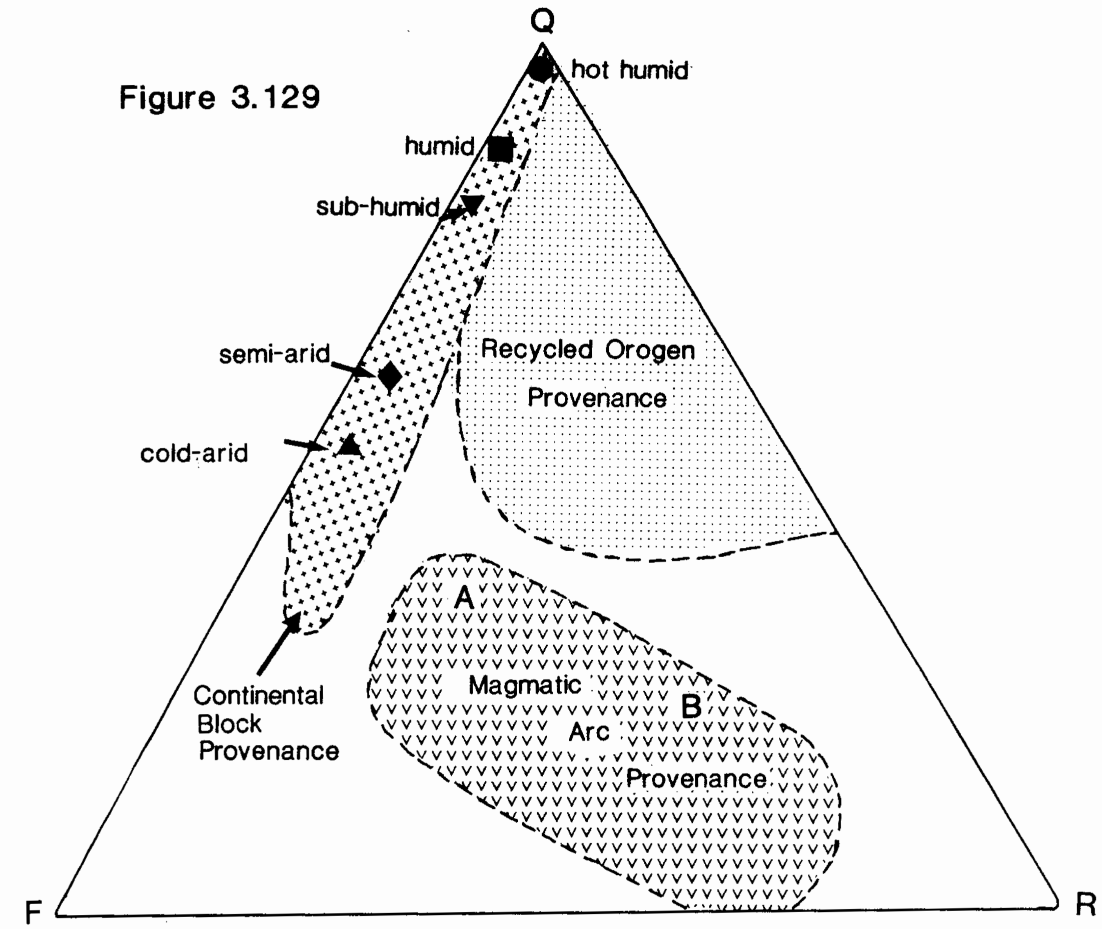

FIG. 3.130: Composition of recent deep sea sands. The dots show mean compositions; each polygon shows the 95% confidence interval about the mean. Note the appreciable overlap between samples from variuos tectonic settings. (from Valloni and Maynard, 1981). Star denotes mean composition of volcaniclastic sandstones from this study.

Figure 3.130

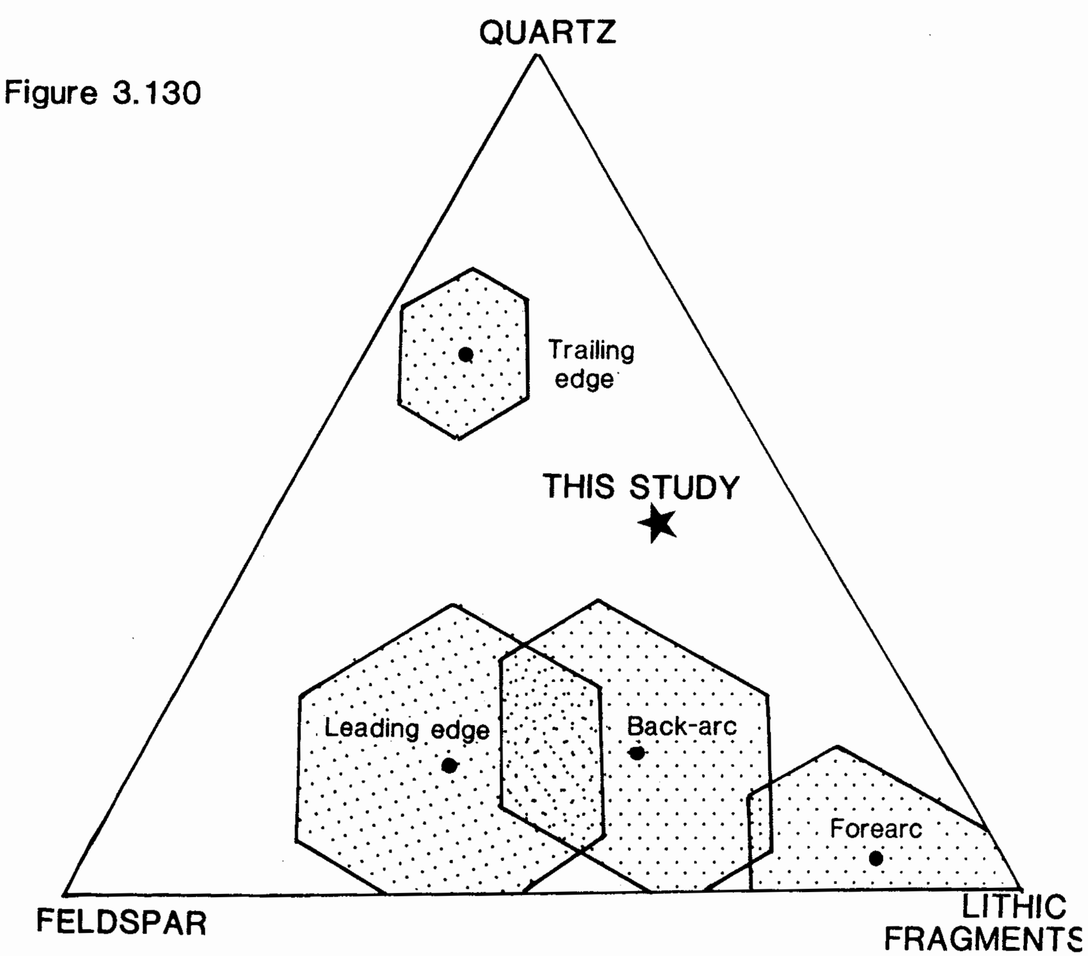

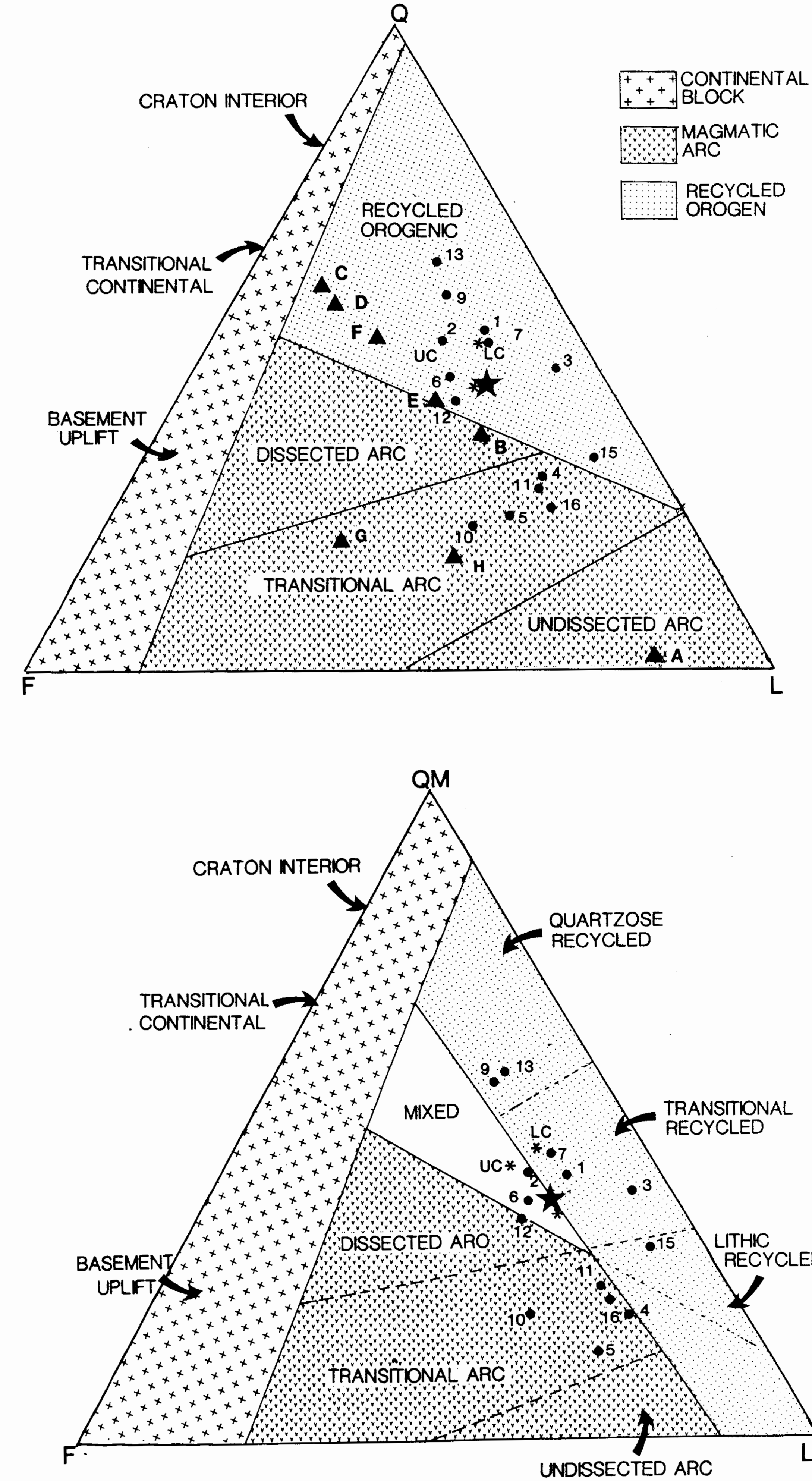

FIG. 3.131: QFL (upper) and QmFLt (lower) plots of mean composition of volcaniclastic sandstones from this study. See previous ternary diagrams for indentity of petrographic units. Star denotes mean composition for all samples. Provenance fields from the recent analysis of framework modes of North American terrigenous sandstones by Dickinson and colleagues, 1983). Small stars indicate petrographic data from other ensialic marginal basins or continental rifts. These are: A) andesitic volcaniclastics, Cretaceous, Chile (Winn, 1978), B) quartzose volcaniclastics, Cretaceous, Chile (Winn, 1978) C) Tesuque Fm., Miocene, New Mexico (Cavazza, 1986) D) Chama-el rito Mbr., Miocene, New Mexico (Ekas et al, 1984). E) and F) Gueydan fluvial sediments, Cenozoic, Gulf coast Texas (from Pettijohn et al, 1972). G) and H) Currabubula Fm., Carboniferous, SE Australia (sediment derived from rhyolitic volcanic ash; most of the siliceous component was present as glass which has now been altered to clay minerals. (from Whetten, 1965).

TECTONIC SETTING	REGION	Q: F: L	Qm:F: Lt:	Reference
MAGMATIC ARC	Volcaniclastic trench sands, Guatemala	1 43 56	1 43 56	*Enkeboll,1979
	Marginal seafloor, Neogene, Philippine and Japan seas	13 15 72	12 15 73	*Harrold and Moore, 1973
	Atka basin, Neogene Aleutian ridge, Alaska	7 34 59	3 34 63	*Stewart, 1978
TRANSITIONAL UNDISSECTED and DISSECTED ARC	Insular sands, northern Puerto Rican shelf	21 31 48	14 31 55	*Breyer and Ehlmann, 1979
	Noegene turbidites, Komardorsky basin, Bering Sea	21 28 51	9 28 63	*Stewart, 1978
DISSECTED ARC	Japan basin, Neogene Sea of Japan	34 45 21	21 33 45	*Harrold and Moore, 1973
ENSIALIC MARGINAL BASIN or CONTINENTAL RIFTS	Cumberland Bay Group Cretaceous marginal basin, Chile	2 15 82		Winn, 1978
	Sandebugten Formation as above.	35 21 43		Winn, 1978
	Tesuque Formation, Miocene, Espanola Basin Rio grande rift	58 31 11		Cavazza, 1986
	Chama-elrito Mbr, Tesuque Fm., Miocene, Rio grande rift	57 30 13		Ekas et al, 1986
	Gueydan Formation, Late Tertiary, SE Texas	51 27 22 41 23 35	45% opal cement	+McBride et al, 1979.
	Currabubula Fm., Carboniferous, SE Australia	17 35 48 20 49 31	32-45% clay	Whetten, 1965
	Ordovician Plynlimion Group, west central Wales	78 13 9	70 13 17	James, 1971
	THIS STUDY	44 17 39	36 17 48	Orton, 1987

Fig. 3.132: Table of sandstone composition from selected back-arc basins and continental rifts. Asterix denotes data collated from Dickinson and Suczek, 1979; "plus" indicates data from Pettijohn et al, 1972. See these citations for full references. Other sources are indicated on right. Sandstone compositions for ensialic extensional basins are plotted on Fig. 3.131.

Chapter 4

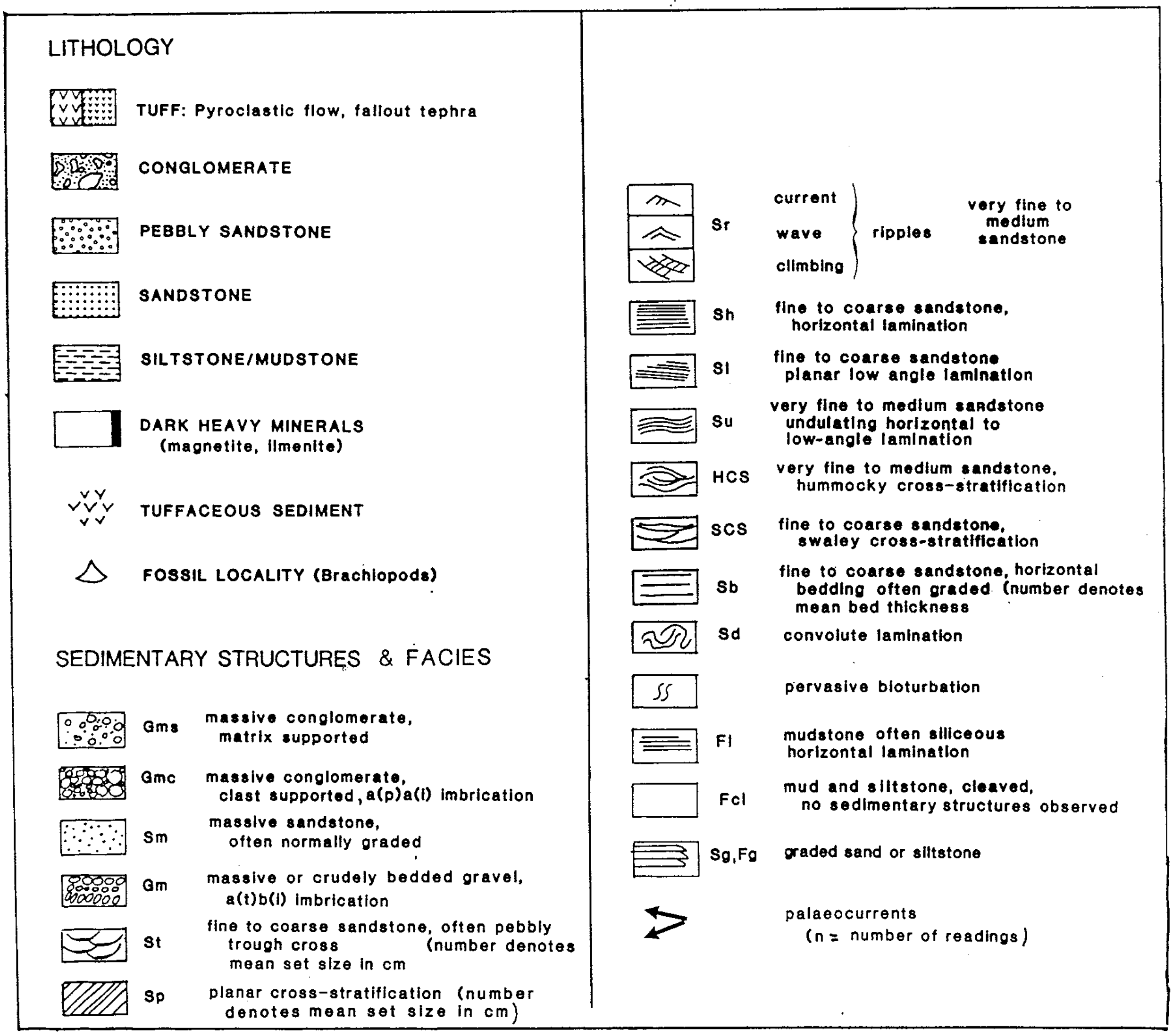

FIG. 4.1: Legend for the stratigraphic sequences shown in the other follwing figures. Facies letter-code modified from Miall (1977).

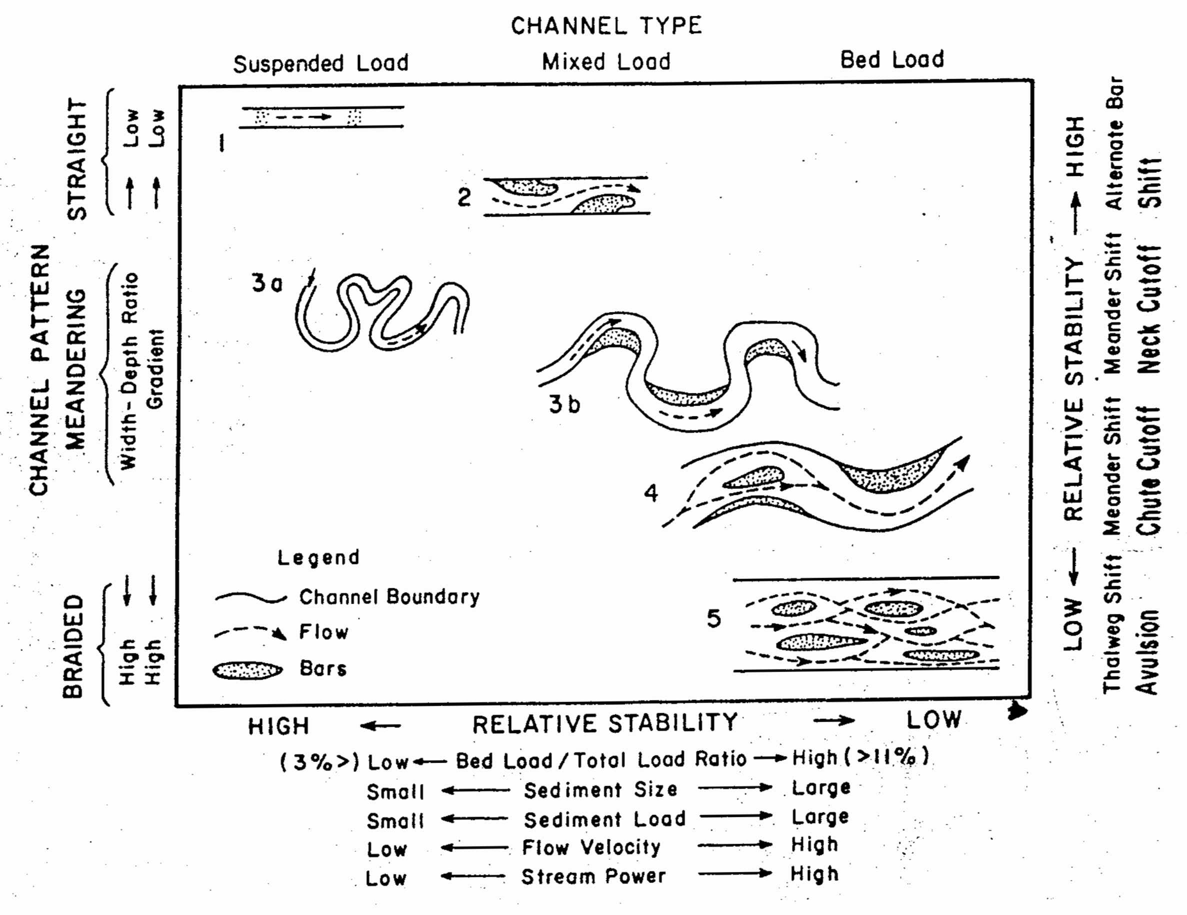

FIG. 4.2a: Classification of fluvial channels based on pattern and type of sediment load (from Schumm, 1981).

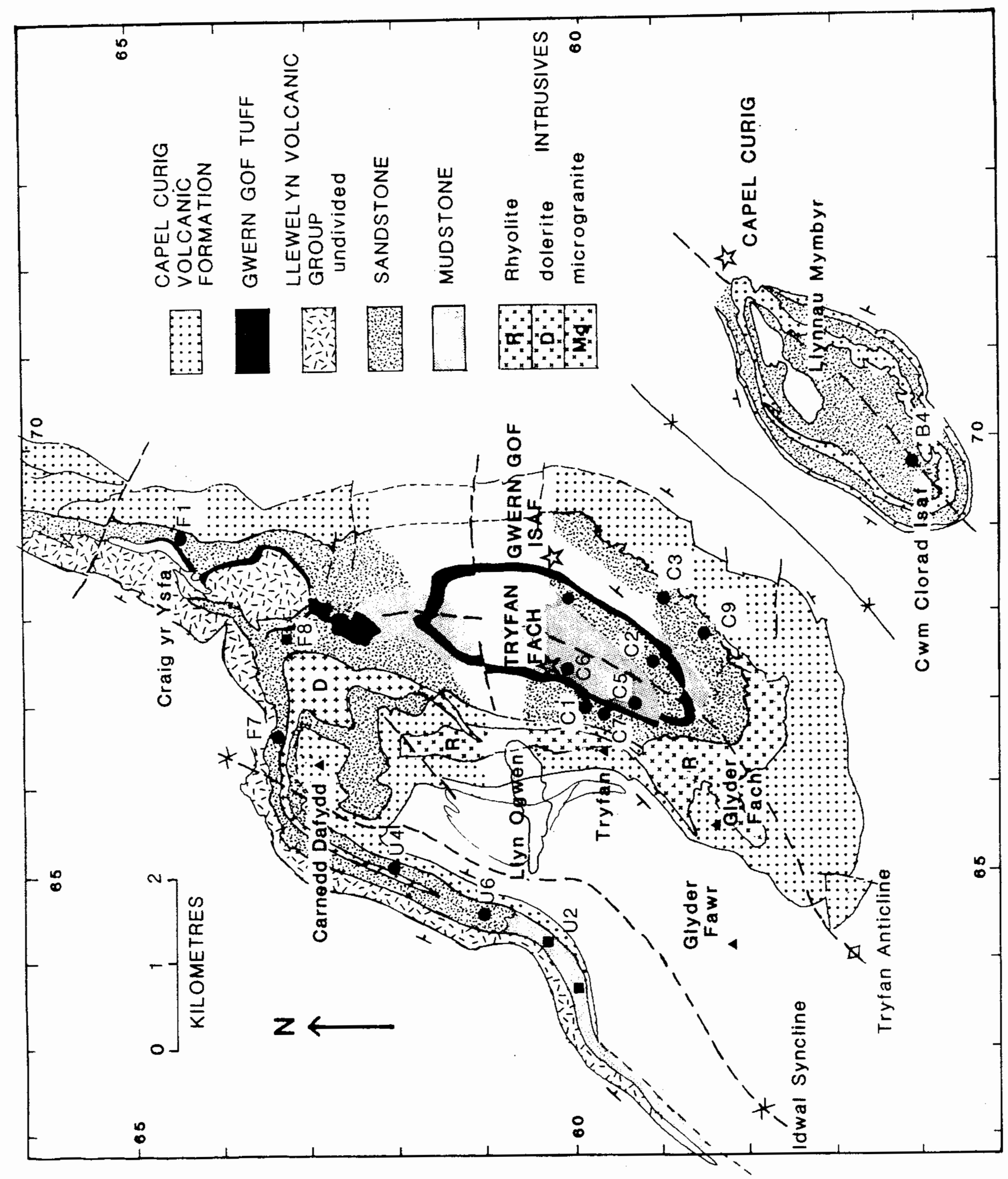

Fig. 4.2b Geological map of the Tryfan anticline and surroundings, showing the distribution of Caradocian volcanics and associated clastics and the locations of the vertical sections (numbered dots) from the LLewelyn Volcanic Group used in this study. Numbers on map margin refer to the national grid.

Fig. 4.3 Stratigraphic sections through the Gwern Gof fan-delta succession (see location of sections in Fig. 4.2B and legend in Fig. 4.1). Time equivelance is implied for the numbered phases of deposition (large numbers, 1 to 8 on section margins). Inset map shows interpreted palaeogeography during maximum progradation (phase 4) of the lower (A) delta; black squares denote other sections used for this reconstruction. Palaeogeography is not corrected for NW-SE shortening of 40%.

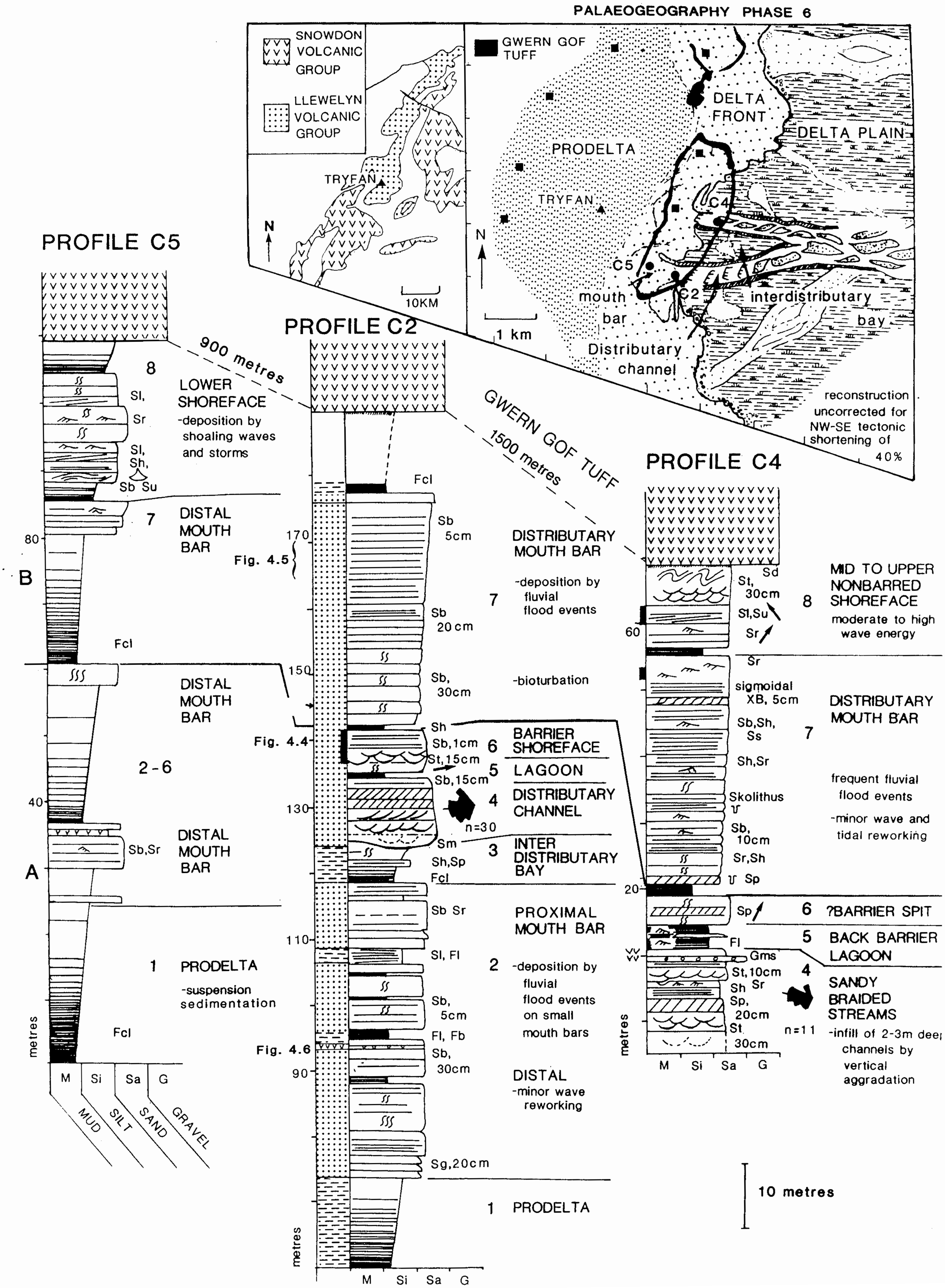

PALAEOGEOGRAPHY PHASE 6
SNOWDON VOLCANIC GROUP
LLEWELYN VOLCANIC GROUP
TRYFAN
N
10KM
GWERN GOF TUFF
DELTA FRONT
DELTA PLAIN
PRODELTA
TRYFAN
C4
C5
C2
mouth bar
interdistributary bay
1 km
Distributary channel
reconstruction uncorrected for NW-SE tectonic shortening of 40%
PROFILE C5
PROFILE C2
PROFILE C4
900 metres
1500 metres
GWERN GOF TUFF
8
LOWER SHOREFACE
-deposition by shoaling waves and storms
Sl, Sr
Sl, Sh,
Sb Su
7
DISTAL MOUTH BAR
80
B
Fcl
DISTAL MOUTH BAR
2-6
40
DISTAL MOUTH BAR
Sb,Sr
A
1 PRODELTA
-suspension sedimentation
Fcl
metres
M Si Sa G
MUD SILT SAND GRAVEL
Fcl
170
Fig. 4.5
Sb 5cm
DISTRIBUTARY MOUTH BAR
7 -deposition by fluvial flood events
Sb 20 cm
150
Sb, 30cm
-bioturbation
Fig. 4.4
Sh
Sb,1cm
St,15cm
Sb,15cm
6 BARRIER SHOREFACE
5 LAGOON
4 DISTRIBUTARY CHANNEL
130
n=30
Sm
Sh,Sp
Fcl
3 INTER DISTRIBUTARY BAY
Sb Sr
PROXIMAL MOUTH BAR
110
Sl, Fl
2 -deposition by fluvial flood events on small mouth bars
Sb, 5cm
Fl, Fb
Fig. 4.6
Sb, 30cm
90
DISTAL -minor wave reworking
Sg,20cm
1 PRODELTA
metres
M Si Sa G
Sd
St, 30cm
Sl,Su
Sr
60
8 MID TO UPPER NONBARRED SHOREFACE
moderate to high wave energy
Sr
sigmoidal XB, 5cm
Sb,Sh, Ss
Sh,Sr
7 DISTRIBUTARY MOUTH BAR
frequent fluvial flood events
-minor wave and tidal reworking
Skolithus
Sb, 10cm
Sr,Sh
Sp
20
Sp
6 ?BARRIER SPIT
Fl
5 BACK BARRIER LAGOON
Gms
St,10cm
Sh Sr
Sp, 20cm
St 30cm
n=11
4 SANDY BRAIDED STREAMS
-infill of 2-3m deep channels by vertical aggradation
metres
M Si Sa G
10 metres

Fig. 4.4 Bioturbated very fine-grained sandstones from distal mouth bar of the Gwern Gof fan delta, Tryfan anticline. (see Fig. 4.3, section C2, phase 7, 145 m.). Pencil for scale.

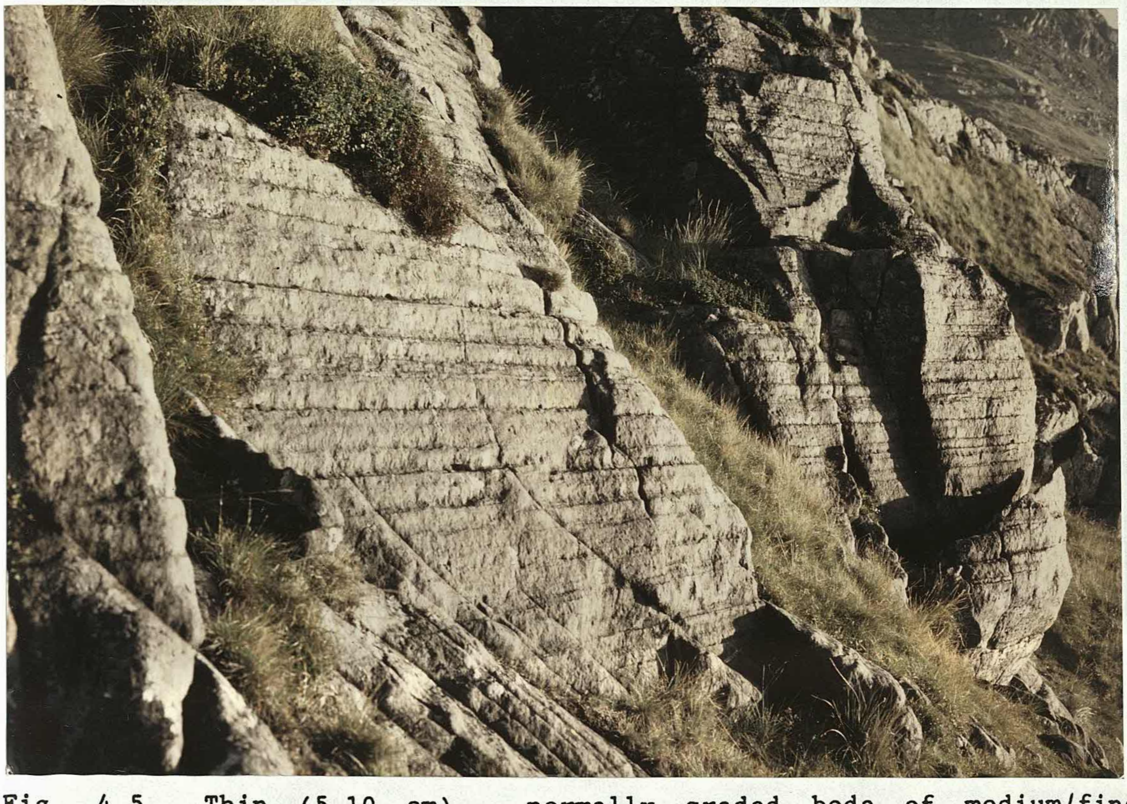

Fig. 4.5 Thin (5-10 cm), normally graded beds of medium/fine sandstones interpreted as stream-effluent flood deposits of a proximal mouth bar, Gwern Gof fan-delta, Tryfan anticline. (see Fig. 4.3, section C2, phase 7, 163 m.) Approximately 2 stratigraphic metres of vertical section are shown.

Fig. 4.6 Thin beds of rhyolitic airfall tuff within bioturbate mouth bar sequences of the Gwern Gof fan-delta, Tryfan anticline. (see Fig. 4.3, section C2, phase 6, 93 m). Lense cap is 6 cm in diameter.

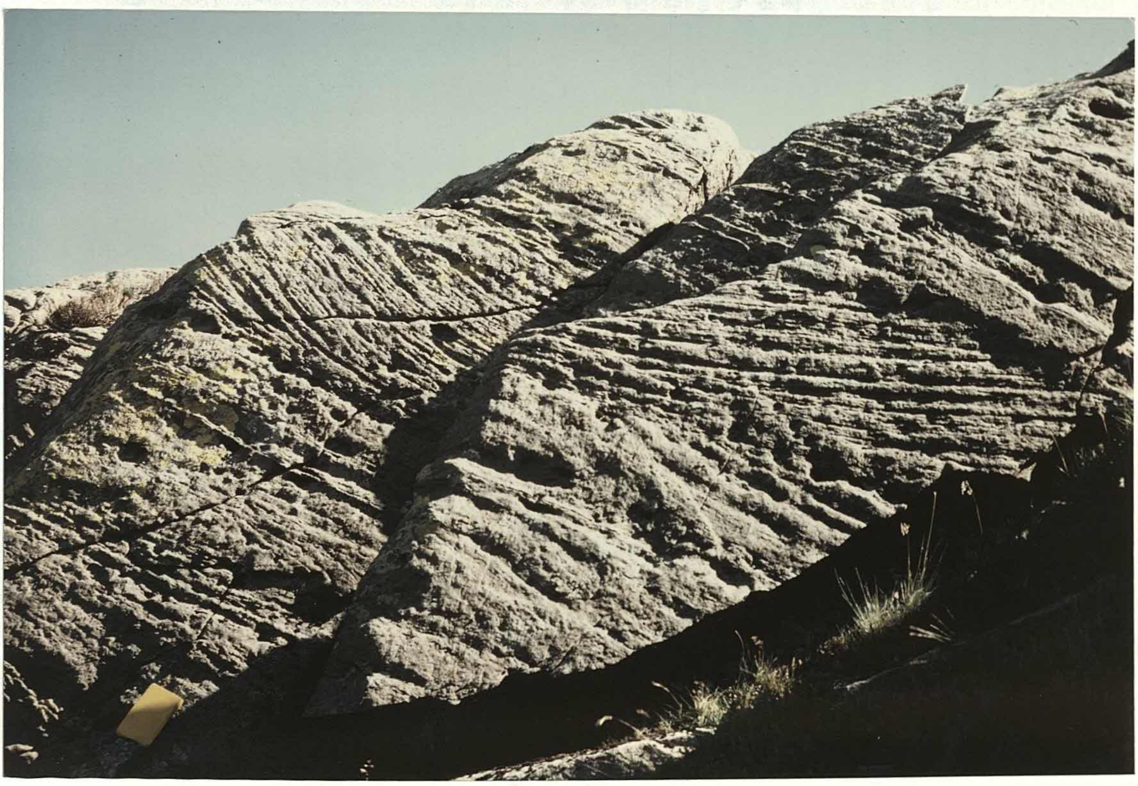

Fig. 4.7 Large scale trough cross-stratification and horizontal lamination from base of distributary channel, Gwern Gof delta-plain. (see Fig. 4.8, Section C2, 126.4 m). Field notebook is 18.5 cm long.

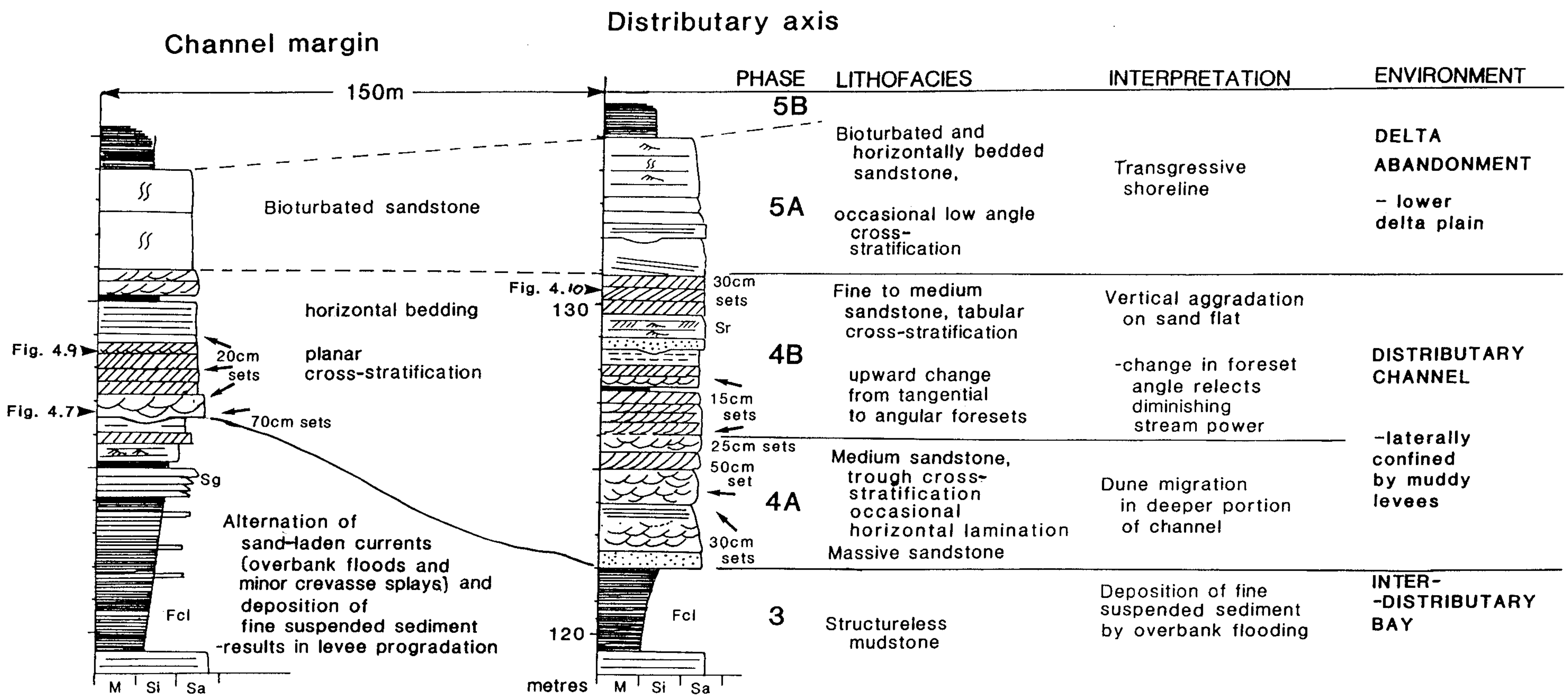

Fig. 4.8 Details of a distributary channel-fill sequence from the Gwern Gof fan-delta (see Fig. 4.3, phase 4 in section C2).

Fig. 4.9 Stacked sets of planar tabular cross-stratification from infill of distributary channel, Gwern Gof Mbr. delta plain. Lateral variation in set thickness, and "hooked" bases to foresets indicates some flow unsteadiness. (see Fig. 4.8, Section C2, 128.5 m). Field notebook is 18.5 cm long.

Fig. 4.10 Stacked sets of planar tabular cross-stratification from infill of distributary channel, Gwern Gof Mbr. delta plain. Lithofacies probably formed part of a large transverse bar complex; its preservation indicates channel was filled by vertical aggradation rather than lateral migration. The angular base to foresets would reflect a lower flow velocity relative to above (Fig. 4.8) lithofacies. (see Fig. 4.8, section C2b, 130 m). Field notebook is 18.5 cm long.

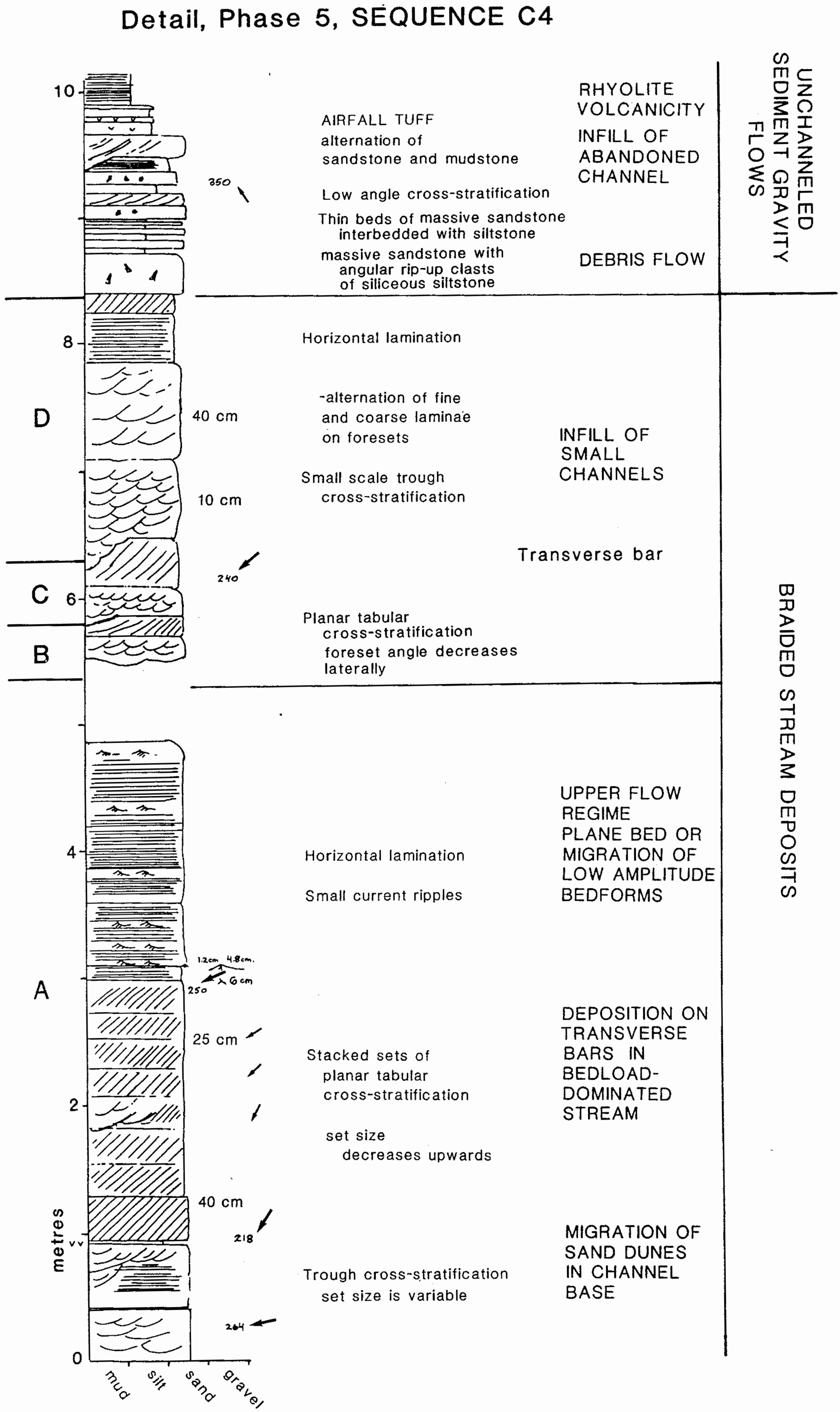

Fig. 4.11 Detail of braided stream deposits from the Gwern Gof fan-delta (see Fig. 4.3, phase 4 in section C4)

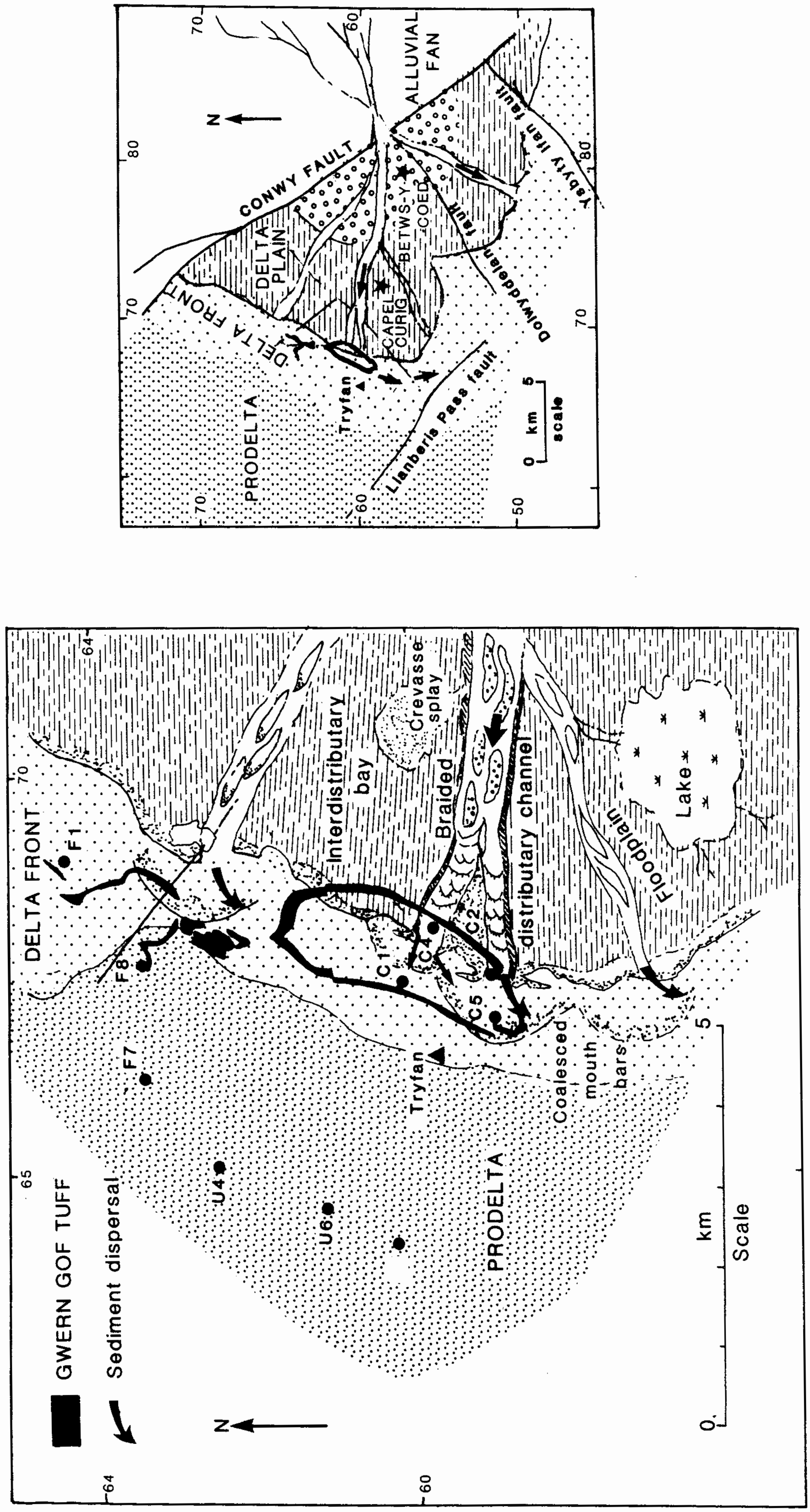

FIG. 4.12: Reconstruction of palaeogeography during maximum progradation (phase 4) of the lower(A) Gwern Gof fan-delta (see Fig. 4.3 and appendix for vertical sections). Palaeogeography not corrected for NW-SE shortening of 40%.

Fig. 4.13 Stratigraphic sections through the Tryfan Fach braidplain delta in the Tryfan anticline (see legend in Fig. 4.1). Inset map shows location of sections and interpreted palaeogeography (phase 4) during maximum advance of the braidplain.

ON FOLLOWING PAGE

FIG. 4.14 Details of braidplain sequences from the Tryfan Fach Mbr., Tryfan anticline. (see Fig. 4.13, phase 4; see also Fig. 4.19 for location of sections).

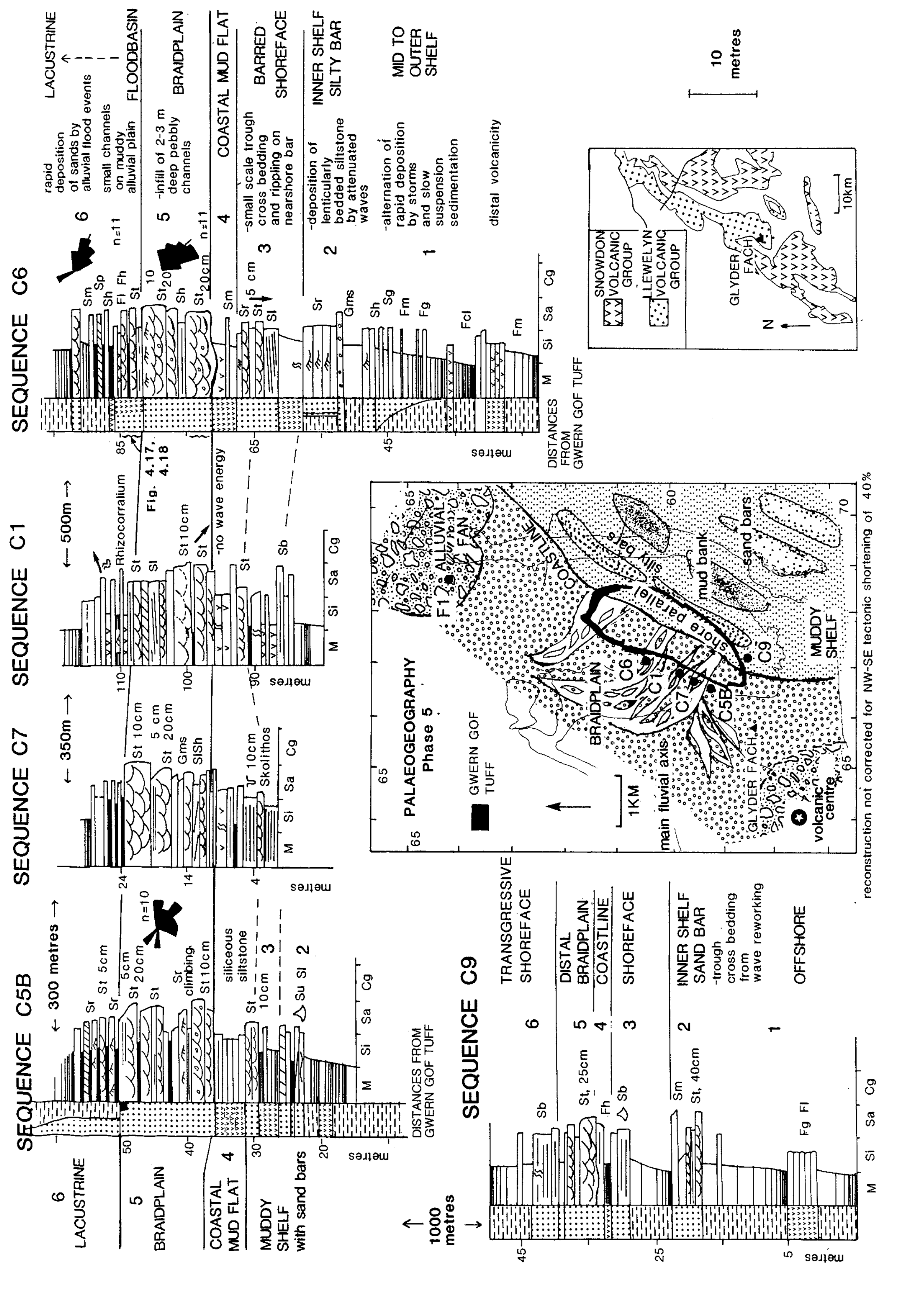

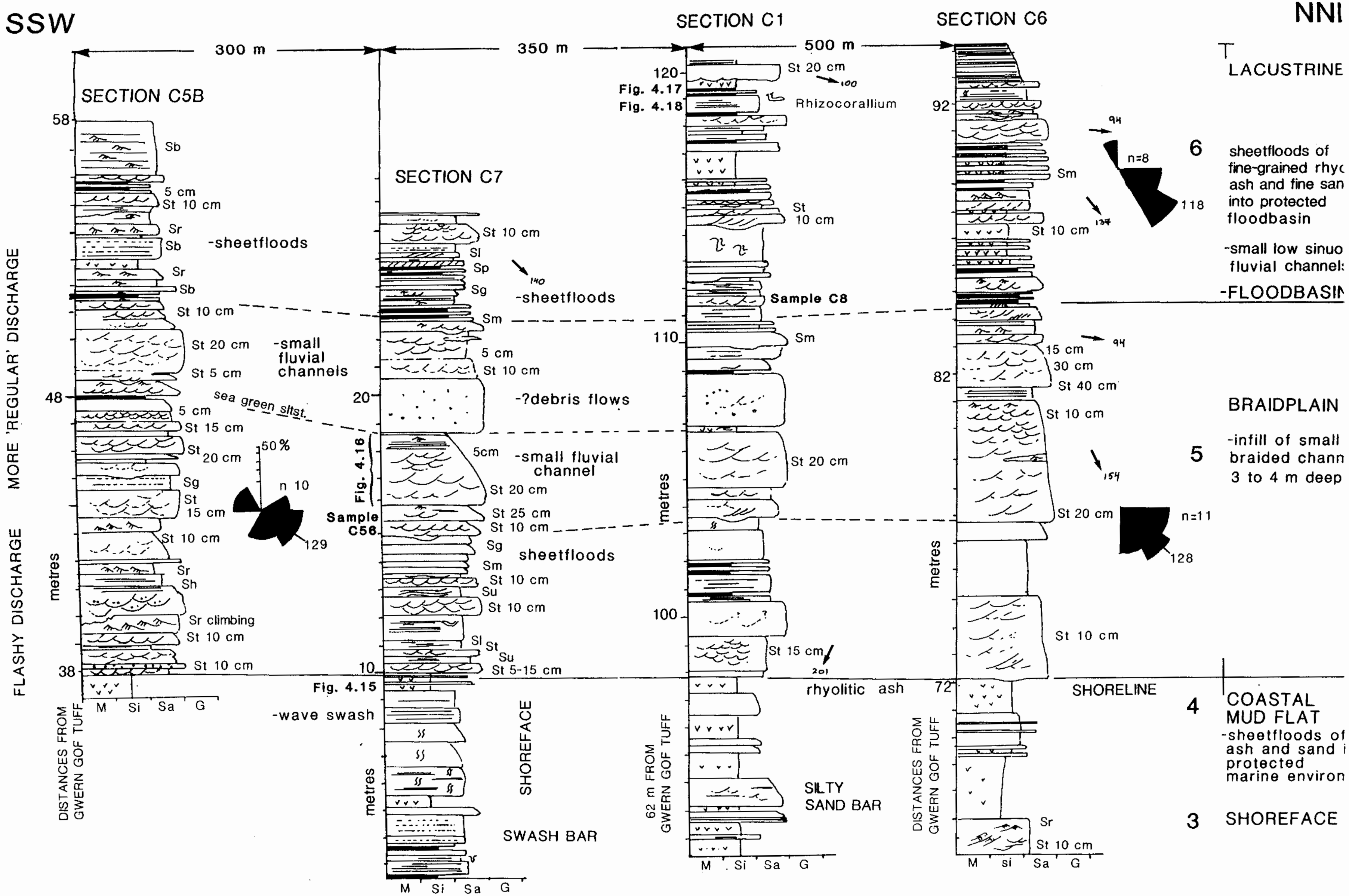
SSW
NNI
SECTION C1
SECTION C6
300 m
350 m
500 m
SECTION C5B
SECTION C7
LACUSTRINE
6
sheetfloods of fine-grained rhyc ash and fine san into protected floodbasin
-small low sinuo fluvial channel:
-FLOODBASIN
BRAIDPLAIN
5
-infill of small braided chann 3 to 4 m deep
SHORELINE
4
COASTAL MUD FLAT
-sheetfloods of ash and sand i protected marine environ
3
SHOREFACE
MORE 'REGULAR' DISCHARGE
FLASHY DISCHARGE
-sheetfloods
-small fluvial channels
sea green sltst.
-sheetfloods
-?debris flows
-small fluvial channel
sheetfloods
-wave swash
SHOREFACE
SWASH BAR
Fig. 4.15
Fig. 4.16
Sample C56
Fig. 4.17
Fig. 4.18
Rhizocorallium
Sample C8
rhyolitic ash
SILTY SAND BAR
DISTANCES FROM GWERN GOF TUFF
62 m FROM GWERN GOF TUFF
metres
M Si Sa G

Fig. 4.15 Cleaved siliceous mudstone deposited on muddy coastal plain/ shoreface overlain by trough cross-stratified coarse-grained volcaniclastic sandstone from infill of a shallow braided stream. Flow of currents was from right to left within fluvial sediments. Tryfan Fach Mbr., Tryfan anticline. (see Fig. 4.13, 4.14, section C7, 9.65 m). Coppertone bottle is 16 cm high.

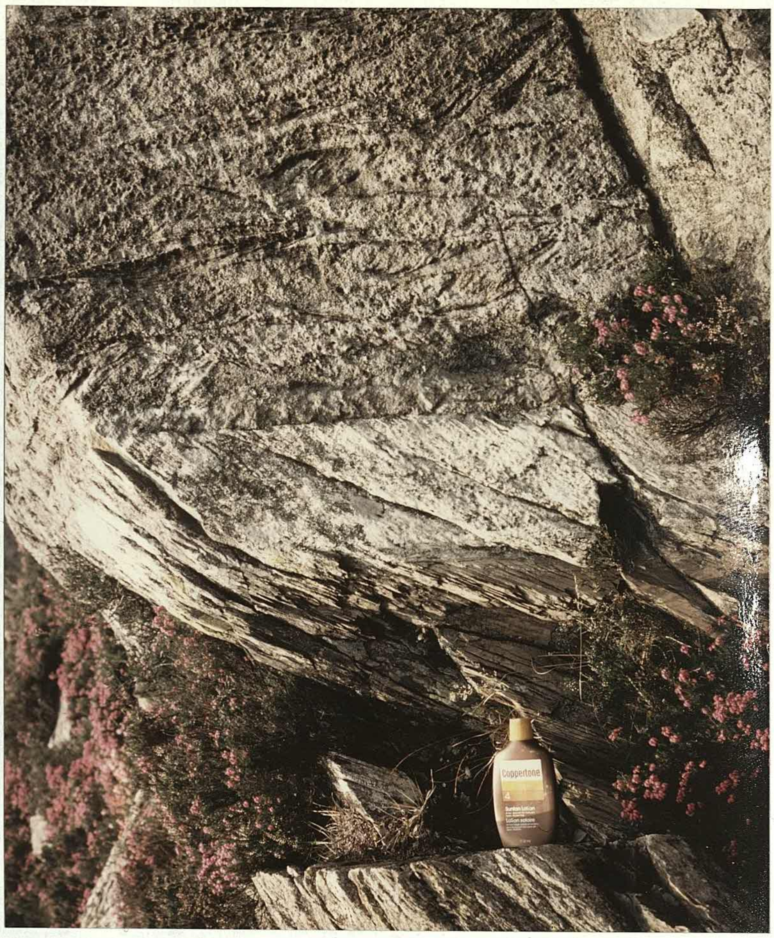

Fig. 4.16 Complete channel-fill sequence from a 2 m deep pebbly braided stream, Tryfan Fach Mbr., Tryfan Anticline. Size of cross-stratification decreases upwards from 20 cm to 4 cm in conjunction with a fining of sediment from very coarse-grained sandstone to siltstone. The poor representation of sedimentary structures would reflect rapid rates of sedimentation. The absence of planar cross-strata suggests channel was infilled by lateral migration rather than vertical accretion. Flow of fluvial currents was towards reader. See Fig. 4.13, 4.14, section C7, 16 m).

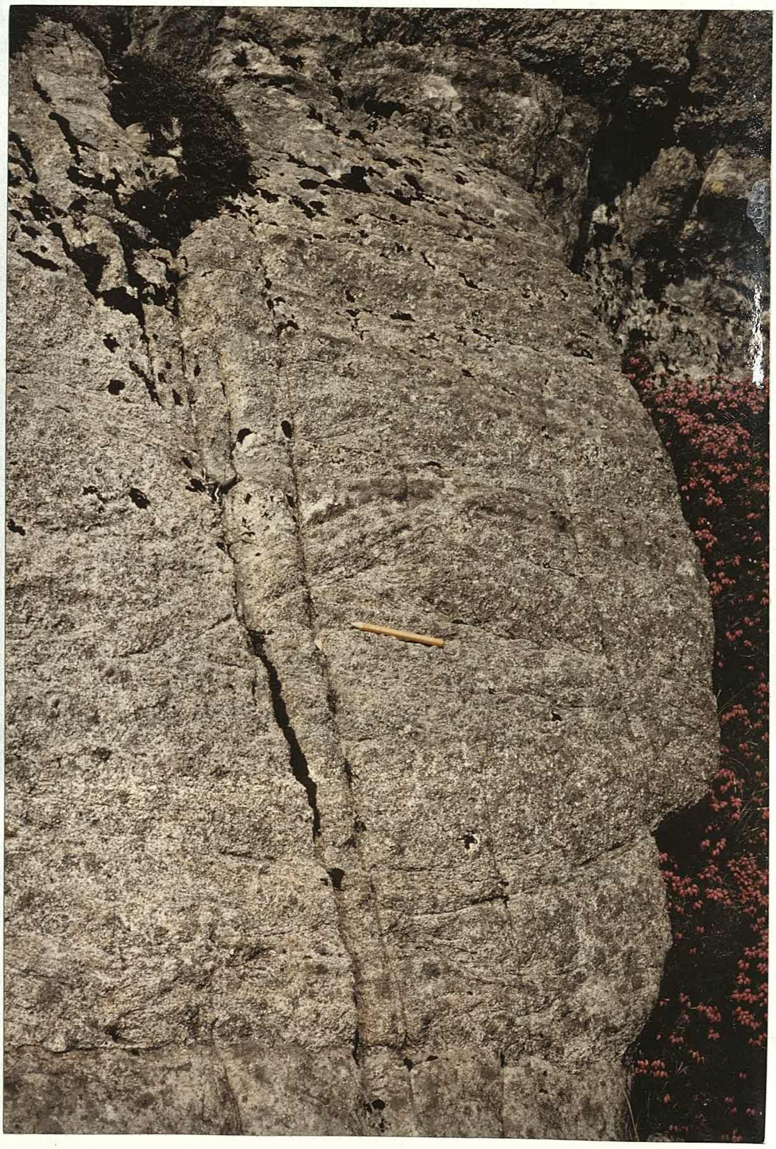

Fig. 4.17 Climbing ?wave ripples (ARROW) and undulose lamination within siliceous siltstones from lacustrine/floodbasin successions deposited during retreat of the Tryfan Fach braidplain. The coarse-grained sandstones at top of photo represent deposits from the base of a small (50 cm deep) ?fluvial channel on the alluvial plain. (see Fig. 4.13, 4.14, section C1, 119.60 m). Pencil sharpener for scale.

Fig. 4.18 Sub-horizontal ?Rhizocorallium burrows (ARROW) (Cruziana ichnofacies) from siliceous floodbasin siltstones. Tryfan Fach Mbr. Tryfan anticline. (see Fig. 4.13, 4.14, section C1, 118.73 m). Pencil sharpener for scale.

PALAEOGEOGRAPHY Tryfan Fach Mbr.

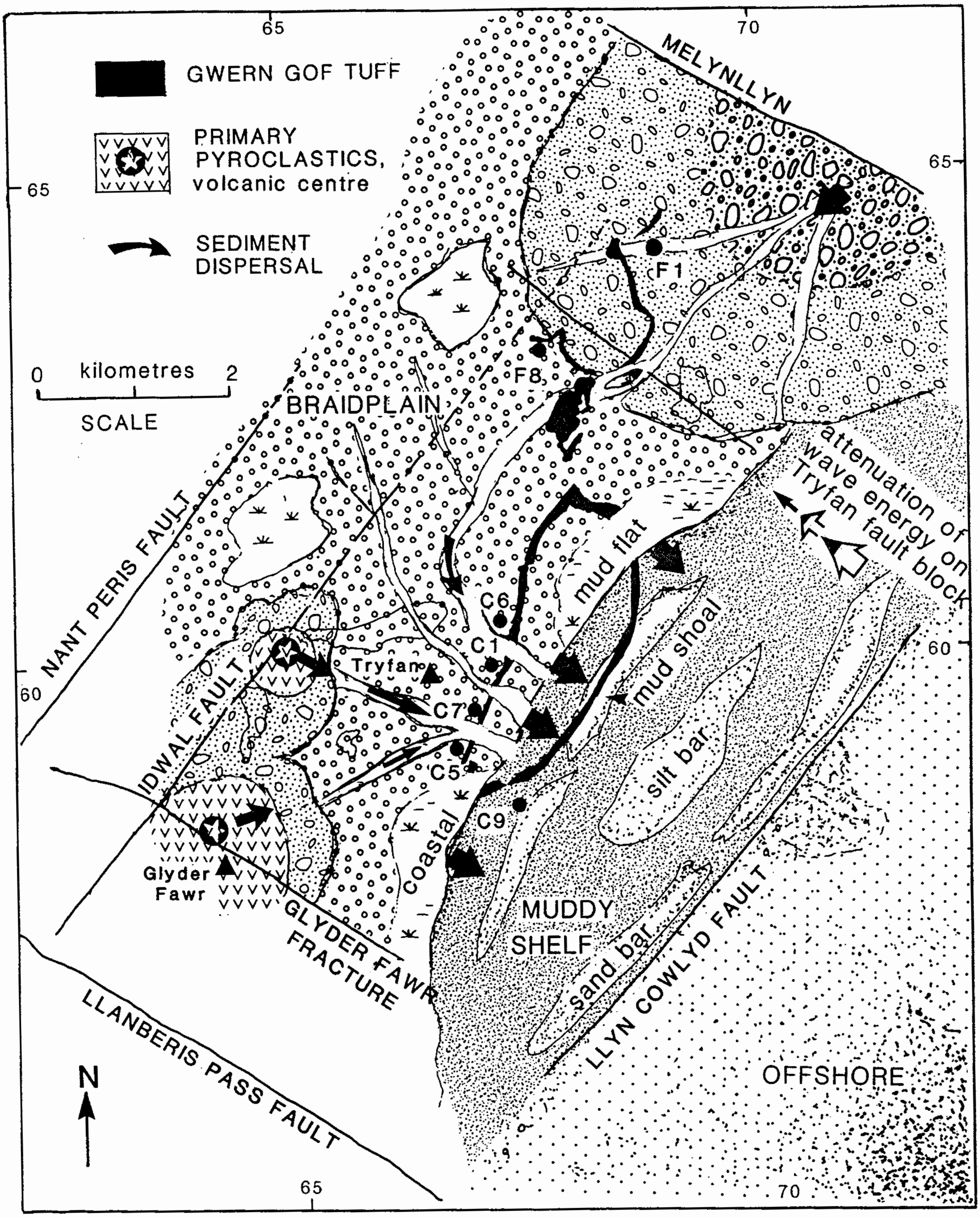

FIG. 4.19 Reconstruction of palaeogeography during maximum advance (phase 4) of the Tryfan Fach braidplain. Palaeogeography not corrected for NW-SE tectonic shortening of 40%. The absence of expected correlative strata of coarse grain size to the NW of the Idwal fault in LLanberis pass (section E6 etc.) suggests that either the Y Garn fault block was uplifted relative to Tryfan fault block or tilt of the Tryfan fault block ensured all sediment produced travelled to the SE. It is likely that some mud was supplied to the braidplain from minor uplift to the NW of the Idwal fault. Possible volcanic sources and related patterns of sediment dispersal are also indicated.

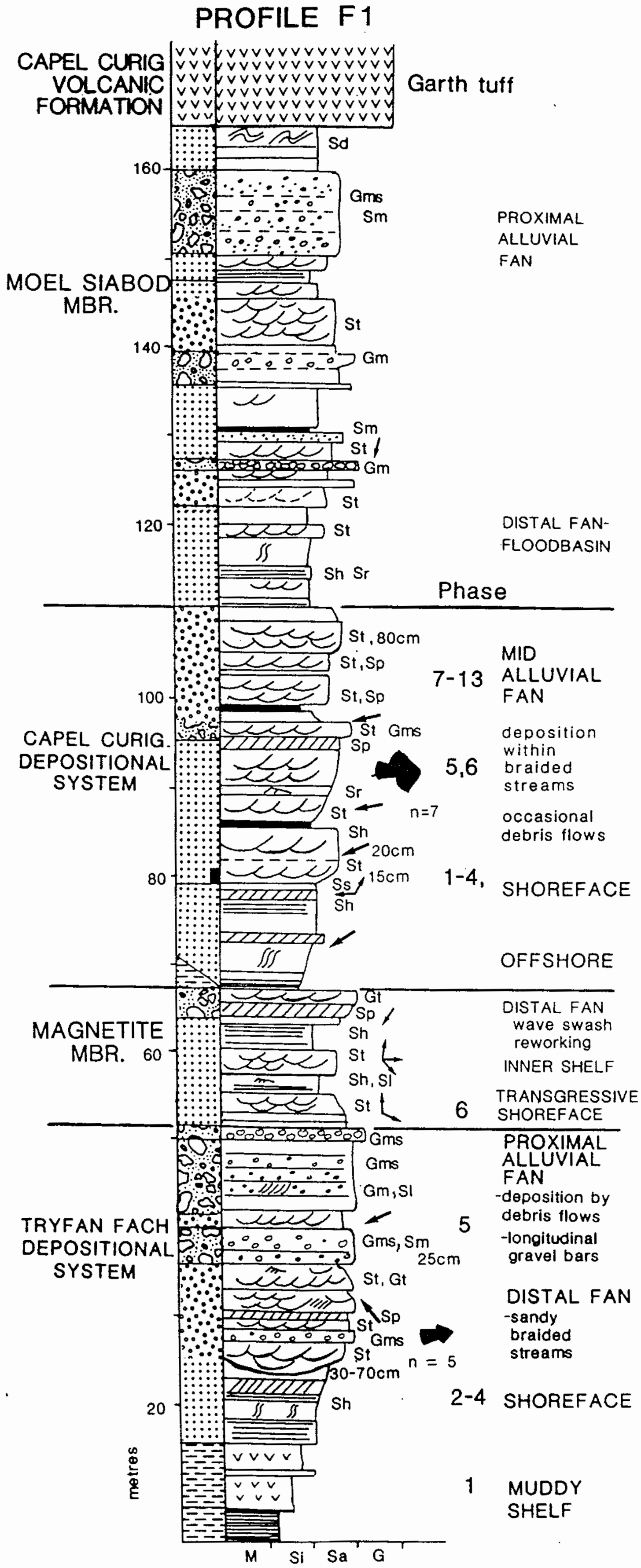

FIG. 4.20 Section through the basin-margin alluvial fan successions at Craig-yr-Ysfa (see section location in Fig. 4.19 and legend in Fig. 4.1).

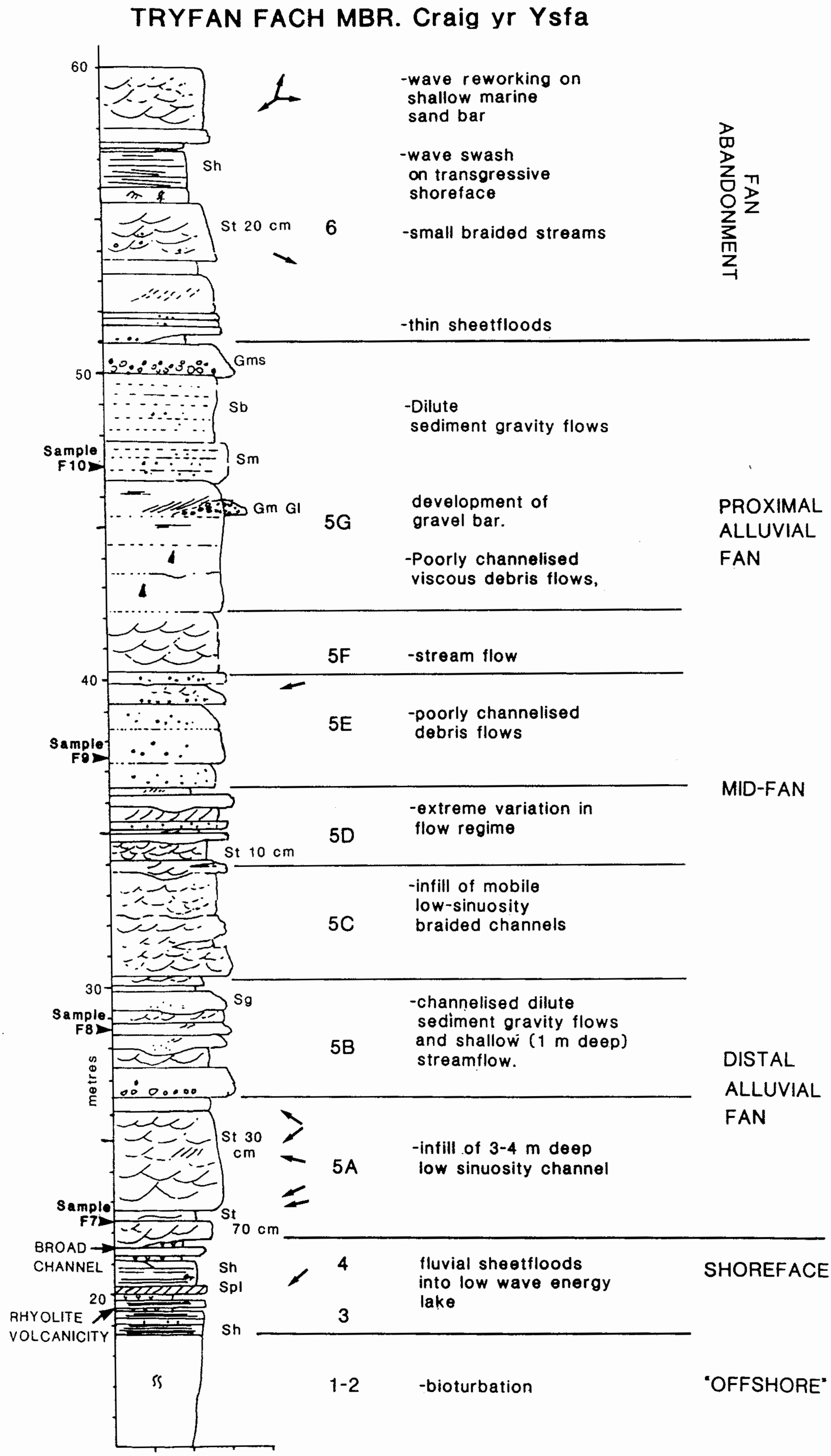

FIG. 4.21 Detail of Tryfan Fach Mbr. alluvial fan at Craig Yr Ysfa. (see Fig. 4.19 for location of section and Fig. 4.1 for lithofacies codes).

FIG. 4.22 Stratigraphic sections through the Magnetite Mbr. braidplain-delta, Tryfan anticline. (see Fig. 4.27 for location of sections and reconstruction of palaeogeography)

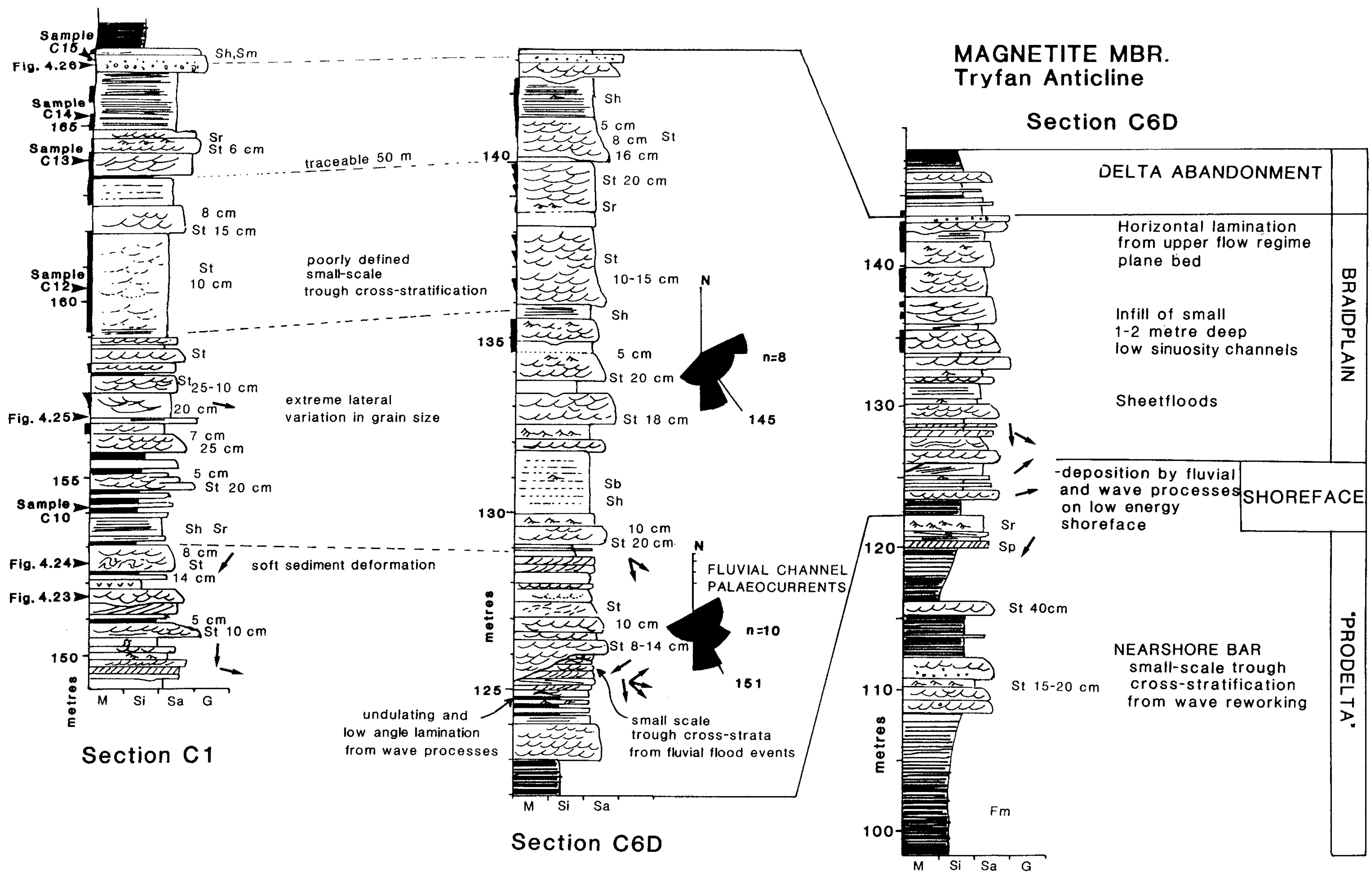

Fig. 4.23 Low-angle cross stratification (S1) and small sets of trough cross-stratification within poorly sorted coarse-grained feldspathic sandstones from braidplain deposits of Magnetite Mbr., Tryfan anticline. Flow of palaeocurrents was towards reader. (see Fig. 4.13, 4.14, section C1, 151.10 m). Pencil for scale.

Fig. 4.24 Thixotropic soft-sediment deformation of medium-grained fluvial sandstones of Magnetite Mbr., Tryfan anticline. Attributed to liquefaction of rapidly deposited sediment by earthquakes. (see Fig. 4.13, 4.14, section C1, 152.19 m). Pencil for scale.

Fig. 4.25 Poorly sorted trough cross-stratified coarse-grained sandstones from base of shallow (1 m deep) fluvial channel. Note rapid variation in grain size within sets of cross-strata and along foresets. Fe-staining from magnetite within fine-grained chloritic sediments. Channel-fill overlies fine-grained sandstones from previous fining-upward fluvial sequence as a tabular sheet. Magnetite Mbr., Tryfan Anticline. (see Fig. 4.13, 4.14, section C1, 155.7 m). Notebook 14 cm long.

Fig. 4.26 Sheetfloods of conglomerate and fine-grained magnetite-rich sandstone (arrow) from top portion of Magnetite Mbr. braidplain, Tryfan anticline. Pebble are predominately rhyolite. Location of sample C10. (see Fig. 4.13, 4.14, Section C1, 166.7 m). Pencil for scale.

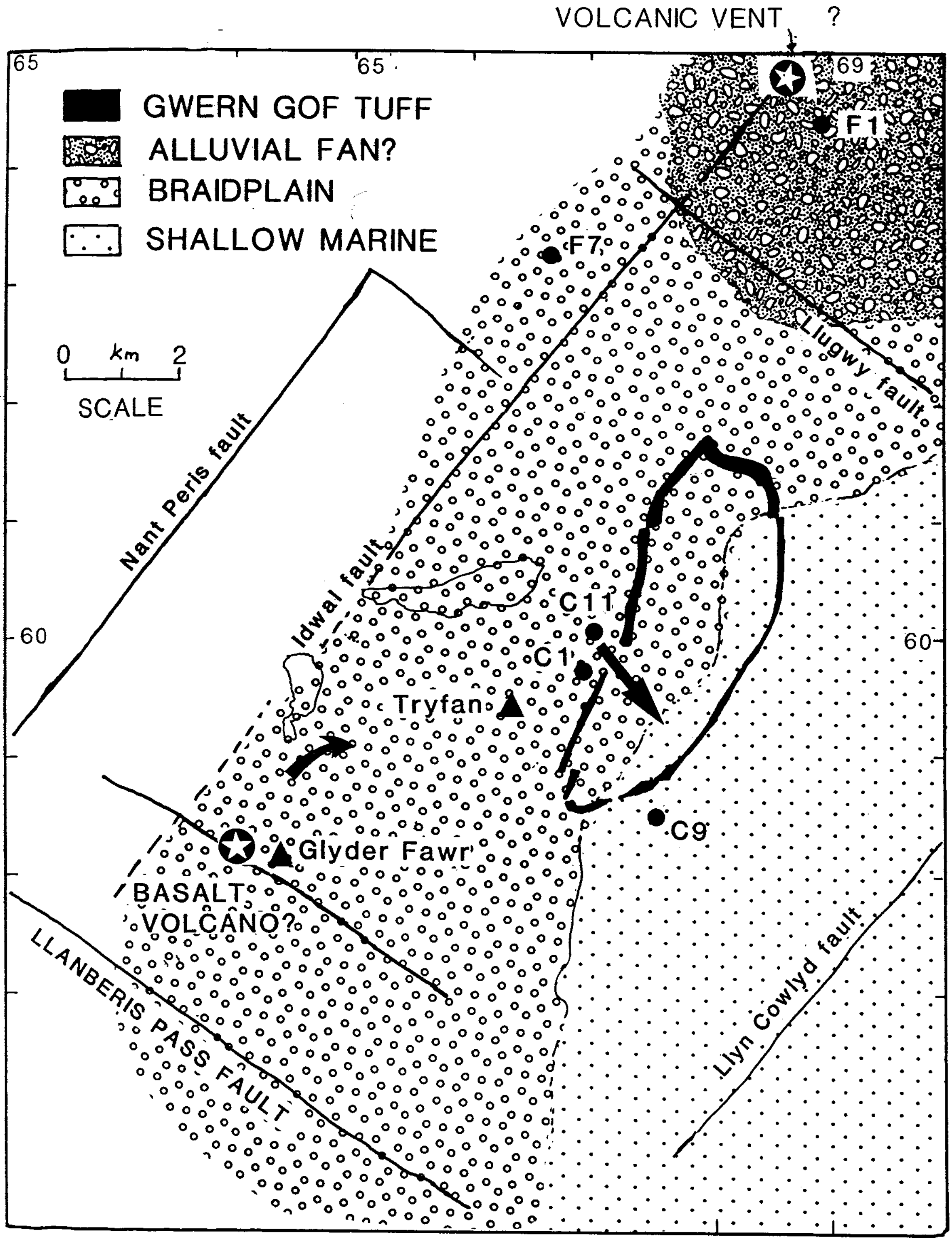

Fig. 4.27 Reconstruction of palaeogeography in the Tryfan depocentre during maximum advance of the Magnetite Mbr. braidplain, showing major faults which were active at this time. Palaeogeography not corrected for NW-SE tectonic shortening of 40%. See Fig. 4.19 for comments regarding activity of Idwal fault and uplift of Y garn fault block.

Fig. 4.28 Stratigraphic profiles through the Capel Curig Mbr. braidplain-delta successions in the Tryfan and Capel Curig anticlines. Time equivalence is implied for the numbered phases of deposition. Inset map shows location of all sections logged. Both map and block diagram show schematic reconstruction of palaeogeography during maximum advance of the braidplain. See text (Chapt. 4.3.4.9) for further discussion.

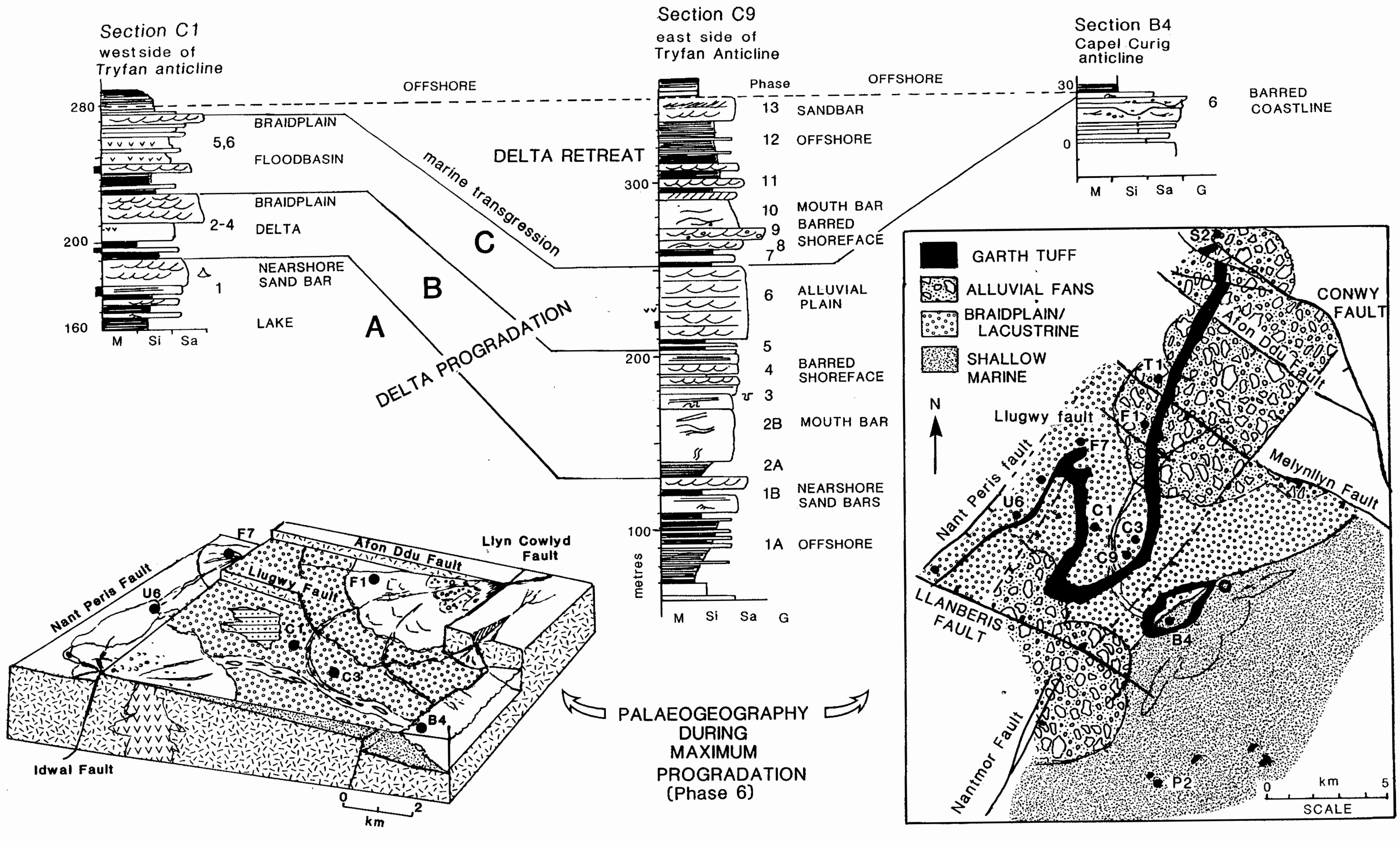

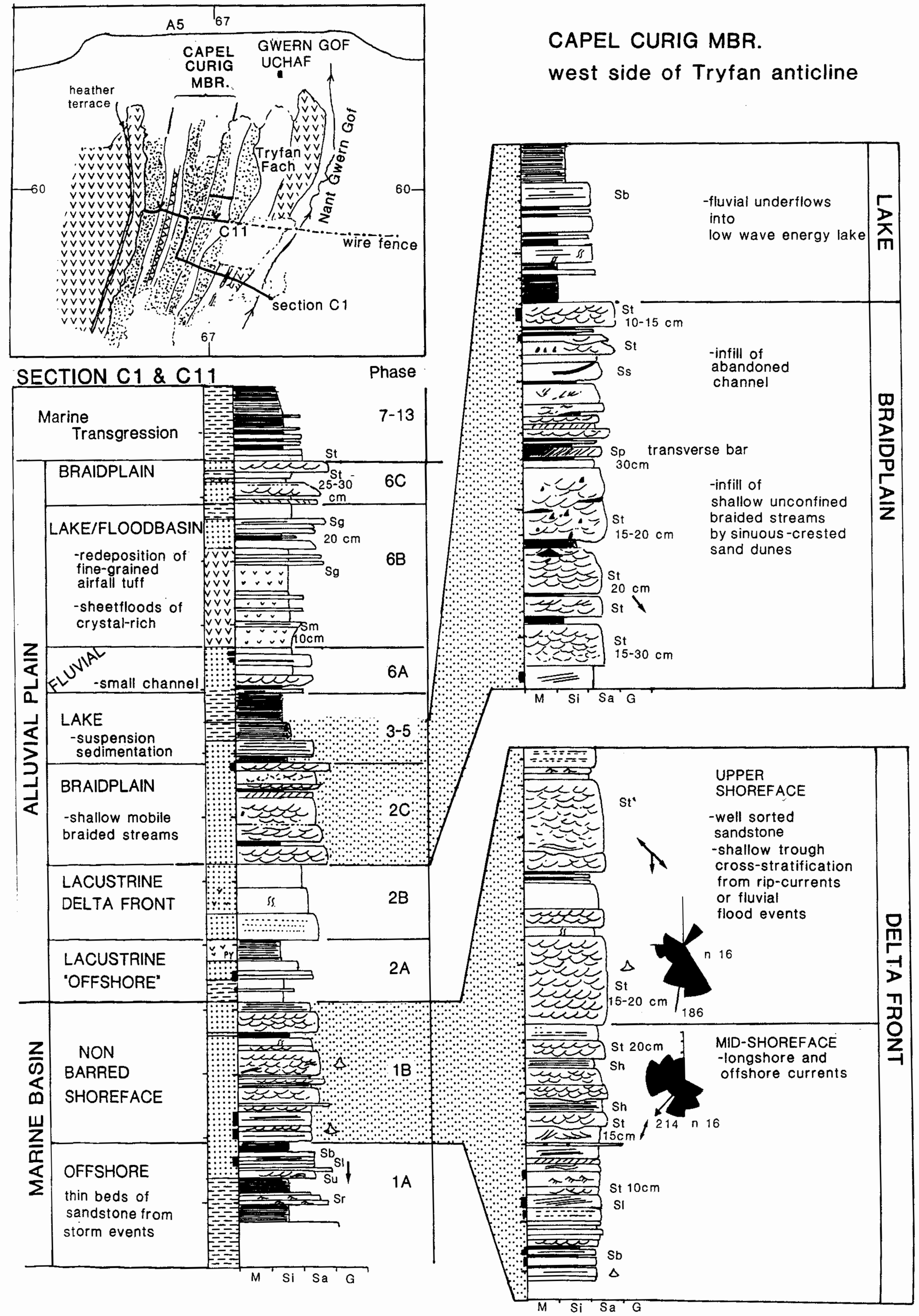

Fig. 4.29 Detailed section(s) through Capel Curig. Mbr. on west side of Tryfan anticline, with enlargements of barred shoreface (Phase 1) and braided stream (Phase 2B) deposits. Inset map shows location of vertical profiles.

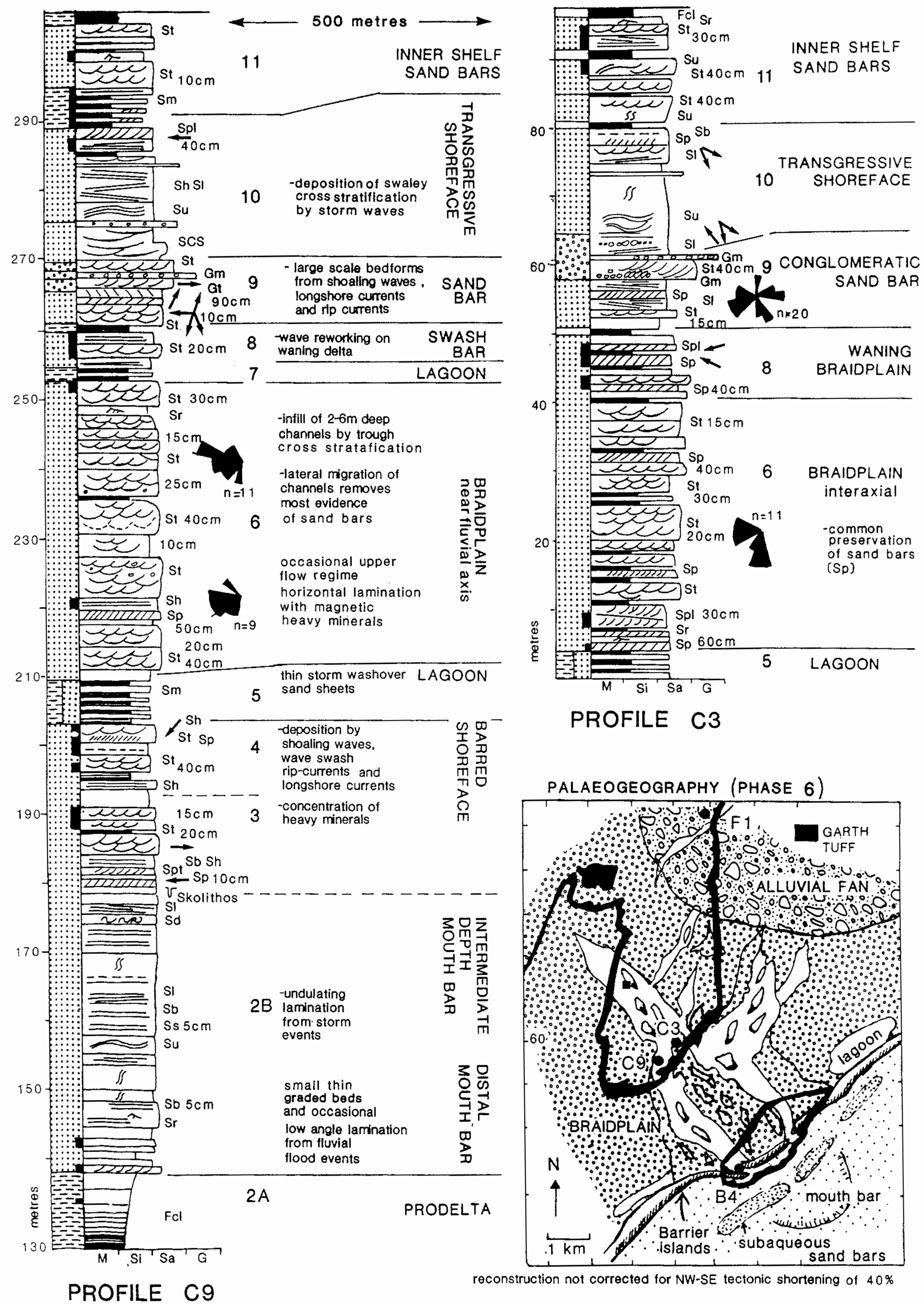

Fig. 4.30 Stratigraphic sections through part of the Capel Curig braidplain-delta succession (see Fig. 4.2b for location of sections and legend in Fig. 4.1). Time equivelance is implied for the numbered phases of deposition (large numbers **2A** to **11** on section margins). Inset map shows interpreted palaeogeography during maximum progradation (phase 6) of the braidplain delta (see Fig. 4.28 for additional palaeogeographical maps). Palaeogeography is not corrected for NW-SE tectonic shortening of 40%.

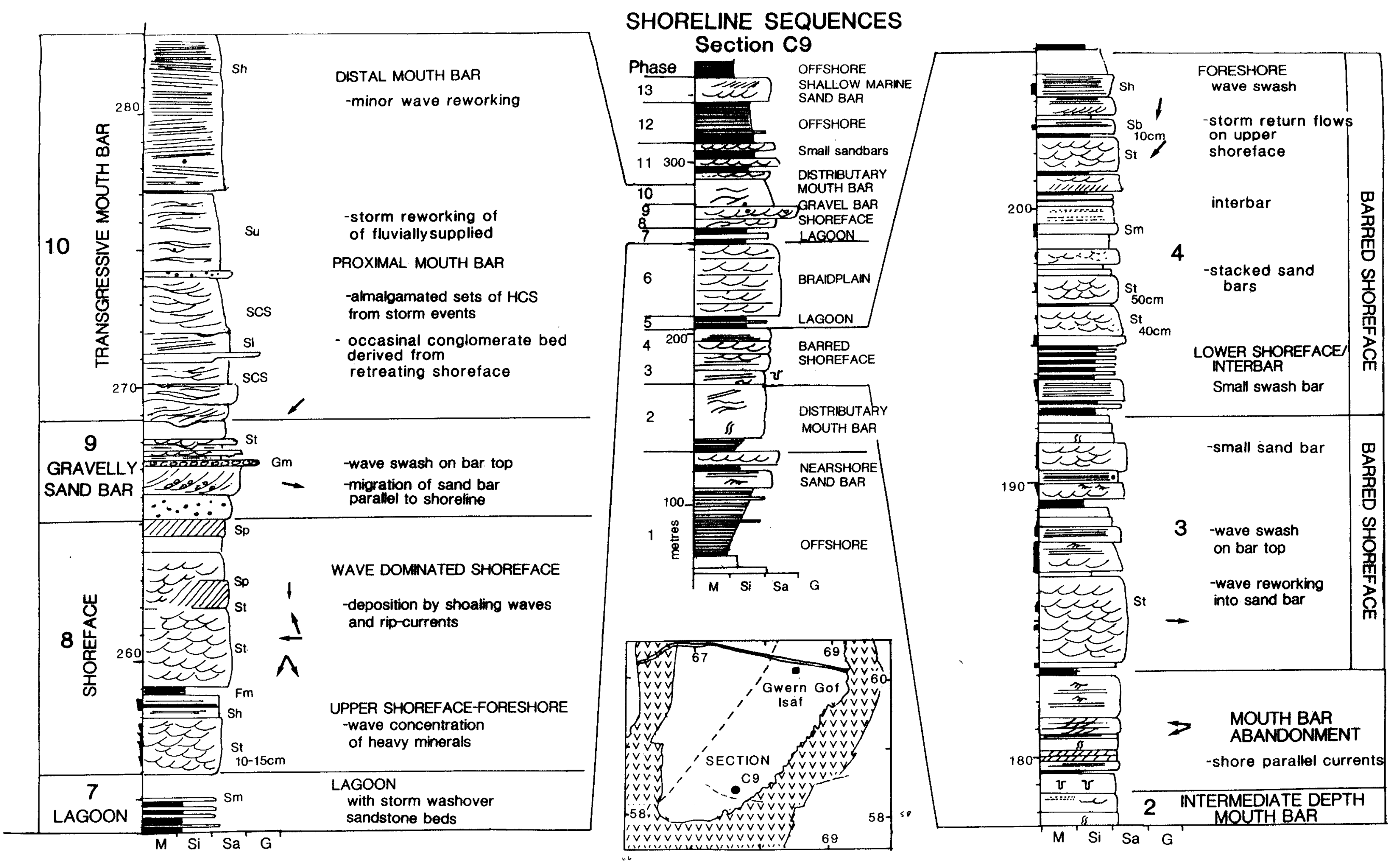

Fig. 4.31 Details of shoreline sequences developed during progradation and retreat of the Capel Curig braidplain-delta. Inset map shows location of section C9. See Fig. 4.28 for correlation with sections on the west side of the Tryfan anticline.

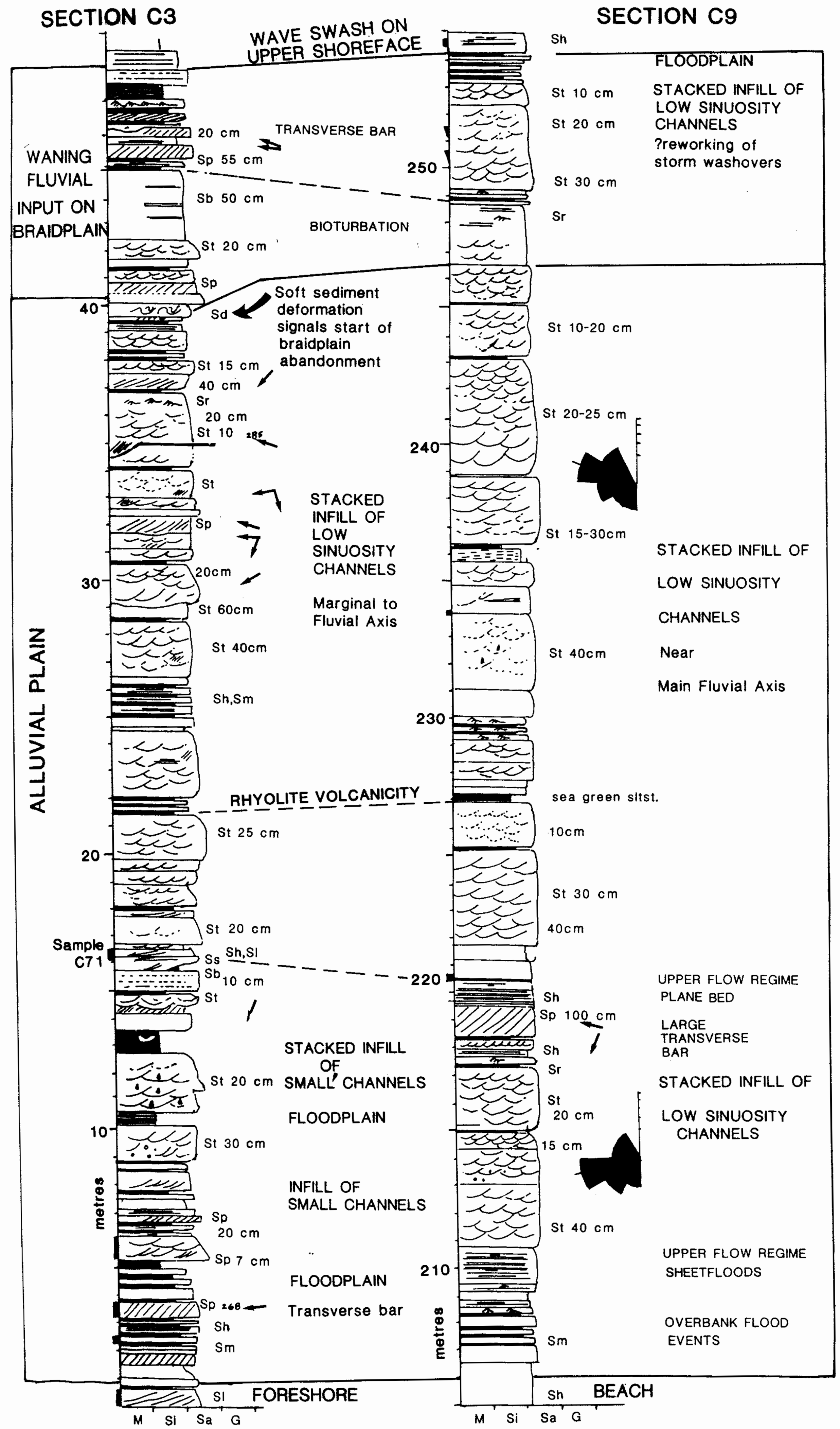

Fig. 4.32 Details of braidplain sequences from Capel Curig Mbr., Tryfan anticline. See Fig. 4.30 (phase 6) for location of sections.

Fig. 4.33 Horizontal to low-angle upper flow regime plane-bed within fluvial sediments of Capel Curig Mbr., east side of Tryfan anticline. Location of sample C71. Horizon can be correlated with similar magnetite rich laminae (Fig. 4.29) on the west side of the Tryfan anticline (*ca.* 2.5 km upstream after unfolding strata). (see Fig. 4.32, section C3, 15.9 m). Lense cap is 6 cm in diameter.

Fig. 4.34 Stacked sets of trough cross-stratification similar to that found within braidplain deposits of the Capel Curig Mbr., Tryfan anticline. Exact source of photo is unknown.

Fig. 4.35 Lithofacies (St, Sp, Sh) from poorly sorted, pebbly, medium- to very coarse-grained braided stream deposits, Capel Curig Mbr. alluvial fan at Craig yr Ysfa. (see Fig. ection F1, 89 m. Field notebook is 18.5 cm long.

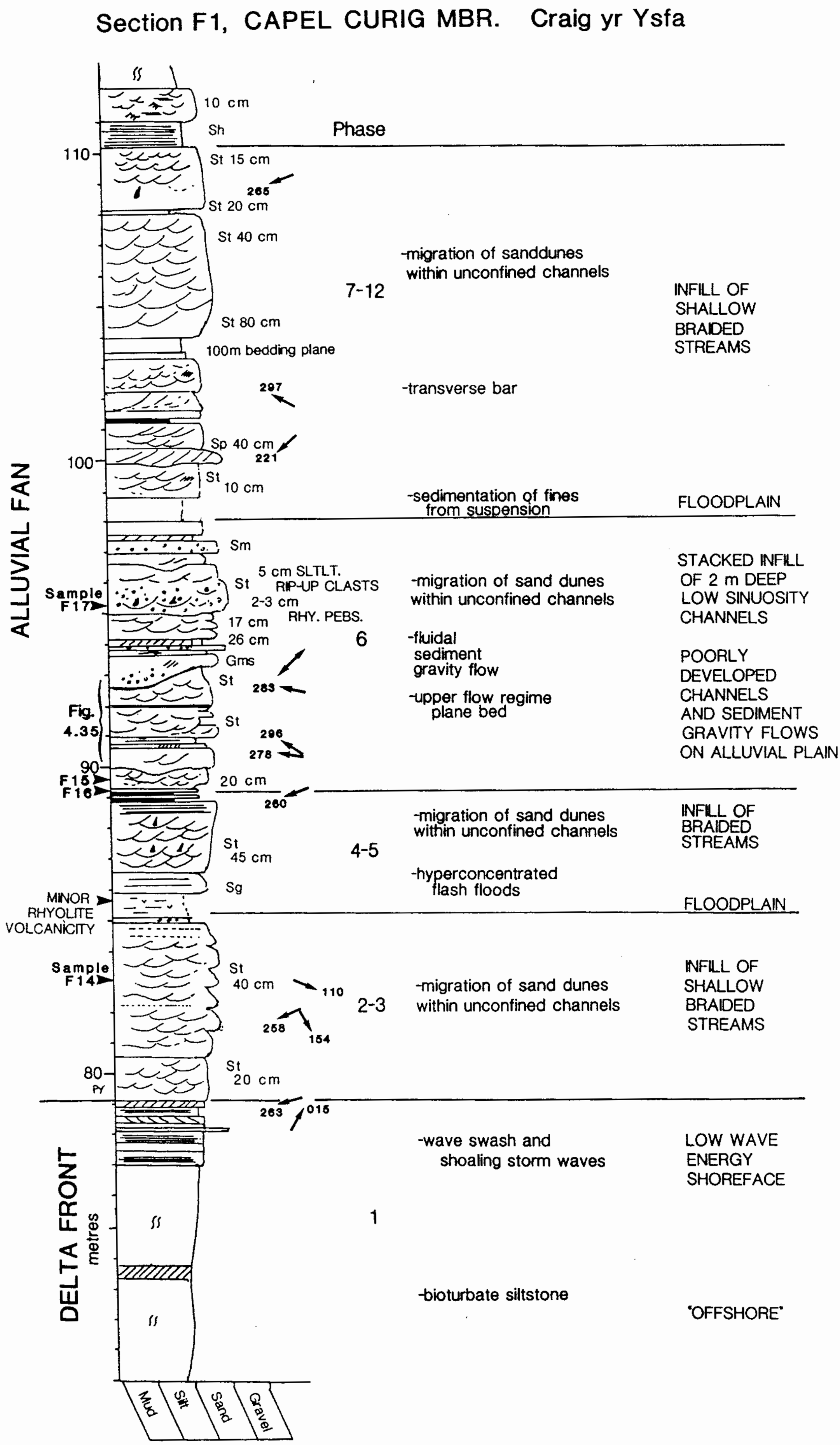

Fig. 4.36 Detail of Capel Curig Mbr. alluvial fan at Craig Yr Ysfa. (see Fig. 4.28 for location of section, Fig. 4.20 for position of sequence within Tryfan Fm, and Fig. 4.1 for lithofacies codes).

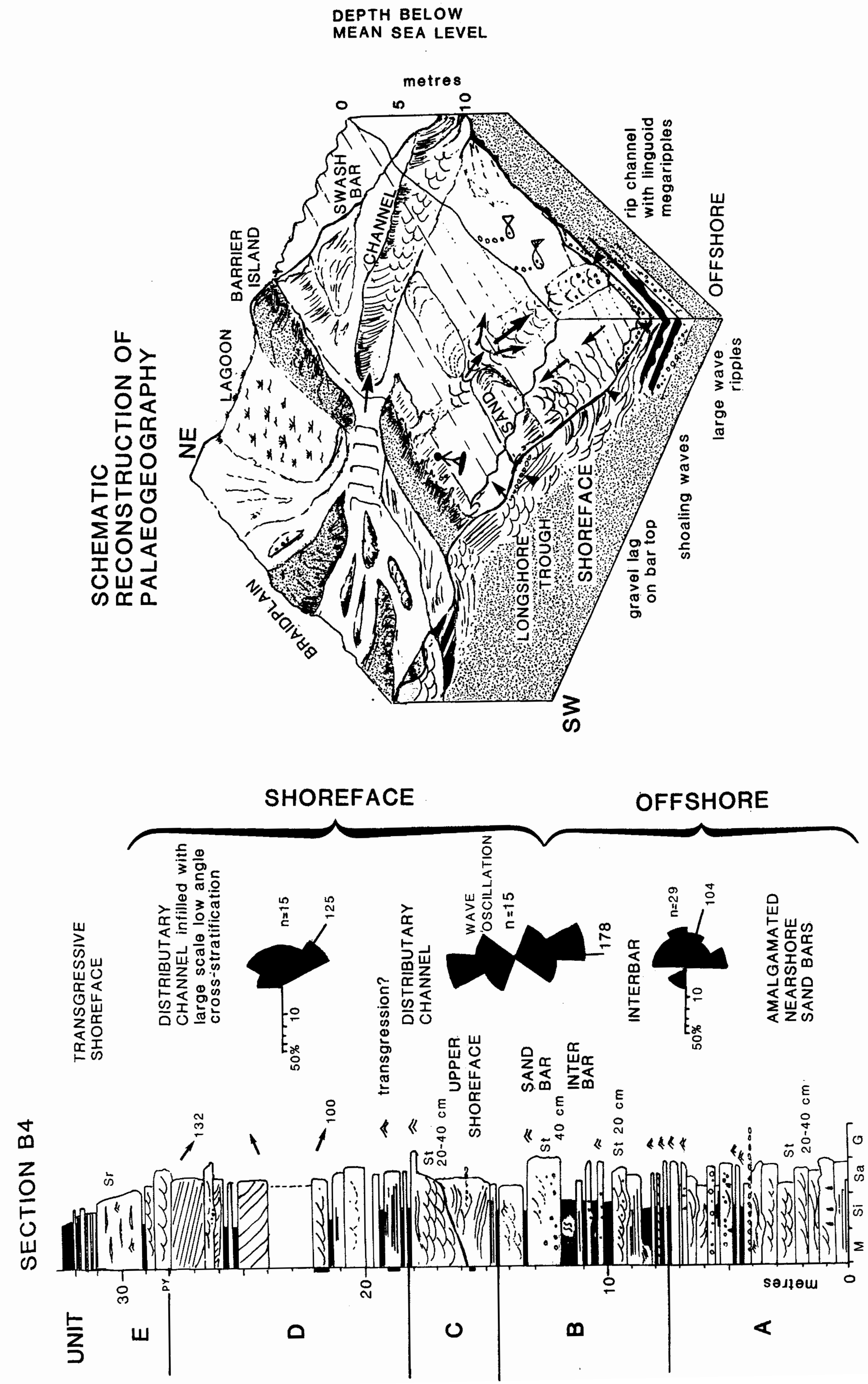

Fig. 4.37 Stratigraphic profile through "terminus" of the Capel Curig Mbr. braidplain-delta at Cwm Clorad Isaf. See Fig. 4.38 for location of section, and Fig. 4.28 for correlation with sequences in the Tryfan anticline. Block diagram shows a schematic reconstruction of depositional environments, process and resultant facies on the wave-dominated delta-front. Analysis of wave ripples (Chapt. 5._) indicates that coastline would have been excellent for surfing; on dissipative coastlines such as this, waves would begin to break a considerable distance from the shoreline. Fish and sedges used to identify deposition environments are varieties as yet undiscovered in the Ordovician.

FIG. 4.38: Lateral variation within Section B4, terminus of Capel Curig Mbr. braidplain delta, Cwm Clorad Isaf. Palaeocurrents oriented relative to outcrop face instead of the conventional N-S oriented diagram, to facilitate comparison of sections.

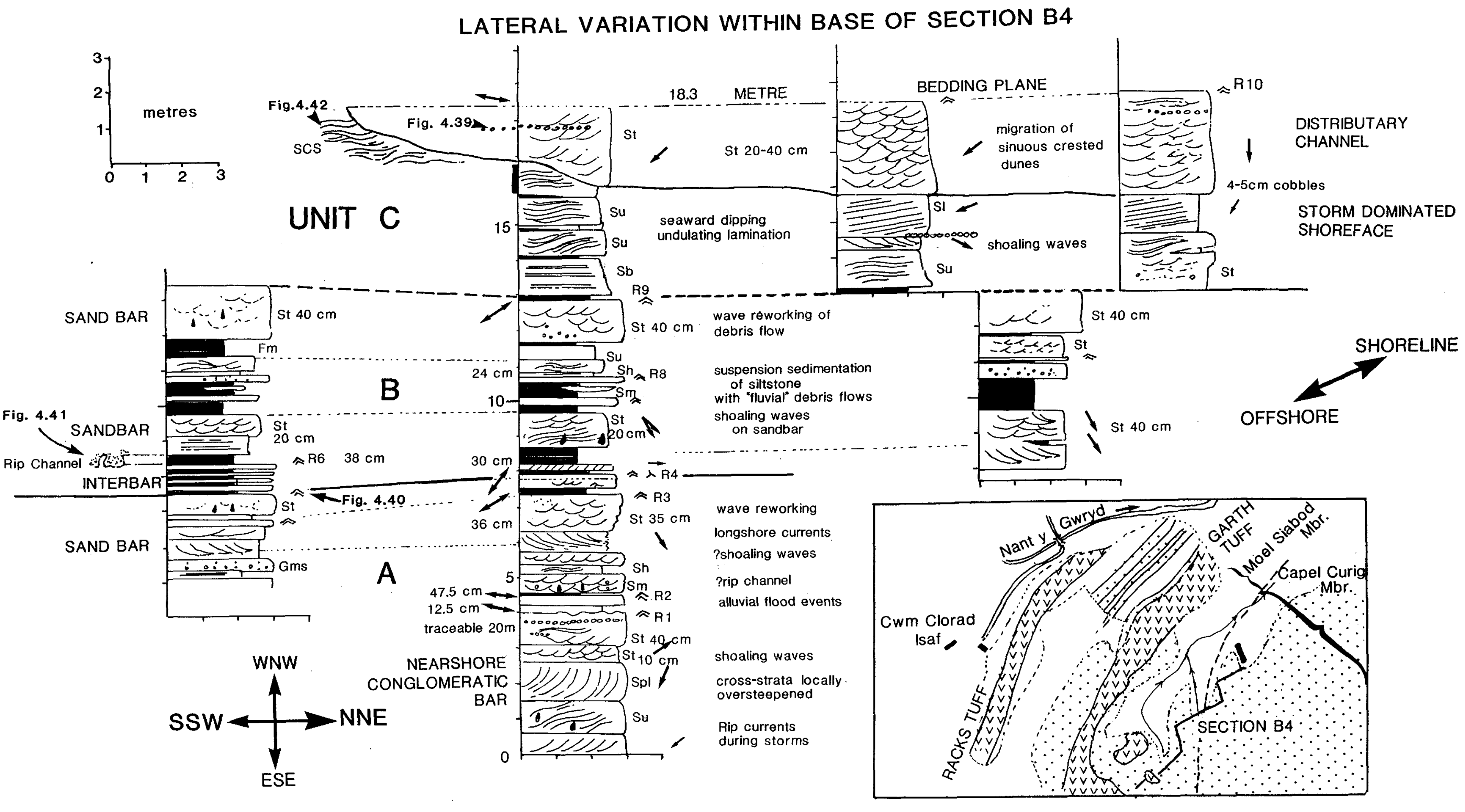

Fig. 4.39 Conglomerate bed of well rounded coarse-grained rhyolite and fine-grained rhyolitic tuff cobbles at base of thin debris-flow of very coarse-grained sandstone. Capel Curig Mbr., Cwm Clorad Isaf. (see Fig. 4.38, section B4/2, succession C, 17.9 m) Lense cap is 6 cm in diameter.

Fig. 4.40: Large wave ripples within very coarse-grained pebbly sandstone. Strike of crestline is parallel to strike of cleavage in Capel Curig anticline. Most of the structural shortening is taken up by troughes of ripples, resulting in the buckled "rod" or "mullion" structure that is seen. From phase 6, Capel Curig Mbr., Cwm Clorad Isaf.(See Fig. 4.38, section B4/1, 6.73 m). Lense cap is 6 cm in diameter.

Fig. 4.41: Siltstone bed (on right: SLTST) is cut-out (to left) by scour filled with medium- to coarse-grained sandstone displaying undulating horizontal lamination. Scour is thought to record eddying from rip-currents on the storm-dominated delta front. The "bum-shaped" load-ball of sandstone (centre) would reflect gravitational intability on the rip-channel margin during its infill; development of the deformation structure probably stems from liquefaction of the delta-front substrate during cyclic loading by storm waves. See text for further explanation. From Capel Curig Mbr., Cwm Clorad Isaf. See Fig. 4.38, section B4/1, 8.1 m). Pen is 15 cm long for scale.

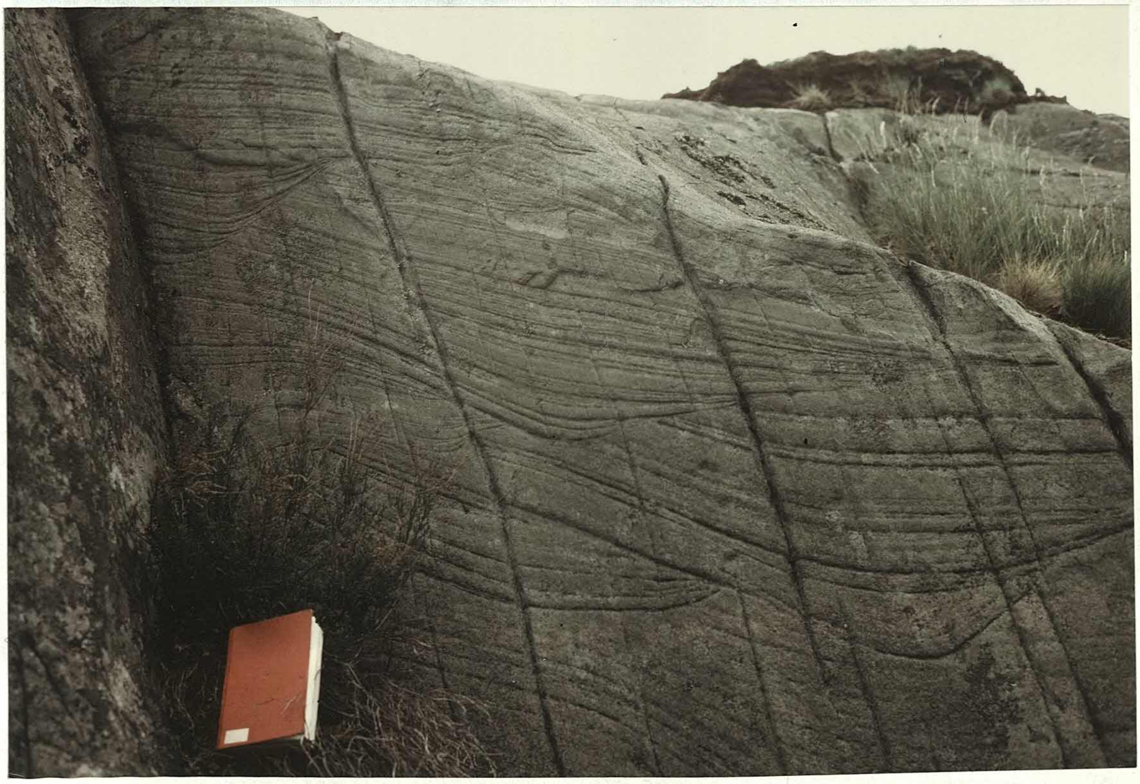

Fig. 4.42: Amalgamated sets of hummocky cross-stratification (*ie.* swaley cross-stratification) transitional to "scour-and-fill" type structures on upper shoreface of Capel Curig Mbr. braidplain delta at Cwm Clorad Isaf. Sub-vertical fractures represent spaced cleavage; strain ratios within sandstone are 1.27: 1.00: 0.73 (I. Wilkinson, pers. comm., 1986). See Fig. 4.38, section B4, ≈16 m. Field notebook is 18 cm in length.

Fig. 4.43: Large wave ripples in very coarse sandstone. Oblique view of bedding surface; measuring stick (centre) is scaled in 10 cm bars. Note straight to sinuous crestlines, common termination of crestlines (T), and varying assymetry to ripple profiles. Ripples are erosively removed by cobble filled channel (C) which progressively cuts deeper into rippled horizon towards the inferred offshore (right in photo). From Capel Curig Mbr., Cwm Clorad Isaf. (see Fig. 4.37, section B4, 18.3 m bedding plane)

Fig. 4.44: Detail of above wave ripples showing termination of a crestline. Note small 1 cm pebbles on tops of ripple profiles.

Fig. 4.45 Trough cross-stratification with opaque magnetite and ilmenite grains defining foresets. Palaeocurrent (direction pencil is pointing) is towards inferred offshore. Cross-strata is thought to represent migration of sinuous-crested megaripples from storm surge return flows, or rip-currents. The contained heavy minerals were probably derived from the upper shoreface or foreshore. From Capel Curig Mbr., Cwm Clorad Isaf. (see Fig. 4.37, section B4, 21.27 m). Pencil for scale.

Fig. 4.46: Sketch of distributary mouth bar/barrier island complex from blocky crags near top of Capel Curig Mbr., Cwm Clorad Isaf. (detail from section B4, Fig. 4.37, 24 to 29 metres). Vertical exaggeration is 250%.

PHOTO A: Solitary set of large-scale (1.5 metres) low-angle tangentiall cross-strata from infill of small distributary channel cut into the underlying and adjacent (PHOTO B) wave reworked deposits of a nearshore bar. Overlain by wave-reworked deposits containing undulating horizontal lamination, or small sets of trough cross-stratification. (view of section B4, 24 to 29 m, outcrop face A) Field notebook (at bottom) is 18 cm long for scale.

PHOTO B: Amalgamated sets of hummocky cross-stratification showing upwards growth of bedform. Silty horizon with field notebook (18.5 cm long) represents a sub-horizontal bedding plane. Top surface of hummocky bedform shows some signs of "fairweather" wave reworking, containing discontinuous pebble lags, trough cross-stratification and ?small wave ripples. Section B4, ≈ 27 m, outcrop face U.

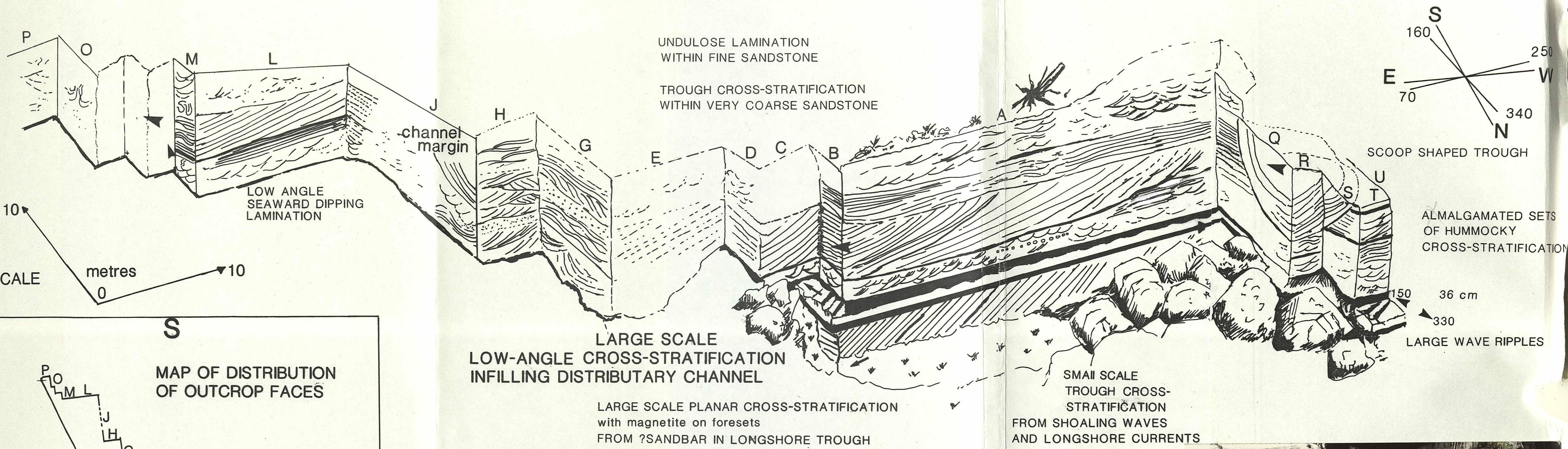

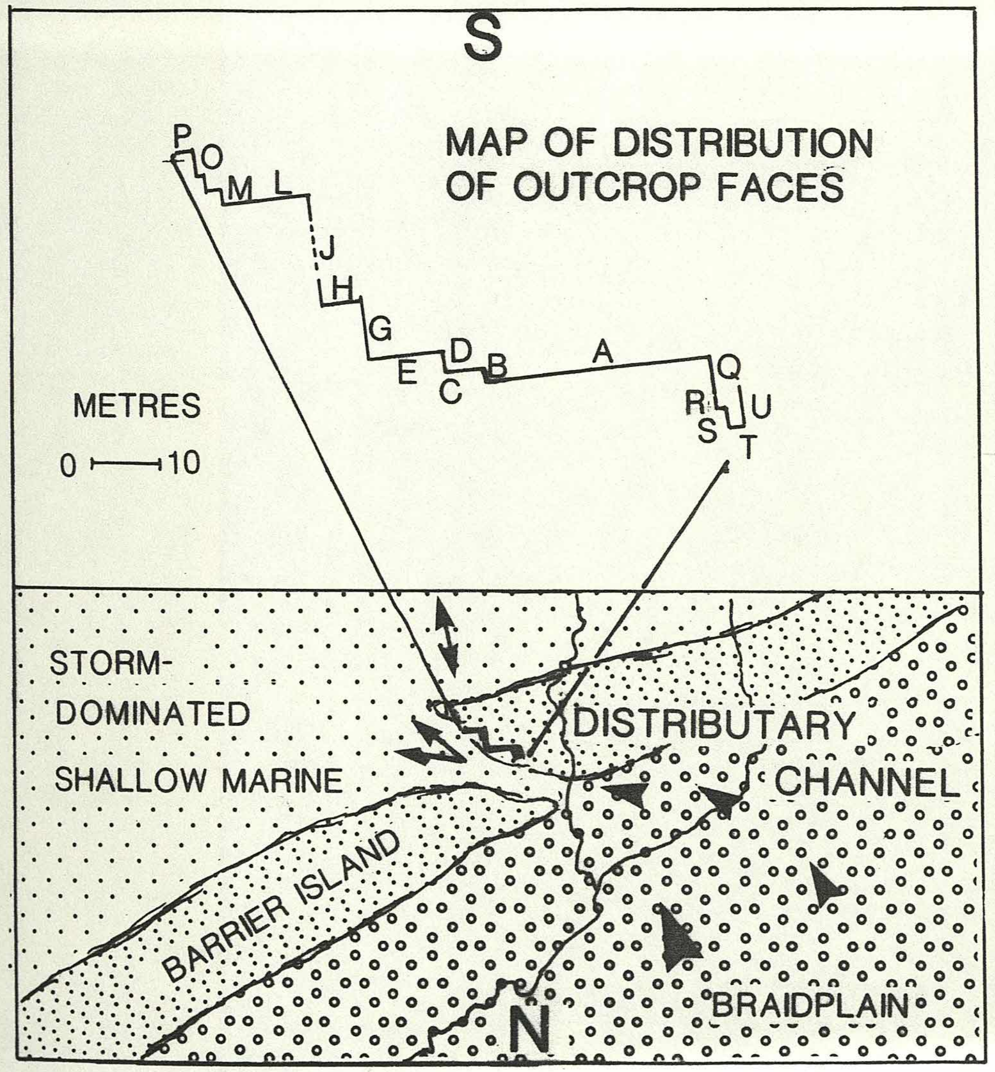

SCHEMATIC PALAEOGEOGRAPHY
LOOKING SOUTH

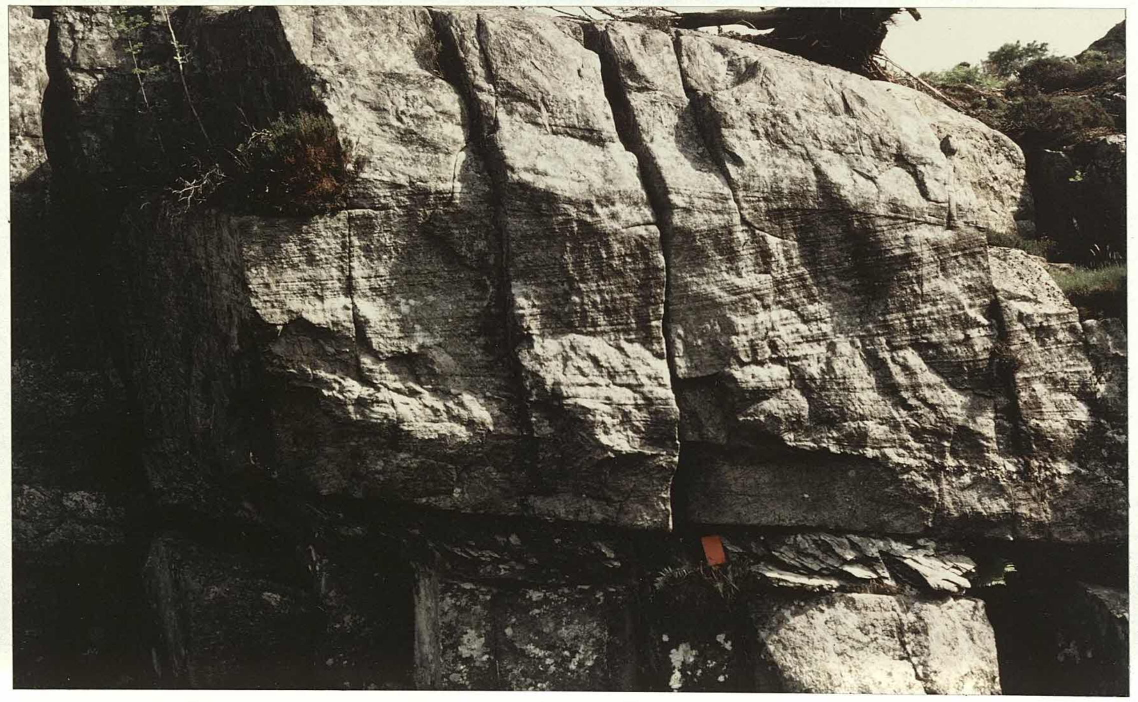

A

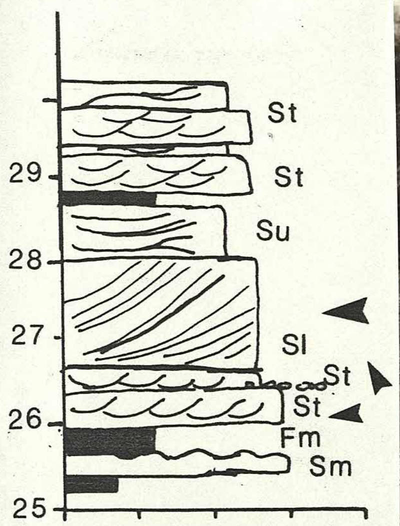

GRAIN SIZE VARIATION THROUGH SECTION ON FACE A

B

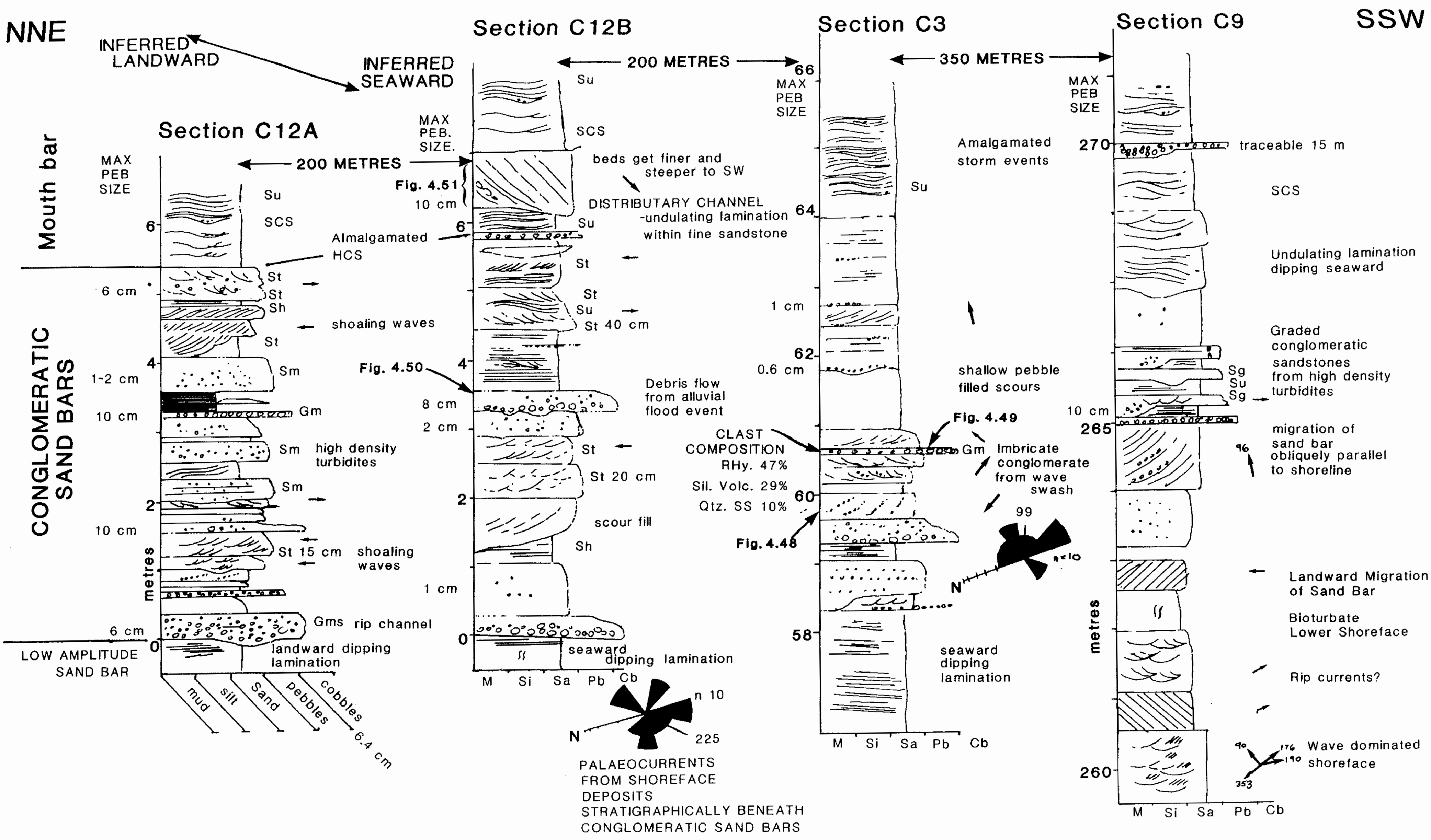

Fig. 4.47: Detail of conglomeratic nearshore deposits (phase 9) developed during retreat of Capel Curig braidplain-delta (see Fig. 4.28, 4.30, phase 9 in sections C9 and C3; see Fig. 4.54 for location of other sections and palaeogeography during marine transgression). Palaeocurrent rose diagrams oriented relative to face of outcrop rather than conventional N-S orientation.

Fig. 4.48 Poorly sorted very coarse-grained sandstones with pebbles in thin horizontal lags or concentrated at the base of cross-strata foresets. View is towards the inferred shoreline. From conglomeratic sand bar (Phase 9) which developed during retreat of the Capel Curig Mbr. braidplain delta.(See Fig. 4.47, section C3, 62.5 m). Field notebook is 18.5 cm long for scale.

Fig. 4.49 Imbricate rhyolite cobbles from nearshore deposits of Capel Curig Mbr. braidplain delta. Pencil points towards inferred offshore. Horizon thought to reflect wave-swash processes on top of a gravelly sand bar. (see Fig. 4.47, section C3, 60.72 m).

Fig. 4.50 Normally-graded conglomerate from high density turbdidity current within nearshore deposits developed during retreat of the Capel Curig Mbr. braidplain-delta. From east side of Tryfan anticline, Fig. 4.47, section C12b, 3.5 m. Lense cap is 6 cm in diameter.

Fig. 4.51 Large-scale low to moderate angle cross-stratification from infill of distributary channel. Grain size of cross-strata fines from left to right in conjunction with increase in foreset angle. Channel scours down an additional 70 cm into subjacent sandstones towards the right (inferred offhore). Channel-fill sequence is overlain by wave-reworked medium- to very coarse-grained sandstones containing undulating horizontal lamination. From delta retreat succession of Capel Curig Mbr. braidplain delta, east side of Tryfan anticline, Section C12B, 6.2 m. Field notebook is 18.5 cm long. Compare with Fig. 4.46a.

Fig. 4.52 Undulating horizontal and low-angle lamination and pebble-lined scours from wave-reworked transgressive mouth bar deposits of Capel Curig Mbr. braidplain delta. From east side of Tryfan anticline, Section C3, 68 m. Pencil for scale.

Fig. 4.53 Middle portion of infill of a rip-channel within "offshore" deposits developed during retreat of the Capel Curig Mbr. braidplain delta. Siltstone bed at top of photo represents the palaeo-horizontal. Channel fill contains numerous rip-up clasts of siliceous siltstone (as shown) and horizontal upper flow regime plane-bed laminae of magnetic heavy minerals (not shown). From east side of Tryfan anticline, section C3, 95.1 m.

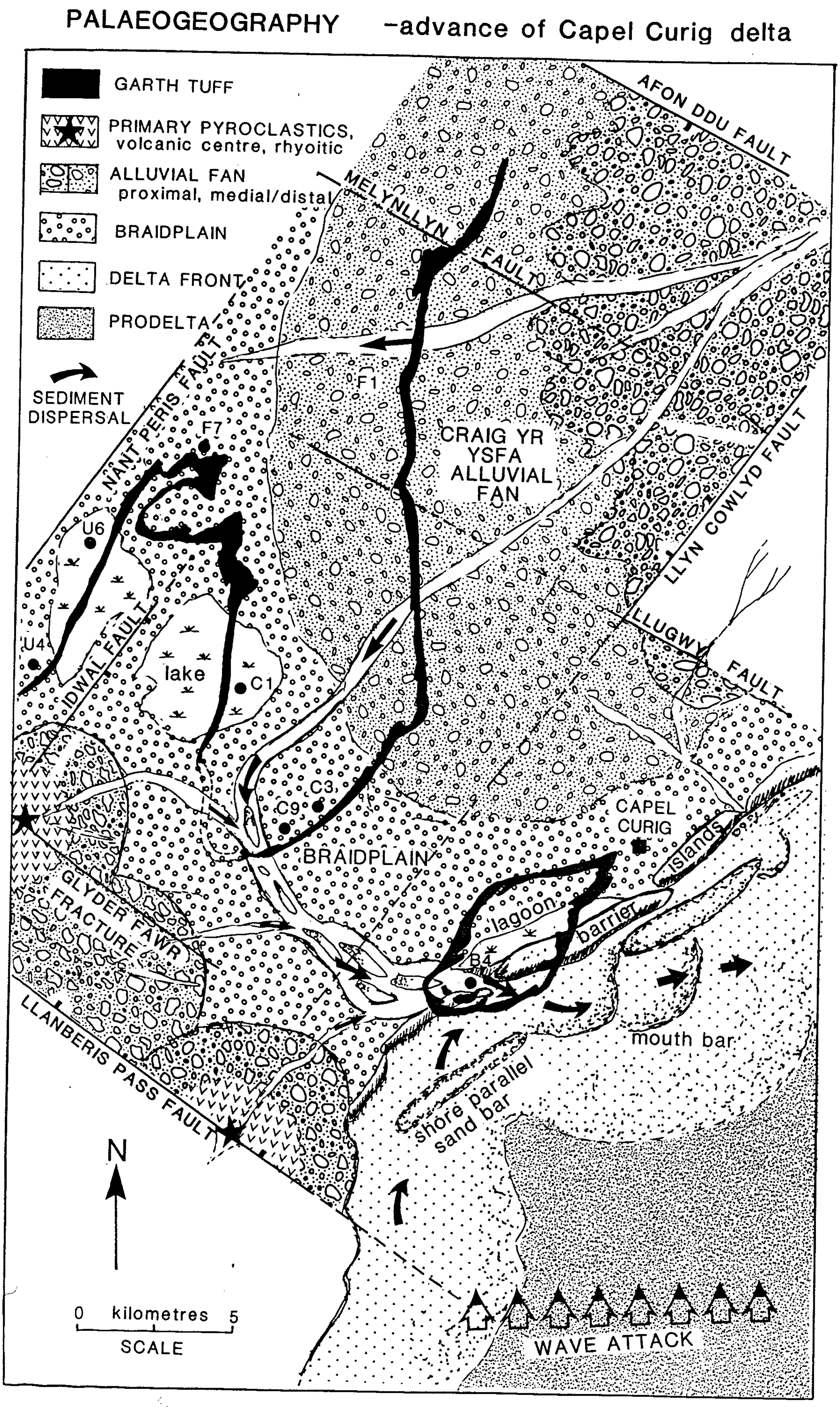

FIG. 4.54: Palaeogeography during maximum progradation of Capel Curig Mbr. braidplain delta.

PALAEOGEOGRAPHY -retreat of Capel Curig delta

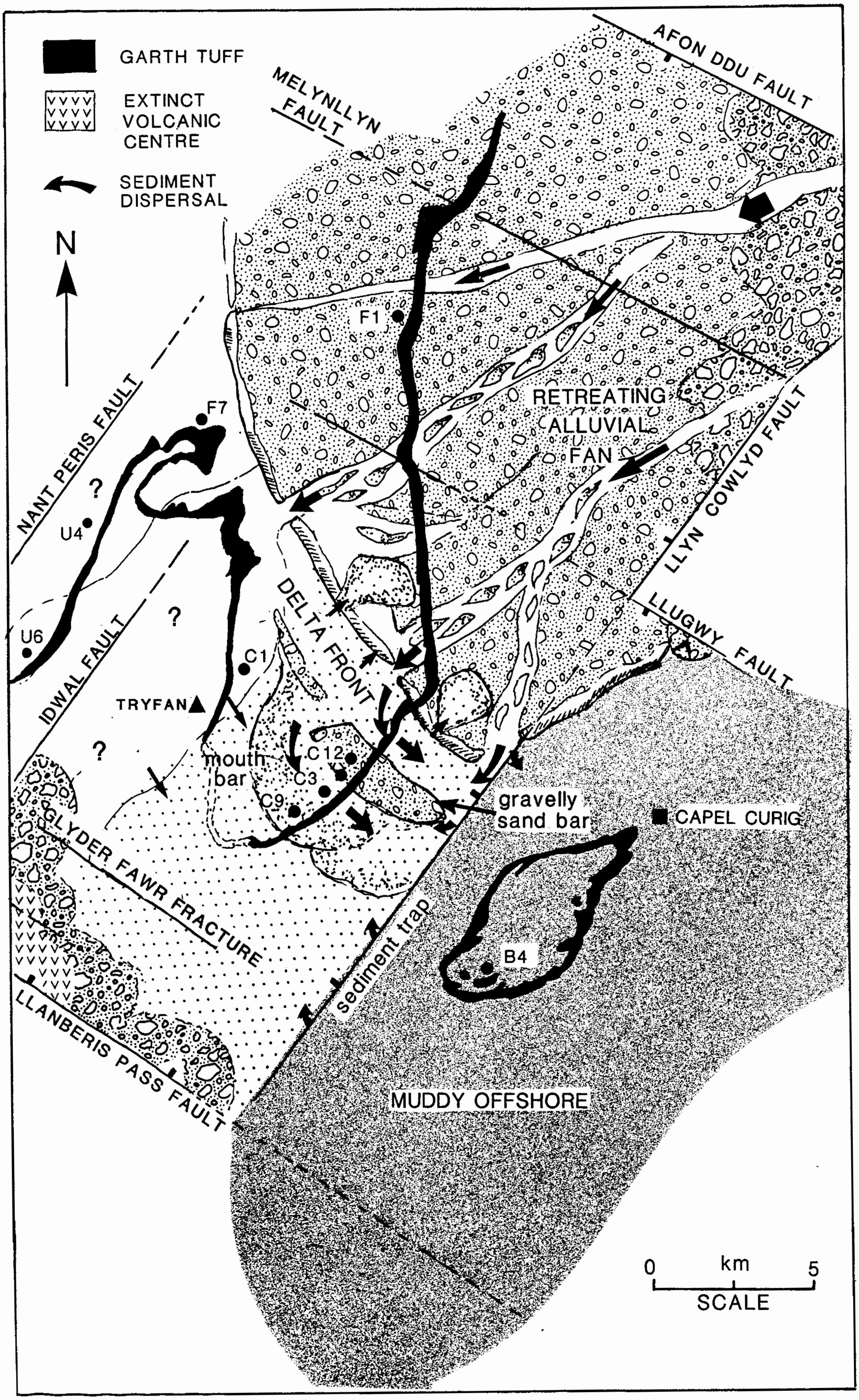

FIG. 4.55: Palaeogeography during retreat of Capel Curig Mbr. braidplain delta. Compare with Fig. 4.54. Note absence of volcanic centre(s) along Llanberis pass and change in shoreline orientation.

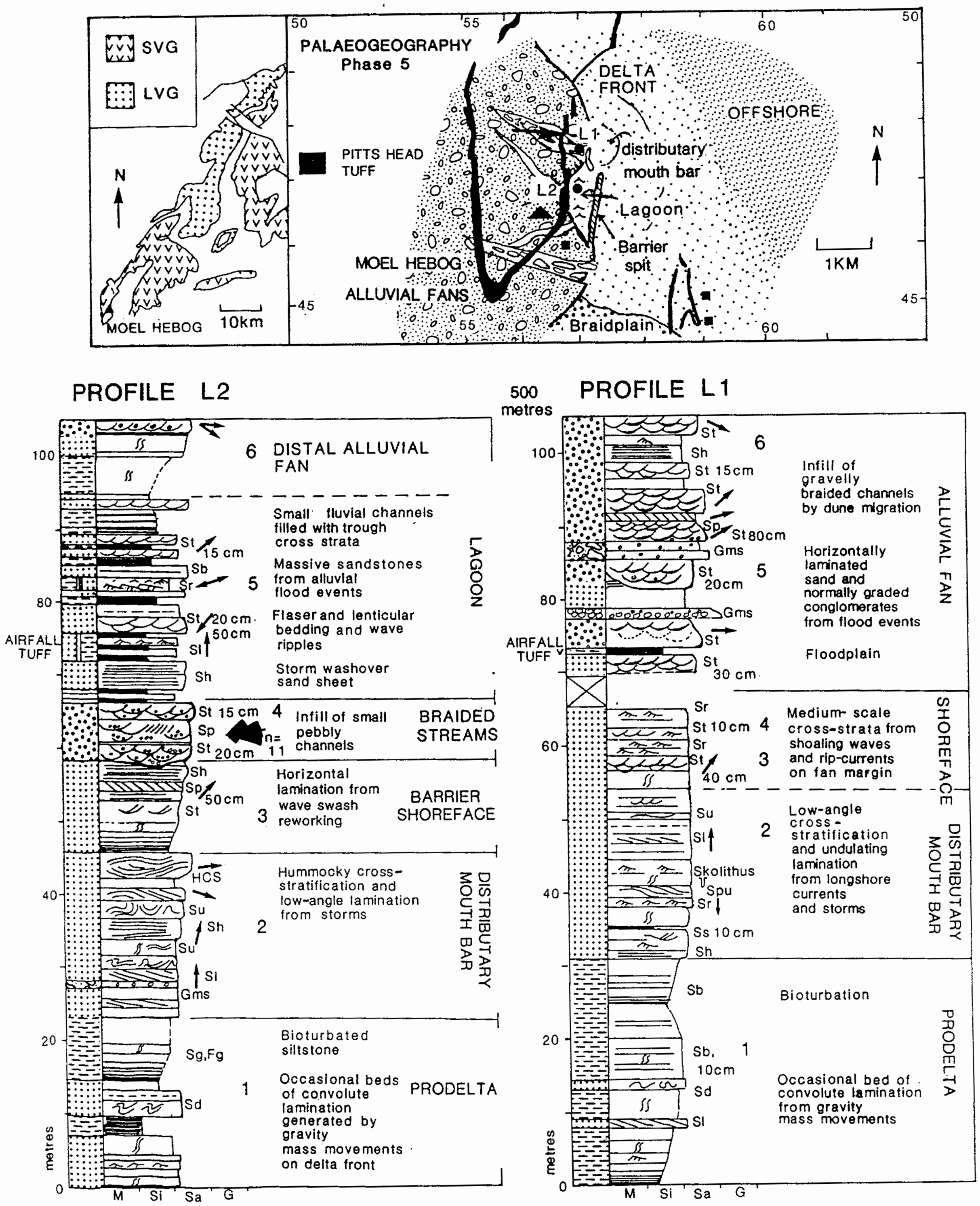

Fig. 4.56: Stratigraphic sections through bottom portion of the Moel Hebog Mbr. showing fan-delta successions. Inset map shows location of sections and interpreted palaeogeography during phase 5 of fan-delta evolution; black squares denote location of other sections used in this reconstruction. See Fig. 4.72 for regional palaeogeographic maps.

Fig. 4.57: Complete vertical profile through Lower Cwm Eigiau Formation at Moel Hebog with enlarged sections of lagoon deposits (Phase 6) of Moel Hebog Mbr. Inset map depicts location of section L2. See Fig. 4.71 for reconstructions of palaeogeography during evolution of the fan-delta.

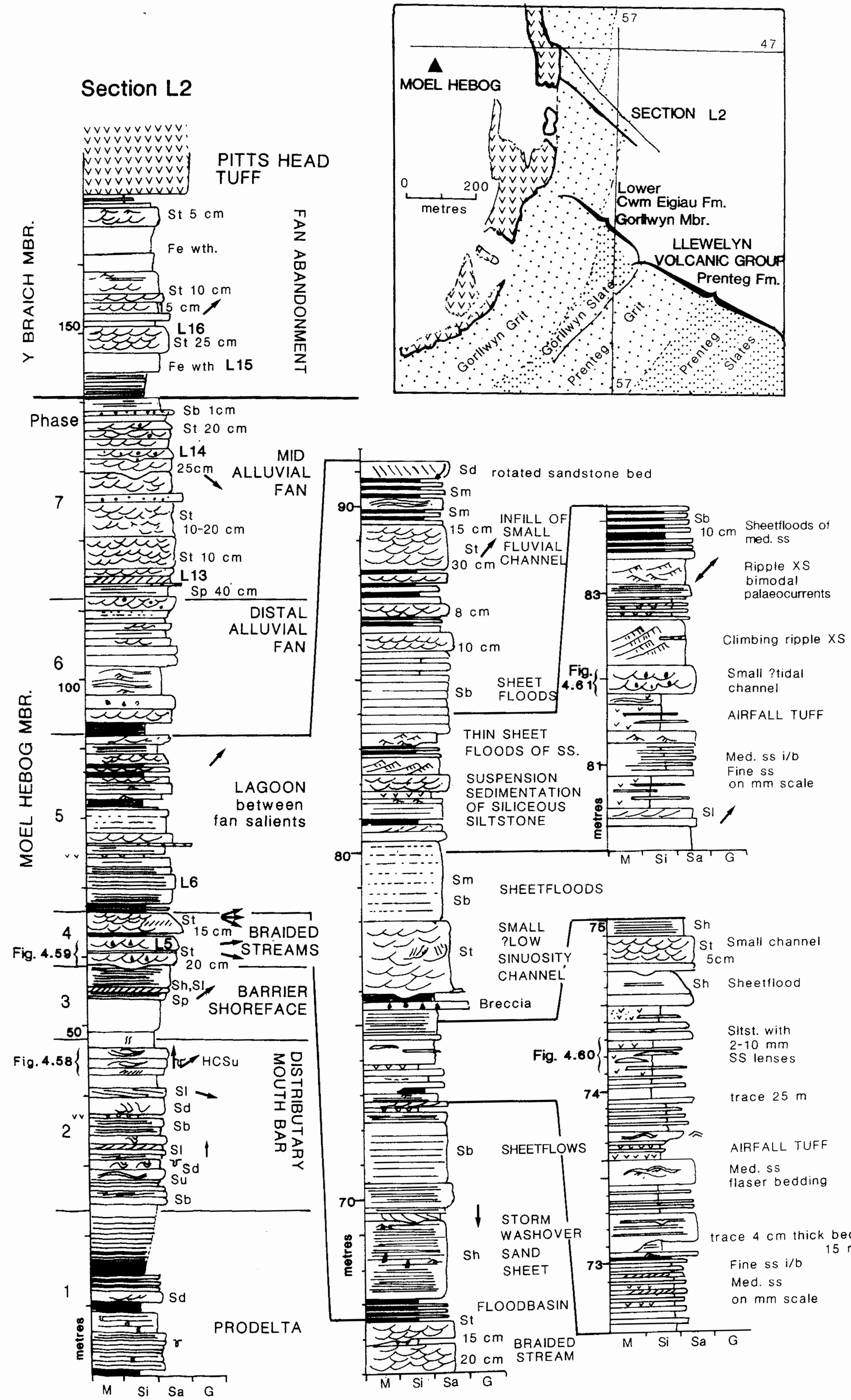

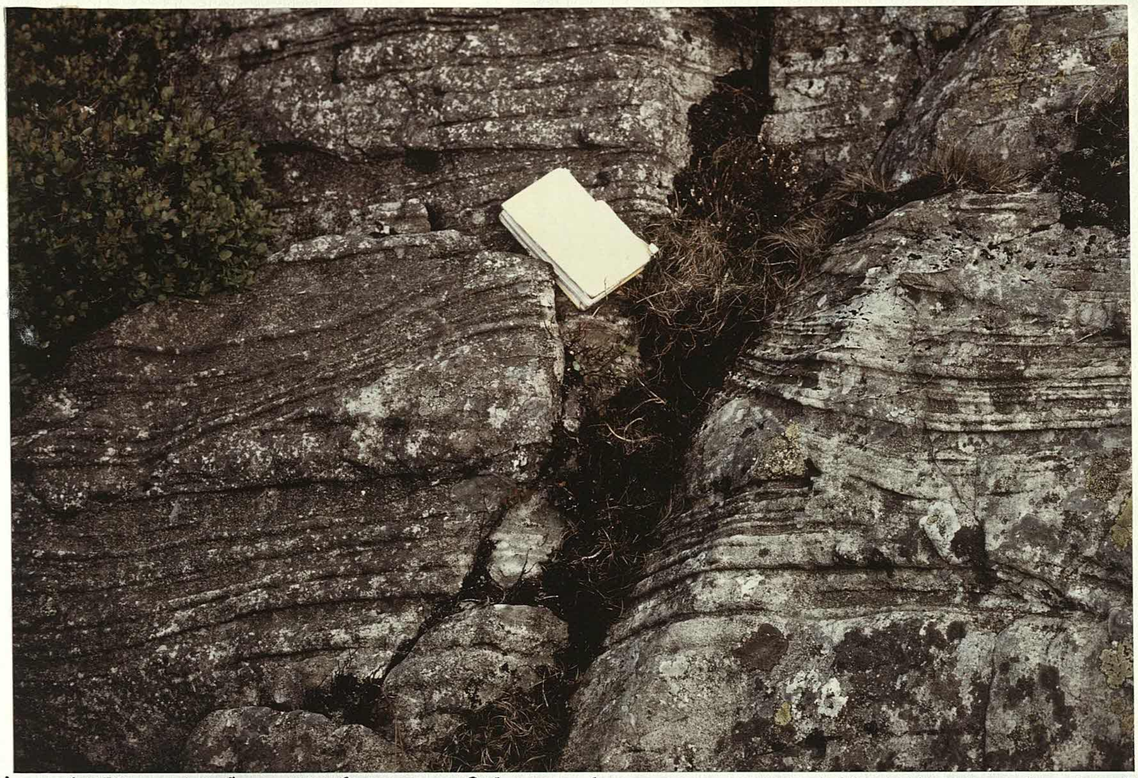

Fig. 4.58: Amalgamated sets of hummocky cross-stratification typical of wave reworked mouth-bar sands (*ie*. phase 2 in section L2, Fig. 4.56). (Photo is actually from Upper Cwm Eigiau Formation at Bwlch Trimarchog, section F5, __ m; a consistent spell of bad weather (3 months) prevented access to the Hebog slopes to obtain representative photo from this locality.

Fig. 4.59: Trough cross-stratification and horizontal lamination within pebbly medium- to coarse-grained sandstones from braided fluvial deposits (phase 4) of Moel Hebog fan-delta. (see Fig. 4.56, section L2, 60 m).

Fig. 4.60: Interbedding of siliceous siltstone with thin (2-10 mm) beds of medium sandstone from fine-grained lacustrine/lagoon deposits of Moel Hebog delta plain. Most of the sandstone beds would represent alluvial sheetfloods, whereas siltstones record minor wave and ?tidal activity within the floodbasin. (see Fig. 4.57, section L2, 74.1 m)

Fig. 4.61: Trough cross-stratification within fine-grained sandstones. attributed to infill of small ?fluvial channel on the Moel Hebog alluvial plain. Surrounding strata comprises bioturbate horizontally stratified very fine-grained sandstone or coarse siltstone from floodbasin. (see Fig. 4.57, section L2, 81.8 m)

Fig. 4.62: Stratigraphic sections through the Lower and Upper Moel DDu Mbrs.. Time equiv l nce is implied for any numbered phases of deposition. Large letters indicate the three distinct depositional packages which are interpreted within text (Chapt. 4.3.6). Inset map depicts location of sections.

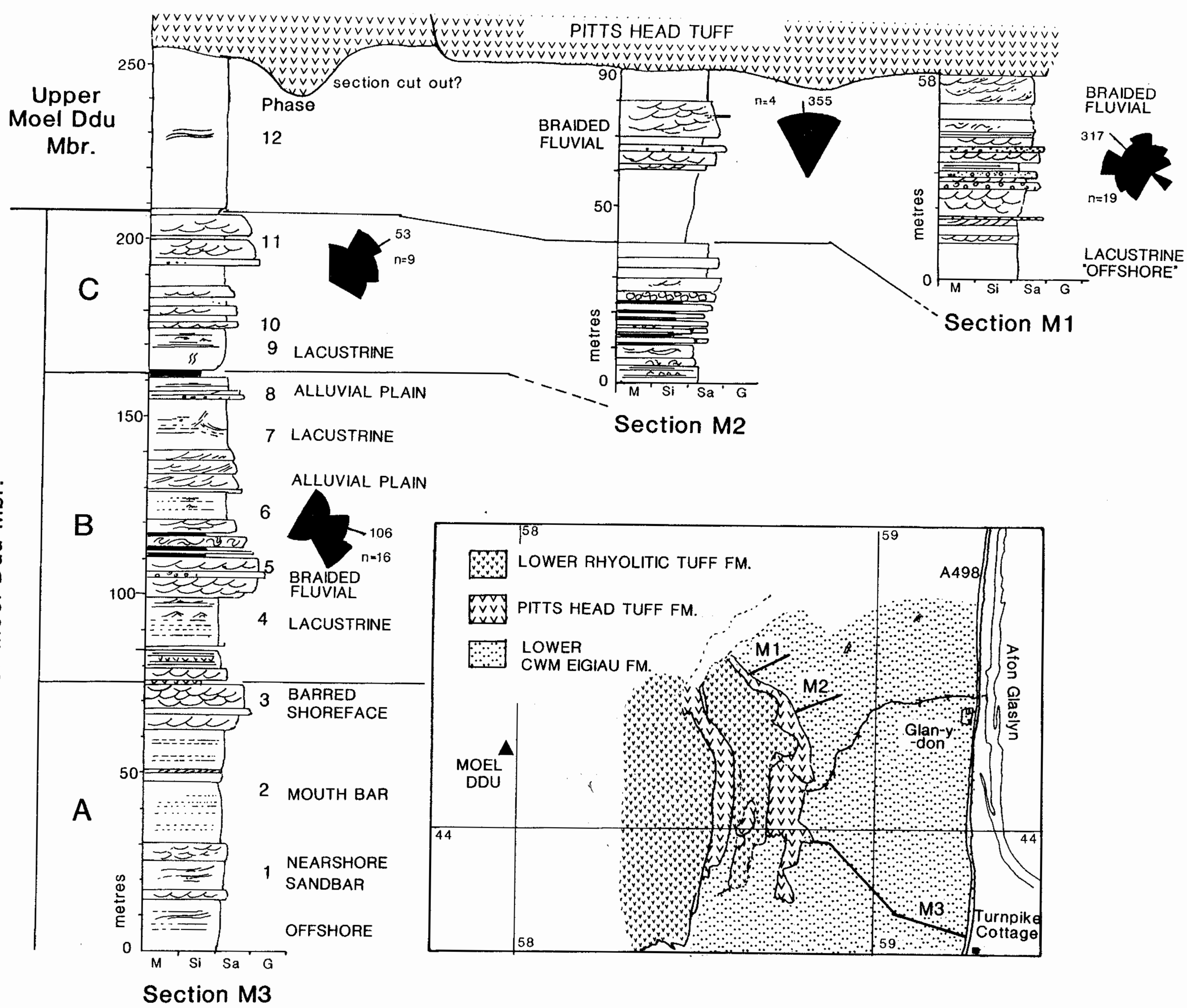

Fig. 4.63: Detail of braid-delta and alluvial plain successions from **SECTION M3** of the Lower Moel Ddu Mbr., Moel Ddu, with selected enlargements of braided and meandering stream, unconfined sheetfloods, and lacustrine shoreface sequences. (see Fig. 4.62 for stratigraphic position and location of section, and Fig. 4.1 for explanation of lithofacies codes).

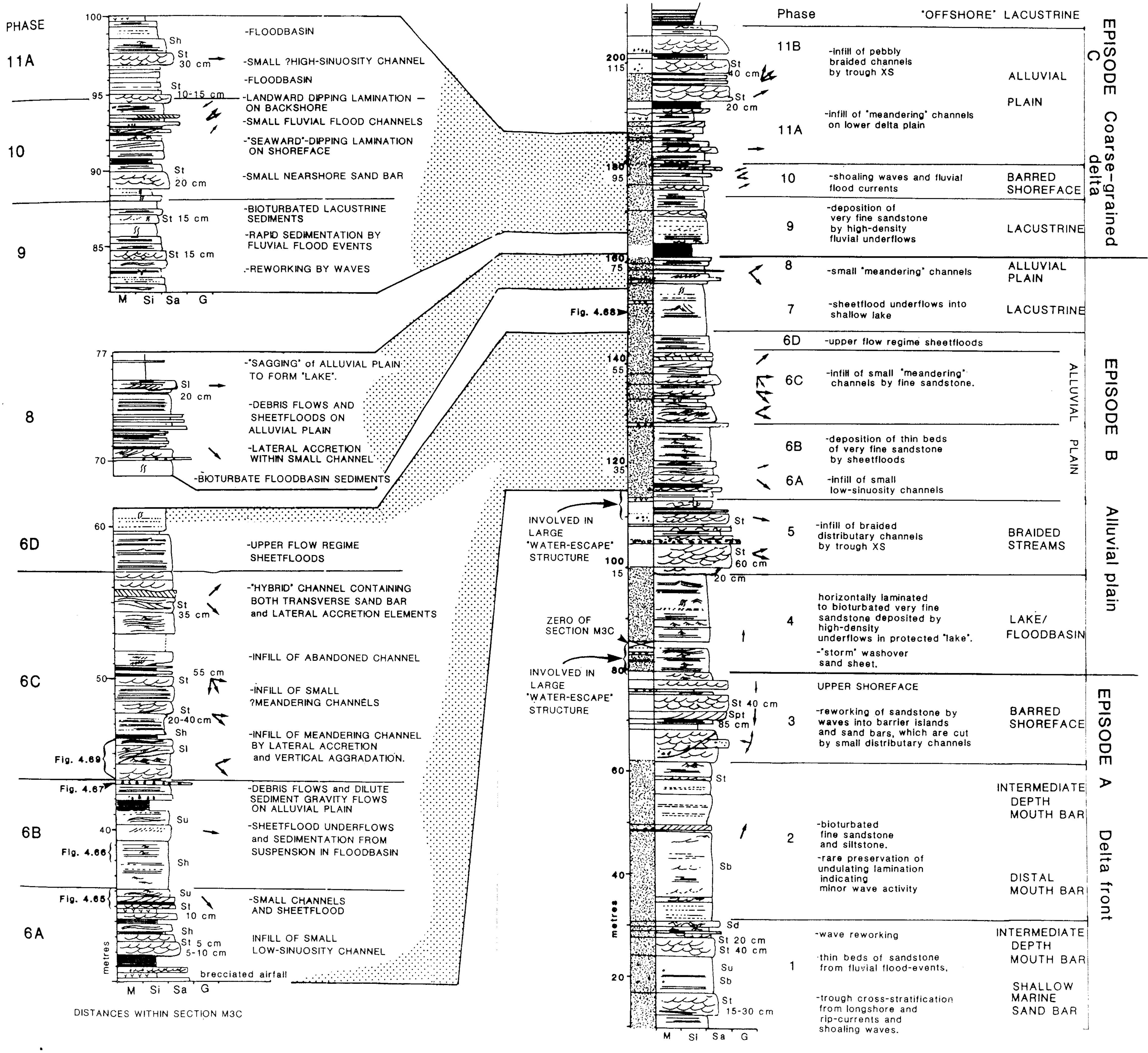

PHASE
11A
-FLOODBASIN
-SMALL ?HIGH-SINUOSITY CHANNEL
-FLOODBASIN
-LANDWARD DIPPING LAMINATION — ON BACKSHORE
-SMALL FLUVIAL FLOOD CHANNELS
-"SEAWARD"-DIPPING LAMINATION ON SHOREFACE
10
-SMALL NEARSHORE SAND BAR
9
-BIOTURBATED LACUSTRINE SEDIMENTS
-RAPID SEDIMENTATION BY FLUVIAL FLOOD EVENTS
-REWORKING BY WAVES
Sh
St 30 cm
St 10-15 cm
St 20 cm
St 15 cm
St 15 cm
M Si Sa G
8
-"SAGGING" of ALLUVIAL PLAIN TO FORM "LAKE".
-DEBRIS FLOWS AND SHEETFLOODS ON ALLUVIAL PLAIN
-LATERAL ACCRETION WITHIN SMALL CHANNEL
-BIOTURBATE FLOODBASIN SEDIMENTS
Sl 20 cm
6D
-UPPER FLOW REGIME SHEETFLOODS
6C
-"HYBRID" CHANNEL CONTAINING BOTH TRANSVERSE SAND BAR and LATERAL ACCRETION ELEMENTS
-INFILL OF ABANDONED CHANNEL
-INFILL OF SMALL ?MEANDERING CHANNELS
-INFILL OF MEANDERING CHANNEL BY LATERAL ACCRETION and VERTICAL AGGRADATION.
St 35 cm
55 cm
St
St 20-40 cm
Sh
Sl
Fig. 4.69
Fig. 4.67
6B
-DEBRIS FLOWS and DILUTE SEDIMENT GRAVITY FLOWS ON ALLUVIAL PLAIN
-SHEETFLOOD UNDERFLOWS and SEDIMENTATION FROM SUSPENSION IN FLOODBASIN
Su
Sh
Fig. 4.66
6A
-SMALL CHANNELS AND SHEETFLOOD
INFILL OF SMALL LOW-SINUOSITY CHANNEL
brecciated airfall
Fig. 4.65
Su
St 10 cm
Sh
St 5 cm
5-10 cm
metres
M Si Sa G
DISTANCES WITHIN SECTION M3C
100 95 90 85 77 70 60 50 40
Phase
'OFFSHORE' LACUSTRINE
11B
-infill of pebbly braided channels by trough XS
St 40 cm
St 20 cm
ALLUVIAL PLAIN
11A
-infill of 'meandering' channels on lower delta plain
10
-shoaling waves and fluvial flood currents
BARRED SHOREFACE
9
-deposition of very fine sandstone by high-density fluvial underflows
LACUSTRINE
EPISODE C Coarse-grained delta
8
-small 'meandering' channels
ALLUVIAL PLAIN
7
-sheetflood underflows into shallow lake
LACUSTRINE
Fig. 4.68
6D
-upper flow regime sheetfloods
6C
-infill of small 'meandering' channels by fine sandstone.
6B
-deposition of thin beds of very fine sandstone by sheetfloods
6A
-infill of small low-sinuosity channels
ALLUVIAL PLAIN
EPISODE B Alluvial plain
INVOLVED IN LARGE "WATER-ESCAPE" STRUCTURE
5
-infill of braided distributary channels by trough XS
BRAIDED STREAMS
St
St 60 cm
20 cm
4
horizontally laminated to bioturbated very fine sandstone deposited by high-density underflows in protected 'lake'.
-"storm" washover sand sheet.
LAKE/ FLOODBASIN
ZERO OF SECTION M3C
INVOLVED IN LARGE "WATER-ESCAPE" STRUCTURE
UPPER SHOREFACE
3
-reworking of sandstone by waves into barrier islands and sand bars, which are cut by small distributary channels
BARRED SHOREFACE
St 40 cm
Spt 85 cm
St
2
-bioturbated fine sandstone and siltstone.
-rare preservation of undulating lamination indicating minor wave activity
INTERMEDIATE DEPTH MOUTH BAR
DISTAL MOUTH BAR
Sb
Sd
1
-wave reworking
-thin beds of sandstone from fluvial flood-events.
-trough cross-stratification from longshore and rip-currents and shoaling waves.
INTERMEDIATE DEPTH MOUTH BAR
SHALLOW MARINE SAND BAR
St 20 cm
St 40 cm
Su
Sb
St 15-30 cm
EPISODE A Delta front
metres
200 115 180 95 160 75 140 55 120 35 100 15 80 60 40 20
M Si Sa G

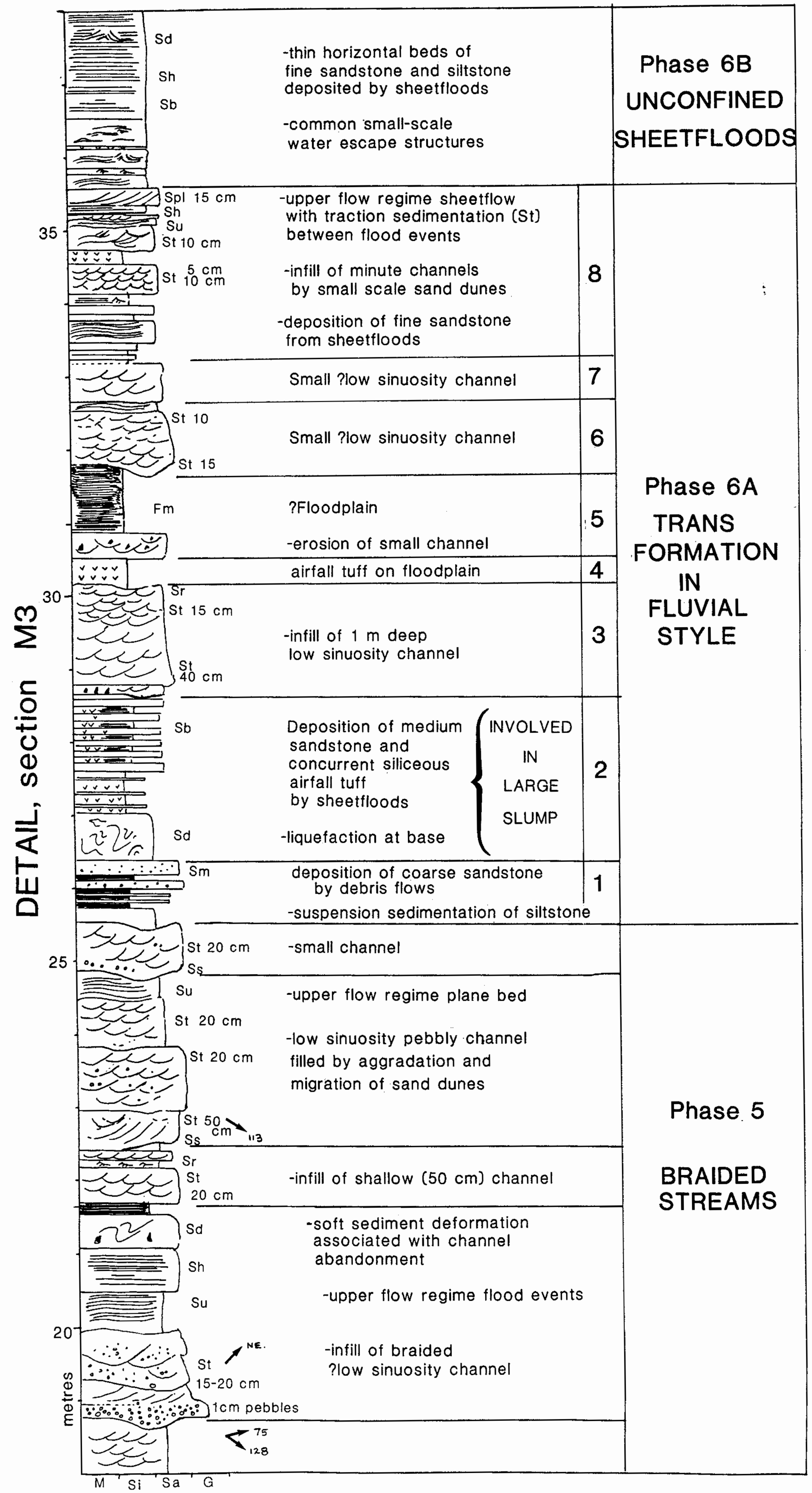

Fig. 4.64: Illustration of a transformation in fluvial style (from braided streams to unchannelised sheetfloods) associated with rhyolite volcanicity. (see Fig. 4.62, 4.63, section M3c, phases 5 & 6A).

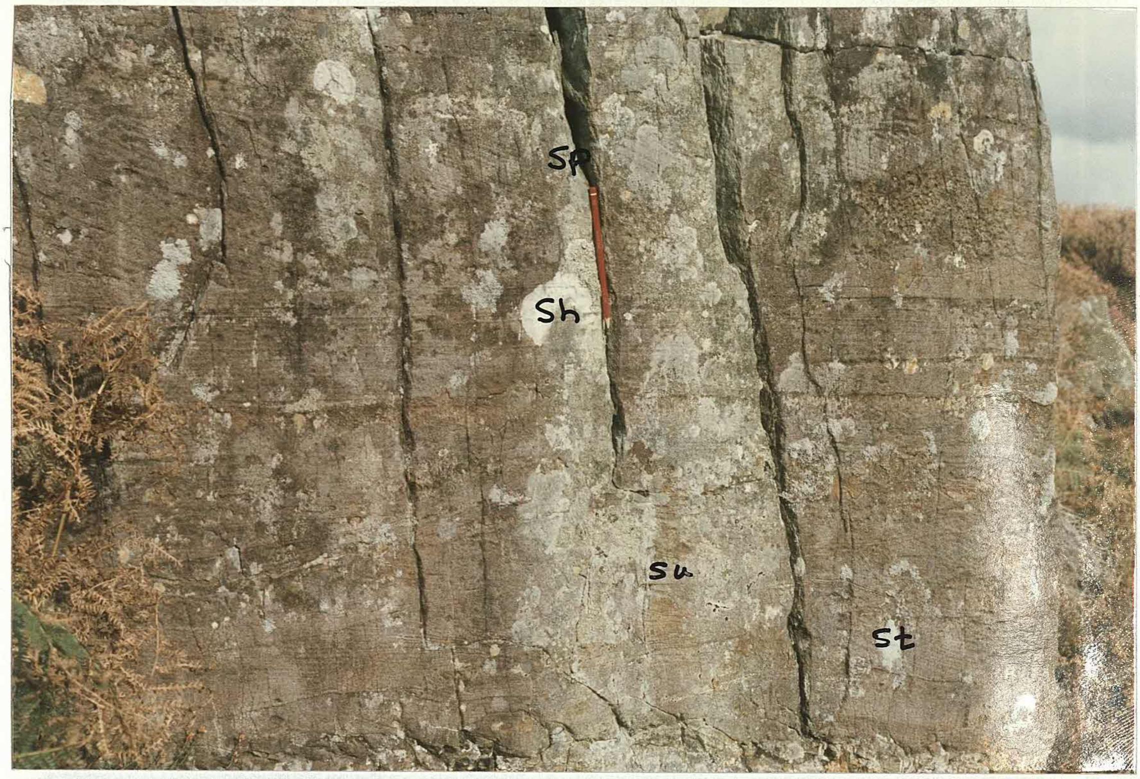

Fig. 4.65: Small-scale trough (St) or planar (Sp) cross-stratification from infill of small (50 cm deep) fluvial channels, and distinct horizontal lamination from upper flow regime plane-bed during a "transformation" in fluvial style associated with rhyolitic volcanicity. (see Fig. 4.64, section M3c, phase 6a, unit 8, 35 m).

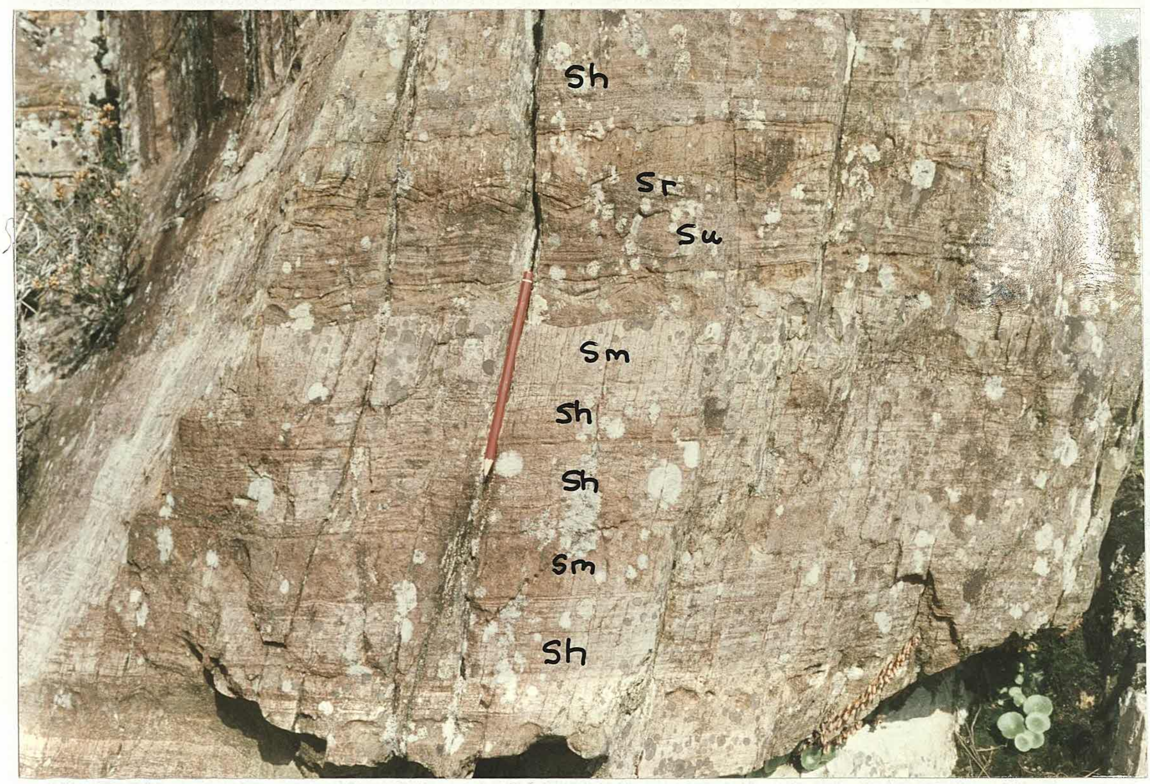

Fig. 4.66: Thinly bedded (*ca.* 5 cm) very fine-grained sandstones which are either structureless (Sm) or contain planar (Sh) or undulating (Su) horizontal lamination, or more rarely climbing-ripple cross-lamination. Beds are attributed to sheetfloods on the distal alluvial plain. (see Fig. 4.63, section M3c, phase 6b, 38.5 m)

Fig. 4.67: Thin (15 cm) normally-graded sandstone bed containing rip-up clasts of rhyolitic airfall tuff, attributed to dilute sediment gravity flow on the alluvial plain. (see Fig. 4.63, phase 6c, 43.0 m and Fig. 4.69)

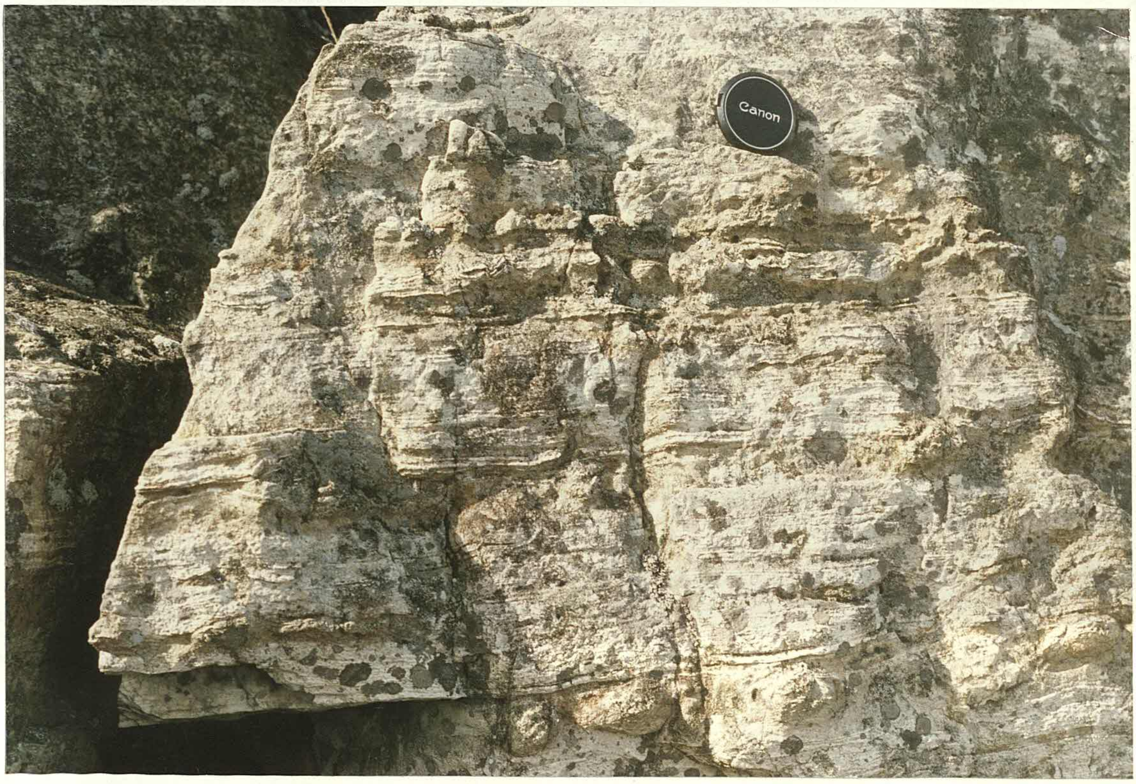

Fig. 4.68: Bioturbated very fine-grained sandstone and coarse siltstone within lacustrine successions on the Moel Ddu Mbr. alluvial plain at Moel Ddu (see Fig. 4.63, section M3c, phase 4, 5 m). Compare with alluvial sheetflood deposits in Fig. 4.66.

Fig. 4.69: Detail of distribution of lithofacies within a "meandering" channel-fill sequence. See Fig. 4.63, section M3c, phase 6c, 43 to 46 metres).

PHOTO A: Stacked sets of trough cross-stratification attributed to migration of sinuous-crested dunes and undulating horizontal lamination from upper flow-regime flood events.

PHOTO B: Epsilon cross-stratification (Sl) attributed to lateral migration of the fluvial channel.

PHOTO C: Climbing-ripple cross-lamination within lateral accretion bedding units. Palaeocurrents are transverse (to left) to the direction of lateral accretion (towards reader).

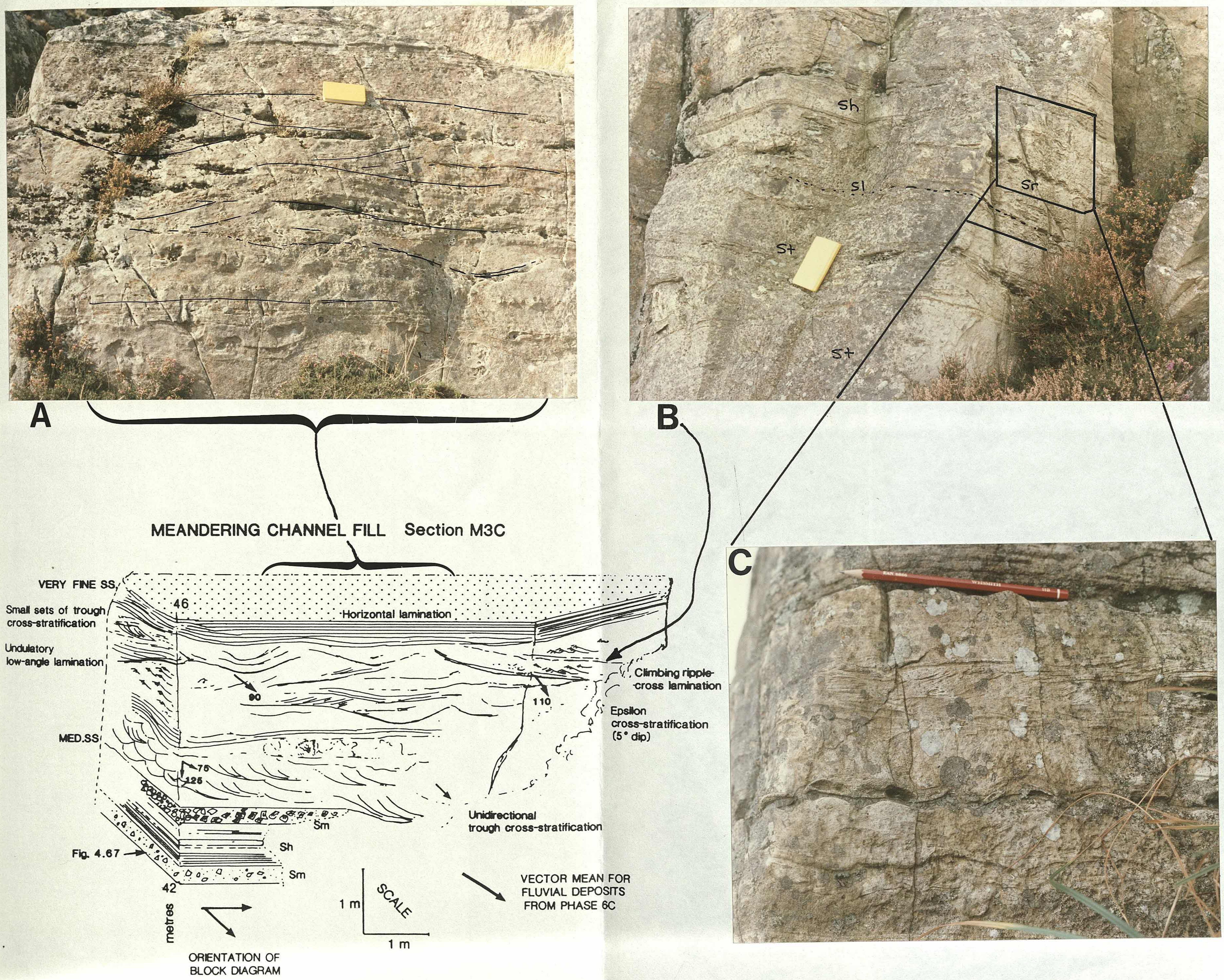
A
B
Sh
Sl
Sr
St
St
C
MEANDERING CHANNEL FILL Section M3C
VERY FINE SS
Small sets of trough cross-stratification
Undulatory low-angle lamination
MED.SS
46
Horizontal lamination
Climbing ripple-cross lamination
Epsilon cross-stratification (5° dip)
90
110
75
125
Unidirectional trough cross-stratification
Sm
Sh
Sm
Fig. 4.67
42
metres
ORIENTATION OF BLOCK DIAGRAM
1 m
SCALE
1 m
VECTOR MEAN FOR FLUVIAL DEPOSITS FROM PHASE 6C

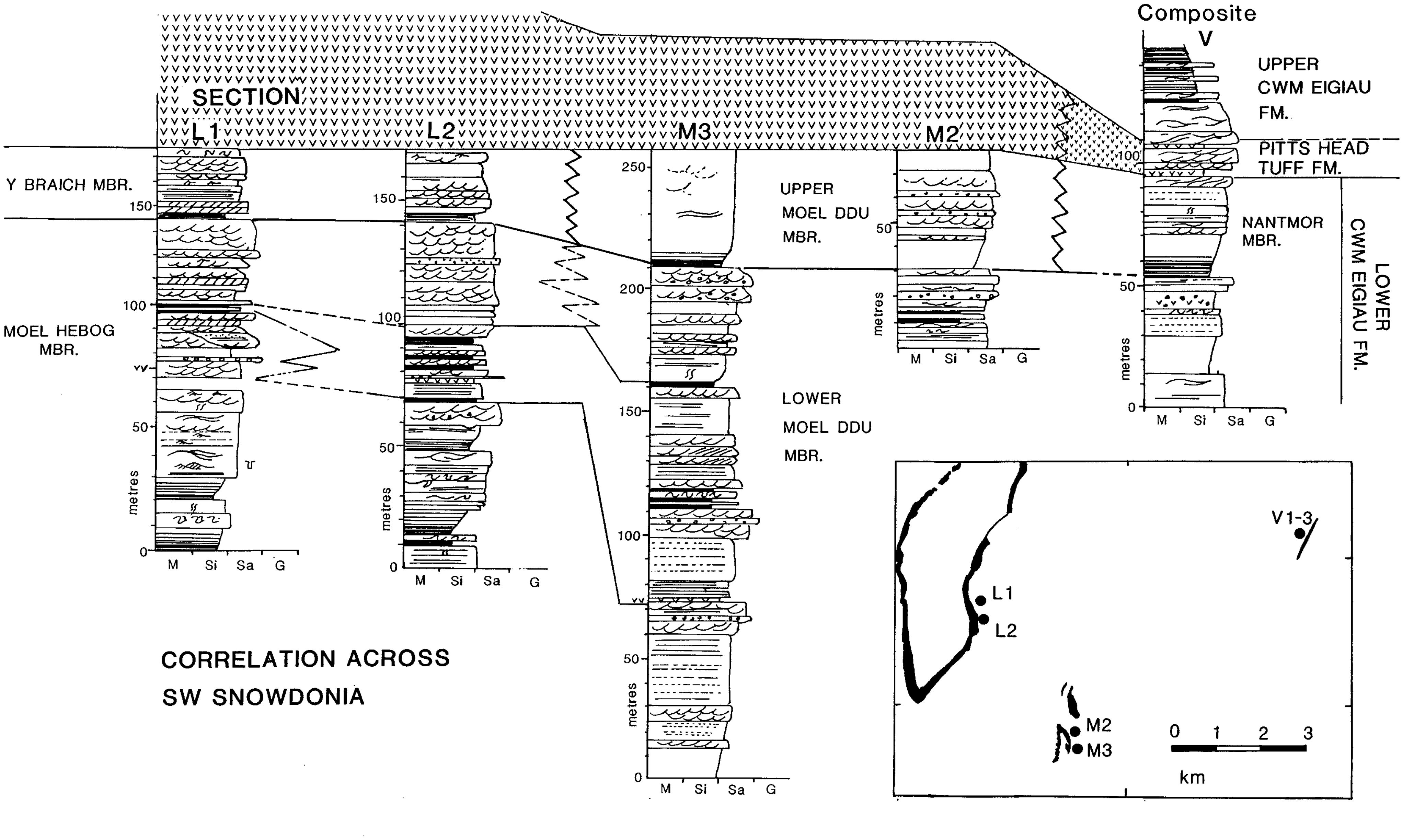

Fig. 4.70: Correlation of sequences between Moel Hebog, Moel Ddu and Yr Arddu.

Fig. 4.7]: Simplified reconstructions of palaeogeography in southern Snowdonia (*ie.* Moel Hebog, Moel DDu, Yr Arddu) during deposition of the Lower Cwm Eigiau Formation. It must be stressed that further research is need (*eg.* at Mynydd Gorllwyn) before: (1) the full importance of sources to the south (*ie.* towards Harlech ?dome) can be ascertained and, (2) the nature of "mixing" between the basalt/mudstone rich depositional system at Moel Hebog, and the quartzose volcaniclastics found at Moel Ddu can be determined.

A) Palaeogeography during intial advance of the Moel Hebog (phase 4) and Moel Ddu (phase 3) Mbrs. Additional palaeocurrents are needed from Section M3 to confirm the suggested orientation of coastline.

B) Palaeogeography during the middle portion of the Moel Hebog (Phase 5) and Moel DDu (phase 5/6) Mbrs.. A possible source of rhyolite volcanicity (lower left), and faults which are thought to have been active during this time period ("ticks" on downthrown side) are also shown. During volcanically active periods, there was probably less spatial variation in alluvial environments (and facies) than depicted, with deposition of fine-grained sheetfloods **everywhere.** Walther's Law, can thus not be directly applied depositional sequences with a **direct** volcanic influence.

C) Palaeogeography during maximum advance of Moel Hebog Mbr. (phase 7). The seaward extent of the Moel Ddu Mbr. (phase 11b) at this time, is slightly less than earlier periods (previous map) when rhyolitie volcanicity assisted its progradation.

D) Palaeogeography beneath the Pitts Head Tuff in southwest Snowdonia (Cwmystraddyn, Y Braich, Upper Moel Ddu, and Yr Arddu Mbrs.). The change in palaeogeography with uplift to the east of the Nantmor and Yr Arddu 'fractures', restricted the distribution of the Pitts Head Tuff, and led to vertical stacking and "ramping" of the outflow sheets at Moel Ddu (see Reedman *et al* , 1987; Chapt. 7.__).

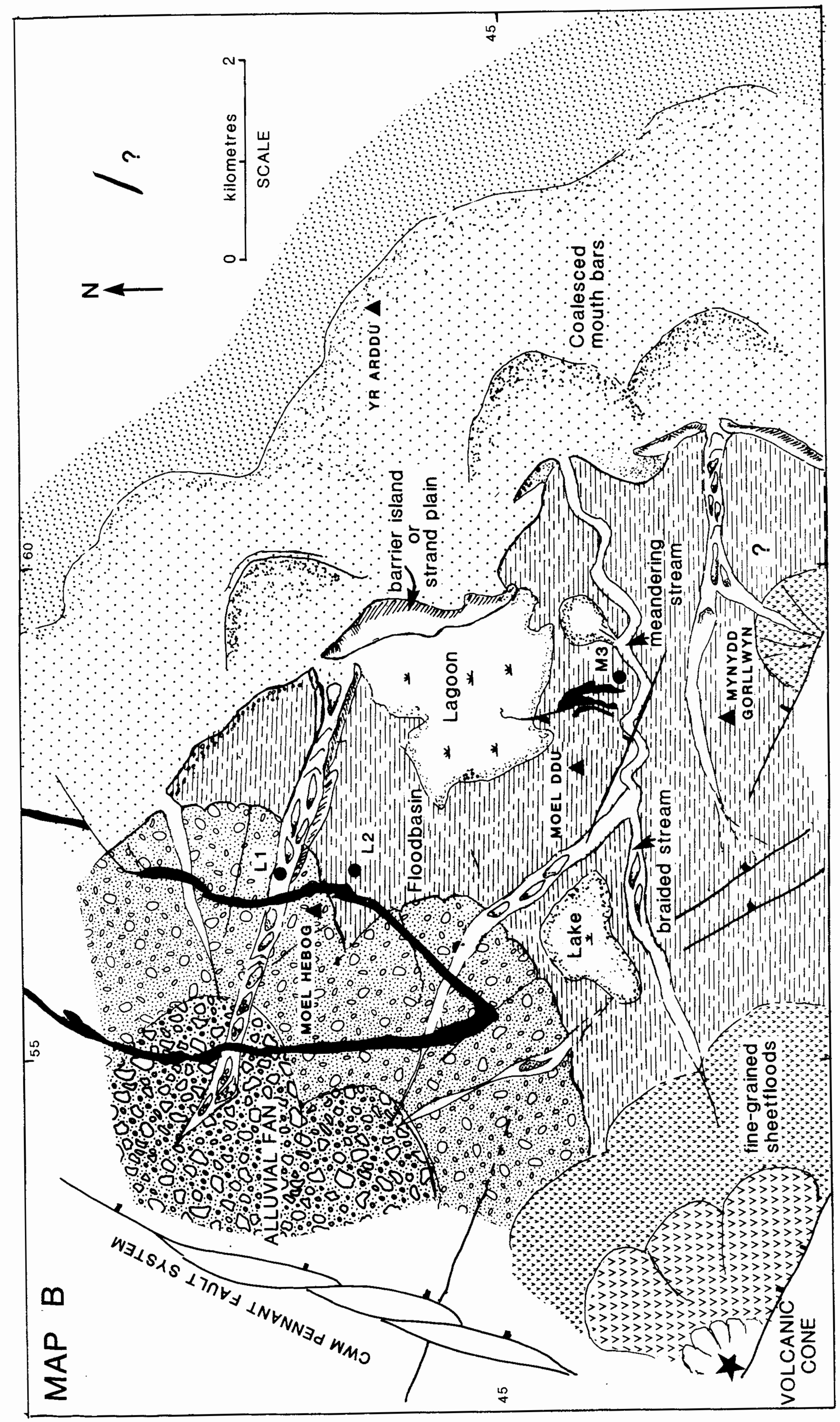

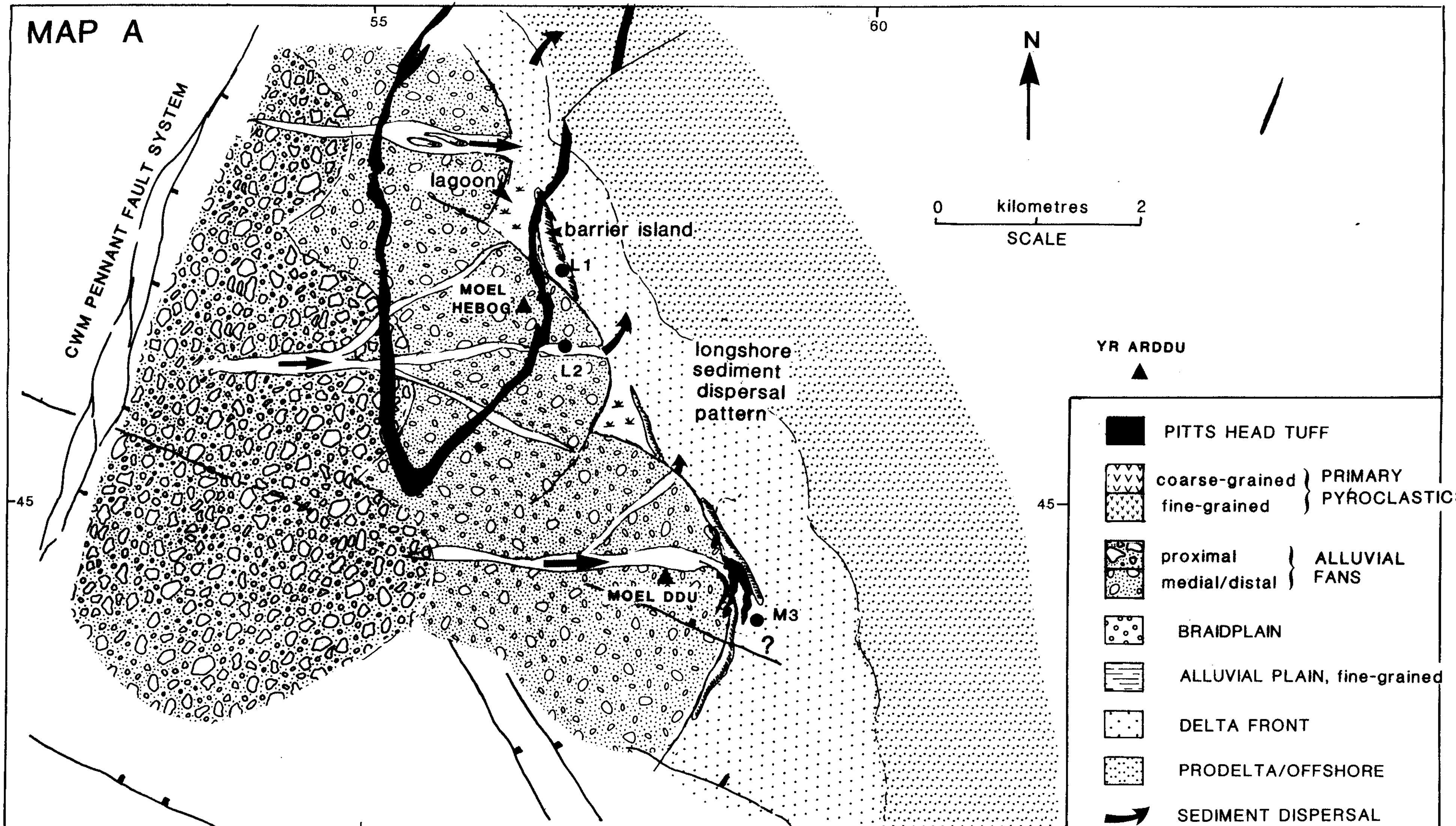

MAP A
55
60
45
45
N
0 kilometres 2
SCALE
CWM PENNANT FAULT SYSTEM
lagoon
barrier island
L1
MOEL HEBOG
L2
longshore sediment dispersal pattern
YR ARDDU
MOEL DDU
M3
?
PITTS HEAD TUFF
coarse-grained
fine-grained
PRIMARY PYROCLASTICS
proximal
medial/distal
ALLUVIAL FANS
BRAIDPLAIN
ALLUVIAL PLAIN, fine-grained
DELTA FRONT
PRODELTA/OFFSHORE
SEDIMENT DISPERSAL

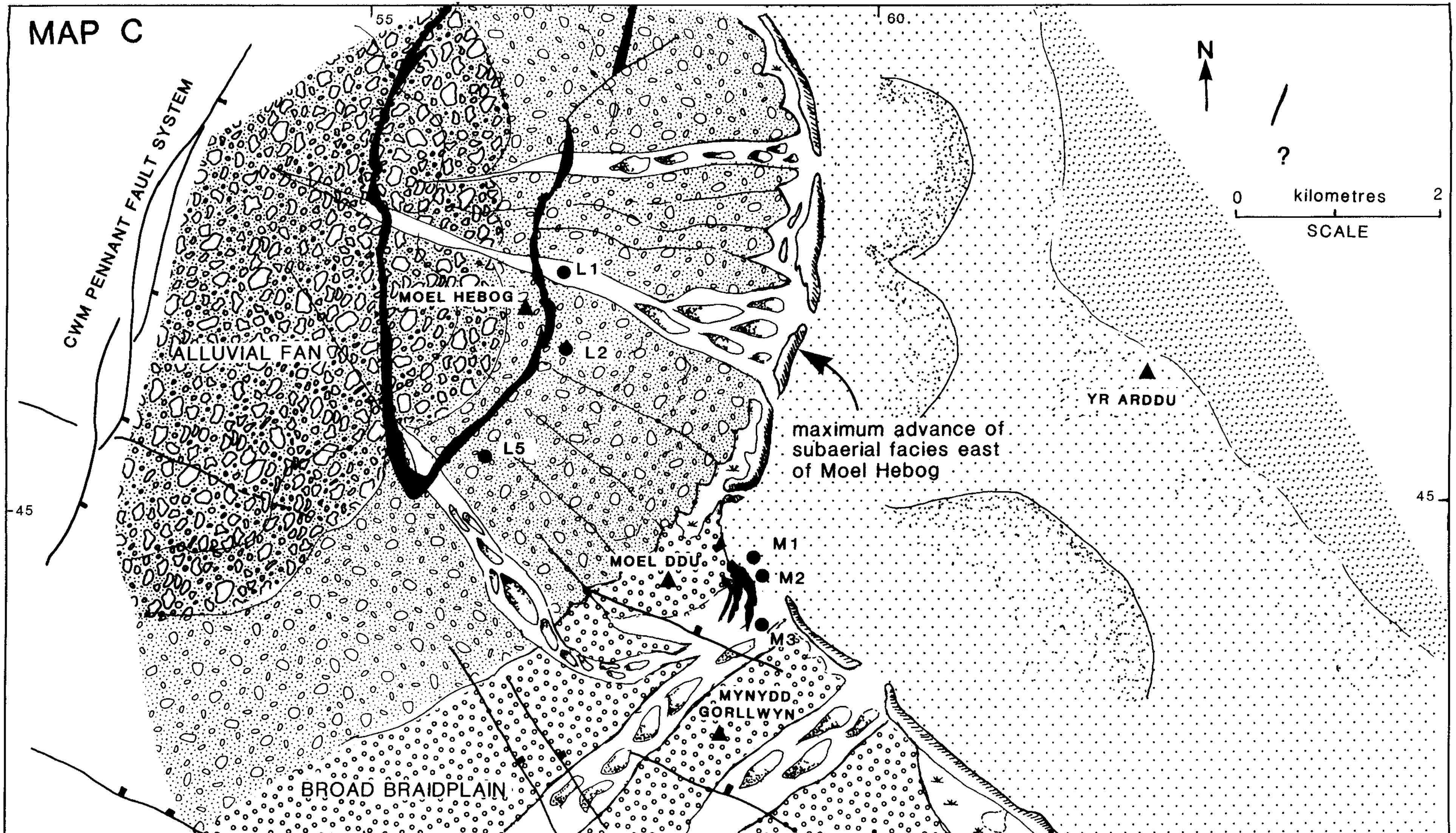
MAP C
55
60
N
?
0 kilometres 2
SCALE
CWM PENNANT FAULT SYSTEM
ALLUVIAL FAN
MOEL HEBOG
L1
L2
L5
maximum advance of
subaerial facies east
of Moel Hebog
YR ARDDU
45
45
M1
M2
M3
MOEL DDU
MYNYDD
GORLLWYN
BROAD BRAIDPLAIN

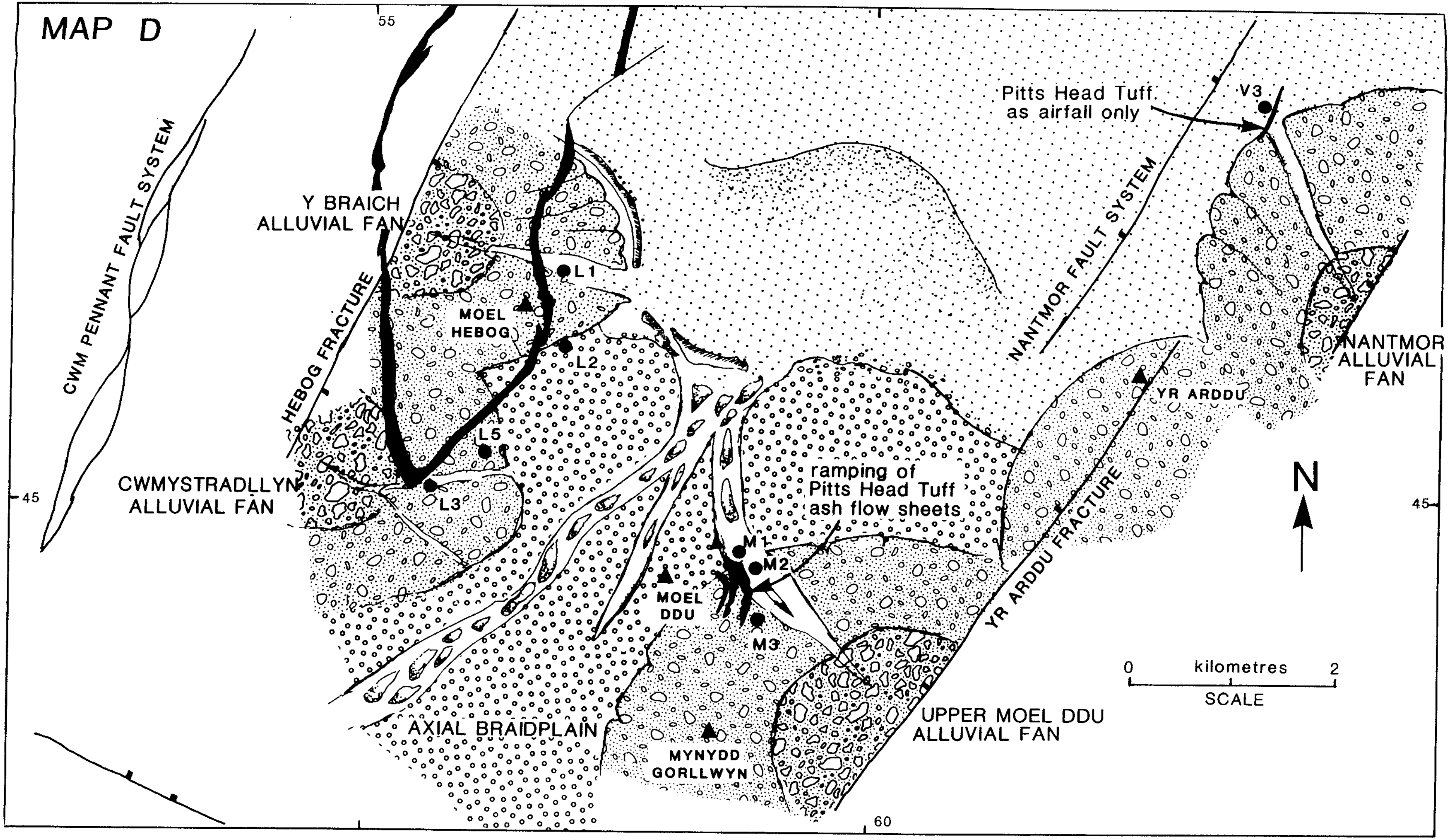
MAP D
55
CWM PENNANT FAULT SYSTEM
Y BRAICH
ALLUVIAL FAN
HEBOG FRACTURE
MOEL
HEBOG
L1
L2
L5
L3
CWMYSTRADLLYN
ALLUVIAL FAN
45
Pitts Head Tuff
as airfall only
V3
NANTMOR FAULT SYSTEM
NANTMOR
ALLUVIAL
FAN
YR ARDDU
ramping of
Pitts Head Tuff
ash flow sheets
N
45
M1
M2
M3
MOEL
DDU
YR ARDDU FRACTURE
0
kilometres
2
SCALE
UPPER MOEL DDU
ALLUVIAL FAN
AXIAL BRAIDPLAIN
MYNYDD
GORLLWYN
60

Fig. 4.72: Stratigraphic section in the Yr Arddu syncline, through a portion of the Upper and Lower Cwm Eigiau Formations. The air fall tuffs at V3 25-30 m (Tuff 102), can be correlated geochemically with the Pitts Head Tuff (Chapt. 2.2.4.3). Location of the top and bottom of section is indicated by National Grid References (see also Fig. 4.71d). See Fig. 4.70 for correlation of sequence with those at Moel Hebog, Moel Ddu, and Dolwyddelan.

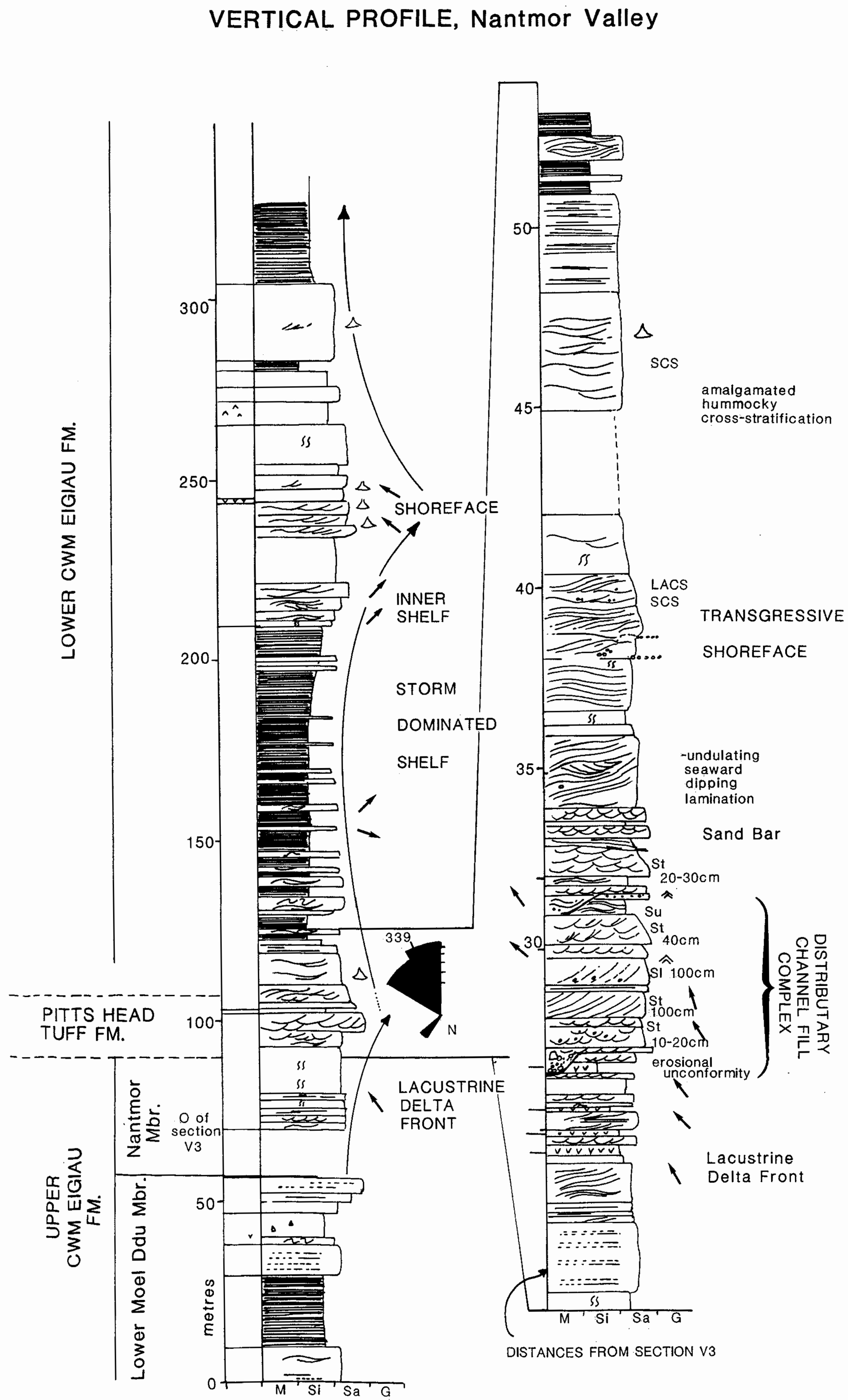

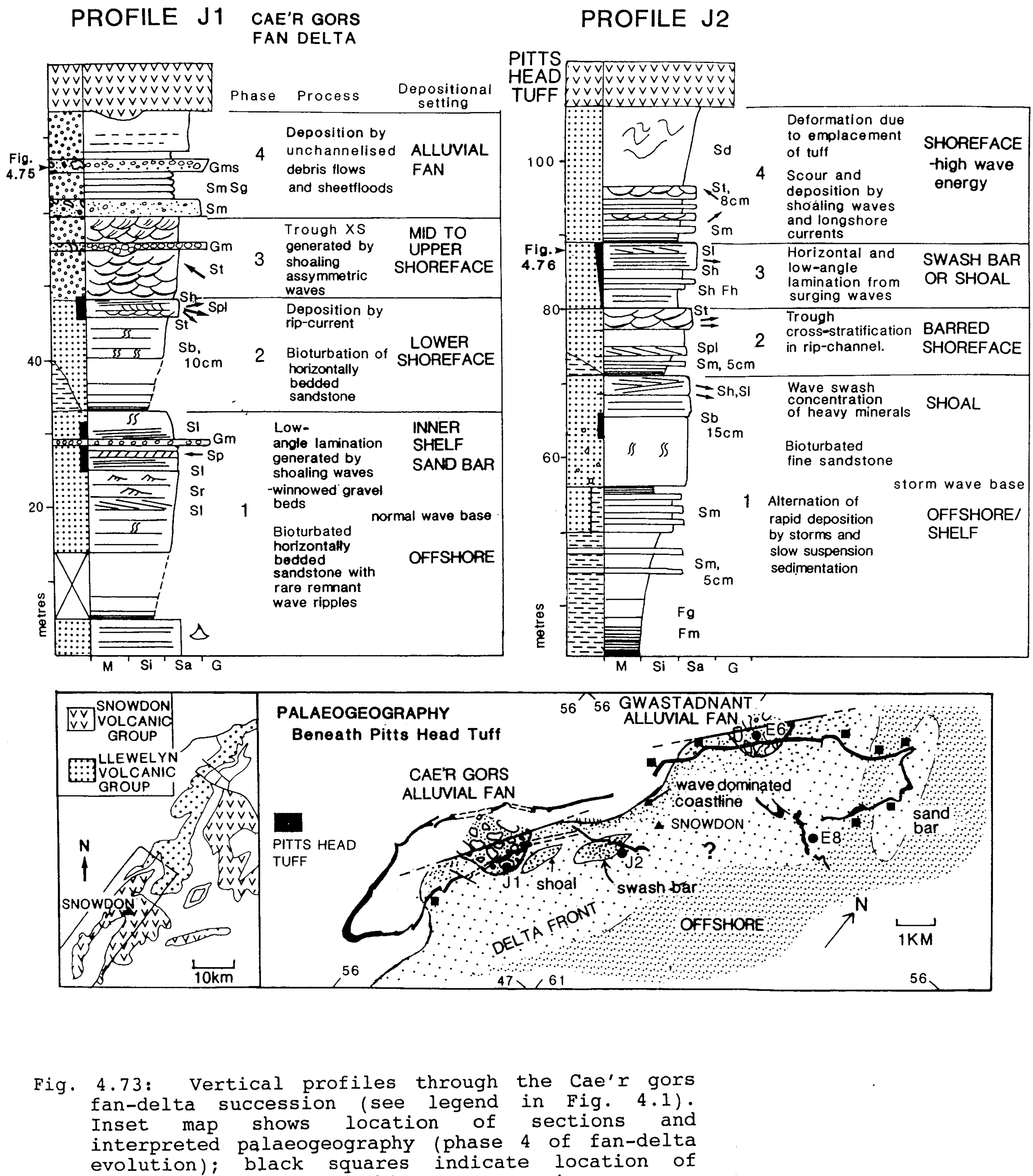

Fig. 4.73: Vertical profiles through the Cae'r gors fan-delta succession (see legend in Fig. 4.1). Inset map shows location of sections and interpreted palaeogeography (phase 4 of fan-delta evolution); black squares indicate location of other sections used in this reconstruction.

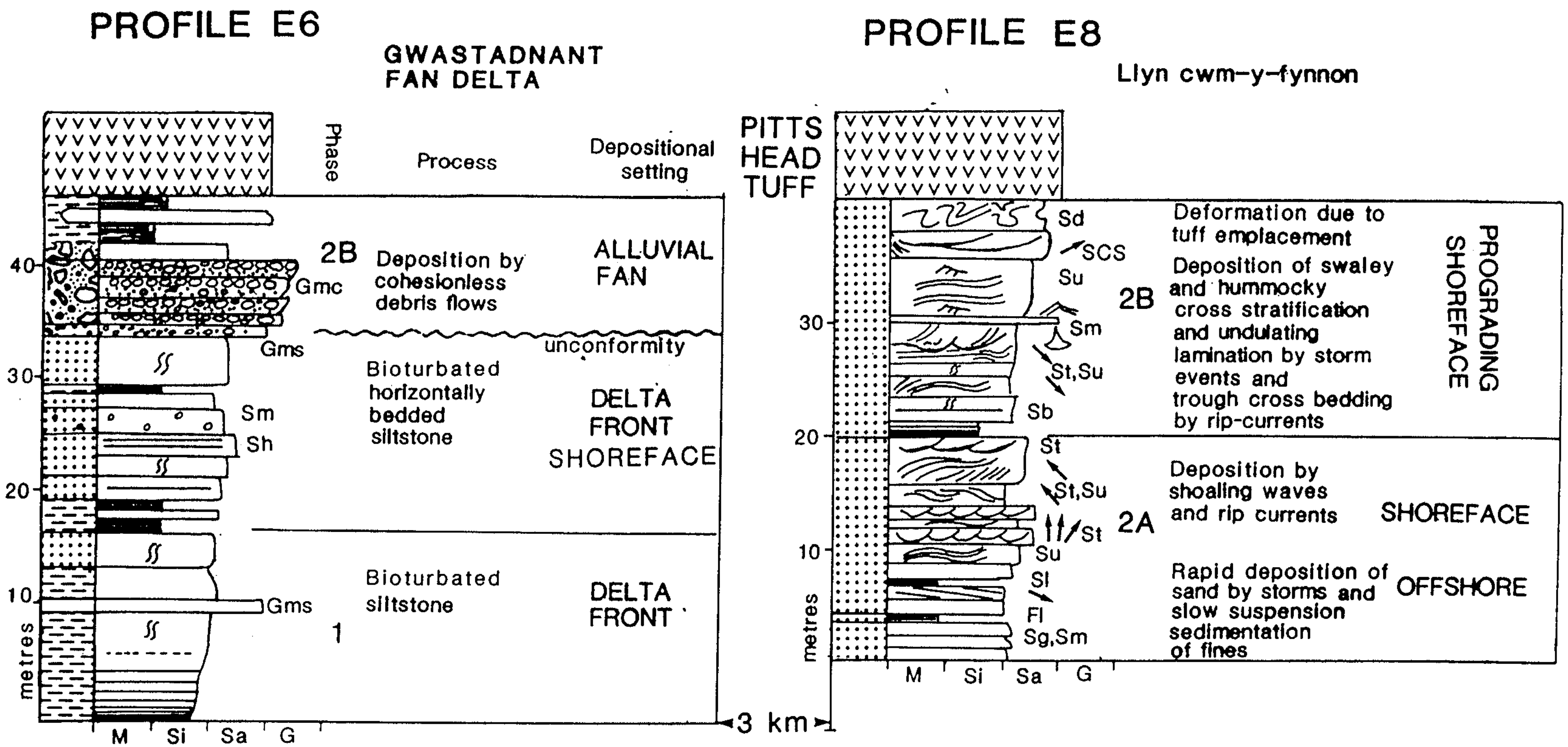

Fig. 4.74: Vertical profiles through the Gwastadnant fan-delta succession (see legend in Fig. 4.1, and locations in Fig. 4.73). Interpreted palaeogeography (phase 2B) is shown in the inset map in Fig. 4.73.

Fig. 4.75: Inversely graded matrix-supported bed of debris-flow conglomerate from the delta plain deposits of the Cae'r gors fan delta (phase 4 in section J2, Fig. 4.73); lens cap is 6 cm in diameter.

Fig. 4.76: Horizontal and low-angle lamination in magnetite-rich, fine-grained swash-bar sandstone deposited some 3 km (alongshore) off the axis of the Cae'r gors fan delta (from phase 3 in section J4, Fig. 4.73); lens cap is 6 cm in diameter.

Fig. 4.77: Details of alluvial plain facies from the Gwastadnant fan-delta.

A) Vertical section through alluvial deposits showing texture of conglomerate beds (*eg.* grading) as well as maxium particle size (MPS: average of 10 largest) and largest clast values. Diameter of actual clast used for sub-spherical shapes, whereas with elongate cobbles, the length and width values were recalculated to give an average diameter for a spherical shape.

B) Plot of maximum particle size (MPS) versus bed thickness (Bth). Solid line represents slope using an "undivided" Bed C, wheras dashed line shows results from linear regression if Bed C is split into two portions.

C) Disorganised clast-supported conglomerates (beds B, C, D) from alluvial plain deposits attributed to viscous sediment gravity flows (see text for further discussion). Field notebook is 18.5 cm in length.

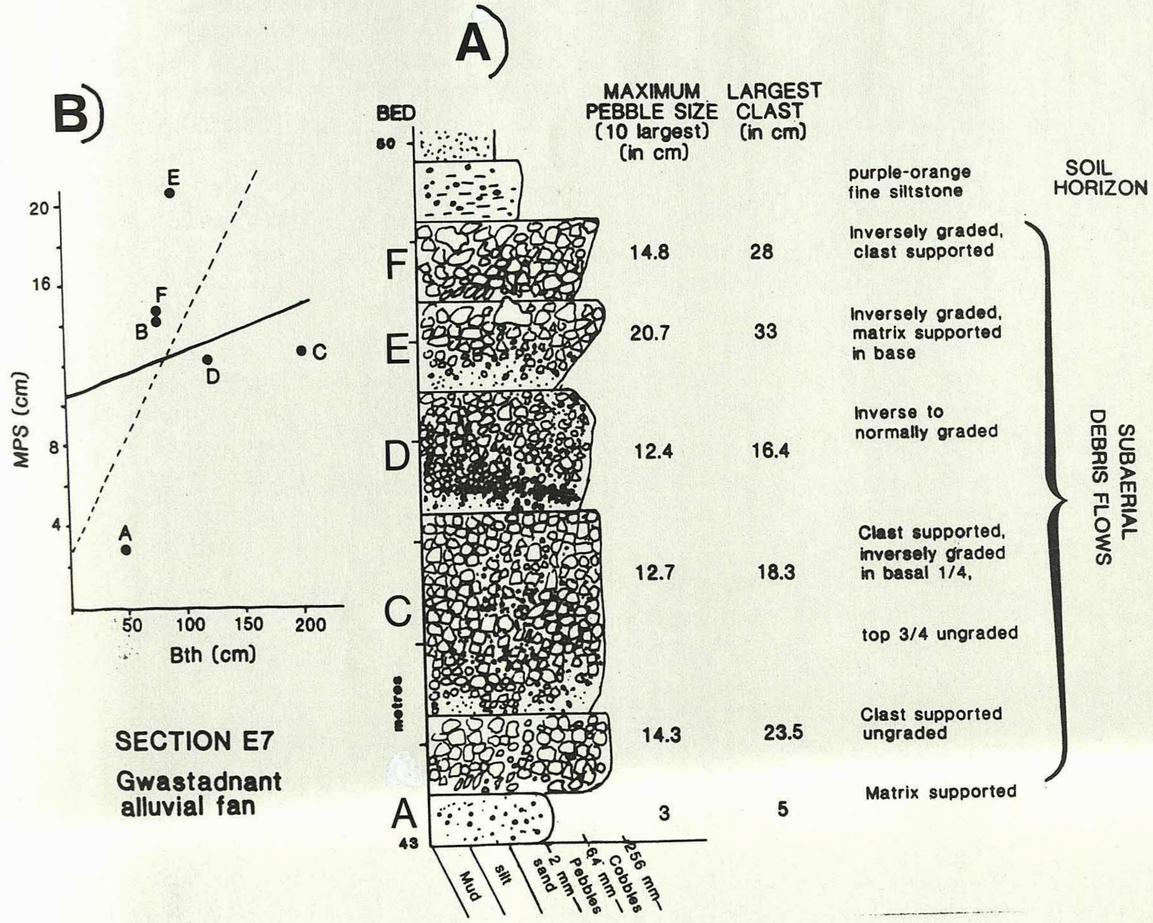

Fig. 4.78: Detail of vertical profiles through the Gwastadnant fan-delta at Llyn Cwm-y-ffynon, and postulated correlation with the succession at Gwastadnant itself. Inset map shows location of sections; a crude interpretation of palaeogeography (phase 2B) is shown in the inset map in Fig. 4.73. Palaeocurrent directions are oriented relative to the NW-SE transect rather than the conventional N-S diagram to facilitate comparison between logs. The listric faulting at section E9/E12, and rotation of section E12 by 20° about a horizontal NE-SW axis will be discussed later in reference to entry of the Pitts Head Tuff into the sea (Chapt. 7.3.2.1).

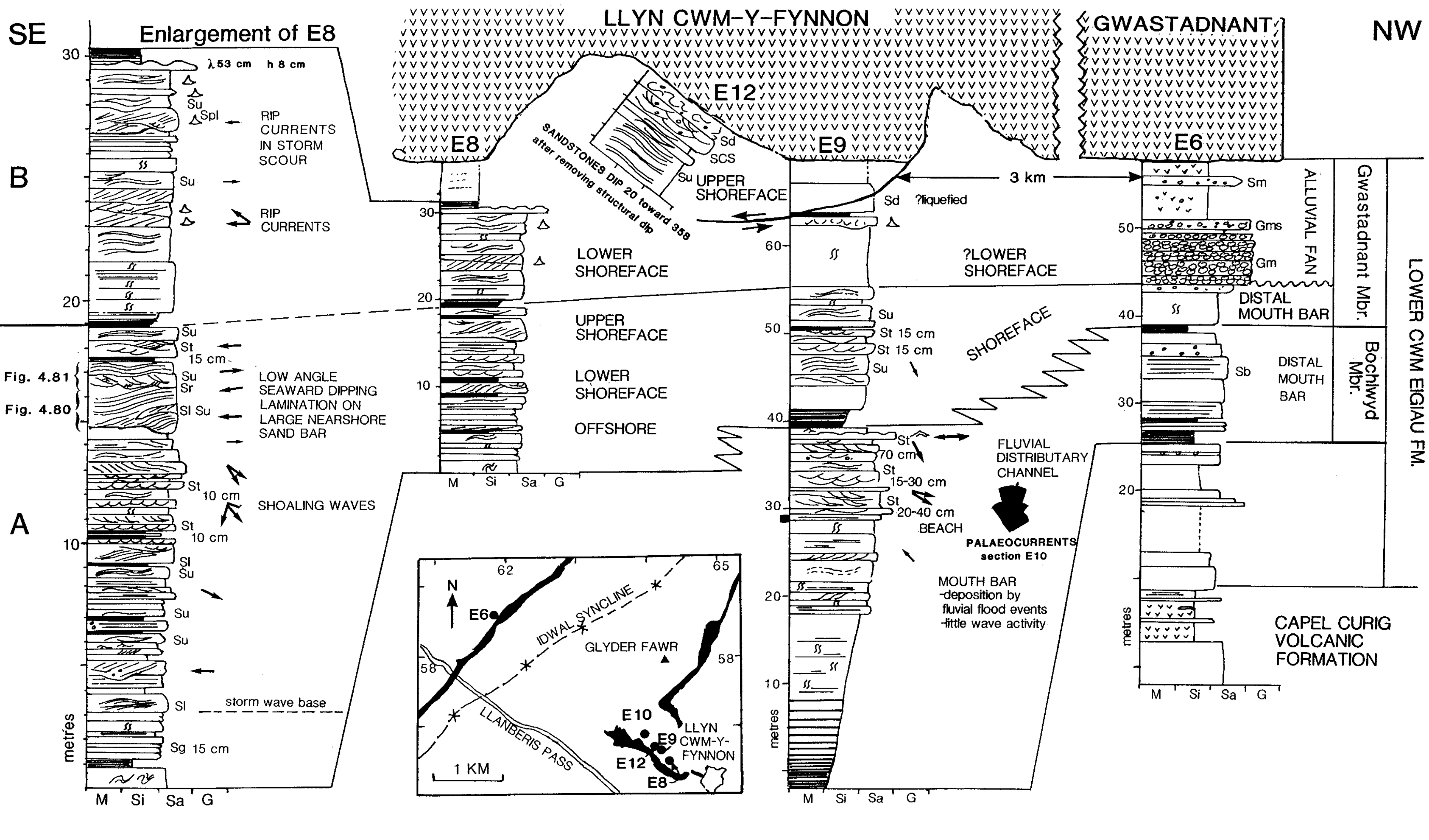

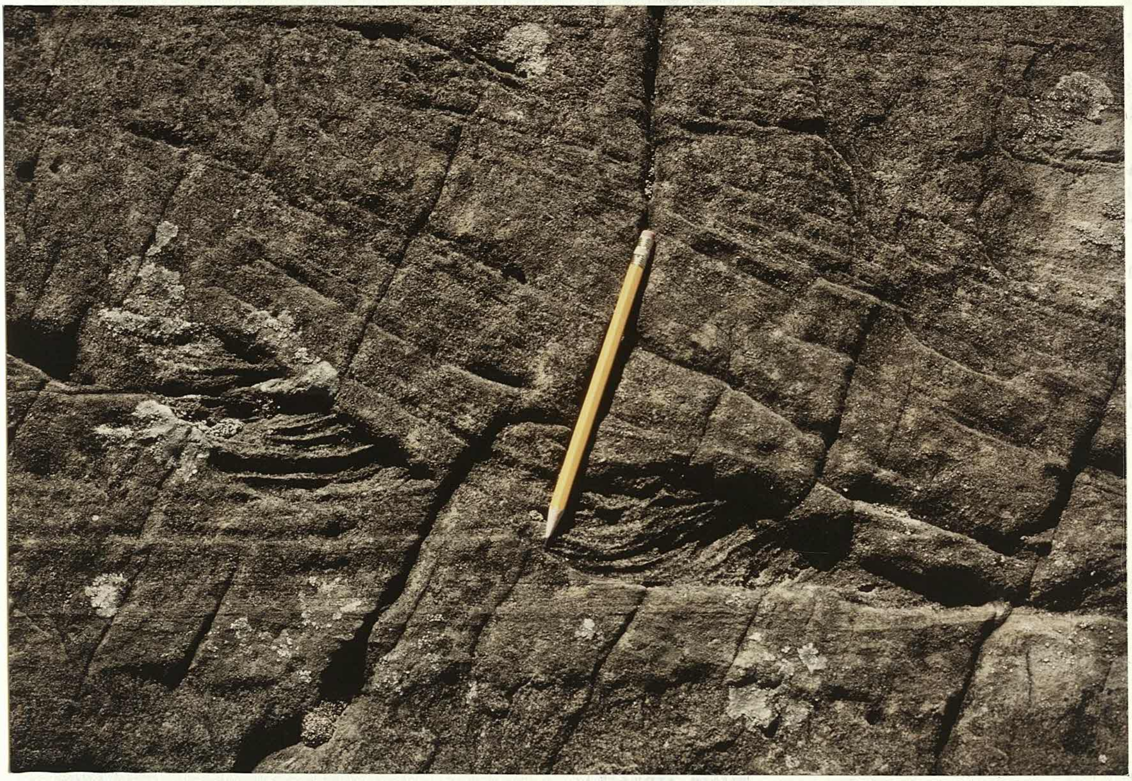

Fig. 4.79: Facies details from the Gwastadnant delta-front (shoreface) sequence in the Llyn Cwm-y-fynnon area (phase 2A in section E8, Fig. 4.78).

(A) Low-angle, seaward-dipping planar to undulatory lamination in medium-grained sandstone, attributing to shoaling storm waves. Note the intervening solitary set of medium-scale cross-strata (arrow). Vertical thickness of strata shown is approximately 2 metres.

(B) Detail of intervening set of low-moderate angle cross-strata within medium-grained sandstone attributed to landward-migration of a small sand-bar. The scooped-base to foresets, and smaller scale "back-set" cross-stratification probably reflects interaction with other nearshore currents (*eg.* edges waves, longshore currents, storm-return flows) rather than "unsteadiness" in the migration of the larger bedform.

	FLUVIAL REGIME Depositional system	NATURE of FLUVIAL SYSTEM	SEDIMENT CALIBRE	RATE OF SUPPLY	DELTAIC RESPONSE N 1 km sediment dispersal	BASINAL REGIME WAVE ENERGY	WATER DEPTH (deposits based on)
FAN DELTAS	GWERN GOF	FIXED DISTRIBUTARY CHANNEL	fine to medium sand	HIGH	FLUVIALLY DOMINATED 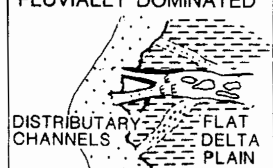 DISTRIBUTARY CHANNELS FLAT DELTA PLAIN	MODERATE TO HIGH	65m section C2 phase 1,2
FAN DELTAS	MOEL HEBOG	MOBILE BRAIDED STREAMS	pebbly coarse sand	MODERATE	FLUVIAL WAVE INTERACTION 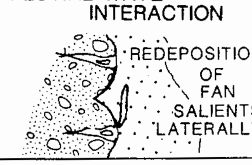 REDEPOSITION OF FAN SALIENTS LATERALLY	HIGH	70m section L2 phase 1-3
FAN DELTAS	CAER GORS	UNCHANNELED DEBRIS FLOWS AND SHEETFLOODS	fine sand to gravel	LOW	WAVE DOMINATED 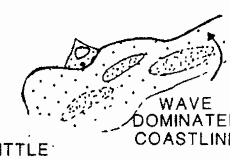 WAVE DOMINATED COASTLINE	HIGH	25m section J2 phase 2 & 3 65m corrected for volcanotectonic uplift
FAN DELTAS	GWAS TADNANT	UNCHANNELED DEBRIS FLOWS AND SHEET FLOODS (inferred)	medium coarse sand to gravel	LOW	LITTLE PRESERVATION OF ALLUVIAL FACIES 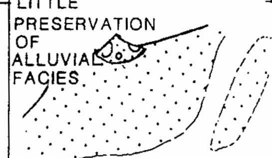	EXTREMELY HIGH	20m section E6 phase 2 60m corrected for volcanotectonic uplift
BRAIDPLAIN DELTAS	TRYFAN FACH	SMALL CHANNELS AND SHEETFLOODS MOBILE BRAIDED STREAMS	siliceous mud very coarse pebbly sand	EXTREMELY HIGH associated with period of volcanicity	FLUVIALLY DOMINATED PROGRADATION AS SHEET 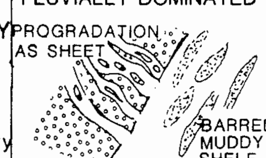 BARRED MUDDY SHELF	MODERATE	40m section C6 phase 1-4
BRAIDPLAIN DELTAS	MAGNETITE	SMALL MOBILE BRAIDED STREAMS	fine to very coarse sand	HIGH -associated with basaltic volcanicity	FLUVIALLY DOMINATED 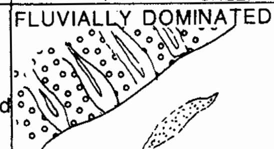	LOW	25 m section C6D phase 1, 2
BRAIDPLAIN DELTAS	CAPEL CURIG	MOBILE BRAIDED STREAMS	medium to very coarse pebbly sand	MODERATE	FLUVIAL WAVE INTERACTION BARRIER ISLANDS FOCUS FLUVIAL INPUT  MOUTH BAR	EXTREMELY HIGH	75m section C9 phase 1-4
BRAID DELTA	MOEL DDU	SINGLE BRAIDED STREAM	medium to coarse sand	HIGH	FLUVIALLY DOMINATED 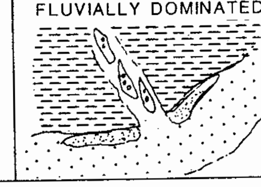	MODERATE	75m section M3 phase 1-3

Fig. 4.80: Salient features of the Caradocian fan, braidplain, and braid-deltas, North Wales.

ALLUVIAL
UNIT

Gwern Gof
Mbr.

Tryfan
Fach
Mbr.

Magnetite
Mbr.

Capel
Curig
Mbr.

Moel
Hebog
Mbr.

Moel
Ddu
Mbr.

Middle
portion

Cae'r
Gors
Mbr.

Gwastadnant
Mbr.

FIG. 4.81: Salient features of alluvial successions.

ALLUVIAL UNIT	NATURE OF FLUVIAL SYSTEM	SEDIMENT LOAD	CHANNEL GEOMETRY depth, width	INFILL FACIES	SET SIZE	RATE OF SEDIMENT SUPPLY	DEPOSIT SHAPE	ALLUVIAL MORPHOLOGY
Gwern Gof Mbr.	FIXED DISTRIBUTARY CHANNEL	fine to medium sand	800 cm, 150 m	St, Sp	40 to 70 cm	LOW	LENSOID	DELTA PLAIN, Tryfan anticline
	MOBILE BRAIDED STREAM	medium to coarse sand	50 to 300 cm, ??	St, Sp	20 cm	LOW	????	DELTA PLAIN
Tryfan Fach Mbr.	MOBILE BRAIDED STREAMS & SHEETFLOODS	siliceous mud to granule gravel	100 to 300 cm, 200 m	St	5 to 20 cm	HIGH	TABULAR, 10 m x 3 km x 3 km	BRAIDPLAIN Tryfan anticline
	MOBILE BRAIDED STREAMS & SEDIMENT GRAVITY FLOWS	very coarse pebbly sand	50 to 200 cm ???	St, Sp Gm, Gms	mean 15 cm, maximum 80 cm	MODERATE	?PRISMATIC	ALLUVIAL FAN, Craig yr Ysfa
Magnetite Mbr.	MOBILE BRAIDED STREAMS & UNCHANNELED SHEETFLOODS	fine to very coarse sand	50 to 200 cm, 200 m	St, Sh, Gms	mean 21 cm, maximum 40 cm	VARIABLE	TABULAR, 10 m x 3 km x 2 km.	BRAIDPLAIN Tryfan anticline
Capel Curig Mbr.	MOBILE BRAIDED STREAMS	medium to coarse sand	400 to 700 cm, » 200 m.	St	mean 40 cm	VARIABLE, MODERATE to HIGH	WEDGE-SHAPED, 40 to 80 m x 3 km x 5 km	BRAIDPLAIN Tryfan and Capel Curig anticlines
	MOBILE BRAIDED STREAMS	medium to coarse sand	200 to 400 cm, ???	St	mean 20 to 30 cm, max. 80 cm	MODERATE	? PRISMATIC	ALLUVIAL FAN, Craig yr Ysfa.
Moel Hebog Mbr.	BRAIDED STREAM	fine to coarse sand	100 t0 300 cm ???	St	mean 20 cm maximum 80 cm	MODERATE	prismatic	ALLUVIAL FAN
	UNCHANNELED SEDIMENT GRAVITY FLOWS	fine to coarse sand	20 cm	St, Sh Sb	mean 10 cm	LOW-MODERATE	??	DISTAL ALLUVIAL FAN.
Moel Ddu Mbr.	A) BRAIDED STREAMS	medium to very coarse sand	100 to 200 cm ???	St	mean 20 cm maximum 60 cm	MODERATE	----	ALLUVIAL PLAIN
Middle portion	B) MOBILE MEANDERING STREAM	fine sand	300 cm deep, ???	St, Sr	mean 20 cm, range 5 to 30 cm	LOW	----	ALLUVIAL PLAIN
	C) UNCHANNELED SHEETFLOODS	very fine sand	---------	Sm,Sh	----	EXTREMELY HIGH	----	ALLUVIAL PLAIN
Cae'r Gors Mbr.	UNCHANNELED SEDIMENT GRAVITY FLOWS	gravelly sand (max. peb size 10 cm)	----	Gms, Sm	----	LOW	prismatic, 800 m radius	ALLUVIAL FAN
Gwastadnant Mbr.	UNCHANNELED SEDIMENT GRAVITY FLOWS	boulder gravel (30 cm cobbles)	----	Gm, Gms,	----	LOW	prismatic, 300 m radius	ALLUVIAL FAN

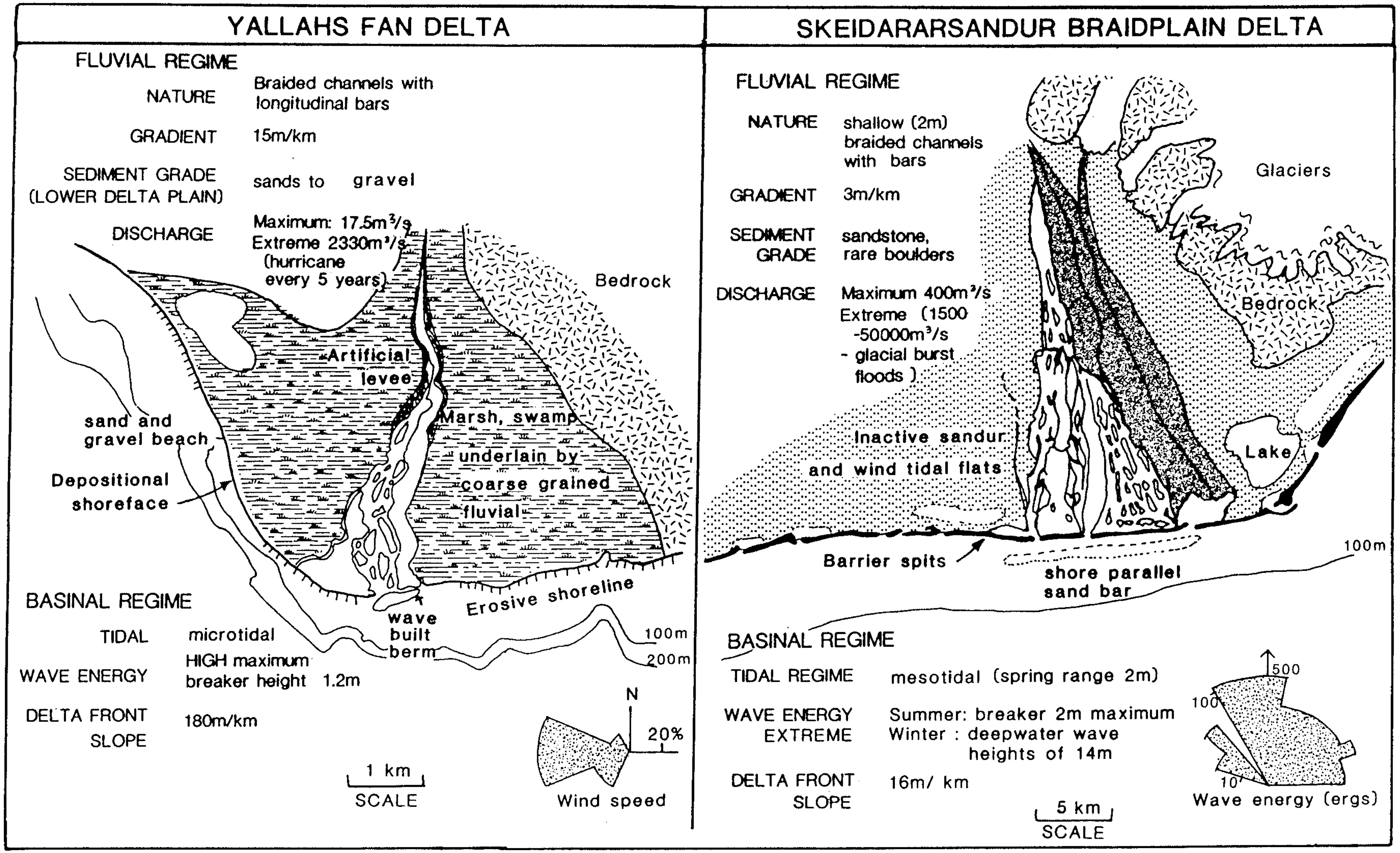

Fig. 4.82: Comparison of the Yallahs fan delta, Jamaica, and the Skeidararsandur (braidplain) delta, Iceland. Data from Wescott and Ethridge (1980), Hine and Boothroyd (1978), and Ward *et al* (1979).

Fig. 4.83: Suggested classification of deltas, based on the dominant processes (fluvial, wave, or tidal) of sediment dispersal at the delta front and on the prevailing grain size of sediment delivered to the delta front. Grain size is used to reflect relative sizes of drainage basins, although this criterion may not apply to alluvial systems affected by active volcanicity or dominated by mass flows. Tidal influence will be minor in coarse-grained deltas because of the relatively steep sope of their alluvial plains. Ancient delta examples are from this study; modern examples are from the literature (Hine & Boothroyd, 1978; Sneh, 1979; Wescott & Ethridge, 1980; Schramm, 1981; Hayes & Michel, 1982; Hayward, 1985; Wright, 1985)

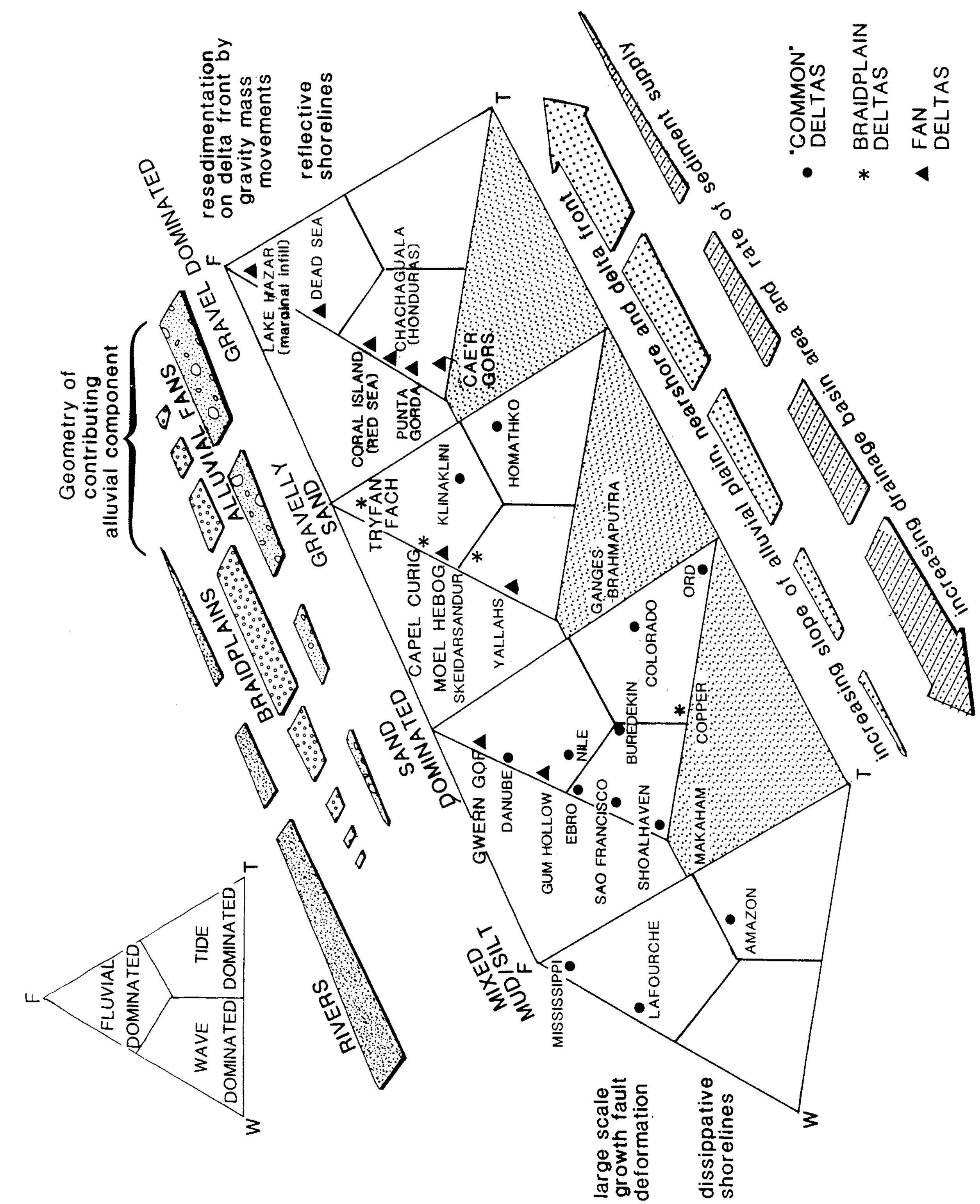

Chapter 5

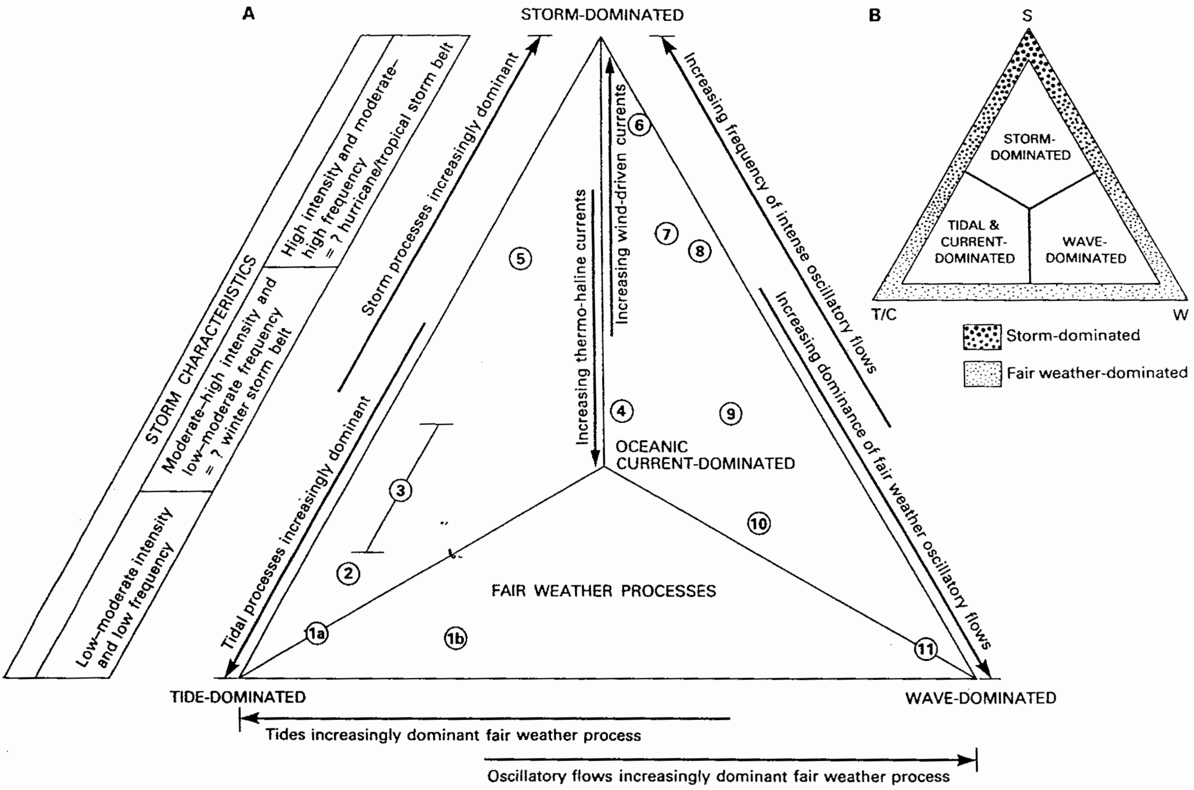

Fig. 9.4. (A) Idealized summary of the main types of offshore/shelf environment based on the nature of the hydraulic regimes and illustrating the relative importance and interaction of fair weather (i.e. tides, oceanic currents and waves) and storm processes. (B) A simplified picture which provides a basis for classifying the main types of modern shelves and for characterizing ancient shallow marine facies (see Sect. 9.9.2). 1a, Macrotidal embayments and estuaries (e.g. Bay of Fundy, Cook Inlet, Kuskokwim Bay, Chesapeake Bay); 1b, mesotidal embayments and estuaries (e.g. German Bight); 2, tidal straits (e.g. St. George's Channel, English Channel, Malacca Straits, Taiwan Strait); 3, tidal seas (e.g. North Sea, Celtic Sea, Yellow Sea, George's Bank); 4, oceanic current-swept shelves (e.g. SE Africa, Blake Plateau, Morocco shelf); 5, storm-dominated (wind-driven) (e.g. NW Atlantic shelf, U.S.A.); 6, storm-dominated (wind- and wave-driven) (e.g. Oregon-Washington shelf, California shelf); 7, storm-dominated (wave-driven) (e.g. SE Bering shelf); 8, storm-dominated (low to moderate energy) (e.g. Gulf of Mexico, Norton Sound); 9, mud-dominated (e.g. Amazon-Orinoco shelf, Niger shelf); 10, non-tidal, low-energy embayments (e.g. Baltic Sea, Hudson Bay); 11, wave-dominated (fair weather) environments (e.g. upper shoreface, wave-built bars etc).

Fig. 5.1 : Processes operating in a shallow marine environment. (from Johnson and Baldwin, 1986).

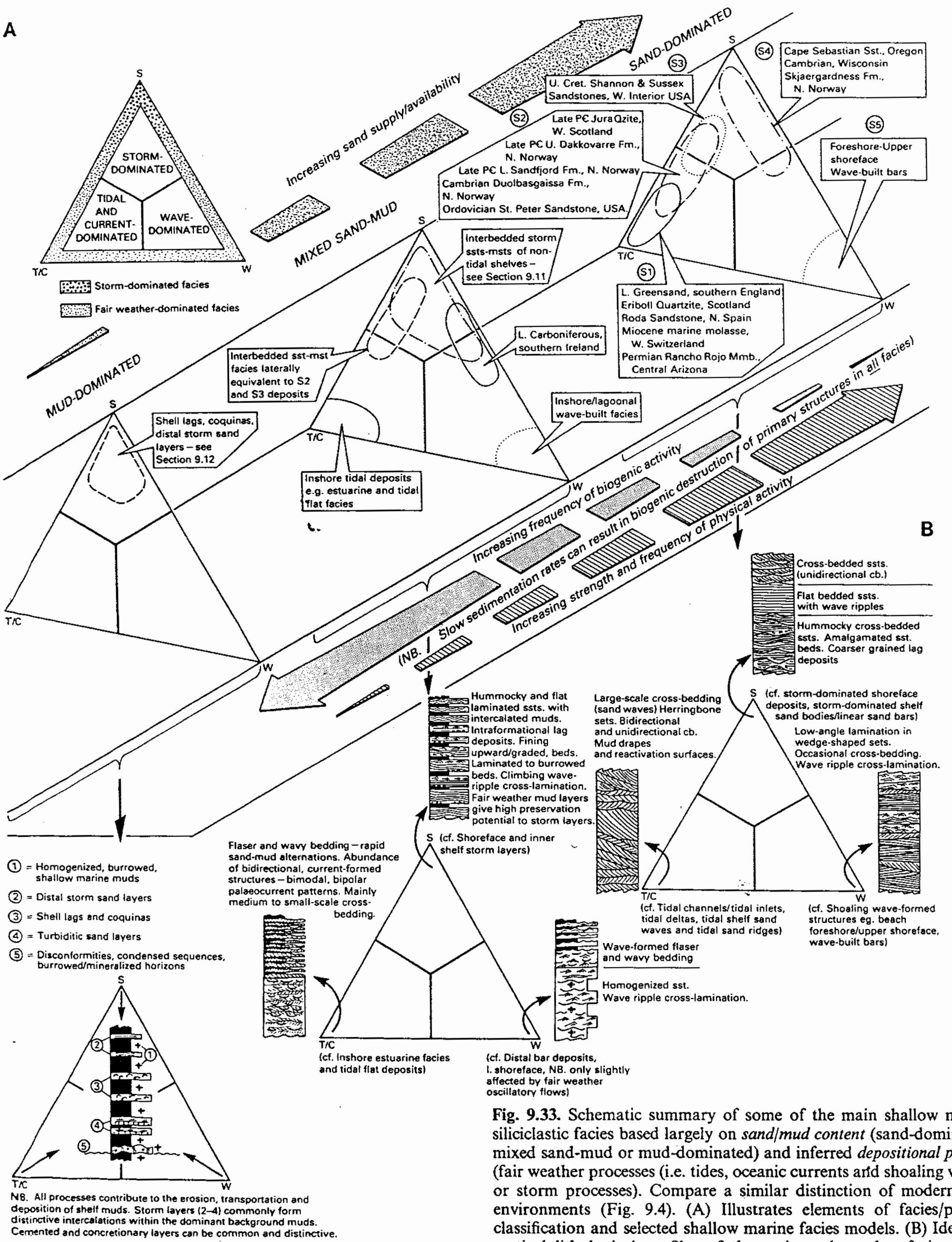

Fig. 9.33. Schematic summary of some of the main shallow marine siliciclastic facies based largely on *sand/mud content* (sand-dominated, mixed sand-mud or mud-dominated) and inferred *depositional process* (fair weather processes (i.e. tides, oceanic currents and shoaling waves) or storm processes). Compare a similar distinction of modern shelf environments (Fig. 9.4). (A) Illustrates elements of facies/process classification and selected shallow marine facies models. (B) Idealized vertical lithological profiles of the main end-member facies types. Inter-relationships (e.g. tide-storm interactive systems) are discussed in the text (Sect. 9.13).

Fig. 5.2: Summary of shallow marine siliclastic facies based on sand/mud content and inferred depositional process. (from Johnson and Baldwin, 1986).

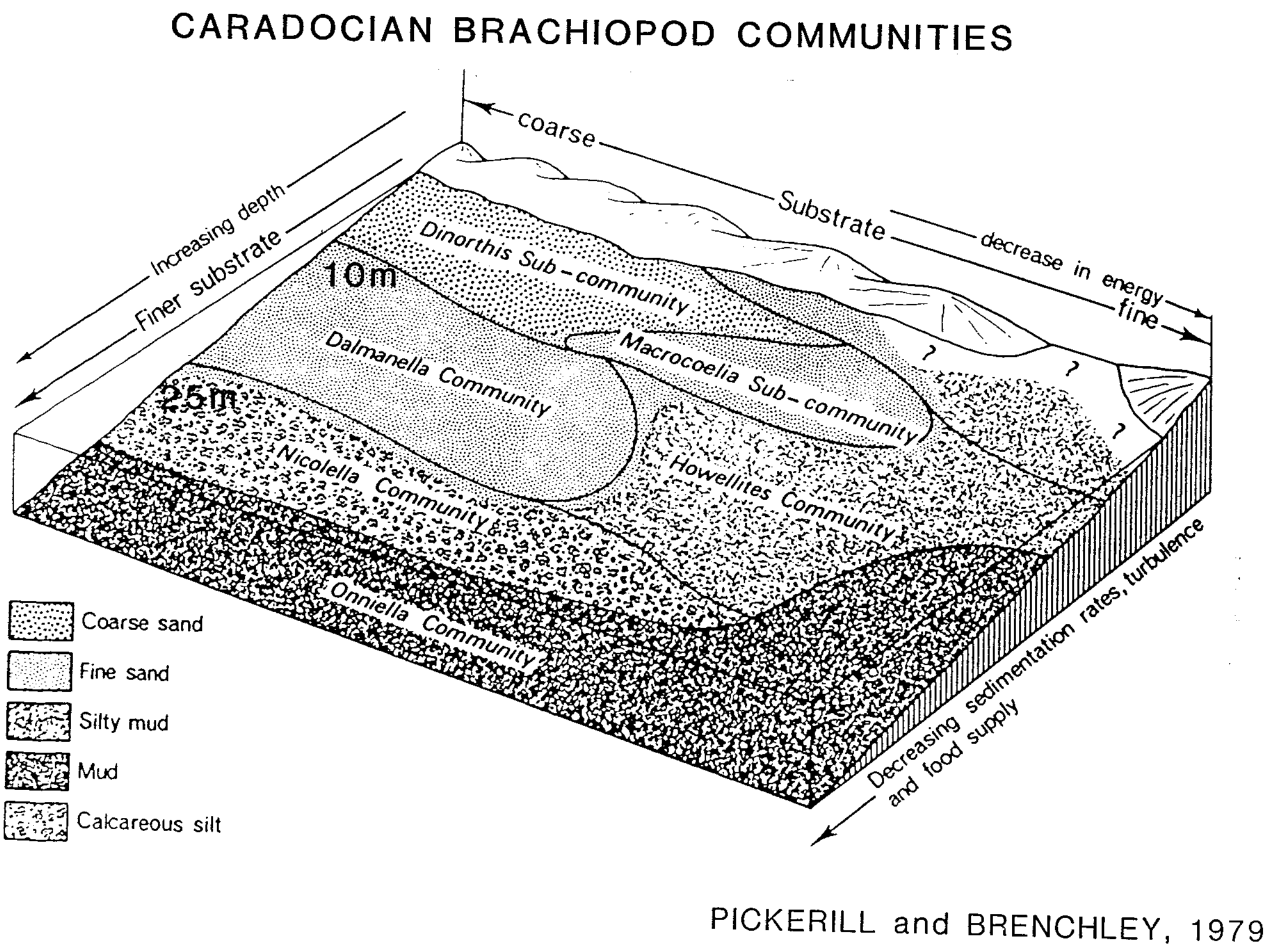

Fig. 5.3: Brachiopod communities postulated for Berwyn Hills. (from Pickerill and Brenchley, 1979).

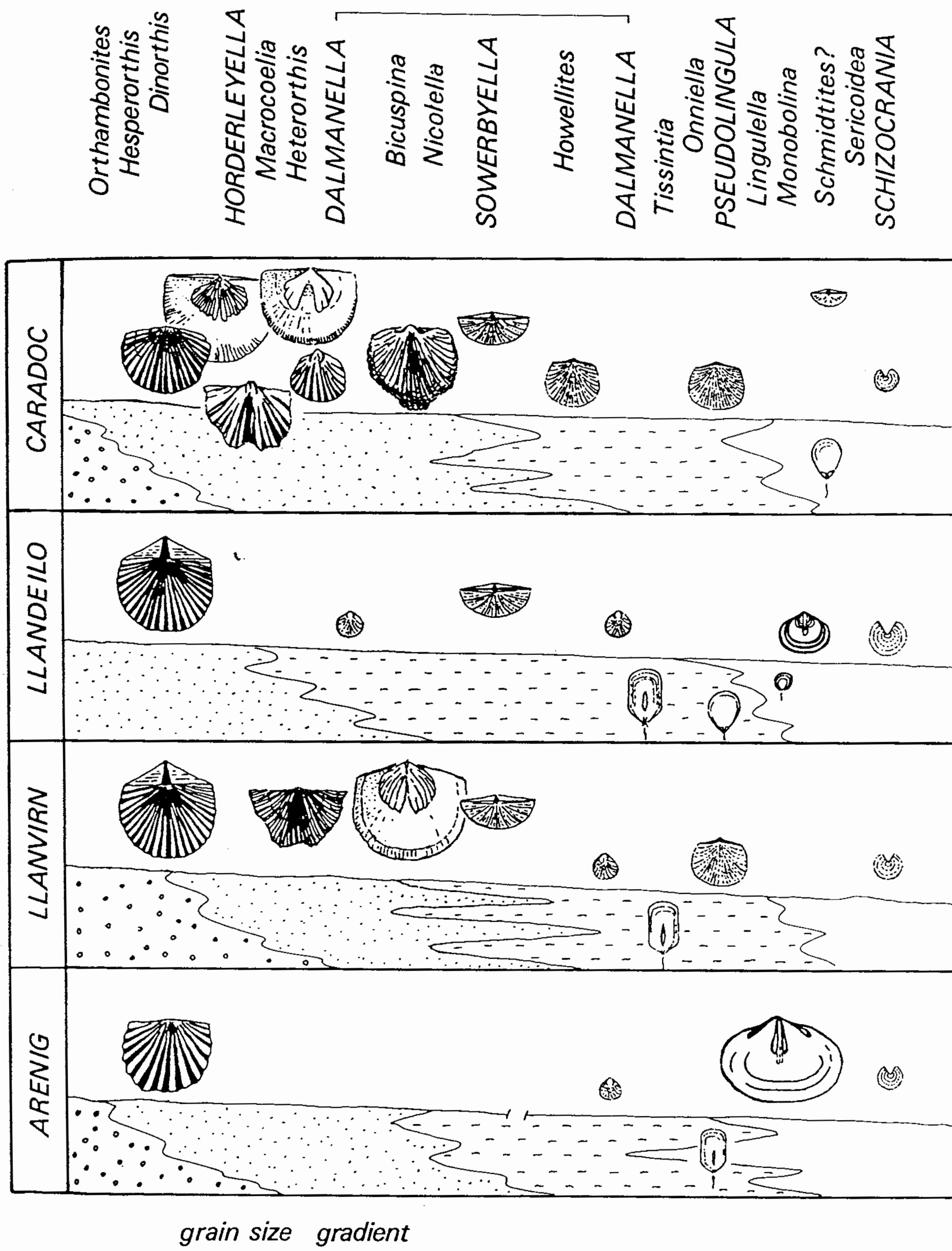

TEXT-FIG. 7. Facies relationships of key brachiopods throughout the Ordovician showing consistent 'preferences' of some taxa.

Fig. 5.4: Control of grain size on faunal distributions. Substrates shown are (from left to right), pebbly sand, sand (stipple), silt, and mud. From Lockley, 1984.

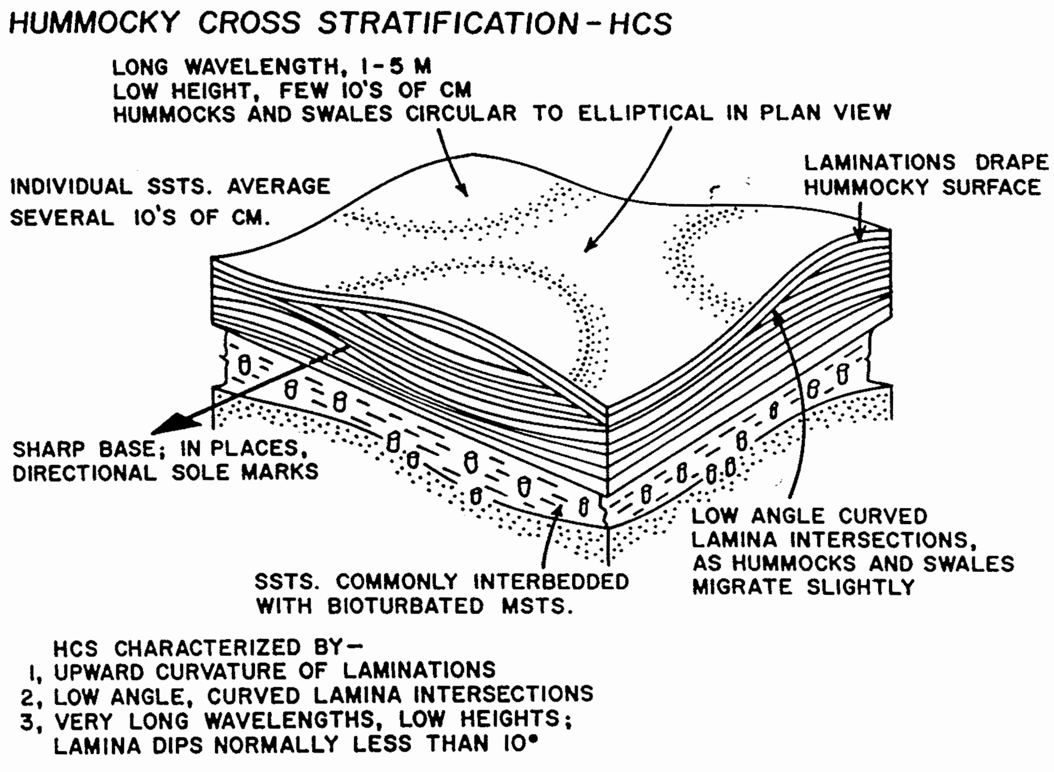

Fig. 5.5: Characteristic features of hummocky cross-stratification. From Walker, 1984.

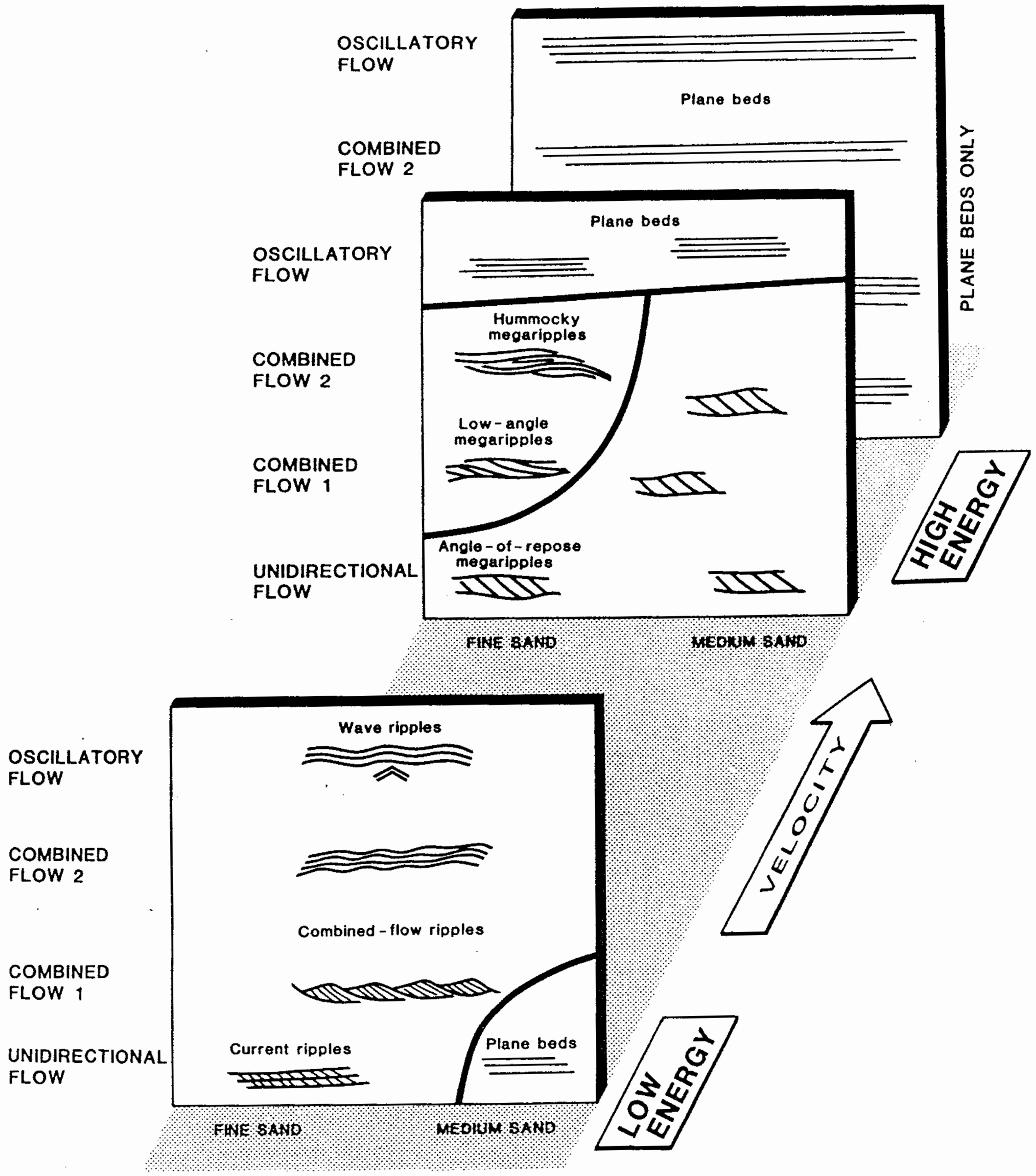

Fig. 5.6: Conceptual bed-form phase diagram. Schematic plot of bedforms as a function of current structure, current velocity, and grain size. Note fine to medium grain size boundary separating low-angle megaripples (including classical hummocky megaripples) from angle-of-repose megaripples. Passage from angle-of-repose, to low-angle, to classical hummocky megaripples is transitional and marked by gradual decrease in foreset inclination and appearance of numerous internal truncation surfaces. This is interpreted to result from increasing suspension sediment-transport caused by changes exclusively in current structure. For increased current velocities, upper-stage plane beds will develop, regardless of current structure. (both diagram and caption from Nottvedt and Kreisa, 1987, Figure 4).

Fig. 5.7a 'Classical' hummocky cross-stratification (HCS) showing upwards curvature and thickening of laminae, low-angle curved lamina intersections and no systemmatic direction of bedform migration. Compare with Fig. 5.7b. From amalgamated storm deposits of Upper Cwm Eigiau Fm., Cwm Cneifion. (section D2, 23.5 m).

Fig. 5.7b Low-angle undulatory cross-stratification (LACS) attributed to downcurrent migration (to right) of storm-produced megaripple. Photograph from the same depositionl unit as above.

Fig. 5.8 Large storm bed from Upper Cwm Eigiau Fm., Bwlch Trimarchog (SH 7048 6283). Section F3, 1.7 m. Scales shown on photographs.

A) Vertical profile to show grain size and lithofacies of adjacent shallow marine deposits. See Fig. 5.43 for position of this detailed section within Upper Cwm Eigiau Formation.

B) Overview of storm bed showing: 1) relation to surrounding facies, 2) undulose base to unit (trough-to-trough spacing of 3-6 m) which results in considerable lateral variation in bed thickness, and 3) development of large-scale (wavelength ca. 2 m) megaripples on top-surface.

C) Detail showing: 1) topographic relief (8 cm) on top surface of megapipple. 2) internal low-angle undulatory cross-stratification migrating to the left (NNE). 3) internal low-angle truncation surfaces.

D) Detail from just to left of overview showing: 1) Scouring at base of storm-bed infilled by moderate-angle trough cross-stratification., 2) Horizontal to very low angle cross stratification within middle of unit., 3) Form discordant planar horizontal lamination in top of unit., 4) Small wave ripples on top of megaripple.

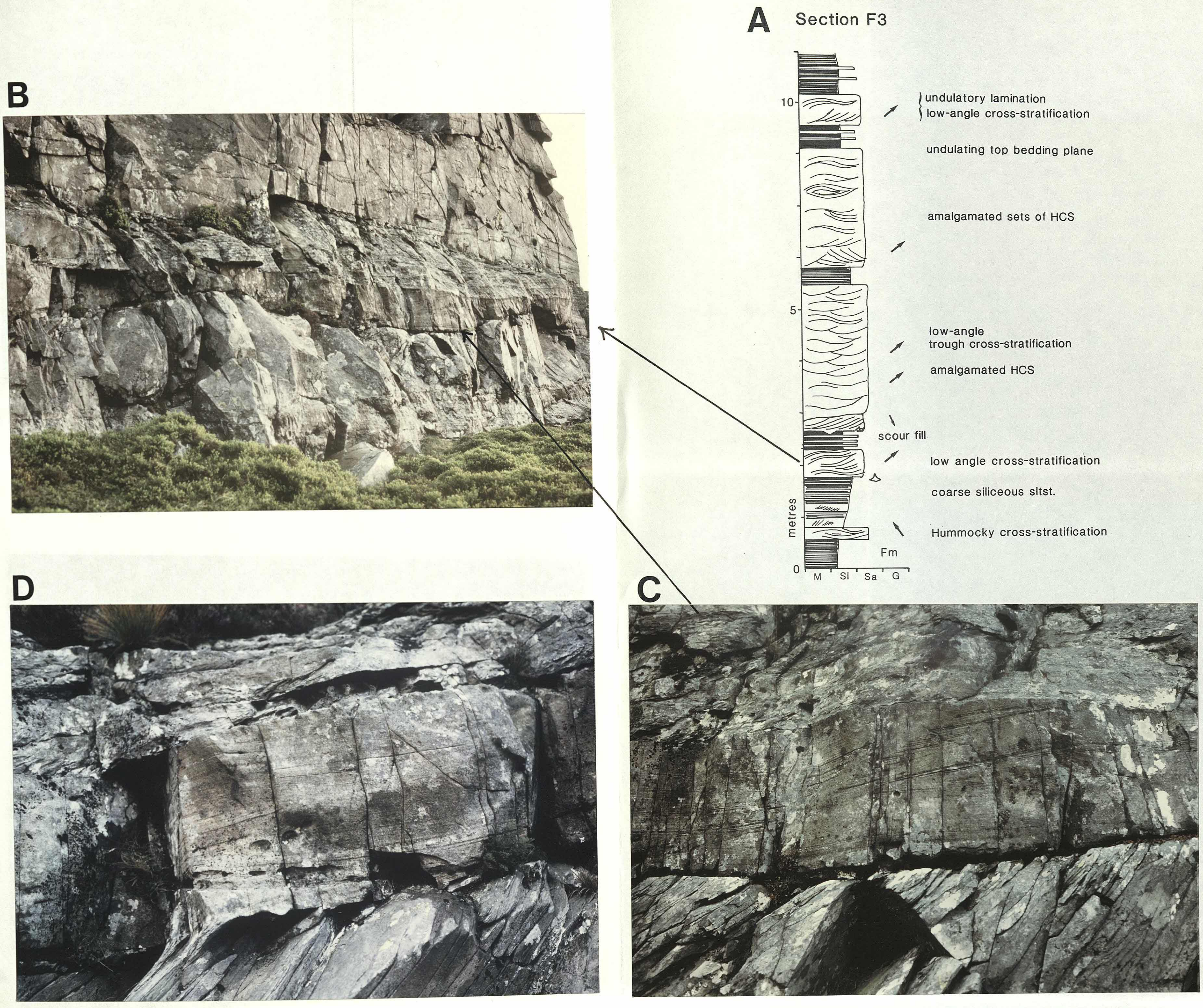
A
Section F3
B
C
D
10
5
0
metres
undulatory lamination
low-angle cross-stratification
undulating top bedding plane
amalgamated sets of HCS
low-angle
trough cross-stratification
amalgamated HCS
scour fill
low angle cross-stratification
coarse siliceous sltst.
Hummocky cross-stratification
Fm
M
Si
Sa
G

Fig. 5.9: Transverse cross-section through subaerial pyroclastic surge deposits, Minoan surge, near Akrotiri, Santorini, Greece. Flow was obliquely away (*ie.* slightly to left) from reader. Note the similarity of bedforms to hummocky-cross stratification (*eg.* Fig. 5.7a.), with the poor sorting that typifies these pyroclastic deposits being the only major difference between these two lithofacies.

Fig. 5.10: Longitudinal cross-section through subaerial pyroclastic base surge deposits, Upper Scoria sequence, near Cape Riva, Santorini, Greece. Small white blebs (arrow) are accretionary lapilli. Flow was from right to left. Compare with low-angle cross-stratification from migration of subaqueous storm megaripples (Fig. 5.7b, 5.8). Pencil for scale.

Fig. 5.11: Transverse cross-section of undulatory low-angle lamination within coarse-grained volcanic ash from 4th volcanic member of Capel Curig Volcanic Formation, Gallt-yr-Ogof. Section C13b, 41.5 m. Beforms probably resulted from internal body waves within surging ?subaqueous pyroclastic flows. Notebook is 18 cm long for scale. See text for further discussion.

Fig. 5.12: Transverse cross-section through "scour-and-fill" type structures developing from surging pyroclastic flows, Bedded Pyroclastic Fm., Cwm Glas, SH 613 557. Individual bedding units would be deposited by high density turbidity currents.

Fig. 5.13: Vertical profiles from Lower, Middle, and Upper Racks Mbrs. of Capel Curig Volcanic Formation, in the Capel Curig anticline. Inset map from unpublished BGS maps and shows location of sections. Identification of fauna from Wright, 1979 (see Fig. 5.15).

TWO
FOLLOWING PAGES

Fig. 5.14: Oblique photograph of the NW side of the Capel Curig anticline showing distribution of the pyroclastic and epiclastic members of the Capel Curig Volcanic Formation.

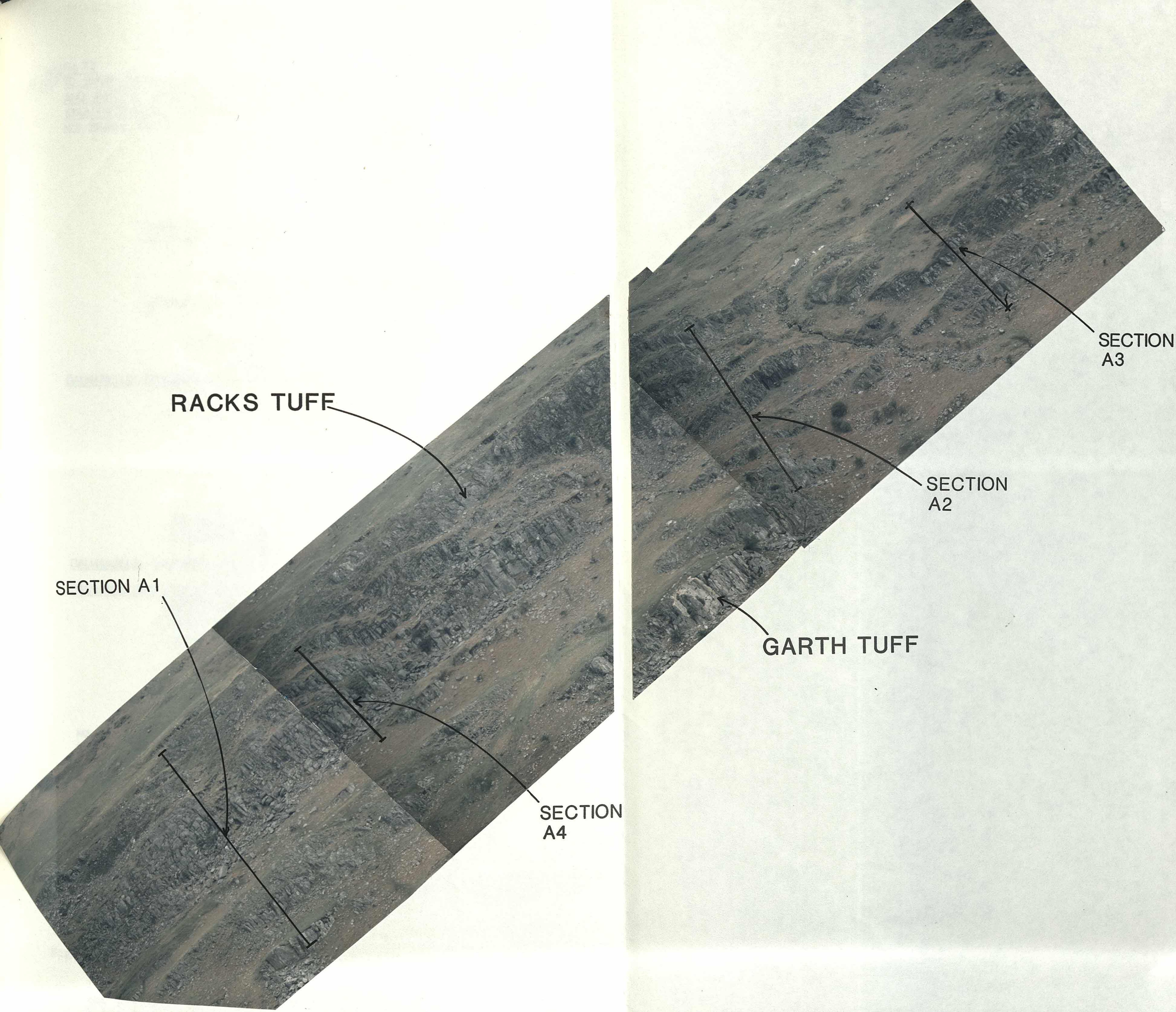
RACKS TUFF
SECTION A1
SECTION A4
SECTION A3
SECTION A2
GARTH TUFF

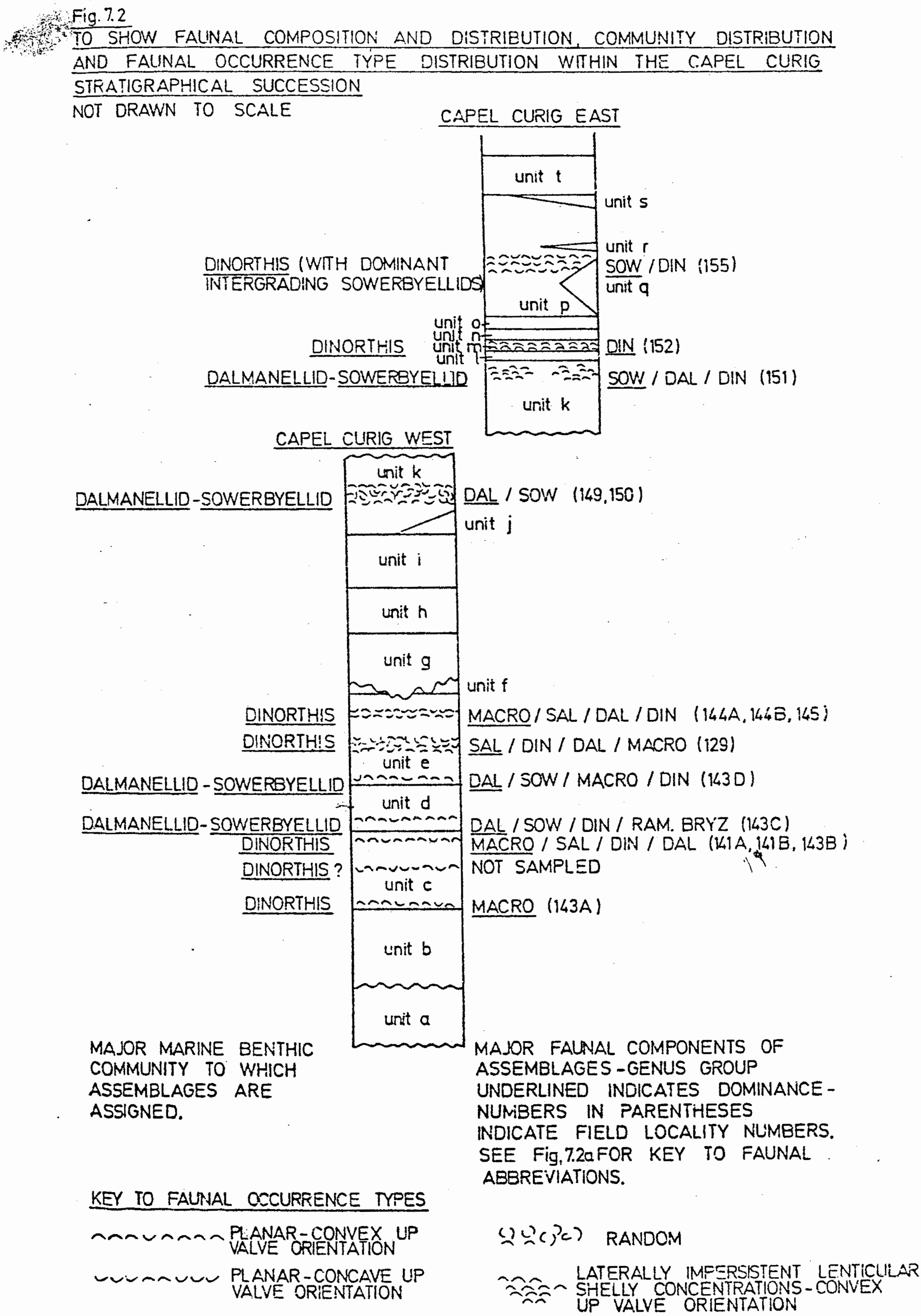

Fig. 5.15: Identification of fauna from the Capel Curig Volcanic Formation, Capel Curig anticline. Reproduced directly from Wright, 1979. As all vertical profiles from Wright's thesis are not to scale, the positioning of his faunal localities on sedimentary logs (*eg.* Fig. 5.13) from this study is only approximate.

FIG. 5.14: VERTICAL PROFILES THROUGH LOWER, MIDDLE, and UPPER RACKS MBRS., CAPEL CURIG ANTICLINE.

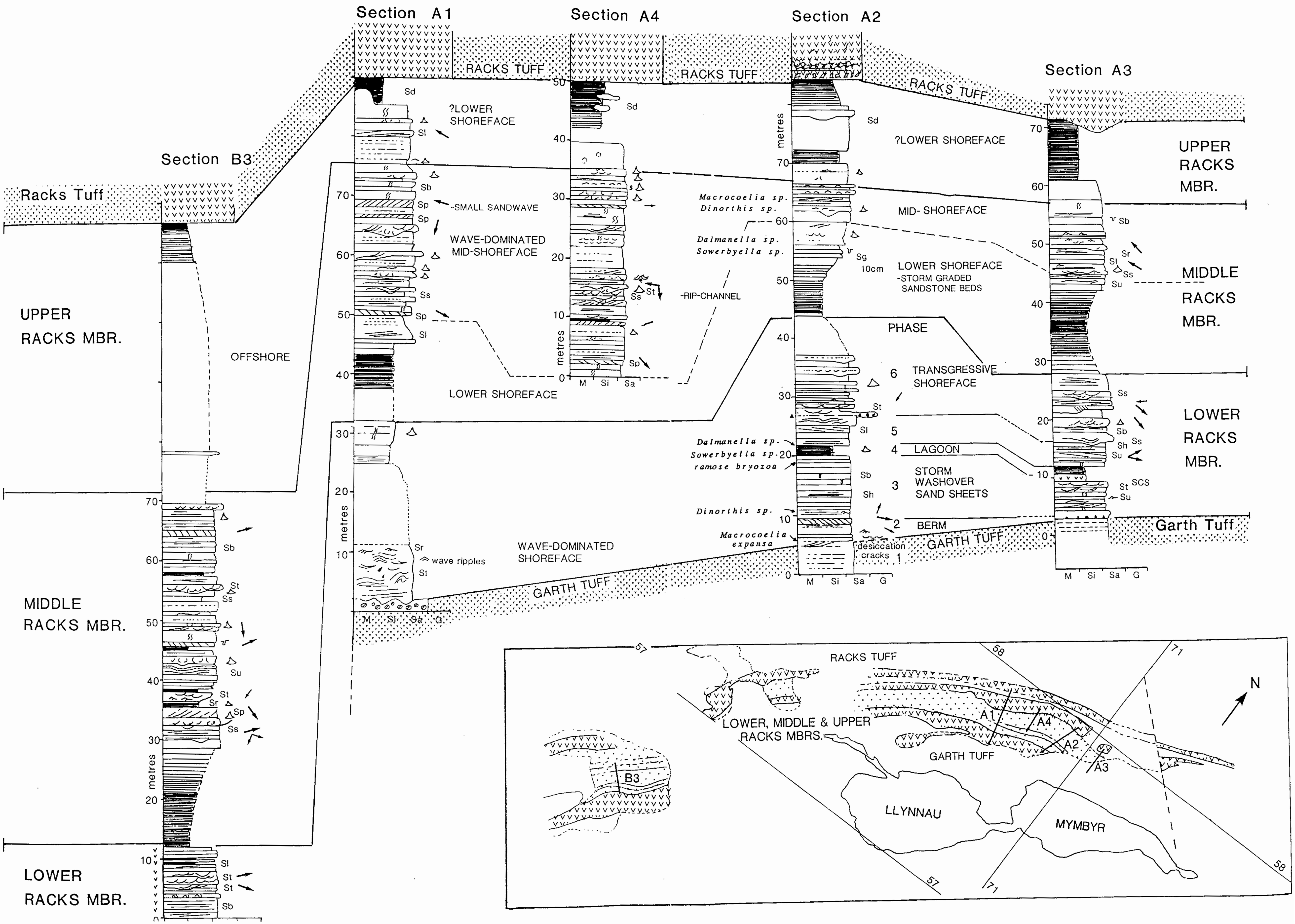

Section B3
Section A1
Section A4
Section A2
Section A3
Racks Tuff
RACKS TUFF
GARTH TUFF
Garth Tuff
UPPER RACKS MBR.
MIDDLE RACKS MBR.
LOWER RACKS MBR.
OFFSHORE
?LOWER SHOREFACE
-SMALL SANDWAVE
WAVE-DOMINATED MID-SHOREFACE
LOWER SHOREFACE
WAVE-DOMINATED SHOREFACE
wave ripples
-RIP-CHANNEL
MID- SHOREFACE
LOWER SHOREFACE -STORM GRADED SANDSTONE BEDS
PHASE
TRANSGRESSIVE SHOREFACE
LAGOON
STORM WASHOVER SAND SHEETS
BERM
desiccation cracks
Macrocoelia sp.
Dinorthis sp.
Dalmanella sp.
Sowerbyella sp.
ramose bryozoa
Macrocoelia expansa
10cm
metres
M Si Sa G
LOWER, MIDDLE & UPPER RACKS MBRS.
LLYNNAU
MYMBYR
N

Fig. 5.16: Low-angle cross-stratification and undulating horizontal lamination attributed to shoaling wave processes. The fine-grained sandstones (recessive weathering) and medium siltstones (white weathering) are rich in quartzo-feldspathic and siliceous vitric components respectively. From mid-shoreface deposits, Lower Racks Mbr. barrier island complex. Section B3, 6.0 m. Pencil for scale. See Fig. 5.13 for location of photograph.

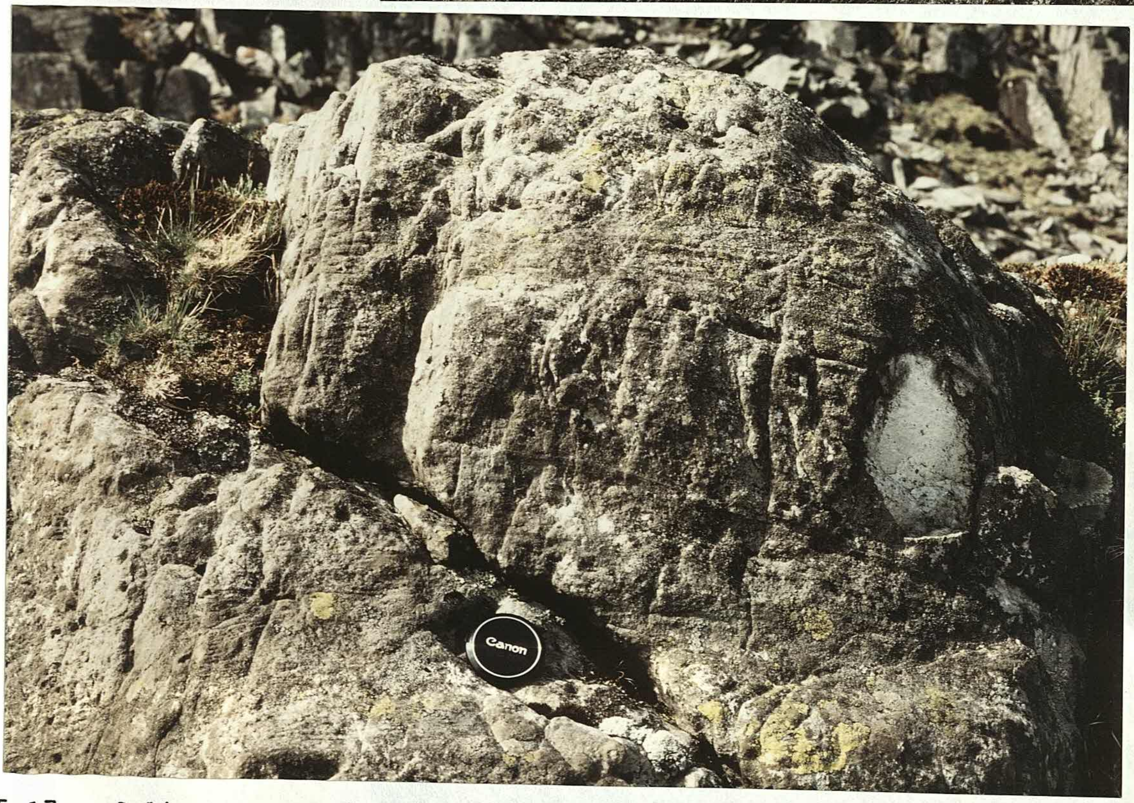

Fig. 5.17: Solitary set of ?sigmoidal low-angle cross-strata from back-barrier deposits, Lower Racks Mbr., Capel Curig Anticline. Bedform attributd to infill of small ?tidal channel. Note siliceous composition of rock on recent fracture. Section A2, 8.80 m. Lens cap is 6 cm for scale.

Fig. 5.18: Polygonal desiccation cracks (tectonically-deformed) from berm-crest facies association of barrier island complex. Lower Racks Mbr., Capel Curig anticline. Section A2, 6.25 m. Lens cap is 6 cm for scale.

Fig. 5.19: Bioturbated horizontally laminated and massive storm washover sheets from back barrier lagoon deposits, Lower Racks Mbr. Capel Curig anticline. Section A2, ca. 16 m. Black mark is 1 cm long for scale.

Fig. 5.20: Siltstone containing ramose bryozoa from inferred lagoon deposits. Lower Racks Mbr. barrier island complex, Capel Curig anticline. Section A2, 25.3 m.

Fig. 5.21: Skolithus-type vertical-escape structures within medium- to coarse-grained high-energy mid-upper shoreface deposits, Middle Racks Mbr., Capel Curig anticline. Section A4, 24.21 m. Black mark 1 cm long for scale.

PALAEOGEOGRAPHY Lower Racks Mbr.

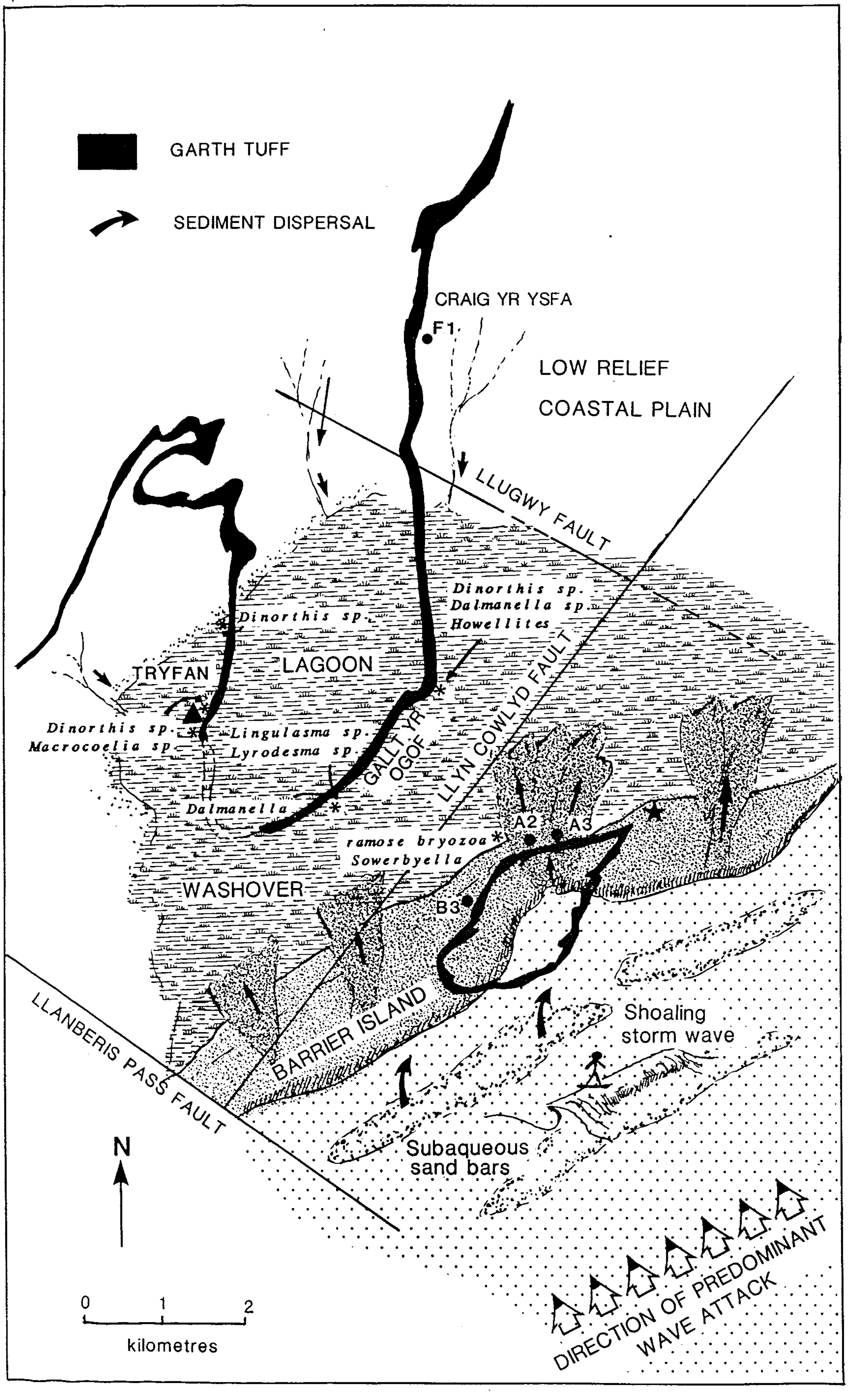

Fig. 5.22: Reconstruction of palaeogeography during deposition of the Lower Racks Mbr.

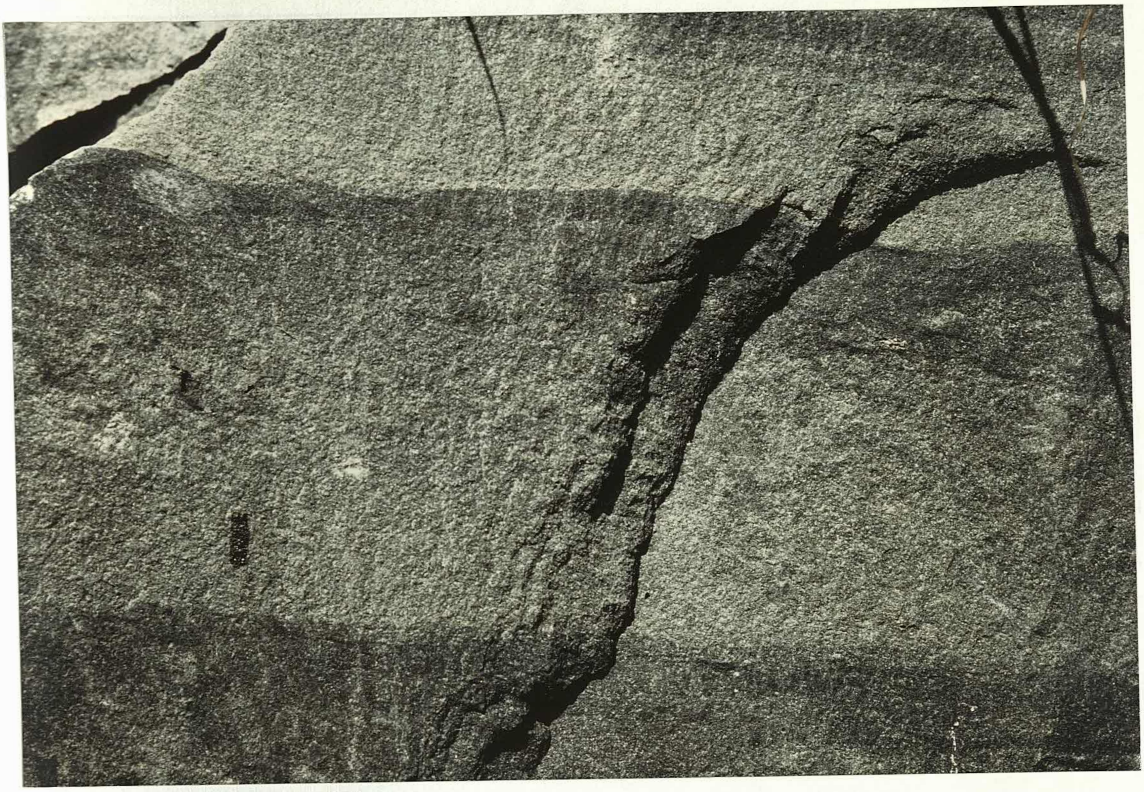

Fig. 5.23: Normally-graded beds of very fine-grained sandstone to siltstone from waning storm events on inner shelf, Middle Racks Mbr., Capel Curig anticline. Section A2, 53.85 m. Black mark is 1 cm long for scale.

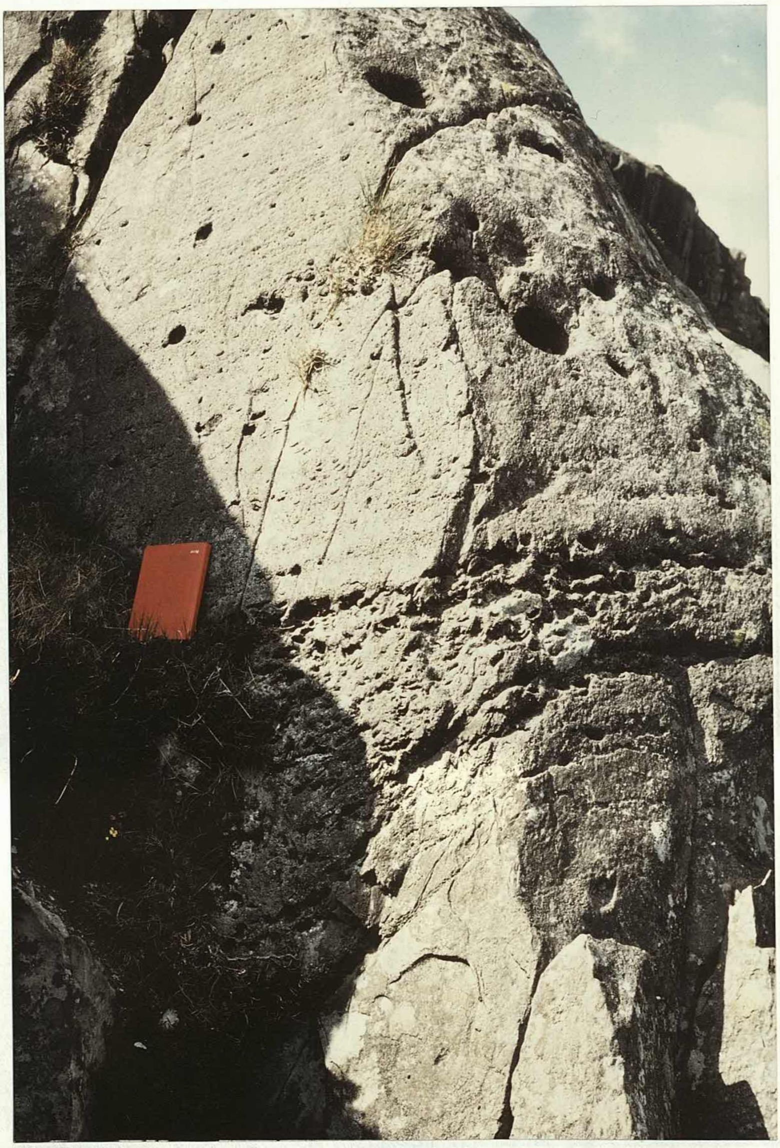

Fig. 5.24: 'Bell-shaped' scour filled with shelly coquina from middle shoreface deposits, Middle Racks Mbr., Capel Curig anticline. Attributed to infill of rip-channel by winnowed bioclastic debris. Section A4, 95 m. Notebook is 18 cm long for scale.

Fig. 5.25: Large (1.2 m) solitary set of planar tabular cross-strata attributed in migration of ?tidally influenced sandwave parallel to shoreline. From Middle Racks Mbr., Capel Curig anticline, Section A1, 103.2 m. Pen on foresets (upper left) is 12 cm long for scale.

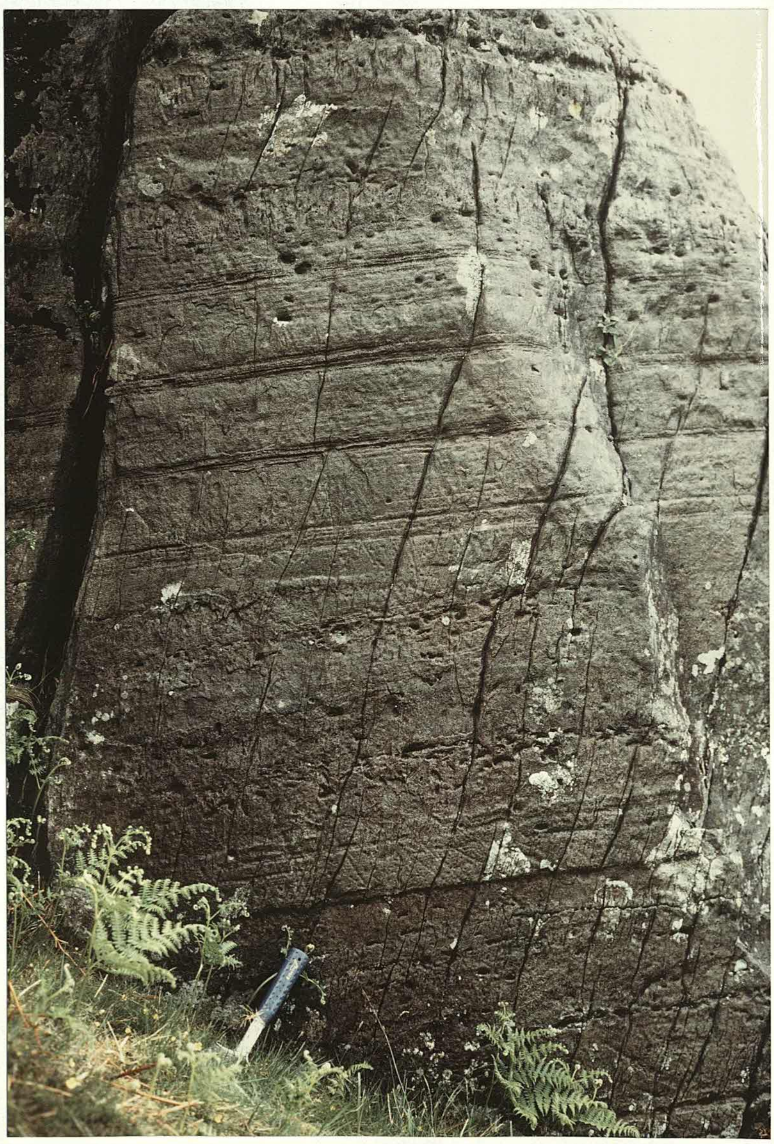

Fig. 5.26: Horizontally laminated to bioturbated ?Upper shoreface deposits from Upper Racks Mbr., Capel Curig anticline. Section A4, 26-30 m. Handle of Estwing rock hammer for scale.

Fig. 5.27: Palaeogeography during deposition of Middle Racks Mbr., in vicinity of Capel Curig anticline.

FOLLOWING PAGE

Fig. 5.28: Palaeogeography during deposition of Middle Racks Mbr., in vicinity of Capel Curig anticline.

PALAEOGEOGRAPHY Middle Racks Mbr

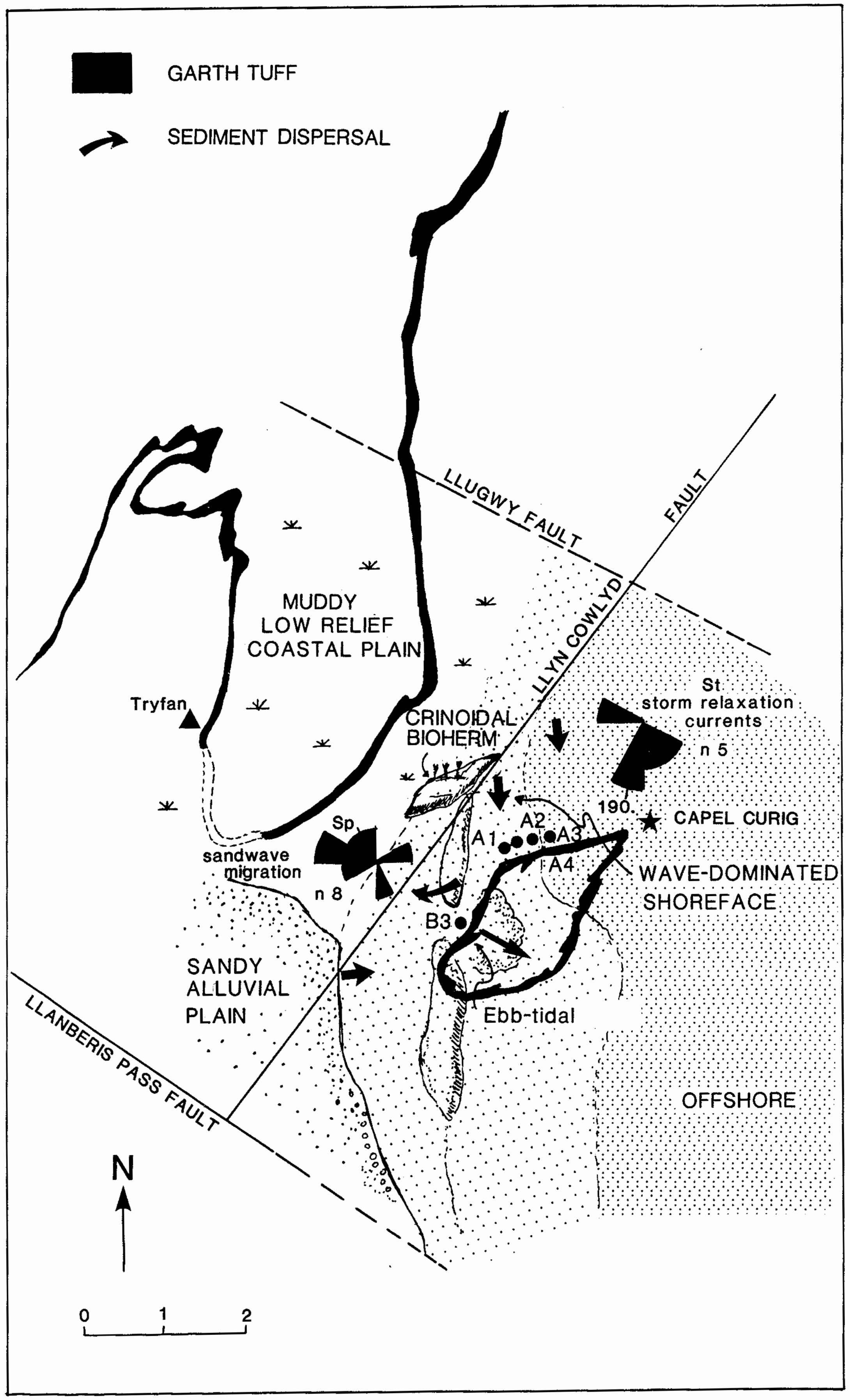

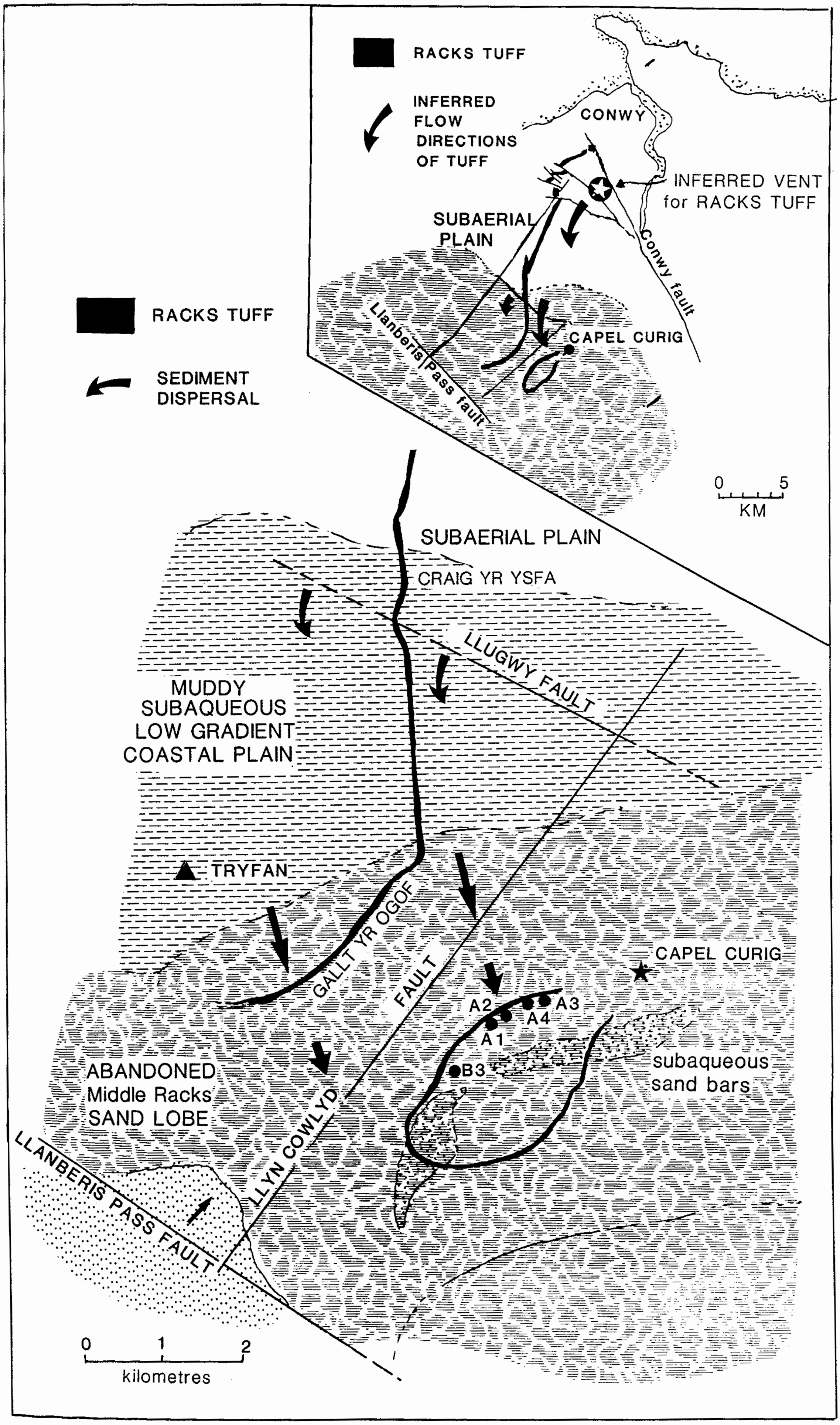

PALAEOGEOGRAPHY Upper Racks Mbr.

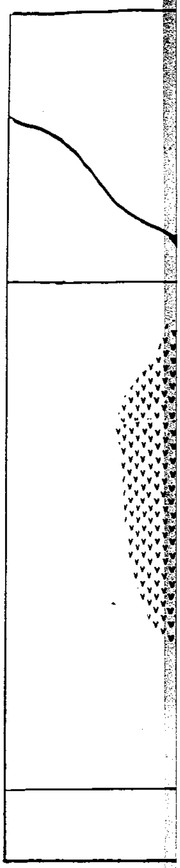

Fig. 5.29: Vertical profiles from the Upper Cwm Eigiau Fm.
at Pont-y-Gromlech.

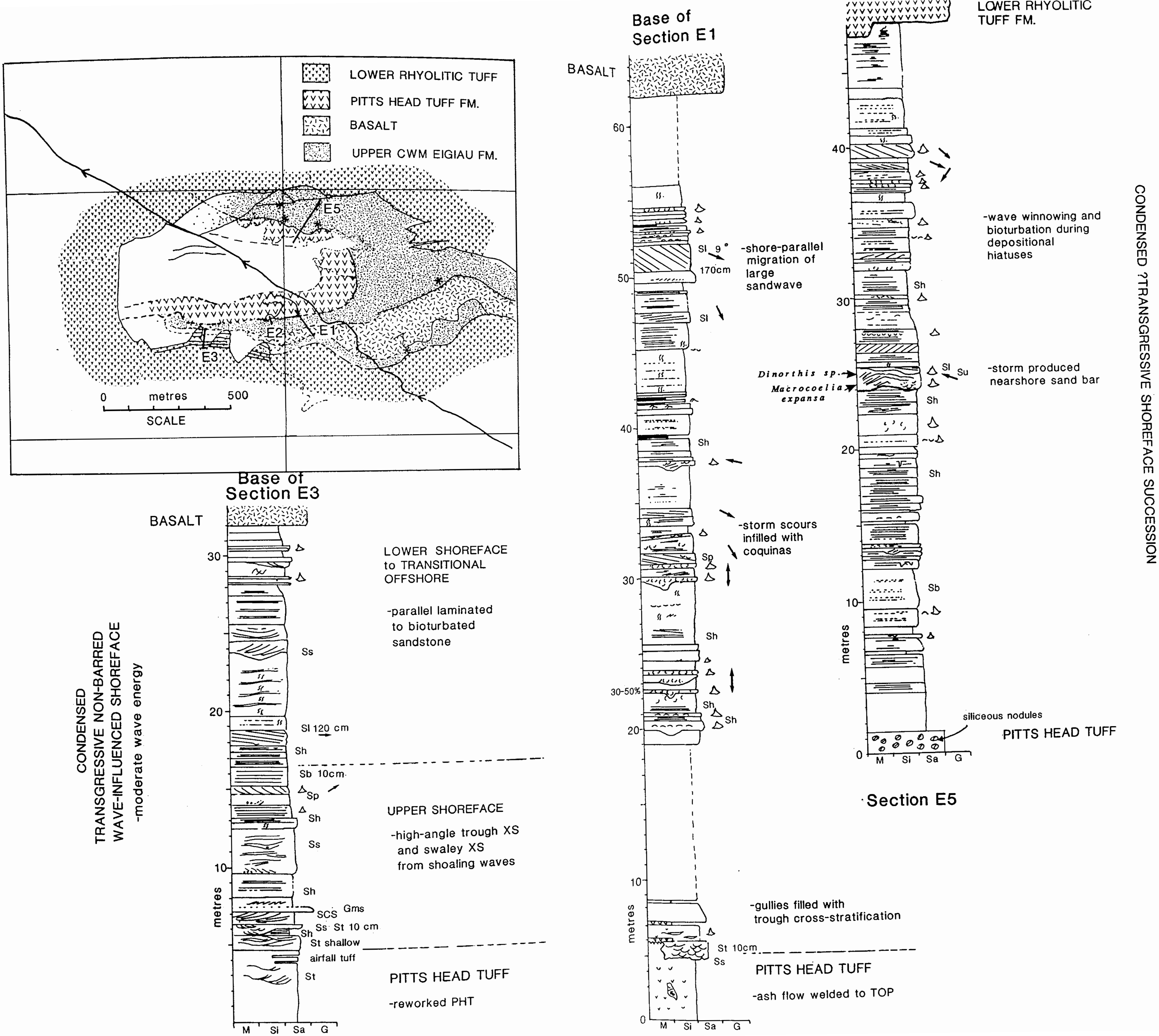

LOWER RHYOLITIC TUFF
PITTS HEAD TUFF FM.
BASALT
UPPER CWM EIGIAU FM.
E5
E2
E1
E3
0 metres 500
SCALE
Base of Section E3
BASALT
LOWER SHOREFACE to TRANSITIONAL OFFSHORE
-parallel laminated to bioturbated sandstone
Ss
Sl 120 cm
Sh
Sb 10cm
Sp
Sh
Ss
UPPER SHOREFACE
-high-angle trough XS and swaley XS from shoaling waves
Sh
SCS
Gms
Ss St 10 cm
Sh
St shallow
airfall tuff
St
PITTS HEAD TUFF
-reworked PHT
CONDENSED TRANSGRESSIVE NON-BARRED WAVE-INFLUENCED SHOREFACE
-moderate wave energy
metres
M Si Sa G
Base of Section E1
BASALT
Sl 9°
170cm
-shore-parallel migration of large sandwave
Sl
Sh
-storm scours infilled with coquinas
Sp
Sh
30-50%
Sh
Sh
-gullies filled with trough cross-stratification
St 10cm
Ss
PITTS HEAD TUFF
-ash flow welded to TOP
metres
M Si Sa G
LOWER RHYOLITIC TUFF FM.
-wave winnowing and bioturbation during depositional hiatuses
Sh
Dinorthis sp.
Macrocoelia expansa
Sl Su
-storm produced nearshore sand bar
Sh
Sh
Sb
siliceous nodules
PITTS HEAD TUFF
metres
M Si Sa G
Section E5
CONDENSED ?TRANSGRESSIVE SHOREFACE SUCCESSION

Fig. 5.30: Incision of erosive gullies into the top of the Pitts Head tuff, Pont-y-Gromlech. Notebook on fine grained siliceous airfall tuff overlying partially welded ash flow of Pitts Head Tuff. This fine grained horizon is cut out on left by 1.5 metre deep channel infilled with horizontal and undulating laminmation from wave-swash processes. Section E2, 0 metres.

Fig. 5.31: Herringbone trough cross-stratification within mid-shoreface deposits of Upper Cwm Eigiau Fm., Pont-y-Gromlech. Section E3, 47 m.

Fig. 5.32a: Overview of condensed sequence horizontally bedded shoreface deposits from Upper Cwm Eigiau Fm., Pont-y-Gromlech. Section E5, *ca.* 14 to 30 m. Several of the numerous tabular coquina beds are indicated by arrows. **THE TOP OF THE CLIFF IS EXTREMELY SLIPPERY WHEN WET; RESEARCHERS ARE ADVISED TO BE CAUTIOUS, for at g=9.8m/s^2 a freefalling object will hit the jagged talus blocks at the bottom at a velocity of 12.5 m/sec. (45 km/hr)** (pers. obs., Sept. 13, 1984).

Fig. 5.32b: Photomosaic showing portion of coquina-rich sandwave complex. Top of photograph approximates a horizontal bedding plane. Note undulose base to bedform (arrows), low angle undulating cross-stratification (LA) with brachiopod valves along foresets which dip predominantly to left, and winnowed shell accumulation (WSA) on stoss side of bedform. Attributed to storm-enhancement of shore-parallel fairweather currents. Section E5, 25 m.

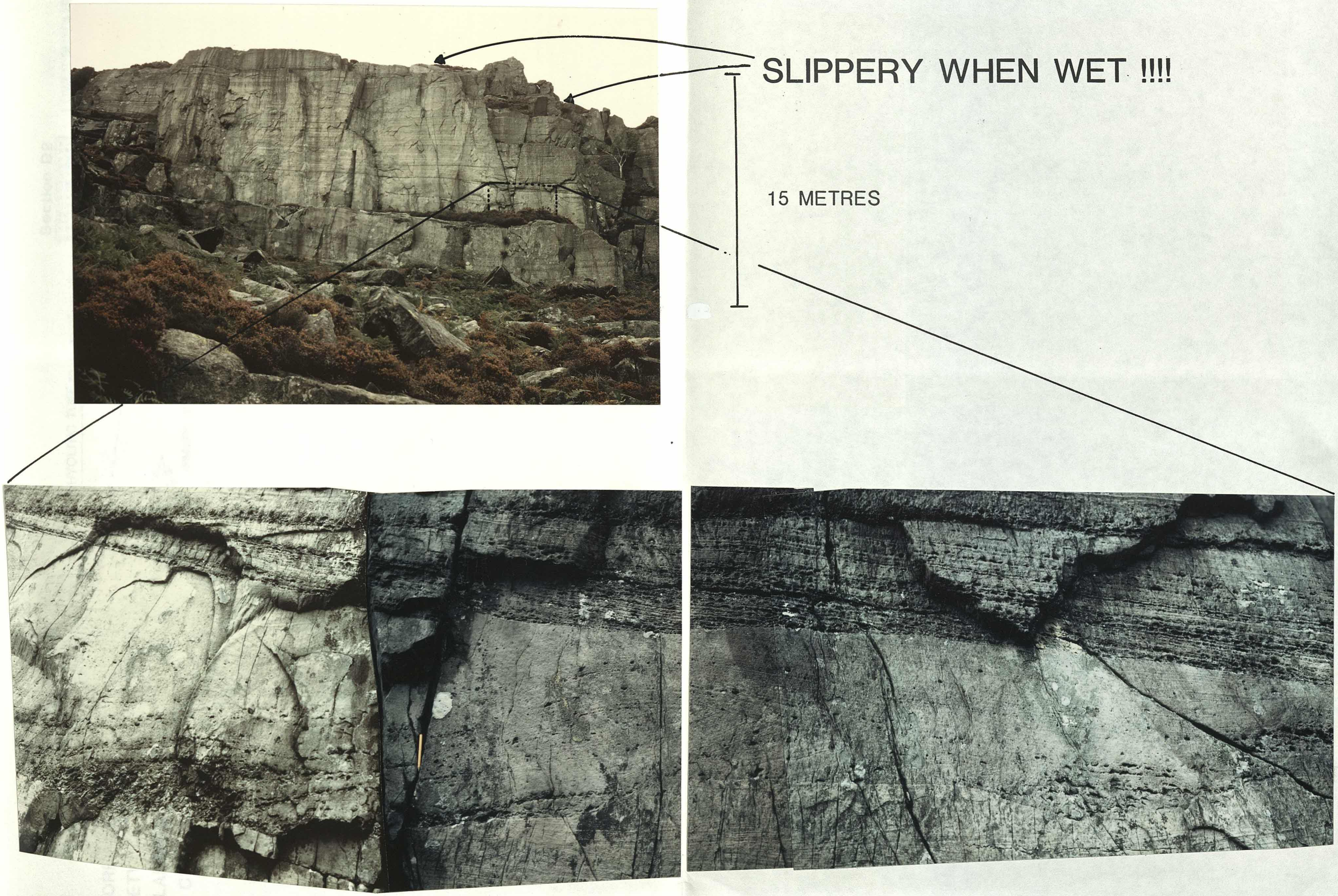
SLIPPERY WHEN WET !!!!
15 METRES

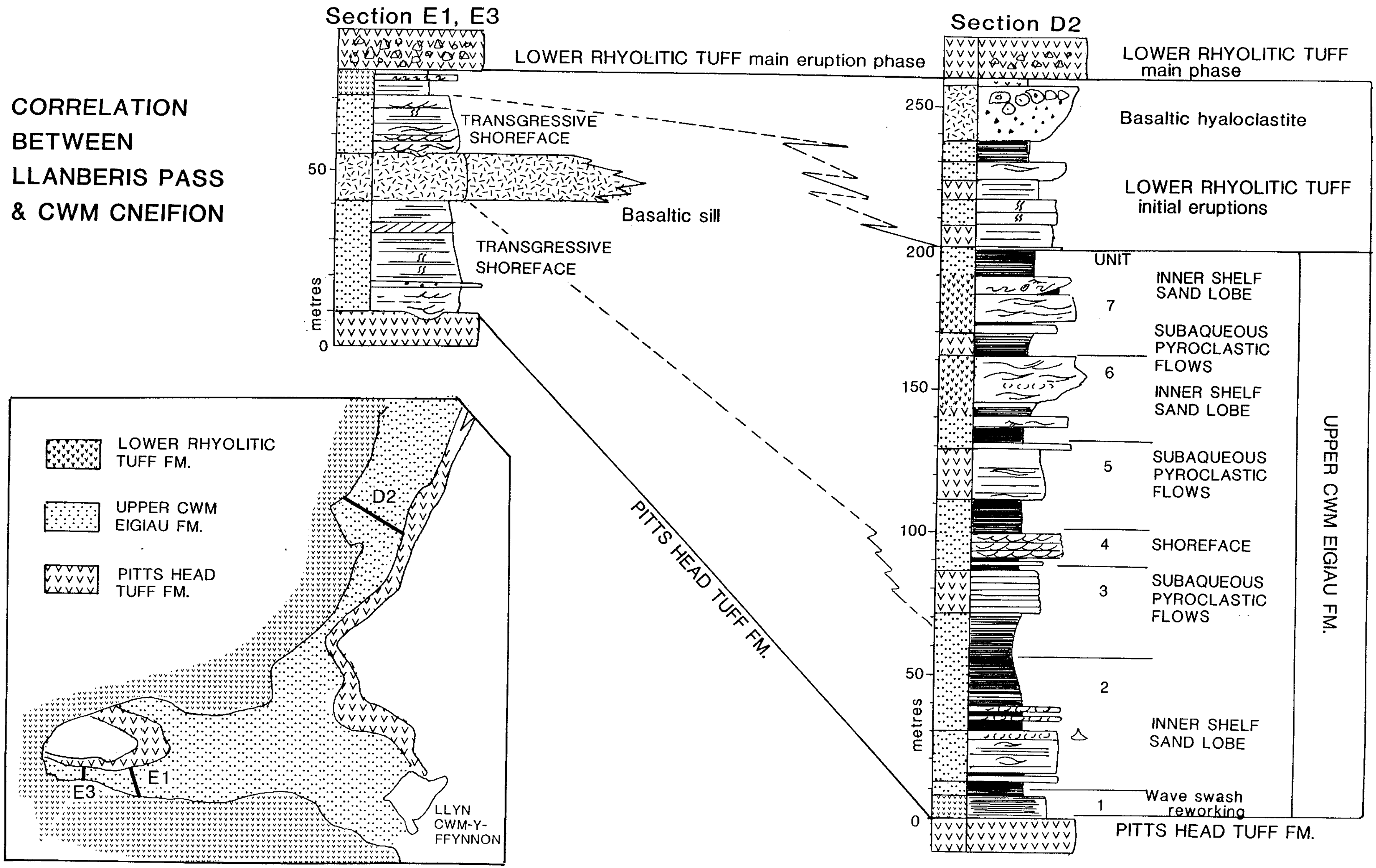

FIG. 5.33: Possible correlation of Upper Cwm Eigiau Fm. between Pont-y-Gromlech and Cwm Cneifion.

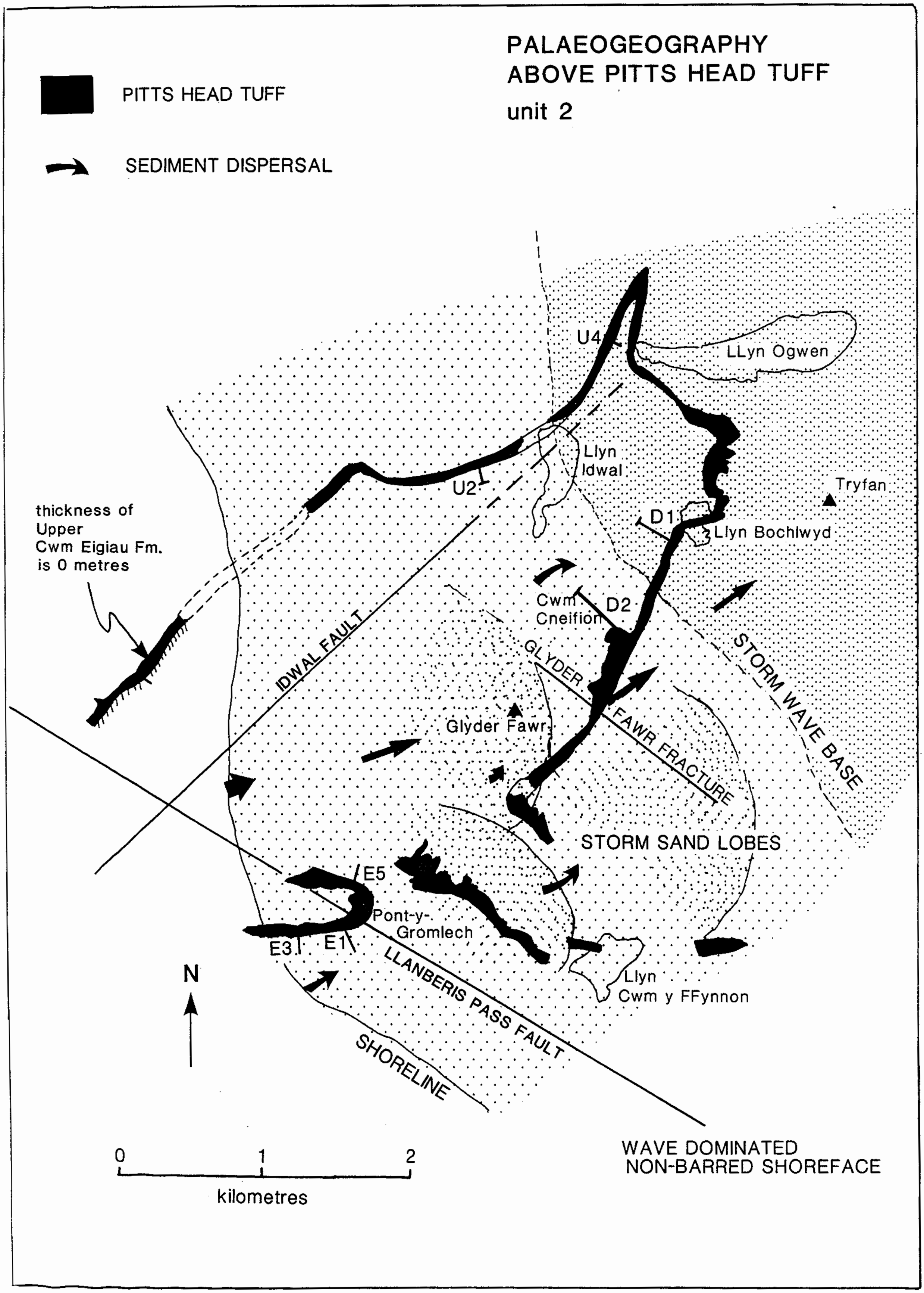

FIG. 5.34: Reconstruction of palaeogeography directly above Pitts Head Tuff near Llanberis pass.

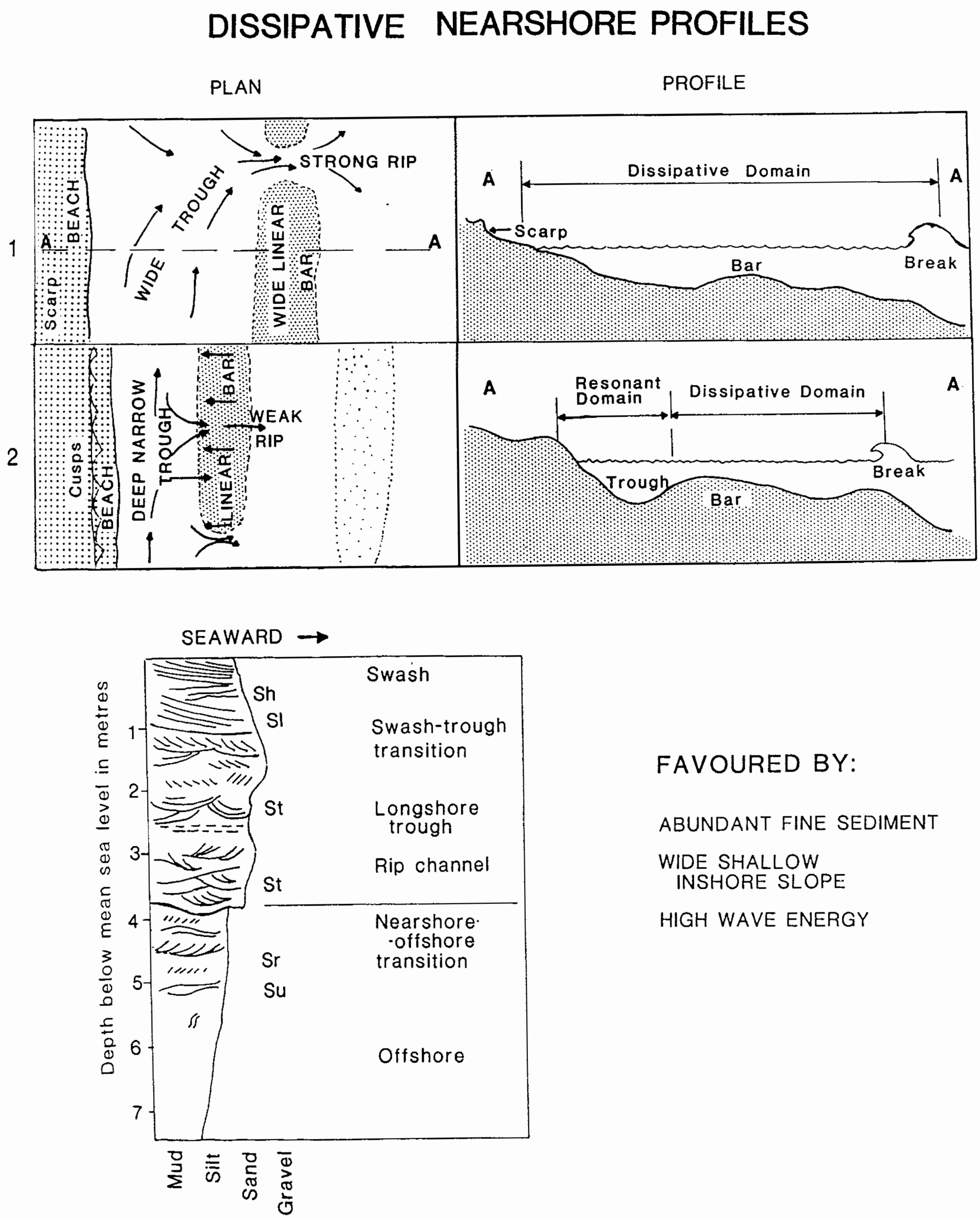

Fig. 5.35: Morphology and typical vertical sequence from barred, dissipative, coastline. (adapted from Wright *et al*, 1979; Hunter *et al*, 1979)

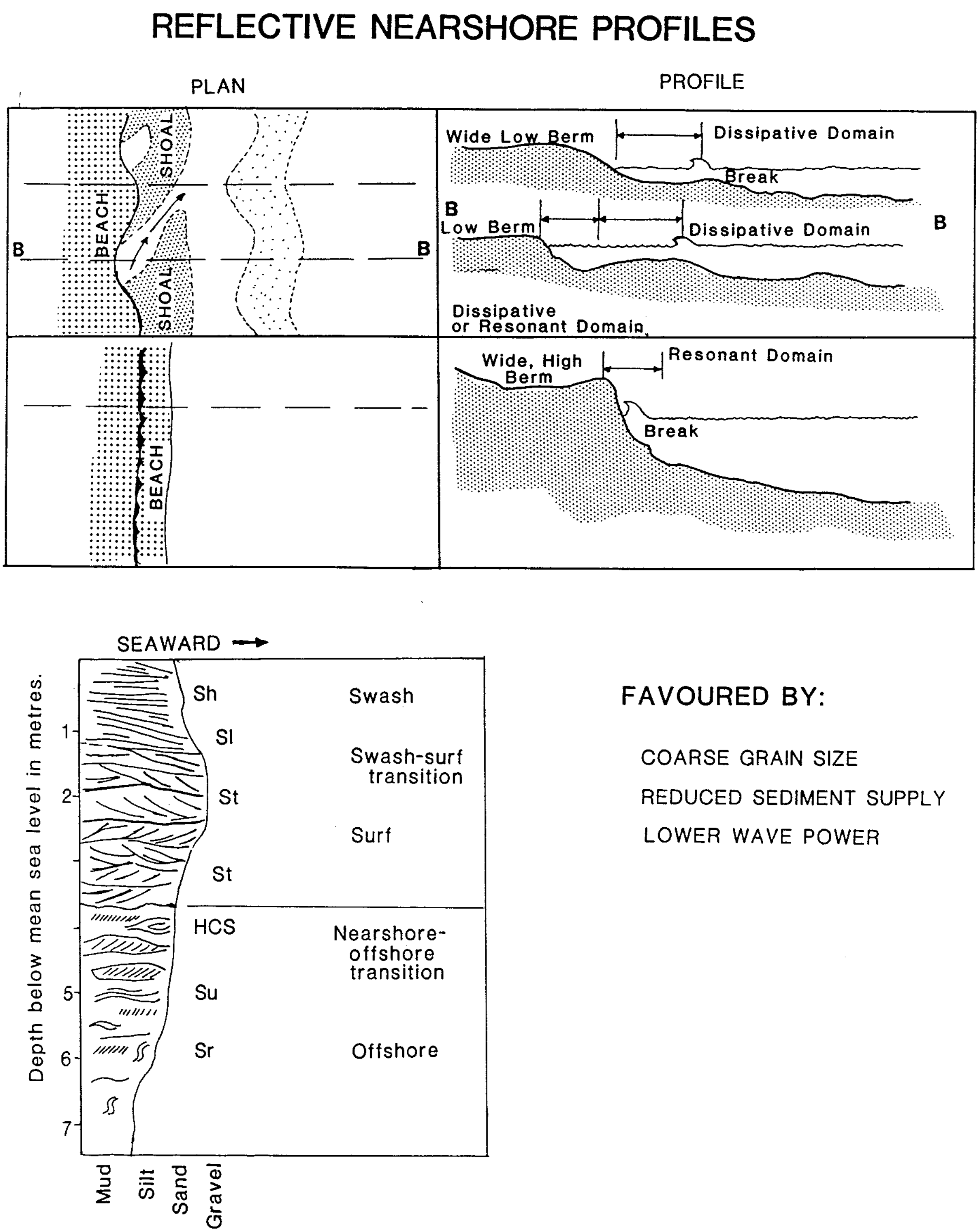

Fig. 5.36: Morphology and typical vertical sequence from non-barred, reflective, coastline. (adapted from Wright *et al*, 1979; Hunter *et al*, 1979)

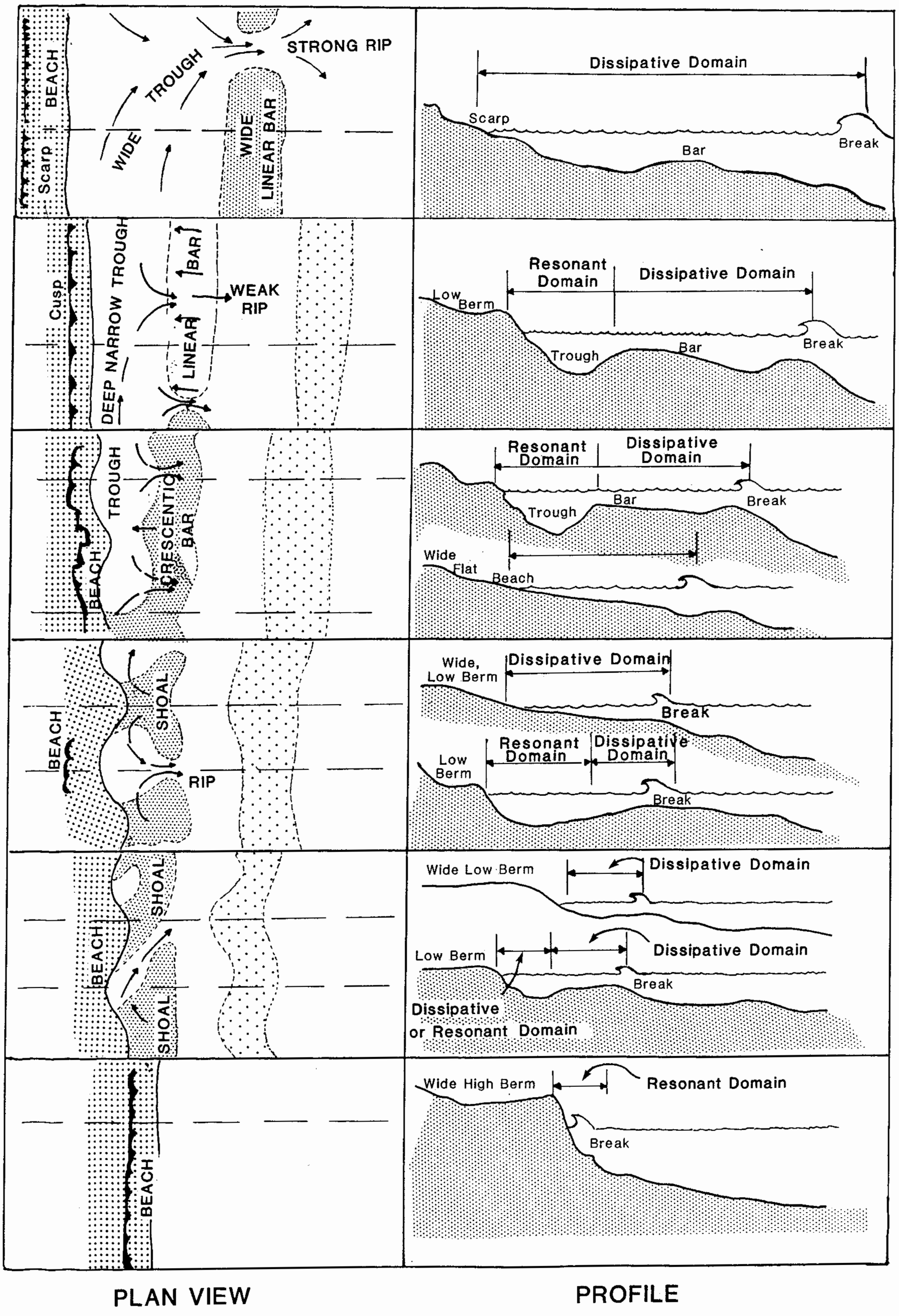

FIG. 5.37: Spectrum of shoreline morphologies on wave-dominated coastlines (from Wright et al, 1979).

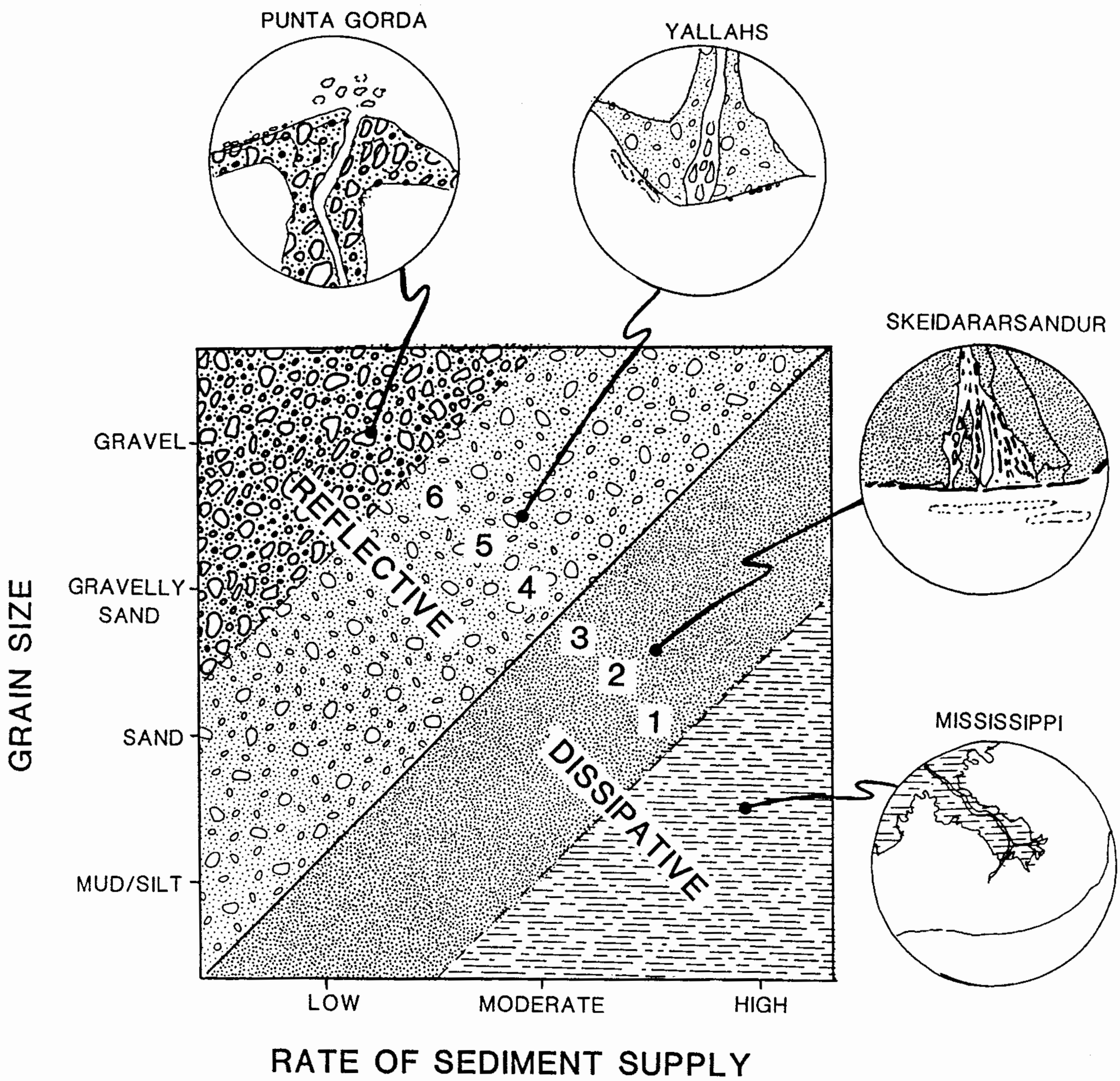

FIG. 5.38: Application of dissipative/reflective coastline concept to deltas. Numbers 1 to 6 refer to morphometric types of coastlines described by Wright (see Fig. 5.37).

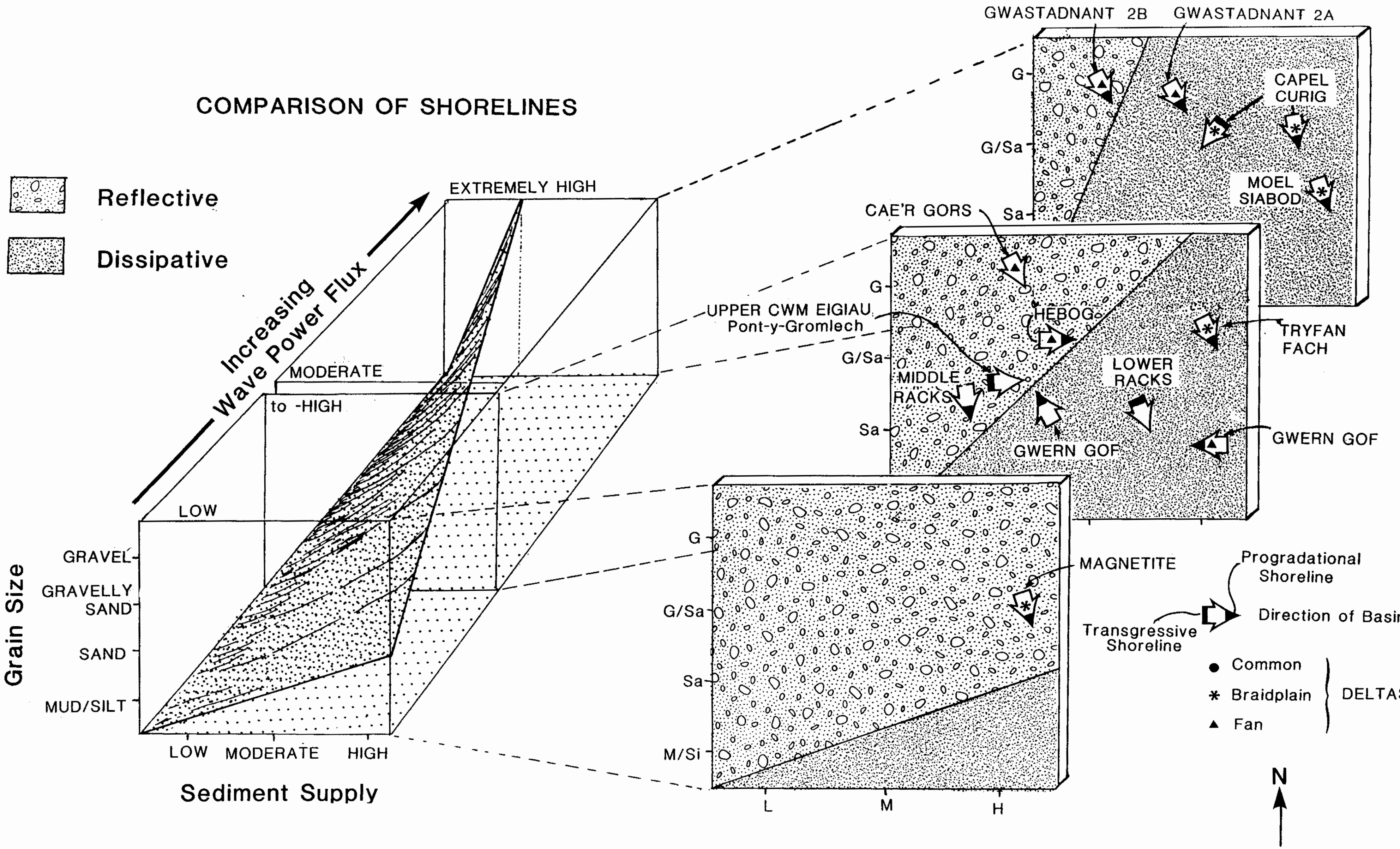
COMPARISON OF SHORELINES
Reflective
Dissipative
Increasing Wave Power Flux
EXTREMELY HIGH
MODERATE
to -HIGH
LOW
Grain Size
GRAVEL
GRAVELLY SAND
SAND
MUD/SILT
LOW
MODERATE
HIGH
Sediment Supply
GWASTADNANT 2B
GWASTADNANT 2A
CAPEL CURIG
MOEL SIABOD
G
G/Sa
Sa
CAE'R GORS
HEBOG
TRYFAN FACH
UPPER CWM EIGIAU
Pont-y-Gromlech
MIDDLE RACKS
LOWER RACKS
GWERN GOF
GWERN GOF
MAGNETITE
M/Si
L
M
H
Progradational Shoreline
Direction of Basin
Transgressive Shoreline
● Common
✱ Braidplain
▲ Fan
DELTAS
N

FIG. 5.39

SHELF SUBDIVISIONS

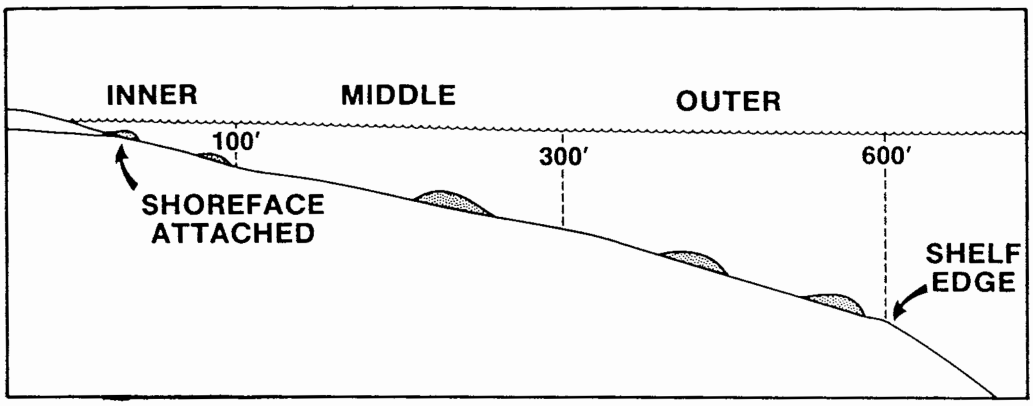

Subidivisions of shelf where sand may accumulate.

SHELF PROCESSES

	Tidal Currents	Wind Induced Alongshore Currents	Wave Modified (Combined flow) Currents	Storm Currents	Permanent or Semi-Permanent Currents	Turbidity Currents
Shoreface Attached	X	X	X	X	X	—
Inner Shelf	X	X	X	X	X	?
Middle Shelf	?	?	X	X	X	X
Outer Shelf	—	—	—	X	X	X

Shelf processes and their distribution on the shelf.

FIG. 5.40: Subdivisions of continental shelf

FIG. 5.41: (BOTTOM) Distribution of processes on the continental shelf.

(both diagrams from Swift, 1983).

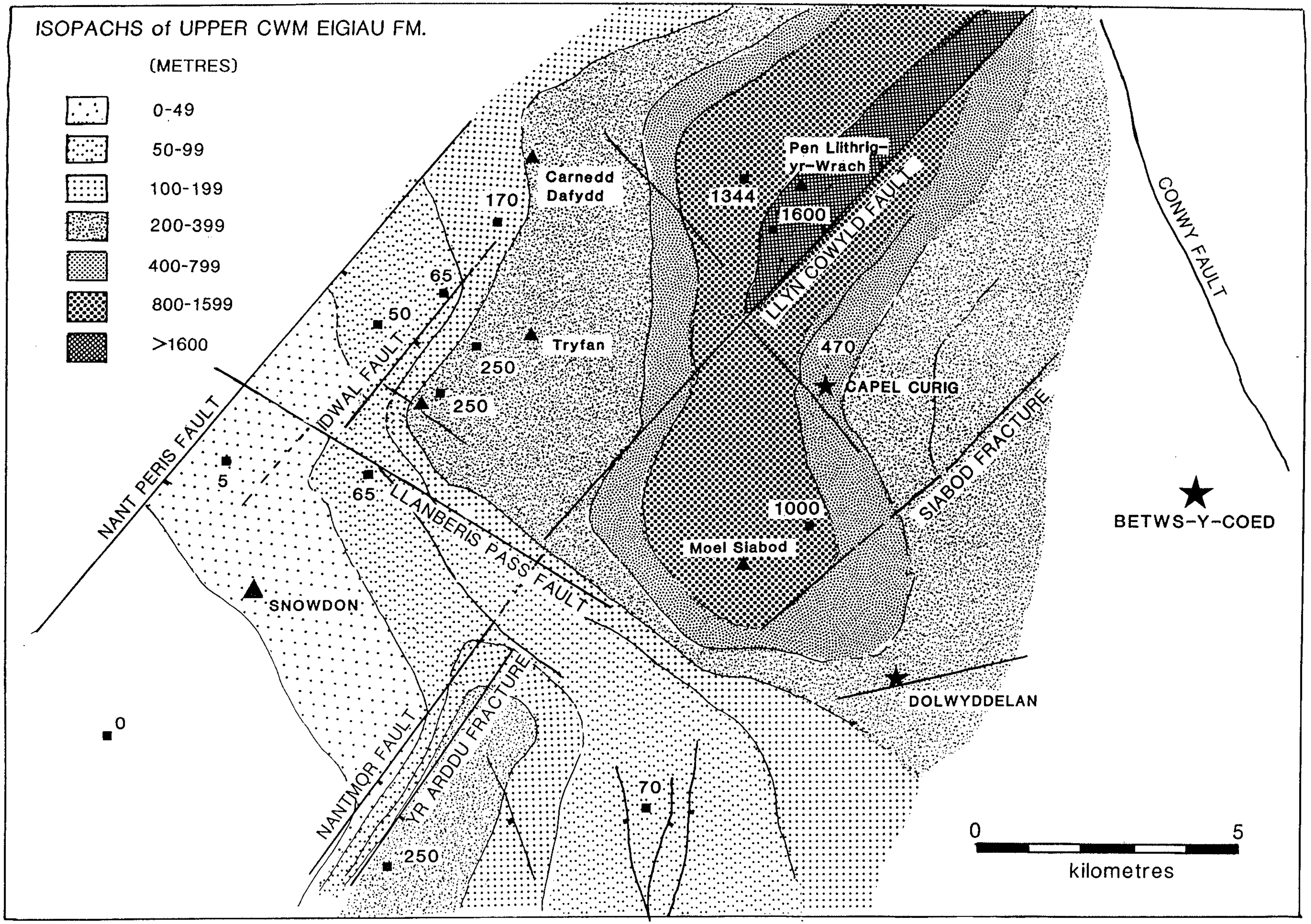

FIG. 5.42: Isopachs of Upper Cwm Eigiau Fm. in NE Snowdonia.

FIG. 5.43: Vertical profiles and correlation of the Upper Cwm Eigiau Fm. in NE Snowdonia.

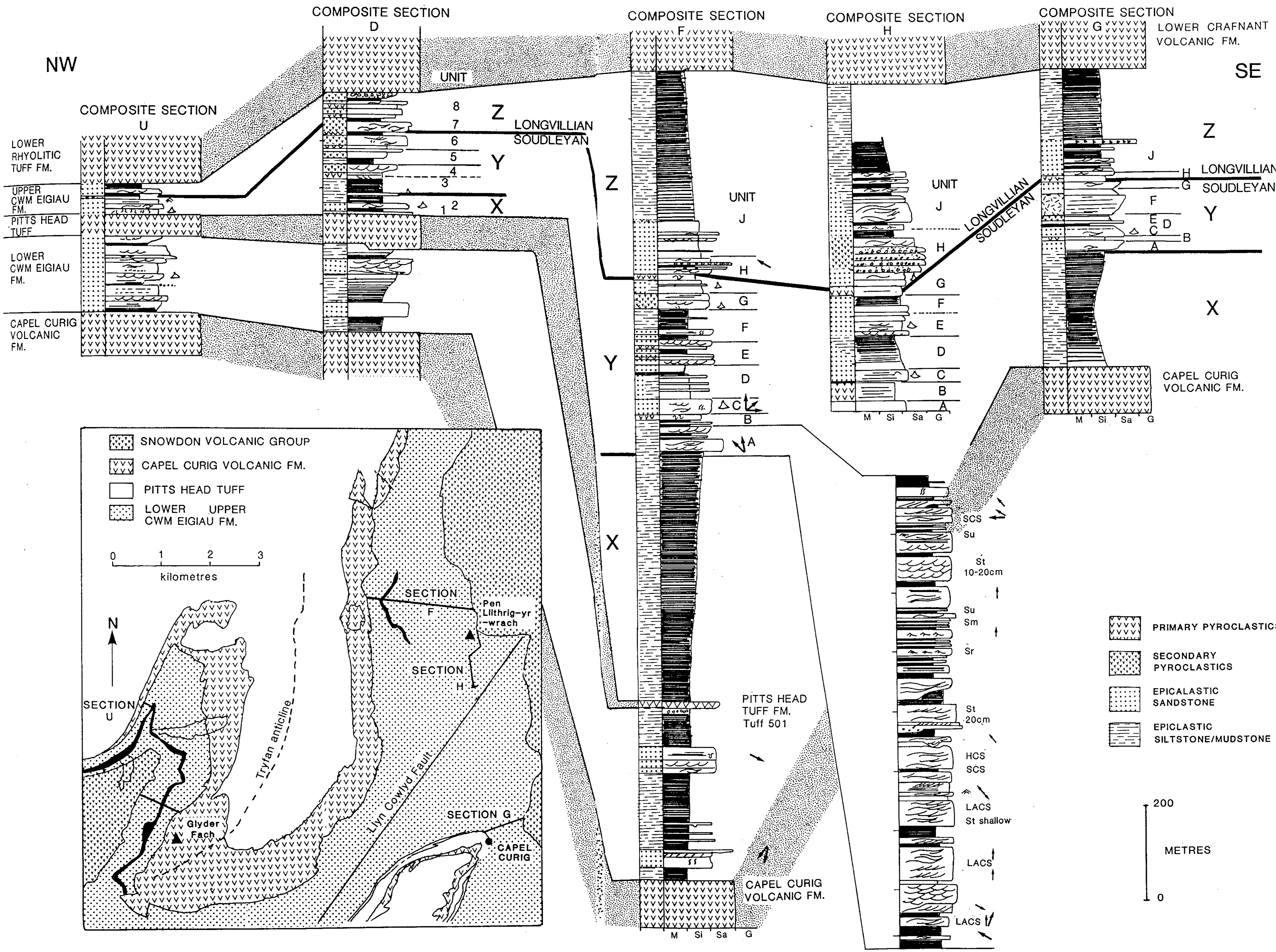

NW
SE
COMPOSITE SECTION U
COMPOSITE SECTION D
COMPOSITE SECTION F
COMPOSITE SECTION H
COMPOSITE SECTION G
LOWER CRAFNANT VOLCANIC FM.
LOWER RHYOLITIC TUFF FM.
UPPER CWM EIGIAU FM.
PITTS HEAD TUFF
LOWER CWM EIGIAU FM.
CAPEL CURIG VOLCANIC FM.
UNIT
LONGVILLIAN
SOUDLEYAN
X
Y
Z
PITTS HEAD TUFF FM. Tuff 501
CAPEL CURIG VOLCANIC FM.
M Si Sa G
SCS
Su
St 10-20cm
Su Sm
Sr
St 20cm
HCS SCS
LACS St shallow
LACS
SNOWDON VOLCANIC GROUP
CAPEL CURIG VOLCANIC FM.
PITTS HEAD TUFF
LOWER UPPER CWM EIGIAU FM.
0 1 2 3
kilometres
N
SECTION F
SECTION H
SECTION U
SECTION G
Pen Llithrig-yr-wrach
Glyder Fach
Tryfan anticline
Llyn Cowlyd Fault
CAPEL CURIG
PRIMARY PYROCLASTICS
SECONDARY PYROCLASTICS
EPICLASTIC SANDSTONE
EPICLASTIC SILTSTONE/MUDSTONE
200
METRES
0

S

FIG. 5.44: Vertical profile through Upper Cwm Eigiau Fm. at Cwm Cneifion. See Fig. 5.45 for explanation of lithologies depicted in log.

FOLLOWING PAGE

FIG. 5.45: Vertical profile through Upper Cwm Eigiau Fm. at Llyn Bochlwyd. See Fig. 5.44 for location of section.

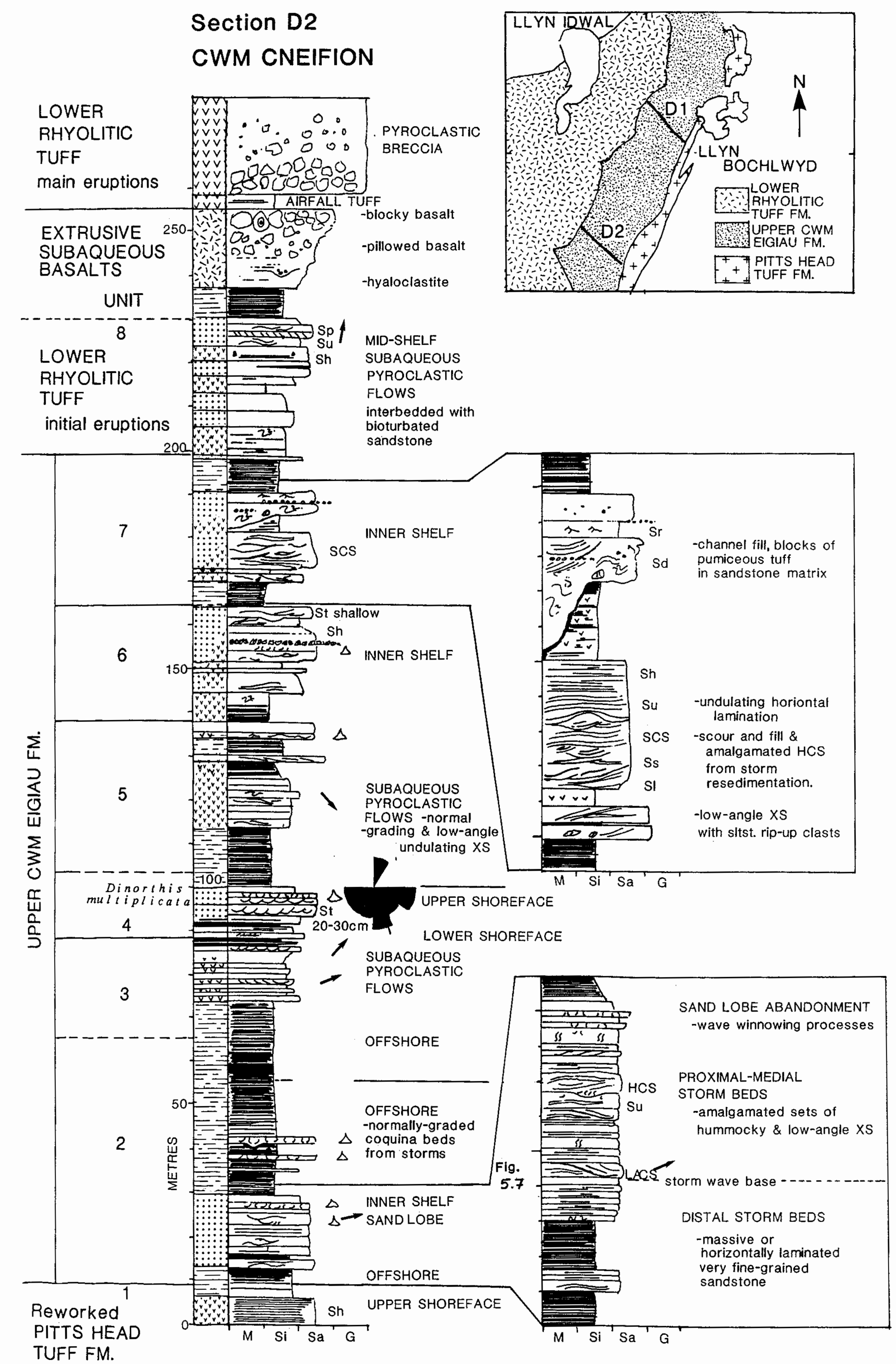

FIG. 5.45

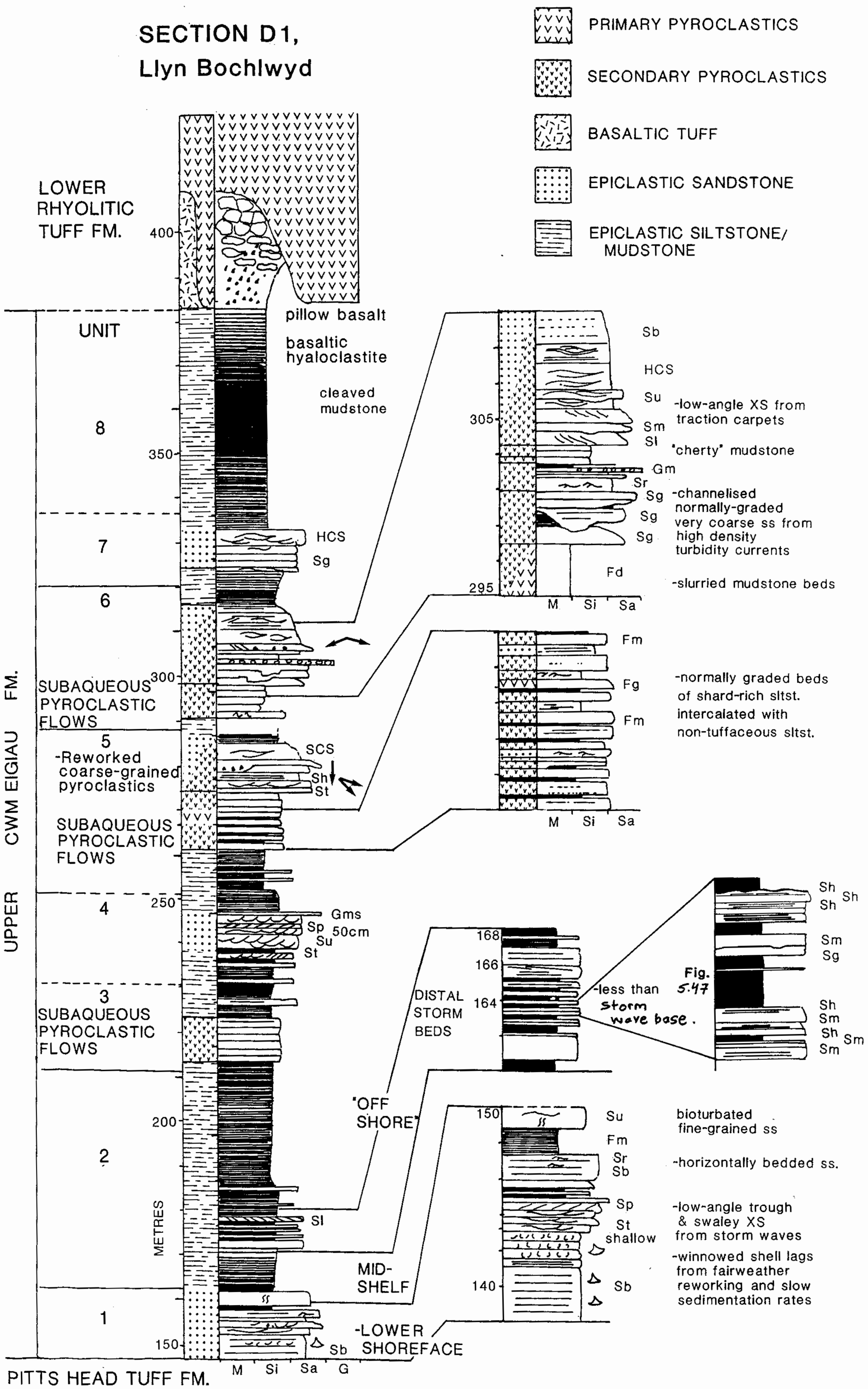
SECTION D1,
Llyn Bochlwyd
PRIMARY PYROCLASTICS
SECONDARY PYROCLASTICS
BASALTIC TUFF
EPICLASTIC SANDSTONE
EPICLASTIC SILTSTONE/ MUDSTONE
LOWER RHYOLITIC TUFF FM.
UNIT
UPPER CWM EIGIAU FM.
PITTS HEAD TUFF FM.
pillow basalt
basaltic hyaloclastite
cleaved mudstone
8
7
6
SUBAQUEOUS PYROCLASTIC FLOWS
5
-Reworked coarse-grained pyroclastics
SUBAQUEOUS PYROCLASTIC FLOWS
4
3
SUBAQUEOUS PYROCLASTIC FLOWS
2
1
HCS
Sg
SCS
Sh
St
Gms
Sp
Su
St
50cm
Sl
Sb
METRES
M Si Sa G
'OFF SHORE'
MID-SHELF
-LOWER SHOREFACE
DISTAL STORM BEDS
Sb
HCS
Su
Sm
Sl
Gm
Sr
Sg
Sg
Sg
Fd
-low-angle XS from traction carpets
'cherty' mudstone
-channelised normally-graded very coarse ss from high density turbidity currents
-slurried mudstone beds
M Si Sa
Fm
Fg
Fm
-normally graded beds of shard-rich sltst. intercalated with non-tuffaceous sltst.
M Si Sa
-less than storm wave base.
Fig. 5.47
Sh
Sh
Sh
Sm
Sg
Sh
Sm
Sh
Sm
Sm
Su
Fm
Sr
Sb
Sp
St
shallow
Sb
bioturbated fine-grained ss
-horizontally bedded ss.
-low-angle trough & swaley XS from storm waves
-winnowed shell lags from fairweather reworking and slow sedimentation rates

Fig. 5.46: Upper flow regime plane-bed lamination within very fine-grained siliceous sandstones directly on top of the Pitts Head Tuff at the head of Cwm Cneifion. Attributed to wave swash processes on retreating transgressive shoreface. Section D2, 3 m. Photograph is approximately 1 metre high. See Fig. 5.44 for stratigraphic position of photo.

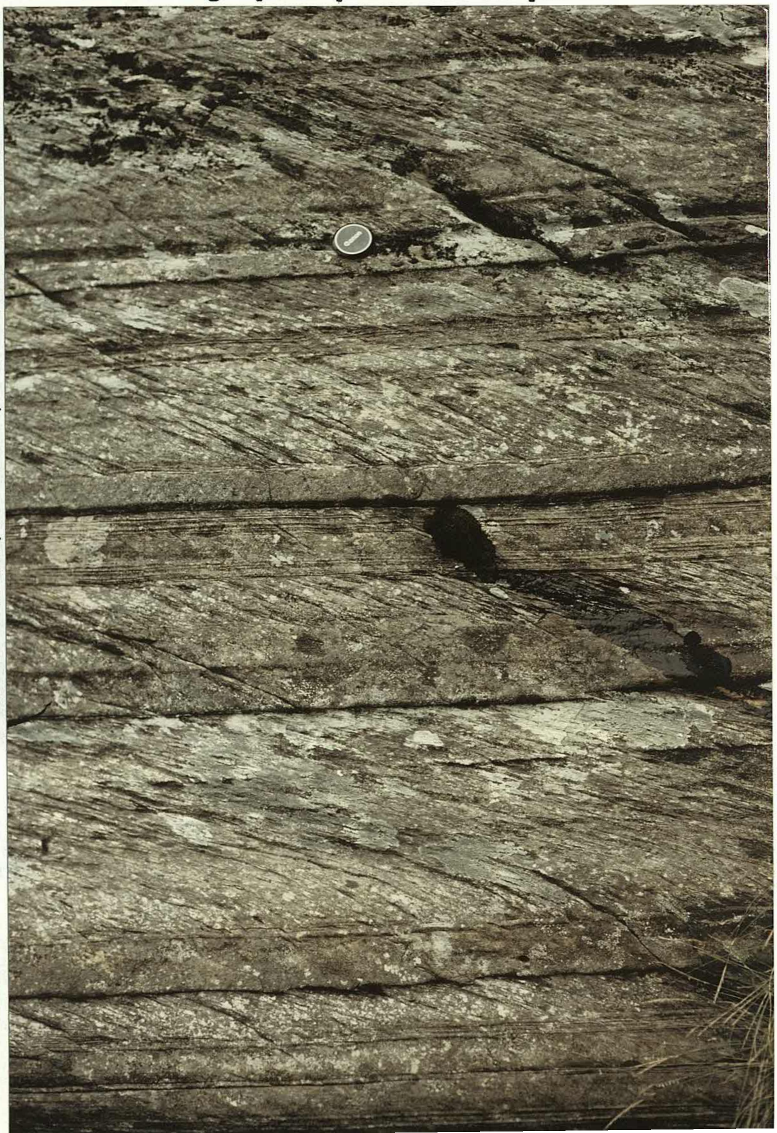

Fig. 5.47: Thin massive and horizontally laminated sandstone beds atrributed to waning storm events below storm wave base. From Upper Cwm Eigiau Fm., Llyn Bochlwyd. Section D1, 175 m. Lens cap is 6 cm wide. See Fig. 5.45 for stratigraphic position of photo.

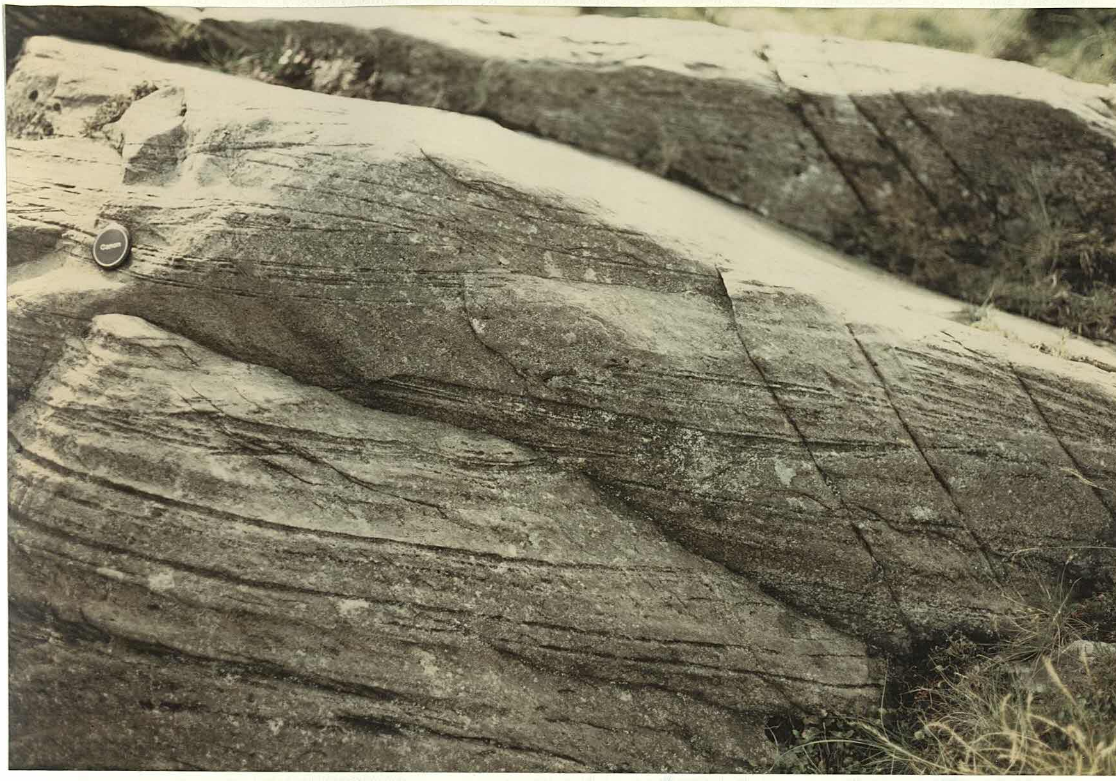

Fig. 5.48: Amalgamated sets of hummocky cross-stratification, Upper Cwm Eigiau Fm. Gribin ridge. Section D1, 332 m.

Fig. 5.49: Pillow of basalt set in lithic-rich hyaloclastic matrix. From Upper Cwm Eigiau Fm, directly beneath Lower Rhyolitic Tuff on Gribin ridge. Section D1, 400 m.

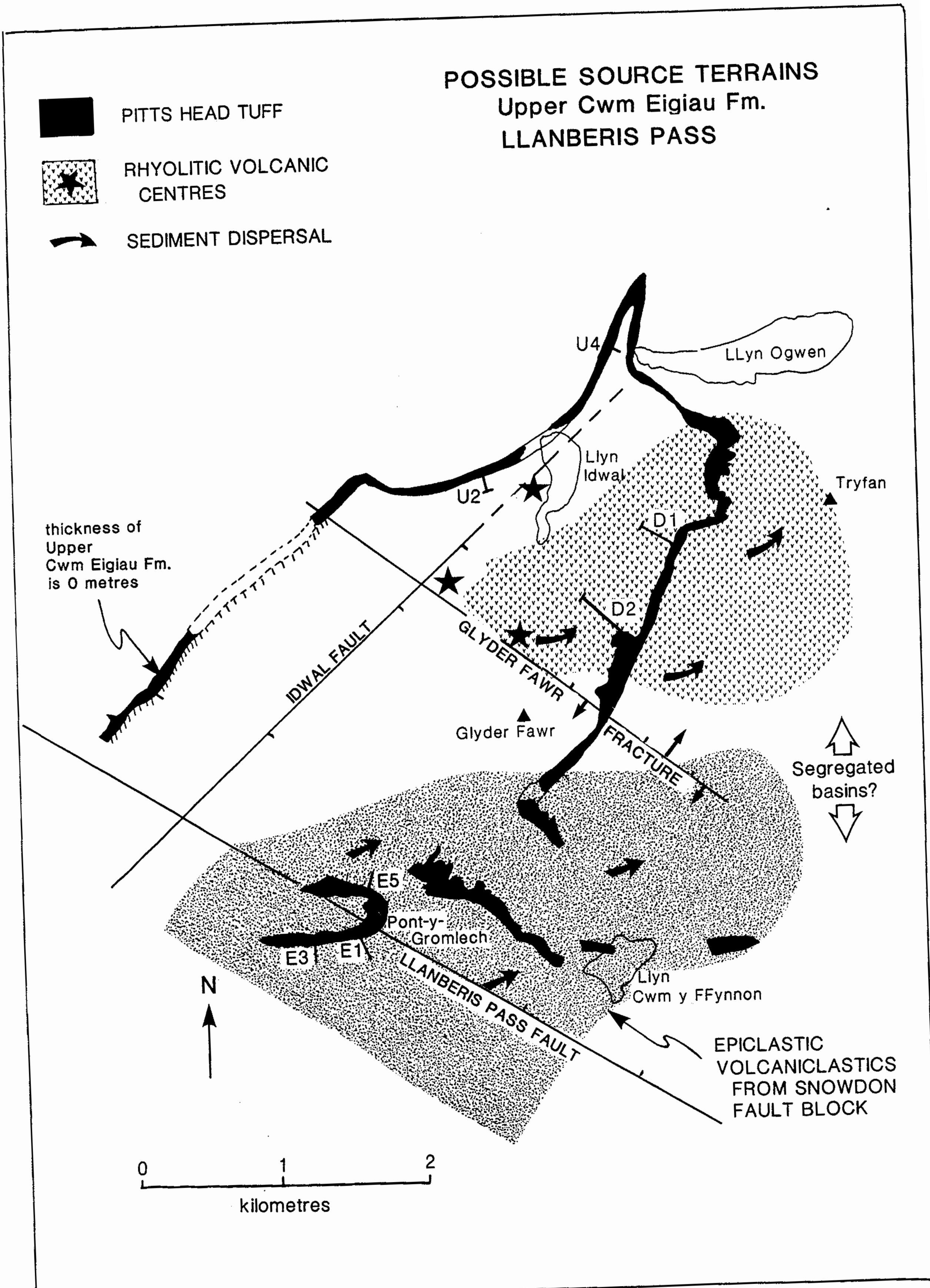

FIG. 5.50: Source terrains and patterns of dispersal of epiclastic and pyroclastic volcaniclastics in the vicinity of Llanberis pass.

UPPER CWM EIGIAU FM. (middle portion)
CAPEL HILL

Section G2 to G8

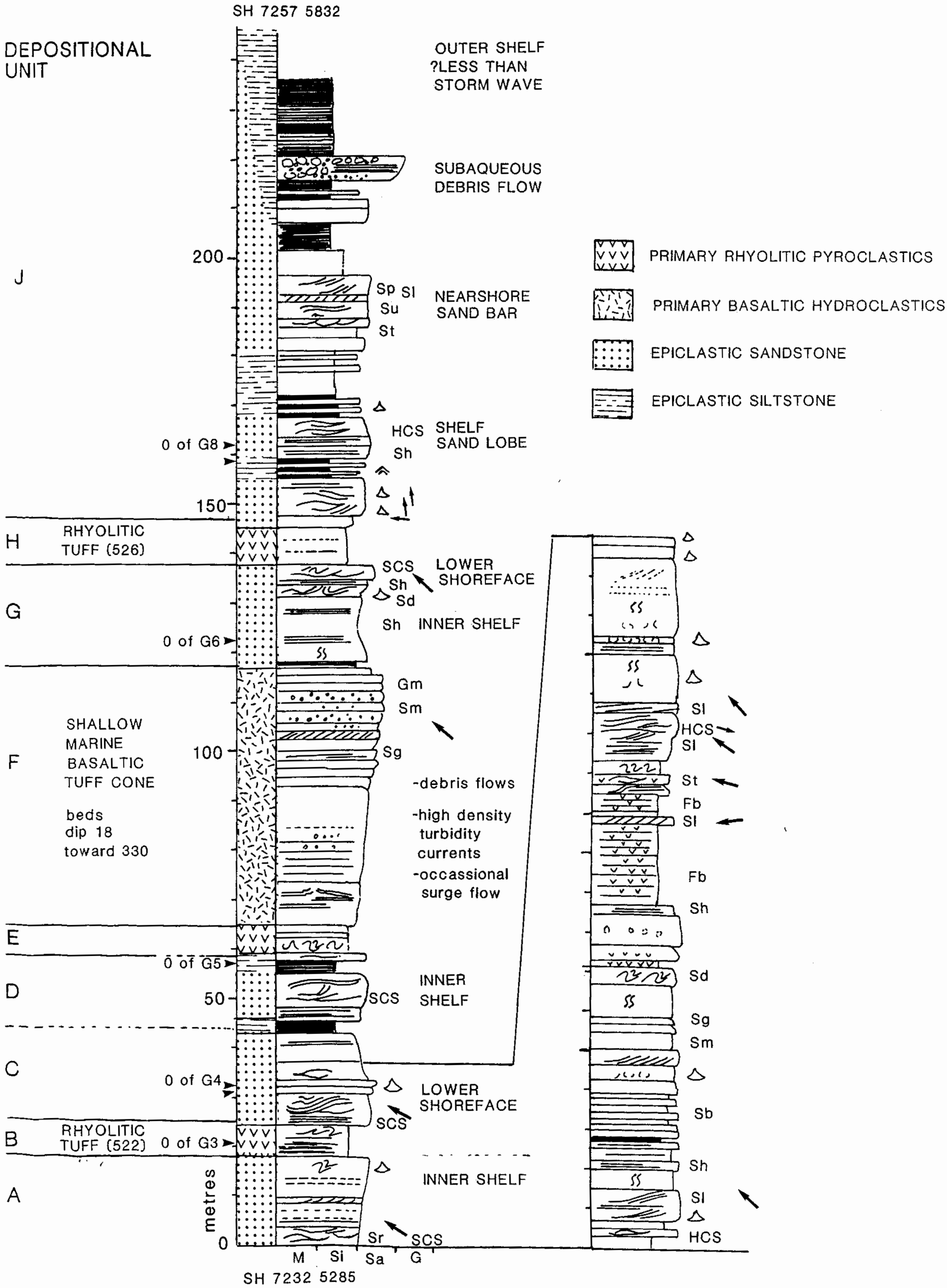

FIG. 5.51: Vertical profile through middle portion of Upper Cwm Eigiau Fm. at Capel Hill.

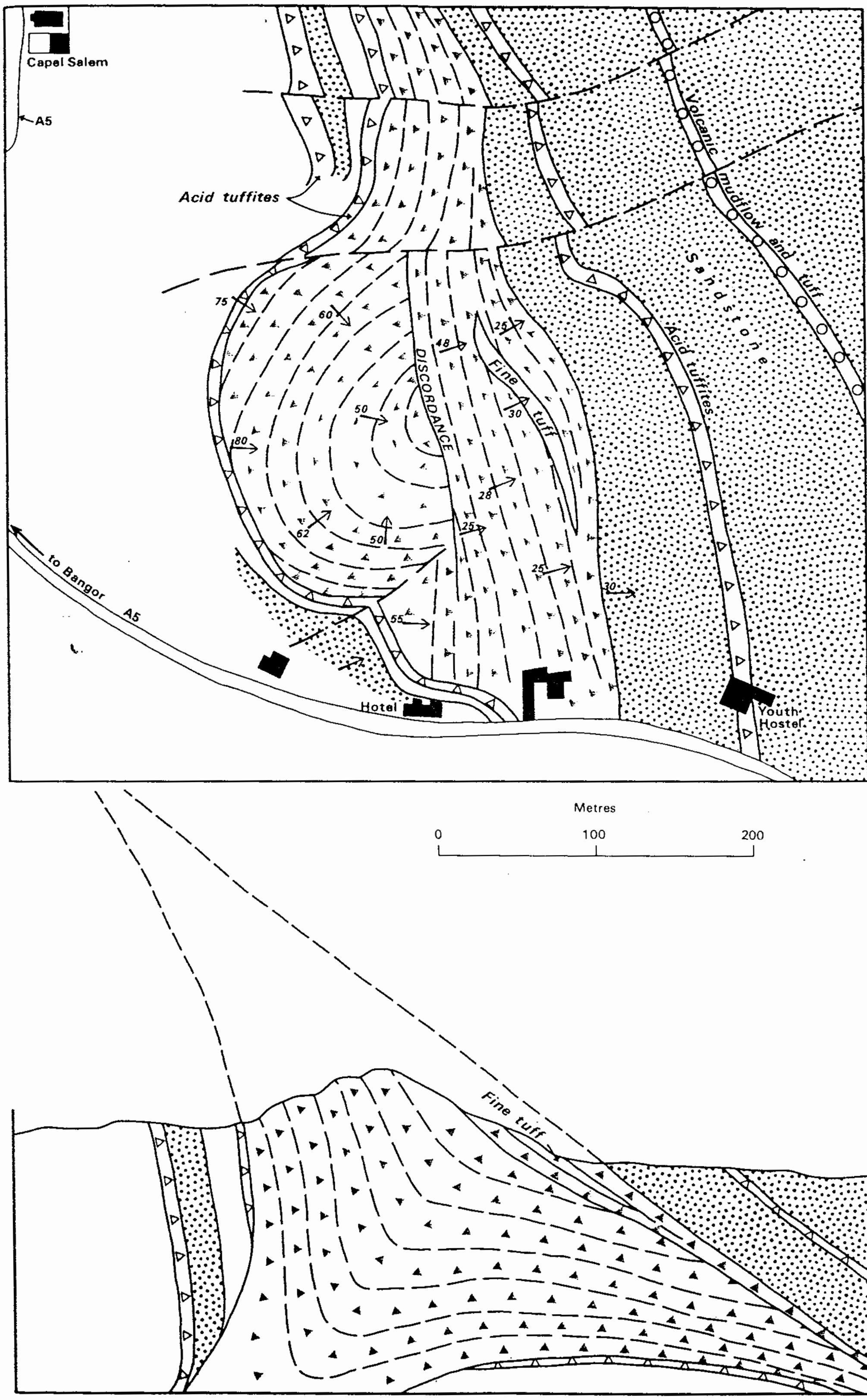

Fig. 5.52: Plan and cross-section of basaltic tuff cone at Capel Hill (From Howells *et al*, 1978).

Fig. 5.53: Normally graded high density turbidites and low-angle cross stratification (LA) from "foreset" of basaltic tuff cone at Capel Hill. Section G5, 41 m.

Fig. 5.54: "Foreset lithic breccia" from sediment gravity flows on slope of a shallow marine basaltic tuff cone, Bedded Pyroclastic Fm., Cwm Glas, SH 614 558, (stratigraphic terminiology and interpretation from P. Kokelaar, pers. comm., 1987)

Fig. 5.55: A) Vertical profiles through heterolithic basaltic mudflow, Upper Cwm Eigiau Fm., north of Capel Hill. Section G8, 56-59 m.

B) Inset map depicting location of vertical profiles with respect to the basaltic vent at Capel Hill.

C) Lateral variation in flow thickness, clast composition and maximum clast sizes with sediment gravity flow at various profile locations.

D) Large angular clast of rhyolitic tuff (RHY) from proximal deposits of uppermost sediment gravity flow, set within pithy pumiceous basaltic matrix. Plastic deformation of clasts suggests many were soft when incorporated. Section 1.

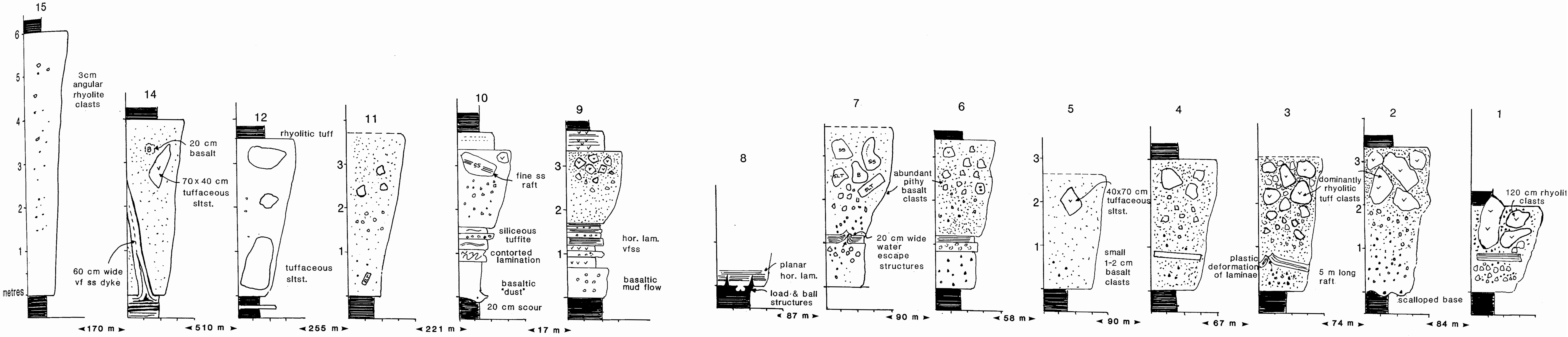
15
14
12
11
10
9
8
7
6
5
4
3
2
1
metres
3cm angular rhyolite clasts
20 cm basalt
70 x 40 cm tuffaceous sltst.
60 cm wide vf ss dyke
rhyolitic tuff
tuffaceous sltst.
fine ss raft
siliceous tuffite
contorted lamination
basaltic "dust"
20 cm scour
hor. lam. vfss
basaltic mud flow
planar hor. lam.
load & ball structures
abundant pithy basalt clasts
20 cm wide water escape structures
40x70 cm tuffaceous sltst.
small 1-2 cm basalt clasts
plastic deformation of laminae
dominantly rhyolitic tuff clasts
5 m long raft
scalloped base
120 cm rhyolite clasts
170 m
510 m
255 m
221 m
17 m
87 m
90 m
58 m
90 m
67 m
74 m
84 m

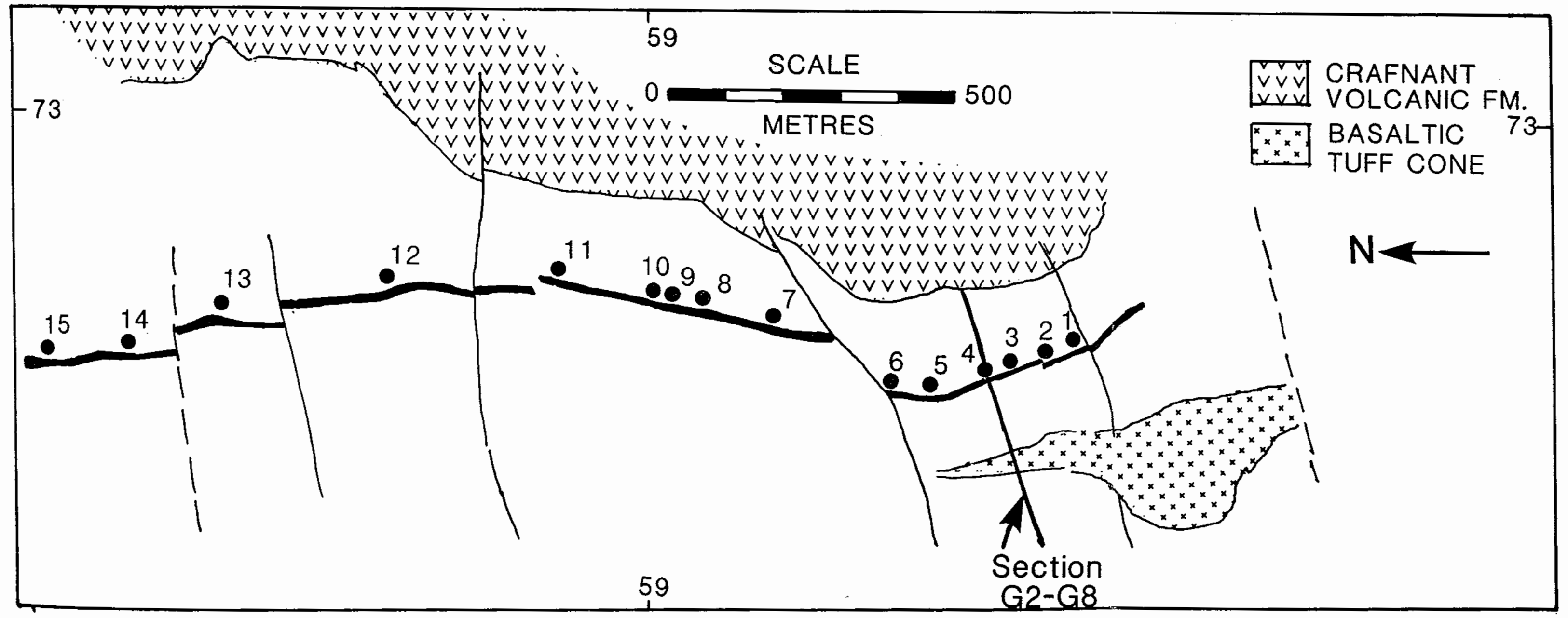
59
73
SCALE
0
500
METRES
CRAFNANT VOLCANIC FM.
BASALTIC TUFF CONE
N
Section G2-G8

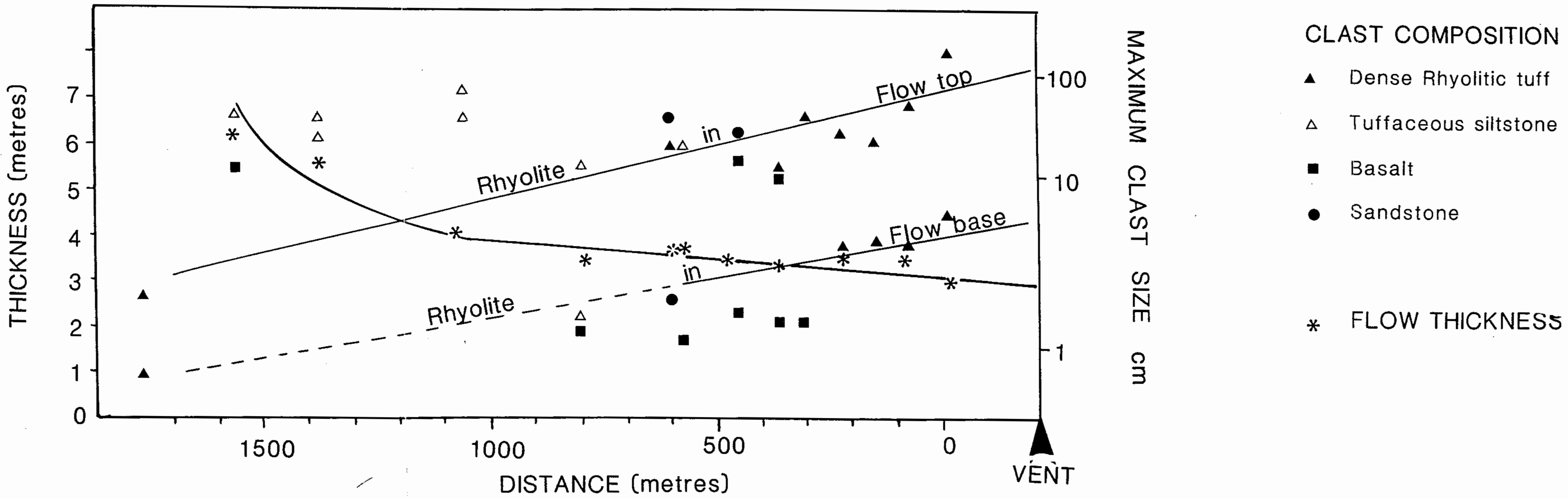
THICKNESS (metres)
MAXIMUM CLAST SIZE cm
DISTANCE (metres)
VENT
Flow top
Flow base
Rhyolite
in
CLAST COMPOSITION
Dense Rhyolitic tuff
Tuffaceous siltstone
Basalt
Sandstone
FLOW THICKNESS

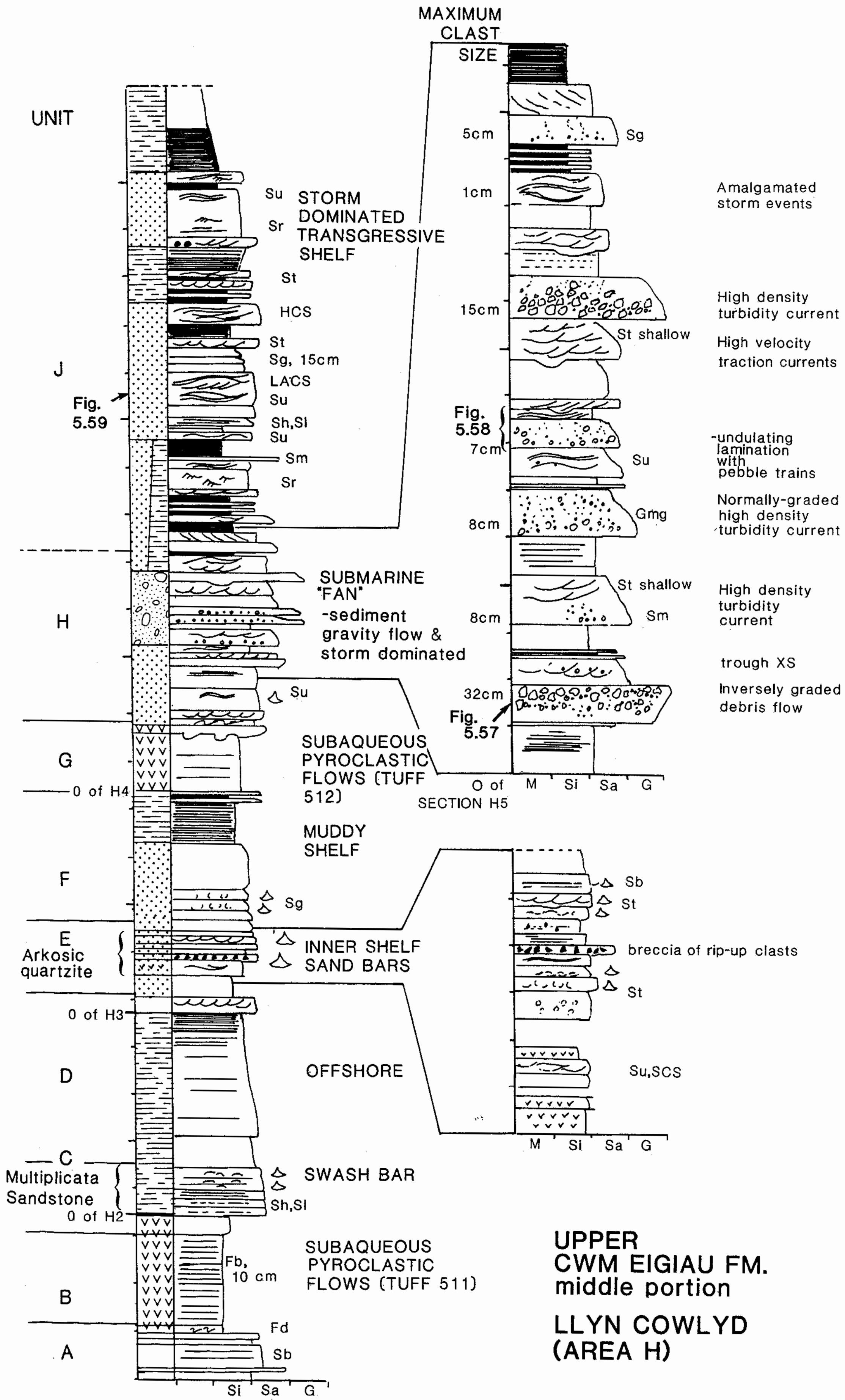

FIG. 5.56: Vertical profile through middle portion of Upper Cwm Eigiau Fm. at Llyn Cowlyd. See Fig. 5.43 for location of section.

Fig. 5.57: Inversely graded matrix-supported debris flow containing angular clasts of fine-grained rhyolitic tuff. Base of flow indicated by arrow. Overlain by medium-coarse grained tuffaceous sandstones displaying low-angle cross-stratification. Section H5, 4.3 m. Notebook is 18.5 cm long for scale.

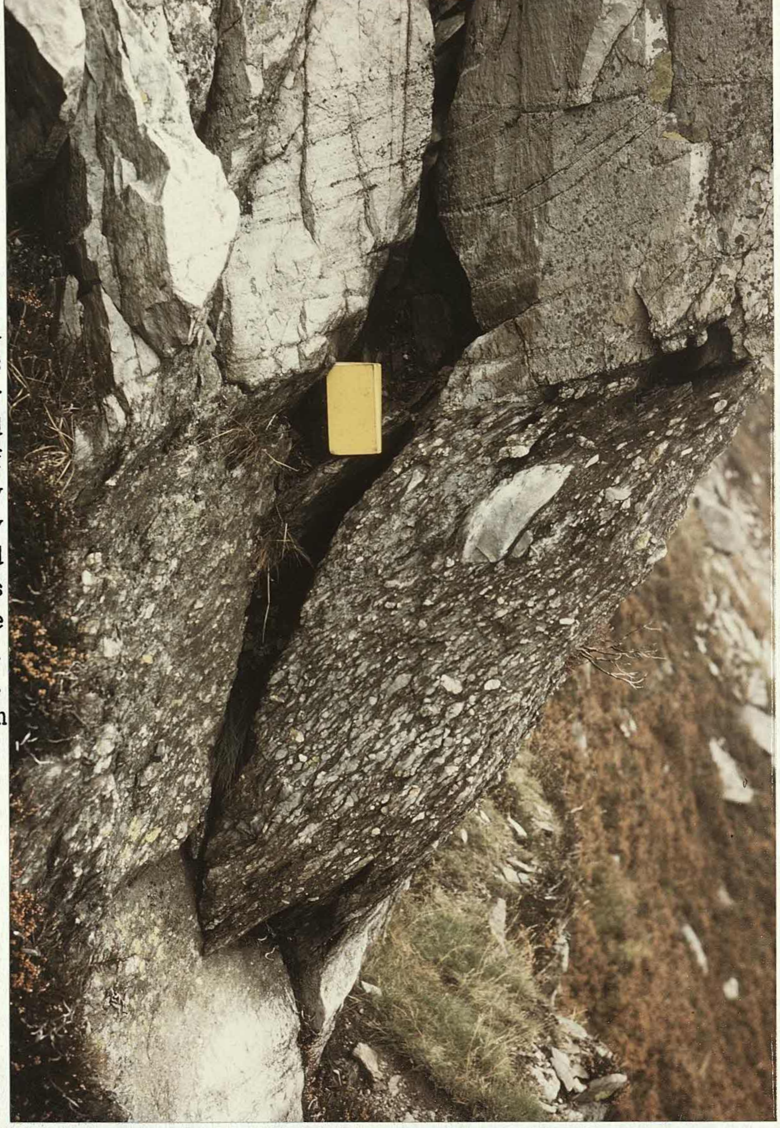

Fig. 5.58: Channelised normally graded high density turbidite containing small sub-angular to sub-rounded clasts of quartzose sandstone and fine-grained rhyolitic tuff. From Upper Cwm Eigiau Fm., Llyn Cowlyd. Section H5, 16 m.

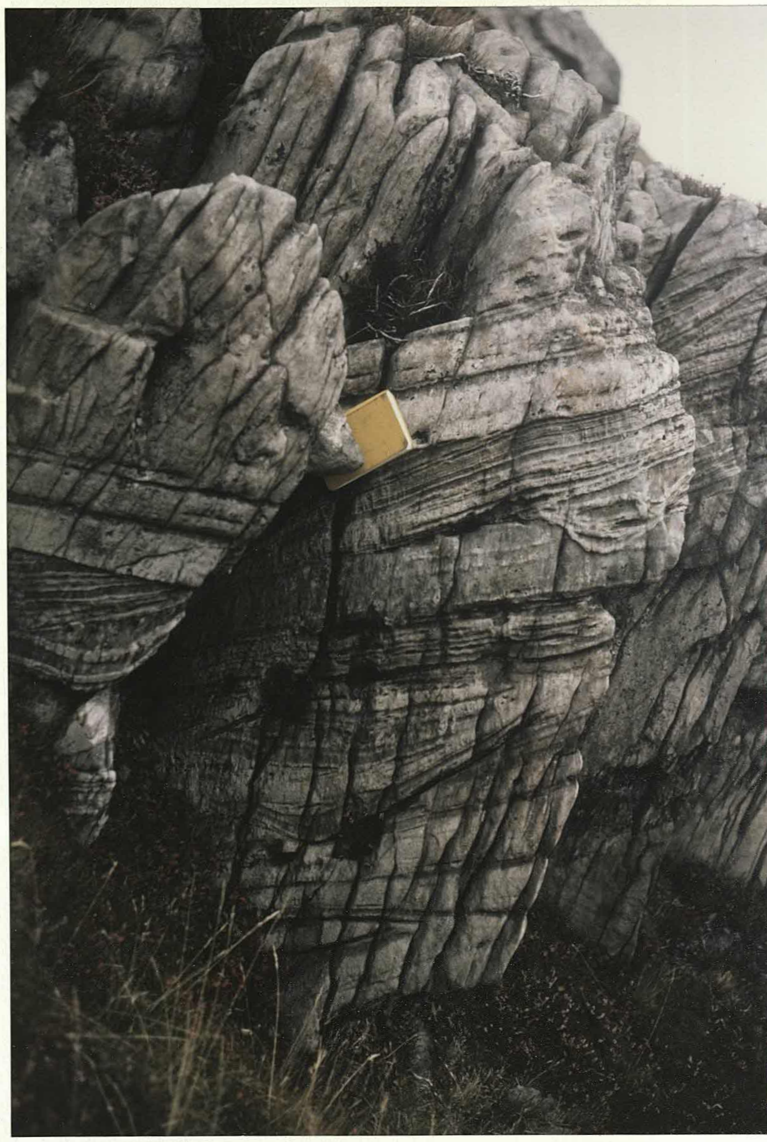

Fig. 5.59a: Low-angle undulating trough cross-stratification and "scour-and-fill" structures attributed to combination of unidirectional currents and wave-oscillation from storms. From Upper Cwm Eigiau Fm., Llyn Cowlyd, Section H4, 58 m.

FIGURE 5.60

MAP A:

1) Lower portion of UCEF (X, units 1,2): Rapid subsidence of the Tryfan depocentre, particularly to the NE where 600 m of mud were deposited. Most sediment, however was probably deposited in much less than 100 m of water. A gradual shallowing of the entire basin occurred before the basin-wide magmatic event (pyroclastic units 3 and B) and onset of the deposition of the sandstone dominated middle portion.

MAP B:

2) Middle portion of UCEF (Y): Deposition of small sand lobes/sand bars in "inner shelf" settings, periodically interrupted by input of either fine-grained pyroclastic flows or more rarely coarse-grained volcanic ash. Limited quantities of sand-grade sediment appear to have been available from most compass directions; regions immediately to the NW of the Llyn Cowld fault, near Llyn Cowlyd itself were furthest from any sediment supplies. Moderation in the amount of differential subsidence between adjacent fault blocks, and lack of resultant topographic relief, allowed development of comparable environments accross the entire basin.

MAP C:

3) Upper portion (C): More pronounced subsidence to the west of the Llyn Cowlyd fault initially resulted in the series of conglomeratic sediment gravity flows at Bwlch Trimarchog, with transgressive storm dominated shoreface or shelf sandstone lobes characterizing other portions of the UCEF.

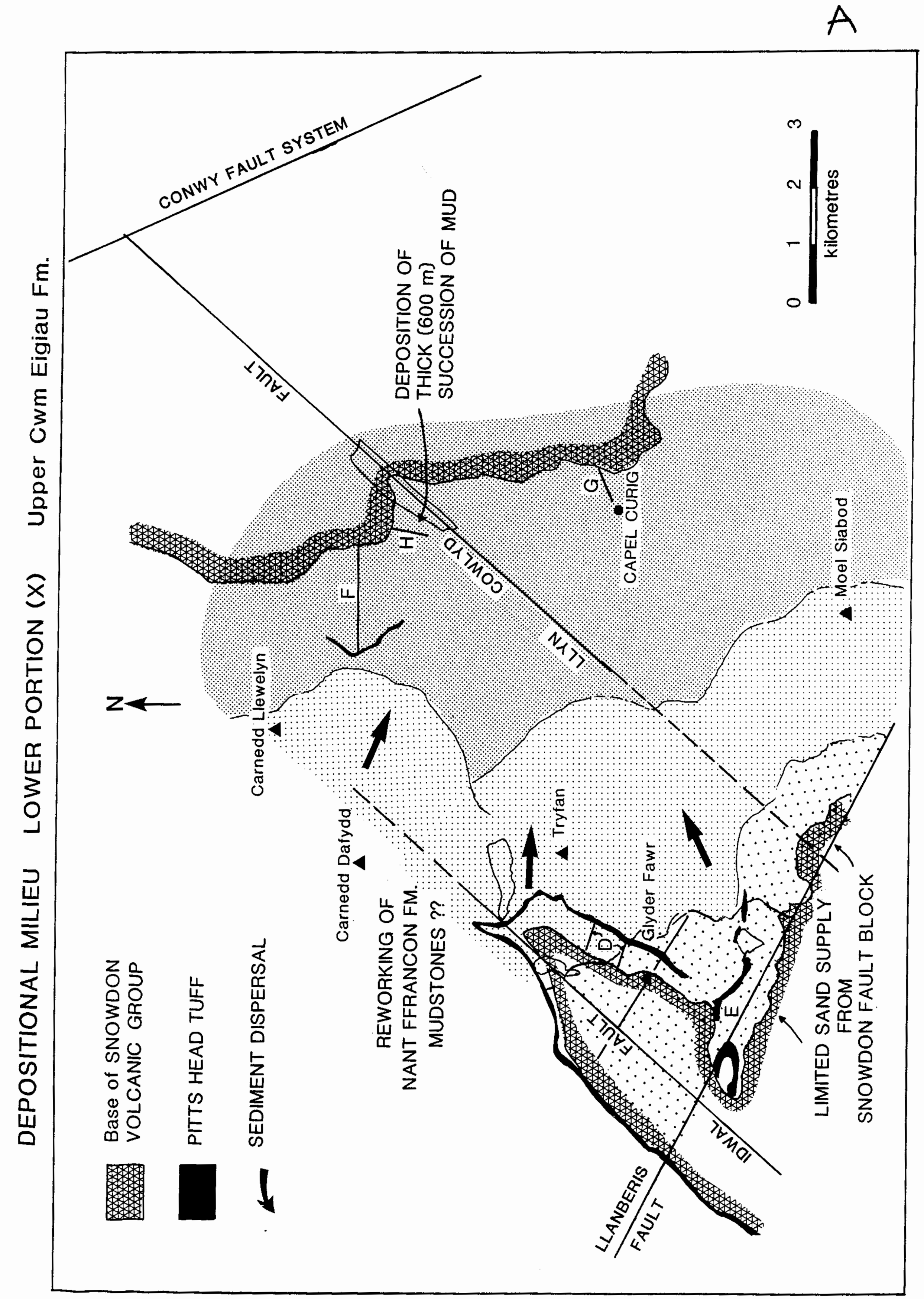

DEPOSITIONAL MILIEU MIDDLE PORTION (Y) Upper Cwm Eigiau Fm.

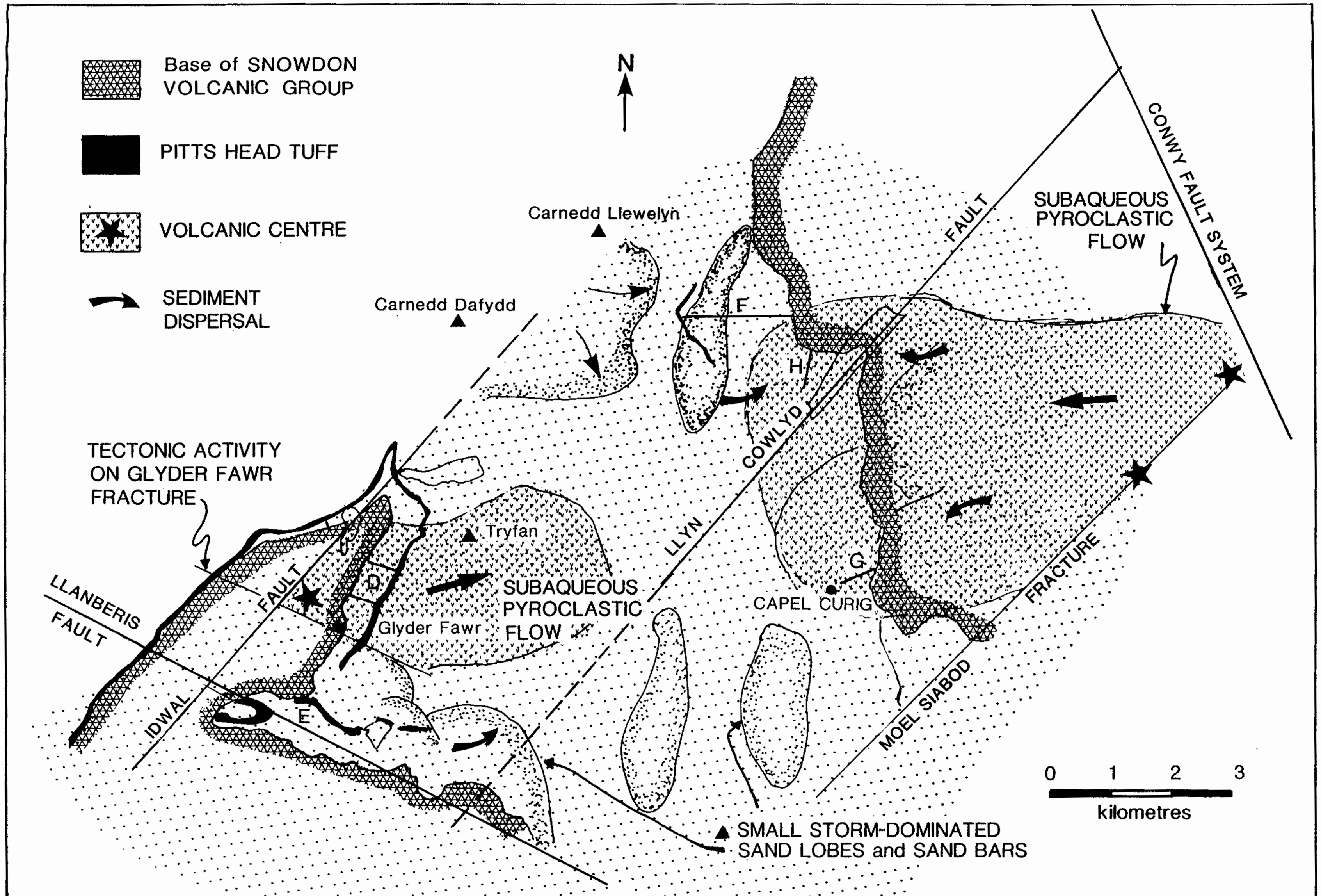

B

DEPOSITIONAL MILIEU UPPER PORTION (Z) Upper Cwm Eigiau Fm.

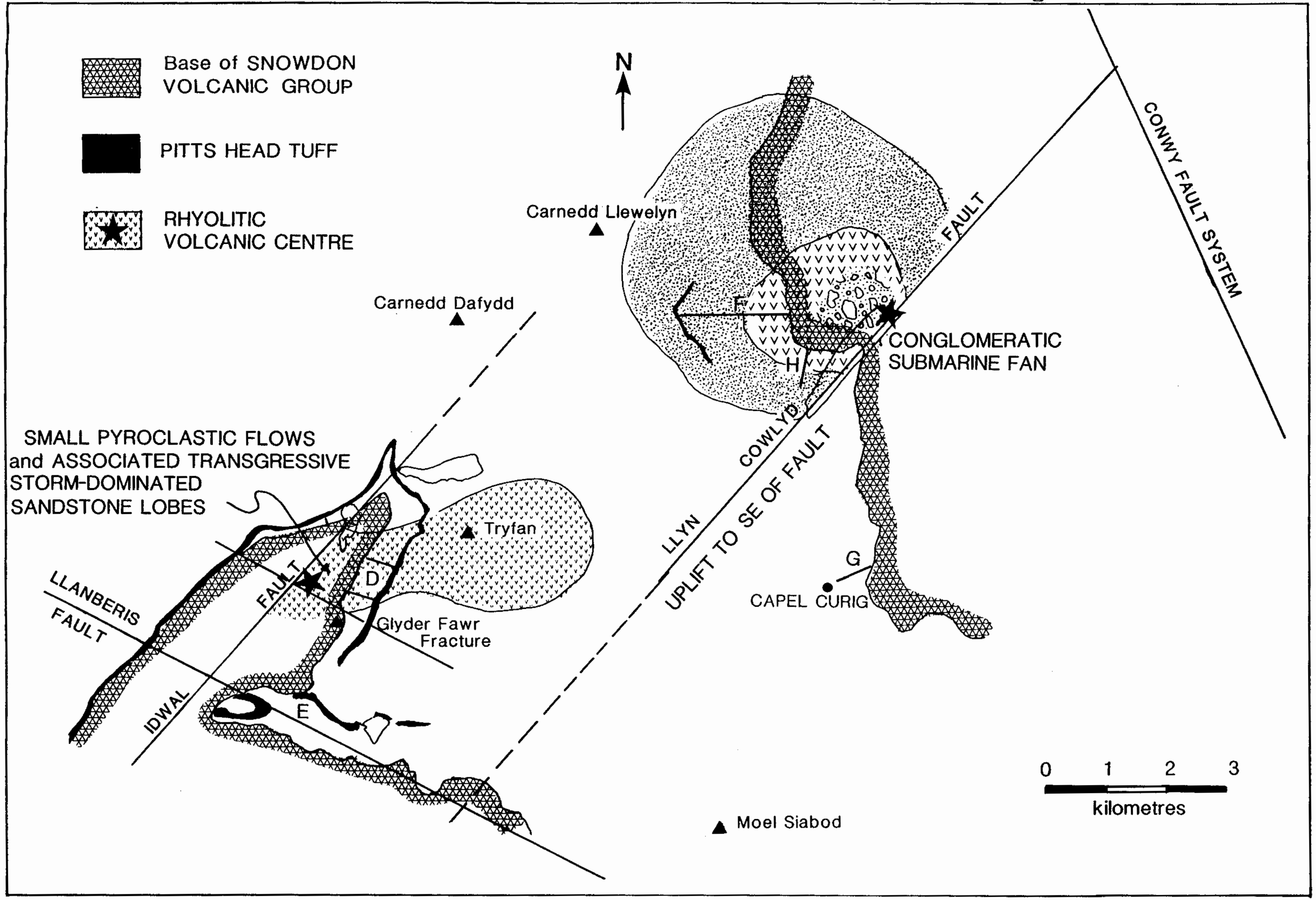

No

lo

FIG. 5.61: Vertical profiles through the Vuggy Mbr. on the east side of Tryfan anticline. Palaeocurrent roses are oriented relative to North-south outcrop face instead of conventional diagram. Photo depicts medium-scale trough cross-stratification from second sandstone unit. Notebook 18 cm fo scale.

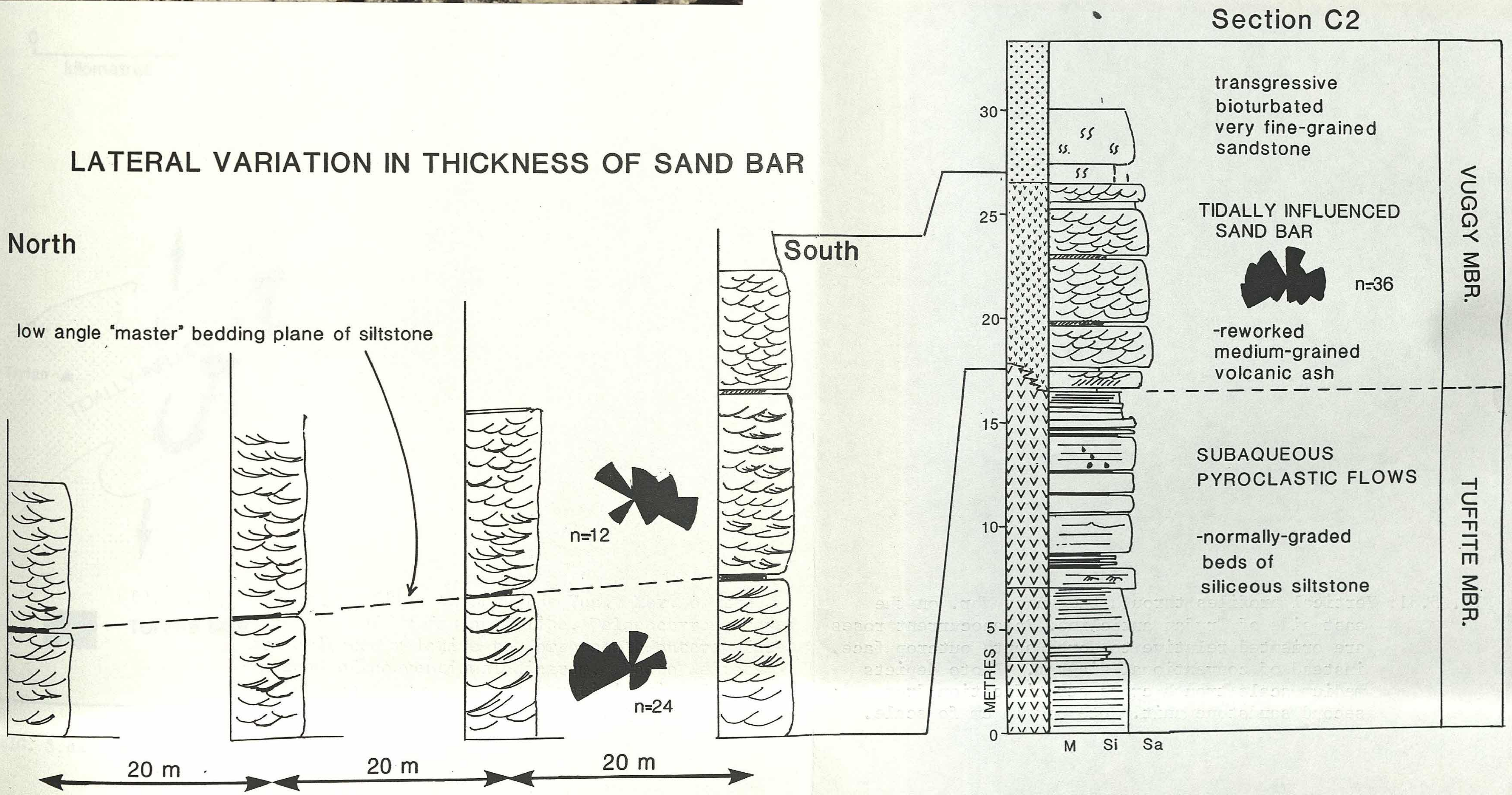
LATERAL VARIATION IN THICKNESS OF SAND BAR
North
South
low angle "master" bedding plane of siltstone
n=12
n=24
20 m
20 m
20 m
Section C2
transgressive
bioturbated
very fine-grained
sandstone
TIDALLY INFLUENCED
SAND BAR
n=36
-reworked
medium-grained
volcanic ash
SUBAQUEOUS
PYROCLASTIC FLOWS
-normally-graded
beds of
siliceous siltstone
VUGGY MBR.
TUFFITE MBR.
METRES
0
5
10
15
20
25
30
M
Si
Sa

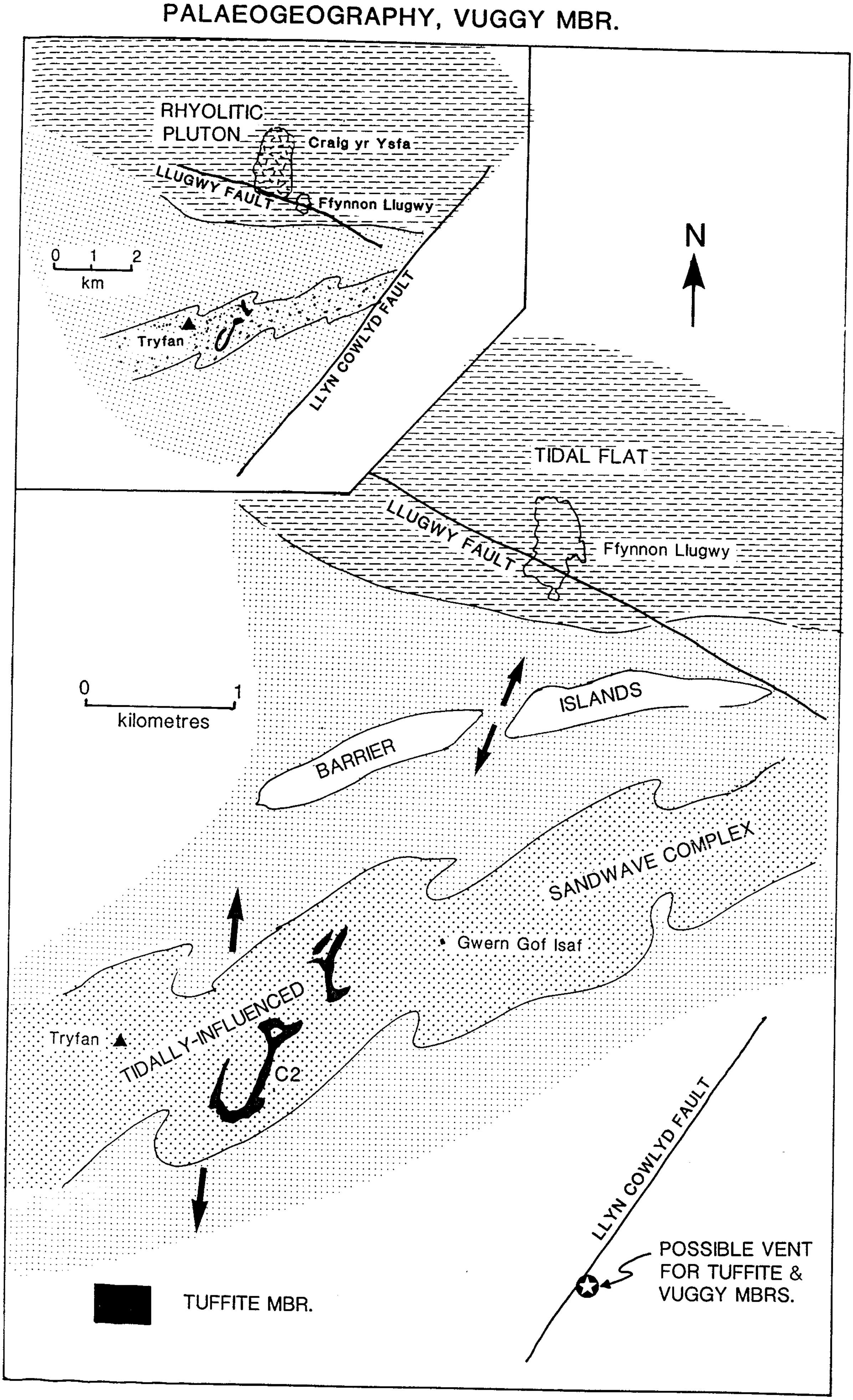

FIG. 5.62: Simplified reconstruction of palaeogeography during deposition of Vuggy Mbr. Also shown is probable vent for both Vuggy and Tuffite Mbrs.

LOCATION	SECTION	RIPPLE SPACING (cm)	RIPPLE HEIGHT (cm)	RIPPLE INDEX	RIPPLE SYMMETRY INDEX	DIRECTION WAVE APPR. FROM	GRAIN SIZE (mm)	ORBITAL DIAMETER (metres)	THRESHOLD VELOCITY m/sec.	MINIMUM WAVE PERIOD	MAXIMUM WAVE PERIOD	DEEPWATER SURFACE WAVELENGTH	MAXIMUM DEPTH (metres)	WAVE POWER kw/m
								0.077	0.11	0.8	2.1	7.0	3.6	2
Gwern Gof Member, Ddeugwm Fm.	C4 35m	5	0.5	10	4	290°	0.18	0.062	0.11	0.7	1.8	5.0	2.5	1
	C4 35.3m	4	1.0	4	1.67	319°	0.18	0.100	0.13	0.90	2.4	8.8	4.5	4
	C4 37.74	6.5	1.2	5.42	1.0	290°	0.25	0.092	0.13	0.90	2.2	7.8	3.9	3
	C4 42m	6	1.7	3.53	?	310°	0.25	0.108	0.13	1.0	2.5	9.8	5.1	5
	C4 43m	7	1.5	4.67	?	310°	0.25							
								0.138	0.14	1.1	3.0	14.3	7.7	12
Cwm Bigiau Fm.	F3 14m	9	0.8	11.25	1	18/198°	0.25	0.123	0.14	1.1	2.8	12.0	6.3	8
	G6	8	2.5	3.20	1									
	P3 339m	9	1.5	6	1	342/162°	0.10	0.138	0.11	1.1	3.8	22.6	13.8	38
	P3 338m	6	1.2	5	1	164/344°	0.10	0.092	0.10	0.9	2.8	12.3	7.1	8
Capel Curig Mbr.- Cwm Clorad Isaf	B4 4.05	12.5ª	3	4.2	2.57	185°	0.20	0.192	0.15	1.3	4.1	26.2	15.2	55.
	B4 4.44m	47.5ª	7.	6.8	4	?	1.2	0.731	0.38	2.6	6.1	57.0	28.1	385.
	B4 6.73	38ª	14.	2.57	1.53	165°	1.5							
	B4 7.23	30ª	7.0	4.28	2.00	140°	1.5	0.462	0.39	2.0	3.7	21.4	8.8	34
	B4 7.58	20ª	3.0	6.67	---	142°	1.5	0.308	0.37	1.7	2.6	10.4	3.7	6.
	B4 8.10	38ª	8.0	4.75	---	---	1.2	0.585	0.40	2.3	4.6	32.8	14.3	95.
	B4 10.05	21.5ª	2.5	8.6	1,52	155°	1.5	0.331	0.37	1.7	2.8	11.9	4.4	8.
	B4 10.80	24.0ª	5	4.8	---	---	0.80	0.369	0.30	1.8	3.9	10.7	10.7	42
	B4 13.30	44.0ª	6.50	6.76	2.14	162°	1.5	0.677	0.41	2.5	5.2	42.4	19.2	181.
	B4 18.30	66.0ª	9.0	7.33	2.30	186°	1.5	1.000	0.43	3.0	7.3	83.6	42.1	1000
	B4 18.30	74.0	8.7	8.50	----	186°	1.5	1.138	0.44	3.2	8.2	104.9	54.5	1763
	B4 18.30	74.0	8.7	8.50	----	186°	**1.0**	1.138	0.37	3.2	9.6	142.7	80.9	3768
	B4 18.30	74.0	8.7	8.50	----	186°	**2.0**	1.138	0.49	3.2	7.4	84.8	40.9	1029.
	B4 18.40	18.0ª	2.50	7.20	2,0	150°	0.17	0.277	0.16	1.6	5.6	49.1	30.7	263.
	B4 19.0	25ª	5??	5.0	1.5	172°	0.25	0.385	0.19	1.9	6.5	66.4	41.1	556.
	B4 25.2	36.0	5.5	6.5	1.76	150°	0.50	0.554	0.26	2.2	6.6	67.9	38.3	591.
	B4 29.0	4.8	1.1	4.4	2.6	150°	0.16	0.074	0.11	0.8	2.1	7.0	3.6	2
	B4 30.0	7.5	1.0	7.5	1.5	170°	0.08	0.115	0.10	1.0	3.5	19.3	11.8	25.
Nantmor	V3 30 m	37.5	----	----	----	318/138°	1.0	0.577	0.34	2.3	5.3	43.4	21.0	193.
	V3 73 m	14.0	2.0	7.0	----	-----	0.18	0.215	0.15	1.4	4.6	32.8	19.6	95
Llanberis Pass	E8 29 m	53.	8.0	6.63	----	304/124°	1.2	0.815	0.42	2.7	6.1	58.7	28.0	410.
	E9 37 m	50	10	5.0	----	310/130°	1.2	0.769	0.41	2.6	5.8	53.0	24.9	317.0
Tudwals Peninsulsa		57.5	----	----	----	SE	2.0	.855	0.47	2.8	5.9	54.2	24.6	341.
Bedded Pyroclastics		40 cm	8.0	----	----	SW	coarse	0.615	0.45	2.3	4.3	28.9	11.7	69.0

FIG. 5.63: Location and parameters of ripples used for application of linear wave theory. All values calculated using equations provided by Diem, 1987. See Appendix 4 for a few cautionary notes.

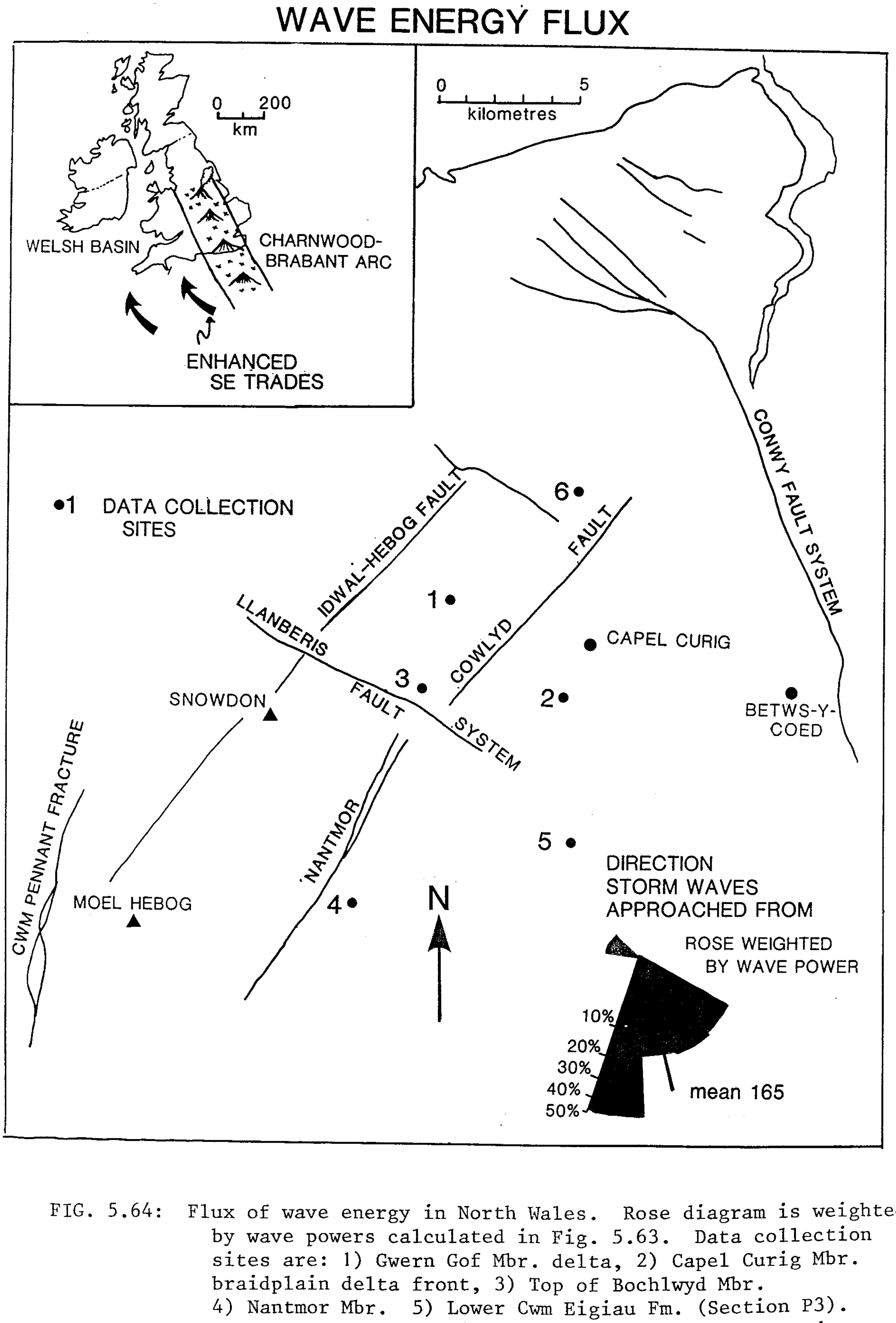

FIG. 5.64: Flux of wave energy in North Wales. Rose diagram is weighted by wave powers calculated in Fig. 5.63. Data collection sites are: 1) Gwern Gof Mbr. delta, 2) Capel Curig Mbr. braidplain delta front, 3) Top of Bochlwyd Mbr. 4) Nantmor Mbr. 5) Lower Cwm Eigiau Fm. (Section P3). Inset map shows relation of wave regime to Charnwood - Brabant arc.

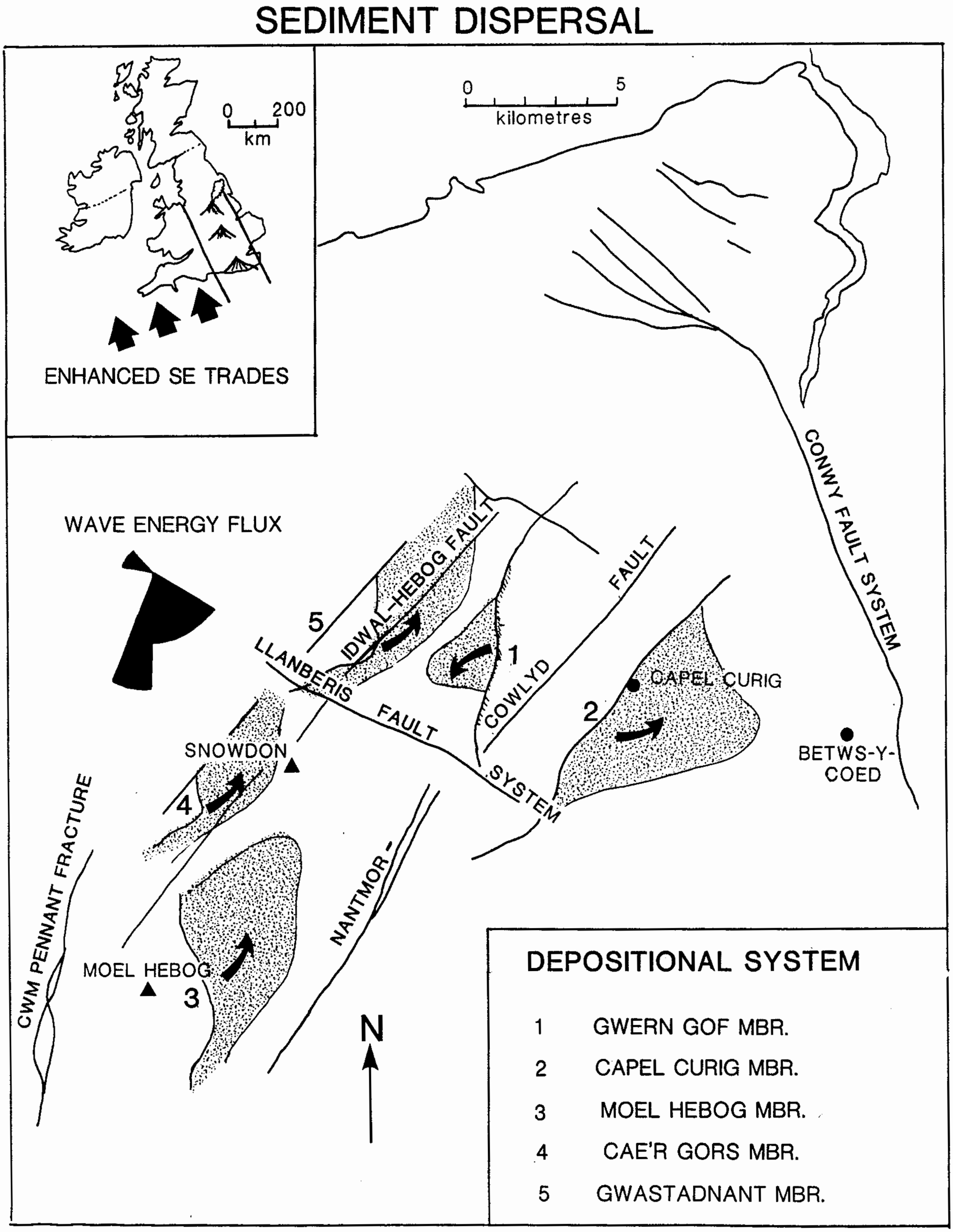

FIG. 5.65: Pattern of sediment dispersal (shaded tone) on several delta fronts. Rose diagram depicts direction that wave energy approached from. Inset map shows inferred wind regime in the NE-SW Welsh basin.

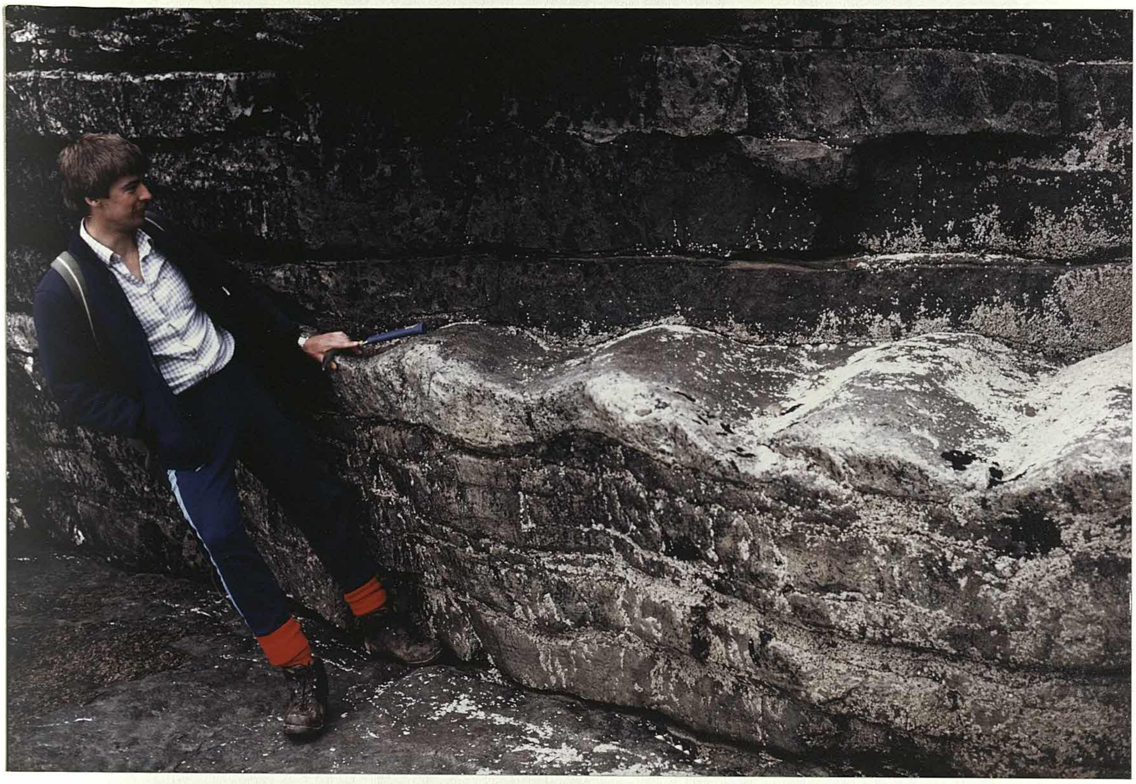

Fig. 5.66: Large, straight crested, slightly asymmetric, in-phase wave ripples from Areing strata on St. Tudwal's Peninsula. Crestline is oriented approximately east-west.

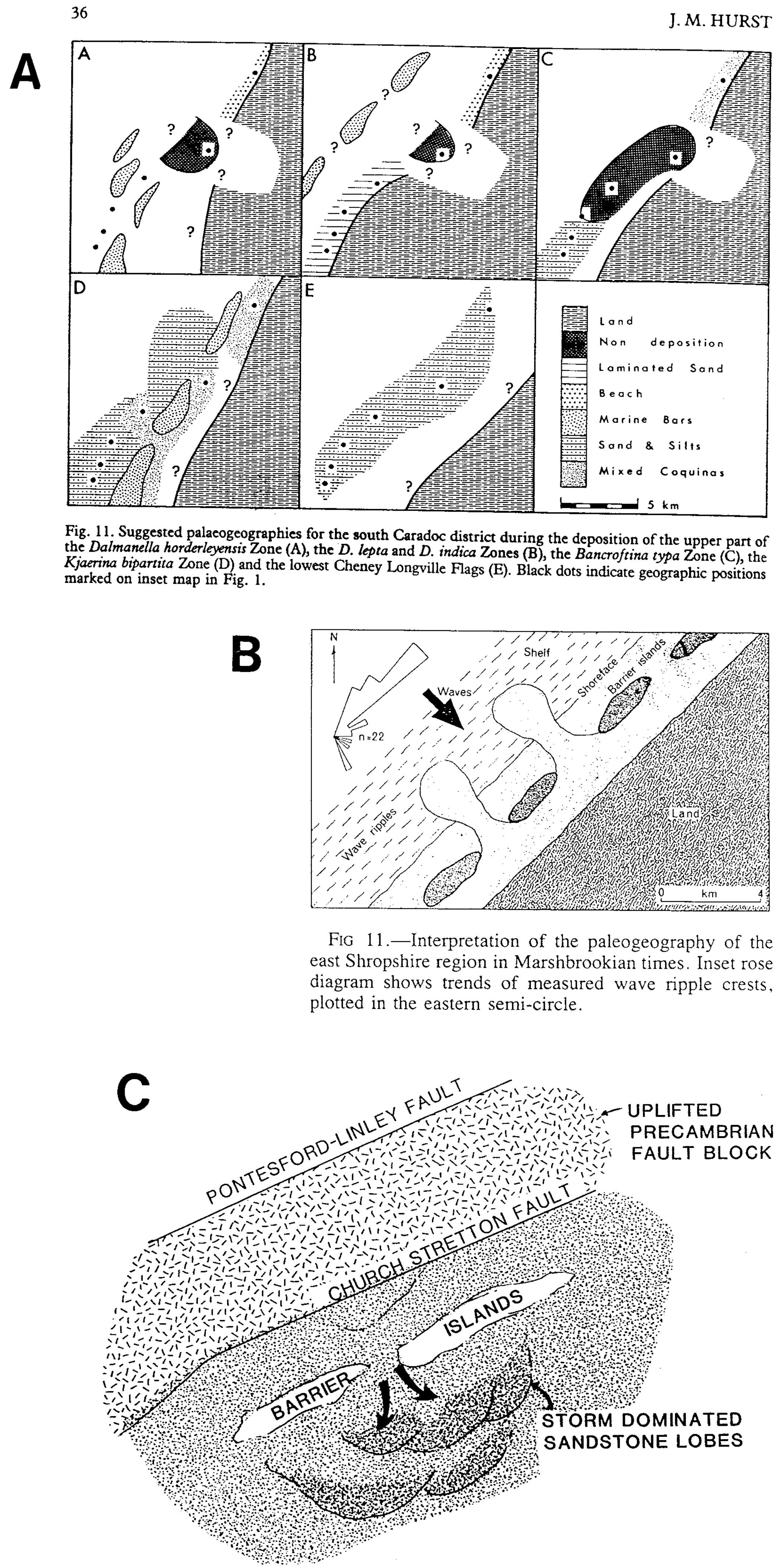

Fig. 5.67: Palaeogeogeography during Caradocian in South Shropshire.

A) Woolstonian (Upper Longvillian) interpretation by Hurst (1979).

B) Marshbrookian palaeogeography suggested by Brenchley & Newall (1980)

(C) Postulated reinterpretation of palaeogeography from this study. See text for further discussion.

Chapter 6

FIG. 6.1: Uplift in modern volcanic fields.

FIG.1 UPLIFT IN MODERN VOLCANIC AREAS

LOCATION	MAXIMUM AMOUNT OF UPLIFT	TIME SPAN	RATE OF UPLIFT	AREA INVOLVED	NATURE OF ERUPTION	ERUPTION SIZE	MAGMA COMPOSITION	TECTONIC SETTING	References
Mt. St. Helens Washington	150m (partly lateral bulge)	2 monthes	2.7m/day	3km2	pyroclastic surge, flow and air fall	0.189km3	mafic dacite	compressional continental arc stratovolcano	Lipman et al, 1981 Moore and Albee, 1981 Rowley et al, 1981 Scandone and Malone, 1985
Kilauea, USA	0.700m	22.5 monthes	.377m/yr	13km2	lava	0.075km3	basalt	intraplate "hot spot"	Fiske and Kinoshita, 1969
White Island, New Zealand	0.256m	5 years	——	<0.20km2	phreato-magmatic to strombolian	0.008km3	andesite	?back arc basin	Clark, 1979 Clark, 1982 Houghton, 1983
Long Valley, CA	0.350m	3 years	0.116m/yr	700km2	* pyroclastic Bishops tuff	*500km3	* rhyolite	extensional, Basin and Range	Denlinger and Riley, 1984 Hildreth and Mahood, 1985 Hill et al, 1985
Yellowstone	>0.700m	53 years	0.014m/yr	up to 8000km2	* pyroclastic eruptions	rhyolite	* andesite	extensional,	Pelton and Smith, 1979 Reilinger et al, 1977 Fritz and Harrison, 1985
Rio Grande Rift Socorro	0.350m	70 years	0.006m/yr	anomaly 70km long	——	——		continental rift	Bachman and Mehnert, 1978 Relinger et al, 1980 Reilinger and Oliver, 1980
Toba, Sumatra	500m	less than 100,000 years	——	2500km2	pyroclastic ash flows	*3000km3	*rhyodacite	extensional, back arc basin	Aldiss and Ghazali, 1984

* PREVIOUS ERUPTIONS

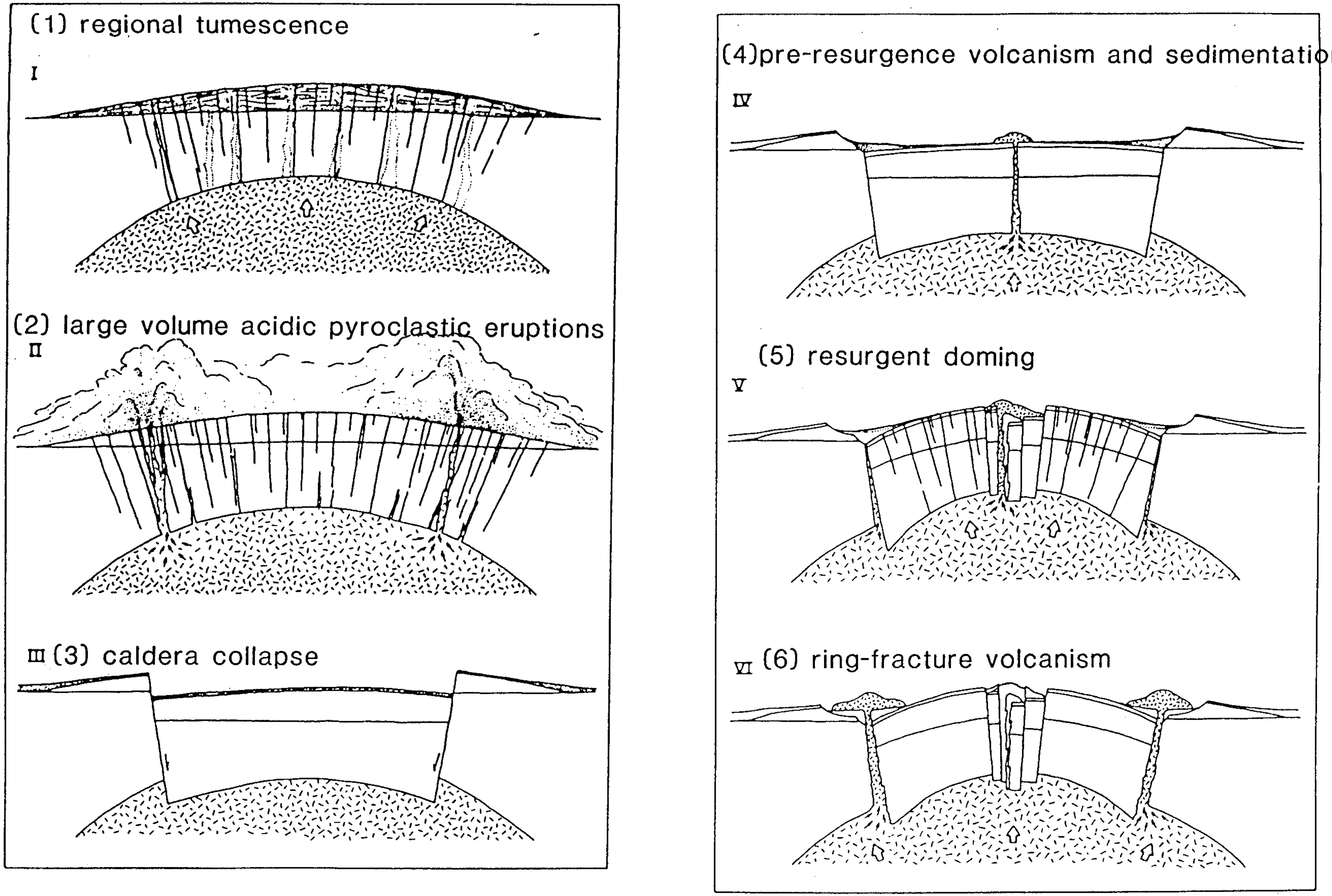

FIG. 6.2: The cycle of uplift, eruption and subsidence associated with many calderas (from Smith & Bailey, 1968).

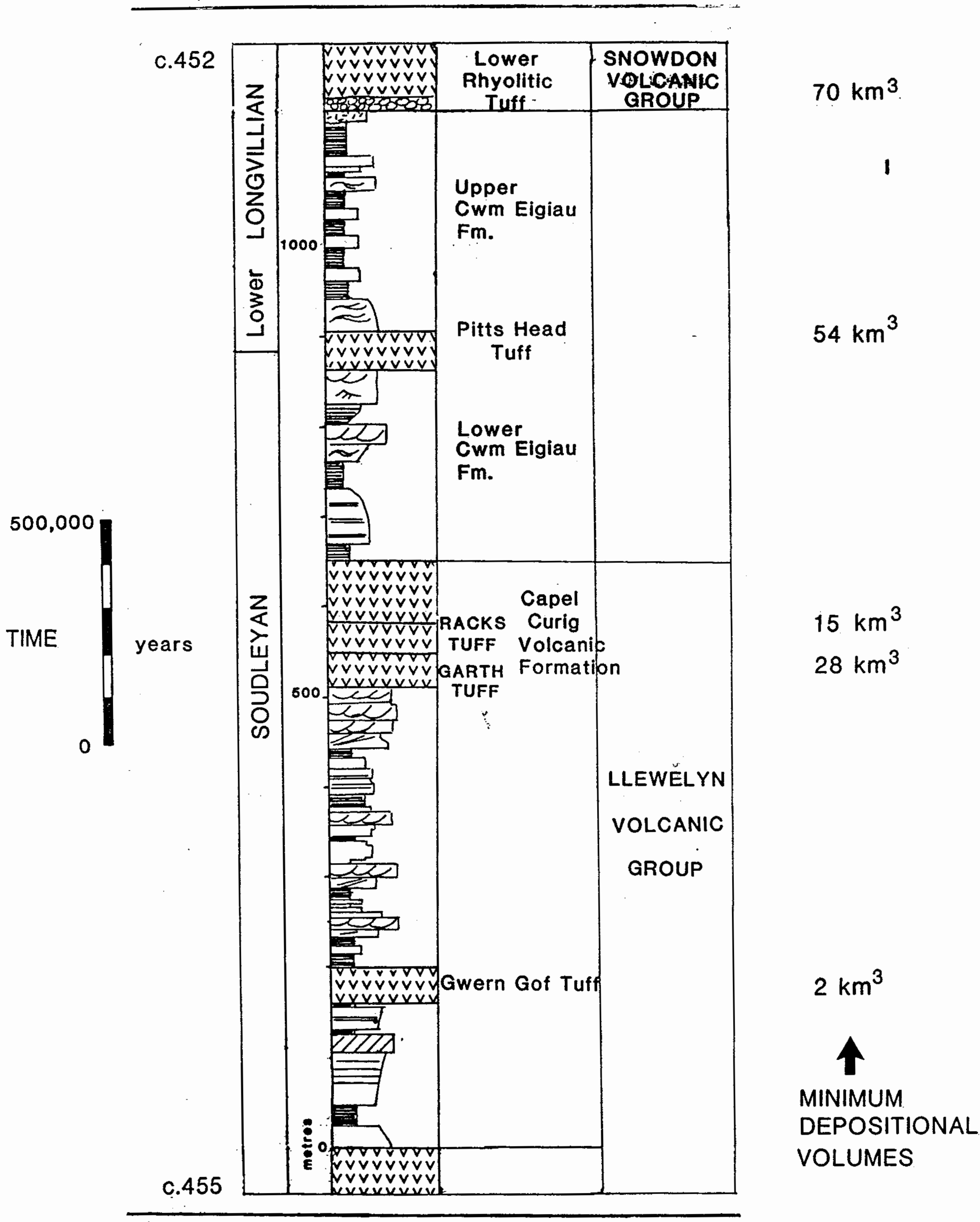

FIG. 6.3: Stratigraphic column showing position of major ignimbrites.

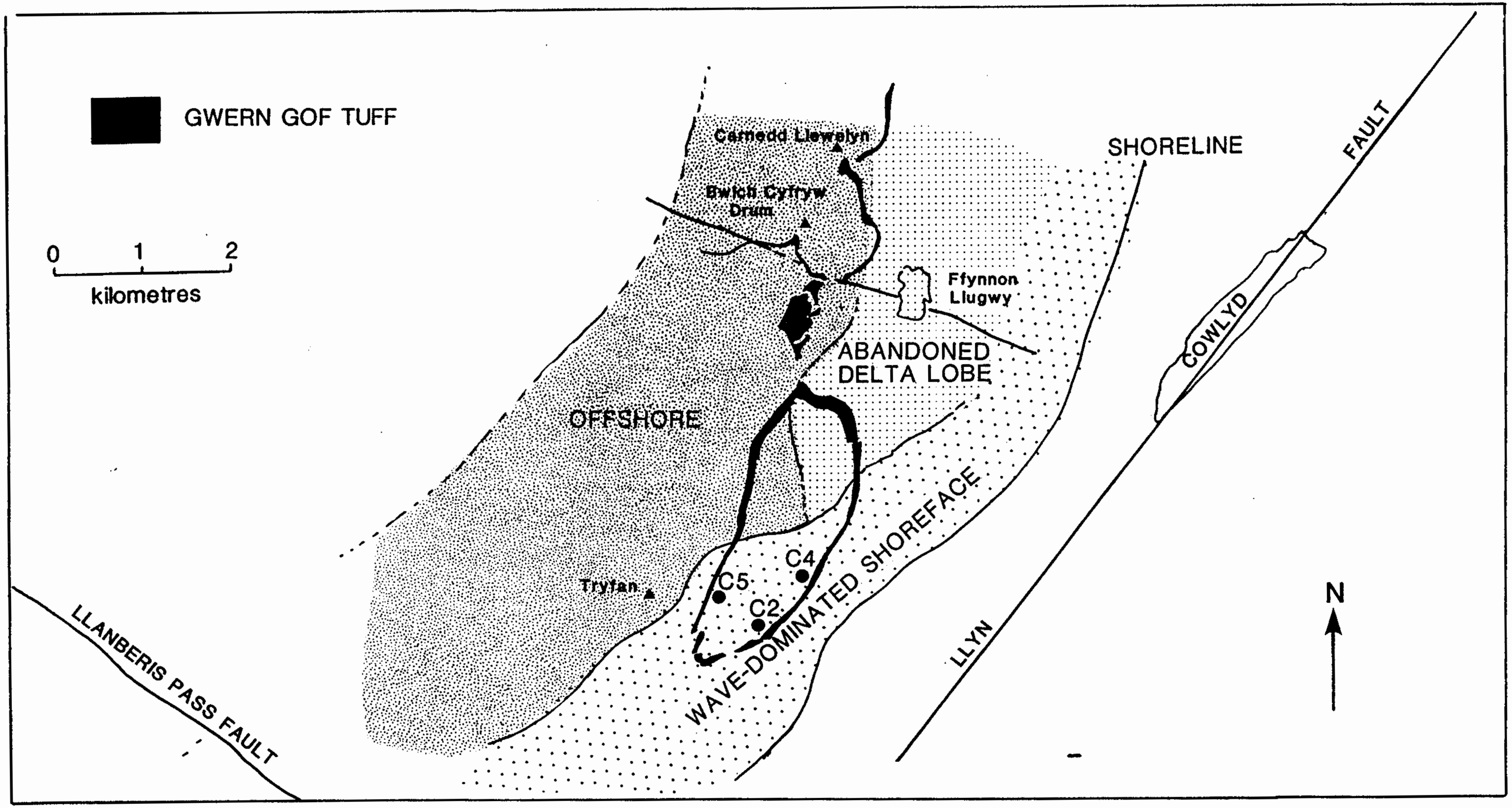

FIG. 6.4: Palaeogeography beneath Gwern Gof Tuff.

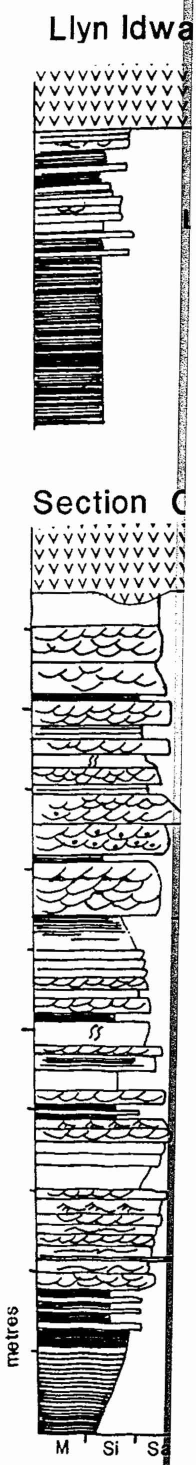

FIG. 6.5: VERTICAL PROFILES BENEATH GARTH TUFF.

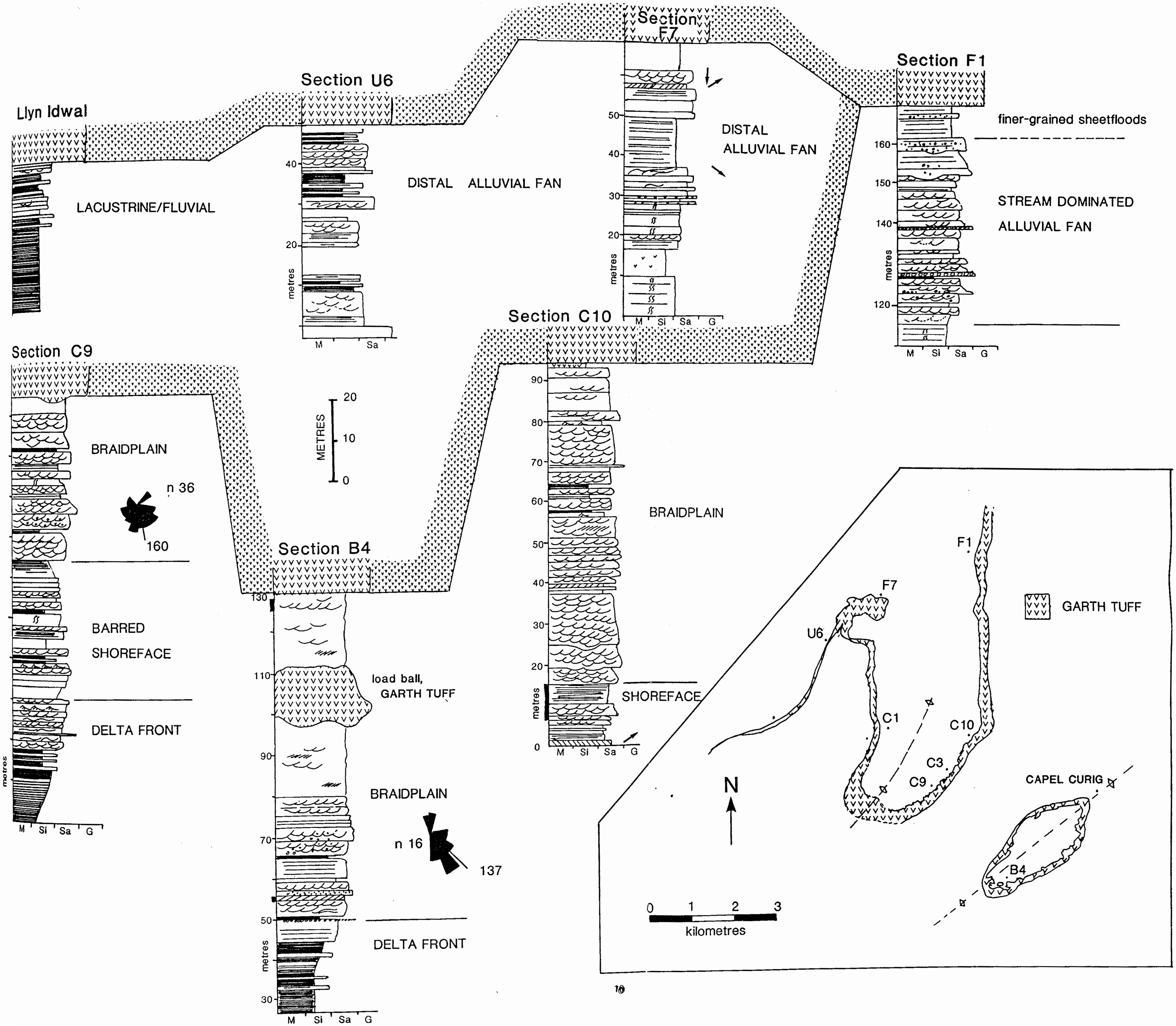
Llyn Idwal
LACUSTRINE/FLUVIAL
Section U6
DISTAL ALLUVIAL FAN
Section F7
DISTAL
ALLUVIAL FAN
Section F1
finer-grained sheetfloods
STREAM DOMINATED
ALLUVIAL FAN
Section C9
BRAIDPLAIN
n 36
160
BARRED
SHOREFACE
DELTA FRONT
METRES
Section B4
load ball,
GARTH TUFF
BRAIDPLAIN
n 16
137
DELTA FRONT
Section C10
BRAIDPLAIN
SHOREFACE
metres
M Si Sa G
F1
F7
U6
C1
C10
C3
C9
CAPEL CURIG
B4
GARTH TUFF
N
kilometres

FIG. 6.6: Planar-tabular cross stratification containing abundant magnetic heavy minerals from fluvial deposits of Moel Siabod Mbr., Cwm Clorad Isaf, Capel Curig anticline.

FIG. 6.7: Micro- hummocky cross-stratification associated with load ball of Garth Tuff at Rolwyd (SH 765 508).

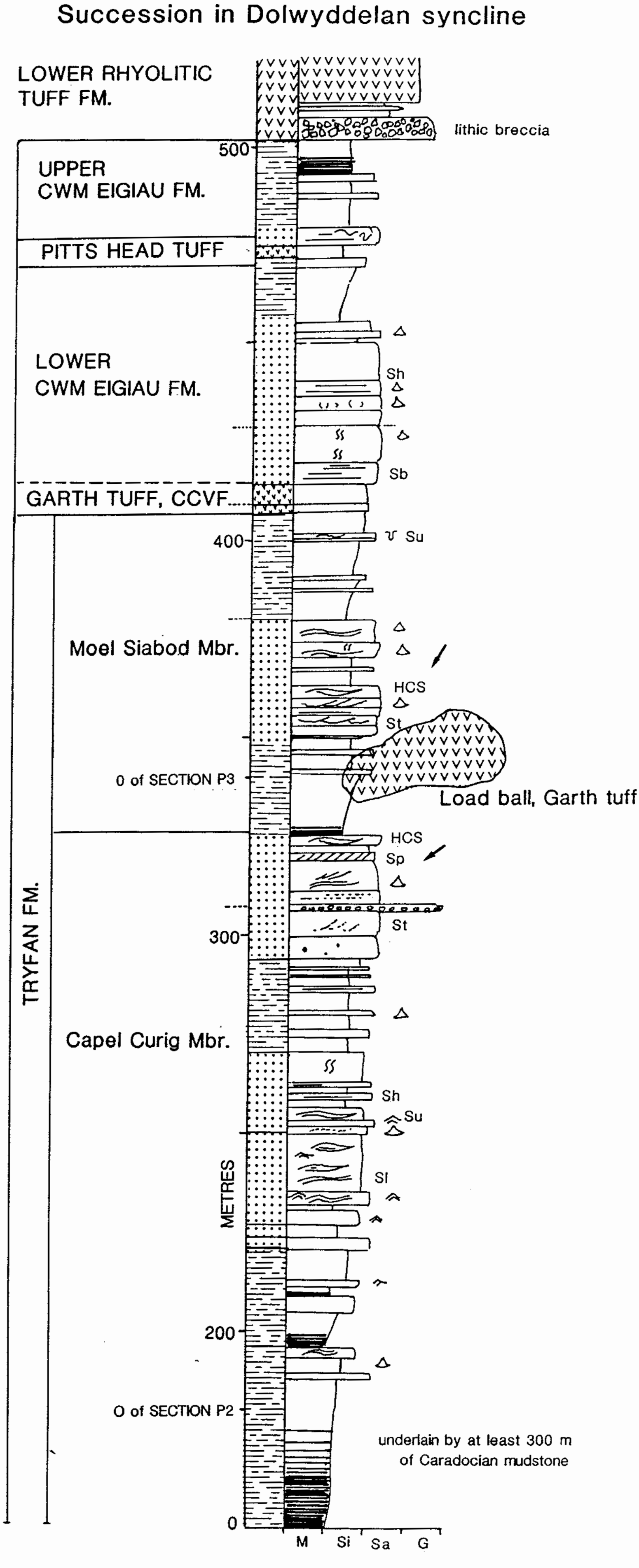

FIG. 6.8: Vertical profile of Llewelyn Volcanic Group and Lower and Upper Cwm Eigiau Fms. in Dolwyddelan syncline. Section from SH 685 501 to SH 686 504 to west of railway tracks near Cwm Fynhadog Isaf.

PALAEOGEOGRAPHY Beneath Garth Tuff

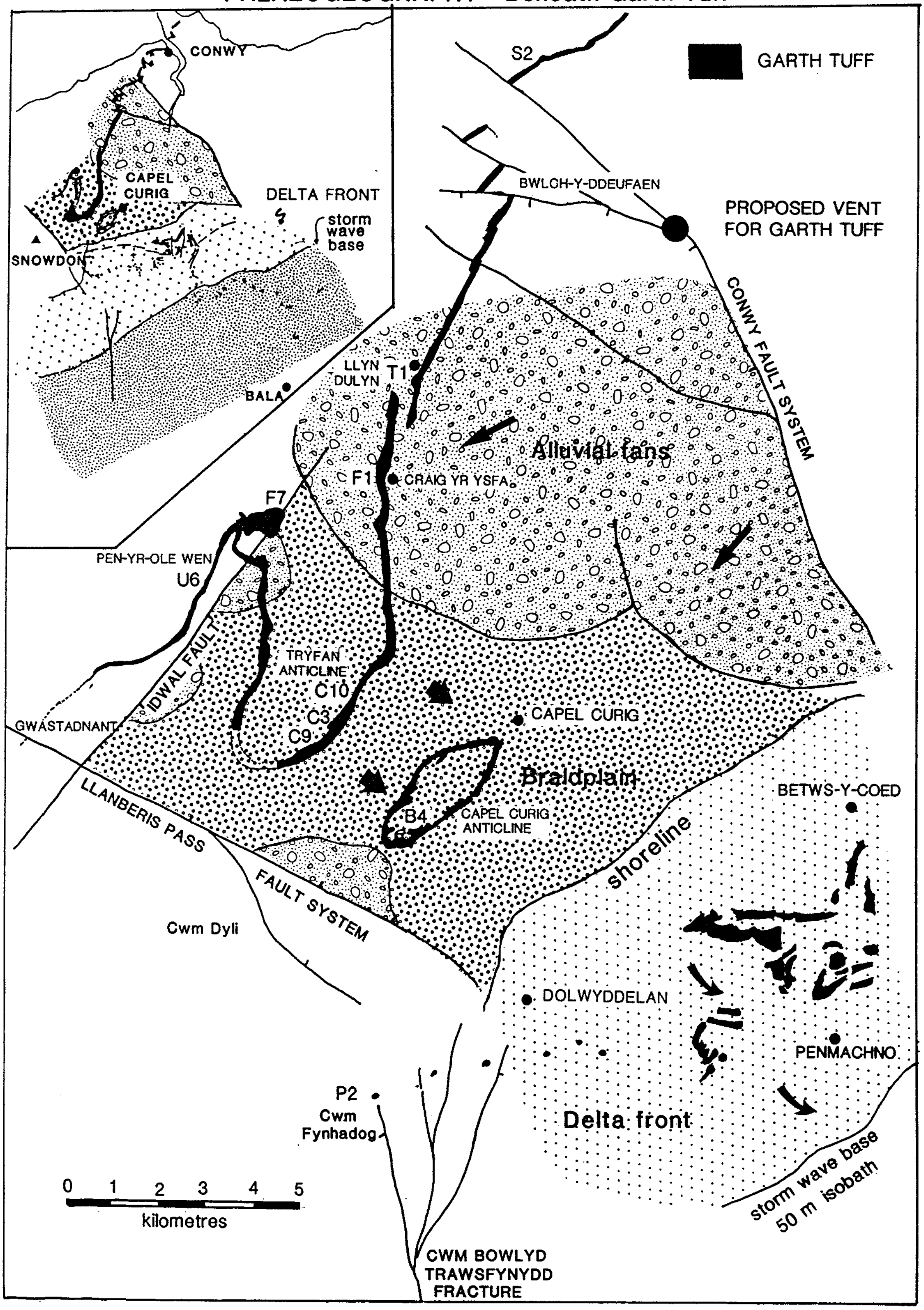

FIG. 6.9a: Palaeogeography beneath Garth tuff in Snowdonia. (Moel Siabod depositional system). See Fig. 6.9b for more regional picture.

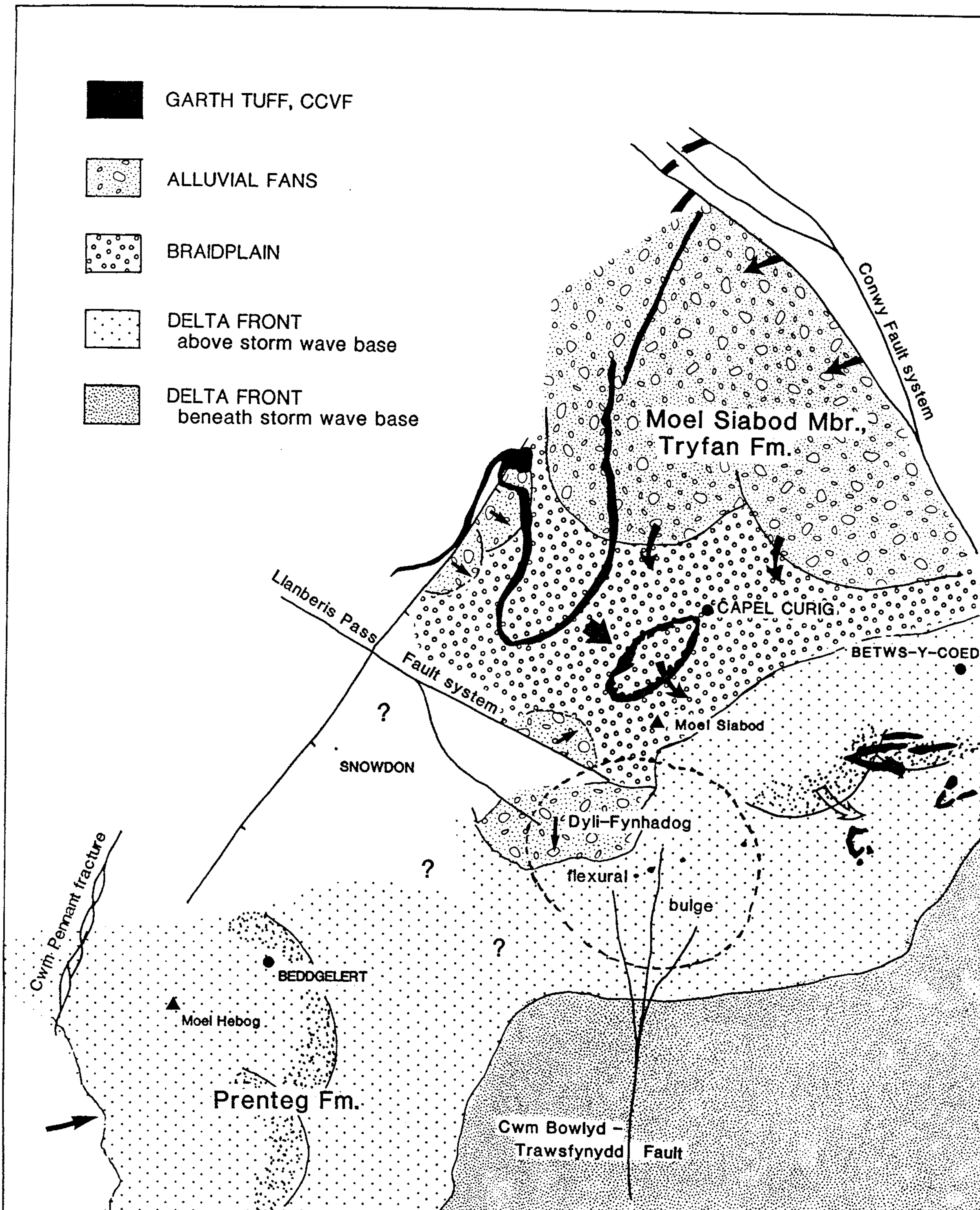

FIG. 6.9b Regional map showing palaeogeography immediately beneath Garth tuff in Snowdonia.

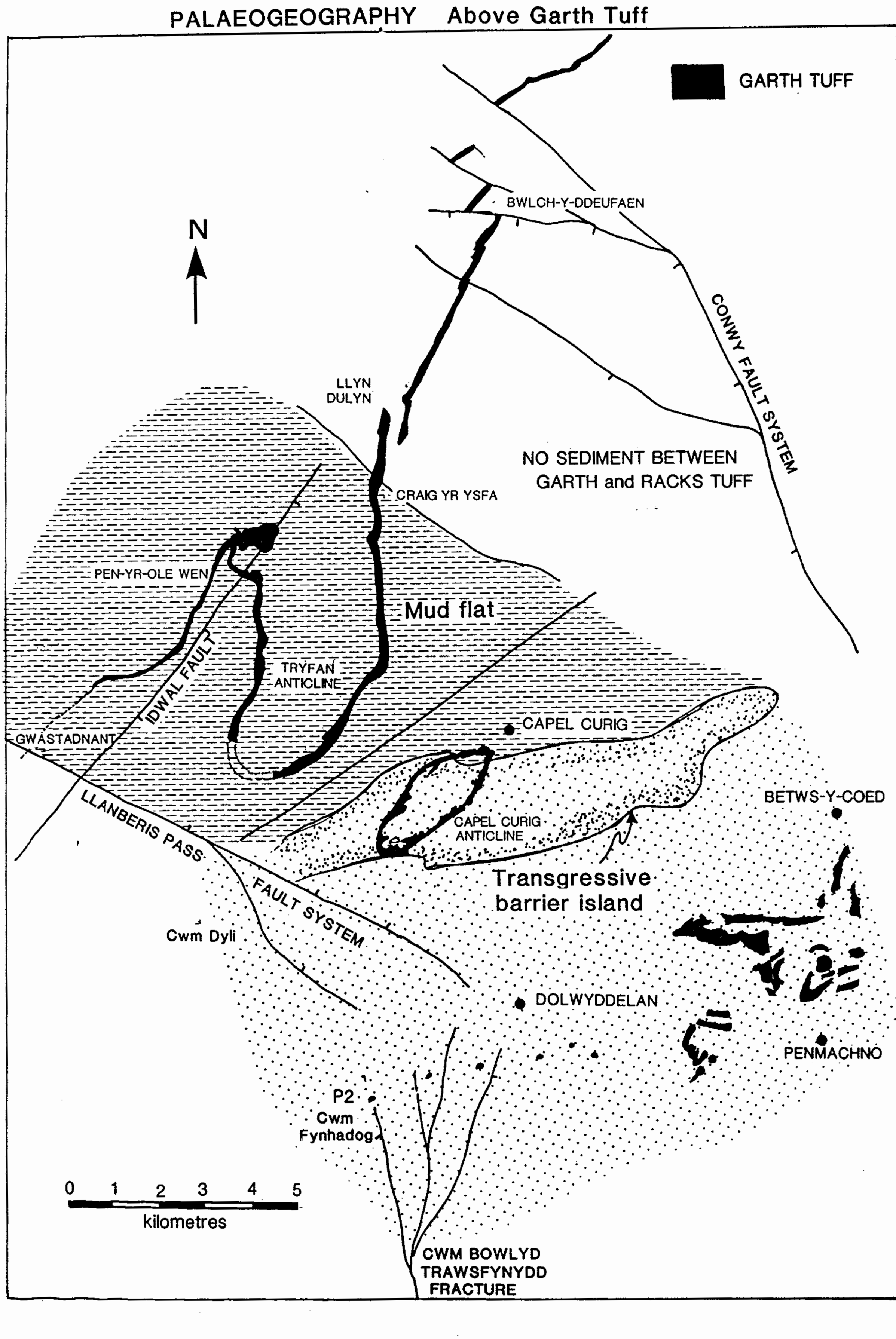

FIG. 6.9c: Palaeogeography above Garth tuff.

PALAEOGEOGRAPHY Beneath Racks Tuff

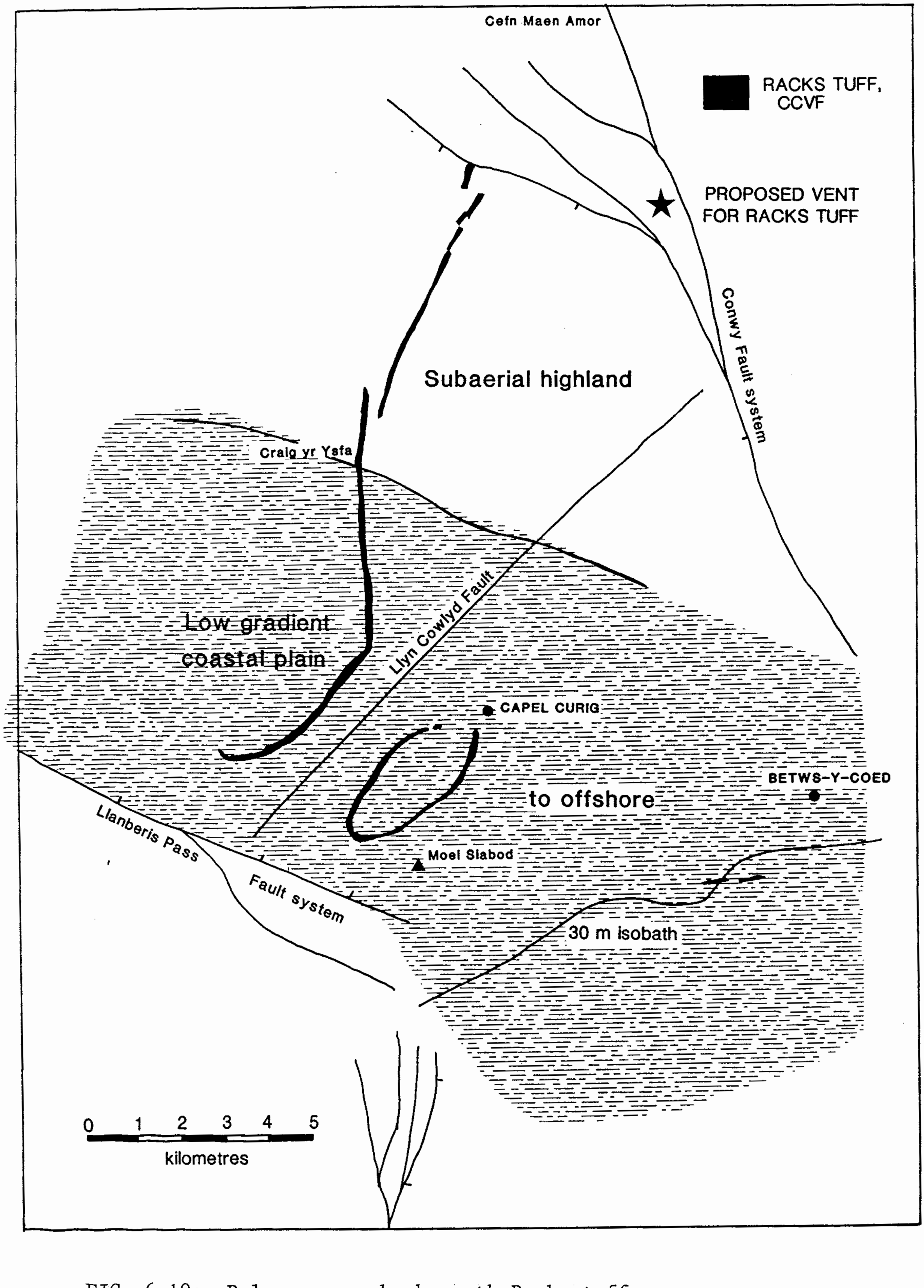

FIG. 6.10: Palaeogeography beneath Racks tuff.

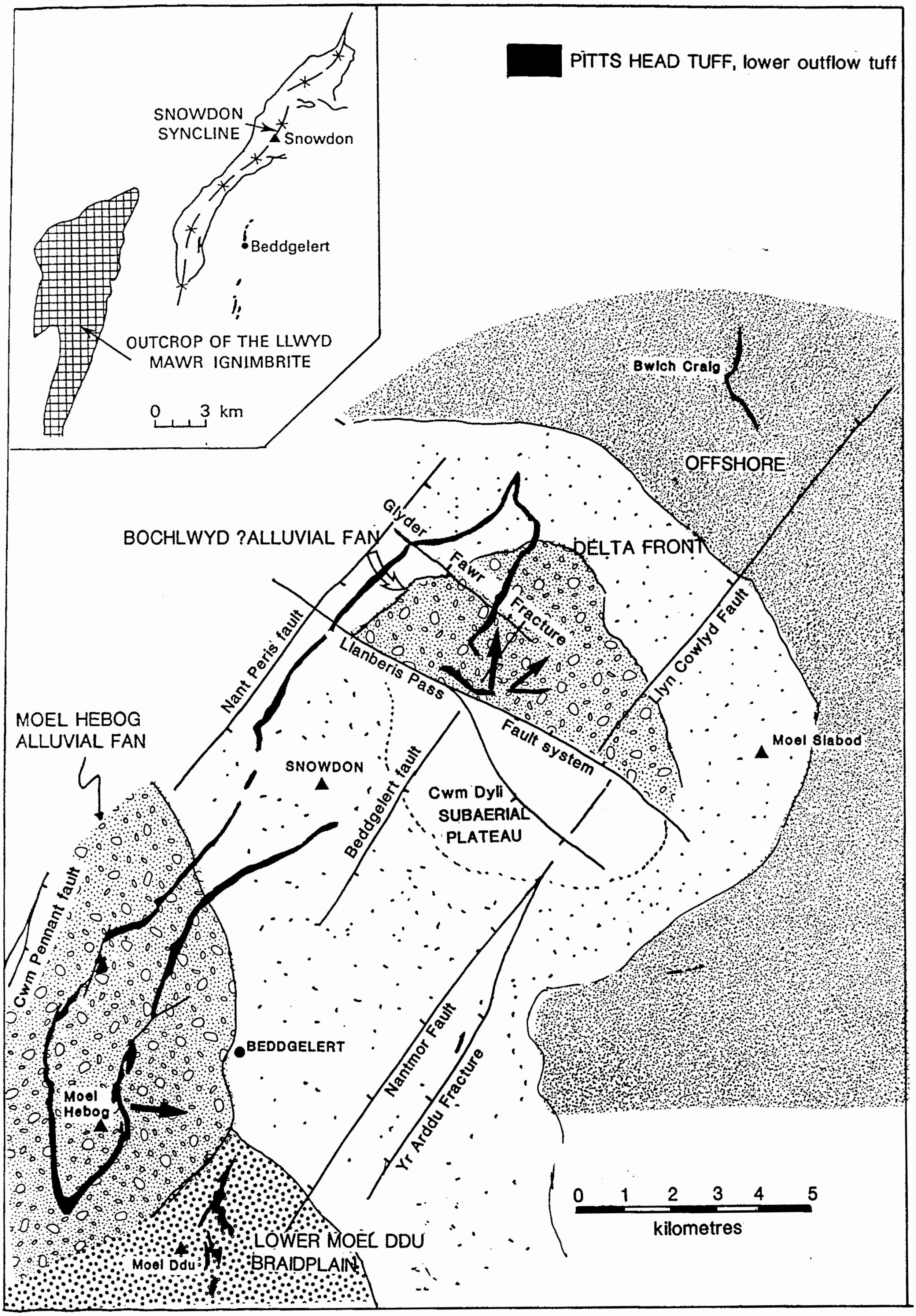

FIG. 6.11a: Palaeogeography at time of deposition of Moel Hebog Mbr. and Bochlwyd Mbr. alluvial fans.

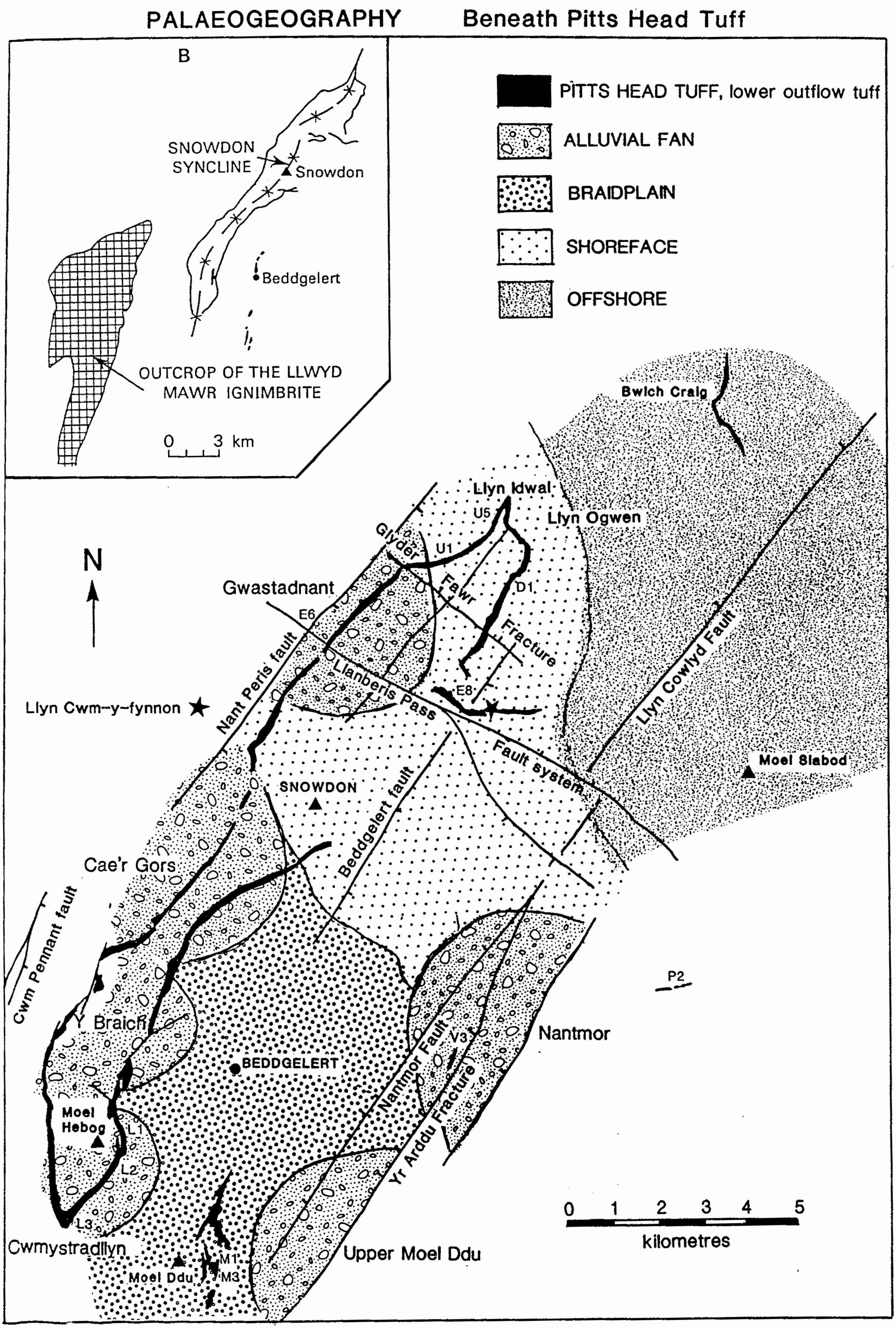

FIG. 6.11b: Palaeogeography immediately beneath Pitts Head Tuff Showing deposition of Gwastadnant Cae'r gors, Y Braich, Cwmystradllyn, Upper Moel Ddu and Nantmor Mbr. alluvial fans.

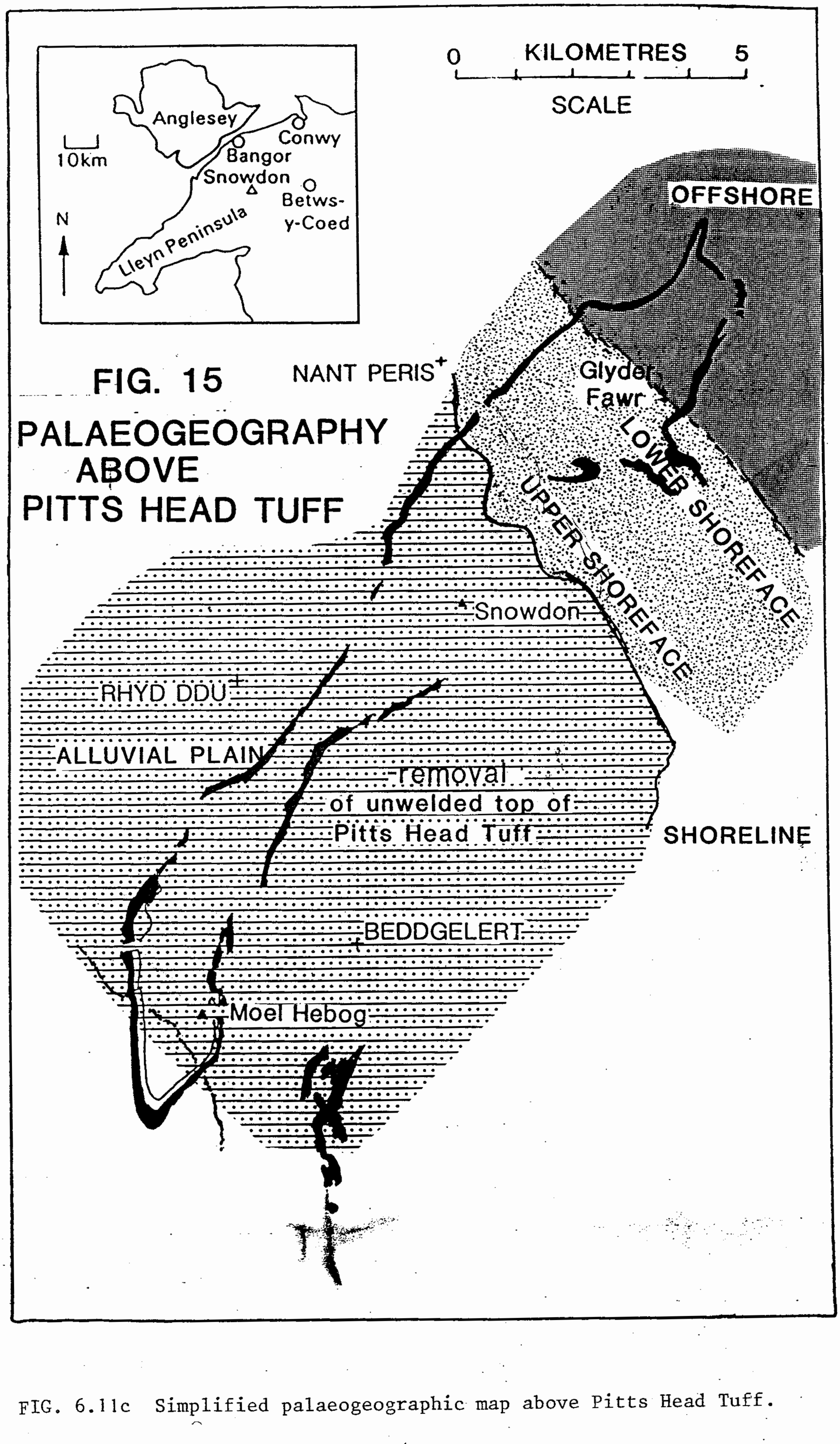

FIG. 6.11c Simplified palaeogeographic map above Pitts Head Tuff.

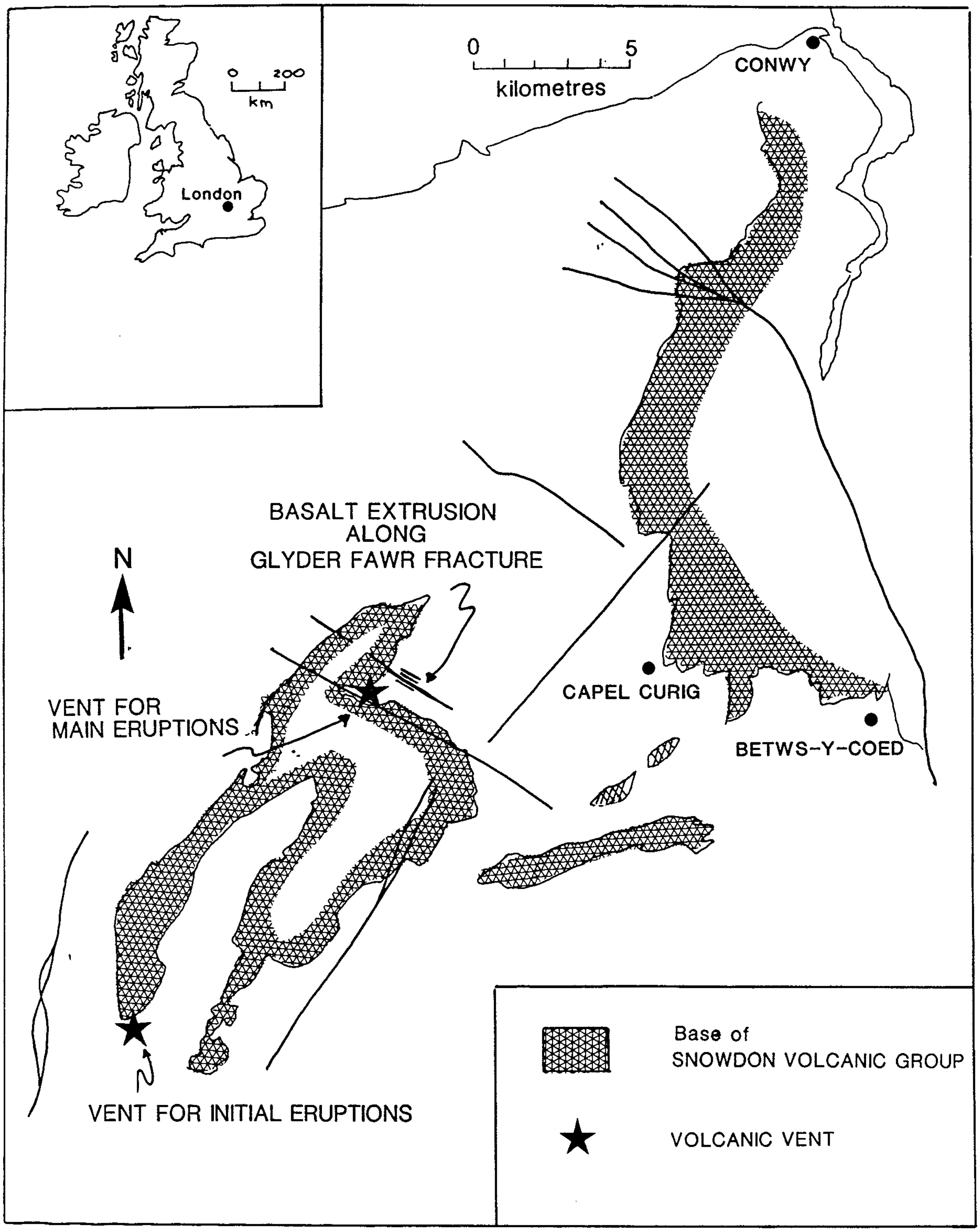

FIG. 6.12a: Outcrop of Lower Rhyolitic tuff Fm. and correlative Lower Crafnant Volcanic Fm., with eruption centres for two phases of LRTF.

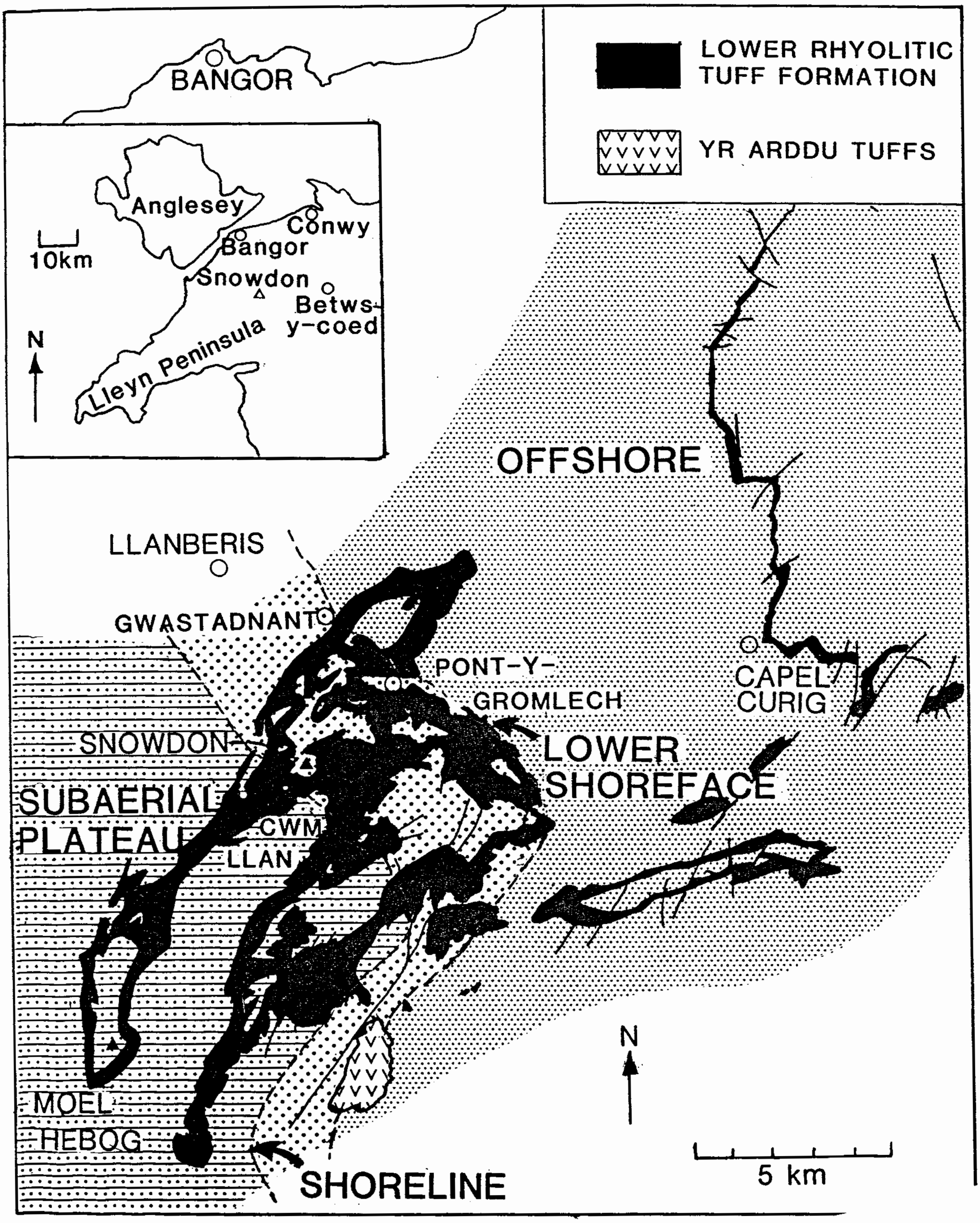

FIG. 6.12 b: Simplified view of palaeogeography immediately prior to eruption of initial phase of Lower Rhyolitic Tuff Fm. caldera.

INFLUENCE OF BASIN FRACTURING

AMOUNT OF INTRABASINAL FAULTING CONTROLS EVENT SIZE AND AMOUNT OF UPLIFT.

CAPEL CURIG VOLCANIC FORMATION

SMALLER EVENTS	1) Garth Tuff (28km3, 20 - 150m thickness)
LESS EXPLOSIVE	2) Racks Tuff 10km3
LESS UPLIFT	3) 3rd member - dominated by 4m flows
	4) 4th member, -numerous small pulses,, formation of volcanic cone.

PITTS HEAD TUFF

-substantial regional uplift

-one single eruption c.70km3

LOWER RHYOLITIC TUFF c.54km3

-little observable uplift

-basin fracturing due to the PHT/CCVF events resulted in

a) initial eruption of 10km3 from vents on deep lineaments

b)later eruptions consisted of numerous small events.

FIG. 6.13: INFLUENCE OF CRUSTAL STRENFTH ON THE AMOUNT OF UPLIFT and NATURE OF VOLCANIC ERUPTIONS IN NORTH WALES.

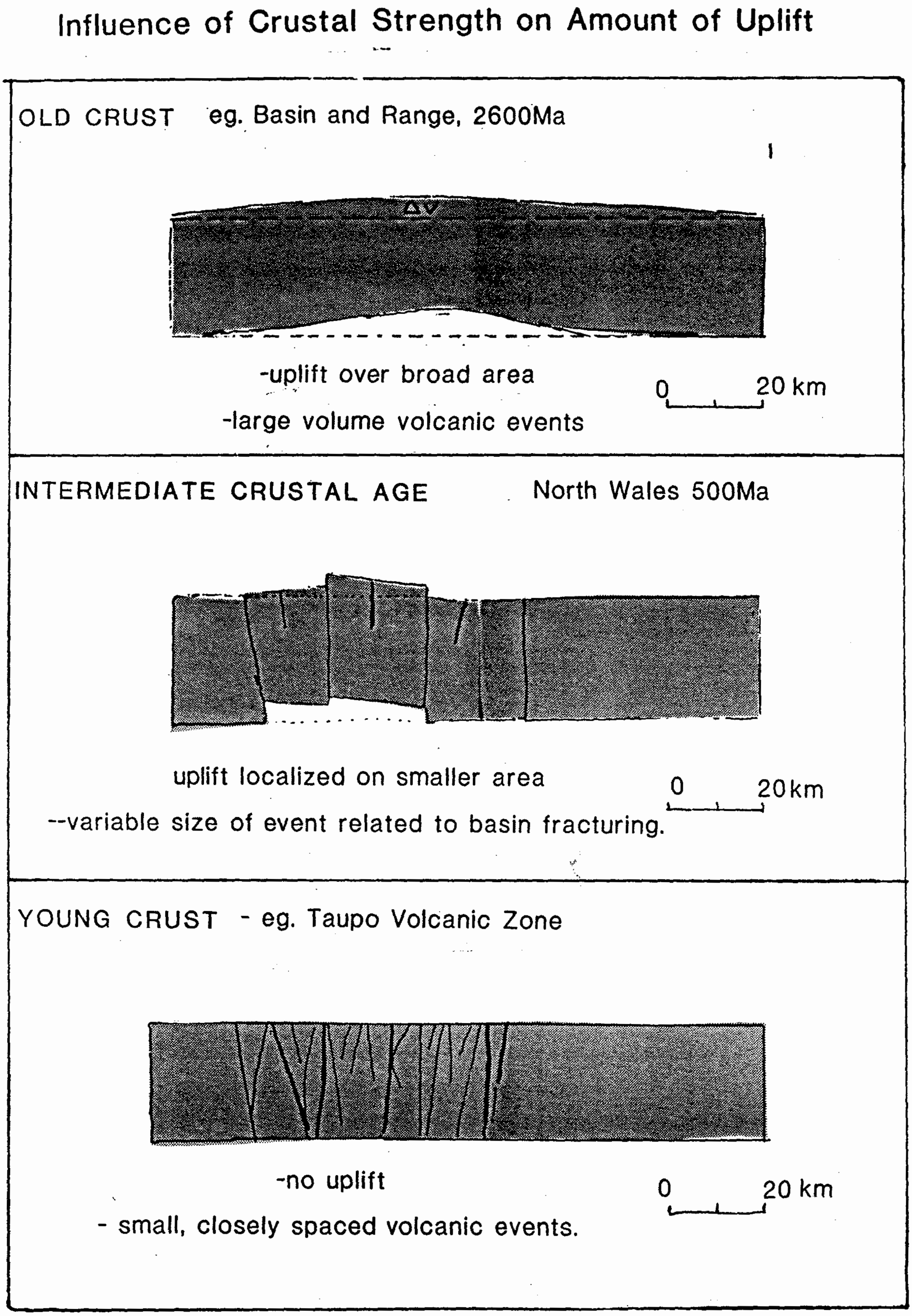

FIG. 6.14: INFLUENCE OF CRUSTAL STRENGTH ON TYPE OF VOLCANIC ERUPTION

Chapter 7

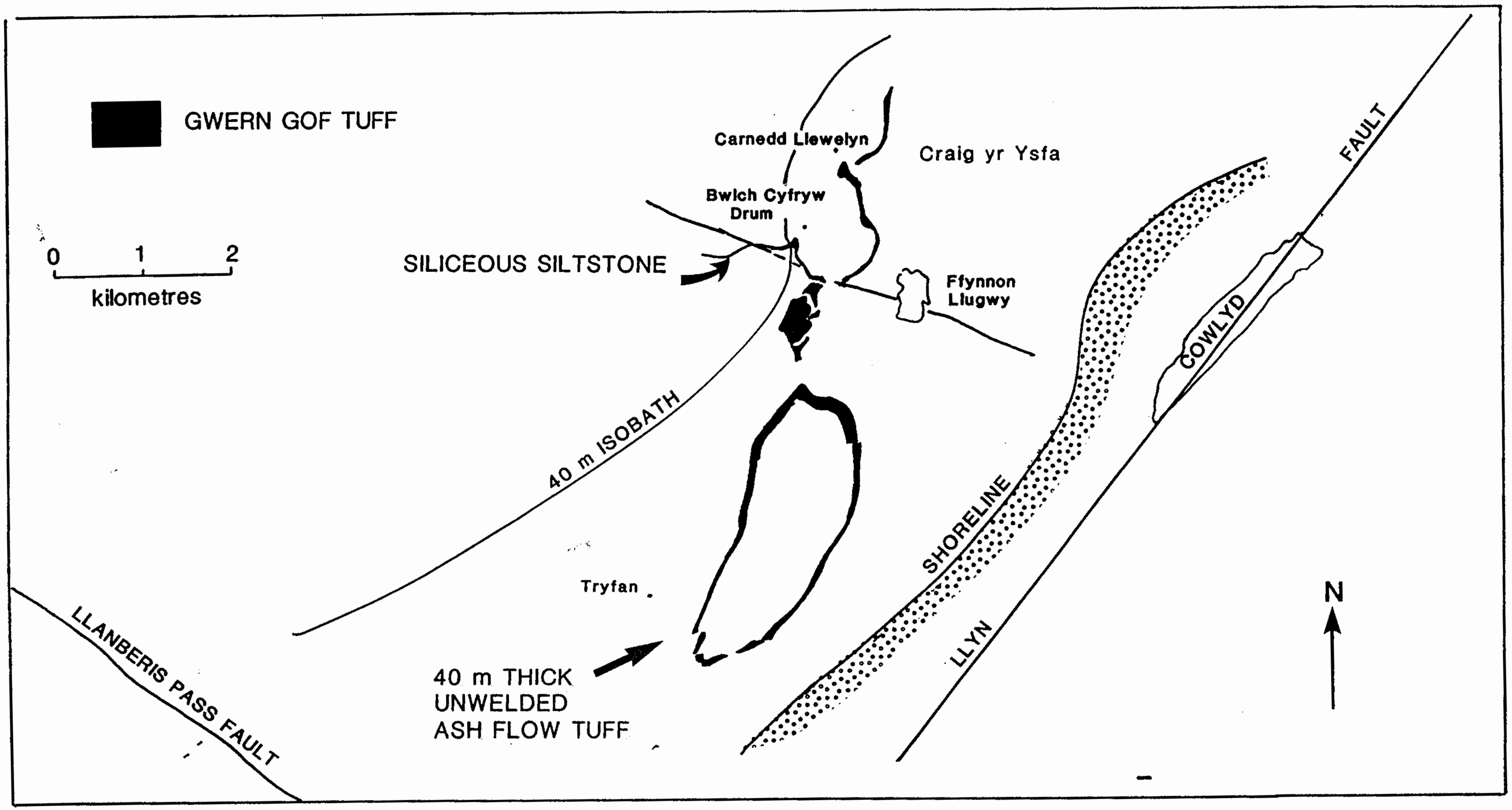

FIG. 7.1: Outcrop and facies of Gwern Gof Tuff Fm.

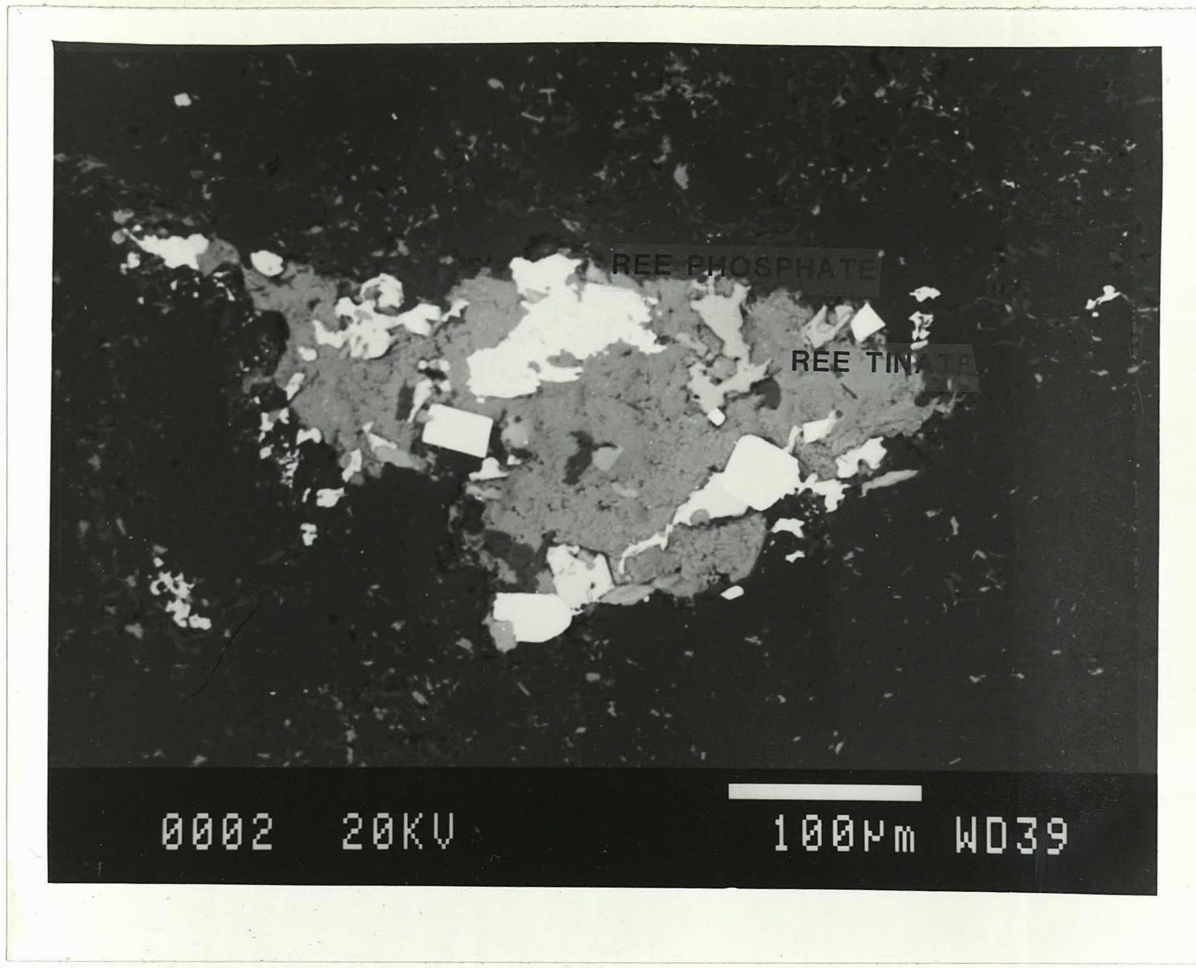

FIG. 7.2a: Vapour-phase crystallization of REE phosphastes and silicates within pumice fragment. Gwern Gof Tuff Fm., Tryfan anticline. Chemical elements dtermined using EDS include Th, Y, Nb, Ti, Ca, Ce, and Gd.

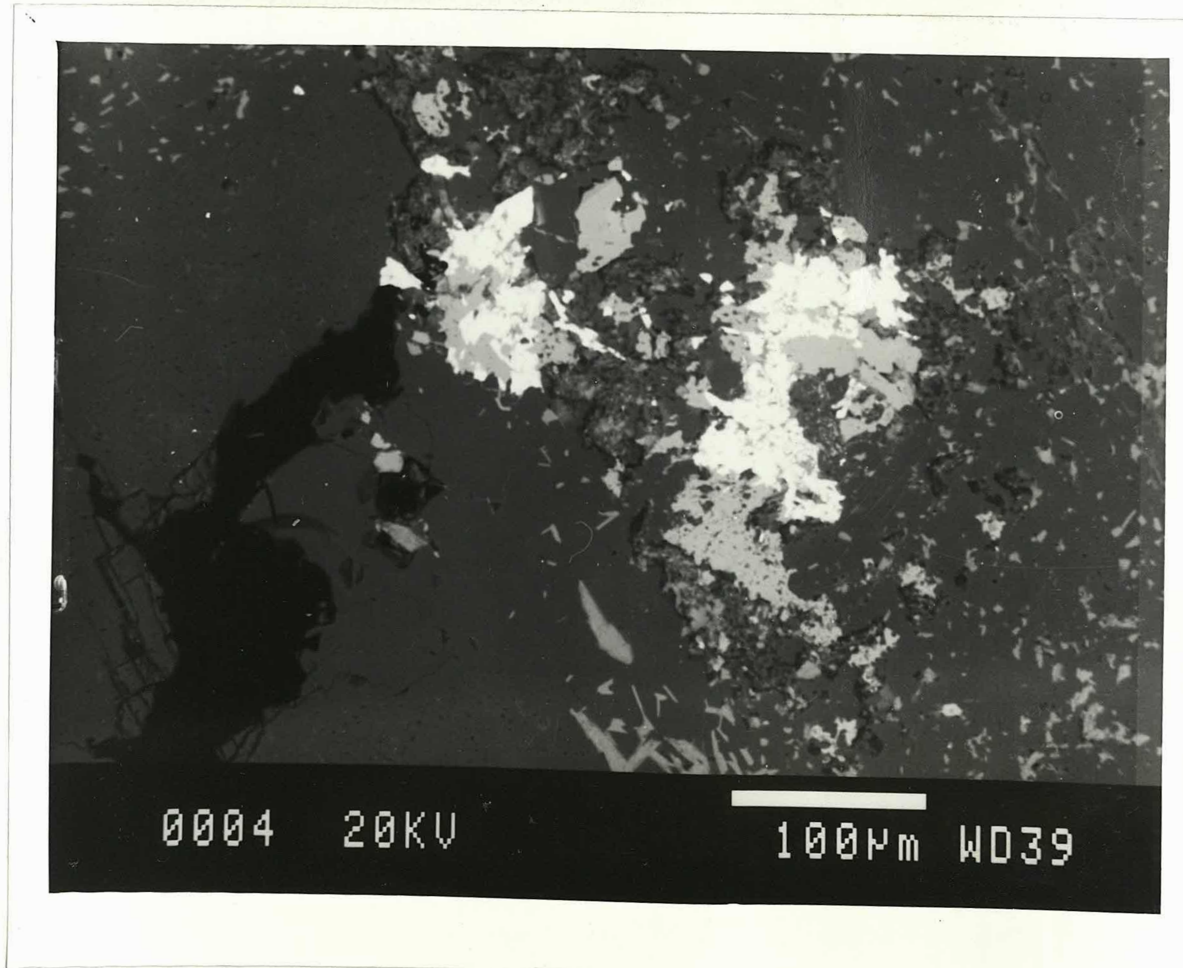

FIG. 7.2b: As above.

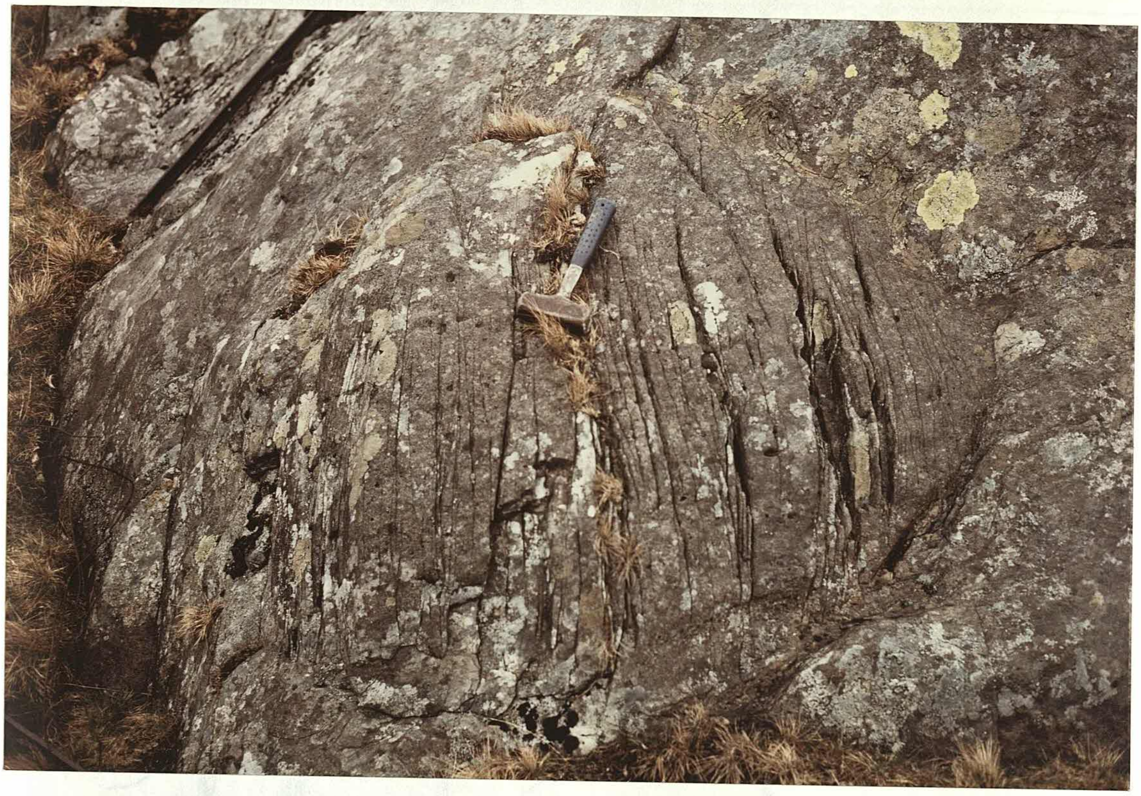

Fig. 7.3: Load ball of medium sandstone (with spaced cleavage) set in fine siltstone approximately 5 metres beneath the Gwern Gof tuff on Ddeugwm ridge, Tryfan anticline. SH 6873 5959.

Fig. 7.4: Lobate protrusions of Garth tuff (white weathering) into underlying braidplain sandstones (brown weathering), Gallt yr Ogof. View looking SE. Spacing of protrusions is approximately 140 metres at this locality.

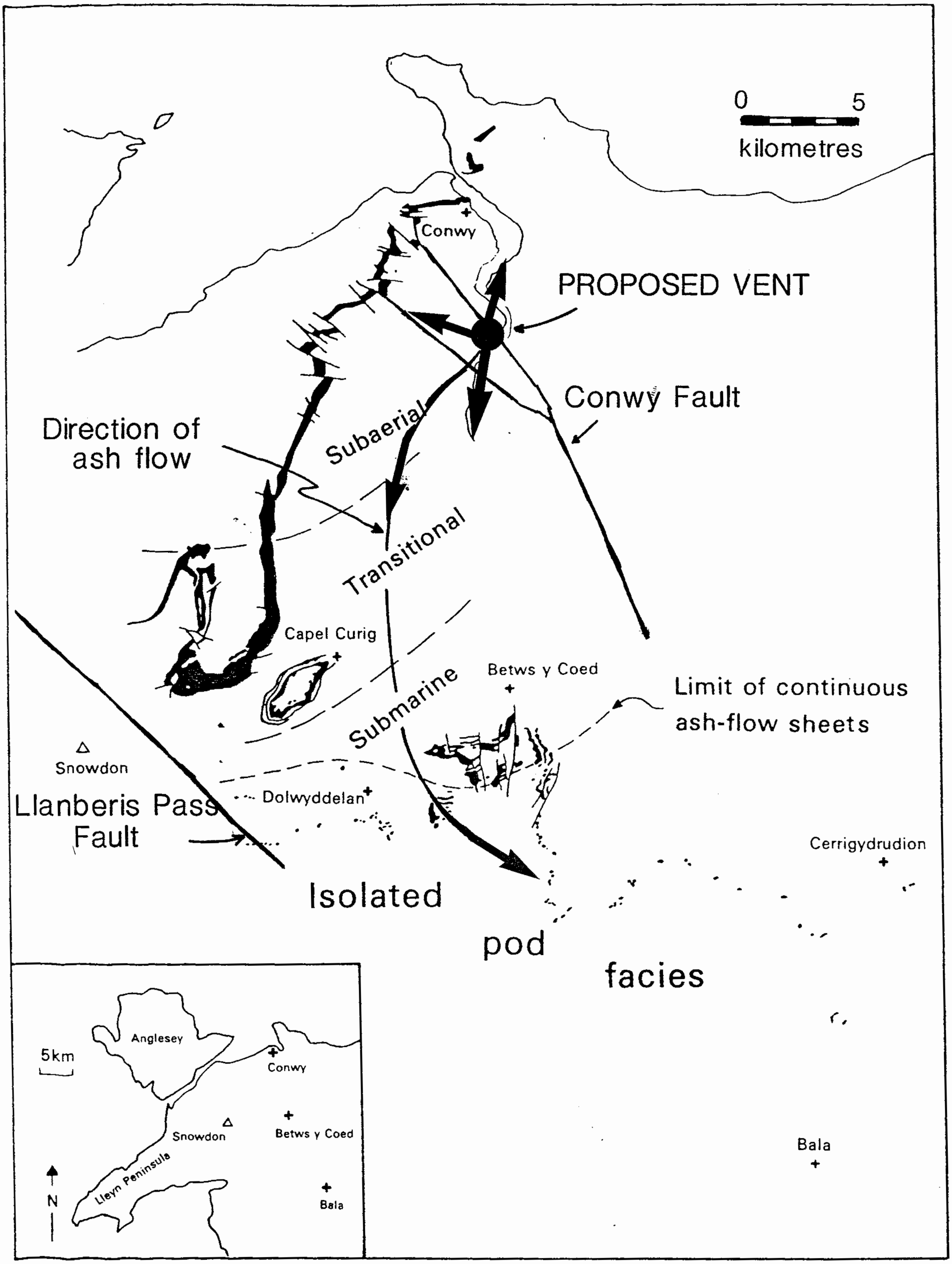

FIG. 7.5: DISTRIBUTION OF GARTH TUFF IN NORTH WALES. Proposed vent and direction of ash flow from this study. Depositional environments shown are from Howells et al, 1985. Results from this thesis suggest that the southern boundary of the "Transitional" zone would be a good approximation for coastline immediately before tuff emplacement.

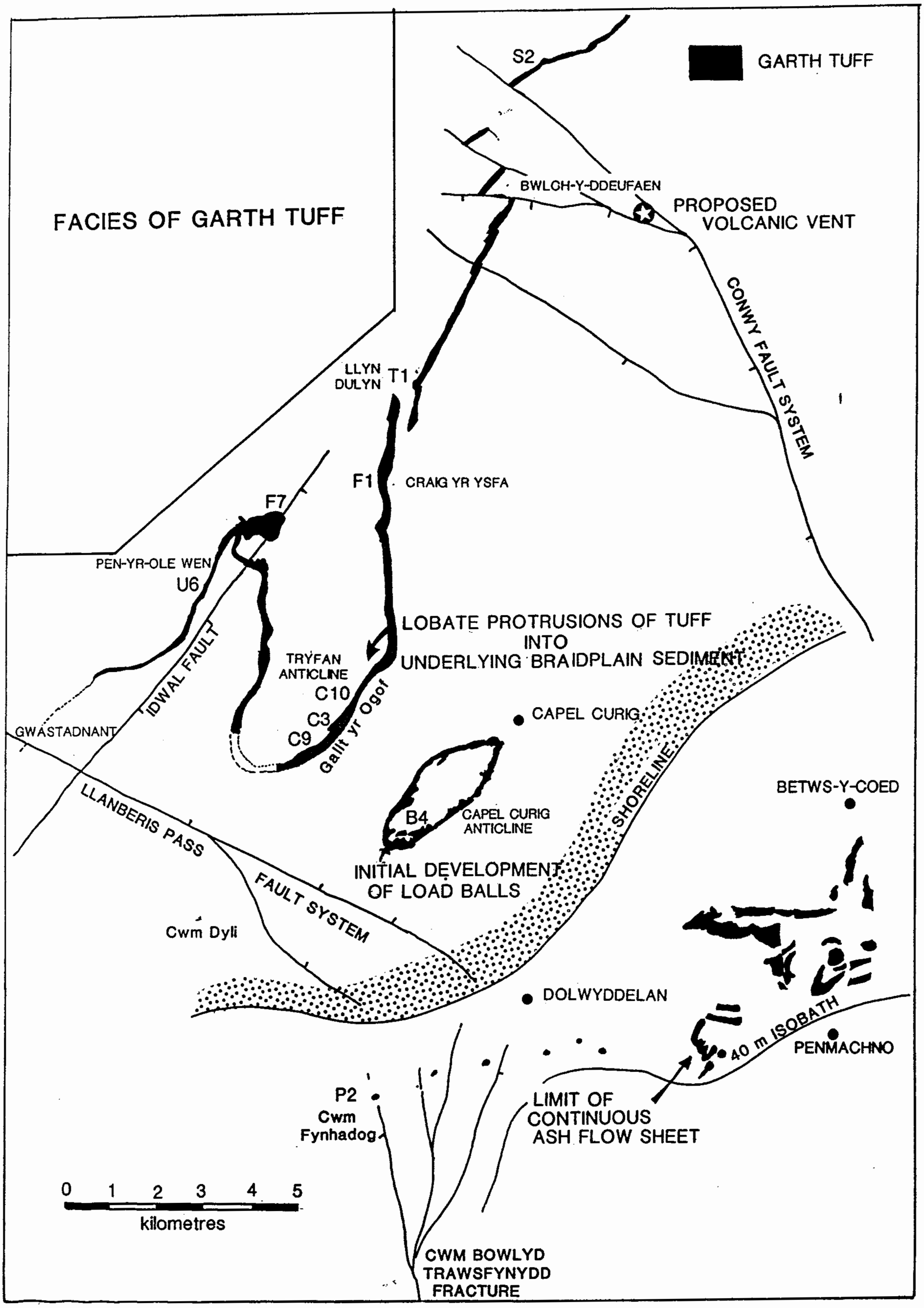

FIG. 7.6: Distribution of Garth tuff with major facies.

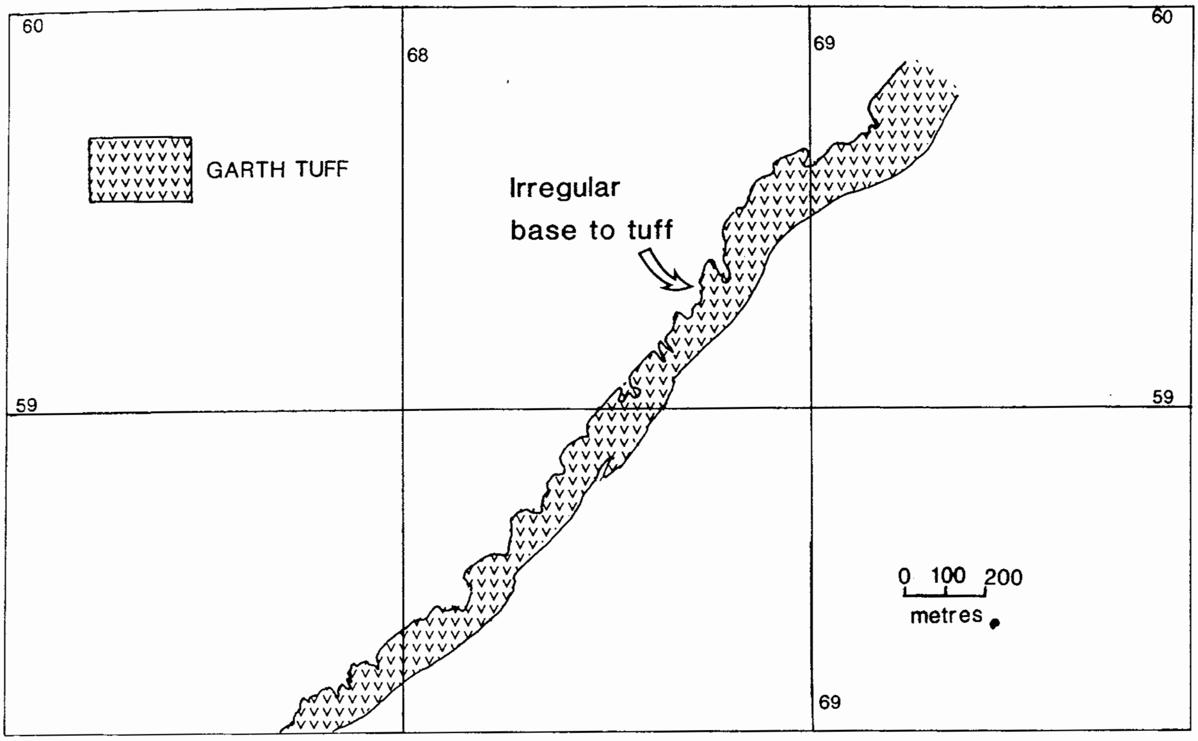

Fig. 7.7: Irregular base to Garth Tuff along Gally yr Ogof ridge, Tryfan anticline. Traced from unpublished BGS 1:10,000 maps.

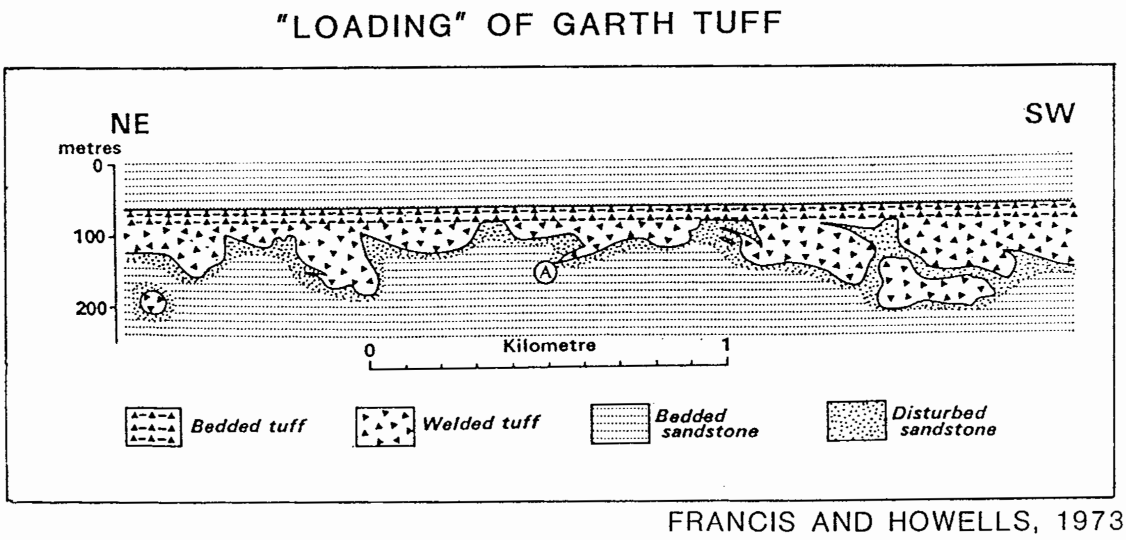

Fig. 7.8: Base of Garth Tuff along SE side of Capel Curig anticline. From Francis & Howells, 1973.

FIG. 7.9: Distribution of Capel Curig volcanic Fm. in Capel Curig anticline. (from Francis and Howells, 1973.

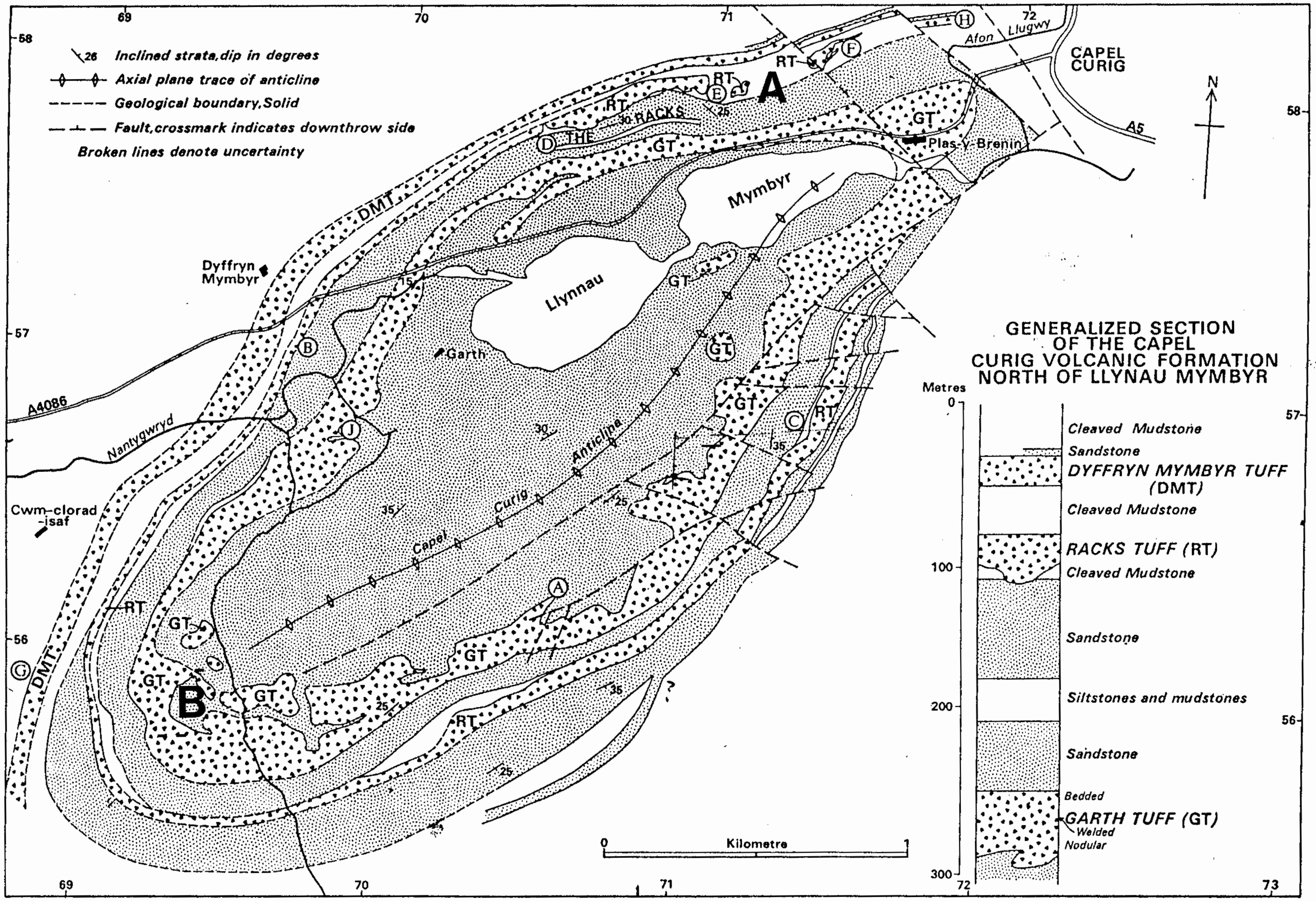

FIG. 2. Map and vertical section of the Capel Curig Volcanic Formation in the Capel Curig Anticline. Drift omitted.

Fig. 7.10: Columnar jointing within load ball of Garth tuff, near Cwm Clorad Isaf, SH 6941 5596

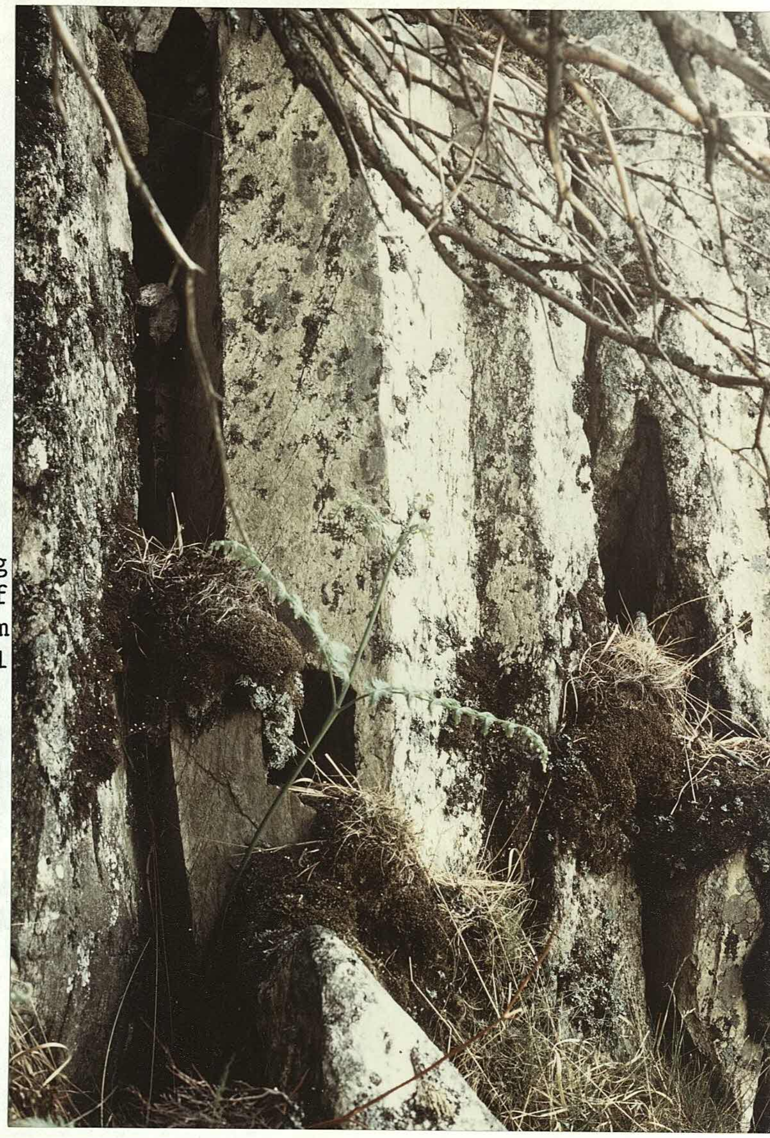

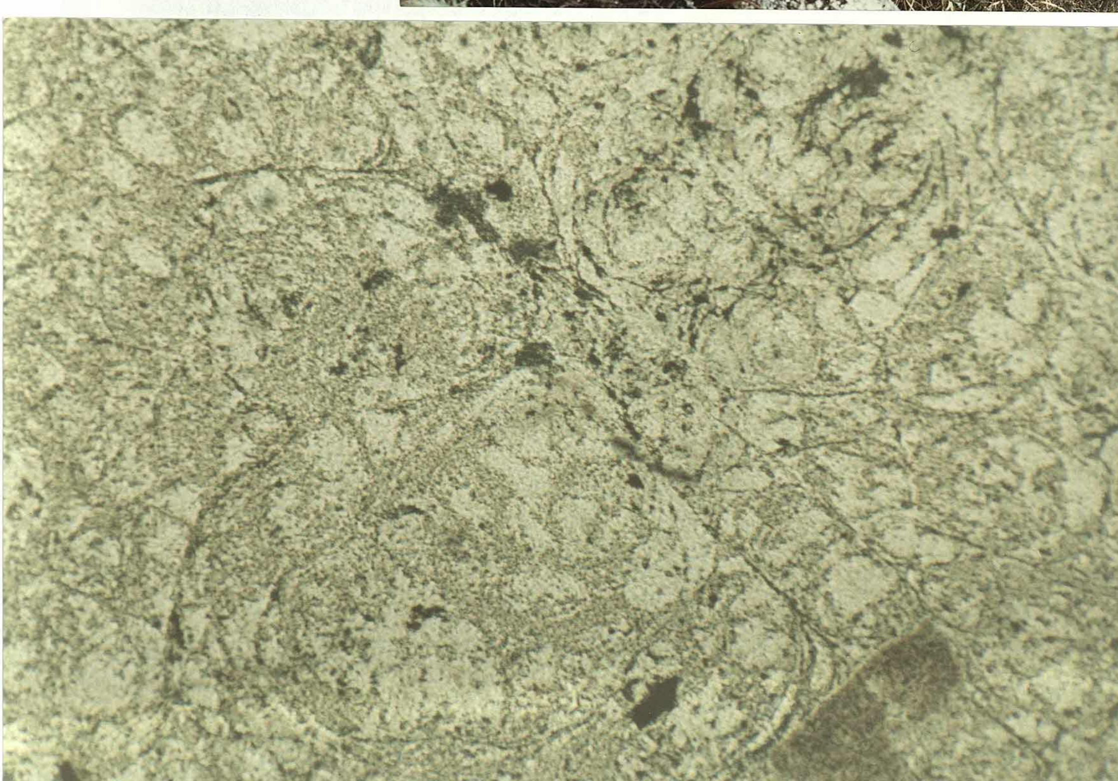

Fig. 7.11: Perlitic fracture from middle portion of Garth tuff in Capel Curig anticline, SH 7060 5770. Sample GO 6. See Appendix 1.__ for chemical composition.

Fig. 7.12: Glass fragment with perlitic fracture, abraded cuspate glass shards, and occasional quartz crystal from reworked Garth tuff. Sample A5A, Section A2, __m, Capel Curig anticline.

Fig. 7.13: Densely packed siliceous nodules near top of unreworked portion of Garth tuff, Capel Curig anticline. SH 7067 5770

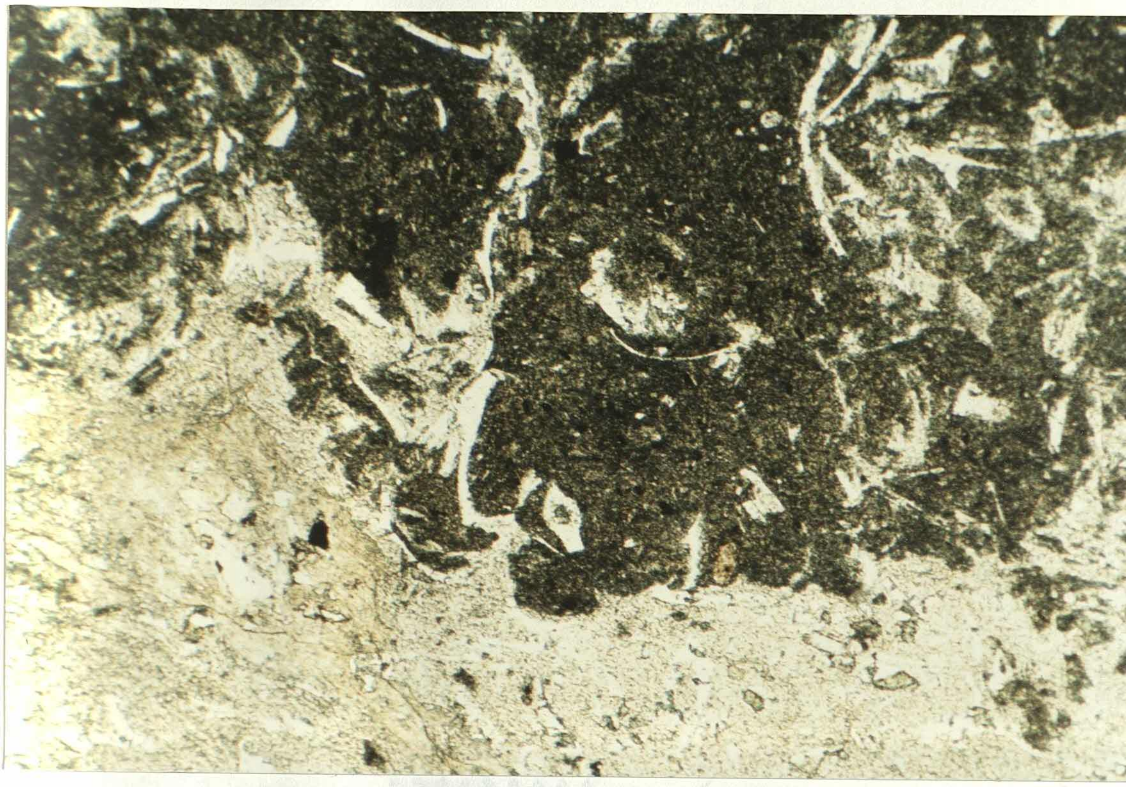

FIG. 7.14: Delicate interfingering of mudstone and vitric-tuff at base of Racks Tuff, Capel Curig Anticline. Photo from top of section A2, __m. SH 7063 5784.

FIG. 7.15: Edge of upwards intrusion of sandstone (on right) into mudstone (cleaved) related to soft-sediment deformation from emplacement of Racks Tuff. See Fig. 7.16 for location of deformation structure in Capel Curig anticline.

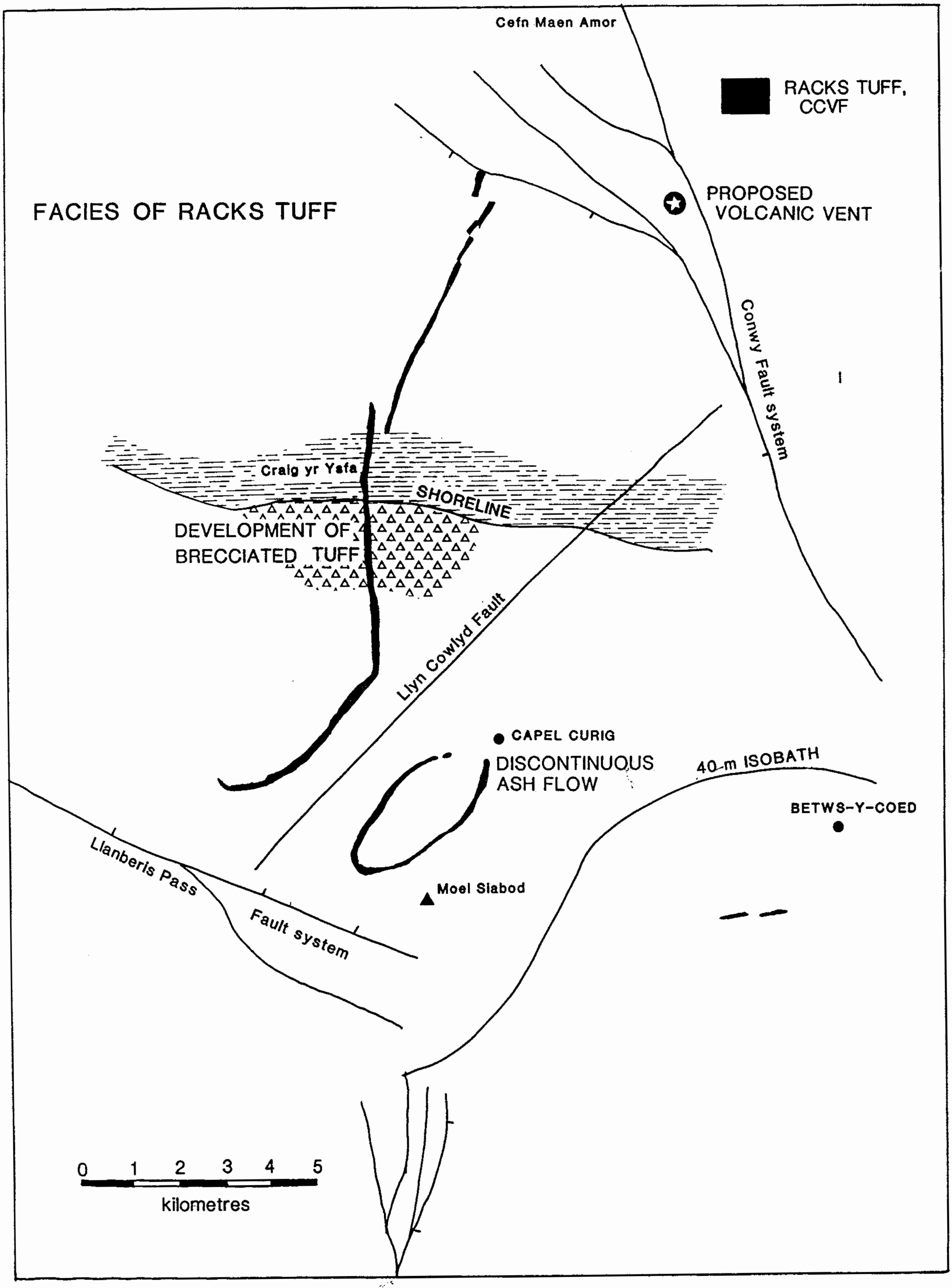

FIG. 7.16: Distribution and facies of Racks Tuff.

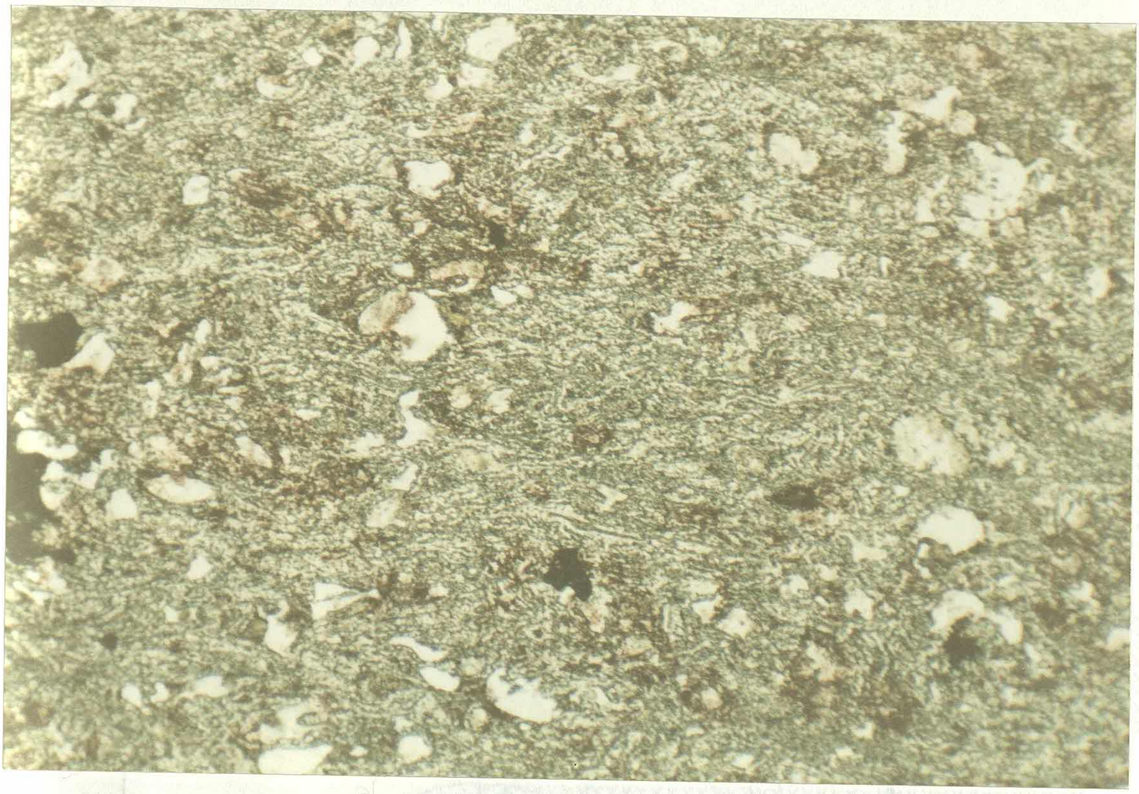

Fig. 7.17: Welded crystal-rich base to Racks Tuff, Capel Curig anticline. Sample from approximately 2 m above base of ash flow. SH 7088 5795.

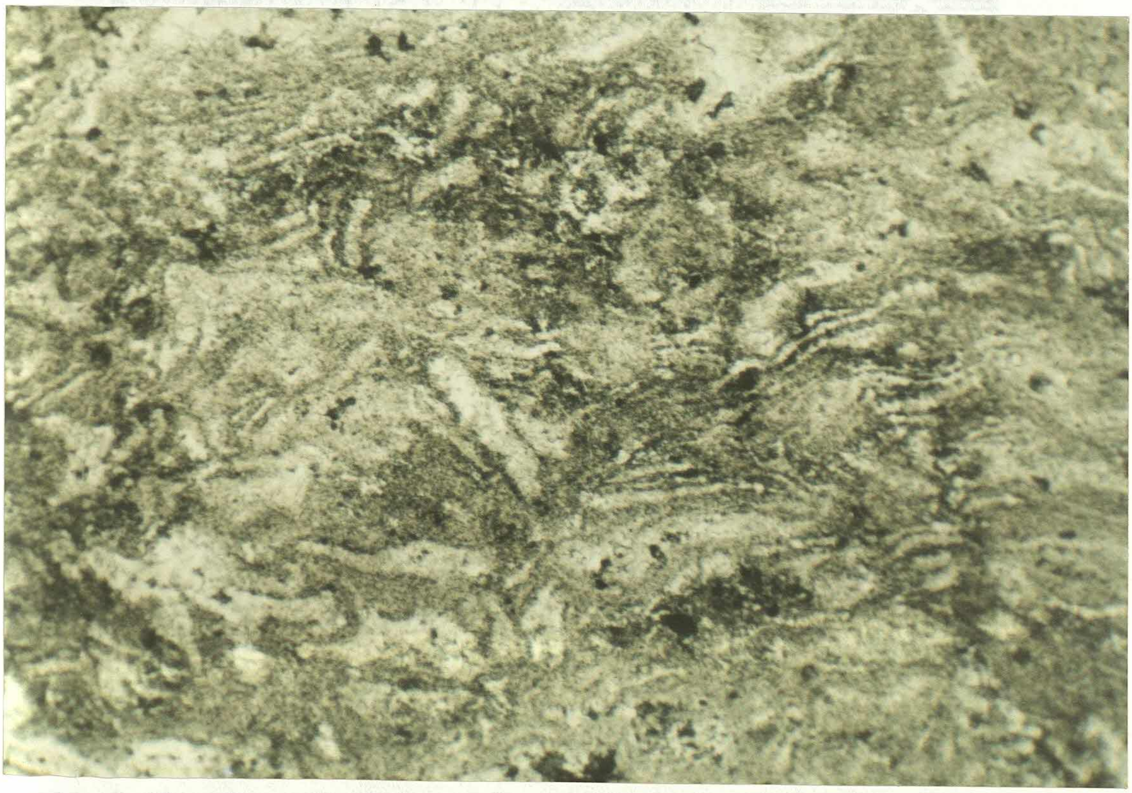

Fig. 7.18: Eutaxitic foliation from middle of Racks Tuff, Capel Curig anticline. SH 7088 5796.

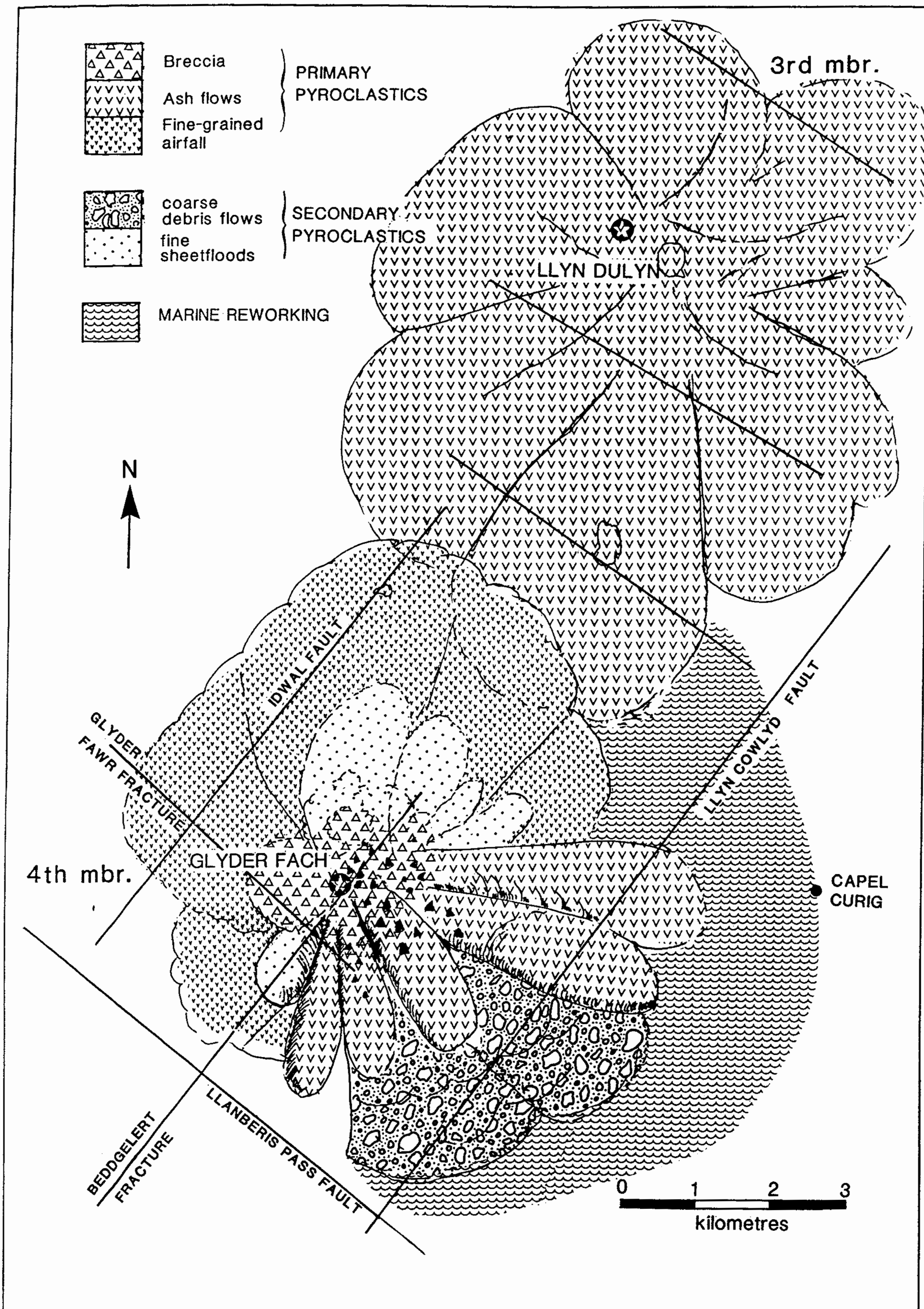

FIG. 7.19: Distribution and facies of coeval 3rd and 4th volcanic members of the Capel Curig Volcanic Fm..

Fig. 7.20: Thin primary ash flow tuffs, 3rd volcanic member of CCVF, Llyn Dulyn. SH 700 663.

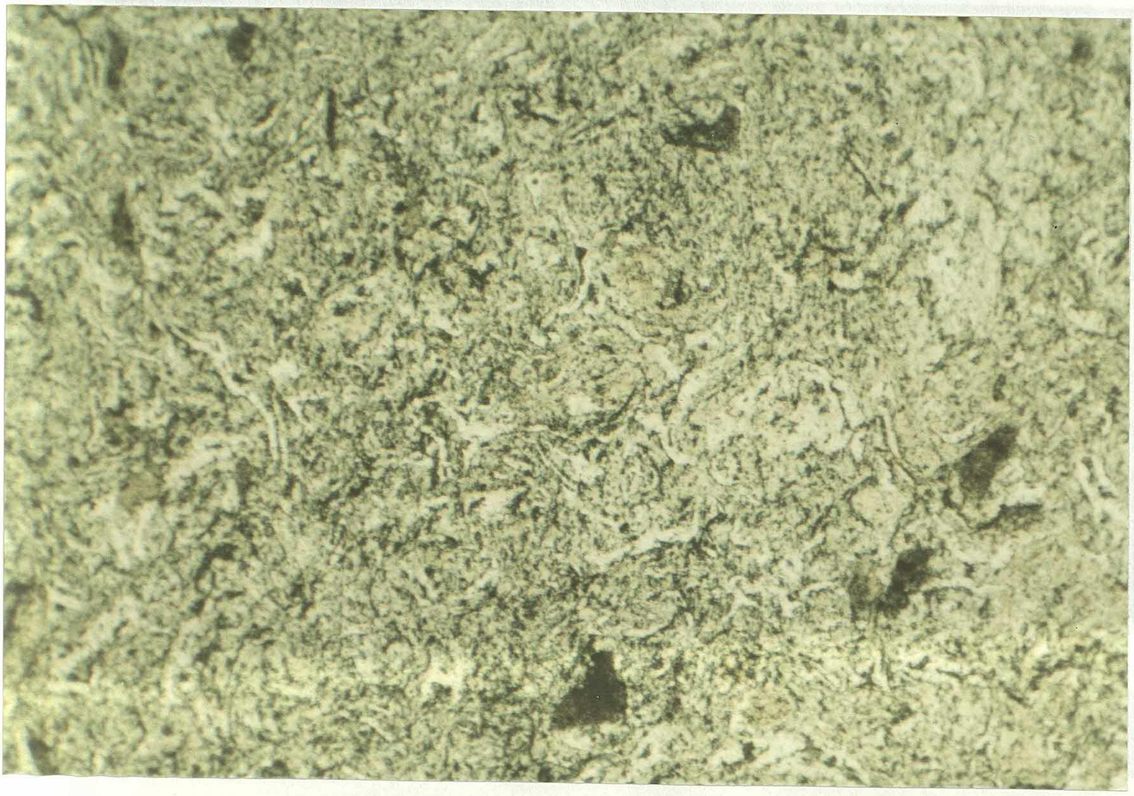

Fig. 7.21: Unwelded vitroclastic texture, 3rd volcanic member of CCVF, Ffynnon Lloer. Section F9, 65 m, SH 6573 6203

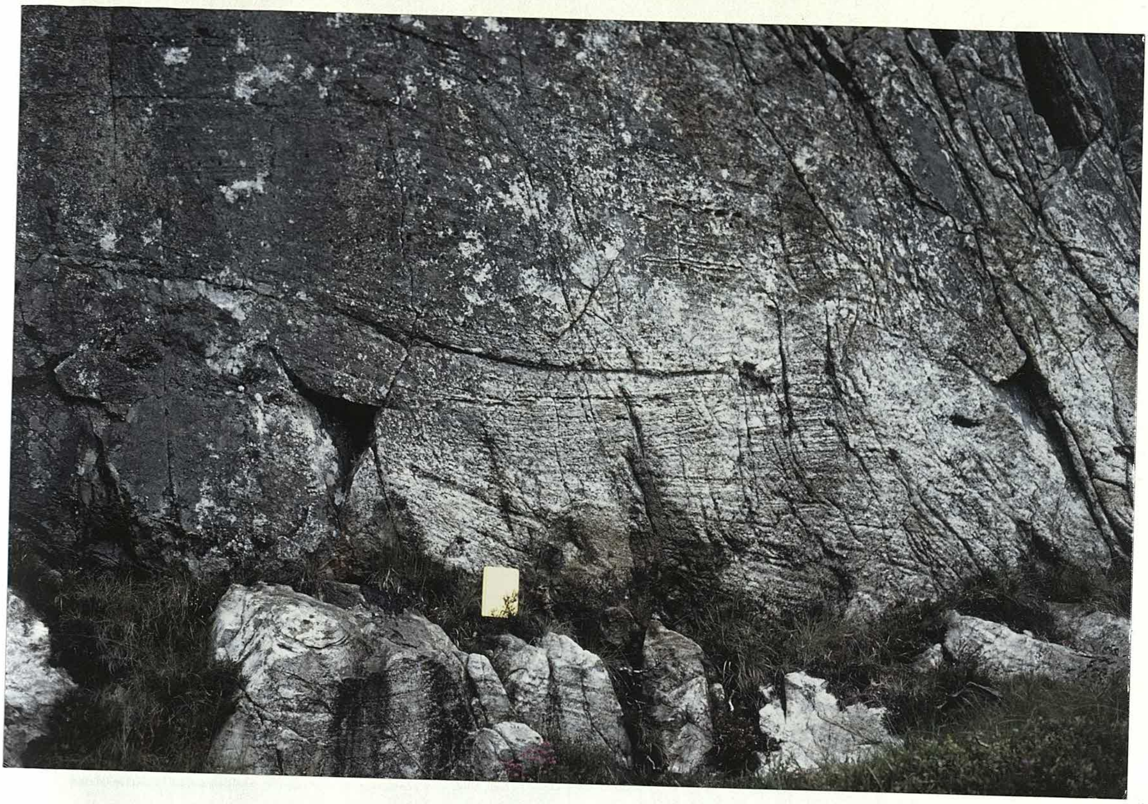

Fig. 7.22: "Swaley cross-stratification" from surging pyroclastic flows. Bedform would reflect internal body waves within pyroclastic flow. 4th volcanic Mbr. of CCVF, Gallt yr Ogof. Section C13b, 45.5 m, SH 6852 5817. Notebook is 18.5 cm long for scale.

Fig. 7.23: Coarse-grained crystal-rich volcaniclastics, 4th volcanic Mbr. of CCVF, Gallt yr Ogof. "Scour-and-fill" and undulating lamination from surging pyroclastic flow. Bedforms later deformed by slumping and soft sediment deformation. Pencil for scale.

Fig. 7.24: View of thin-section showing portion of a welded tuff clast contained within subaqueous debris flow, 4th volcanic mbr. of CCVF, Gallt yr Ogof. Section C13a, __ m. SH 688 585

Fig. 7.25: Inversely and normally graded pumiceous debris flows, 4th volcanic Mbr. of CCVF, Capel Curig anticline, SH 7070 5797. Section __, _ m. Notebook is 18.5 cm long for scale.

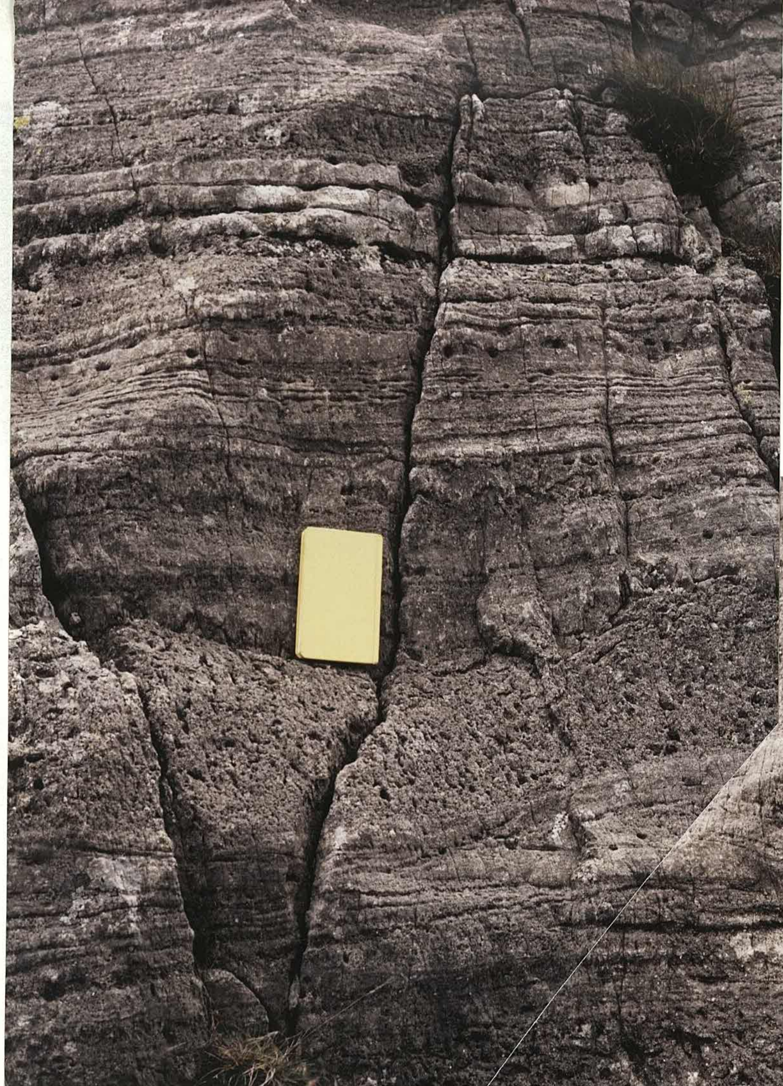
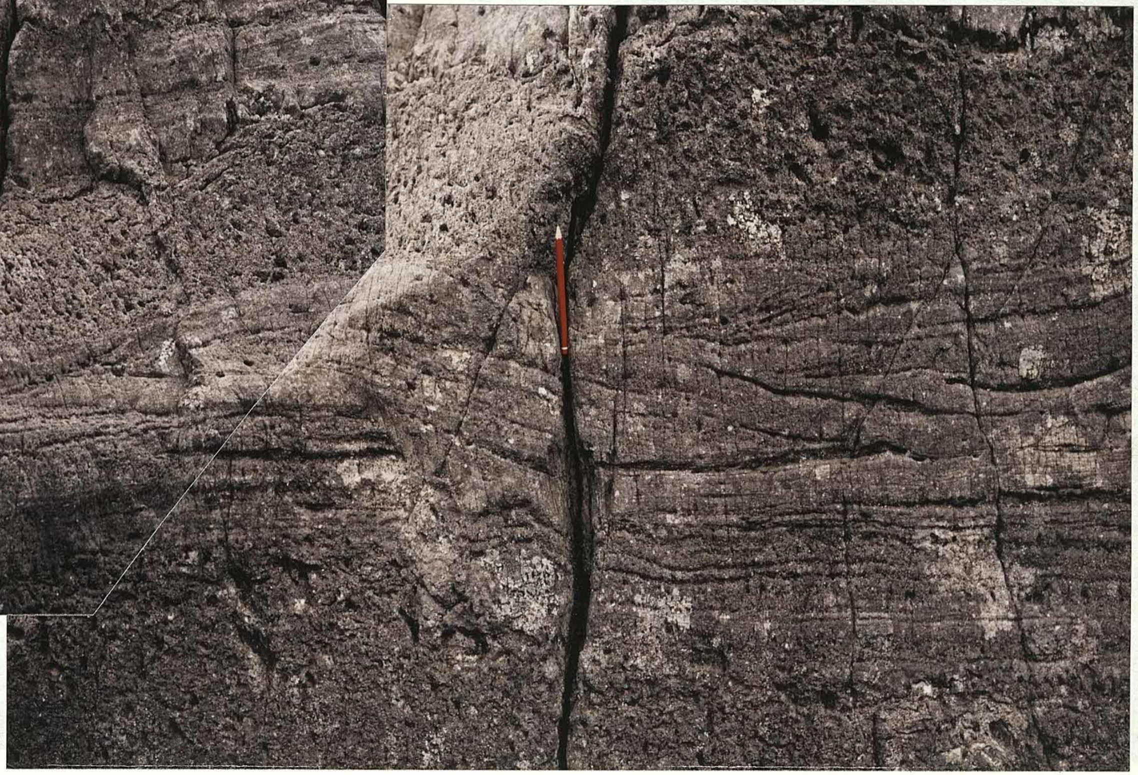

Fig. 7.26: Pumiceous debris flows, thin normally graded high-density turbidites and low angle cross-stratification from turbulent pyroclastic surge. From 4th volcanic Mbr. of CCVF, Ffynnon Lloer, SH 6580 6203.

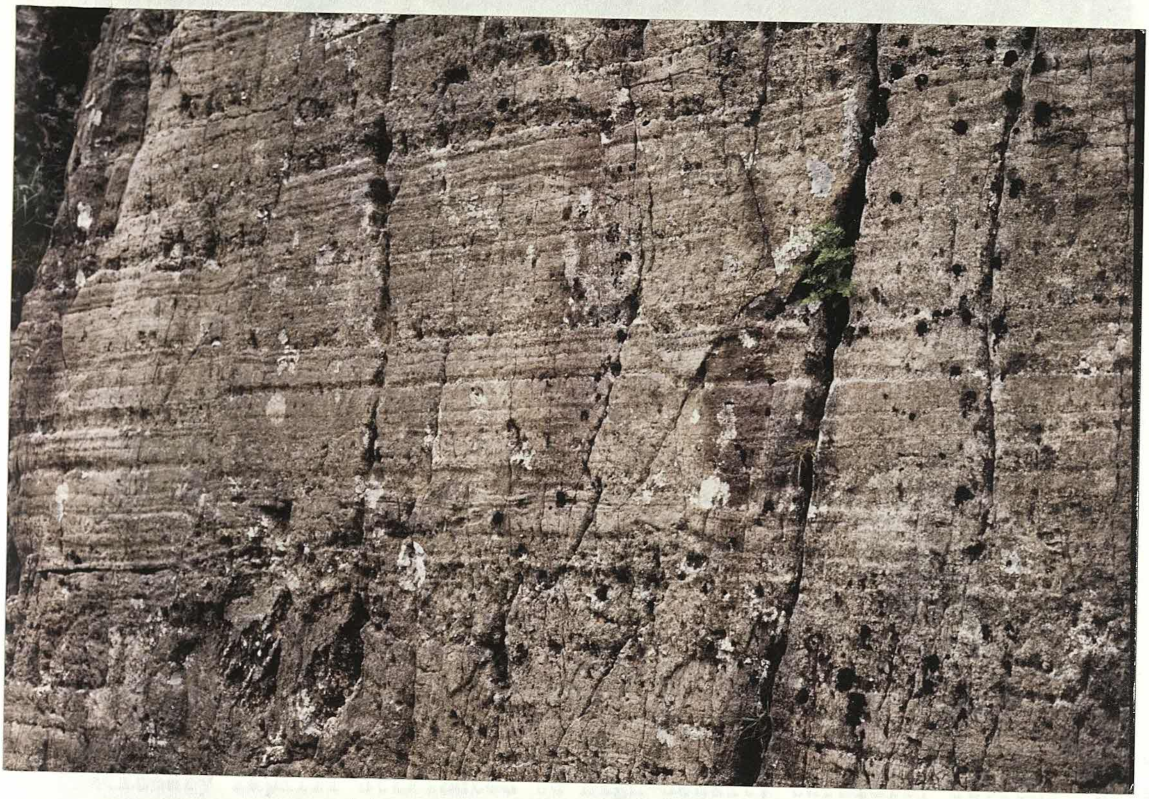

Fig. 7.27: Thinly bedded sheetflows of fine to medium-grained volcaniclastics, isolated large blocks (*eg*. bottom) of pumiceous tuff. Fynnon Lloer, SH 658619, Section F9, 30 m.

Fig. 7.28: Airfall tuff and cross-stratified fine-grained ash containing accretionary lapilli. 4th volcanic Mbr. of CCVF, Pen yr Ole Wen. Section U5, 26 m.

Fig. 7.29: Normally-graded bed of very fine-grained sandstone containing accretionary lapilli attributed to high-density turbidity current. Base of sediment gravity flow denoted by arrow. Accretionary lapilli are not found within basal 4 cm of flow which probably reflects boundary layer shear during deposition. Black mark (centre right) is 1 cm long for scale. From 4th volcanic Mbr. of CCVF, Dyffryn Mymbyr, SH 6965 5732.

Fig. 7.30: Broken fragments of accretionary lapilli from graded sandstone bed. Note fine-grained coated margins. Texture emphasizes durability of accretionary lapilli once formed. Chemical reactions between glass shards rather than electrostatic attraction were probably the dominant binding force (*cf*. Schmid, 1981). From 4th Mbr. of Capel Curig Volcanic Fm.., Capel Curig anticline.

Fig. 7.31: Sediment gravity flow of accretionary lapilli, 4th volccanic Mbr. of CCVF. Alignment of lapilli is tectonic. Pen Yr Ole Wen. Section U5, 61 m. SH 6512 6160.

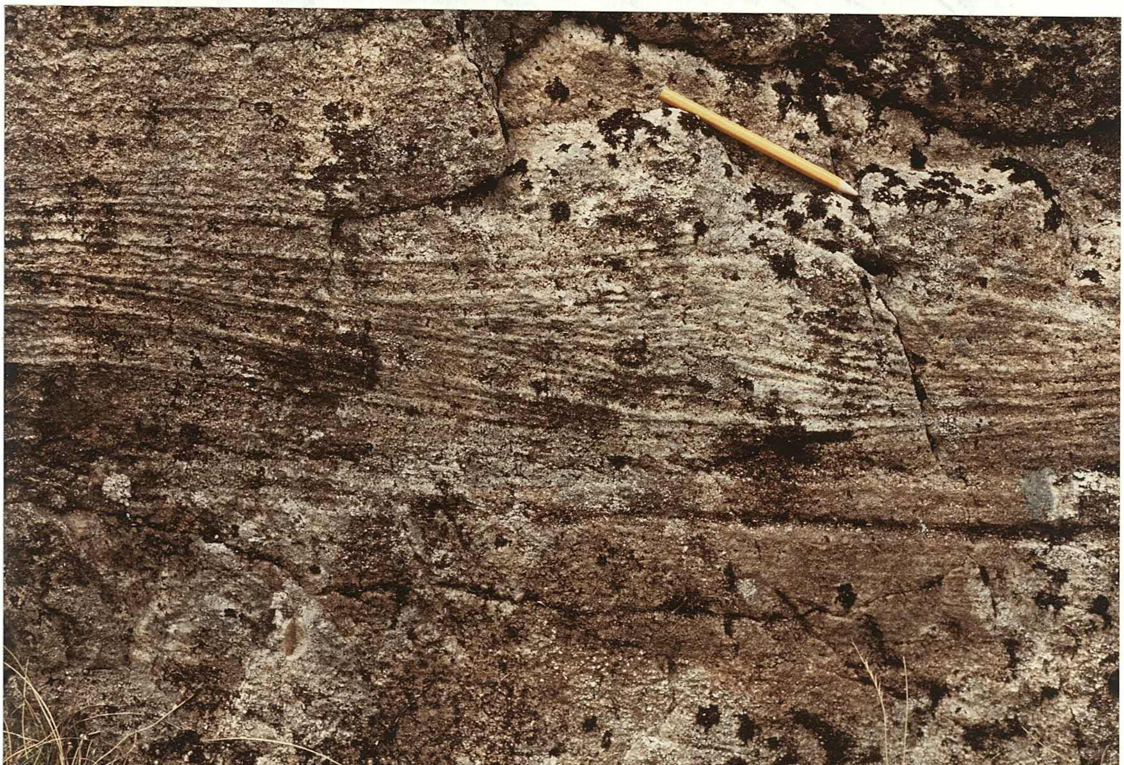

Fig. 7.32: Chevron wave-ripples from distal margins of 4th member volcanic cone, Gallt yr Ogof, north. SH 6968 5952.

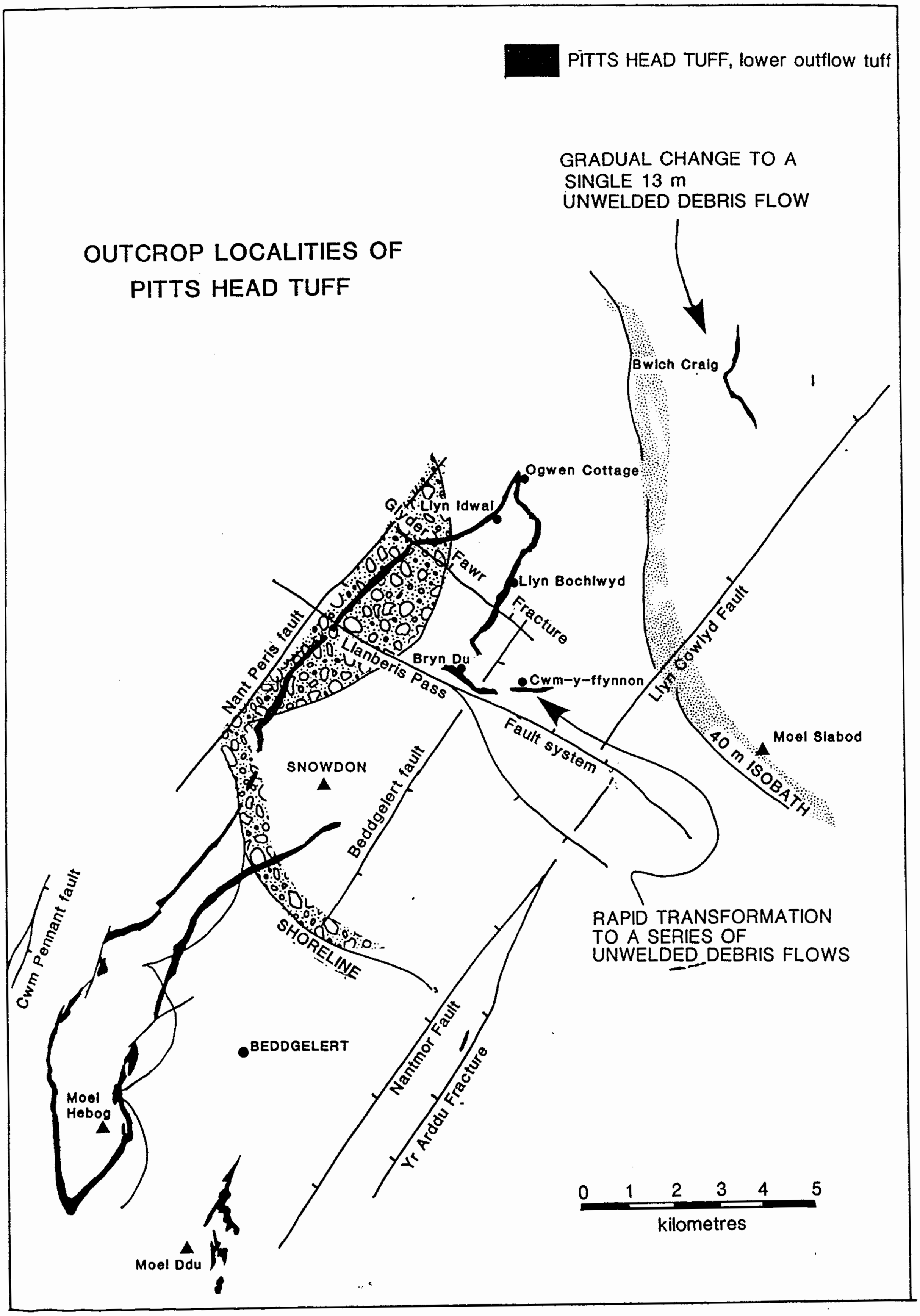

FIG. 7.33: OUTCROP LOCALITIES OF PITTS HEAD TUFF.

Fig. 7.34: Parataxitic welding texture and rotated tuff fragment within Pitts Head Tuff, Moel Ddu. SH 587 442 Evidence for primary welding within ash flow tuff? Portion of rock chisel approximately 15 cm long for scale.

Fig. 7.35: Eutaxitic foliation demarked by flattened pumice fragments. Pitts Head Tuff, near Gwastadnant, Llanberis Pass. SH 610 573.

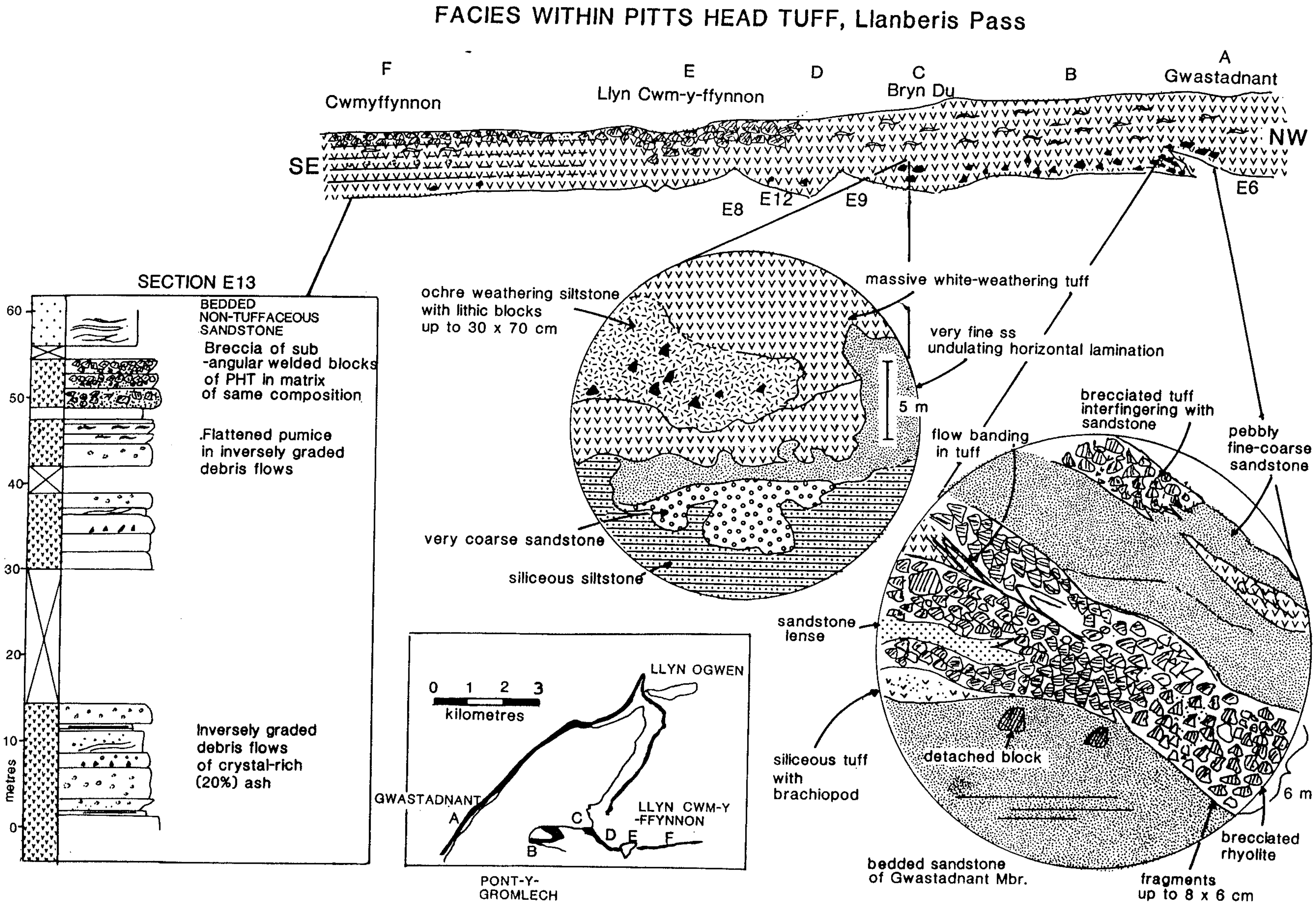

FIG. 7.36: Depositional facies within Pitts Head Tuff along Llanberis Pass.

Fig. 7.37: Airfall tuff at base of Pitts Head Tuff, near Gwastadnant. (SH 613 582) It is not certain whether the lateral pinching and swelling of tuff beds is tectonic, or related to associated surge activity? Similar undulatory bedforms can be witnessed along the base of the Pitts Head Tuff on upper portion of Bochlwyd ridge (SH 652 586).

Fig. 7.38: Large sub-angular to sub-rounded lithic clasts of fine-grained rhyolitic ?tuff within cleaved micaceous tuffaceous siltstone at base of Pitts Head Tuff, near Bryn Du (SH 643 566). Notebook 18.5 cm long for scale. See Fig. 7.33 and 7.49 for location of photograph.

Fig. 7.39: Breccia of angular clasts of parataxitically welded Pitts Head Tuff with comminuted matrix of same composition. From slide blocks of Pitts Head Tuff, Moel Ddu (see Fig. 6 in Reedman *et al*, 1987 and discussion therein). Field notebook is 18 cm long for scale. Compare with Fig. 7.40 & 7.41.

Fig. 7.40: Breccia of sub-rounded clasts of Pitts Head Tuff within unwelded tuff matrix, Llyn cwm-y-ffynnonn. Tuff clasts show considerable variation in texture (*ie*. degree of welding, crystal-content, amount of pumice) and several accidental clasts of uncertain composition (?sandstone) are also visible. Pencil for scale. See section in Fig. 7.36 for stratigraphic location of photo.

Fig. 7.41: Rounded clast of welded Pitts Head Tuff within unwelded tuff matrix, Llyn cwm-y-ffynnon. Lens cap is 6 cm for scale. See section in Fig. 7.36 for stratigraphic location of photo.

Fig. 7.42: Inversely graded debris flows within distal portion of Pitts Head Tuff, from pulsating entry of ash flow into sea. Thin sections are not yet available to determine whether matrix is welded. It is suspected, however that the flattened pumice fragments were formed during movement of the flow on land and transported into the marine setting where they were deposited (*ie.* they <u>do not</u> represent *in situ* pumice flattening).

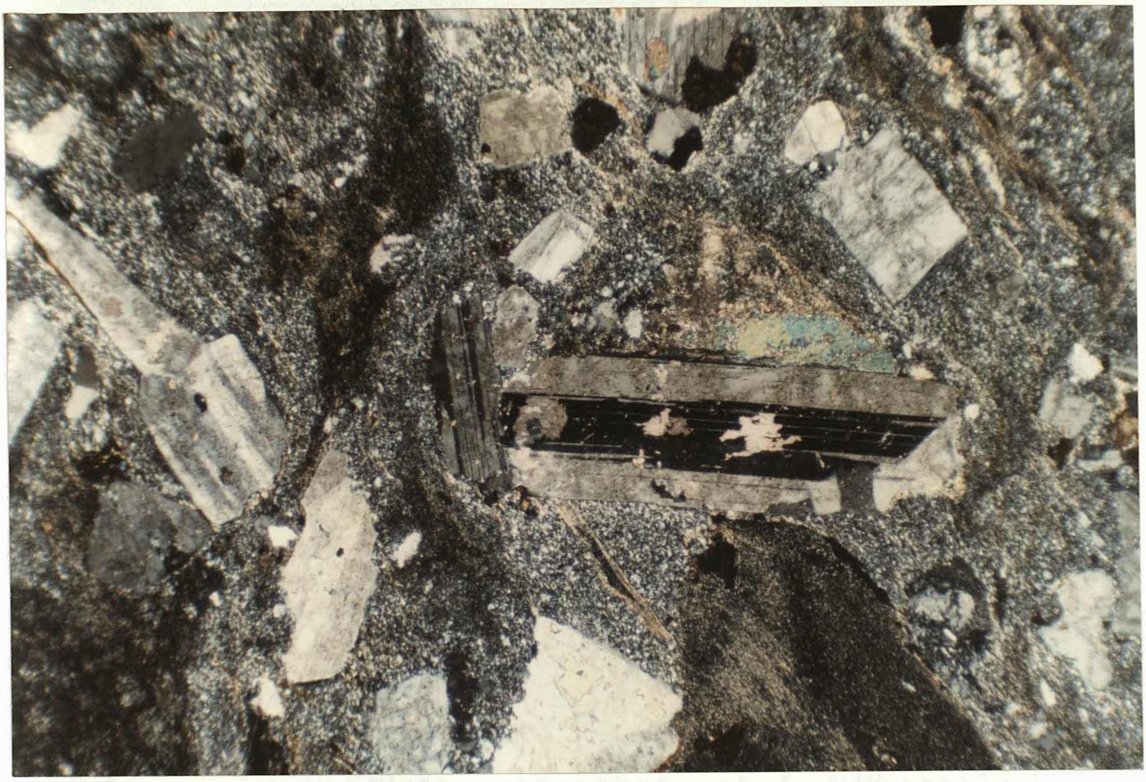

Fig. 7.43: Crystal-rich tuff from debris flow within distal succession of Pitts Head Tuff at Cwmffynnon (SH 656 564). The plagioclase and k-feldspar phenocrysts are set in a "matrix" of microcrystalline quartz. Sample X13. See appendix 1.6+1.7 for chemical composition.

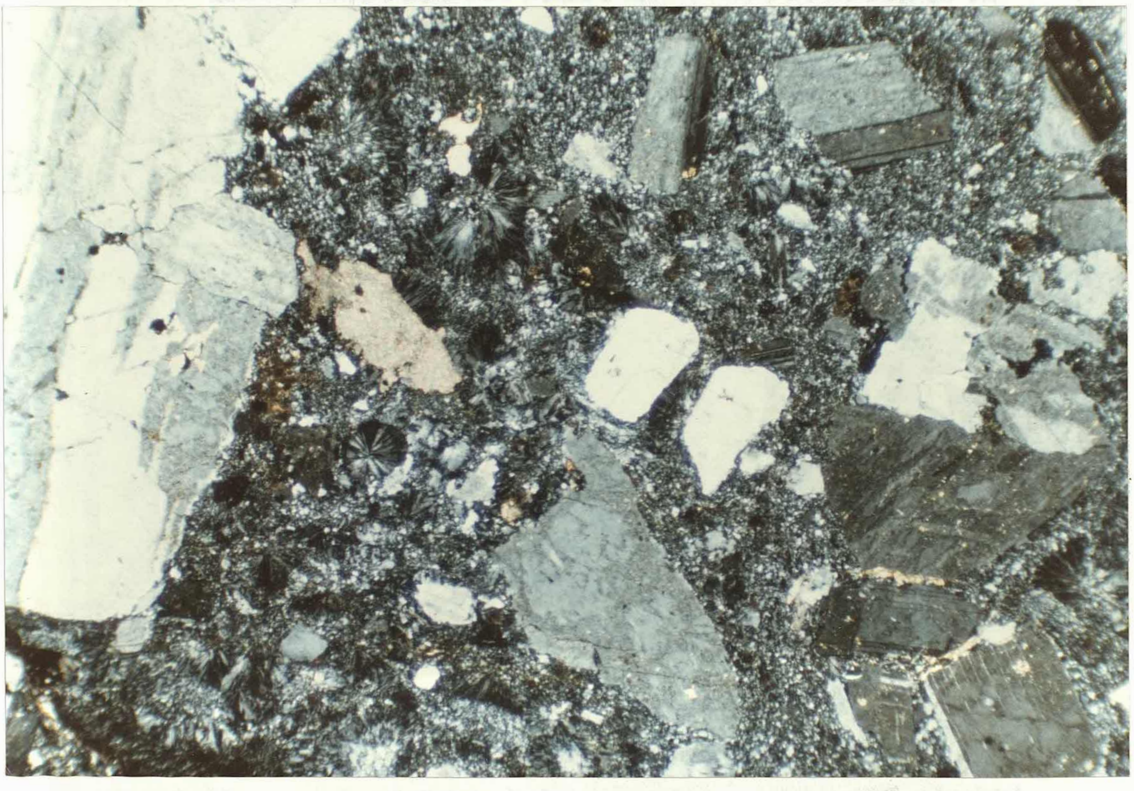

Fig. 7.44: Similar to above. Radial spherulites from devitrified glass shards can be recognised within the matrix. Sample X13. See appendix 1.xx for chemical composition.

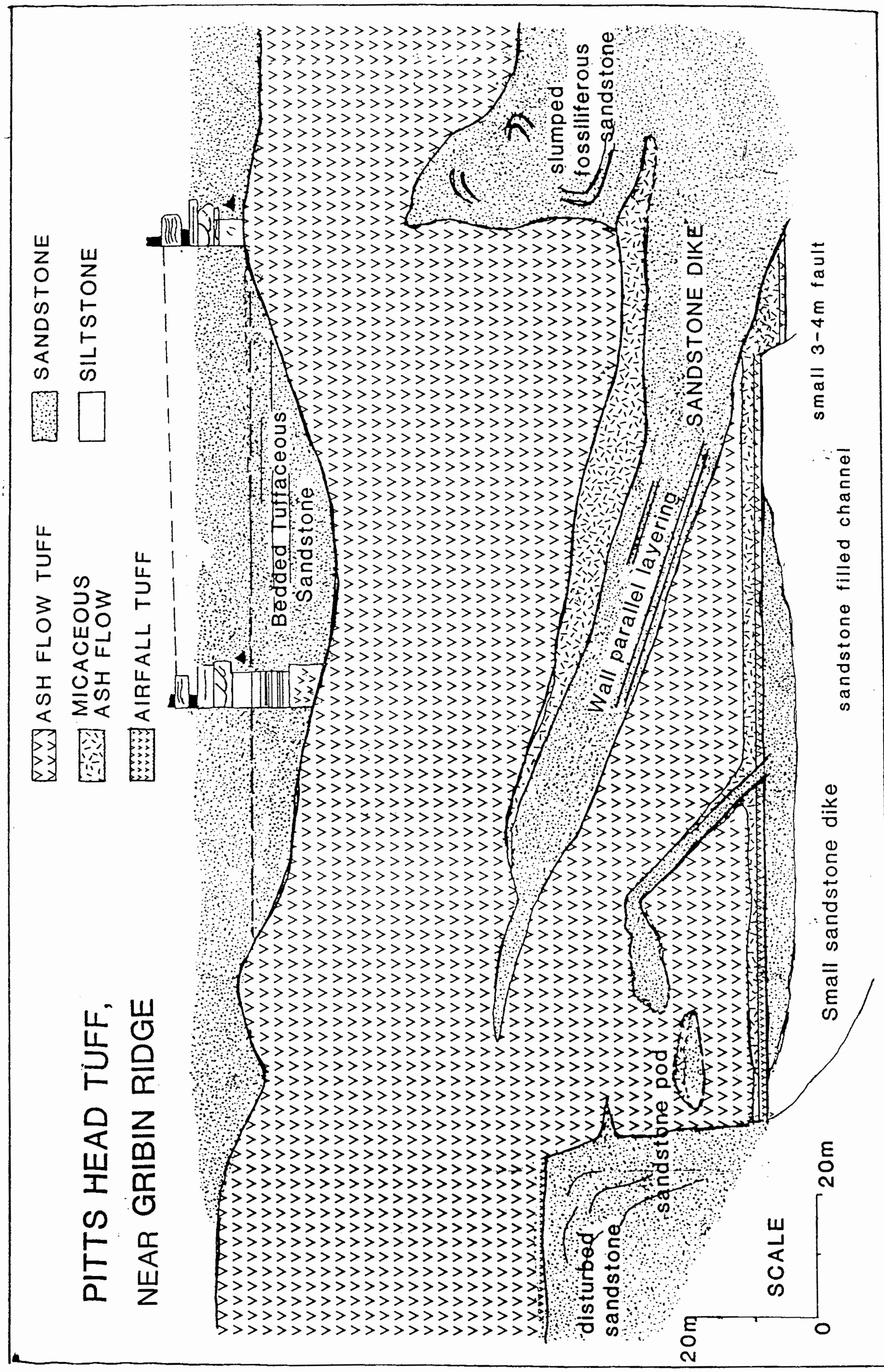

FIG. 7.45: Sketch of half graben, sandstone dyke relationships on Bochlwyd Ridge (SH 653 588). See Fig. 7.46 for oblique phot of dyke, and Fig. 7.47 for stages in its development.

Fig. 7.46: Oblique photo of Bolchlwyd ridge showing outcrop of:

1) Deltaic succession of Bochlwyd Mbr., Lower Cwm Eigiau Fm.
2) Shoreface sequences of Gwastadnant Mbr., Lower Cwm Eigiau Fm.
3) Infill of half-graben by Pitts Head tuff, with thickening of tuff against footwall fault scarp.
4) Large sandstone dyke, with wall parallel layering (4a).
5) Small sandstone dyke
6) Location of apophyses and small pods of sandstone adjacent to main dyke.
7) Secondary pyroclastic flows infilling sag at top of Pitts Head Tuff.

See Figure 7.47 for stages in development of succession, and Figures 7.48- 7.53 for details of particular aspects of tuff/sediment relations.

Fig. 7.47: Sequence of events envisaged for formation of sedimentary and tectonic relationships on Gribin ridge. Field location of numbered features indicated on Fig. 7.46.

A) Emplacement of air fall tuff at base of Pitts Head Tuff. Development of half-graben synchronous with emplacement of ash flow tuff results in local thickening of ash flow to 70 metres along hanging-wall (1) and induces soft sediment deformation and slumping in opposing sediments (2)

B) Continued listric rotation at base of Pitts Head Tuff and tensional opening of fissure leads to intrusion of several sandstone dykes (4,5). Dykes were intruded just after welding commenced towards the base of the ash flow but before any cohesion or cementation had developed in the middle of the flow (see text for further discussion).

C) Final movement on sole fault produced sag (7) which was quickly infilled by a series of thin debris flows derived from reworking of unwelded, partially welded and brecciated top to Pitts Head tuff.

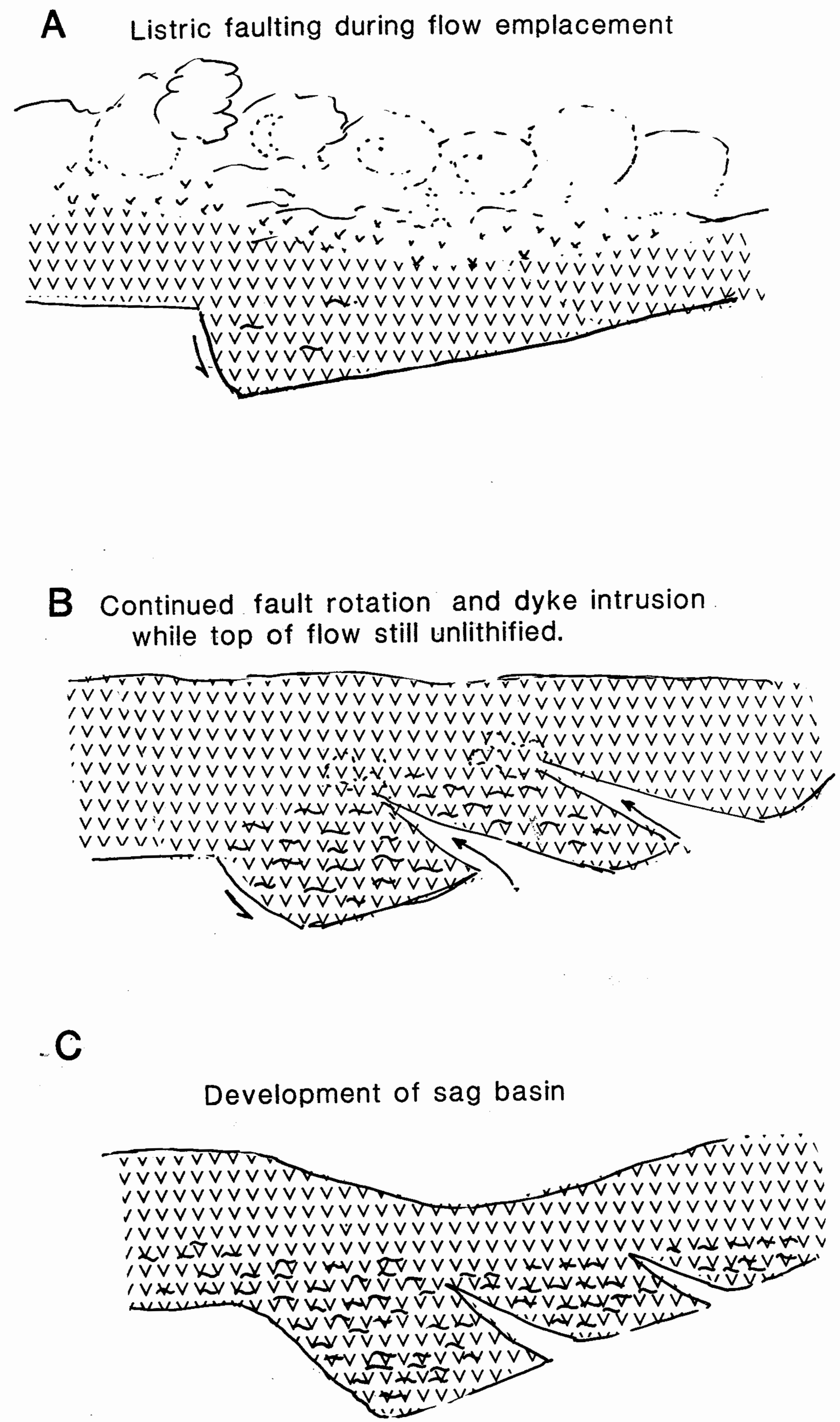

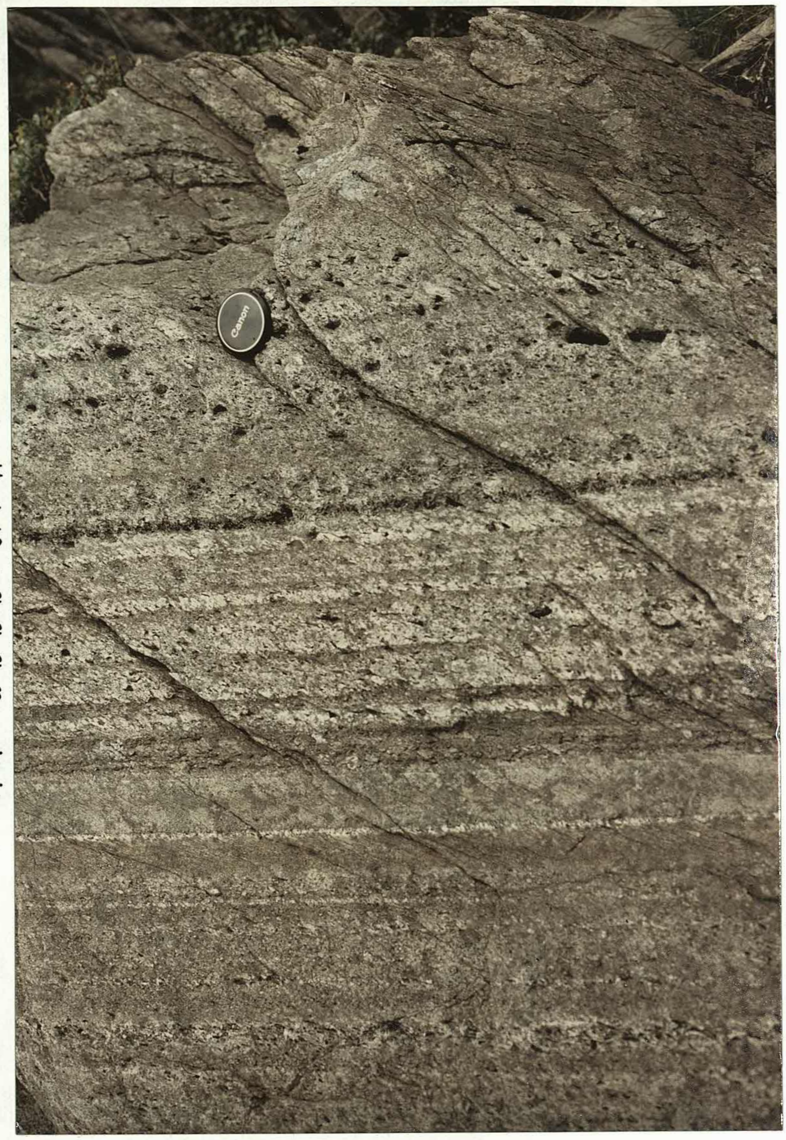

Fig. 7.48: One-metre thick sequence of air-fall tuff succession along base of Pitts Head Tuff, Bochlwyd Ridge. The individual centimetre thick layers can be traced for 200 metres parallel to strike. Lens cap is 6 cm for scale. See Fig. 7.37 for field local of photo.

Fig. 7.49: Base of Pitts Head Tuff, Bochlwyd Ridge showing:

1) Bedded airfall tuffs
2) Micaceous base of the ash flow tuff.
3) Intrusion of thin sandstone dyke into Pitts Head Tuff. Dyke is bound on both sides by the unwelded micaceous tuff from the base of Pitts Head Tuff.

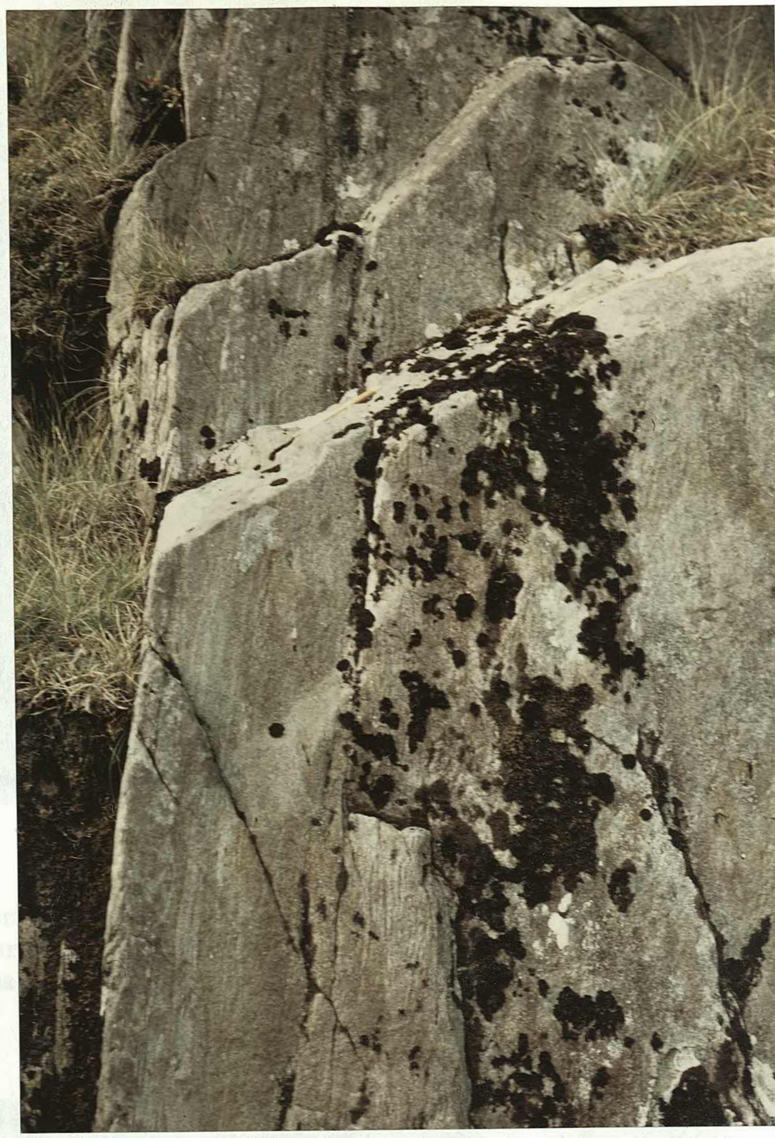

Fig. 7.50: Wall-parallel layering near edge of large sandstone dyke. Partially hidden pencil (arrow) for scale. See Fig. 7.37 for field location of photograph.

Fig. 7.51 View of large sandstone dyke showing both, 1) the thick zone of wall-parallel layering, and 2) an internal massive zone where preservation of textures transverse to dyke margins suggests plug flow. Field notebook is 18.5 cm for scale. See Fig. 7.37 for location of photograph.

Fig. 7.52: Apophyse of sandstone (under 6 cm lens cap) protruding into ash flow tuff on margin of large sandstone dyke. Note that ?welded tuff with eutaxitic foliation extends locally to within 20 cm of sandstone indicating limited interaction of water/sediment mixture and hot tuff at this locality. Compare with Fig. 7.53. See Fig. 7.46 for location of phot.

Fig. 7.53: Detached "pod" of sandstone adjacent to large sandstone dyke within Pitts Head Tuff, Bochlwyd ridge. Radial fractures within sandstone pod would reflect rapid contraction resulting from expulsion of contained water as steam. Surrounding tuff shows no evidence of welding at this locality. Compare with Fig. 7.52. See Fig. 7.46 for location of photo.

Fig. 7.54: Large raft of sandstone (?originally a large sandstone dyke) near top of Pitts Head Tuff at Llyn Idwal. Margins of raft are either extremely distinct (A) or diffusely grade into surrounding tuff; these relationships indicate extreme variance in the amount and style of interaction between hot ash flow and incorporated sand/water mixture. See text for further discussion. Location: SH 641 597.

Fig. 7.55: "Cannon-ball"-sized siliceous nodules 8 m above base of welded Pitts Head Tuff, Moel Hebog. From top of section L2, SH 569 467.

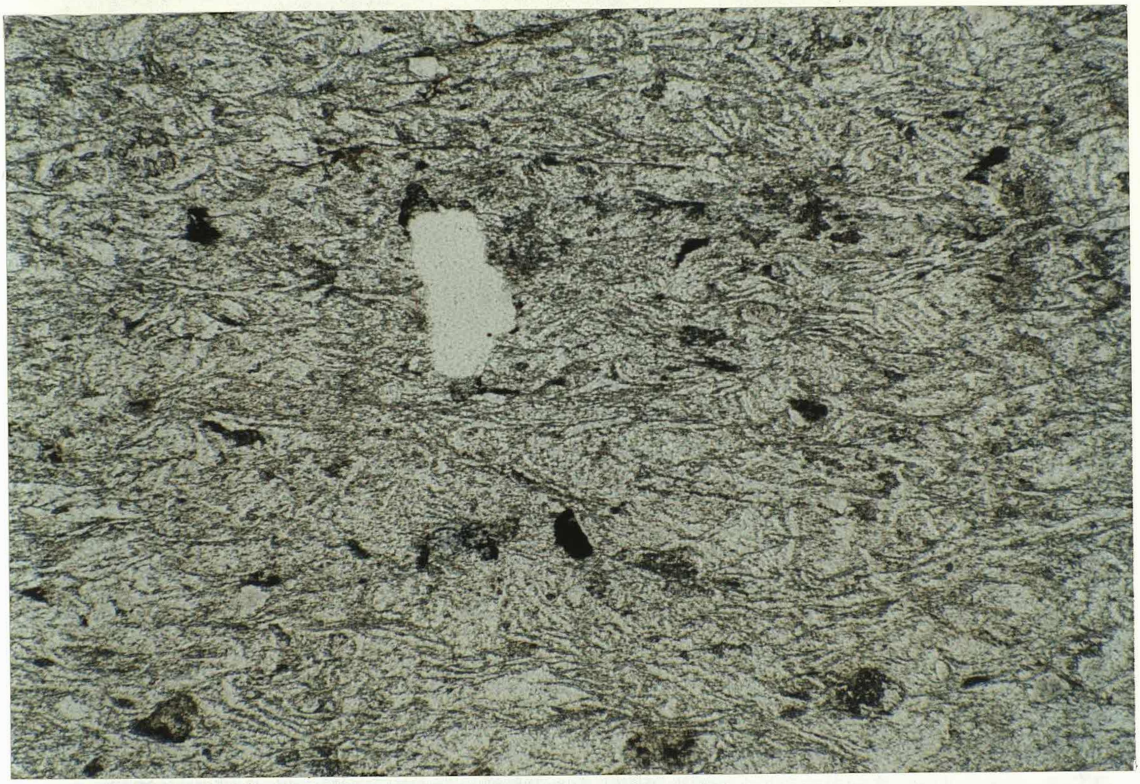

Fig. 7.56: Vitroclastic texture within Pitts Head Tuff at Bwlch Craig. Texture originally interpreted as incipient welding but M. Howells (pers. comm, 1988) suggests that it represents tectonic deformation. Further petrographic research with orientated thin sections is currently in progress to validate which hypotheses is correct. It should be noted that adjacent samples display perlitic fracturing of glass shards indicating that they were hot upon emplacement. Sample X23, *ca.* 5 m from base of 13 m thick flow. See Fig. 7.33 for location and Appendix 1.7 for trace element geochemistry.

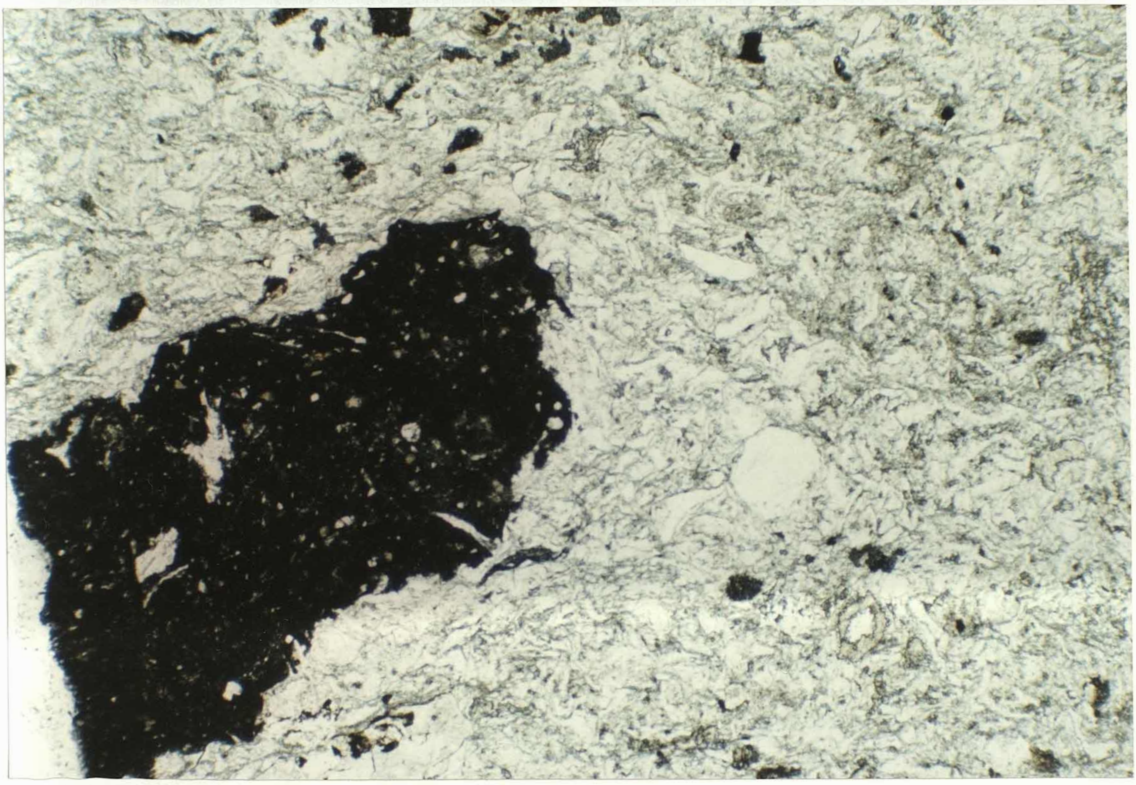

Fig. 7.57: Unwelded glass shards and "clot" of mudstone within Pitts Head Tuff, Bwlch Craig. See Fig. 7.33 for location and Appendix 1.7 for trace element geochemistry.

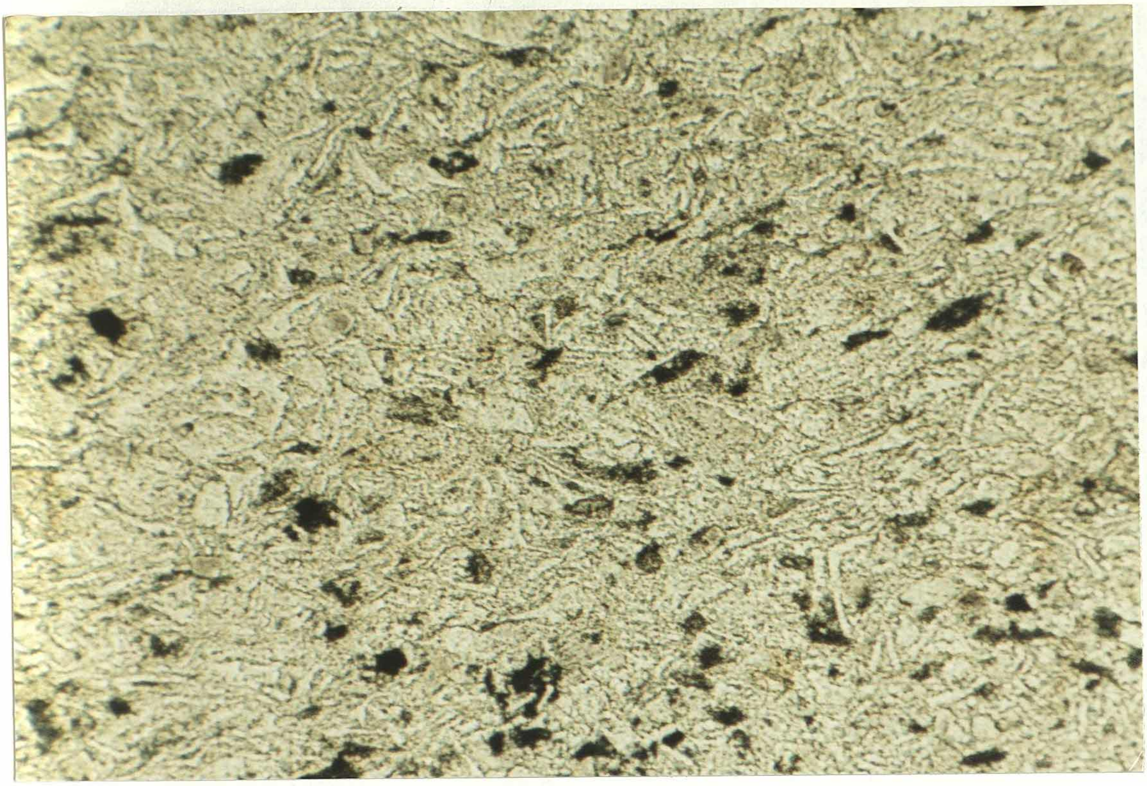

Fig. 7.58: Unwelded cuspate glass shards from fine-grained "tuffite", Gribin ridge. Section D1, 251 m. Sample D41.

Fig. 7.59: "Slurried" texture in subaqueous rhyolitic pyroclastic flow, Tuff 512, Llyn Cowlyd.

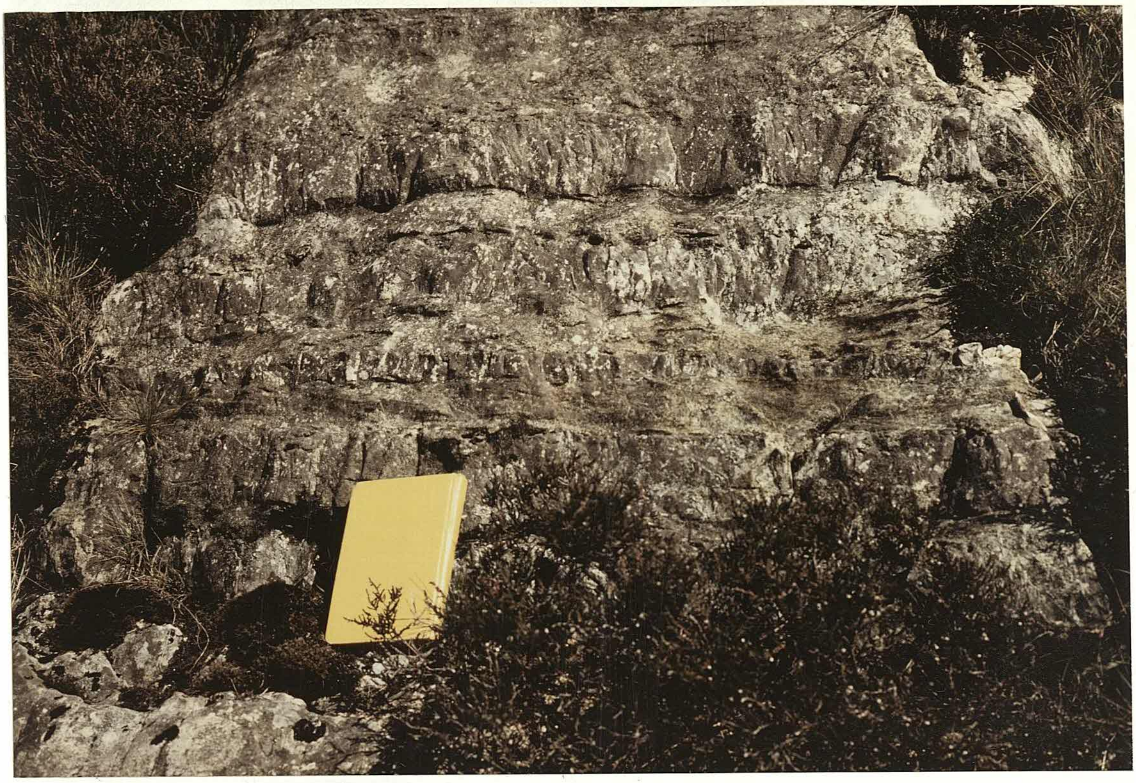

Fig. 7.60: Thin (5-15 cm), normally-graded beds of white weathering fine-grained tuff separated by thinner beds of less tuffaceous siltstone. From Tuffite Mbr., Tryfan anticline. See Fig. 5.61 for stratigraphic position. Notebook 18 cm long for scale.

Fig. 7.61: Water-escape structure within horizontally-laminated siltstone from top of Tuffite Mbr., Tryfan anticline. See Fig. 5.61 for stratigraphic position. Black mark (centre bottom) 1 cm long for scale.

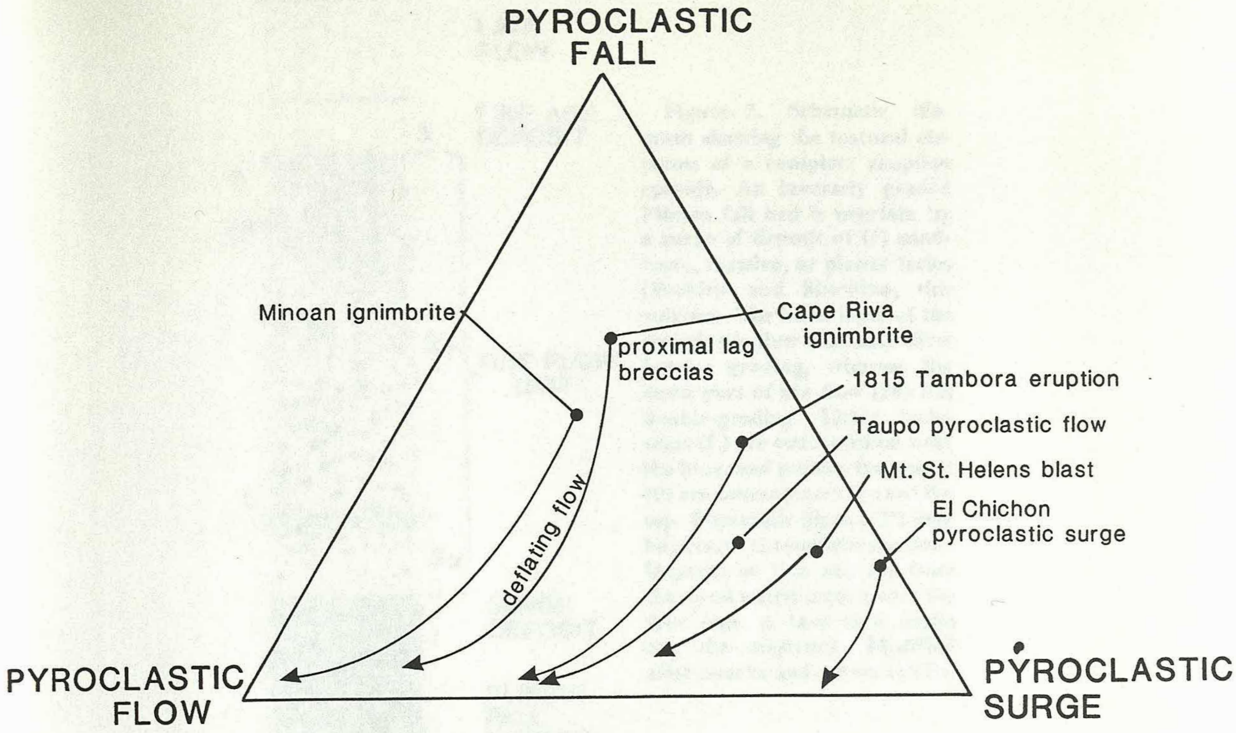

Fig. 7.62: Triangular framework for examination of subaerial pyroclastic processes with relative position of several recent deposits. Also shown is hypothetical pathway that would be followed by evolving pyroclastic flows

Fig. 7.63: Small lobate sandflows cascading down slopes of quarry within Cretaceous Lower Greensands near Leighton Buzzard during a wet June. Note cleft-and-lobe structure on flow front of each depositional lobe. Notebook 18 cm long for scale.

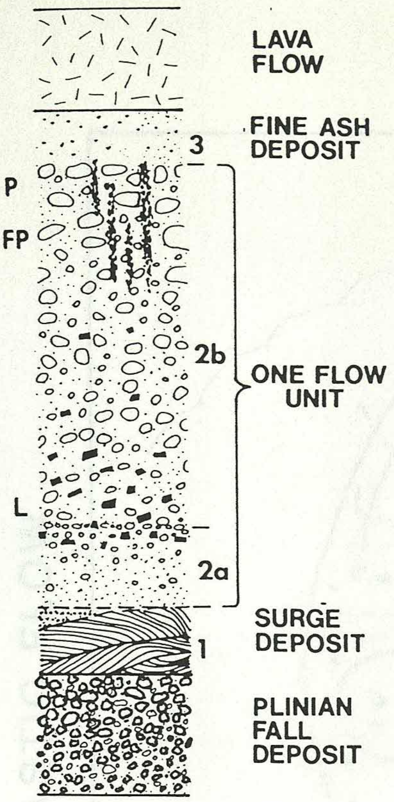

Figure 3. Schematic diagram showing the textural elements of a complete eruption episode. An inversely graded Plinian fall bed is overlain by a surge of deposit of (1) sandwave, massive, or planar facies (Wohletz and Sheridan, this volume). The basal layer of the pyroclastic flow (2a) may show inverse grading, whereas the main part of the flow (2b) has double-grading. Lithic inclusions (L) are concentrated near the base, and pumice fragments (P) are concentrated toward the top. Fumarolic pipes (FP) may be present throughout the flow. Deposits of fine ash (3) from the cloud would occur above the flow unit. A lava flow might cap the sequence. Modified after Sparks and others (1973).

Fig. 7.64 Standard ignimbrite sequence. From Sparks & Walker, 1973.

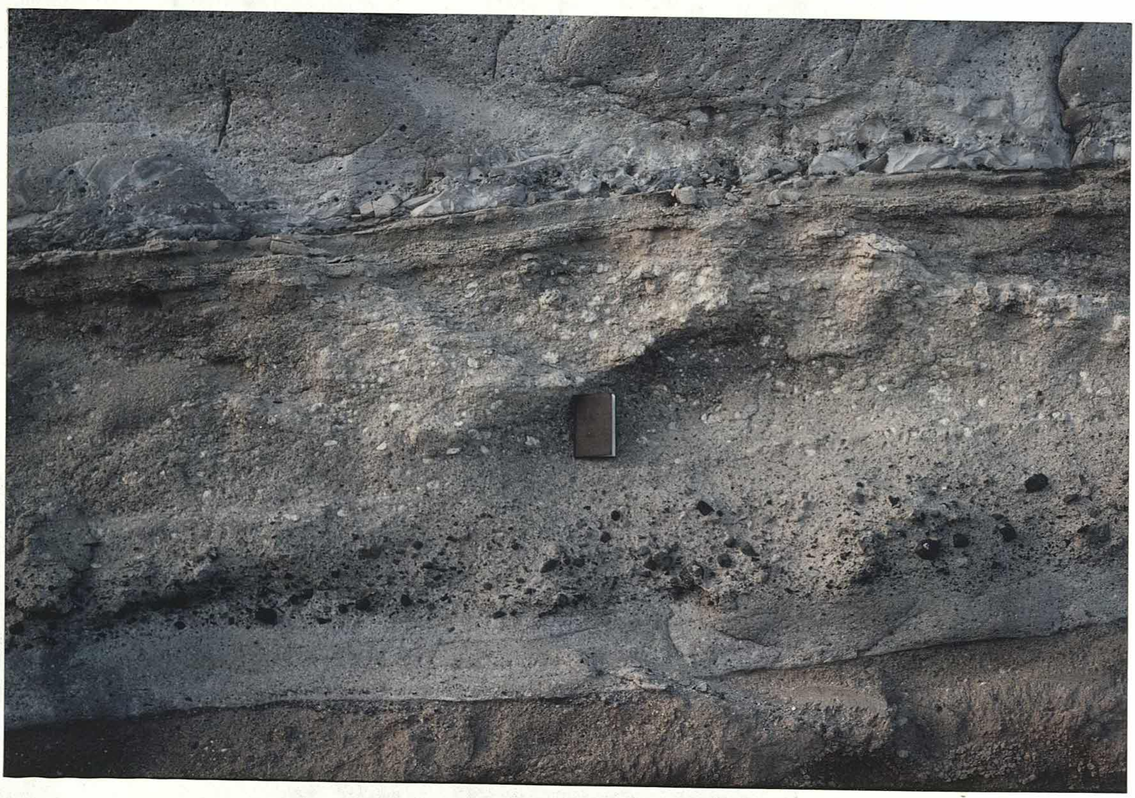

Fig. 7.65: Ideal sequence that one would expect from small-intermediate volume pyroclastic flow. Depositional units that can be recognised are number from Sparks & Walker, 1973 (shown above)

SCHEMATIC PYROCLASTIC FLOW

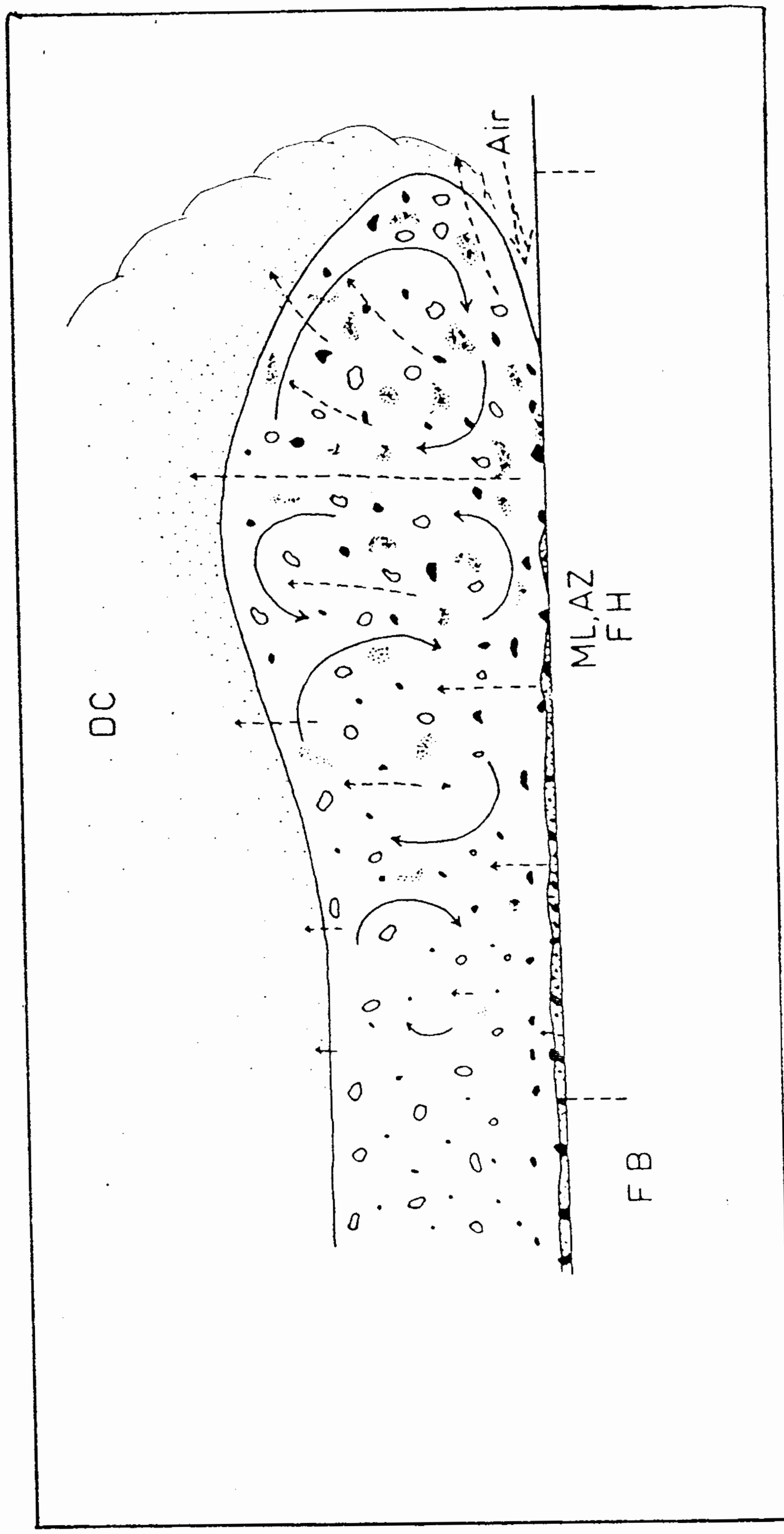

WILSON, 1980

FIG. 7.66: Front of a fluidised pyroclastic flow showing turbulent mixing of air into head along base of flow. (From Wilson, 1980)

FIG. 7.67: Tracing of powdergraphs from sediment gravity flows travelling over a horizontal surface. Illustrates the degree of mixing into the flow in the wake of the head in both viscid and inviscid situations. (traced from Simpson & Britter, 1979).

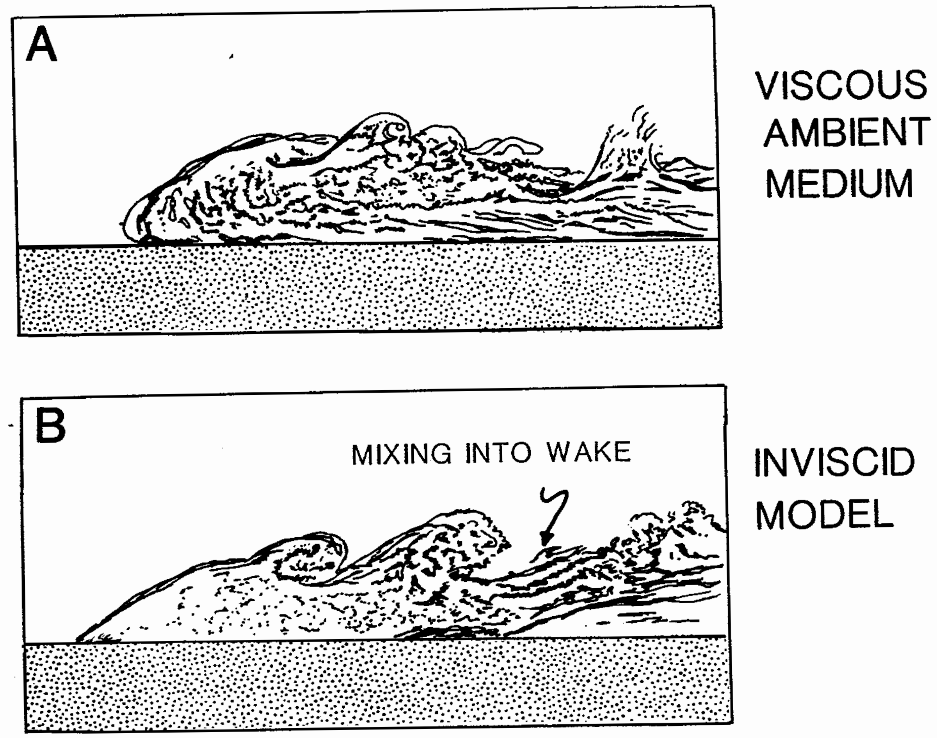

FIG. 7.68: The control of slope on the size and amount of mixing in a gravity current head. Traced from Britter & Linden, 1980.

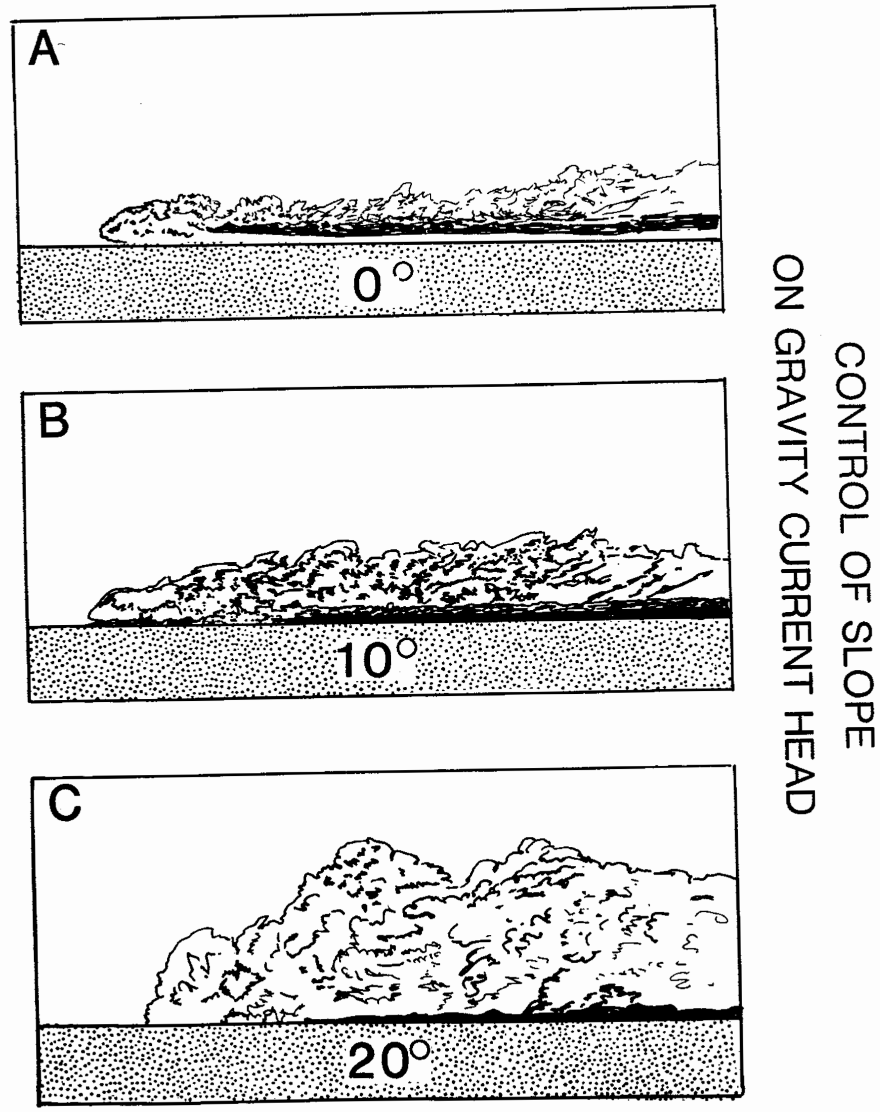

FIG. 7.69: Characteristic features of a boundary layer of a sediment gravity flow. (From Middleton & Southard, 1984)

A: Development of a turbulent boundary layer in a mature flow.

B: Style of mixing with a non-turbulent flow and its turbulent boundary layer.

C: Position of viscous sub-layer.

A

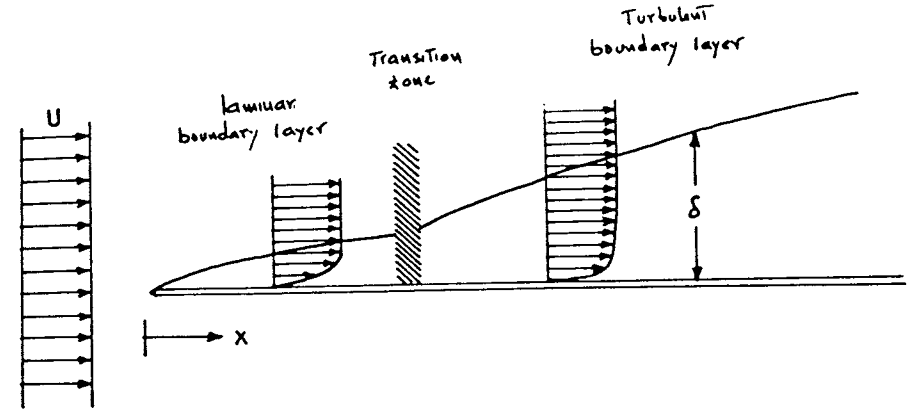

Figure 3.18 Transition from laminar flow to turbulent flow in the boundary layer developed next to a flat plate held parallel to the flow.

B

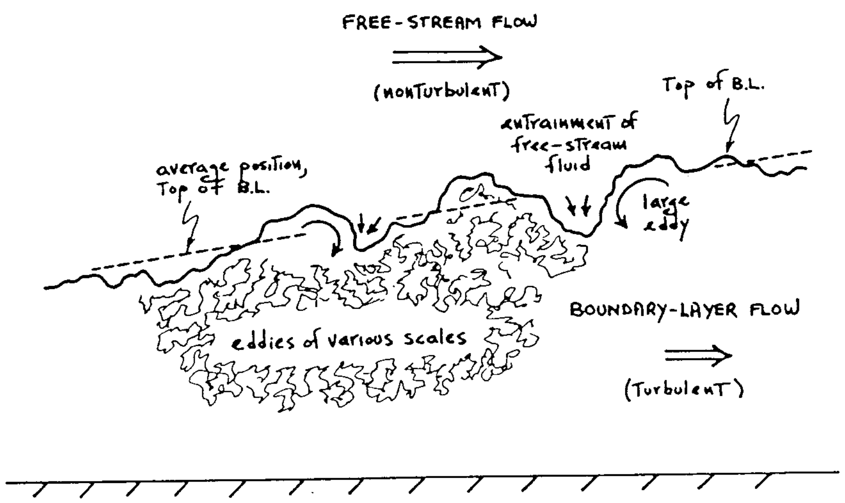

Figure 3.19 Mixing of ambient free-stream fluid into the outer part of a turbulent boundary layer.

C

5-7

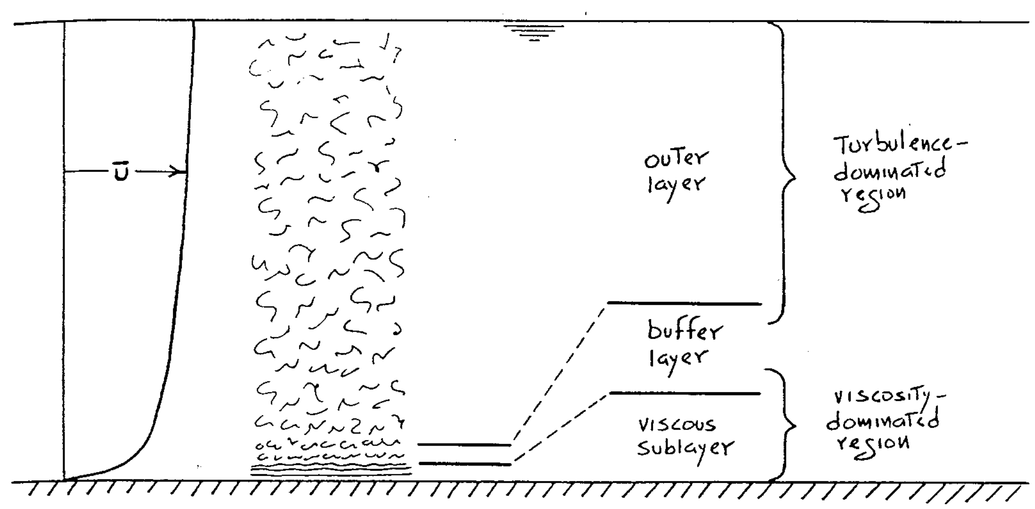

Figure 5.4 Zones of turbulence structure in steady uniform turbulent flow down a smooth plane. Eddy structure (schematic) is as seen by an observer moving with flow.

Fig. 7.70: Flow parallel alignment of foam on Llyn Cwm-y-ffynnon attributed to Langmuir circulation cells. A steady wind was blowing from upper right to lower left at *ca.* 30 mph. whilst photograph was taken. The development of the contra-rotating vortices responsible for pattern would result from complex boundary layer interaction between waves and wind.

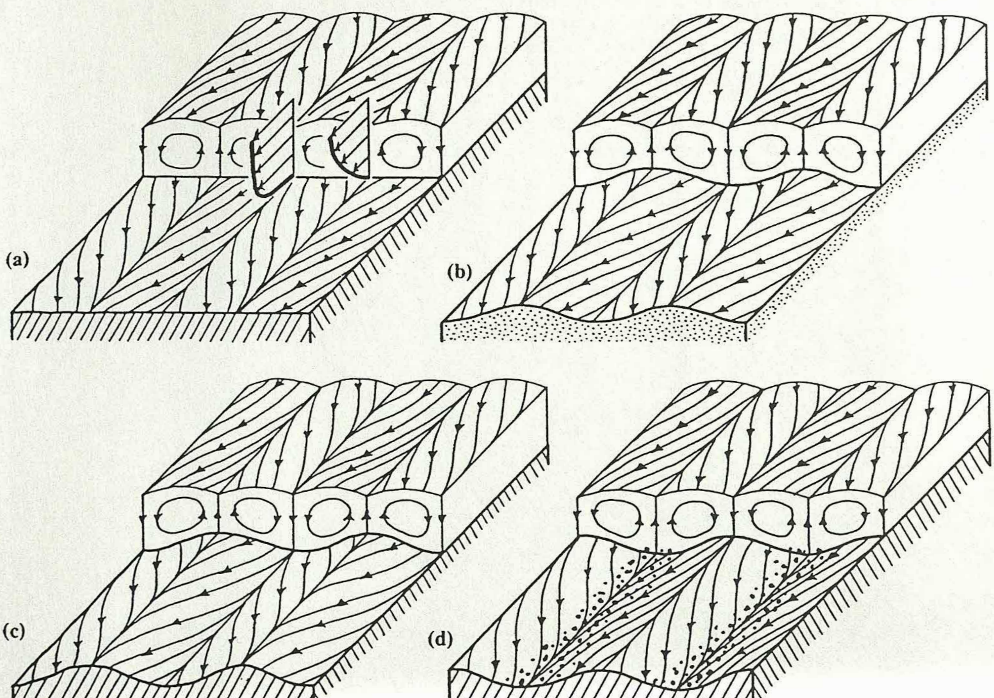

Figure 11.15 Corkscrew vortices (secondary flows) and their effects. (a) General character of motion. (b) Shape of deformable granular surface adjusted to the motion. (c) Shape of a mud bed adjusted to the motion in the absence of bedload. (d) Shape of a mud bed adjusted to the motion in the presence of bedload particles.

Fig. 7.71 Wind patterns associated with formation of seif dunes (from Allen, 1985)

FIG. 7.72: Sketch of the front of a sediment gravity flow showing development of cleft and lobe structures. (From Allen, 1971).

FIG. 7.73: Geometry of deep marine pahohoe basalt flows in the Archean. Map illustrates the control of volume and effusion rate on the degree of development of cleft and lobe structures. (From Dimroth et al, 1985)

A

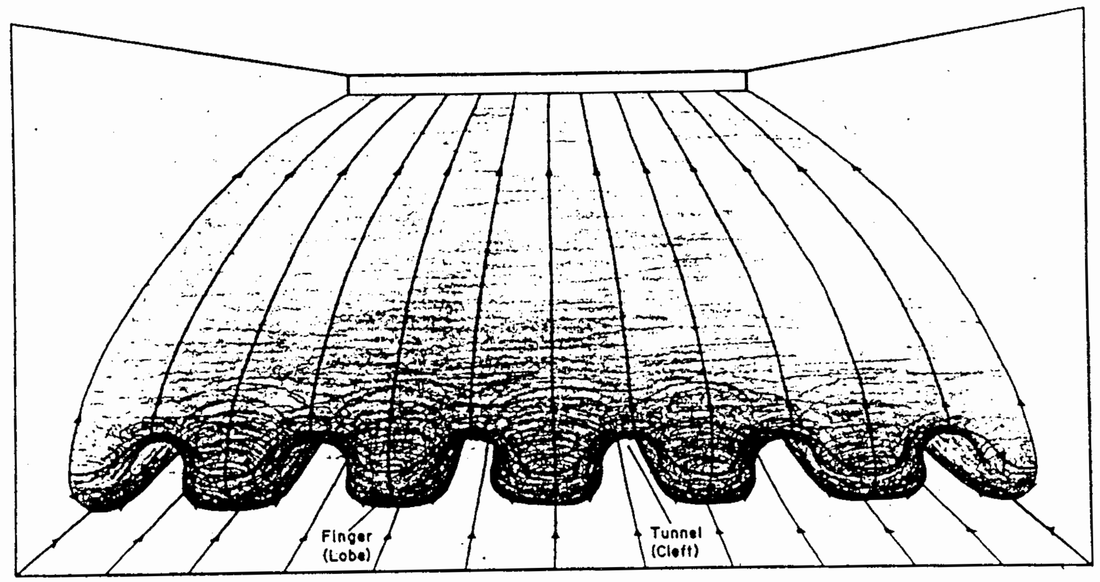

B

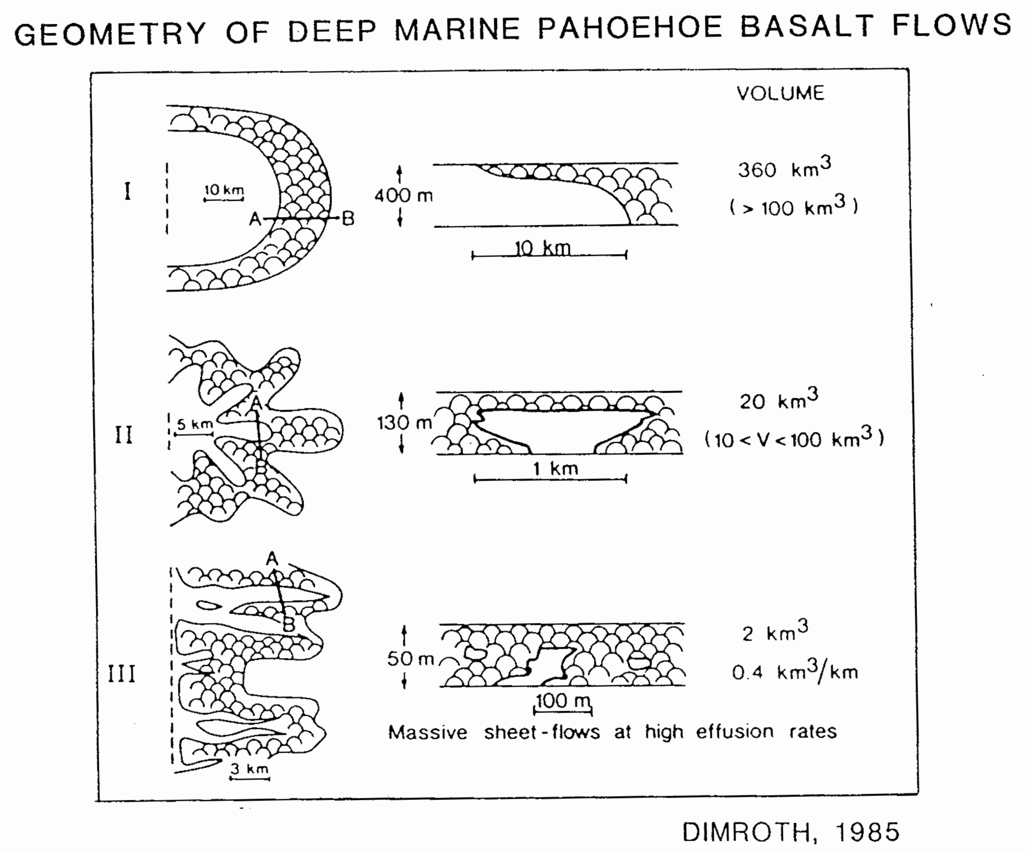

Fig. 7.74: Hydraulic jump induced by change in depositional slope when water within overflow chute from reservoir mid-Wales passes into fluvial channel. The transition from upper flow regime sheetflow to lower flow regime currents is marked by several turbulent "standing" waves and a substantial increase in the thickness of the flow. Ignore unrelated plume of water at top of photo.

Fig. 7.75: Small lense of lithic blocks within pyroclastic flow on Tenerife. Attributed to local fluctuations in flow regime such as a supercritical to subcritical transition which were perhaps related to a change in subjacent topography. Taken from lower slopes of volcano.

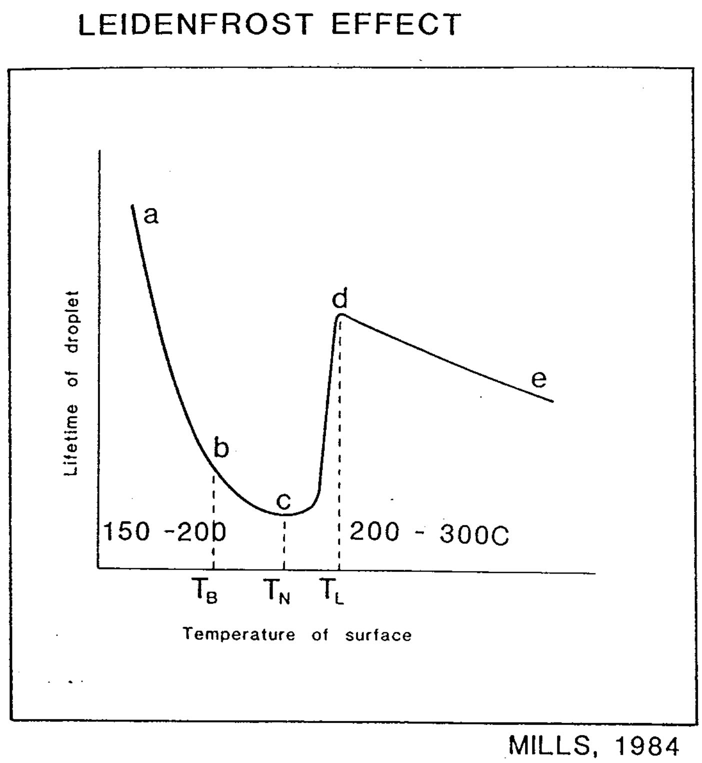

FIG. 7.76: The Leidonfrost effect. At Tl (d) non-nucleated film boiling replace "normal" vigorous boiling. (from Mills, 1984).

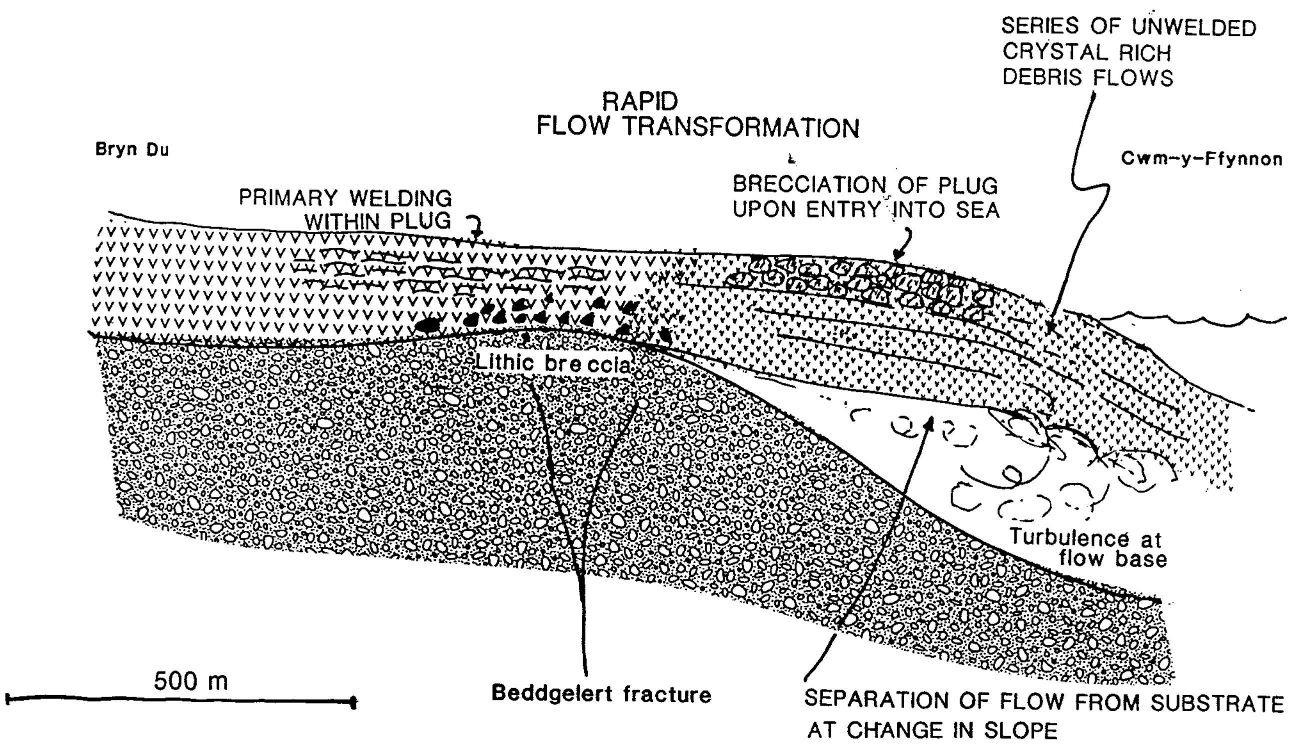

FIG. 7.77: Emplacement dynamics of the Pitts Head Tuff along Llanberis Pass.

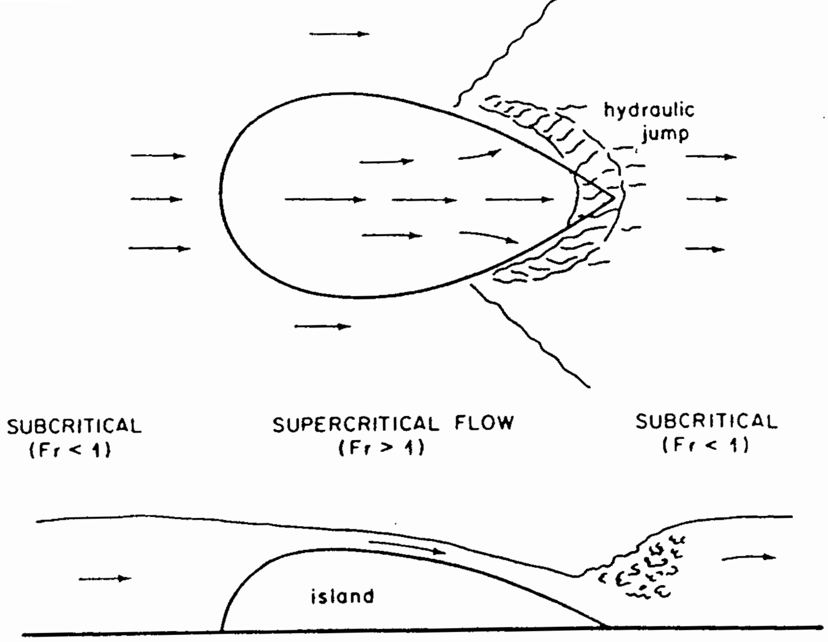

Figure 4. Schematic drawing of flow over submerged island, modifying it into streamlined form. Flow over island becomes supercritical due to Fr = $u/\sqrt{gh} > 1$ so that hydraulic jump occurs on its downstream side.

FIG. 7.78: Schematic drawing of supercritical flow over submerged island. An analog for development of laminar shear within the Pitts Head Outflow tuff which was able to top the caldera wall???? (From Komar, 1983).

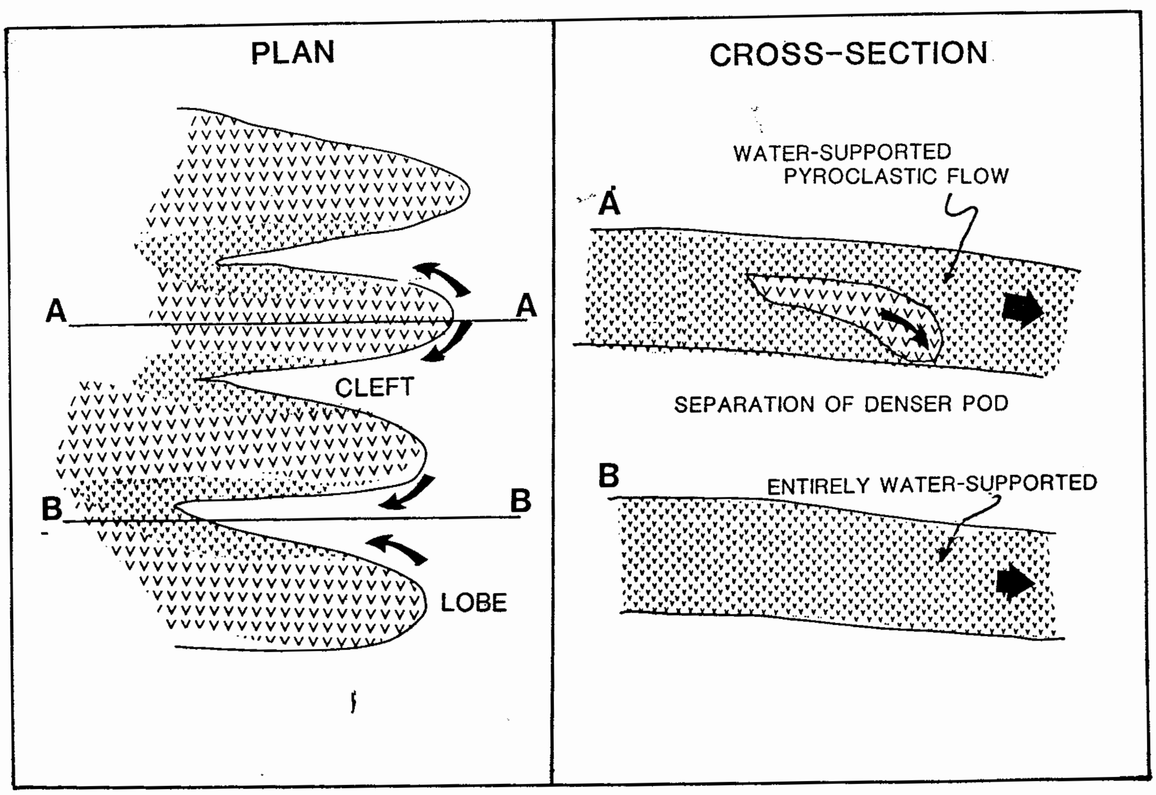

FIG. 7.79: Schematic drawing of development of a Capel pod within a lobe of a poly-lobate pyroclastic flow.

Fig. 7.80: Outsized clast of rhyolite (R) in mudflow which is only 5 cm thick (arrow). From Upper Cwm Eigiau Fm., near Capel Hill. Section G6b, 17.6 m.

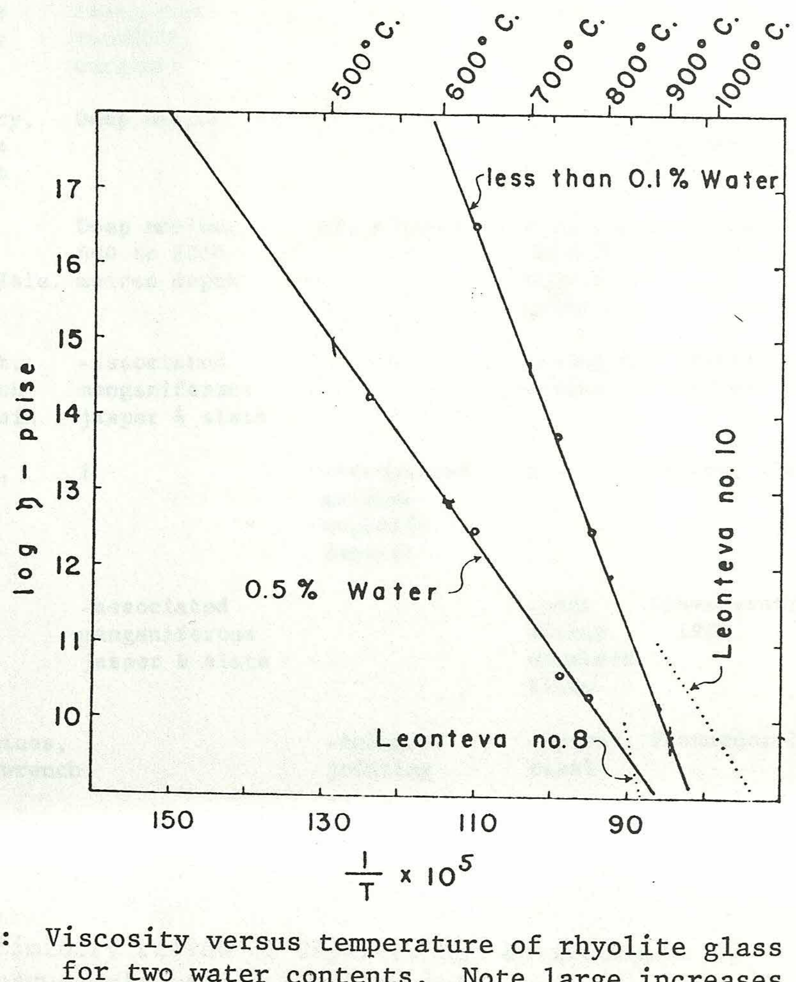

FIG. 7.81: Viscosity versus temperature of rhyolite glass for two water contents. Note large increases in viscosity for slight decreases in temperature. (From Friedman et al, 1963)

REALMS OF SUBAQUEOUS WELDING.

	AGE	LOCATION	ENVIRONMENT	FEATURES	GEOMETRY	REFERENCE
SHALLOW WATER (< 50 m)	Archean Canada	Yellowknife	Shallow marine, associated with XS conglomerate	10-15 m thick, i/b pillowed andesites	lensoid	Padgham, 1980
	Archean	Ontario	Shallow marine	-2 flows,50 & 100m -underlain subaqueous ash flows, - overlain stromatolites	16 km lateral extent	Thurston, 1980
	Ordovician	Ireland, Back-arc basin	Alluvial plain	Laterally extensive, 3-36 m thick	Sheet-like	Stanton, Dewey, Pudsey,
	Ordovician	North Wales	Nearshore marine (25 m maximum water depth)	Laterally extensive	Sheets	this study
	Devonian	Germany	Tidal flat			Scherp & Grabert, 1981.
DEEP MARINE (>500 m)	Protero-zoic	Colorado, Immature back-arc basin	Deep marine, associated turbidity currents	?	?	Condie, 1981
	Lower-Middle	Roseberry, Tasmania Cambrian	Deep marine	?	?	Corbett, 1981 Braithwaite, 1974 Green, 1976
	Ordovician	South Wales, Ramsay Isle.	Deep marine, 500 to 2000 metres depth	161 m thick	laterally restricted within gully	Kokelaar & Bevins, 1985
	Ordovician	Bathurst, N.B. Back-arc basin	-associated manganiferous jasper & slate		-submarine caldera	-Patari, 1977 Hurley, 1970
	Silurian	Buchans, NFLD	?	-associated massive suplhide deposit	?	Thulow, 1980
	Lower Carb.	Spain, Pyrite Belt	-associated manganiferous jasper & slate		-pods within unwelded flows	Schermerhorn, 1980.
	Palaeogene	Phillipines, -along wrench		-columnar jointing	-patchy basal	Fernandez,1977

FIG. 7.82: Preliminary review of depositional environments of subaqueously welded ash flow tuffs.

FIG. 7.83: A classification of rhyolitic magmas using proprtions of Nb and Zr. (From Leat et al, 1986).

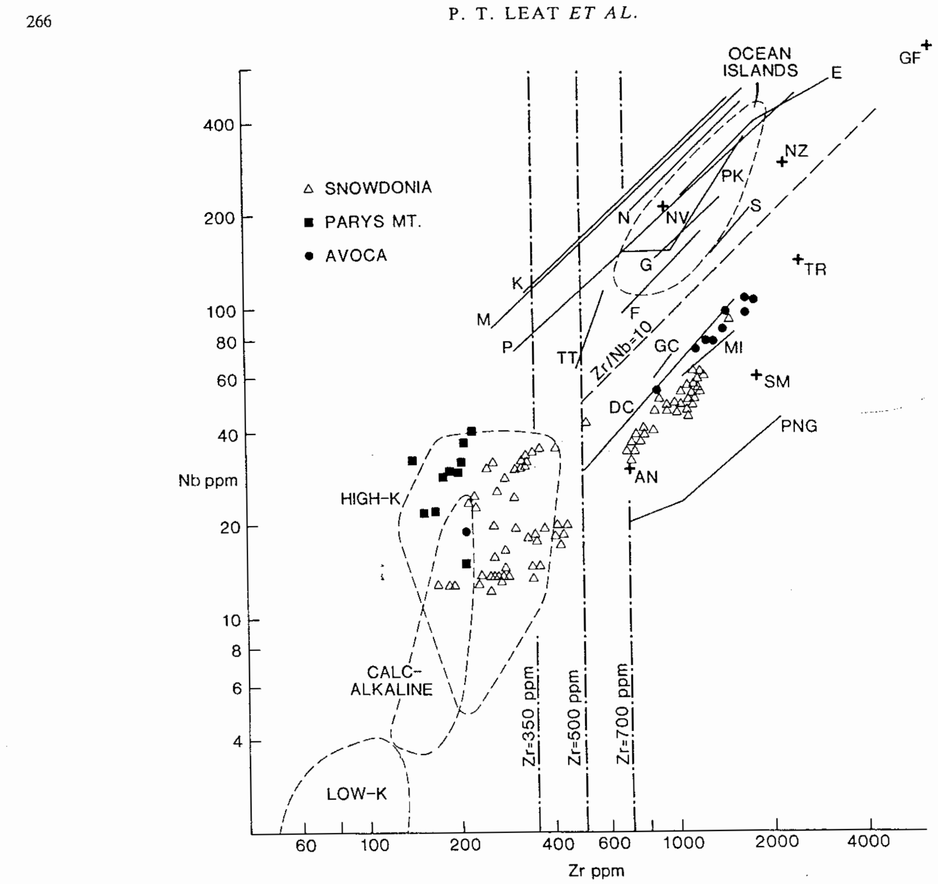

FIG. 7.84: Nb versus Zr plot for ash flow tuffs from this study.

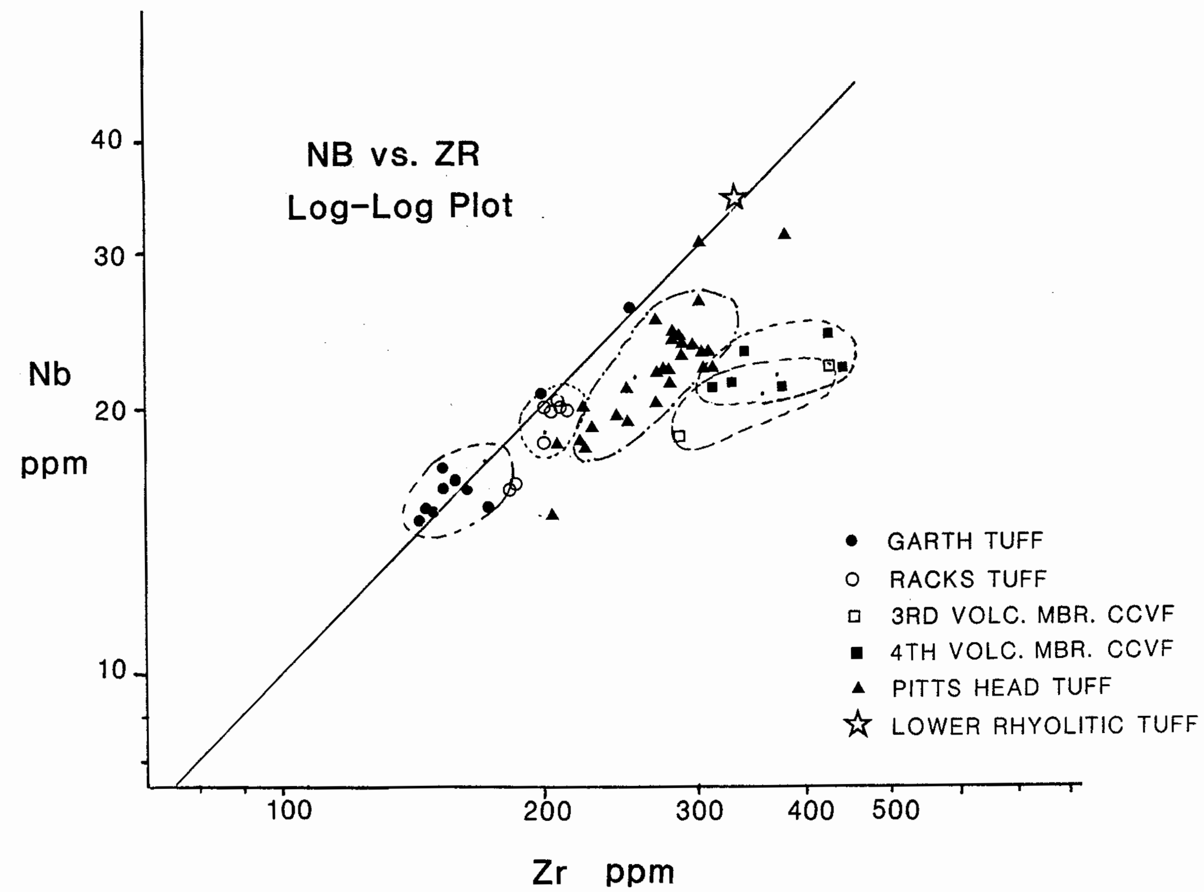

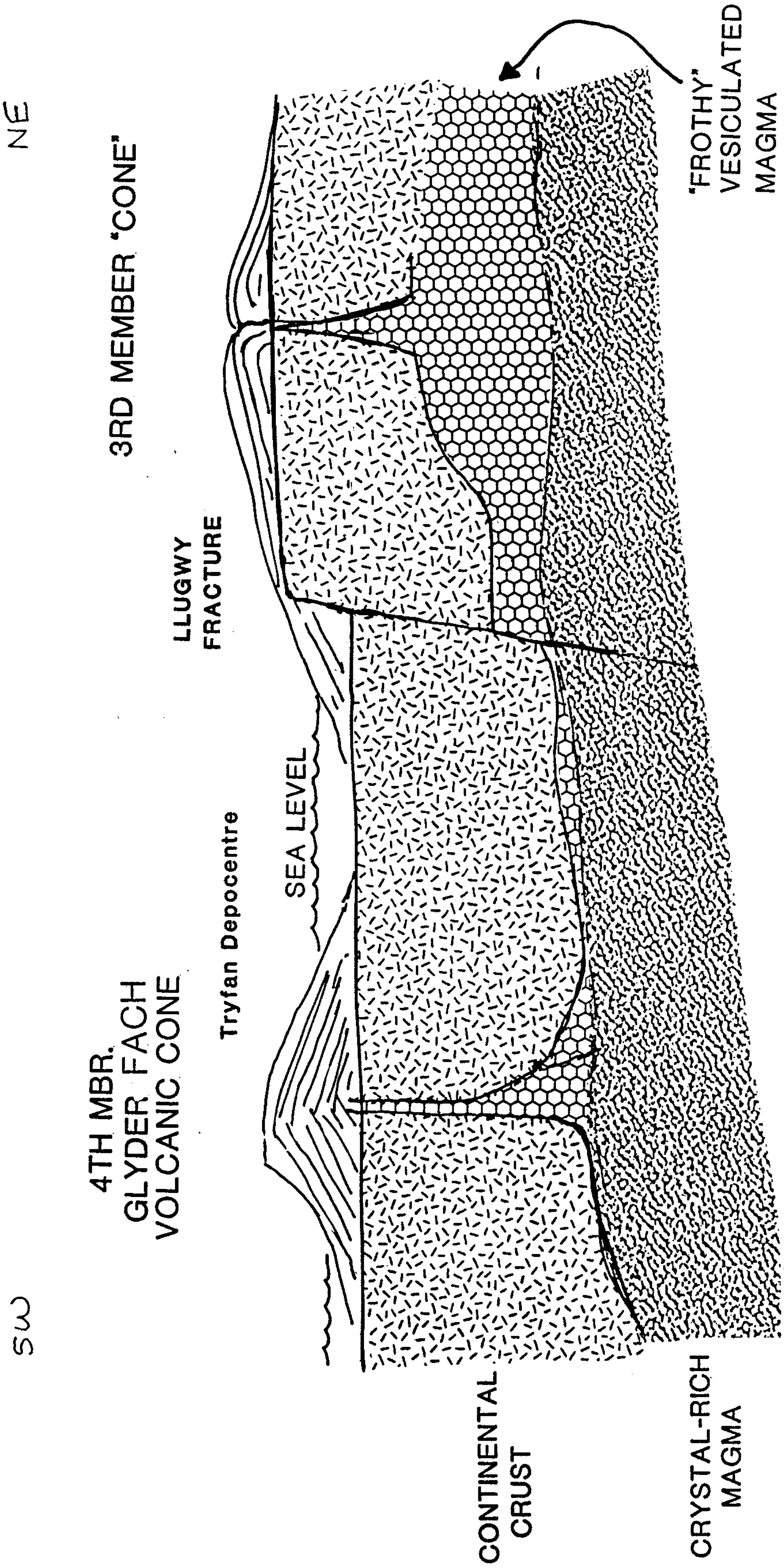

FIG. 7.85: Possible scenario to explain coeval eruption of explosive vitric-rich pyroclastics atLlyn Dulyn and crystal-rich volcaniclastics at Glyder Fach from the same magma chamber.

Chapter 8

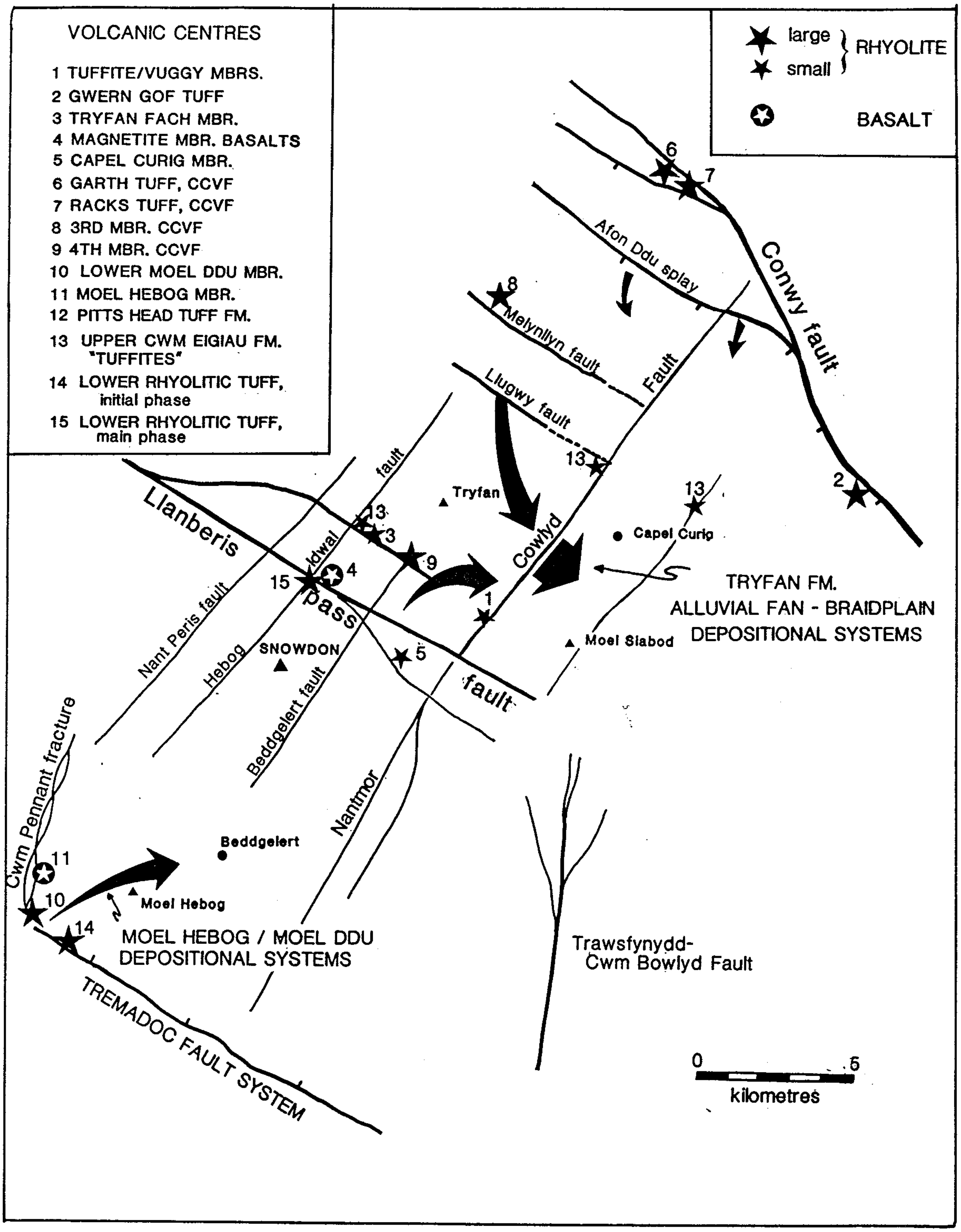

FIG. 8.1: TECTONIC FABRIC OF NORTH WALES showing location of volcanic centres and major depositional systems. Centres 8,9 from Howells & Leveridge, 1980; 15 from Kokelaar et al, 1984: Remainder from this study.

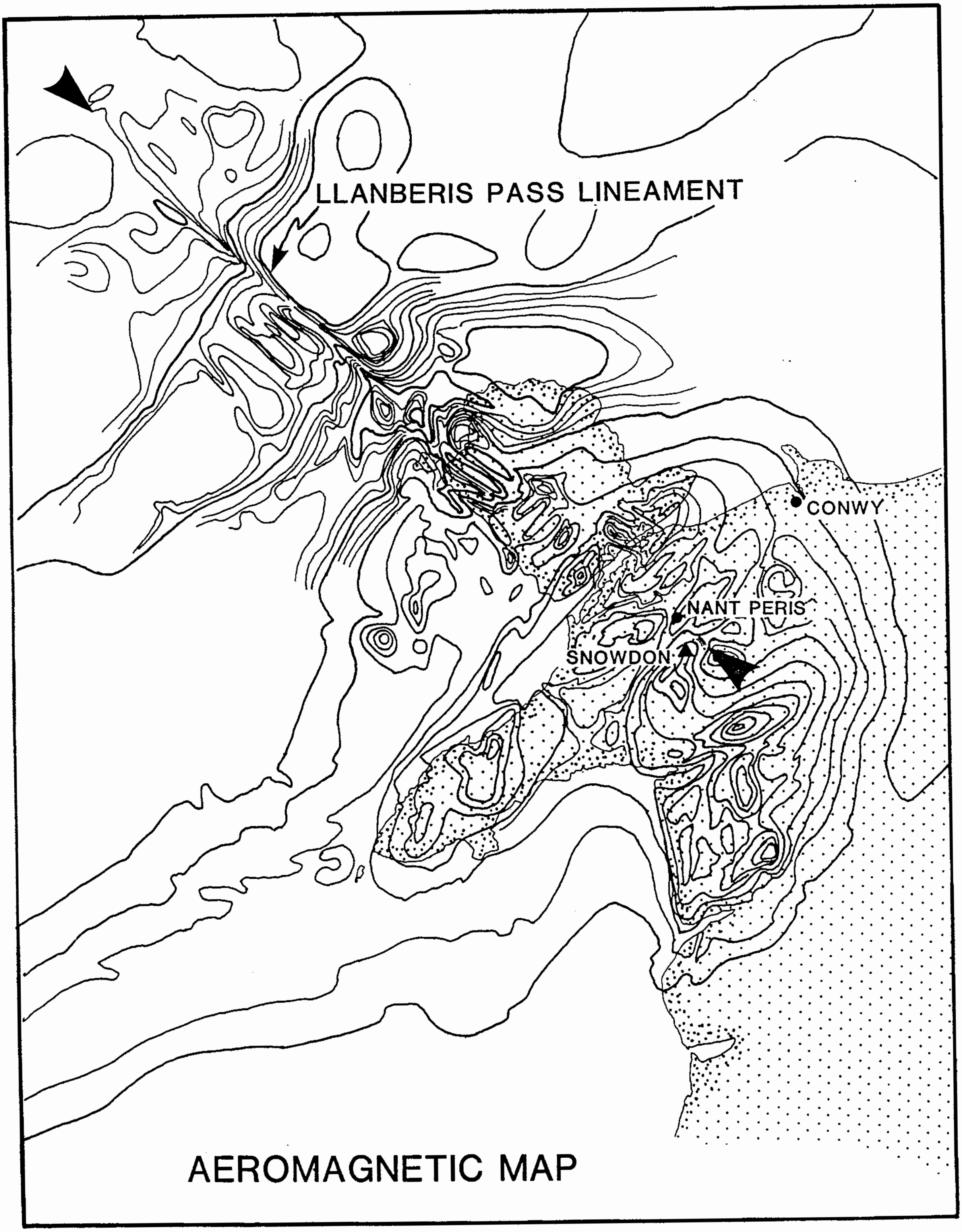

FIG. 8.2: Tracing of aeromagnetic map of North Wales showing extension of the Llanberis pass structure into the Irish Sea.

EVIDENCE FROM NORTH WALES

1) NW-SE structural alignment of depositional basin (Fig. 8.1)
2) basalt intrusions at Glyder Fawr indicate NE-SW extension
3) largest volcanic eruptions were from NW-SE trending faults
4) wave ripples require fetches in excess of distance to Church Stretton fault.
5) No evidence for uplift of Anglesey-Rosslare Horst ie. it was not the NW margin of the basin

EVIDENCE FROM OTHER PORTIONS OF WELSH BASIN

1) NNE-SSW extension associated with emplacement of sheeted basalt dyke complex at Rhobell Fawr (Kokelaar, 1979).

2) The basin deepens from NE to SW with 1) an uplifted NW-SE subaerial volcanic arc along the Midland Platform, 2) dominantly shallow marine facies in North Wales, Berwyn Hills, Builth Inlier area with uplift related to volcanic episodes, 3) deeper marine environments in Lleyn, Fishguard and SE Ireland with common pillow basalts and turbidites.

EVIDENCE FROM OTHER PORTIONS OF THE AVALON MICROCONTINENT and SE SIDE OF IAPETUS

1) The Midland platform (and Lake district) formed am uplifted NW-SE volcanic arc with varying amounts of preservation of subaerial volcaniclastic facies. In areas of weaker continental crust (eg. Lake district) the basement subsided; in areas of stronger crust (eg. about Birmingham), the volcanic arc never subsided and igneous intrusions are the only record of mid-Ordovician volcanic activity. This volcanic arc can be correlated with a coeval volcanic suite in the Brabant massif of Begium (Le Bas, 1972, Andre et al, 1986; Pharaoh et al, 1988)

2) No Lower Palaeozoic volcanicity in SE Newfoundland (ie. no evidence for SE directed subduction of Iapetus lithosphere).

3) No nappe sheets in Scandanavia with Baltic fauna contain volcanic successions. (ie. no evidence for subduction of Iapetus lithosphere beneath Baltica in Lower Palaeozoic) (Spjeldnaes, 1985; Stephens and Gee, 1985)

4) Igneous geochemistry from the Brabant massif, Belgium suggests SW directed subduction of the Tornquists sea (Andre et al, 1986).

FIG. 8.3: Some of the evidence to be presented by Orton and McKerrow in a later publication.

Fig. 8.4 View from Cwm Cneifion to NW showing proximity of Anglesey to Welsh mainland, being separated by the narrow Menai Straits. Despite this proximity there is no evidence for any input of sediment into Snowdonia from an uplifted Anglesey-Irish sea horst, which was its own self-contained sedimentary story by this time.

Fig. 8.5: Barranco (narrow valley) on south slopes of Tenerife which only receives epiclastic sediment during rare flash floods. Sedimentation is dominated by deposition of pyroclastic flows.

Fig. 8.6 Rubbly top to lava flow and a succession of ash flow tuffs in road cutting on southern flanks of Tenerife volcano. The shorter of two supervisors is shown for scale.

Fig. 8.7: Depositional succession on the southern flanks of Tenerife showing: A) mudflow, B) ignimbrite, C) erosive channel, D) ignimbrite, E) airfall tuff, F) soil horizon, G)

Fig. 8.8: Depositional succession on south flanks of Tenerife showing: A) ignimbrite, B) steep-sided channel infilled with muddy bedris flows, C) pyroclastic surge overlain by thin ash flow, and D) blocky debris flow.

Fig. 8.9: Development of small-network of braided streams by-passing toe of lava flows and ?volcanic cone on floor of caldera near Teide, Tenerife.

Fig. 8.10: Debris flow of rounded basaltic clasts in matrix of similar composition on north slopes of the Tremadocian volcanic edifice at Rhobell Fawr, southern Snowdonia.

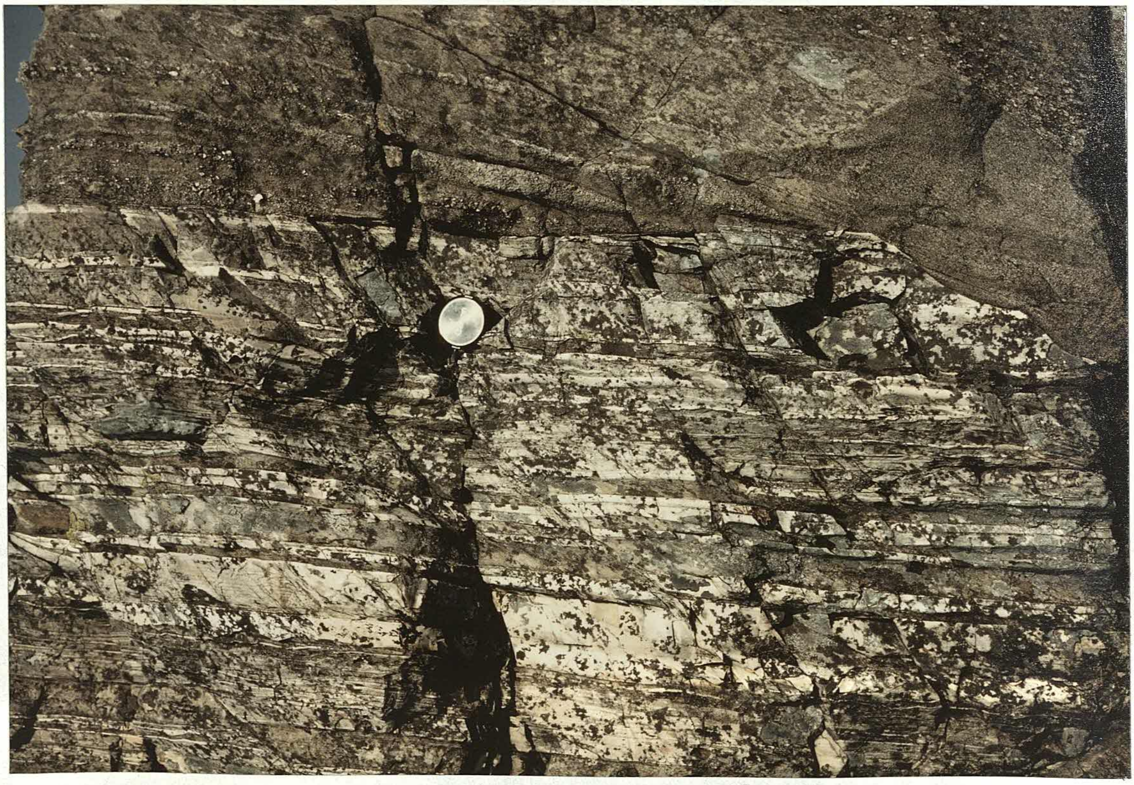

Fig. 8.11: Airfall tuff erosively removed by pebbly fluvial channel, near Rhinos Pass, Lake District.

FIG. 8.12: Heterolithic, blocky debris flows and sheetfloods, Lake district.

Fig. 8.13: Thin normally graded, pumice and lithic rich debris flows from mid-Ordovician volcaniclastic successions, Lake district.

FIG. 8.14:

USEFUL TOPICS OF FUTURE RESEARCH IN WALES

A: GENERAL INTEREST

1) Combination of whole-rock geochemistry of rhyolitic tuffs and sedimentology to establish a chronostratigraphic framework for the Ordovician from North Wales to the Berwyn Hills.

2) Geochemistry of mudrocks to determine both proportion of basaltic/rhyolitic source rocks and variation in anoxicity of Welsh basin in relation to volcanic events.

3) Re-examination of the type section of the Caradoc in south Shropshire to determine if plate-tectonic model proposed in this thesis (Chapt. 8.1) is viable.

4) Examination of ?analagous volcaniclastic successions on Cader Idris and the Arans.

B: SPECIFIC INTEREST

1) Influence of volcanic load on fluvial channels. Measurement and correlation of additional sedimentary sections at Moel Ddu (SH 588 443).

2) Coarse-grained nearshore sedimentation. Map of lithofacies of Capel Curig Mbr. shoreface successions along Gallt yr Ogof. (SH 677 584), and Gwastadnant Mbr. successions at Llyn Cwm-y-fynnon (SH 642 567).

3) Rare-earth element geochemistry to correlate "tuffites" within the Upper Cwm Eigiau Fm. to the NE of the A5 and recognize Capel Curig Volcanic Fm. and Pitts Head Tuff in successions near Dolwyddelan.

4) Sedimentology and geochemistry of the Lower Rhyolitic Tuff Fm., with aim to unravel the spatial and temporal evolution of the ?subaqueous caldera.

5) Detailed petrographic and sedimentological examination of the base of the Pitts Head Tuff near Llyn cwm-y-ffynnon, Llyn Bochlwyd, and Llyn Idwal to determine the pattern of mixing of ash flow and sediment during entry into the sea.